

DISSERTATION

INVESTIGATING THE BIOSYNTHETIC MECHANISMS OF THE BREVIANAMIDES &  
PENICIMUTAMIDES THROUGH THE TOTAL SYNTHESIS OF SECONDARY  
METABOLITES

Submitted by

Morgan McCauley

Department of Chemistry

In partial fulfillment of the requirements

For the Degree of Doctor of Philosophy

Colorado State University

Fort Collins, Colorado

Fall 2020

Doctoral Committee:

Advisor: Jeff Bandar

Alan Kennan  
Grzegorz Szamel  
Richard Slayden

Copyright by Morgan Taylor McCauley 2020

All Rights Reserved

## ABSTRACT

### INVESTIGATING THE BIOSYNTHETIC MECHANISMS OF THE BREVIANAMIDES & PENICIMUTAMIDES THROUGH THE TOTAL SYNTHESIS OF SECONDARY METABOLITES

The class of prenylated indole alkaloids containing a bicyclo[2.2.2]diazaoctane ring system consists of secondary metabolites isolated from fungal genera that possess diverse biological activities. Recent findings have established three ways in which the bicyclic core in this class can be constructed: (1) Generation of the monoxopiperazines (malbrancheamides and related families) by an NADPH-dependent bi-functional reductase/Diels-Alderase; (2) An enantiodivergent generation of the dioxopiperazines by some cytochrome P450 creation of achiral azadienes and successive enzyme-mediated stereoselective intramolecular hetero-Diels-Alder (IMDA) reaction in the notoamide/stephacidin families; and (3): non-Diels-Alderase generation of the bicycle of the brevianamides directed by a novel cofactor-independent pinacolase, culminating in a spontaneous IMDA reaction. The goal of the current work was to employ total synthesis to assist with the full characterization of unknown metabolites and decipher biochemical mechanisms employed in fungal organisms. Through this, the first total synthesis of brevianamide X and penicimutamide E, along with the synthesis of brevianamide A, and an improved, enantioselective synthesis of brevianamide Y were completed. The details of the novel synthetic work carried out by the author can be found in Chapters 3 and 5. Further synthetic efforts to better understand and access a variety of natural products are in progress to decipher the intrinsic transformations organism found in nature harness.

## ACKNOWLEDGEMENTS

First, I need to thank Professor Robert M. Williams. Bob was instrumental in developing me into the scientist that I am today. He was always there when I had questions and fully backed any of the ideas that I was interested in trying out. Working with him also allowed me to get experience in a variety of chemistry applications besides total synthesis, like acting as a science consultant on a patent case. While many may have found him to be a bit gruff and hard to approach, it did not mean that Bob was not there. Also, through working for him, I have learned to be confident in my ideas, even when talking with people who are experts in their field. This confidence that I have fostered is what will propel me forward in my career. Even though you are not with us anymore and cannot read this, I just want to say thank you.

Over my time at CSU I have been lucky to work with so many amazing chemists and people. Thank you to the members of the Williams group, both past and present. You all have listened to me complain, helped me get past ruts with my syntheses, always been there to discuss whatever comes to mind (not only science-related things), and have been an incredible support system. Thank you for being incredible friends, both in and outside of the lab. It has been a blessing to work with every one of you and I cannot wait to see what your futures hold.

Before coming to CSU for graduate school, I went to a small university in Nashville, Belmont University. The faculty there, especially Dr. Kimberly Entsminger and Dr. Duane Hatch, were crucial in fostering my love for chemistry. Without them and their loving, but insistent, push for me to continue with chemistry, I would not be here. I would never have seen going to graduate school as an option without them, much less be graduating so soon with a Ph.D. Even though it took me a bit longer than most (i.e. towards the end of the fall semester of my senior year), you both kept pushing me to the right choice for my future, so thank you for

being more stubborn than I was. With Dr. Entsminger being my PI for almost 4 years, and Dr. Hatch helping through the graduate school process, they both sparked my curiosity for chemistry and gave me a tool to further explore it all.

While I would not be the scientist that I have become without the people mentioned above, I would not be here nor be there person that I was without my family. Mom and Dad, I can never fully thank you for everything that you have done for me. Although most of the time you may not quite understand what I may be talking about, you were always there to listen. I cannot put into words how blessed I have been to have you both as parents. Even though you both worked full-time jobs, never once in my childhood did I (or my siblings) ever feel neglected or unable to do things; you both allowed all three of us to do activities outside of school and yet still managed to always be there when it counts. Through this, Mom and Dad, you have shown that it is possible to have a career and a family, without sacrificing one for the other. On top of that, both of you have never stopped encouraging me, even when my path took me somewhere new to all of us and made for little time for our family to be fully together. For all of this, and so much more that I would not ever be able to put into words, thank you.

Nicholas and Ryan, you have always been amazing brothers. While we used to fight A LOT when we were younger, I know that you have and will continue to always have my back. I am so lucky to say that I have a good relationship with both of my siblings, and I cannot wait to see what both of your futures will hold, and how our relationship will continue to grow. Also, to my niece, Reese, at the moment you are a middle schooler. I know now it may seem like you know everything, but it will all change, and quickly. I just hope that you continue through your life with an open mind and a caring heart. Do not let other people's opinions hold you back and do what you love. Life may seem like it will go on forever, but it is short, and we should be

thankful for every moment. I love you Reese and cannot wait to see you mature into the person you will be in the future.

## DEDICATION

To Professor Robert M. Williams, known by all by Bob

Thank you. I began my graduate career with you and am sad that you had to leave us too soon.

## TABLE OF CONTENTS

ABSTRACT.....	ii
ACKNOWLEDGEMENTS.....	iii
DEDICATION.....	vi
Chapter 1: Prenylated Indole Alkaloids.....	1
I. Introduction.....	1
II. Monooxopiperazines: Diels-Alderase Generation of the Bicyclic Core.....	4
III. The Enantiodivergent Synthesis of the Notoamides and Stephacidins.....	6
IV. Conclusions and Perspective.....	7
Chapter 2: <i>Penicillium brevicompactum</i> Proposed Biosynthetic Proposals and Total Syntheses for Brevianamide A and B.....	9
I. Early works (1969-1973).....	9
II. Williams initial synthesis and biosynthetic proposal (1988-1989).....	11
III. Williams 1993 <sup>13</sup> C study and Biosynthesis.....	14
IV. Williams 1998 Synthesis of Brevianamide B and C-19- <i>epi</i> -brevinanamide A.....	16
V. Halligan-Investigation Towards the Total Synthesis of Brevianamide A.....	18
VI. Williams 2005 Synthesis of Brevianamide B.....	20
VII. Williams 2007 Synthesis of Brevianamide B.....	21
VIII. Simpkins 2010 Synthesis of Brevianamide B.....	23
IX. Scheerer's 2016 and 2017 Formal Syntheses of Brevianamide B.....	24
X. Lawrence's Total Synthesis of Brevianamides A and B and Biosynthetic Proposal.....	26
XI. Minor Metabolites Isolated From <i>Penicillium Brevicompactum</i> : Brevianamides X and Y.....	29
i. Marine Drugs.....	29
ii. Glinka.....	30
iii. Greshock: First synthesis of oxindole without PG.....	31
iv. Miller: A new Approach to establishing the Oxindole Core.....	32
v. Qin's Total Synthesis of Brevianamide Y (depyranoversicolamide B).....	34
XII. Conclusions and Perspective.....	36
Chapter 3: Elucidation of Brevianamides A and B Biosynthesis.....	37
I. Background.....	37
II. Biosynthesis of Brevianamides A and B.....	38

III. BvnE Knock Out Study: The Total Synthesis of Unstable Intermediates and Mechanistic Investigations .....	42
IV. Total synthesis of N-methyl-deoxybrevianamide E and BvnE Substrate Model Study .....	52
V. BvnE Crystal Structure and Catalytic Mechanism Insight.....	54
VI. Total Synthesis of Brevianamide Y and X.....	56
VII. Indoxyl Species: Total synthesis of brevianamide A and Syn Indoxyl 204 .....	65
VIII. Computational Analysis .....	71
IX. Conclusions and Future Directions .....	76
Chapter 4: <i>Penicillium purpurogenum</i> : Biosynthetic isolate and proposals .....	78
I. Penicimutamide A-C: Isolation and Biosynthetic proposal.....	78
II. Total Synthesis of the Enantiomers of Aspeverin and Penicimutamide A .....	80
III. Isolation of Penicimutamides D-E .....	84
IV. Conclusions.....	86
Chapter 5: Synthetic Investigation of metabolites from <i>P. purpurogenum</i> .....	87
I. Introduction.....	87
II. Total synthesis of penicimutamide E and synthetic studies towards the synthesis of penicimutamide D .....	87
III. Towards the Total Synthesis of Penicimutamide A-C and Aspeverin.....	88
IV. Conclusions and Future direction .....	91
References .....	93
Appendix I: Contributions to Work .....	107
Appendix II: Supporting Information .....	108
Chapter 1: Experimental.....	108
i. General Procedures.....	108
Chapter 2: NMR Data .....	140
Appendix IV: Publications.....	257
List of Abbreviations .....	274

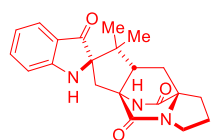
## Chapter 1: Prenylated Indole Alkaloids

### I. Introduction

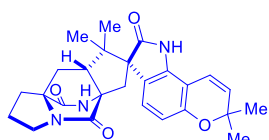
The class of prenylated indole alkaloids comprising a bicyclo[2.2.2]diazaoctane ring system consists of a variety of polycyclic and functionally unique secondary metabolites. These alkaloid metabolites have been isolated from both marine and terrestrial sources of *Aspergillus sp.*, *Malbranchea sp.*, and *Penicillium sp.*<sup>1-3</sup> Based upon biochemical and genetic origins, these natural products are divided into two structural sub-families (*Figure 1.1*).<sup>1,4</sup> First, there are the dioxopiperazines which contain two amides in the bicyclic system (*Figure 1.1*). Brevianamide A, a dioxopiperazine, was the first metabolite in the prenylated indole alkaloids family to be isolated with the bicyclic core. The second family of compounds is the monooxopiperazines that contain only one amide in the bicycle like seen in paraherquamide A. The monooxopiperazines can be further broken down into an entirely new family of biogenetically related decarbonylated alkaloids. While little is known of the decarbonylated compounds, such as citrinalin A<sup>5</sup>, it is theorized that they are a result of decarbonylation of the bicyclo[2.2.2]diazaoctane core. Despite the prenylated indole alkaloid class of compounds being around for over 50 years, the interest from both a biological and synthetic standpoint remains strong.

The continued interest in the prenylated indole alkaloids stems from their structural complexity and diverse biological activity. For example, paraherquamide A and 2-deoxyparaherquamide (derquandel), a semi-synthetic derivative, possess strong anthelmintic properties (*Figure 1.1*). In combination with abamectin, derquandel has been found to be effective at removing a large range of nematodes, even multi-resistant GI varieties, from sheep.<sup>6</sup>

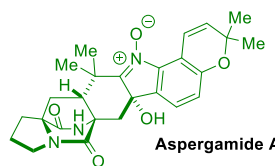
## Dioxopiperazines



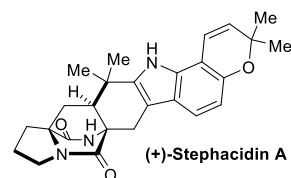
(+)-Brevianamide A



(+)-Versicolamide B



Aspergamide A



(+)-Stephacidin A



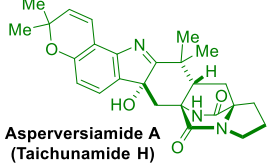
(+)-Brevianamide B



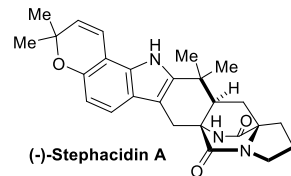
(-)-Notoamide A, X=OH; Y=H

(-)-Notoamide B, X=Y=H

(-)-Sclerotiamide, X=H; Y=OH



Asperversiamide A  
(Taichunamide H)



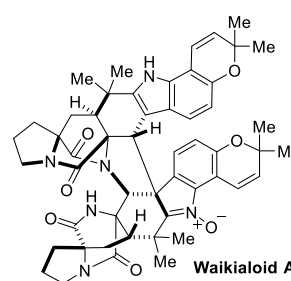
(-)-Stephacidin A



Amoenamide B

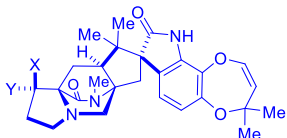


Taichunamide A

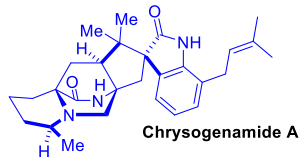


Waikialoid A

## Monooxopiperazines



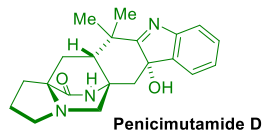
(-)-Paraherquamide A, X=OH, Y=Me  
(-)-Paraherquamide B, X=Y=H



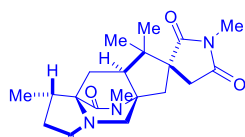
Chrysogenamide A



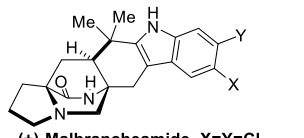
Citrinalin C



Penicimutamide D

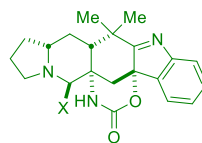


Asperparaline A, X=H<sub>2</sub>  
(Aspergillimide; VM<sub>55598</sub>)  
SB<sub>202327</sub>, X=O



(+)-Malbrancheamide, X=Y=Cl  
(+)-Malbracnamide B, X=H, Y=Cl  
(+)-Pre-malbrancheamide, X=Y=H  
(+)-Malbracnamide C, X=H, Y=Br

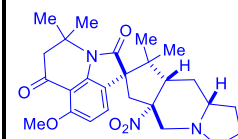
## Decarboxylated



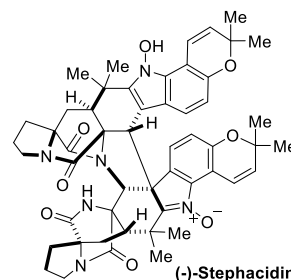
Penicimutamide B, X=OH  
Penicimutamide C, X=H  
Aspeverin, X=CN



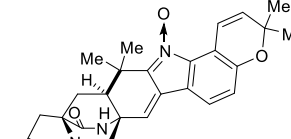
Citrinalin A



Cyclopiamine A



(-)-Stephacidin B



Avrainvillamide

**Figure 1.1: Representative fungal indole alkaloids containing bicyclo[2.2.2]diazaoctane.**

Compounds with 3-*spiro-ψ*-indoxyls, *spiro*-2-oxindoles and 3-hydroxyindolenines are presented in red, blue, and green respectively; compounds in black lack derivatization of the indole functionality.

Other biological activities shown by alkaloid metabolites includes anti-parasitic (marcfortines<sup>7,8</sup>, asperparalines<sup>9,10</sup>, brevianamides<sup>11,12</sup>), antibacterial (waikialoids<sup>13</sup>, aspeverin<sup>14</sup>, avrainvillamide<sup>15,16</sup>, speramide A<sup>17,18</sup>), anti-fungal (waikialoids<sup>13</sup>), neuroprotective<sup>19</sup>, anti-tumor (stephacidins<sup>20,21</sup>, notoamides<sup>22</sup>), and calmodulin inhibitory<sup>23</sup> properties.

While these indole alkaloids have been found to be biologically important, many enzyme transformations in the fungi are unique; as such, interest has also been drawn towards the biogenesis of the prenylated indole alkaloids. Harnessing the power of biomimetic and biocatalytic synthesis, the biochemical mechanisms of these fungal metabolites have been intensely investigated.<sup>24</sup>

Among the fungal genera *Aspergillus*, *Penicillium*, and *Malbranchea*, it was theorized that the bicyclo[2.2.2]diazaoctane ring system was constructed by an intramolecular hetero-Diels Alder (IMDA) reaction catalyzed by some Diels-Alderase enzyme. When performing the IMDA reaction, four distinct stereochemical outcomes are possible (*Figure 1.2*). The relationship between the bridged amide and the C-H proton at the bridgehead can be identified as being *syn*- or *anti*- to one another. Historically, *syn*-metabolites are more common than *anti*, and selectivity through synthesis also has displayed favorability towards the formation of *syn*-products.<sup>1-3</sup>

Recently, three distinct biogenetic pathways have been identified to be exploited by the producing fungi to construct the bicyclic core. First, the monooxopiperazines (malbrancheamide, paraherquamide, and related families) use NADPH-dependent bifunctional reductases/Diels-Alderase to build the bicyclic core (see Chapter 1.2). Second, a stereoselective construction of the bicycle in the dioxopiperazines is derived through an enantiodivergent Diels-Alderase cycloaddition of catalytically generated achiral azadienes through enzymatic oxidation for the notoamides and stephacidins (see chapter 1.3). Lastly, the construction of the

bicyclo[2.2.2]diazaoctane system in the brevianamides is directed by a cofactor-independent pinacolase, followed by a spontaneous IMDA reaction (see chapter 3).

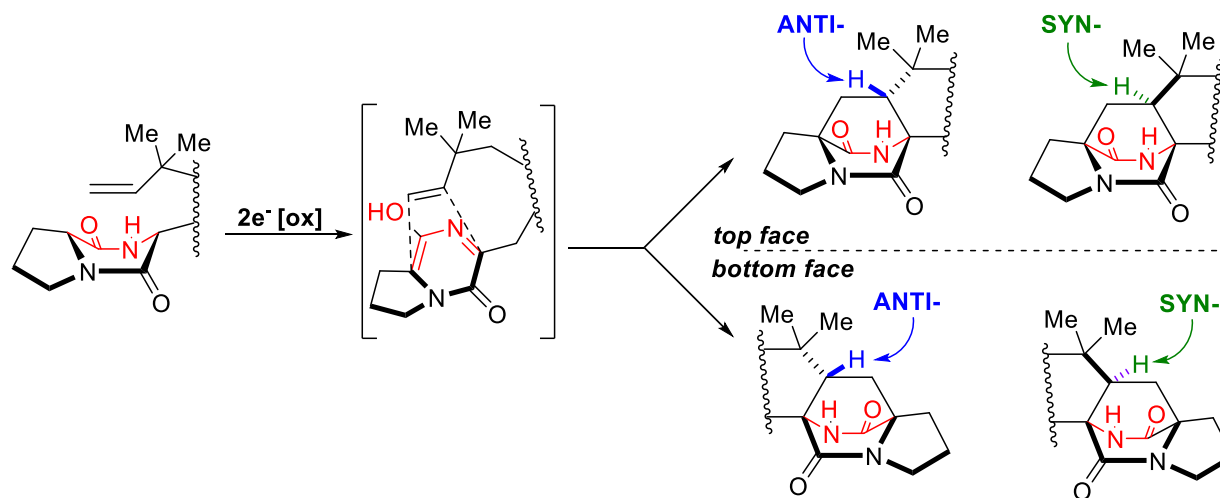


**Figure 1.2: Stereochemical outcomes of the IMDA cyclization across the diketopiperazine moiety to form the bicyclo[2.2.2]diazaoctane ring system.** *Anti*- and *syn*- designations are referring to the relation of the bridged amide (red) and C-H proton (blue = *anti*; green = *syn*) at the bridgehead.

## II. Monooxopiperazines: Diels-Alderase Generation of the Bicyclic Core<sup>1</sup>

By biomimetic total synthesis and *in vitro* enzymatic reconstitution, the biosynthesis of monooxopiperazines' malbrancheamide and paraherquamide were elucidated. For malbrancheamide, the coupling of proline and tryptophan is accomplished with dimodular NRPS (non-ribosomal synthetase) MalG, producing aldehyde **1** (Figure 1.3). Upon loss of water, the aldehyde rearranges to form monoketopiperazine **4**. Reverse prenylation by MalE and spontaneous oxidation will lead to zwitterionic species **5**. The structure of zwitterion **5** and its functionality in the biosynthesis was confirmed through biomimetic total synthesis of the substrate. Zwitterion **5** is reduced to azadiene **6** by MalC in the presence of NADPH, which also catalyzes an enantio- and stereoselective IMDA cycloaddition to (+)-premalbrancheamide (**7**).

<sup>1</sup> The work discussed was originally reported in *Nature Catalysis*<sup>25</sup>.

Similar results were found in the phqE genome of paraherquamide; the reductase/Diels-Alderase was identified as PhqE.

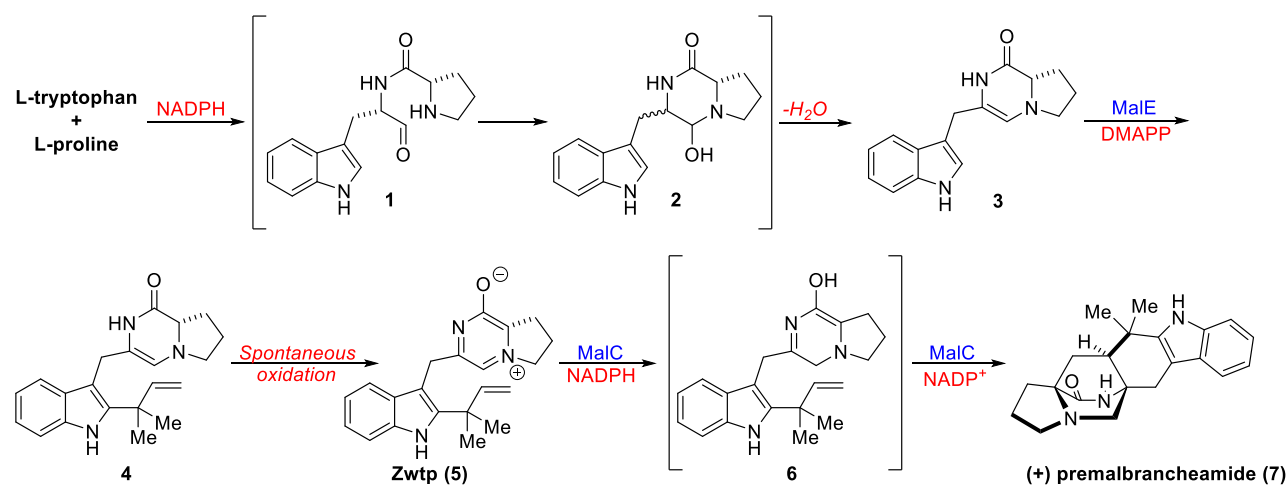


**Figure 1.3: Biogenesis of premalbrancheamide in *Malbranchea aurantiaca*.**

MalC is the first known reductase-dependent Diels-Alderase, and the first example of a Diels-Alderase in the prenylated indole alkaloid family. Interestingly, MalC was found to derive its selectivity for the cycloaddition from NADPH; in the presence of NADH the enantioselectivity between (+)-premalbrancheamide (**7**) and its enantiomer was 63:37. The necessity of NADPH appears to be a result of the high level of preorganization of the enzyme, which prevents the diene of **6** from exploring both faces of the pyrazinone ring. The discovery of novel enzymes, such as MalC and PhqE, represents “tools” that can be applied to various indole alkaloids to be able to selectively access more diverse substrates in a less step-heavy fashion. Identifying the reductase/Diels-Alderase enzymes for two species of the monooxopiperazines also acts as precedence for the Diels-Alderase construction of the bicycle in the family and decarbonylated sub-family of metabolites. Highly homologous proteins have already been identified by the Sherman group in the Citrinalin (CitL; *P. citrinum* F53) and Citrinadin (CtnO;

*P. citrinum* IBT 29821) pathways that could perform an *anti*-diastereoselective IMDA reaction to build the bicyclic precursor for some decarbonylated indole alkaloids.

### III. The Enantiodivergent Synthesis of the Notoamides and Stephacidins

The Gloer's laboratory was the first to isolate (-)-stephacidin A from *Aspergillus amoenus* (formerly *A. versicolor*), a terrestrial fungus.<sup>26</sup> The enantiomer, (+)-stephacidin A, was originally isolated from terrestrial fungi, *A. ochraceus* by Bristol-Meyer Squibb.<sup>27</sup> The stephacidins have also been isolated from marine fungi: (+)-stephacidin A from *A. protuberus* and (-)-stephacidin A from *Aspergillus sp. XS2009006*<sup>28</sup>. For each species, stephacidin A, and following metabolite derivatives, were optically pure.<sup>2,3,29-31</sup> This indicates that there likely is some enzymatic process that enantioselectively assists with the construction of the bicyclo[2.2.2]diazaoctane ring system in each species.

The identity of the enzyme, and its native substrate, is not known. After numerous feeding studies, it was theorized that isolated metabolite, notoamide S, could be the biosynthetic precursor to stephacidin A (*Figure 1.4*).<sup>4</sup> An oxidation of the diketopiperazine unit of notoamide S could occur (**8**), followed by the construction of the bicyclic core to form proposed metabolite notoamide T through a facial selective enzyme-mediated IMDA cycloaddition. The pyran ring could be formed by oxidation and cyclization to yield stephacidin A.<sup>3</sup> While the specific biological intermediates and enzymes have not been elucidated for the biosynthesis of stephacidin A, the gene clusters of the various fungi have been analyzed and determined to be orthologous to one another.<sup>2</sup> Further evolutionary implications of this finding are currently being investigated.

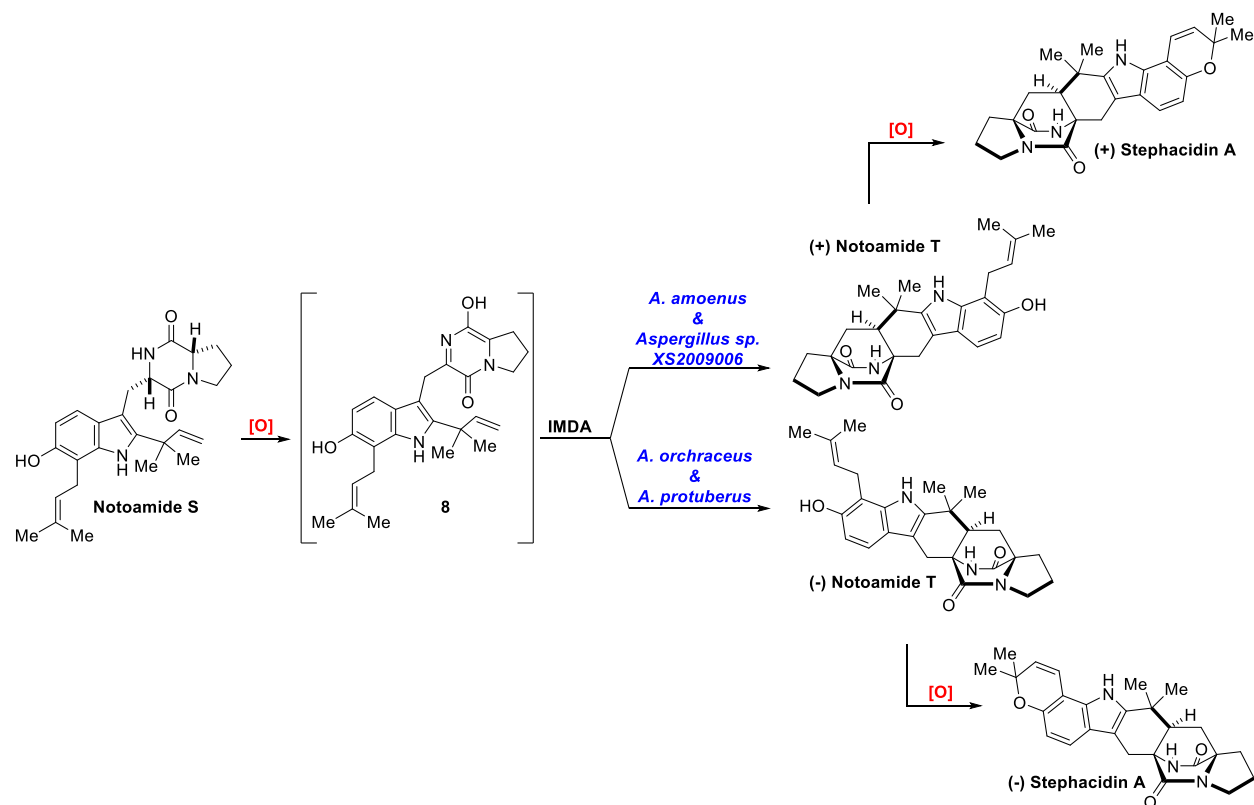


**Figure 1.4: Proposed biosynthesis of stephacidin A.** Fungal species *A. amoenus* and *Aspergillus sp. XS2009006* produce (+) stephacidin A while *A. orchraceus* and *A. protuberus* produce (-) stephacidin A in an optically pure manner.

#### IV. Conclusions and Perspective

The prenylated indole alkaloids are a class of compounds isolated from fungal genera *Aspergillus*, *Penicillium*, and *Malbranchea*. While this class of compounds has been studied for over a half a century, starting with the dioxopiperazine Brevianamide A, much is still unknown. The continued interest stems from the diverse biological activity and the continued ingenuity found in the biosynthetic construction of the structurally intriguing analogs. The recent discovery of the three pathways towards the construction of the characteristic bicyclo[2.2.2]diazaoctane ring system has provided us with a better framework for the biochemical mechanics that these fungi possess. With each new discovery of functionally unique enzymes, access to more complex

natural products, such as Waikialoid A, can be more readily studied. Also, reactions that were either not practical or not selective in the past, can easily be done on a variety of substrates through the application of the newly discovered enzymes.

This chapter was a brief overview of the current understanding of the prenylated alkaloids. Future chapters will focus on dioxopiperazines from the brevianamides, with specific interest on how our understanding of the biosynthetic construction of the metabolites has changed over the years through synthetic and biochemical studies (Chapters 2 & 3). Specifically, chapter 2 will discuss pertinent previous works. Chapter 3, on the other hand, will cover the full elucidation of the brevianamide biosynthesis, where all synthetic work was completed by the author (Morgan McCauley), biochemical work by the Sherman group at the University of Michigan, and the computational analysis by the Paton group at Colorado State University. A brief overview of the newly discovered penicimutamides will also be covered, including a proposed synthesis of the natural products through proposed biosynthetic intermediates (Chapters 4 & 5). The background, both isolation and previous relevant synthetic work, will be discussed in chapter 4. In chapter 5, synthetic efforts will be discussed, which, unless otherwise noted, were completed by the author.

## Chapter 2: *Penicillium brevicompactum* Proposed Biosynthetic Proposals and Total Syntheses for Brevianamide A and B

### I. Early works (1969-1973)

In 1969 Birch and Wright isolated brevianamide A, along with brevianamide E, from *Penicillium brevicompactum*.<sup>32</sup> Brevianamide A (**8**) was a groundbreaking discovery as it was the first compound isolated in the prenylated indole alkaloid family that contained the characteristic bicyclo[2.2.2]diazaoctane ring system (*Figure 2.1*). Initial biosynthetic studies revealed that brevianamide A was made from tryptophan, proline, and an isoprene unit.<sup>33,34</sup> While the exact structure of the compound was unknown at the time, the *spiro-ψ*-indoxyl skeleton was confirmed by the UV chromophore. In future isolation studies, Birch and Russell were able to identify four new brevianamides: B, C, D, and F.<sup>35</sup> Most notably, brevianamide B (**9**) was theorized to be a stereoisomer of brevianamide A, which was later confirmed through the total synthesis of the metabolite. Additional biological testing found brevianamide A to be a potent anti-parasitic agent against an assortment of insect species.<sup>11,12</sup> The most pressing mystery for the structure determination of brevianamide A was how, biosynthetically, the organism could establish the bicyclic core.

The bicyclo[2.2.2]diazaoctane ring system was first theorized by Porter and Sammes to arise from some spiro-5-intramolecular [4+2] Diels-Alder (DA) reaction (*Figure 2.2*).<sup>36</sup> To test the theory, Porter and Sammes attempted Diels-Alder reactions between various substrates. Most notably, a trial was performed with norbornadiene and a pyrazine derivate. The reaction was found to not only readily form the Diels-Alder product, but also to favor product

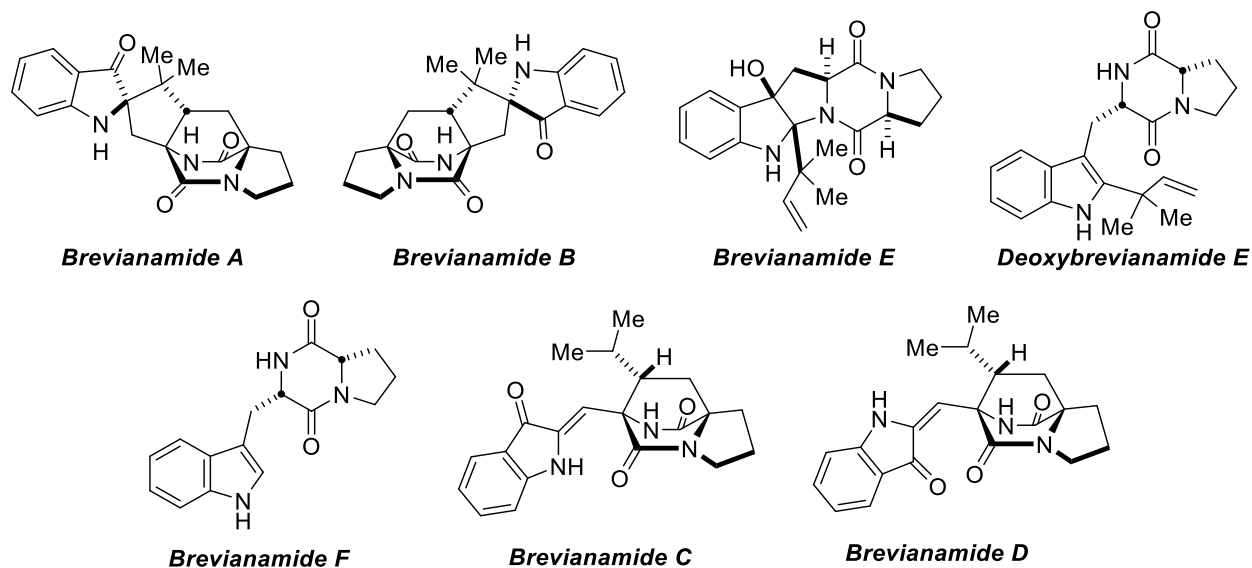


**Figure 2.1: Fungal metabolites isolated from *P. brevicompactum*.** Brevianamides C and D were found to be photolytic artifacts of brevianamide A

formation over reforming the reactants, likely due to favorability towards amide formation over the dihydropyrazine system. With support towards the formation of the bicyclic system of brevianamide A through some IMDA reaction, attention was shifted towards understanding the inherent selectivity. This could not be established at the time, as the stereochemistry of brevianamide A was unknown. It was not until the first total synthesis of brevianamide B that the absolute configuration of the compound, and a vital relationship in the biogenesis of brevianamides A and B, was revealed.<sup>37,38</sup> The biogenesis, while unknown, needed to account for the tricyclic ring systems of the two compounds functioning as enantiomorphs.<sup>39</sup>

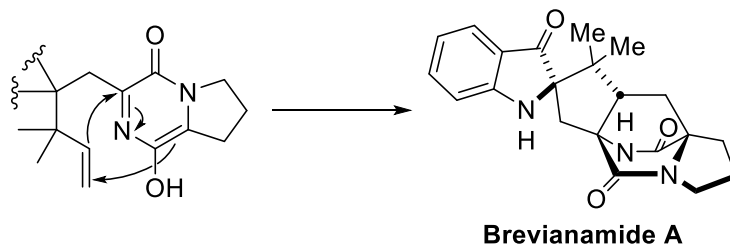


**Figure 2.2: Early suggestions by Sammes and Birch for the biosynthetic construction of the bicyclo[2.2.2]diazaoctane ring system.** While the exact substrate of the IMDA reaction was not proposed, the proposal suggests some spiro-derivative of the indole.

## II. Williams initial synthesis and biosynthetic proposal (1988-1989)<sup>2</sup>

The first total synthesis of brevianamide B was carried out by Williams and coworkers in 1988 (*Figure 2.3*). To start, proline derivative **8** was allylated following Seebach's<sup>40</sup> procedure to afford **10**. Aminolysis with pMB, accompanied by condensation with bromoacetyl bromide, and the consecutive ring closer, yielded diketopiperazine derivative **13**. Ozonolysis of **13** provided aldehyde **14**. Access to **16** was achieved by a Wittig reaction between aldehyde **14** and *E*-allylic alcohol **15**, succeeded by a NaBH<sub>4</sub> reduction. Silylation of **16** and carboxymethylation yielded **17** in a 4:1 mixture. Compound **19** was synthesized through Kametani-type coupling of gramine (**18**) with **17**. Successive silyl deprotection, indole protection, and allylic chlorination resulted in **20**. The resultant product (**20**) was exposed to the key intramolecular S<sub>N</sub>2' cyclization, an essential step to establish the desired *anti*-stereochemistry of the bicyclic core. The desired isomer (**21**) was formed by NaH treatment of **20**, but the undesired isomer could also be accessed by addition of 18-crown-6 to the reaction mixture.

Hexacyclic indole **22** was constructed from **21** by consecutive removal of the N-t-BOC group and cyclization with concentrated HCl. Oxidation of the indole double bond with mCPBA gave a single hydroxyindolenine (**23**) diastereomer, which upon treatment with a strong base went through a semi-pinacol rearrangement to indoxyl species **24**. Lastly, the pMB group was removed with excess *t*-BuLi in THF to afford (-) brevianamide B. With their total synthesis of brevianamide B, a compound that is produced in extremely low quantities in *P. brevicompactum*, the absolute configurations of both brevianamides A and B were revealed, as well as a critical biosynthetic relationship between the two compounds.

---

<sup>2</sup> The work discussed can be found in references 37-39.

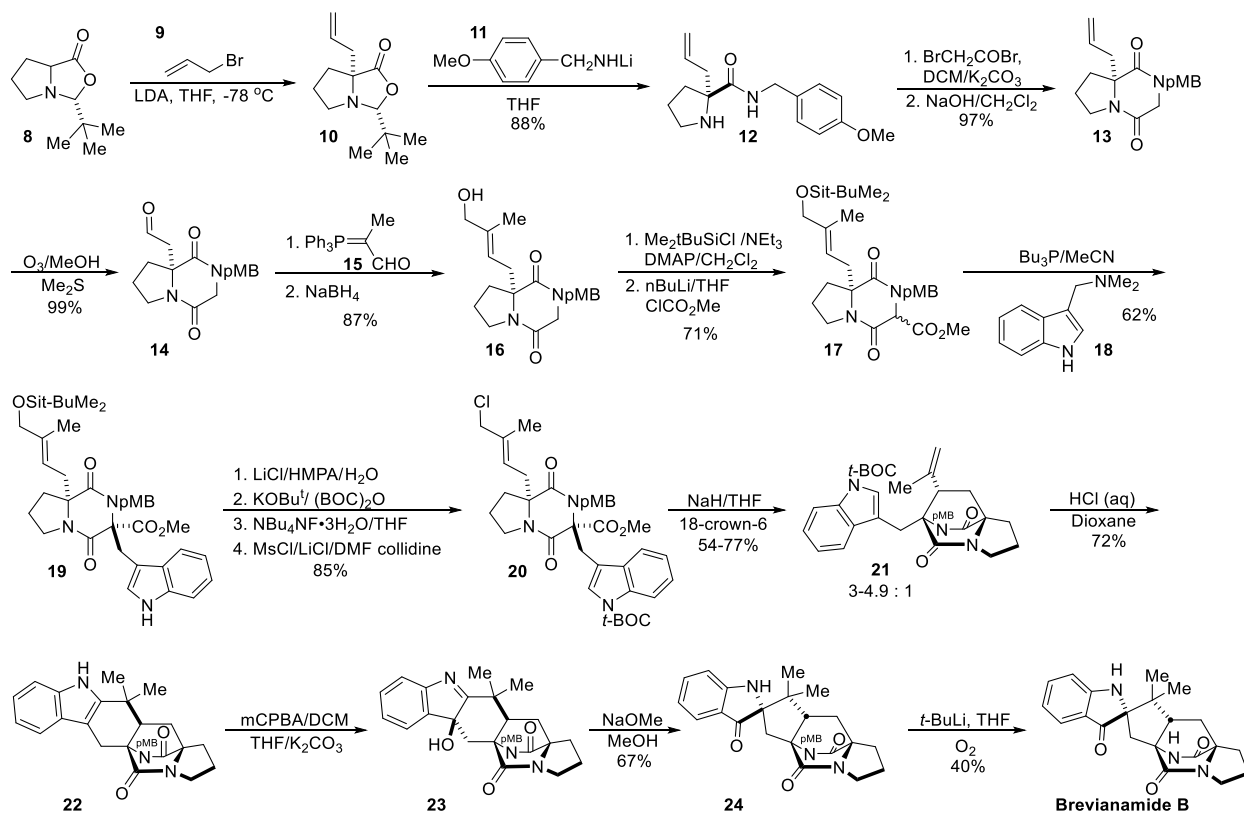


**Figure 2.3: Williams 1988 synthesis of brevianamide B.** Accounted for first total synthesis of brevianamide B.

From this discovery, the Williams group developed their first biosynthetic proposal for the brevianamides (*Figure 2.4*). Based on Birch's feeding study, it was believed that brevianamide F was constructed from *L*-tryptophan and *L*-proline.<sup>34</sup> Brevianamide F could then be prenylated with dimethylallyl pyrophosphate (**32**) to give deoxybrevianamide E. Oxidation of the diketopiperazine unit of deoxybrevianamide E could yield an azadiene species (**33**), which could suffer an intramolecular [4+2] IMDA reaction to give cycloadduct **34**. Oxidation and semi-pinacol rearrangement of the resultant hydroxyindolenine would then provide brevianamides A and B. During the total synthesis of brevianamide B, mCPBA was found to selectively oxidize one face of the cycloadduct. Given that mCPBA only oxidized towards the formation of brevianamide B, the minor product, it was theorized that some enzyme-mediated process must occur to shift the

stereoselectivity to favor the major isomer, brevianamide A, from the specific enantiomer of the cycloadduct.

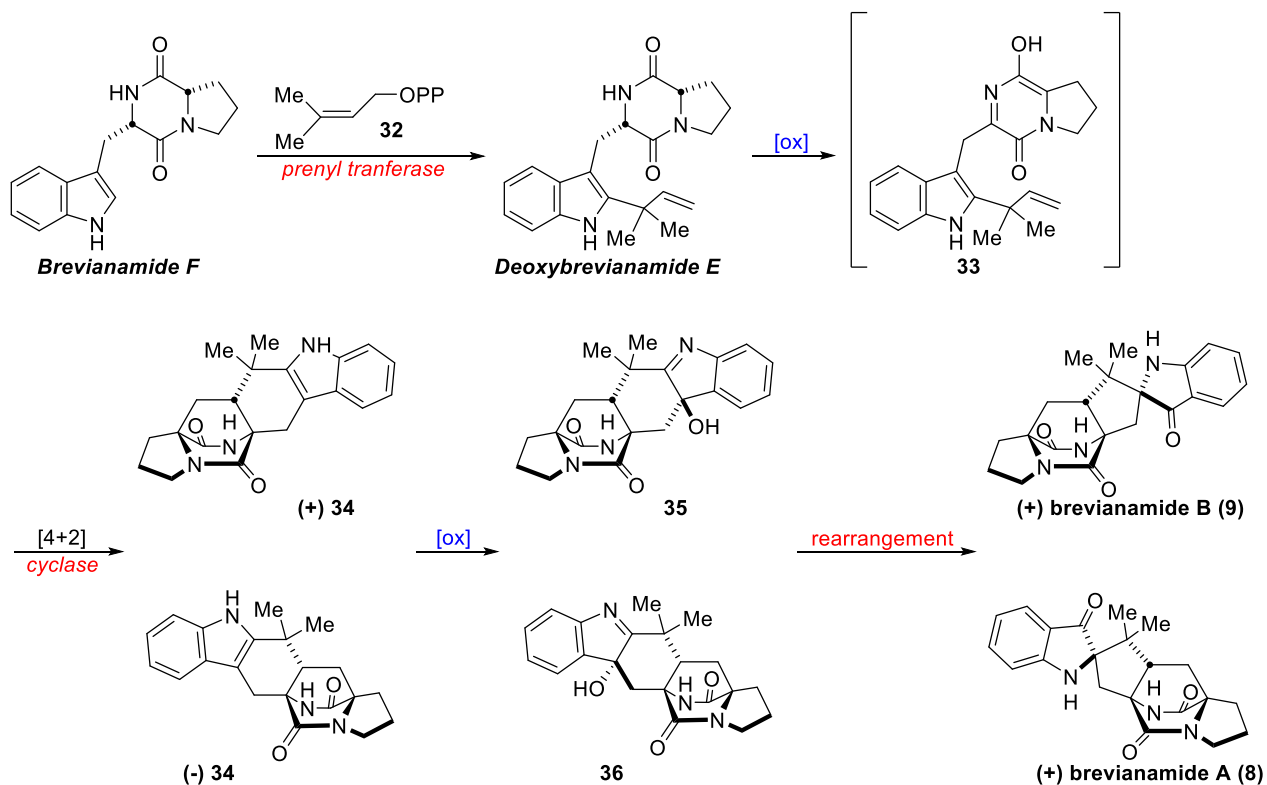


**Figure 2.4: Williams 1989 biogenetic proposal for brevianamides A and B.** The pinacol rearrangement to the indoxyl occurs after the IMDA cycloaddition.

To test the likeliness of their proposed biosynthesis, Williams and co-workers screened for the presence of cycloadduct **34** in extracts from *P. brevicompactum*. Efforts to detect **34** were unsuccessful, which led to two possible conclusions. Either cycloadduct **34** was short-lived in the organism and was immediately transformed by the enzyme to other substrates (i.e. **35/36** or brevianamides A and B). Or the cycloadduct was not present in the fungi, and as a result, not a biological intermediate to the brevianamides.

### III. Williams 1993 <sup>13</sup>C study and Biosynthesis<sup>3</sup>

In the William's 1989 proposed biosynthesis of brevianamides A and B, cycloadduct **34** was proposed to be a key intermediate. The compound was not found when screened for in the organism. To indisputably determine whether **34** was present in *P. brevicompactum*, a <sup>13</sup>C labeled synthesis of the cycloadduct was carried out. The route that was previously used to synthesize brevianamide B (*Figure 2.3*) was followed using <sup>13</sup>C-labeled gramine. When the <sup>13</sup>C-labeled cycloadduct was fed to the organism there was no seen incorporation into either brevianamide A or B.

With **34** ruled out as a biological intermediate in the biosynthesis of the brevianamides, a new target was set. Deoxybrevianamide E, a compound that was first postulated to be a precursor by Birch<sup>34</sup>, was tested next for its intermediacy in the biosynthesis of the brevianamides. A tritium label was utilized to ascertain that the compound could be detected even with the small quantities that would be isolated.

The synthesis of [8-<sup>3</sup>H]labeled deoxybrevianamide E was inspired by the procedure established by Kametani.<sup>43,44</sup> Prenylated indole **27** was prepared by a variation of the Fisher indole synthesis (*Figure 2.5*).<sup>45</sup> Acetonitrile was reacted with **25** and Zn(Ag) to establish a ketone. Imine **26** was formed when the ketone was treated with hydrazine. Upon reflux with ZnCl<sub>2</sub> in diglyme, desired prenylated indole **27** was established. The tritium label was introduced with labeled formaldehyde and reacted with prenylated indole **27** to give gramine derivative **28**. Somei coupling<sup>46</sup> of gramine with diketopiperazine **29**, followed by reduction of the methyl ester gave a mixture of deoxybrevianamide E and its (*R*)-diastereomer.

---

<sup>3</sup> The work discussed can be found in references 41 and 42.

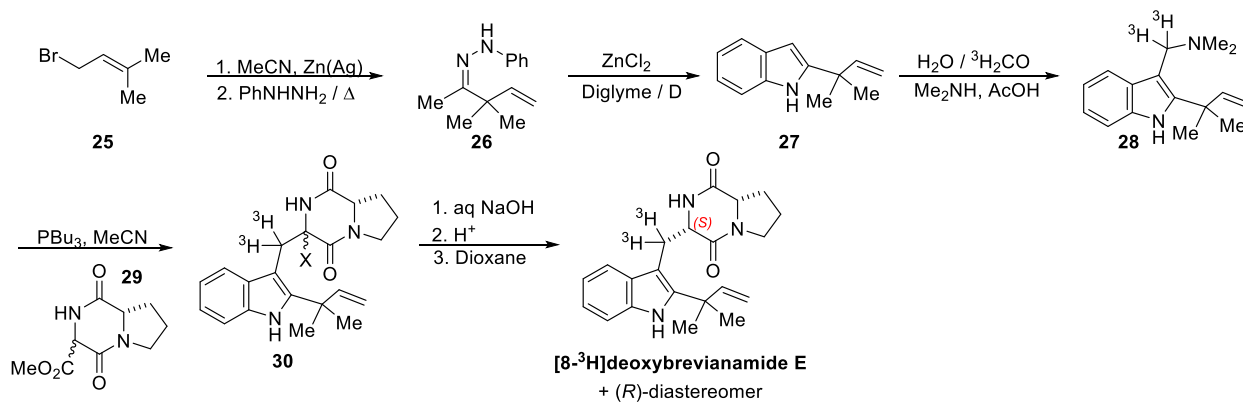


**Figure 2.5: Williams tritium labeled synthesis of deoxybrevianamide E.** The tritium label was introduced by formaldehyde. X= CO<sub>2</sub>Me

A significant amount of incorporation of [8-<sup>3</sup>H]deoxybrevianamide E was found in both brevianamide A (7.8% total incorporation, 12.1% specific incorporation) and brevianamide B (0.9% total incorporation, 1.4% specific incorporation) when fed to *P. brevicompactum*. There was also incorporation found in brevianamide E (24.9% total incorporation, 38.5% specific incorporation). The high values of incorporation confirmed that deoxybrevianamide E is a biosynthetic precursor of brevianamides A, B, and E. The high levels of incorporation of deoxybrevianamide E into brevianamide E, along with its stability in culture conditions and consistent proportion to brevianamide A, implied that brevianamide E is not an artifact of work-up or culture conditions like previously believed; instead, brevianamide E is a dead end in the biosynthetic pathway.

Founded on the results of the feeding studies, Williams and coworkers developed a new biosynthetic proposal (Figure 2.6). The major difference in the 1993 proposed biosynthesis when compared to that from 1989 is a conclusion derived from the <sup>13</sup>C and <sup>3</sup>H feeding studies; the indoxyl is likely constructed before the IMDA cycloaddition. Like previously seen in the 1989 biosynthesis, brevianamide F was thought to be prenylated to form deoxybrevianamide E. Selective oxidation of the indole of deoxybrevianamide E would furnish the hydroxyindolenine

intermediate. The hydroxyindolenine then could experience two fates: either undergo a nucleophilic substitution to form brevianamide E or suffer a pinacol rearrangement to indoxyl **38**. Formation of azadiene species **39** through an oxidation of the diketopiperazine unit, followed by an enzyme-catalyzed DA reaction would yield brevianamides A and B.

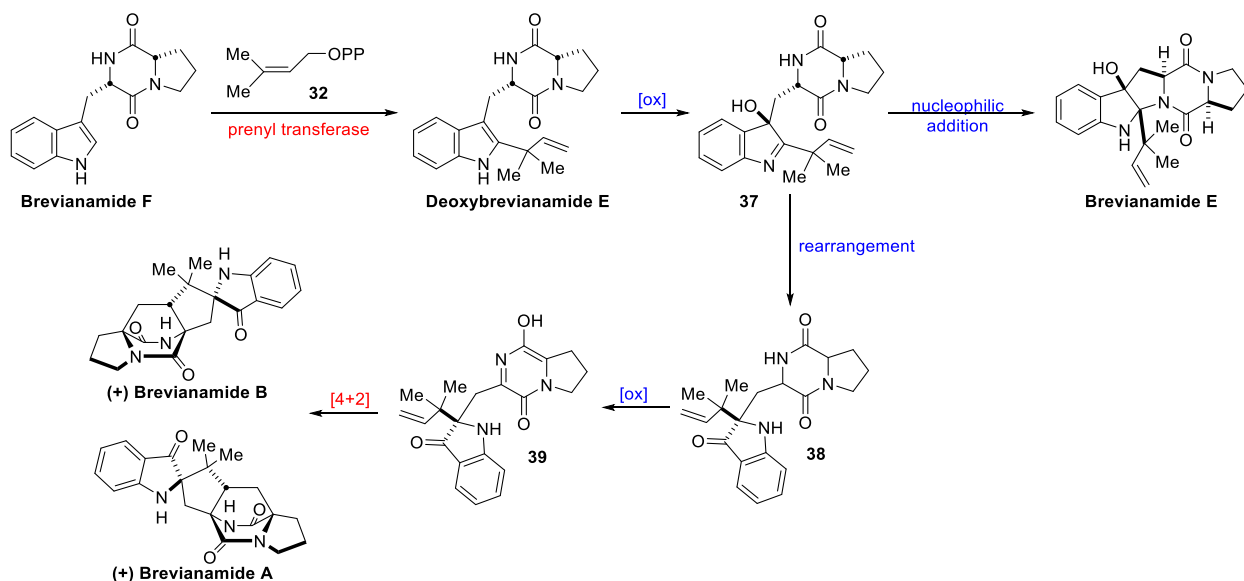


**Figure 2.6: Williams 1993 biosynthetic proposal for brevianamides A and B.** The first biosynthetic proposal to account for the formation of brevianamide E as a shunt metabolite, which was accomplished by the pinacol rearrangement occurring before the IMDA reaction.

#### IV. Williams 1998 Synthesis of Brevianamide B and C-19-*epi*-brevianamide A<sup>4</sup>

An IMDA reaction was proposed to establish the bicyclo[2.2.2]diazaoctane ring system in the Williams 1993 biosynthetic proposal. To establish if an IMDA reaction could occur on the brevianamide substrates, and whether the transformation was likely enzymatic, a biomimetic synthesis was carried out, with a focus on executing the IMDA cyclization.

<sup>4</sup> The work discussed can be found in reference 47.

The synthesis of 9-*epi*-deoxybrevianamide followed the procedure by Kametani.<sup>2</sup> Conversion to lactim ether **40** proceeded with Me<sub>3</sub>OBf<sub>4</sub> (Figure 2.7). DDQ oxidation gave unsaturated compound **41**. Treatment of compound **41** with methanolic KOH caused a tautomerization to azadiene species **42**, which suffered a spontaneous IMDA reaction to cycloadducts **43** and **44** in a 2:1 ratio. Cycloadducts **43** and **44** were separated and converted to C-19-*epi*-brevianamide A and brevianamide B respectively through mCPBA oxidation, semi-pinacol rearrangement of the hydroxyindolenines (**45** and **46**), and lactim ether deprotection.

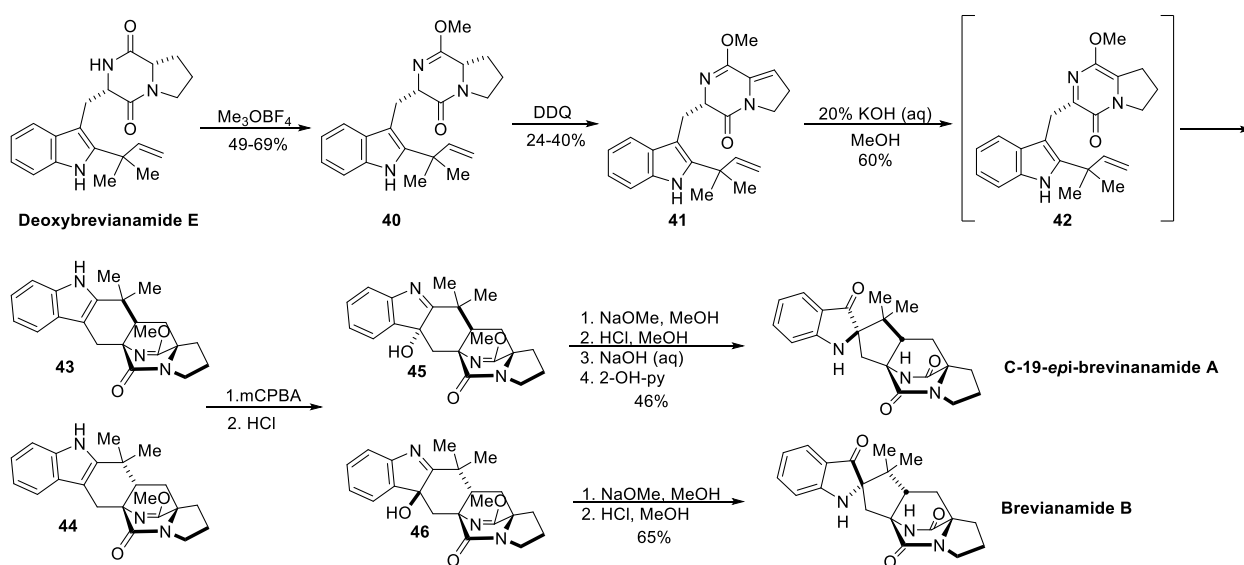
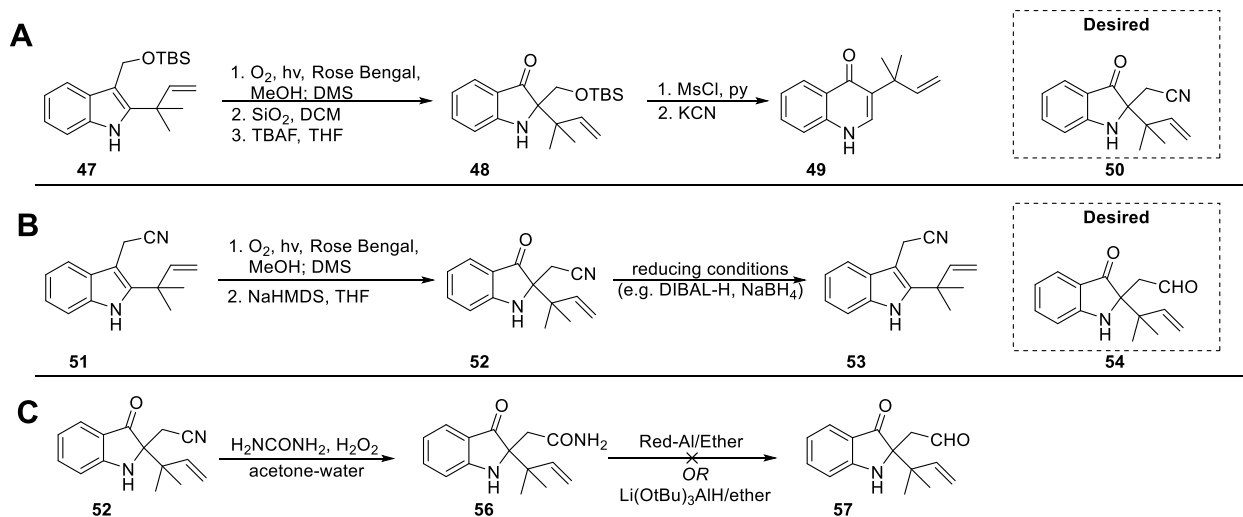


Figure 2.7: Williams 1989 synthesis of brevianamide B and C-19-*epi*-brevianamide A. Synthesis is shown from biosynthetic precursor deoxybrevianamide E.

When investigating the IMDA construction of the bicyclo[2.2.2]diazaoctane ring system, it was found that the choice of solvent did not play a role in the selectivity of the proportion of *syn*- to *anti*-cycloadduct. The major synthetic product was the *syn*-cycloadduct (**43**), of which none have been identified in *P. brevicompactum*. This implied that the organism may possess a mechanism to assure facial exclusivity in the construction of the bicyclic core.

## V. Halligan-Investigation Towards the Total Synthesis of Brevianamide A<sup>5</sup>

Previous syntheses of brevianamide B were accomplished by oxidizing the indole of *anti*-cycloadducts (**22** & **44**) to form the relevant hydroxyindolenine, which would rearrange under basic conditions. The reason that only brevianamide B was synthesized was that oxidation to the hydroxyindolenine was solely occurring on one face; the hydroxyindolenine precursor to brevianamide A was never formed. It was theorized by Halligan that by performing the semi-pinacol rearrangement to the indoxyl before IMDA cyclization, access to both brevianamides A and B would be possible. The idea was to form proposed biosynthetic precursor **38** from Williams' 1993 biosynthetic proposal, the indoxyl of deoxybrevianamide E (**38**; see *Figure 2.6*). Initial attempts to form an indoxyl were done on less functionalized indoles (**47** & **51**; *Figure 2.8*).



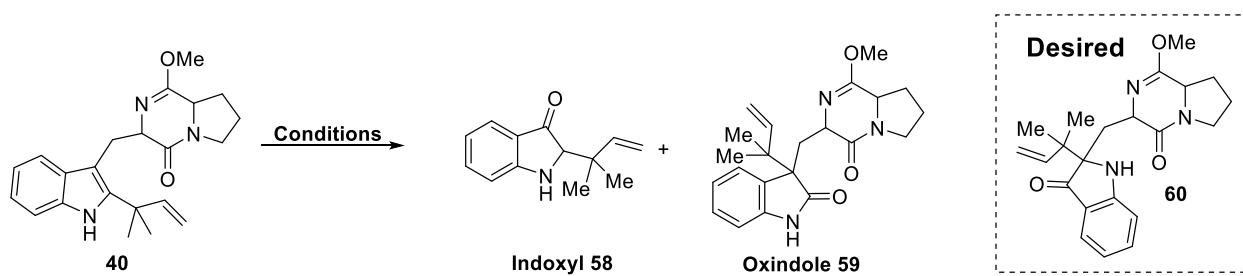
*Figure 2.8: Attempts to synthesize and derivatize indoxyl substrates:* (A) Initial attempts to synthesize indoxyl **50**, which led to a ring expansion; (B) Initial conditions to try to form the indoxyl **54** that resulted in reformation of the indole. (C) Further derivatization of the indoxyl was not possible from **56**.

While indole derivatives **47**, **51** and **52** were able to be transformed to indoxyl derivatives, when any further functionalization, especially even slightly reductive conditions, were attempted

<sup>5</sup> The work discussed can be found in reference 48.

the indoxyl would reform the indole or a ring expansion would occur (*Figure 2.8*). For example, after mesylating indoxyl derivate **48**, exposure to KCN triggered a ring expansion of the pentane ring gives undesired product **49** (*Figure 2.8 A*). Protecting the indoxyl was attempted in hopes of preventing the unwanted side reactions. Boc-protection of the indole was not successful, nor was forming an ether species with  $\text{BF}_4\text{OEt}_3$ . After intense investigation of the indoxyl species, coupling of **57** to a proline derivative was accomplished, but conversion to the diketopiperazine while maintaining the indoxyl was not possible.

As an alternative of carrying forward the indoxyl over a multitude of steps, a semi-pinacol rearrangement was attempted on a lactam ether derivative of deoxybrevianamide E (**40**). A variety of basic and acidic conditions were tested (*Figure 2.9*).



Conditions	Results
1M NaOH, MeOH	Indoxyl <b>58</b>
KOH, PPTS, DMSO-MeOH	Indoxyl <b>58</b>
DBU, THF	SM ( <b>40</b> ) + decomp
KHMDS, PPTS, DCM	SM + decomp
$\text{K}_2\text{CO}_3$ , DMF	Oxindole <b>59</b>
2 M HCl, MeOH	SM ( <b>40</b> ) + decomp
Silica gel	SM ( <b>40</b> ) + decomp
$\text{Al}_2\text{O}_3$ , toluene	SM ( <b>40</b> ) + decomp
$\text{BF}_3(\text{OEt})_2$ , $\text{HC}(\text{OMe})_3$ , DCM	SM ( <b>40</b> ) + decomp

*Figure 2.9: Conditions tested on compound 40 to attempt the formation of indoxyl 60. All attempts either led to elimination of the diketopiperazine ring (**58**), formation of the oxindole (**59**), or recovery of starting material. SM= starting material; decomp= decomposition*

The results of these tested were either recovery of starting material, formation of the oxindole (**59**), or elimination of the diketopiperazine ring upon construction of the indoxyl (**58**).

The formation of oxindole **59** was thought to occur by a simple elimination upon rearrangement from the epoxide (*Figure 2.10 A*). The elimination of the diketopiperazine ring appeared to be a result of deprotonating the tryptophan hydrogen instead of the indole hydrogen (*Figure 2.10 B*). As all attempts to form and maintain the indoxyl moiety were unsuccessful, the synthesis of brevianamide A was not achieved. But, from Halligan's study, the instability of the indoxyl on less functionalized material was established.

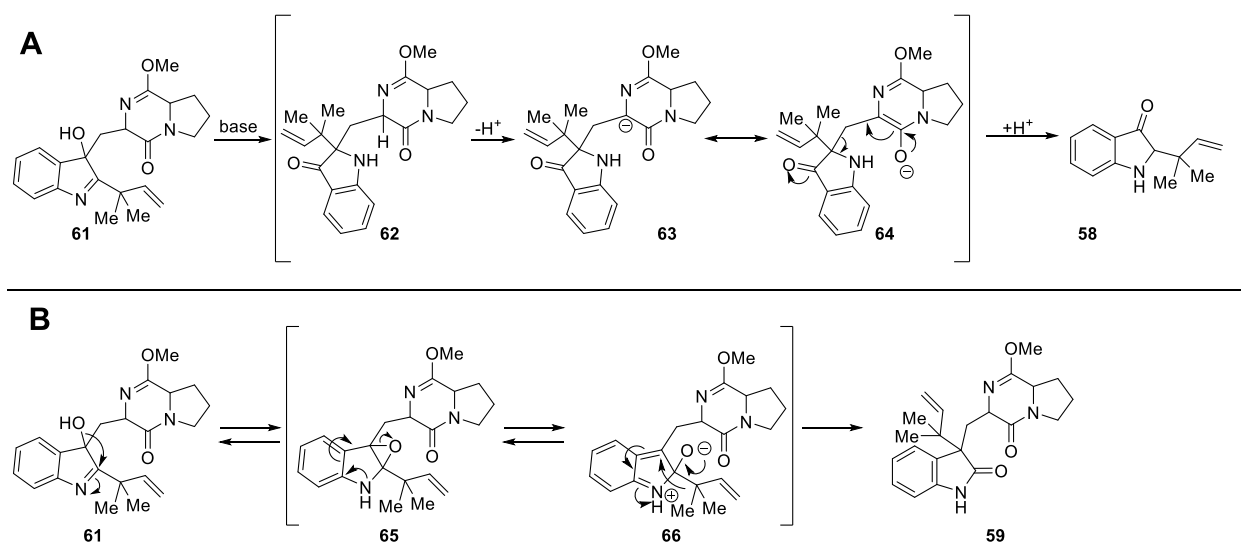


*Figure 2.10: Mechanistic proposals for undesired product selectivity* (see *Figure 2.8* for conditions) (A) Proposed mechanism for the elimination to **58**. (B) Mechanism for favorability of oxindole (**59**) construction.

## VI. Williams 2005 Synthesis of Brevianamide B<sup>6</sup>

To further explore the facial bias of an IMDA reaction, a new route to brevianamide B was developed (*Figure 2.11*). Known ketone **67**<sup>46,50</sup> was subjected to conjugate addition with ethyl 1,3-

<sup>6</sup> The work discussed can be found in reference 49.

dithiane-2-carboxylate. The resultant ester was hydrolyzed with base to carboxylic acid **69**, which was coupled with BOP-Cl to *L*-prolineamide (**71**) to provide peptide **72**. The dithiane was removed by oxidative deprotection to yield a mixture of **73** and an uncyclized amide. The diketopiperazine (**73**) went through a Lewis acid catalyzed IMDA reaction to give solely the *anti*-configuration of the bicycle (**74**). Mimicking the Williams 1993 synthesis, the ketone was converted to a phenylhydrazone and rearranged to indole **34** through a Fischer indole reaction. Applying established steps, cycloadduct **34** was converted to brevianamide B by formation of the hydroxyindolenine and subsequent semi-pinacol rearrangement to establish the indoxyl unit.

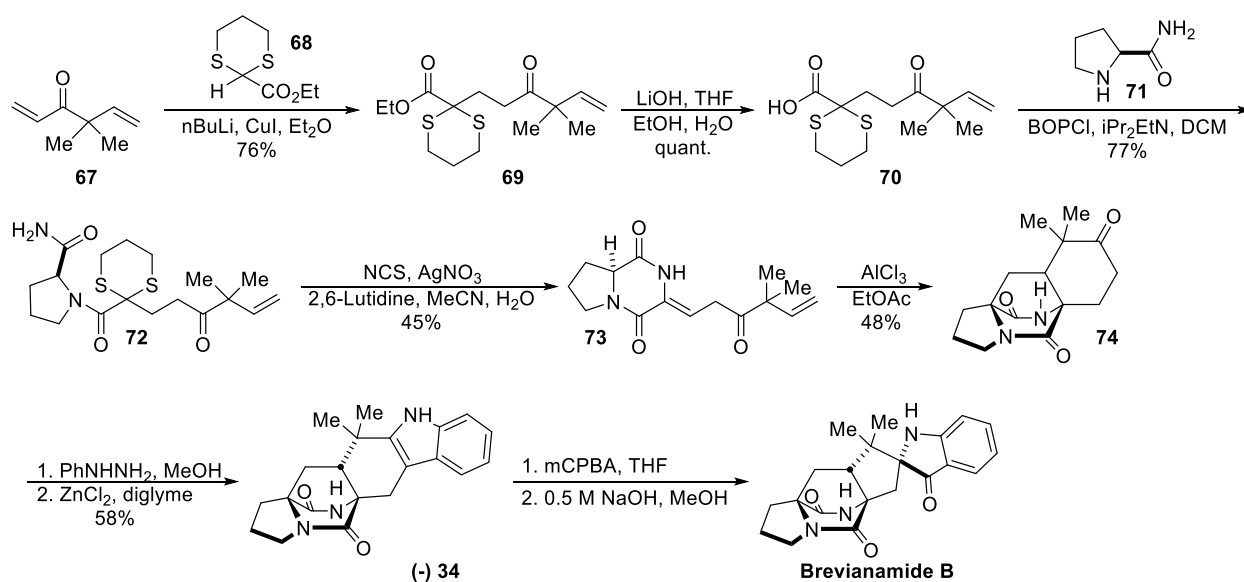


**Figure 2.11: Williams 2005 synthesis of brevianamide B.** Facial bias of the IMDA reaction of **73** was investigated and found only *anti*-cycloadduct **74** was produced.

## VII. Williams 2007 Synthesis of Brevianamide B<sup>7</sup>

Employing a newly developed biomimetic route towards stephacidin A, a new synthetic approach towards brevianamide B was established. Known tryptophan derivative **82** was

<sup>7</sup> The work discussed can be found in reference 51.

synthesized following established protocols (*Figure 2.12*).<sup>52,53</sup> From prenylated gramine (**79**)<sup>53</sup>, Somei-Kametani coupling of benzophenone imine (**80**) in the presence of PBU<sub>3</sub> gave coupled imine **81**. Cleavage of the benzophenone under acidic condition provided the free amine, which subsequently was Boc protected. Basic hydrolysis of the amino ester gave carboxylic acid **83**.

With the newly established conditions applied in the synthesis of stephacidin A, Boc-protected tryptophan derivative **83** was coupled to *cis*-hydroxyproline ethyl ester (**84**) as an acid salt by HATU and DIPEA peptide coupling. The resultant dipeptide was deprotected and cyclized to form diketopiperazine **86** as a mixture of diastereomers. Two different methods were developed to form the IMDA cycloadducts **34** and **126**. One involved a Mitsunobu elimination of the hydroxy group, followed by subjugation to methanolic KOH. The other method involved utilizing equal amounts of DEAD and PBU<sub>3</sub> to both eliminate the alcohol and cyclize the resultant enamide (**87**). Cycloadduct **34** was exposed to the established indoxyl construction conditions to transform the compound to (±) brevianamide B.

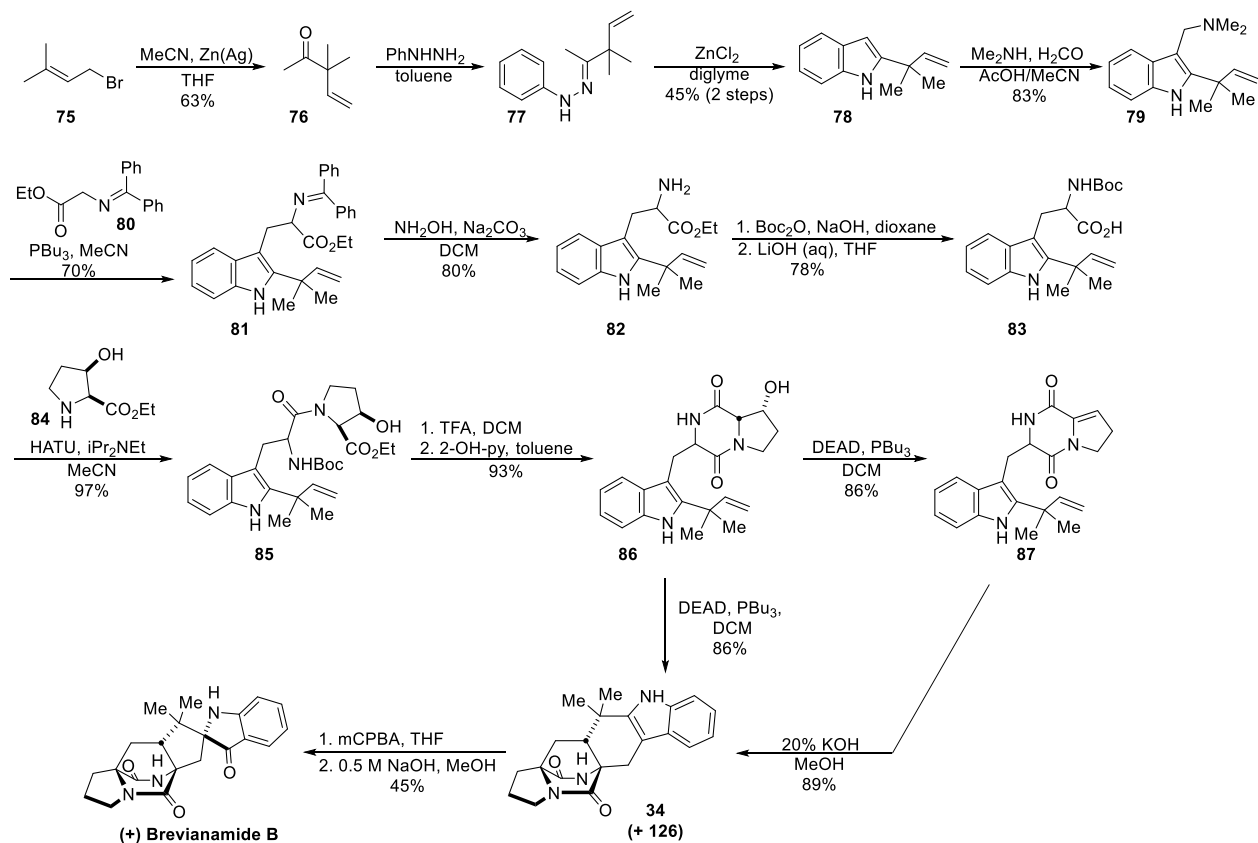


**Figure 2.12: Williams 2007 synthesis of brevianamide B.** One of the first biomimetic construction of the bicyclic core from possible biological precursor. Compounds were racemic mixtures.

### VIII. Simpkins 2010 Synthesis of Brevianamide B<sup>8</sup>

A new method to establishing the bicyclo[2.2.2]diazaoctane ring system was developed in Simpkins synthesis of brevianamide B by utilizing a cationic cyclization. The beginning steps mirror that by Williams' 1988 synthesis of brevianamide B<sup>37</sup> by starting with some proline derivative **88** and prenylating. The oxazolone (**89**) was opened and reacted with lithiated *o*-benzylhydroxylamine. The amine of proline derivative **90** was coupled to indole pyruvic acid **91** to give the hydroxy-diketopiperazine **92**. Cationic cyclization of the diketopiperazine occurred using TMSOTf and resulted in the construction of both *syn* and *anti*-cycloadducts (**93**) in a 1:4

<sup>8</sup> The work discussed can be found in reference 54.

ratio. Standard conditions for indoxyl formation were implemented on **93**.<sup>37</sup> The protecting group on **94** was removed with  $\text{SmI}_2$  and  $\text{LiCl}$ , which simultaneously reduced the indoxyl to a mixture of alcohols (**95**).<sup>55</sup> The alcohol was re-oxidized with Dess-Martin to give (-) brevipianamide B.

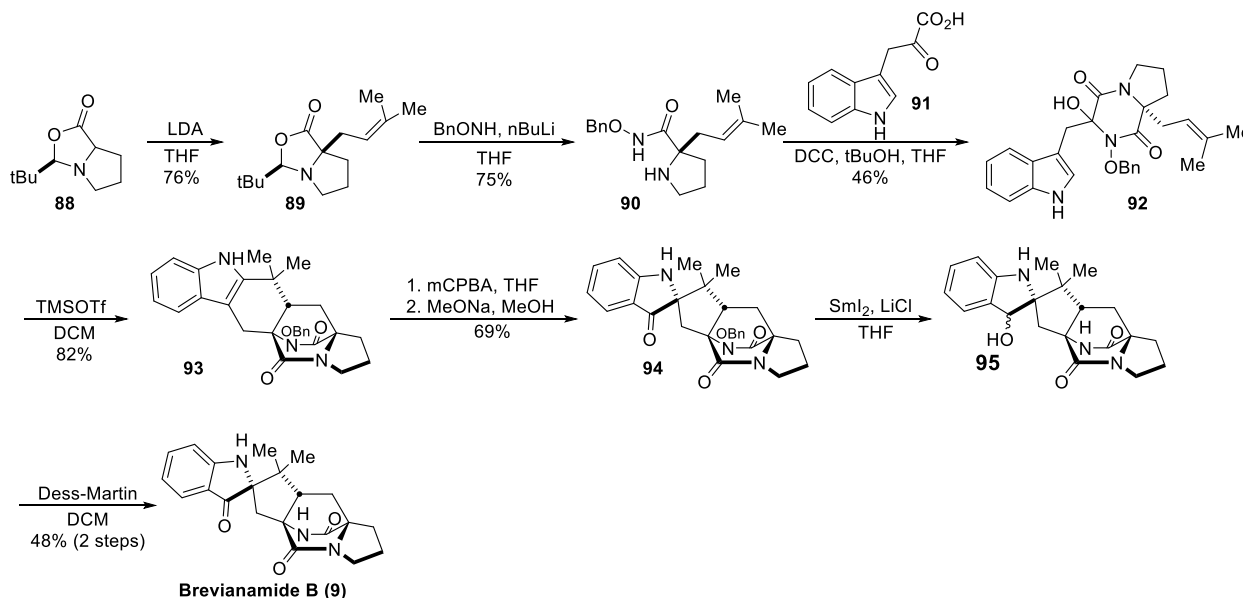


Figure 2.13: Simpkins 2010 total synthesis of brevipianamide B. The key IMDA reaction was initiated by cationic cyclization

## IX. Scheerer's 2016 and 2017 Formal Syntheses of Brevipianamide B<sup>9</sup>

With the goal to selectively synthesize both enantiomers separately, Scheerer and co-workers in 2016 carried out a formal synthesis of brevipianamide B that put attention towards the IMDA reaction. Established in previous work, diketopiperazine **97** was formed in 3 steps from proline methyl ester.<sup>58</sup> Enolization of the **97** with  $\text{LiHMDS}$  was followed by aldol addition to the aldehyde of indole **96** (Figure 2.14). The exocyclic diene was eliminated by acylating the intermediate b-alkoxy and subsequent treatment with base to yield key intermediate azadiene **99**.

<sup>9</sup> The work discussed can be found in references 56 and 57.

Methyl 2-nitroacrylate **100** was employed as the dienophile for the DA reaction with azadiene **99** to control the regioselectivity.<sup>59</sup> Compound **100** also compelled the DA cycloaddition to only occur for the *endo* transition state. Elimination of the nitro group was carried out with DBU. Hydrogenation of the newly formed double bond gave a mixture of *syn*- and *anti*-bicycles (**103**). The ester of **103** was converted to the tertiary alcohol **104** with excess methyl magnesium bromide.

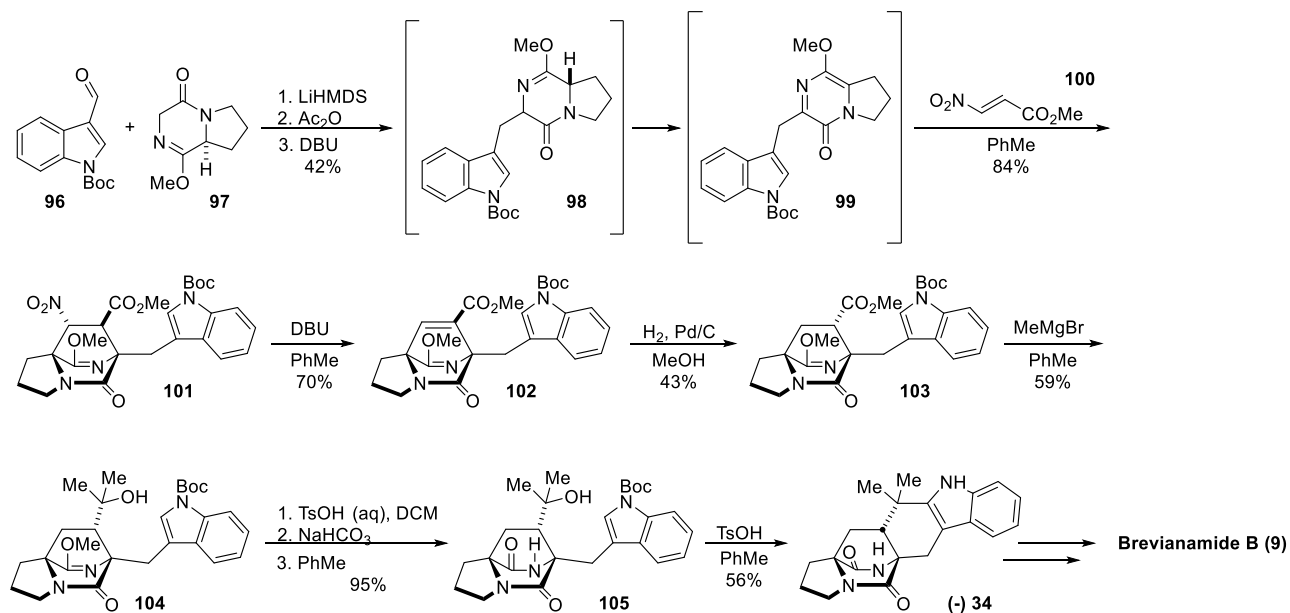


**Figure 2.14: Scheerer's 2016 formal synthesis of brevianamide B.** The route was carried out in hopes of implementing an enantioselective synthesis in which both enantiomers could be isolated.

Employing a variation of the DA reaction done in 2016, Scheerer's formal synthesis of brevianamide B in 2017 started by coupling diketopiperazine **97** and indole derivative **96**. Instead of using methyl-2-nitroacrylate (**100**) for the DA cyclization, maleic anhydride (**106**) was used as the diene to give a 58% yield of cycloadduct **107** (Figure 2.15). Applying excess methanol and DMAP, a selective attack ensued on the carbonyl distal to the indole. The resultant carboxylic acid was benzylated (**108**). Selective acid hydrolysis was accomplished over three steps with an overall 77% yield of **109**. The benzyl ester of **109** was hydrogenated to a carboxylic acid, followed by esterification with N-hydroxyphthalimide (NHPI) to **110** which was more readily capable of

radical decarboxylation to **111**. Established in their 2016 synthesis, the methyl ester was converted to free tertiary alcohol with MeMgBr, which intern was cyclized with TsOH to construct cycloadduct **34** in a 61% yield. The formal synthesis could have been completed by using established indoxyl formation conditions to again yield ( $\pm$ ) brevianamide B.<sup>5</sup>

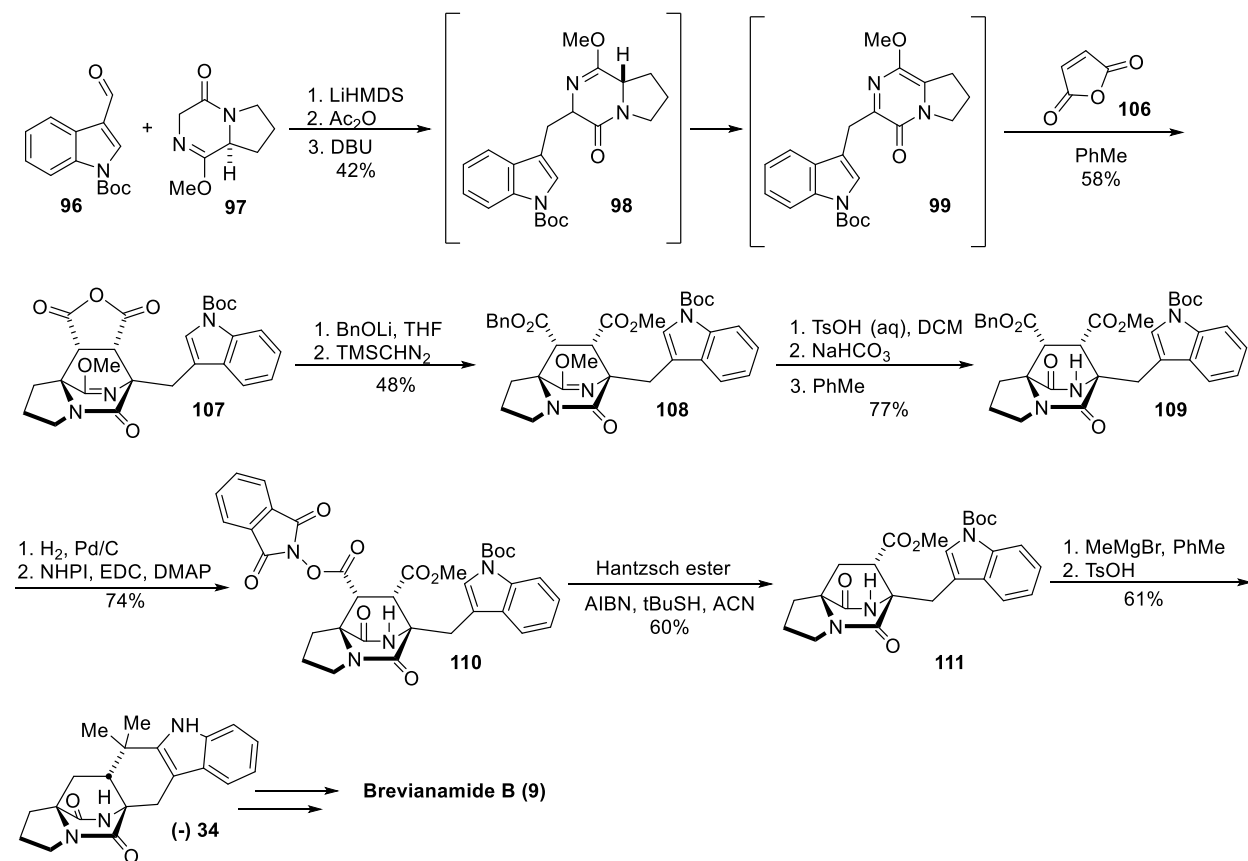


Figure 2.15: Scheerer's 2017 formal synthesis of brevianamide B. Focus was placed on optimization of the DA reaction. Compound **34** was synthesized in a racemic mixture.

## X. Lawrence's Total Synthesis of Brevianamides A and B and Biosynthetic Proposal<sup>10</sup>

Brevianamide A was first isolated in 1969, but its total synthesis had been a challenge for synthetic chemists for almost 50 years. Lawrence's methodology was the first instance in which not only brevianamide A was synthesized, but also both enantiomers of brevianamide A were

<sup>10</sup> The work discussed can be found in reference 60.

accessible separately, resulting in optically pure substrates. What was likewise remarkable about the first total synthesis of brevianamide A was that the ratio of brevianamide A to B that was synthesized mimicked the ratio that these compounds were produced in *P. brevicompactum*.

The first total synthesis of brevianamide A started with phthaloyl (**113**) protection of commercially available tryptophan methyl ester (**112**; *Figure 2.16*). Danishefsky prenylation of tryptophan derivative **114** gave intermediate **116** on a 20-gram scale.<sup>61</sup> A S<sub>N</sub>2 style demethylation was employed on the methyl ester of **116** using LiCl and DMF. The resultant lithium carboxylate (**117**) was subjected to a one-pot acyl chloride formation and imine acylation to give enamine **119**.

Deprotection of the primary amine was accomplished by using mild nucleophilic conditions, ammonia in methanol, which simultaneously was able to cyclize and construct the diketopiperazine ring, synthesizing dehydrodeoxybrevianamide E (**120**). Oxidation of **120** with mCPBA gave diastereomers of brevianamide E, in a 3:2 ratio. Treatment with LiOH caused the brevianamide E diastereomers to go through a DA reaction and construct the bicycle while simultaneously performing a retro-5-*exo-trig* [1,2]-alkyl shift to the indoxyl, providing both brevianamides A and B. Each enantiomer of brevianamide A and B could be accessed in an optically pure fashion by exposing either diastereomer of brevianamide E to LiOH.

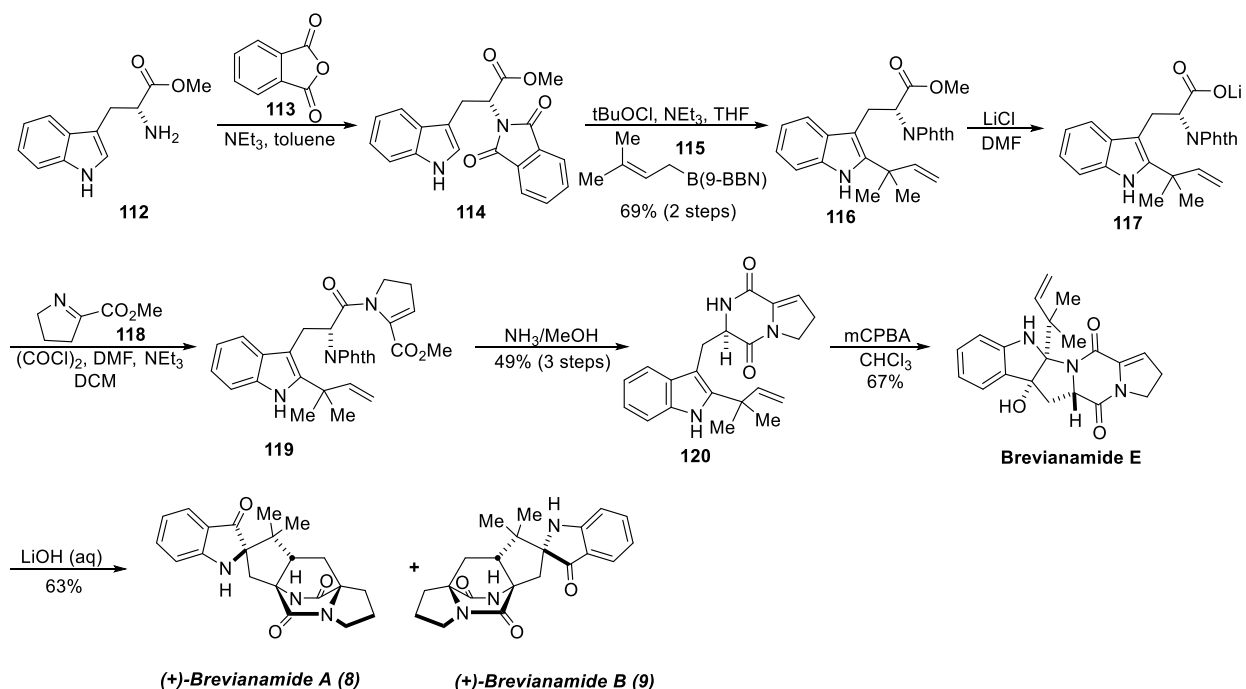


**Figure 2.16: Lawrence's total synthesis of brevianamides A and B.** Marked as the first total synthesis of brevianamide A, which was enantioselective, and mimicked the selectivity that is seen in *P. brevicompactum*. The enantiomer of brevianamides A and B depended on which diastereomer of brevianamide E was carried forward; the diastereomer to (+) brevianamides A/B is shown above.

From their synthetic studies, Lawrence and co-workers developed a new biosynthetic proposal that centered on a newly proposed biosynthetic precursor, dehydrodeoxybrevianamide E, which has previously been isolated from some *Penicillium* and *Aspergillus* species.<sup>62-64</sup> The proposal suggests that the fungi could take dehydrodeoxybrevianamide E and oxidize the indole to the hydroxyindolenine (**122**; *Figure 2.17*). Rearrangement of the indolenine could give the indoxyl (**123**) or brevianamide E if a 5-*exo*-trig reaction occurred instead. Tautomerization of the diketopiperazine unit to form the azadiene species (**39**) would then set up the molecule to perform a diastereoselective DA reaction.<sup>41,65</sup> Whether this was enzymatically catalyzed or not was undecided. Overall, the biosynthetic proposal by Lawrence was incredibly similar to Williams' 1993 biosynthetic proposal<sup>41</sup> but used a different starting material (dehydrodeoxybrevianamide E vs. deoxybrevianamide E).

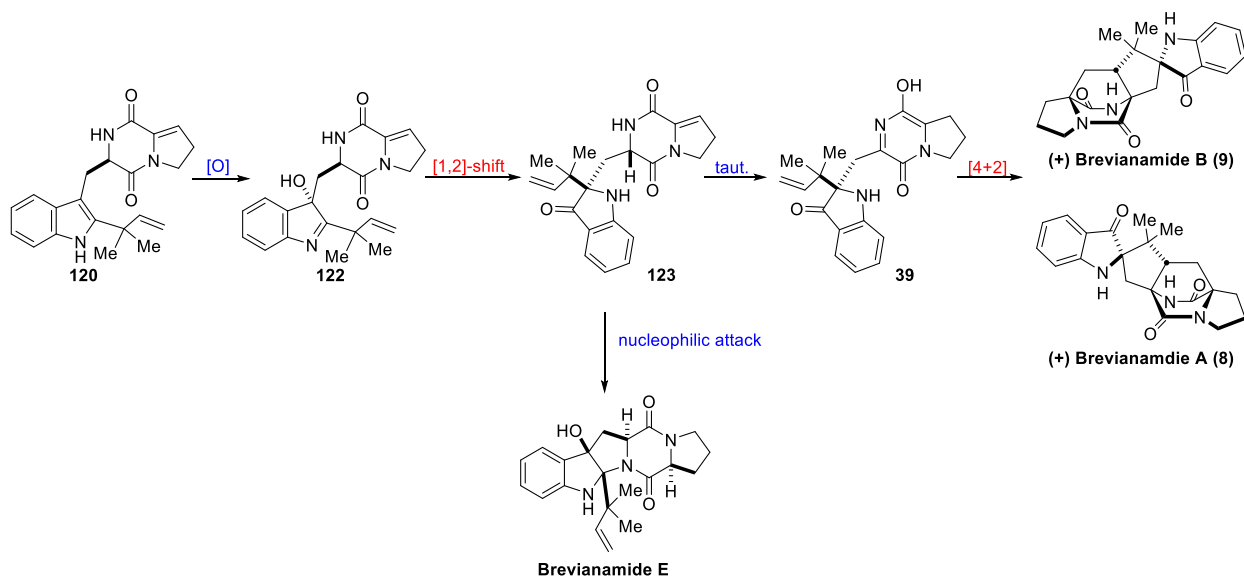


Figure 2.17: Lawrence's 2019 brevianamides biosynthetic proposal. Key difference to other biosyntheses is noted by compound 20, an enamine derivative of deoxybrevianamide E.

## XI. Minor Metabolites Isolated From *Penicillium Brevicompactum*: Brevianamides X and Y

### i. Marine Drugs<sup>11</sup>

New metabolites were identified from *Penicillium brevicompactum* (DFFSCS025) in 2017, brevianamide X and Y. These compounds both contain an oxindole core, a new structural component to the brevianamides. Oxindoles have been seen previously in the prenylated indole alkaloid family from compounds such as versicolamide B (*Aspergillus sp.*) and paraherquamide A (*Penicillium sp.*).<sup>67,68</sup> The exact stereochemistry of brevianamides X and Y were not known at the time that this paper was published; neither crystal structures nor optical rotation values were determined.

The best-known metabolites that have been isolated from *P. brevicompactum* are brevianamides A and B. Both brevianamides A and B are *anti*-cycloadducts and contain an indoxyl

<sup>11</sup> The work discussed can be found in reference 66.

core. All previous biosyntheses have only planned for how the fungi would be constructing the indoxyl. With the isolation of brevianamides X and Y, the new mystery was how the organism constructed both indoxyls and oxindoles, but also how selectivity of the various metabolites was controlled.

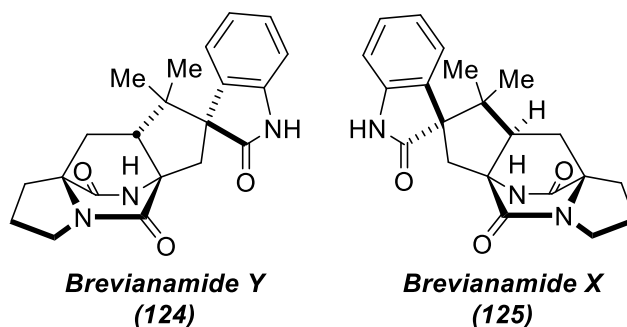


**Figure 2.18: Structures of newly isolated oxindole metabolites.** First instances of the oxindole metabolites in *P. brevicompactum*, especially with the identification of a syn-metabolite, brevianamide X. The exact stereochemistry of the compounds was later elucidated.<sup>107</sup>

## ii. Glinka<sup>12</sup>

When paraherquamide A was isolated, synthetic chemists were enthralled with the idea of synthesizing the compound, especially as it had been shown to possess potent anti-parasitic properties.<sup>70</sup> One key characteristic that was somewhat unique to paraherquamide A was the oxindole core. To study the synthesis of paraherquamide A, a model study was carried out with non-substituted indole *syn*-cycloadduct **126** (Figure 2.19).

It has been previously established that when indole cycloadducts, like **126**, were exposed to mCPBA followed by base, a semi-pinacol rearrangement to the indoxyl proceeded. Following literature precedent, tBuOCl was applied on **126** to form chloro-indolenine **127**, which when refluxed in aqueous acetic acid and methanol caused the rearrangement to the oxindole. This

<sup>12</sup> The work discussed can be found in reference 69.

protocol was found to be somewhat stereoselective towards formation of the less hindered diastereomer (**129**; 58%) over the more hindered diastereomer (**130**; 15%). It is important to note that a protecting group was used on the secondary nitrogen located in the bicycle and was not removed. In later synthetic studies by the Williams group it was found that the pMB (*p*-methoxybenzyl) group was not removable under established conditions (e.g. ceric ammonium nitrate), so much harsher conditions had to be employed to trigger deprotection.<sup>39</sup>

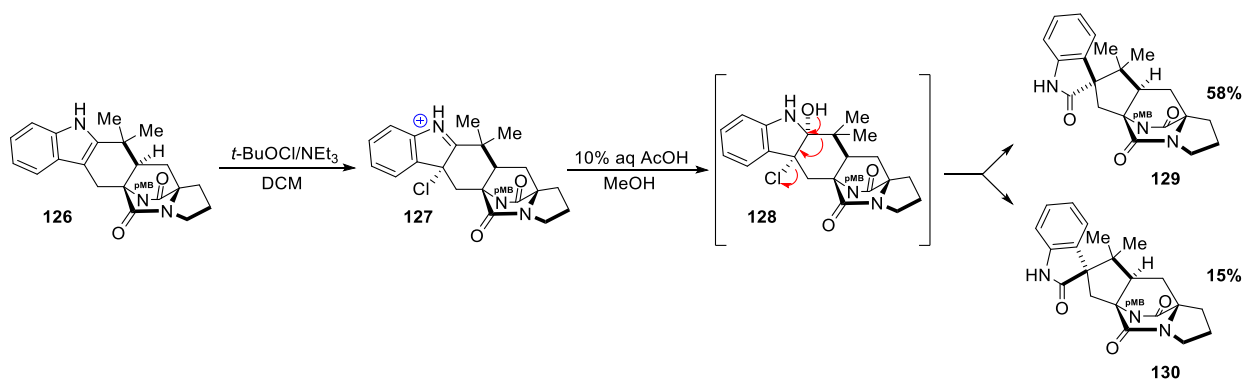


*Figure 2.19: First instance of oxindole formation from DA substrate (126). Note the present of a pmb (*p*-methoxybenzyl) protecting group.*

### *iii. Greshock: First synthesis of oxindole without PG<sup>13</sup>*

Along with the total synthesis of brevianamide B, a new route to the oxindole was developed by Williams and coworkers in 2007 (*Figure 2.20*). Treating the anti-cycloadduct with Davis oxaziridine **131** gave the hydroxyindolenine as one diastereomer (**36**). When the hydroxyindolenine was treated with a biphasic solution of 2M HCl and DCM a clean conversion to oxindole **132** was achieved. With this work, a definitive synthesis of the oxindole can not only be achieved but can also be accomplished stereoselectively. Note the difference in selectivity of the pinacol rearrangement on **34** and **126**. When a protecting group was present (**126**) two products

<sup>13</sup> The work discussed can be found in reference 51.

(**126** and **130**) were formed; on the other hand, when no protecting group was on the molecule (**34**) only one product (**132**) was isolated.

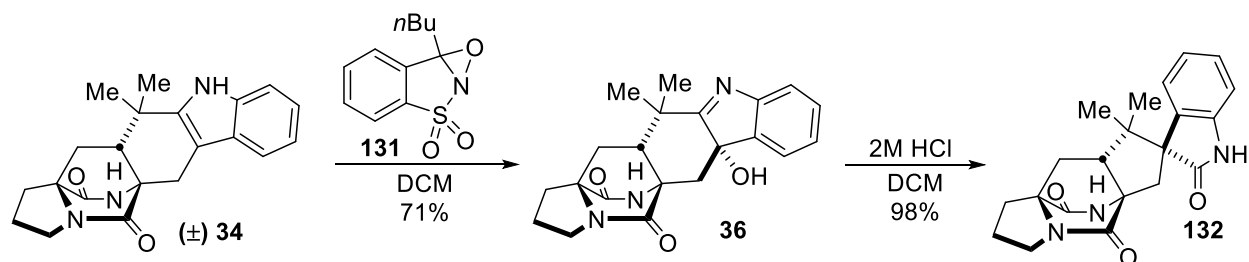


*Figure 2.20: Synthetic catalyzed pinacol rearrangement from DA substrate **34**. Absence of protecting groups, and selective oxidation to the hydroxyindolenine (**36**) was possible with Davis oxaziridine (**131**). All products were racemic mixtures.*

#### *iv. Miller: A new Approach to establishing the Oxindole Core<sup>14</sup>*

After isolating both (+) and (-) versicolamide B, a new synthetic scheme was proposed and carried out to model a feasible biogenetic pathway that would produce both enantiomers of versicolamide B. All previous syntheses of prenylated indole alkaloids that contain an oxindole have been accomplished by first establishing the bicyclo[2.2.2]diazaoctane ring system and then focusing on the formation of the oxindole (*see Figures 2.19 & 2.20*). In Miller's synthesis of versicolamide B, a new methodology was developed; the oxindole was formed before the bicyclic core was established (*Figure 2.21*).

The pinacol rearrangement of the indole was carried out on separated diastereomers of diketopiperazine **133**<sup>71</sup> when treated with oxaziridine **131** (*Figure 2.21*). The rearrangement gave both the (*S*) and (*R*) stereochemistry for the oxindoles, but at different ratios depending on the diketopiperazine diastereomer (*cis* vs. *trans*). A Mitsunobu elimination was utilized to eliminate

<sup>14</sup> The work discussed can be found in reference 68.

the alcohol on oxindoles **134** and **135**. Tautomerization and subsequent DA cycloaddition was achieved by treatment with methanolic KOH to yield four diastereomers of versicolamide B as

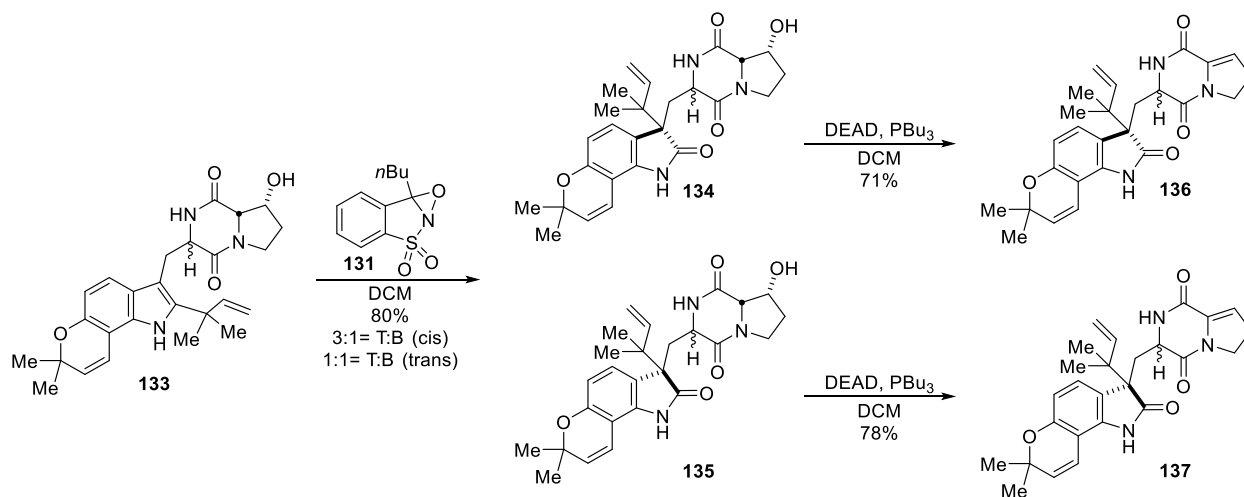


**Figure 2.21: Pinacol rearrangement from diketopiperazine **133** to oxindoles **134** and **135**.** Both diastereomers of **133** (referencing the hydrogen shown) were separated when carried forward. The cis- and trans-diastereomeric nomenclature refers to the relative stereochemistry of the proline- and tryptophan-derived  $\alpha$ -methine protons.

optically pure products (*Figure 2.22*). An interesting result of performing the DA reaction on the oxindole was that only the *anti*-cycloadducts were synthesized, when in all previous works using similar conditions the *syn*-cycloadduct was favored in an approximate 2:1 ratio.

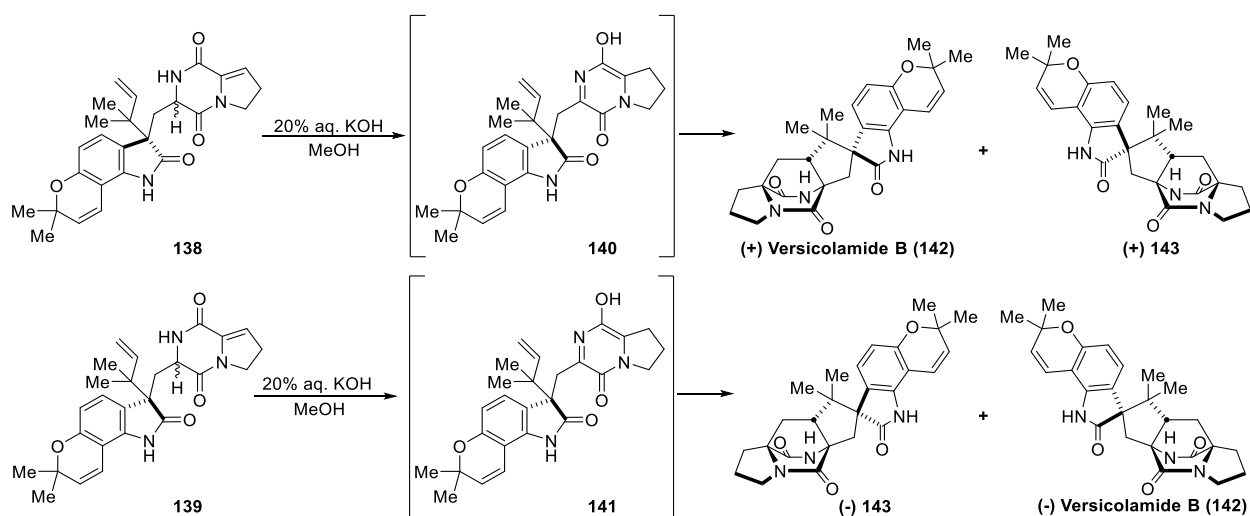


**Figure 2.22: Diels-Alder rearrangement of oxindoles to versicolamide B (142) and diastereomer (143).** Compounds were optically pure. Only *anti*-cycloadducts were isolated.

#### *v. Qin's Total Synthesis of Brevianamide Y (depyranoversicolamide B)*<sup>15</sup>

While conducting an experiment to obtain complete stereoselectivity for the *anti*-cycloadduct from the DA reaction, Qin was able to complete the first total synthesis of brevianamide Y (Figure 2.23). The synthesis began with the prenylation of the C-3 position on Boc-protected indoline derivative **144**.<sup>73</sup> Deprotection of the Boc groups of **146** was followed by re-Boc protecting one nitrogen selectively while methylating the other. By using a combination of TiCl<sub>4</sub> and NaBH<sub>3</sub>CN, ring opening of compound **148** occurred, leaving tryptophan derivative **151**. Once the Boc group was again removed, a HATU coupling to proline **152** was achievable. The new dipeptide (**153**) was deprotected with piperidine, which simultaneously cyclized to form diketopiperazine **154**. The methyl lactim ether derivative **155** was prepared before a thiophenyl group was introduced to the C-17 position of the diketopiperazine moiety. Treatment with KMnO<sub>4</sub> allowed for the oxidation of the N-methyl group to aldehyde **157**. Further oxidation of the aldehyde intermediate with magnesium monoperoxyphthalate caused the elimination of the thiophenyl

<sup>15</sup> The work discussed can be found in reference 72.

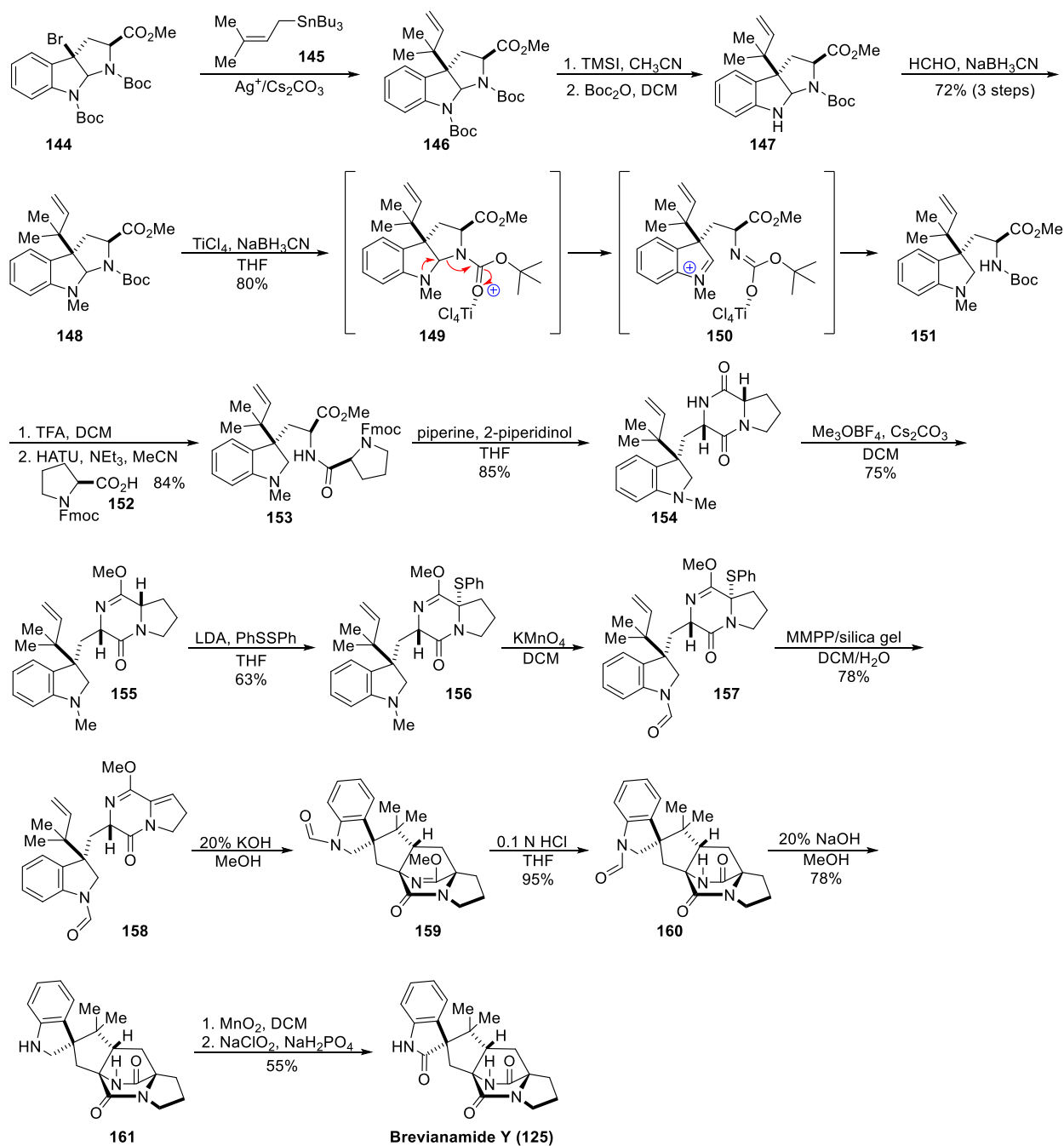


Figure 2.23: Qin's total synthesis of brevianamide Y.

group to give DA precursor **158**. Treatment with the standard Williams conditions<sup>68</sup> of methanolic KOH allowed for the DA cyclization to occur, but in this instance only yielding the desired *anti*-cycloadduct **160**. The lactim ether was removed with acid and deformylation of the aldehyde

occurred upon treatment with base. The oxindole was constructed by oxidizing indoline **161** to an imine with MnO<sub>2</sub>, which was further oxidized with NaClO<sub>2</sub>/NaH<sub>2</sub>PO<sub>4</sub> to brevianamide Y.

## **XII. Conclusions and Perspective**

From Birch to Lawrence, a variety of biosyntheses have been proposed for the brevianamides isolated from *P. brevicompactum*. Through the application of total synthesis, the absolute configurations of many metabolites were determined. To better understand what the biosynthetic route in the fungi entailed, feeding studies with synthesized deuterium/tritium labeled compounds were carried out. These feeding studies were able to disprove some biosynthetic proposals, but also foster the development of others. For example, the role that brevianamide E played as a shunt metabolite towards the biosynthetic construction of brevianamides A and B was revealed through feeding studies.

While many syntheses of brevianamide B have been completed in the past, as well as a variety of biosynthetic routes to the metabolites had been proposed, little was known with certainty of the biochemical mechanism carried out by the fungi. No biochemical analysis had yet been performed to fully elucidate the enzymes, and their exact substrates, yet. It was not until recently that the biosynthesis of the brevianamides, from full characterization of the enzymes and their native substrates, were revealed. The use of biochemical analysis, gene manipulation, total synthesis (completed by the author), and computation analysis allowed for the full elucidation and the discovery of a novel cofactor-independent pinacolase (Chapter 3).

## I. Background

Brevianamides A and B have continued to hold the attention of both synthetic chemists and biologists for over 50 years. While brevianamide A was recently synthesized for the first time, there were still many unknowns for the biochemical mechanisms that led to its generation in native fungi, *Penicillium brevicompactum*. The key unanswered question was still: where does the oxidation occur, before or after the crucial IMDA cycloaddition to establish the bicyclo[2.2.2] diazaoctane core, and on what is the structure of this intermediate? Another intriguing aspect of brevianamide A and B was their 3-*spiro-ψ*-indoxyl functionality. Most prenylated indole alkaloids that have an oxidized indole core have been 2-*spiro*-oxindoles, while only a small number contains an indoxyl (*Figure 1.1*). Both indoxyls and oxindoles have been theorized to arise biosynthetically from some form of a pinacol rearrangement.

Pinacol, or semi-pinacol, rearrangements have been of great importance to the biogenesis of natural products by way of a 1,2-alkyl shift to generate a new carbonyl group. Besides the previously mentioned indole alkaloids, many other species have been found to utilize this rearrangement, including aflatoxin B1<sup>108</sup>, (+) liphagal<sup>109</sup>, tropolone<sup>110</sup>, aurachin<sup>111</sup>, and (+) asteltoxin<sup>112</sup>. Natural product biosynthetic pathways that have been found to include a (semi)-pinacol rearrangement are rare and all known cases contain pinacolases that are cofactor-dependent. Examples of which include the FAD-dependent monooxygenase NotB in the biosynthesis of notoamides C and D<sup>113</sup>, the two-enzyme system AuaG/AuaH (FAD/NADH

---

<sup>16</sup> This chapter is based on a publication from *Nature Catalysis*<sup>107</sup>

dependent) responsible for aurachin<sup>114</sup>, and the non-heme deoxygenase TropC involved in the biosynthesis of tropolone<sup>115</sup>. In each case the enzyme is bi-functional; it has both oxireductase availability and is responsible for directing the 1,2-alkyl shift. In the recently elucidated biosynthesis of brevianamides A and B a cofactor-independent pinacolase, the first of its kind, was discovered. The novel enzyme was also found to assist in directing the construction of the bicyclo[2.2.2]diazooctane ring system in an enantioselective manner. All synthetic work covered in the current chapter was completed by the author (Morgan McCauley). The biochemical techniques employed were carried out by the Sherman group, mostly by Dr. Ying Ye, at the University of Michigan and the computational analyses were performed by the Paton group from Colorado State University.

## II. Biosynthesis of Brevianamides A and B

The isolation of the brevianamide gene cluster was achieved through genome mining by employing the notoamide nonribosomal peptide synthetase (NRPS) gene *note*.<sup>116</sup> Through genome mining, a biosynthetic (*bvn*) gene cluster was identified in *P. brevicompactum*. The gene cluster was smaller than that of its homolog, notoamide, which reflected the differences in their corresponding complexities. A combination of gene deletion, heterologous gene expression, precursor feeding, chemical total synthesis, computational analysis, and *in vitro* biochemical assays were utilized to determine the enzymes and substrates that compose the biosynthetic pathway for brevianamides A and B.

As seen in both the notoamide and fumitremorgin biosynthesis, *L*-proline and *L*-tryptophan were converted to brevianamide F by NRPS enzyme BvnA (*Figure 3.1*).<sup>117,118</sup> The function of BvnA was also confirmed by heterologous gene expression in *Aspergillus oryzae* (*Ao*).

The remaining enzymes, *bvnB-E*, functionalities were analyzed by creating single-gene knockout (KO) strains of *P. brevicompactum*.

An accumulation of brevianamide F, the product of BvnA, was found in the *bvnC*-KO strain. The *bvnB*-KO and *bvnD*-KO strains accumulated deoxybrevianamide E and brevianamide E, respectively. It was proposed that brevianamide E could be a shunt metabolite that resulted from a 2,3-indole epoxidation of deoxybrevianamide E by flavin monooxygenase BvnB. To test the hypothesis, recombinant *N*-His<sub>6</sub>-tagged BvnB was exposed to deoxybrevianamide E, which showed complete and efficient conversion to brevianamide E *in vitro* likely through a similar mechanism as seen by NotB (a BvnB homolog with 62%/75% identity/similarity) from the notoamide biosynthesis.<sup>119</sup> As the *bvnD*-KO did not generate a compound containing the bicyclo[2.2.2]diazaoctane structure, BvnD was reasoned to be the key enzyme for the proposed IMDA reaction. When *bvnE* was deleted, seven unique compounds were observed, brevianamides A, B, X, and Y, along with what was later determined to be novel hydroxyindolenine intermediates. The details of the *bvnE* KO study and the following conclusions will be discussed later in a later section of this chapter (*see section III*).

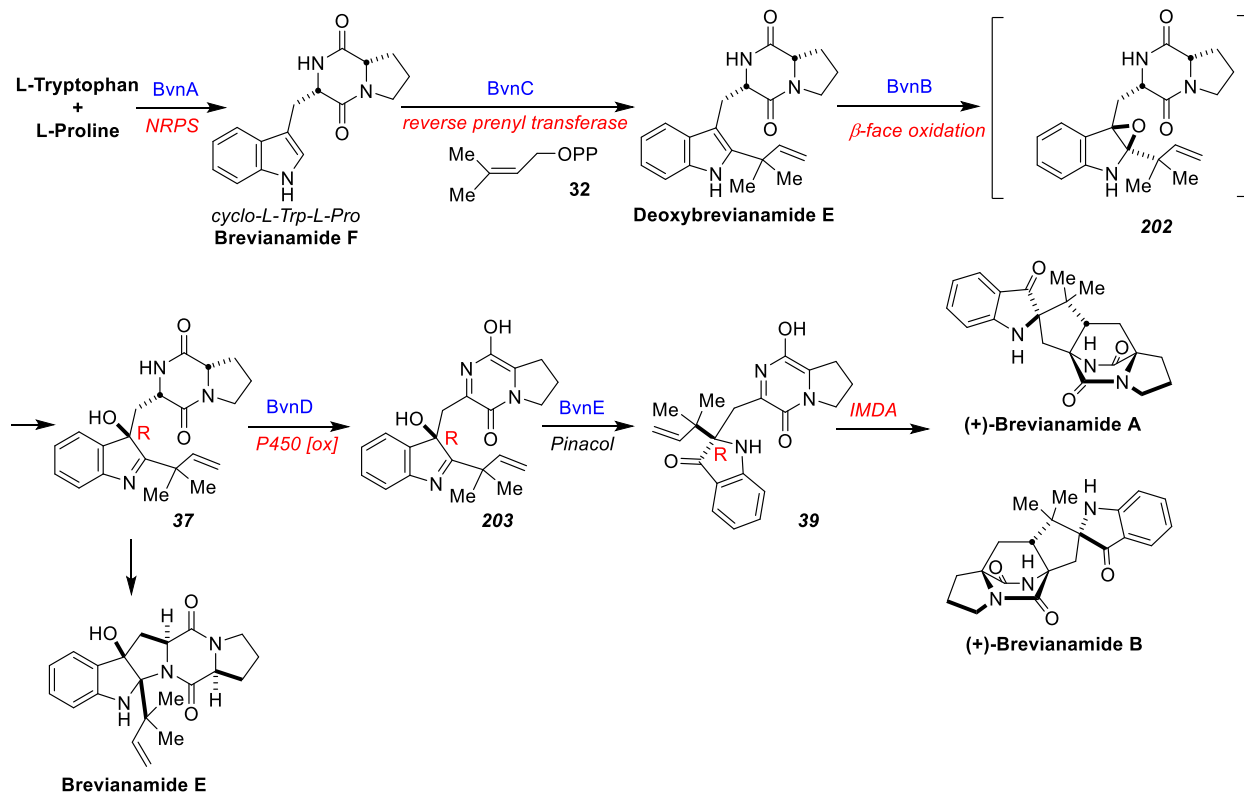


**Figure 3.1: Biosynthesis of the breviriamides.** Enzymes are shown in blue and functions/transformations in red.

To further validate the function of the *bvn* genome and to clarify the biosynthetic order for each transformation, heterologous gene expression with a variety of gene combinations was carried out in *A. oryzae*. It was found that breviriamide F was reverse prenylated to form deoxybrevianamide E both by *Ao-bvnC* *in vivo* and by purified BvnC *in vitro* when in the presence of DMAPP and  $Mg^{2+}$ . The results confirmed that reverse prenyl transferase BvnC was a synthase for deoxybrevianamide E, holding the same role as NotF in the notoamide biosynthesis.<sup>117</sup> Trying to determine the role of BvnB, an *Ao-bvnCDE* strain was tested, which observed only accumulation of deoxybrevianamide E in the feeding experiment, while *Ao-bvnBC* and *Ao-bvnBCE* both saw breviriamide E as the solitary product. The combined results gave credence to the idea that BvnB must be a flavin monooxygenase that performed an indole

epoxidation (**202**) before the BvnD-mediated and the BvnE catalyzed steps. Introducing brevianamide F to the *Ao-bvnBCD* strain resulted in the identification of 5 products with a  $m/z$  of 366 ( $[M+H]^+$ ) with relative abundances of 1:1:5:2:6 (brevianamide A: brevianamide B: **45**: brevianamide X: brevianamide Y). These results were reminiscent of that found by the KO study of *bvnE* in *P. brevicompactum*. Lastly, when the enzyme BvnE was incorporated, and brevianamide F was fed to *Ao-bvnBCDE*, brevianamides A and B were isolated in a ratio of 10:1, the same as what is found when produced in *P. brevicompactum*.

Combining the results of the KO study and gene manipulation/biotransformation carried out in *Ao*, a reaction sequence was developed. The enzymatic pathway could be deduced to be  $BvnA \rightarrow BvnC \rightarrow BvnB \rightarrow BvnD \rightarrow BvnE$  (Figure 3.1). The exact role of BvnD was not fully elucidated. Attempts to incorporate the P450 enzyme in *E. Coli* and *Saccharomyces cerevisiae* were unsuccessful, preventing further functional analysis. Seeing that the *Ao-bvnBCD* strain transformed brevianamide F into multiple IMDA products, as well as *Ao-bvnCDE* not being able to react with deoxybrevianamide E, along with the knowledge of P450 enzymes and Diels-Alder reactions, suggested that BvnD might oxidize a non-isolable intermediate (**37**), derived from a ring-opening of epoxide **202** to azadiene **203**. The azadiene could then readily go through some IMDA reaction, either spontaneously or enzymatically, later in the biosynthetic pathway. It appeared that BvnE played a crucial role in the proportion and type of products isolated, suggesting that BvnE may be mediating the formation of the indoxyl, as well as directing the selectivity of the presumed IMDA cycloaddition.

### III. BvnE Knock Out Study: The Total Synthesis of Unstable Intermediates and Mechanistic Investigations

To understand the function of the newly identified enzymes in the biosynthesis of brevianamides A and B, KO studies were carried forward. While the findings for many of the enzymes were simplistic (*see section II*), the *bvnE*-KO study gave a variety of products (*Figure 3.2*). In total, eight compounds with the molecular weight of 365 Da were detected. Four of the eight compounds were readily identified as indoxyls brevianamides A and B, and oxindoles brevianamides X and Y. Three of the remaining compounds were theorized to be hydroxyindolenine forms of the DA cycloadducts (**45**, **46**, & **216**), while the last was theorized to be a *syn*-indoxyl based on HPLC analysis.

Although compounds **46** and **216** were too unstable to isolate, **34** was isolated and characterized. The C-2=N bond of compound **34** was identified by the chemical shift of the C-2 as 189.29 ppm, along with a peak at 81.31 for the C-3 position. Most reported hydroxyindolenines in literature have a C-2 value between 187-193 ppm.<sup>51</sup> Further 2D NMR analysis was utilized to validate the structure, as well as electric circular dichroism (ECD) experimental and computational analysis, to confirm the absolute stereochemistry of hydroxyindolenine **34**. Based upon stereochemistry, **34** appeared to be a possible biosynthetic precursor to brevianamide A. As such, it was possible that the isolated brevianamide A from the *bvnE*-KO strain was a result of a small portion of **34** suffering a semi-pinacol rearrangement. While NMR and ECD analysis was attained, a crystal structure was not possible to obtain for **34** because of its instability. To further confirm the structure of hydroxyindolenine **34** and to also identify the two unstable compounds, a total synthesis of all diastereomers of the hydroxyindolenines was carried out.

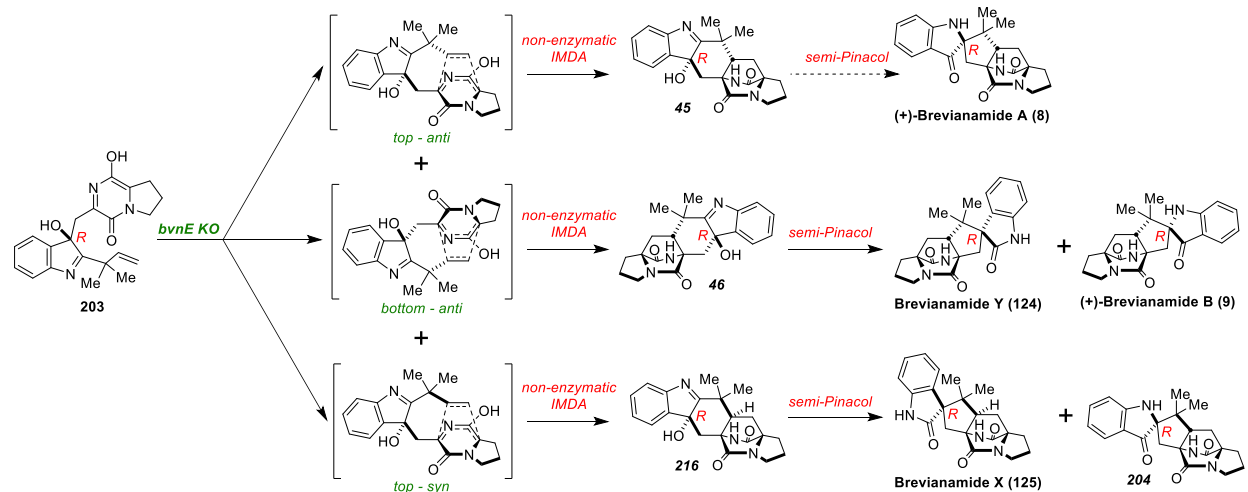


**Figure 3.2: *bvnE* KO study and resultant metabolites isolated.** The structures of hydroxyindolenines **46** and **216** were confirmed through total synthesis as the compounds were too unstable to isolate. Brevianamides X and Y had been previously isolated as well in the natural species, but at drastically lower levels than found in the current study. An unknown metabolite was also isolate, the identity of which is theorized to be indoxyl **204**.

Previous syntheses of brevianamide B accessed some hydroxyindolenine intermediates, but full characterization was never attained or protecting groups were present somewhere in the molecule.<sup>37,47,51,54</sup> It was theorized to be possible to synthesize the hydroxyindolenines from DA cycloadducts **126** and **34**, which were known compounds.<sup>51</sup> Before beginning the route to **34** and **126**, a crucial reagent needed to be synthesized, 1,1-dimethylallene (*Figure 3.3*).

The synthesis of 1,1-dimethylallene (**207**) was two-steps and began with commercially available 2-methyl-3-butyn-2-ol (**205**). Bromoallene (**206**) was synthesized on a 100 g scale from compound **205** in a respectable 70% yield. Whereas the reaction to form **206** was both scalable and reproducible, the same was not true for the formation of **207**. To synthesize allene, **206** was added dropwise to a flask containing acetic acid and zinc, while simultaneously distilling the product. The reaction proved to be difficult to reproduce, part of which had to do with the volatility of allene. It was found that carrying out the reaction on a smaller scale with excess heating gave more consistent results even though acetic acid would be distilled along with **207**.

The acetic acid was easily removed by cooling the mixture below the acid's melting point and quickly removing **207**, which was still a liquid. Optimization of temperature conditions was able to increase the yield from 30% to 86% on a 70 g scale. Once **207** was in hand, the general synthetic scheme shown in *Figure 3.4* was followed.

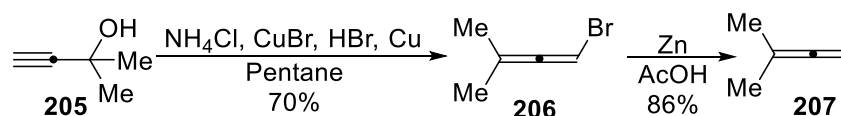


*Figure 3.3: Synthesis of dimethyl allene (207).*

Commercially available indole was treated with NCS to form light-sensitive chlorinated indole (**209**; *Figure 3.4*). The reaction was performed on a 20 g scale and was quantitative in yield. Reverse prenylation of **209** provided **78**, which was readily converted to gramine **79**. Somei-Kametani type coupling with glycine derived benzophenone imine **80** and subsequent treatment with acid yielded tryptophan **81**.<sup>43,120</sup> Peptide coupling of **81** and Fmoc-hydroxy *L*-proline (**210**) gave dipeptide **211** as a rotameric mixture of diastereomers. Cyclization of **211** to form diketopiperazine **86** occurred upon deprotection of the Fmoc group. The cyclization reaction, which previously had only been done on sub-gram scales, was performed on a 2.5 g scale and maintained a 75% total yield. Mitsunobu elimination of the alcohol gave enamine **87** with an almost quantitative yield. Upon treatment with methanolic KOH, enamine **87** was able to rearrange to its corresponding azadiene before suffering an IMDA cycloaddition to construct *syn*- and *anti*-cycloadducts (**34** & **126**) in a 2.1:1 ratio. The IMDA cycloaddition was carried out on a gram scale with an 81% yield and an approximate 15% recovery of starting material (**87**). This was an improvement on the IMDA reaction of **87**, which had previously only been performed on a 100 mg scale. It is important to note that the cycloadducts were separated, but the

*syn*- and *anti*- products were mixtures of enantiomers. With the *anti*-cycloadduct in hand, hydroxyindolenine reaction conditions were assessed.

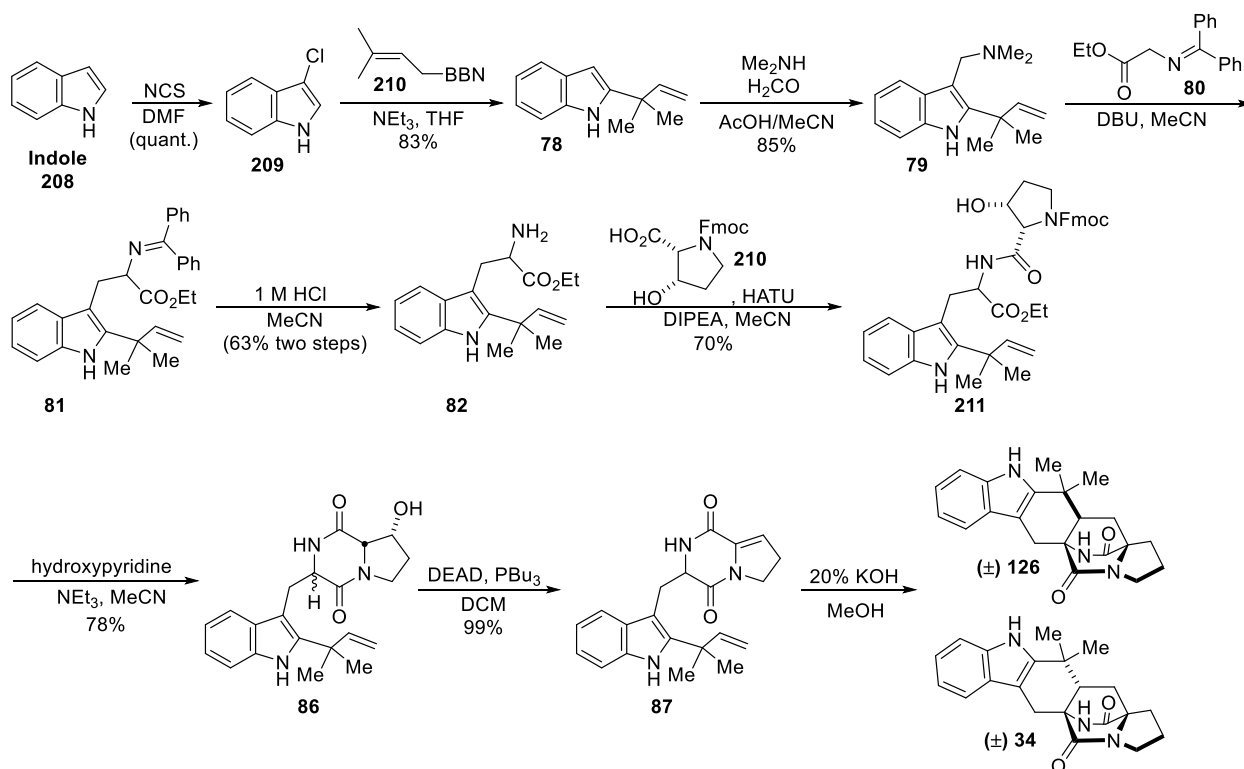


**Figure 3.4: Synthesis of cycloadducts from commercially available indole.** Both cycloadducts were mixtures of enantiomers.

As hydroxyindolenine **45** had been identified and appeared to be a possible biosynthetic precursor to brevianamide A, the other plausible hydroxyindolenine diastereomers (**46** & **216**) were thought to likely be the hydroxyindolenines that could form brevianamide B/Y and brevianamide X, respectively. The hydroxyindolenine that would form brevianamide B/Y would have the hydroxy group on the less hindered face of the *anti*-cycloadduct indole, like hydroxyindolenine intermediates proposed in previous brevianamide B syntheses.<sup>37,47 51, 54</sup> The hydroxyindolenine that could form brevianamide X would need to be from the *syn*-cycloadduct (**216**) with the hydroxy group also on the less sterically hindered face of the indole.<sup>47</sup>

Initial attempts to form the *anti*-hydroxyindolenine precursor of brevianamide B/Y were carried out with tBuOCl to form the *anti*-chloroindolenine (**212**), which was theorized to become a hydroxyindolenine when exposed to aqueous acid (*Figure 3.5 A*). After intense NMR analysis, it was proven that *anti*-hydroxyindolenine **46** was not formed from these conditions, but instead the *anti*-chloroindolenine remained. An interesting finding in this process was that the NMR spectra of **212** and **46** were incredibly similar; both spectra had almost identical splitting and ppm values for their <sup>1</sup>H-NMR spectra, as well as similar carbons, with the key C-2=N signal around 190 ppm. The only major difference between the <sup>13</sup>C NMR spectra of **212** and **46** was one signal; **212**'s spectrum did not contain a signal at 80 ppm for the C-3-OH as seen in hydroxyindolenine spectra, but instead an additional peak around 70 that represented the C-3-Cl bond.

While the tBuOCl sequence did not supply the hydroxyindolenine, there were some interesting findings for the reactivity of the species, along with insights into the *bvnE-KO* species. When kept at 0 °C or higher, the *anti*-chloroindolenine would rearrange to form brevianamide Y and trace amounts of another substance that matched one of the unknown compounds (**46**) in the *bvnE-KO* HPLC trace (*Figure 3.5 B*). The fact that the compound was in a similar place as the hydroxyindolenine that had been synthesized, together with the polarity of the compound and the accessibility of the *anti*-hydroxyindolenine from an *anti*-chloroindolenine, gave more credibility to the idea that the unknown compounds were hydroxyindolenines. The eagerness of **212** to rearrange demonstrated that the compound was incredibly reactive and favored the formation of the oxindole rather than the indoxyl. These results were also seen in the *bvnE-KO* study when referencing the relative abundances the isolated compounds (1:1:5:2:6 with brevianamide A: brevianamide B: **45**: brevianamide X: brevianamide Y).

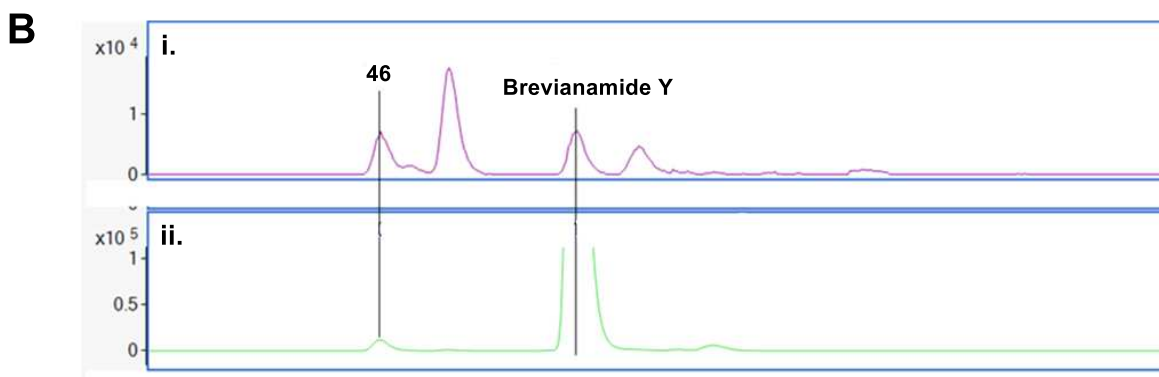
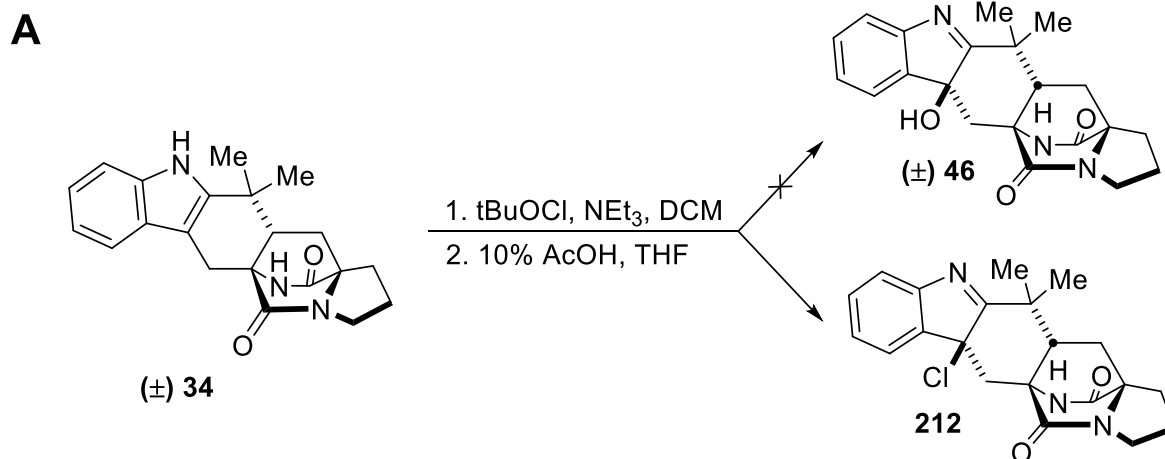


**Figure 3.5: Initial attempts to synthesize hydroxyindolenine 46.** (A) synthetic undesired chloroindolenine **212**. All compounds are racemic. (B) i. HPLC trace of BvnE mutant (pink) ii. chloroindolenine **212** after treatment with 0.05% formic acid (green). Note the rearrangement to brevianamide Y, complete disappearance of **212** and minor levels of **46**.

Since the tBuOCl conditions were not able to produce the anti-hydroxyindolenine, new conditions were sought out. As almost all brevianamide B syntheses employed mCPBA to form the hydroxyindolenine, the conditions were investigated next. The only concern with using mCPBA as the oxidizing agent was that a pinacol rearrangement would occur too readily, thus preventing the isolation of the desired product. Care was taken with the reaction, limiting the amount of time the compound was in solution. By doing so, two *anti*-hydroxyindolenine products, **46** as the major and **45** as the minor, were isolated, in addition to trace amounts of Brevianamide Y (*Figure 3.6*). Previous uses of mCPBA to form **46** as an intermediate to

brevianamide B, never mentioned the formation of another hydroxyindolenine product (**45**); if **45** had been present then it is likely that a small amount should have converted to brevianamide A. The reasoning for not seeing brevianamide A, or its hydroxyindolenine precursor, could either be from it not being formed under previous reaction conditions (i.e. the reaction was run too long; basic conditions were too harsh) or that it was not identified. Nevertheless, both *anti*-hydroxyindolenines were formed, with the less sterically hindered compound, **46**, being the major product.

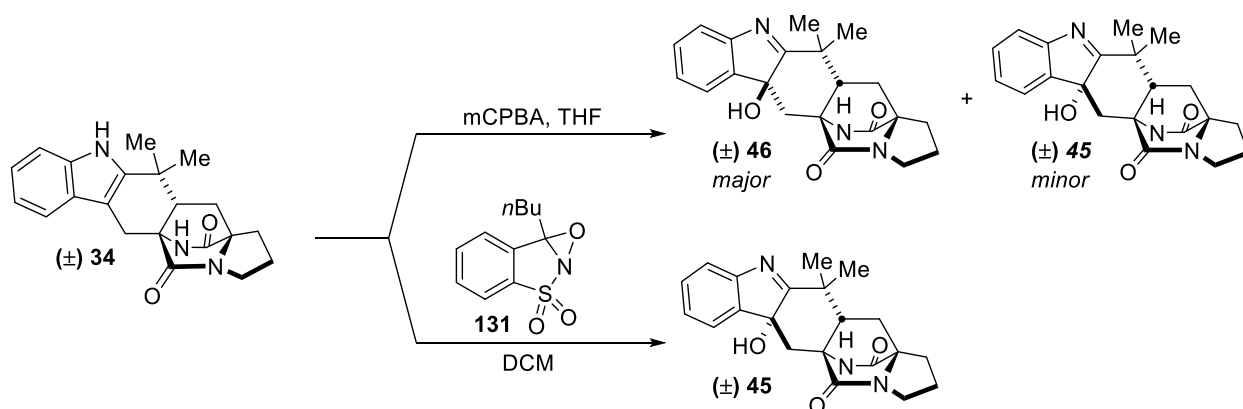


**Figure 3.6: Hydroxyindolenine selectivity of *anti*-cycloadduct **34** upon treatment with different oxidizing agents.** Compound **45** was the minor product for mCPBA oxidation, but the only product for **131** oxidation. **46** was found to be incredibly reactive and quickly rearranged to brevianamide Y.

To better access **45**, a different oxidizing agent was used, Davis oxaziridine (**131**). The synthesis of **131** followed a simple three step pathway, starting with saccharin. (*Figure 3.7*)<sup>121</sup> Conversion of the carbonyl group of the amide to an ether was possible when treated with PCl<sub>5</sub> and ethanol. The ether of **214** was replaced with an *n*-butyl group upon exposure to *n*-BuLi. For the reaction to work, the source of *n*-BuLi had to be fresh, if not starting material (**214**) would be recovered. With the *n*-butyl imine in place, mCPBA epoxidation of the double bond was carried out to give Davis oxaziridine (**131**). With the new oxidizing agent in hand, the synthesis of characterized hydroxyindolenine **45** commenced.

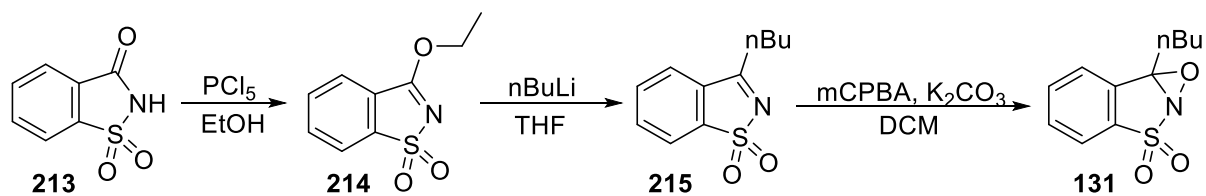
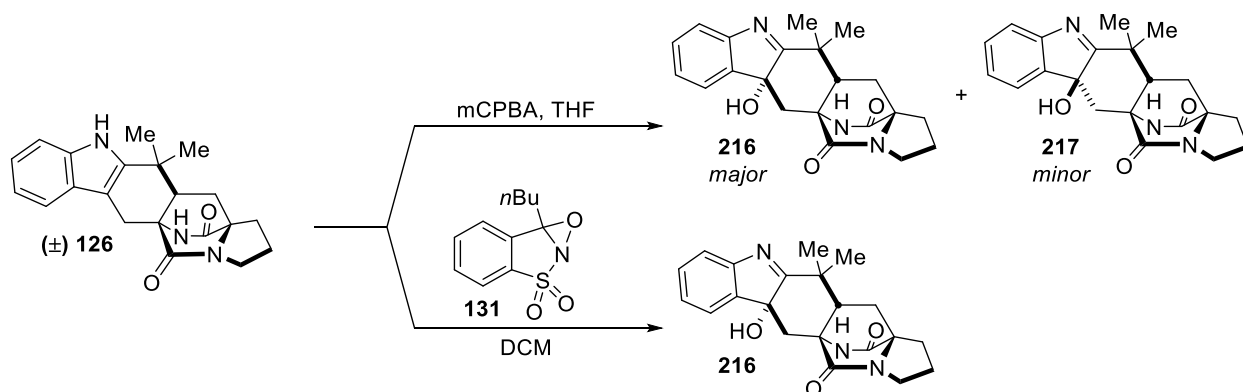


Figure 3.7: Synthesis of Davis oxaziridine 131.

Upon treating anti-cycloadduct **34** with oxaziridine **131**, hydroxyindolenine **45** was formed (Figure 3.6). All data for the synthesized compound matched that from the isolated compound from the *bvnE*-KO strain. While treatment with mCPBA gave both hydroxyindolenines, oxaziridine oxidation was much more selective, with the selectivity towards the previously minor product (**45**). In contrast to both *anti*-hydroxyindolenine **46** and *anti*-chloroindolenine **212**, **45** was relatively stable at room temperature and would not spontaneously rearrange like the other synthesized indolenines. With two of the three hydroxyindolenines synthesized, attention was moved towards the synthesis of the remaining hydroxyindolenine, which was formed from the *syn*-cycloadduct (**126**).

When *syn*-cycloadduct **126** was exposed to mCPBA, both diastereomers of the hydroxyindolenine were formed, with the desired compound (**216**) as the major and almost trace amounts of the more sterically hindered hydroxyindolenine **217** (Figure 3.8). Surprisingly, the hydroxyindolenines from the mCPBA reaction with the *syn*-cycloadduct were found to be more reactive. In fact, the reaction had to be terminated before complete consumption of starting material (**126**) to suppress the formation of brevianamide X. Oxidation of *syn*-cycloadduct **126** with oxaziridine **131** was selective towards the same product that was major from the mCPBA oxidation; the opposite results as to what was found for the *anti*-cycloadduct (Figure 3.6). From the combination of the results of oxidation of **34** and **126**, it was theorized that the selectivity of oxaziridine **131** arose from hydrogen bonding interactions between the bridged amide and the

nitrogen of the oxaziridine. As a result of the bridged amide going back (as currently drawn), the hydroxy group would then add on the same face such that the two components would be *syn* to one another. With all the hydroxyindolenines now in hand, each was tested by HPLC analysis to confirm their identity.



**Figure 3.8: Hydroxyindolenine selectivity of *syn*-cycloadduct 126 upon treatment with different oxidizing agents.** Compound 217 was only found in trace amounts from mCPBA epoxidation. All compounds were racemic mixtures.

Comparison of the HPLC chromatograms from synthetic hydroxyindolenines **46** and **216** with the *P. brevicompactum-bvnE*-KO chromatogram confirmed that the hydroxyindolenine was in fact the previously unknown and un-isolatable compounds (*Figure 3.9 C*). As compounds **46** and **216** were seen to rearrange to form brevianamides Y and X, respectively, the stereochemistry of the compounds was set to show such (*Figure 3.9 A*). For further evidence to support the claim, the stability of synthesized and isolated hydroxyindolenines were analyzed by HPLC (*Figure 3.9 D, E*). It was found that hydroxyindolenine **46** would completely rearrange into brevianamide Y and B within 24 hours when kept in a 30% methanol-water solution. Along the same lines, brevianamide X was formed when hydroxyindolenine **216** was kept in the same conditions for 24 hours. Regardless of whether synthesized or isolated, **46** and **216** both gave similar results when exposed to a 30% methanol-water solution. Together, the HPLC data, as

well as synthetic data, was able to confirm that the hydroxyindolenines were the previously unknown intermediates in the *P. brevicompactum-bvnE-KO* strain.

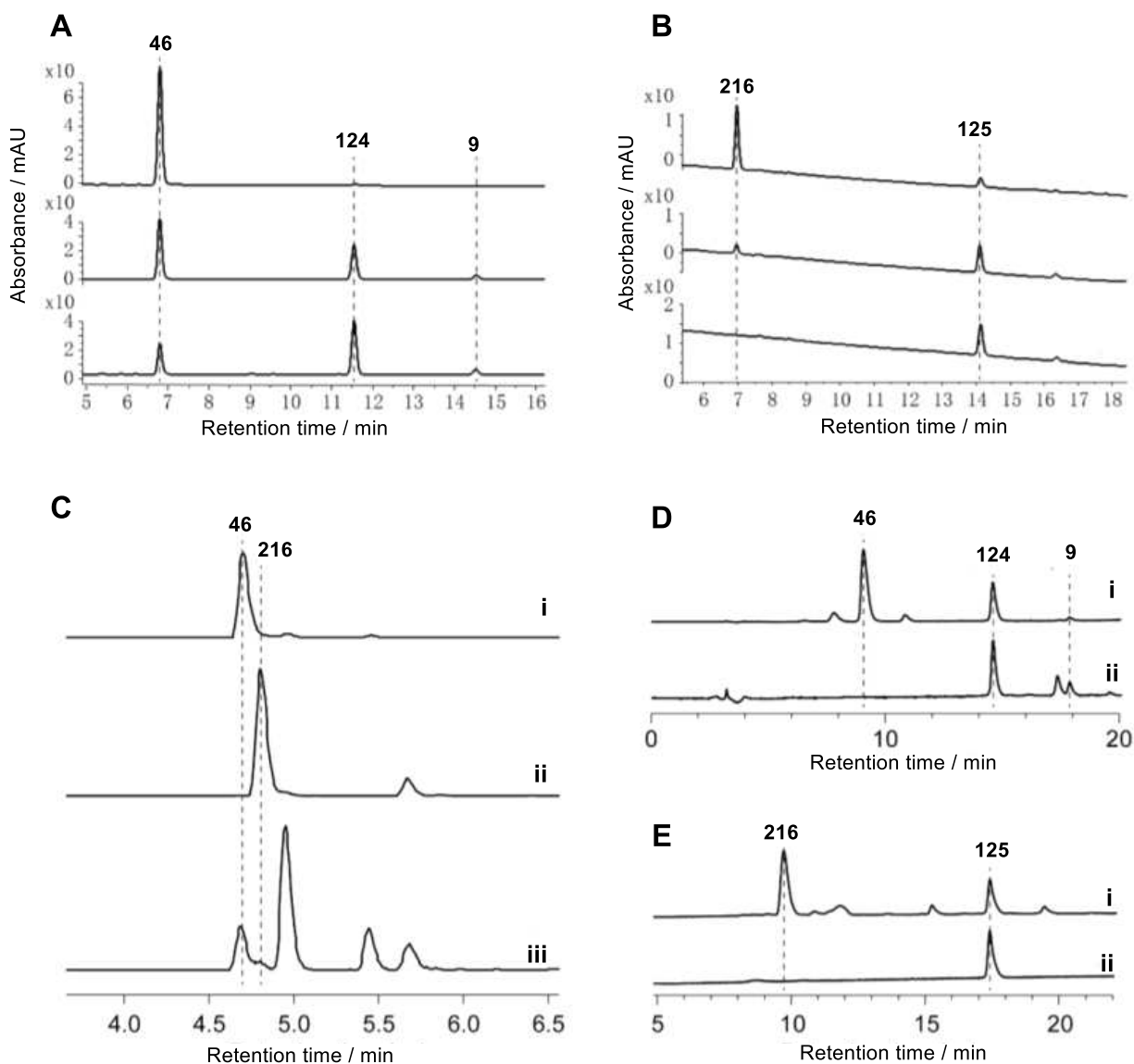


**Figure 3.9: HPLC analysis (230 nm) of isolated and chemically synthesized 46 and 216.** Stability assays of **46** (A) and **216** (B) in 30% methanol-water solution. HPLC analysis of **46** and **216** after 30 min (i), 24h (ii), and 48h (iii). (C) Comparison of synthetic **46** (i) and synthetic **216** (ii) with the *bvnE-KO* profile (iii). (D) Stability assays of **46** (i, synthetic **46** in 30% methanol-water solution after 24 h; ii, authentic standards of Brevianamide Y (**124**), Brevianamide X (**125**) and Brevianamide B (**9**)). (E) Stability assays of **216** (i, synthetic **216** in 30% methanol-water solution after 24 h; ii, the authentic standard of **125**)).

By utilizing total synthesis, the identity of non-isolable substrates was elucidated. The synthesis of the hydroxyindolenines also allowed for a more thorough understanding of their

roles as intermediates for the pinacol rearrangement to corresponding products seen in the *bvnE*-KO strain (*Figure 3.2*). Overall, it appeared that by knocking out the BvnE enzyme selectivity was lost; both *syn*- and *anti*-cycloadducts were produced. The study mainly clarified the role of BvnE as a control for selectivity in the biosynthesis, but it did not clarify the exact function of the enzyme. To establish the role that BvnE plays in *P. brevicompactum*, an *in vitro* study was carried forward with synthetic *N*-methyl deoxybrevianamide E.

#### **IV. Total synthesis of N-methyl-deoxybrevianamide E and BvnE Substrate Model Study**

Seeing that BvnE appeared to be a crucial enzyme in the biosynthetic pathway to brevianamides A and B, the native substrate was investigated. It was found that hydroxyindolenines **45** and **46**, along with brevianamides X, Y, and E, were not transformed when fed to BvnE, isolated from *N*-His<sub>6</sub>-tagged BvnE produced in *E. Coli*. It was then hypothesized that compound **203** may be the enzymatic substrate for BvnE. To assist in the determination of the native substrate of the BvnE enzyme, especially with the inaccessibility of **203**, a model study was carried out with *N*-methyl-deoxybrevianamide E. The reasoning for *N*-methylating the dioxopiperazine nitrogen was to prevent any N-C ring closures (brevianamide E) and possible oxidation to the azadiene.

Following a similar protocol set out in the synthesis of *N*-methyl-notoamide E<sup>90</sup>, the total synthesis of *N*-methyl-deoxybrevianamide E commenced with a HATU coupling of Boc-protected tryptophan derivative **83** with proline derivative **218** (*Figure 4.10*). Deprotection of the Boc group with TFA, followed by reflux in toluene with catalytic amounts of 2-hydroxypyridine gave deoxybrevianamide E and its diastereomer. Carrying forward only deoxybrevianamide E, the diketopiperazine was selectively methylated with MeI and NaH. It appeared that the geminal

methyl groups to some degree shielded the indole nitrogen from being methylated preferentially, but it did still occur if care was not taken with the addition of the MeI. To prevent N-methylating the indole nitrogen, MeI was added in several small aliquots with sufficient time in-between each. The reaction also had to be terminated early, which contributed to the 50% yield for the reaction as starting material (deoxybrevianamide E) was also recovered. When an adequate quantity of the substrate was synthesized, a chemoenzymatic synthesis of compound **222** was investigated.

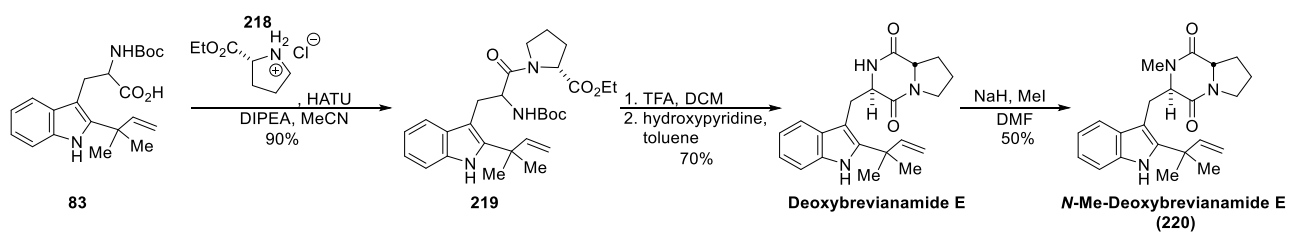


**Figure 3.10: Synthesis of *N*-Me-Deoxybrevianamide E from Boc-protected tryptophan **83**.** The diastereomer of deoxybrevianamide E was also produced (1:1 ratio) but was not carried forward.

Hydroxyindolenine **222** was prepared by BvnB-catalyzed *in vitro* conversion of *N*-methyl-deoxybrevianamide E through an epoxide intermediate and its simultaneous ring-opening (Figure 3.11). Interestingly, indoxyl **224** and oxindole **223** were also isolated as minor products from hydroxyindolenine **222** formation, with the oxindole formation being major over indoxyl formation. Although the indoxyl and oxindole would form from the hydroxyindolenine spontaneously at room temperature, the transformation was slow. Incubation of **222** with BvnE, on the other hand, resulted in full conversion to the indoxyl (**223**). As BvnE selectively gave one product, it indicated that the enzyme acted as a semi-pinacolase that is responsible for the selectivity of the 3-spiro- $\psi$ -indoxyl. The stereocontrol in the IMDA cycloaddition, in terms of *top/bottom* enantiomer face (brevianamide A/X vs. brevianamides Y/B) and *anti/syn* selectivity, was lost in the absence of BvnE (Figure 3.2). This strongly suggests that the isomers are

constructed from non-enzymatic IMDA reactions. Computational calculations are consistent with the results seen and the selectivity of the IMDA from structure **203** (see section VIII for more details; Figure 3.28). As the overall role of BvnE was identified, attention shifted towards determining how the enzyme catalyzes the formation of the indoxyl species.

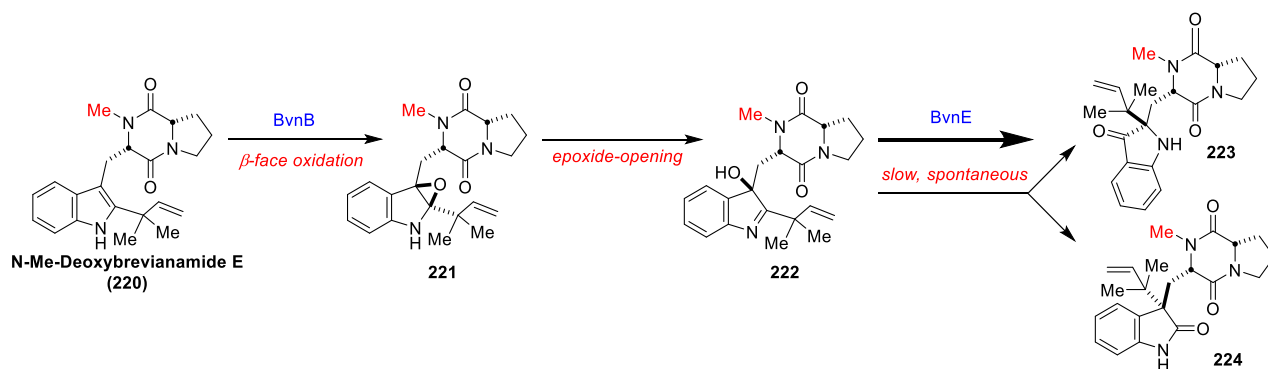


**Figure 3.11: Probing the functionality of BvnE using substrate mimic, *N*-Me-deoxybrevianamide E (220).** BvnB was used to oxidize the indole before the catalytic properties of BvnE were tested. Compound **222** was found to be completely converted by BvnE in indoxyl **223**, but in the absence of BvnE the substrate would spontaneously convert to **223** and **224**.

## V. BvnE Crystal Structure and Catalytic Mechanism Insight

The catalytic mechanism of BvnE toward the selective formation of the indoxyl species was sought out. The NTF2-like superfamily enzymes have been studied in the fungal meroterpenoid biogenesis and are related to BvnE.<sup>87</sup> As such, homolog PrHC (PDB ID:2085X9J) was used as a search model by molecular replacement to assist in solving the crystal structure of BvnE at 1.8 Å resolution (PDB ID: 6U9It; Figure 4.12 A). The crystal structure revealed that BvnE is a symmetric homodimer that adopts an  $\alpha$ + $\beta$ -barrel fold with the active site at the end of each barrel. The cavity that is created is hydrophobic and contains several polar residues, which could be performing acid-base chemistry (Figure 4.12 B).

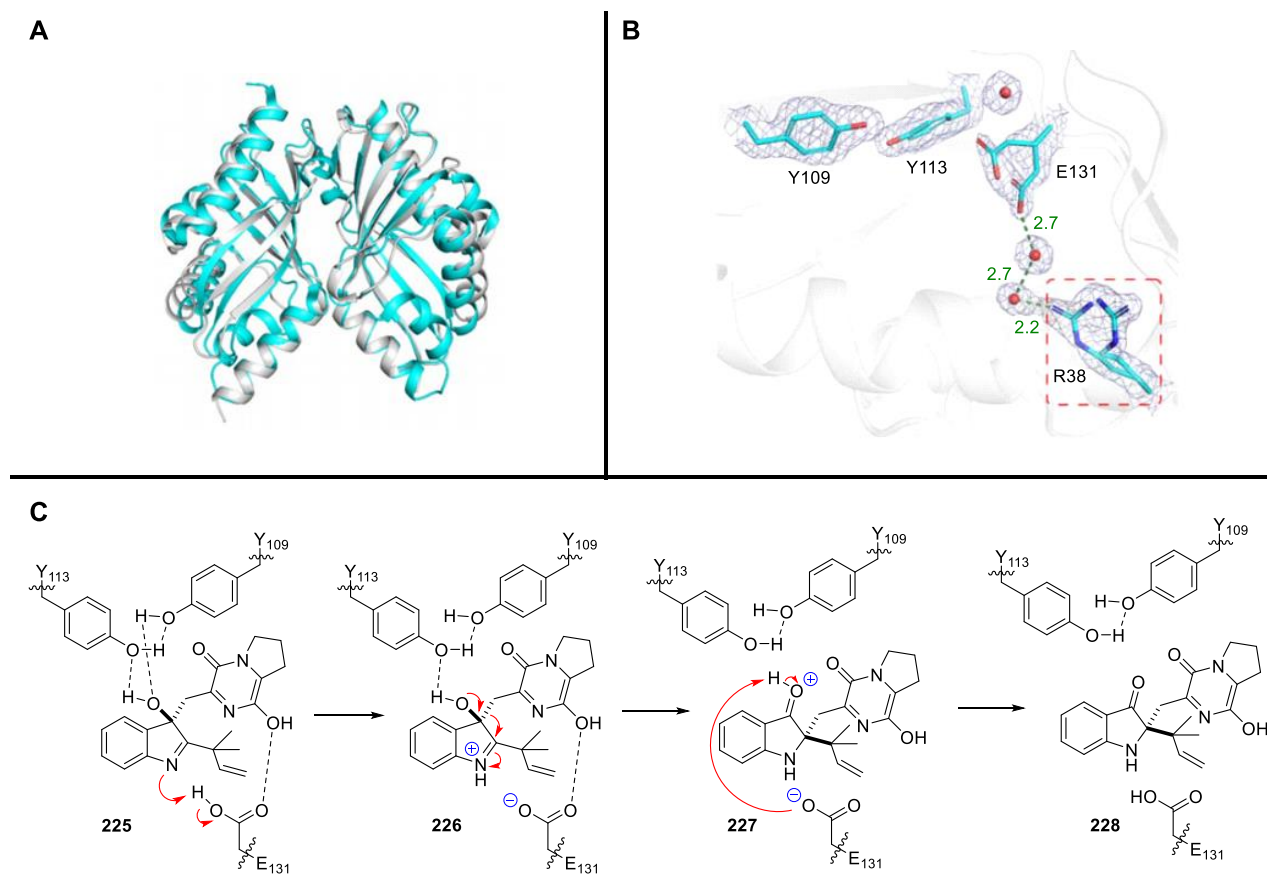


**Figure 3.12: BvnE crystal structure, docking and the proposed catalytic mechanism.** (A) cartoon crystal structure of BvnE. (B) Electron density ( $2F_o-F_c$ ,  $1\sigma$ ) for the active site residues of BvnE (PDB ID: 6U9I) shows conformational flexibility at Arg38 and Glu131 suggestive of potential active site remodeling during catalysis. Arg38 (red box) which is essential for catalytic activity does not make direct interactions with the docked ligand or active site residues. However, the structure reveals two ordered water molecules (red spheres) in a hydrogen bonding network between Arg38 and Glu131. (C) The proposed BvnE reaction mechanism for isomerization. Glu131-mediated proton transfer could be assisted by Arg38, which interacts with Glu131 via an ordered water network

By docking presumed native substrate **203**, the active site of BvnE was revealed. From *in vitro* enzyme assays with **222** residues Arg38, Tyr109, Tyr113, and Glu131 were identified as candidates for site-directed mutagenesis. Specifically, Arg38, Tyr113, and Glu131 were found to adopt multiple conformations in the crystal structure, implying these residues were flexible for molecular docking. Based on the docking studies, a 2-step reaction mechanism was proposed (Figure 4.12 C). First, Glu-131 mediated a proton transfer to initiate the semi-pinacol

rearrangement and stabilize charge in the intermediate. Second, Tyr108 and Tyr113 activate the semi-pinacol rearrangement by hydrogen bond-assisted activation. The remaining two residues, Arg38 and Glu131, do not directly catalyze the rearrangement, but instead create a hydrogen bonding network by supplying two ordered water molecules.

## VI. Total Synthesis of Brevianamide Y and X

At the time of initial synthesis, only the relative stereochemistry of brevianamide Y was known, which indicated that the bicyclo[2.2.2]diazaoctane core was in the *anti*-configuration; therefore, a scheme like seen in Miller's versicolamide B synthesis where only *anti*-compounds were synthesized was the model. Following the versicolamide pathway, the Diels-Alder reaction would need to occur after the pinacol rearrangement. Brevianamide Y could come from **229** by a hetero-IMDA (*Figure 3.13*). Compound **229** could be obtained by elimination of the alcohol of compound **230** in a Mitsunobu-type fashion. A pinacol rearrangement of known compound **86** could then yield compound **230**. The pinacol rearrangement would likely be more challenging in this case, for unlike the versicolamide B precursor **133**<sup>68</sup>, there were no extra electron donating components on the benzene ring of the aromatic system to aid in the rearrangement.

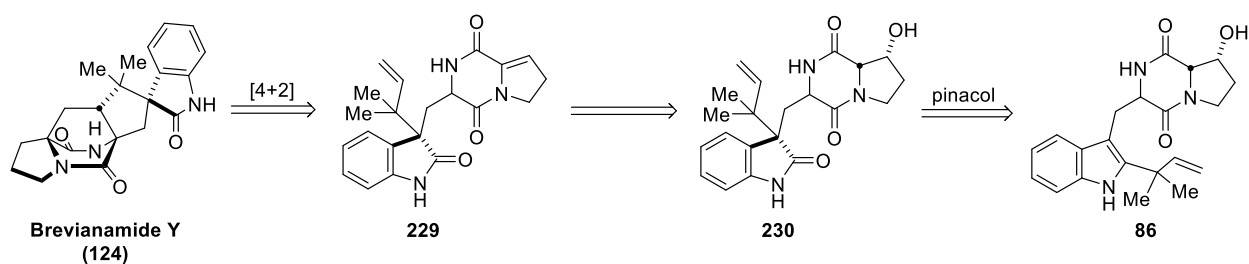


*Figure 3.13: Retrosynthesis of brevianamide Y*

To study the pinacol rearrangement, the diastereomers of diketopiperazine **86** were carried forward separately. Initial attempts were done without any protecting groups, testing conditions developed by Miller<sup>68</sup> and Glinka<sup>69</sup>.

When diketopiperazine **86** was treated with oxaziridine **131**, no reaction occurred. Although the treatment of compound **133** with oxaziridine **131** worked, it was plausible that the electron donation from the pyran ring assisted the oxindole formation as seen in *Figure 3.14*.<sup>122</sup> This claim is further supported by work done by Grubbs and coworkers who found that a reaction with **131** did not occur with a Boc-protected phenol.<sup>122</sup> It is interesting to note that oxaziridine **131** was able to convert both *syn*- and *anti*-cycloadducts to hydroxyindolenines, which could then be pushed through a pinacol rearrangement to the oxindole. Due to Miller's synthesis of versicolamide B being one of the few sources of reactions to form early-stage oxindoles, a new approach that was often applied to a Diels-Alder cycloadduct (e.g. compound **34**) was explored.

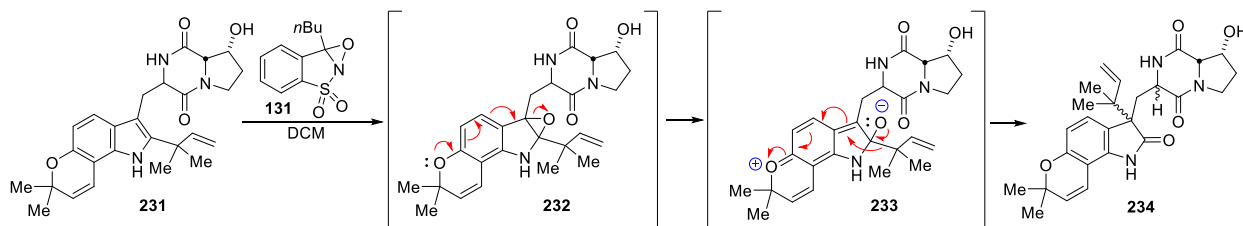
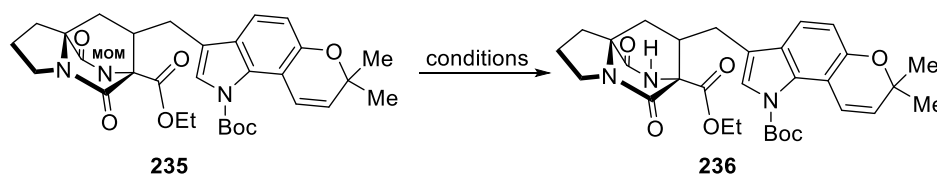


*Figure 3.14: Mechanism for oxindole formation on pyran substituted indole substrates (231). Oxaziridine 131 was used as the oxidizing agent, and both *R* and *S* oxindoles were made.*

Addition of *tert*-butyl hypochlorite to diketopiperazine **86** provided the chloroindolenine intermediate, which immediately was refluxed in methanolic acetic acid. The only product furnished was brevianamide E, a shunt metabolite seen in the biosynthesis of brevianamides A and B. The cyclization was interesting to note as, during KO studies of the enzymes in *P. brevicompactum*, brevianamide E was exclusively formed in the absence of BvnD.<sup>46</sup> The

formation of brevianamide E suggested that a protecting group might be necessary to overcome the nucleophilicity of the amide nitrogen upon reflux.<sup>107</sup>

The choice of protecting group for the amide nitrogen was crucial; it needed to be able to withstand slightly acidic conditions and not readily protect the indole nitrogen. As seen in past work by the Williams group, para-methoxy benzyl (pMB) protecting groups do work but were incredibly difficult to remove from prenylated indole alkaloid substrates.<sup>39</sup> The next plausible protecting group was a methoxyl methyl group (MOM), as it is somewhat acid stable and has been removed from a related substrate in the total synthesis for a compound in the indole alkaloid family (*Figure 3.15*).



Conditions	Product (% yield)
BF <sub>3</sub> OEt <sub>2</sub> , EtSH, DCM	Recover S. M.
BBr <sub>3</sub> , DCM	Complete decomposition
<i>B</i> -Br-9-BBN, DCM	35%
TMSI, DCM	49%
<i>B</i> -bromocatecholborane, DCM	68%

*Figure 3.15: MOM-deprotection conditions tested on compound 235 by the Baran group.*

In Baran's paper on the total synthesis of avrainvillamide and the stephacidins, a MOM group deprotection was carried out on a compound similar to diketopiperazine **86**.<sup>123</sup> When testing deprotection conditions, they found that strong acids at reflux temperatures tended to cause decompositions and refluxing with weaker acids only gave small amounts of deprotected product. In a later model study performed on compound **235**, it was found that various Lewis acids were able to deprotect the MOM group with varying degrees of success, but *B*-bromocatecholborane was able to mildly remove the MOM group with no noticeable

decomposition and later was applied to a target compound much like **235** (Figure 3.15).<sup>123</sup> With this in mind, *B*-bromocatecholborane appeared to be a good candidate for MOM-deprotection, making a MOM protecting group a good candidate for the amide nitrogen (Figure 3.16).

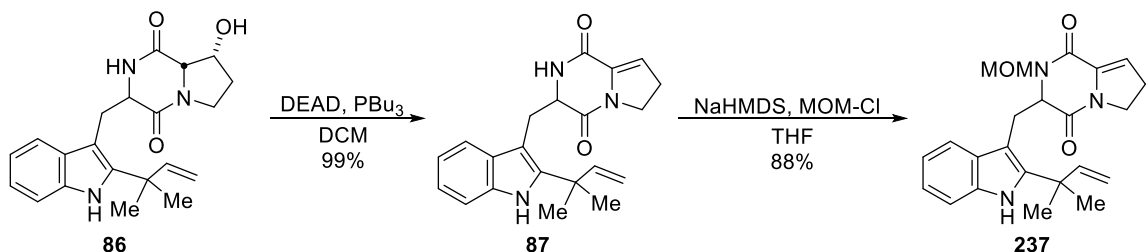
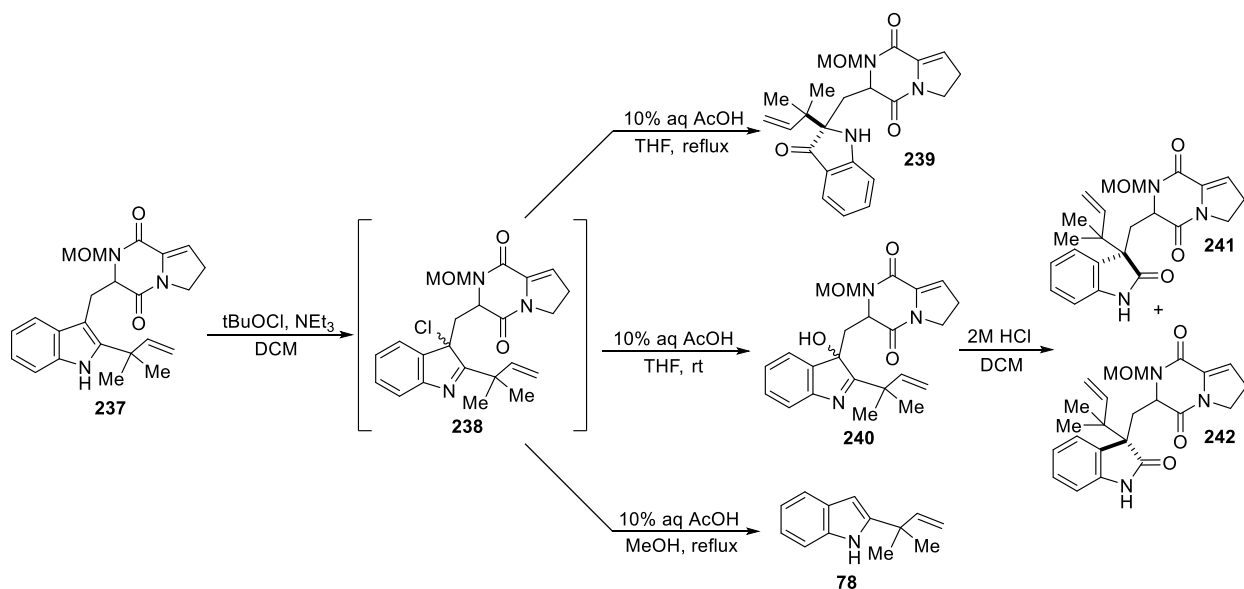


Figure 3.16: **Mom protection of diketopiperazine 86**. Diastereomers of **86** were carried forward separately for subsequent reactions.

The MOM-protection was carried out on enamine **87**. To prevent protection of both the indole and the amide, MOM-Cl was added in multiple small increments and monitored closely by TLC. The selectivity of the amide nitrogen before the indole nitrogen was likely due to the steric hindrance of the geminal dimethyl groups, as mentioned in the total synthesis of *N*-methyl-deoxybrevianamide E (see section IV). The greater selectivity of the MOM-protection was likely a result of its bigger size when compared to the methylation. The chloroindolenine (**238**) was generated upon treatment with *tert*-butyl hypochlorite (Figure 3.17). Immediate reflux in methanolic acetic acid was utilized to trigger the pinacol rearrangement. Instead of forming the oxindole, elimination of the diketopiperazine unit occurred, leaving prenylated indole (**78**) as the only product. To suppress the undesired elimination, a less polar solvent, THF, was substituted for MeOH, a change that was proven to prevent side reactions in the total synthesis of (+) paraherquamide B.<sup>36</sup>

When chloroindolenine **238** was refluxed in THF and acetic acid the elimination was prevented, but instead of forming the oxindole (**241/242**) as the only product, a semi-pinacol rearrangement occurred to create indoxyl **239** (Figure 3.17). The proportion and yield of each

product depended upon the reaction time, but the indoxyl was always the major product by 70% or greater. Since the oxindole was not the product of either reflux reactions under acidic conditions, it was decided to try the reactions at a lower temperature in hopes of suppressing the formation of the indoxyl moiety.



**Figure 3.17: Pinacol rearrangement conditions screened for MOM-protected 237.** Solvent properties and reaction temperature play a role in selectivity of the rearrangement.

When the acetic acid reaction of the chloroindolenine was run at room temperature the hydroxyindolenine was the product. As seen in the biosynthetic studies of the brevianamides, the hydroxyindolenine can readily be converted to the oxindole, which was accomplished with a biphasic solution of 2M HCl and DCM.<sup>64</sup> With the oxindole in place, MOM deprotection conditions from Baran's synthesis of avrainvillamide and the stephacidins were screened.

Even after successive trials with various concentrations of *B*-bromocatecholborane, deprotected product was never isolated; only starting material (**241/242**) was recovered. This was indicative of *B*-bromocatecholborane not being a suitably strong Lewis acid for the removal of the MOM group from the amide. While  $\text{BBr}_3$  was found to only decompose the material in

Baran's model study, it was still tested on oxindoles **241** and **242**.<sup>123</sup> Sadly, only a small amount of deprotected product was recovered, with the major product being decomposed material.

After various trials of deprotection conditions were carried out, deliberation on oxindole formation was reinvestigated. The initial reasoning for a protecting group was that an acidic reflux made the amide nitrogen incredibly reactive towards the C-2 position on the indole. At that moment in time, though, the rearrangement did not necessitate any reflux conditions, as the pinacol rearrangement could occur at room temperature. Because of this, it was theorized that a protecting group may no longer be necessary and so pinacol rearrangement conditions were again tested on diketopiperazine **39** (*Figure 3.18*).

The conditions developed during the MOM protection for the pinacol were implemented on diketopiperazine **86**. With the use of *tert*-butyl hypochlorite, diketopiperazine **86** was transformed into the chloroindolenine intermediate (*Figure 3.18*). Upon treatment with acid, the chloroindolenine executed a pinacol rearrangement to oxindoles *cis*-**230** and *cis*-**243**. The oxindoles were separated and carried forward in the same fashion as seen in Miller's versicolamide B synthesis.<sup>68</sup>

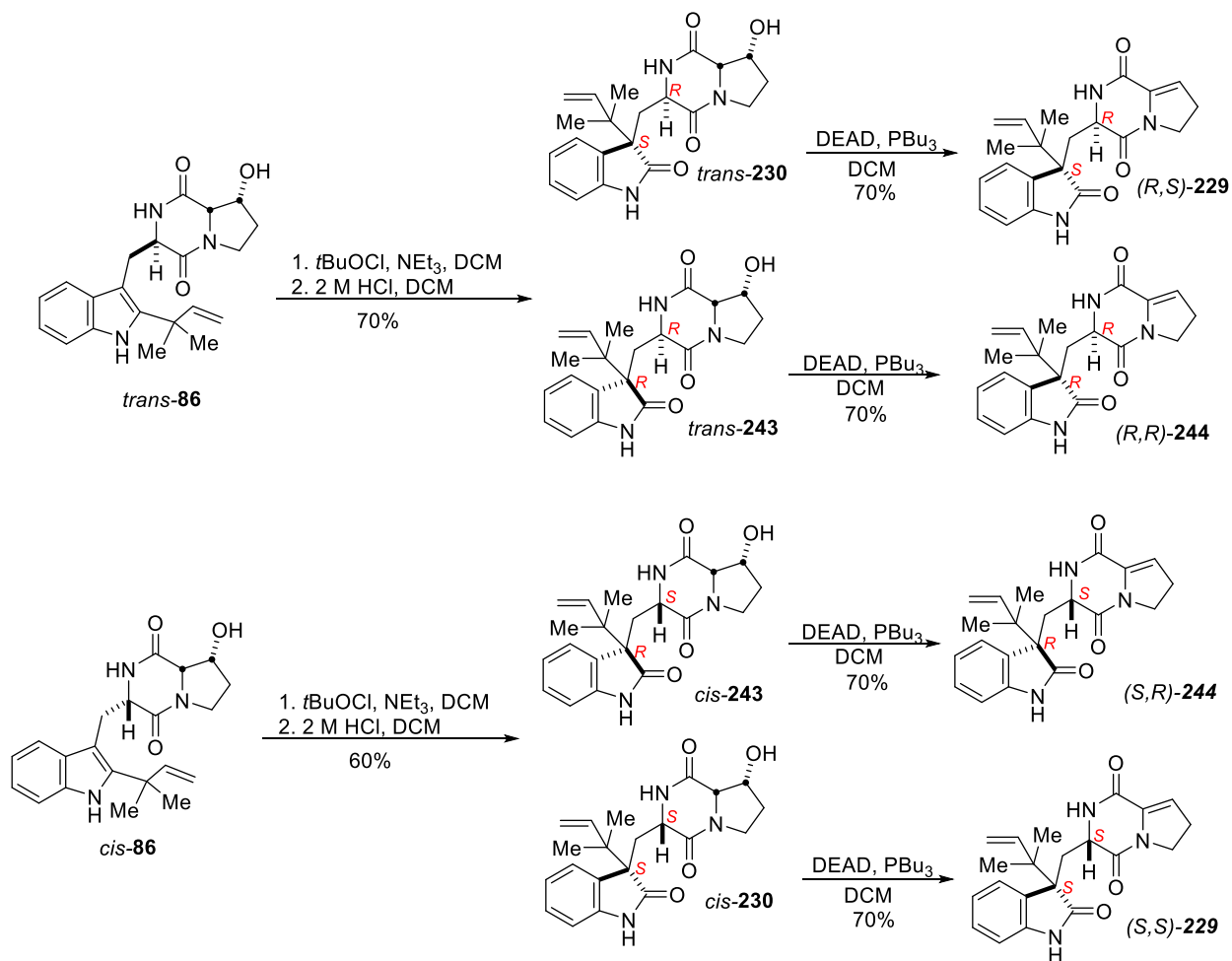


**Figure 3.18: Pinacol rearrangement of diketopiperazine 86.** the cis- and trans-diastereomeric nomenclature refers to the relative stereochemistry of the proline- and tryptophan-derived  $\alpha$ -methine protons. Relative stereocenters for naming are shown in red.

Mitsunobu of oxindoles *cis*-230 and *cis*-243, followed by a Diels-Alder reaction in methanolic KOH, afforded optically active brevianamide Y and corresponding diastereomers (245, *ent*-245, *ent*-124; Figure 3.19). Interestingly, as demonstrated in Miller's versicolamide B synthesis, only anti-cycloadducts were synthesized. All data collected for brevianamide Y matched that isolated from *P. brevicompactum* (Figure 3.20).

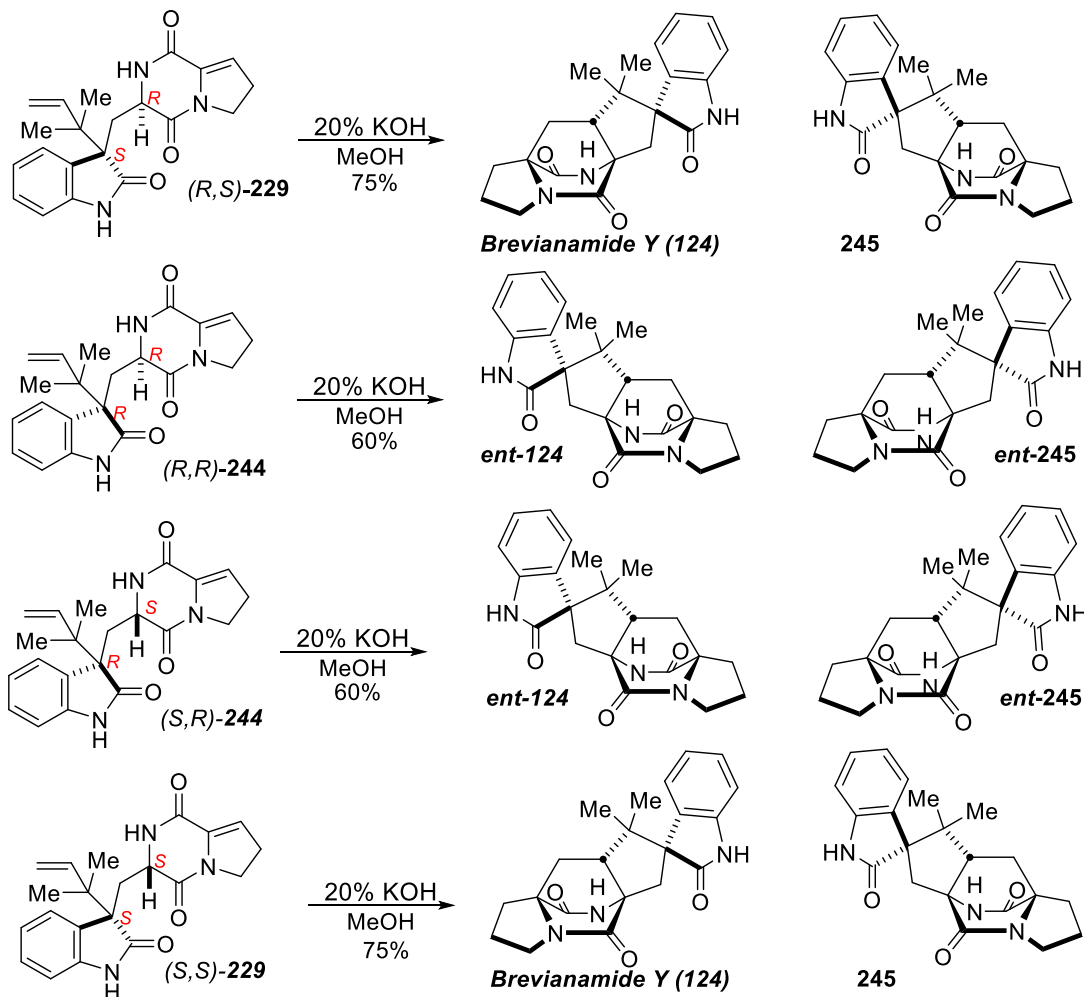


**Figure 3.19: Synthesis of Brevianamide Y and corresponding diastereomers.** All compounds were optically active and readily separated. Brevianamide Y and its enantiomer were the major diastereomers in each reaction.

As only anti-cycloadducts were produced, in order to synthesize brevianamide X, a new approach was sought. Instead of the pinacol rearrangement occurring before the IMDA reaction, the reverse needed to occur; the pinacol must follow the IMDA reaction. The Diels-Alder substrate was accessed through the rearrangement of compound **87** in methanolic KOH to yield a 2.1:1 ratio of *syn:anti*-compounds (**126** & **34**). The *syn*-compound was easily isolated from the *anti*-cycloadduct and carried forward.

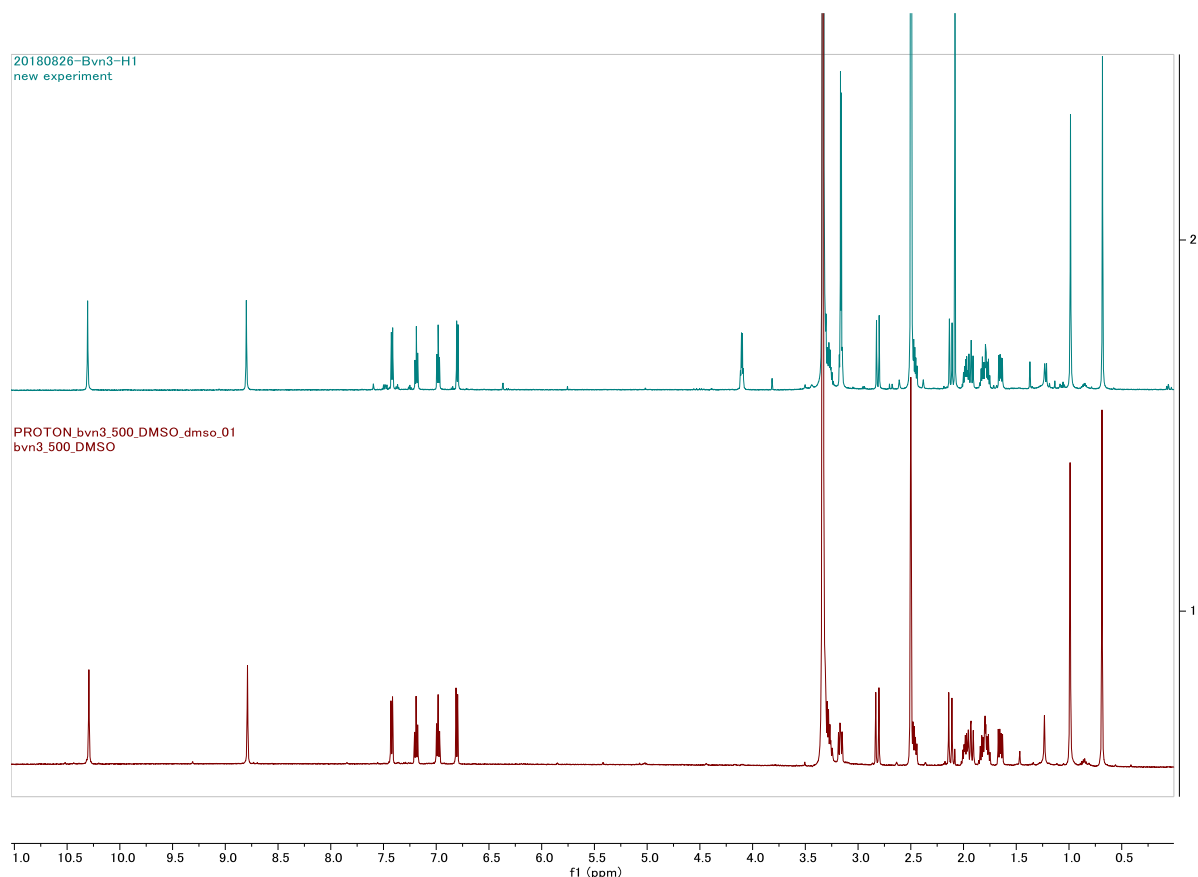


**Figure 3.20:  $^1\text{H}$ -NMR comparison of synthetic vs. isolated brevipamide Y.** Solvent for both spectra was  $d_6$ -DMSO. Synthetic spectra = red; isolated spectra = blue

It was found that the formation of the chloroindolenine and rearrangement into the oxindole brevipamide X via *tert*-butyl hypochlorite and 2M HCl occurred on Diels-Alder cycloadduct **67** readily (Figure 3.21). Later, it was also determined that the formation of hydroxyindolenine **216** or **46**, either by mCPBA or Davis Oxaziridine (**131**), followed by treatment with acid could furnish brevipamide X or brevipamide Y, respectively. Interestingly, the chloroindolenine, while it favored the same face of the DA cycloadduct as mCPBA, was much more selective and converted to the oxindole quicker than the hydroxyindolenines.

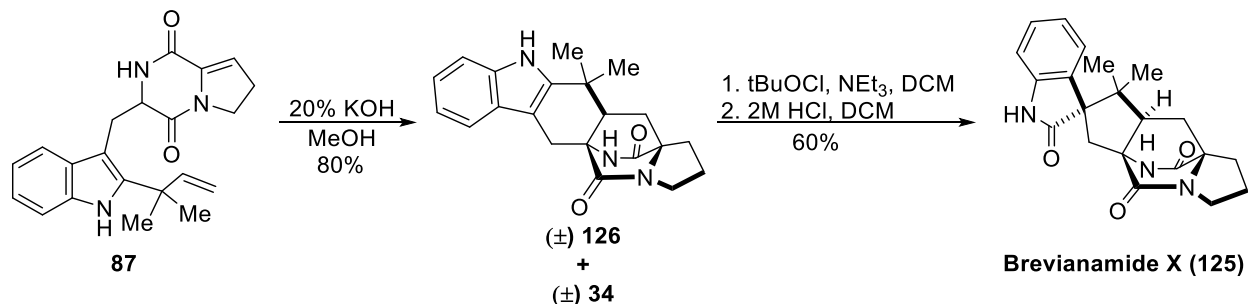


**Figure 3.21: Synthesis of brevianamide X from enamine 87.** Compounds synthesized were racemic. The hydroxyindolenine of **126** synthesized from mCPBA or Davis oxaziridine also converted to brevianamide X upon treatment with acid.

Overall, the total synthesis of brevianamides X and Y were completed. The total synthesis of brevianamide Y was optically active and accomplished in 11 steps from commercially available indole. Brevianamide X was synthesized from indole in 11 steps but was a mixture of enantiomers. Having synthesized both new oxindoles in the biosynthetic pathway of the brevianamides, the compounds were compared to authentic samples isolated from *P. brevicompactum*, which confirmed their identities and, in the case of brevianamide Y, assisted in the determination of the absolute configuration of the natural product. With both hydroxyindolenines (**45**, **46**, **216**) and oxindoles (brevianamides X and Y) synthesized, attention was shifted towards the synthesis of the indoxyl species.

## VII. Indoxyl Species: Total synthesis of brevianamide A and Syn Indoxyl 204

Only one total synthesis of brevianamide A has been completed previously. The main aspect prohibiting an earlier synthesis was the inaccessibility of the corresponding hydroxyindolenine precursor.<sup>60</sup> Now having garnered access to hydroxyindolenine **45**, the total synthesis of brevianamide A and a *syn*-indoxyl (**204**) from hydroxyindolenines **45** and **216** were attempted.

Previous syntheses of brevianamide B applied base treatment on hydroxyindolenine **46** (or derivatives of the compound) to successfully catalyze the semi-pinacol rearrangement to construct the indoxyl. Base treatment to catalyze the semi-pinacol rearrangement was also attempted on hydroxyindolenine **45**. When a small amount of hydroxyindolenine **45** was treated with 0.5 M NaOH, HPLC analysis was able to detect some conversion to brevianamide A (Figure 3.22).

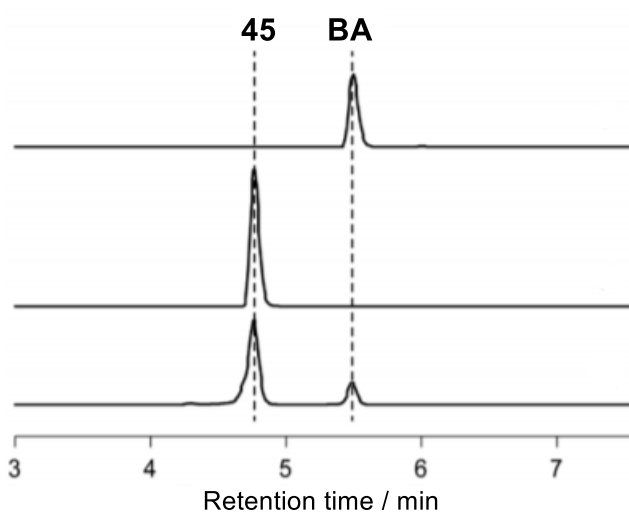


**Figure 3.22: HPLC analysis of base treatment of compound 45.** i, Brevianamide A (BA) standard; ii, **45** treated with 0.5 M NaOH for 0 h; iii, **45** treated with 0.5 M NaOH for 1 h.

Applying the same conditions as seen in Figure 3.22, hydroxyindolenine **45**, synthesized from *anti*-cycloadduct **34**, was treated with NaOH at room temperature (Figure 3.23). No conversion to brevianamide A was detected by TLC after 3 days; instead, hydroxyindolenine **45** remained. It became apparent that **45** was much more stable than the other hydroxyindolenines, more specifically **46** that readily converted to brevianamide B. To better catalyze the semi-pinacol rearrangement, the reaction mixture with NaOH in MeOH was heated to reflux but only provided deoxybrevianamide E and its diastereomer (Figure 3.23). The conventional pathway to establish the indoxyl from a hydroxyindolenine by treatment with base did not appear to be an

adequate methodology to construct the indoxyl of brevianamide A, so other conditions were investigated.

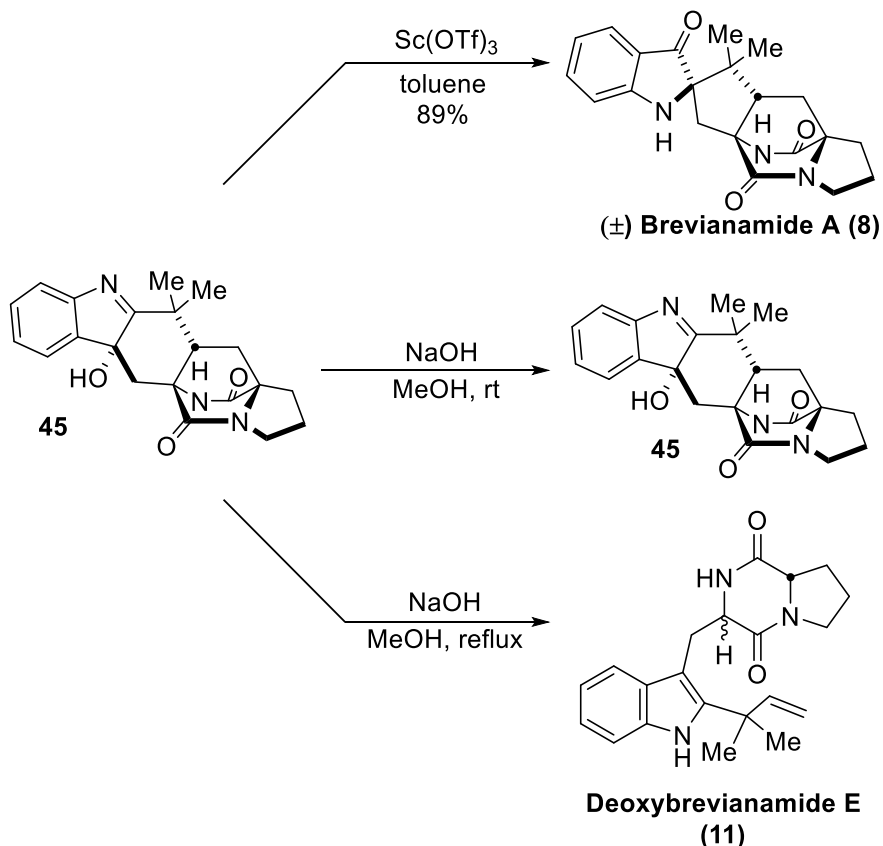


*Figure 3.23: Semi-pinacol rearrangement conditions tested to synthesize brevianamide A. Compounds synthesized were racemic.*

In Sarpong's total synthesis of the enantiomer of citrinalin B, a variety of methodologies were investigated to form the oxindole core.<sup>5</sup> Similar to other pinacol rearrangements carried out in literature, the starting material was a hydroxyindolenine (**246**). A Lewis acid, scandium triflate ( $\text{Sc}(\text{OTf})_3$ ), was used in hopes to catalyze the pinacol rearrangement to the oxindole (*Figure 3.24*). Instead of forming an oxindole, the indoxyl species was formed (**247**) and would not rearrange to the oxindole even when excess heat was applied. In fact, the only way that an oxindole could be synthesized from a hydroxyindolenine like **246** was by treating its

diastereomer, **248**. The favoring of the indoxyl over the oxindole for **246** was intriguing, as many previous studies have shown the opposite.

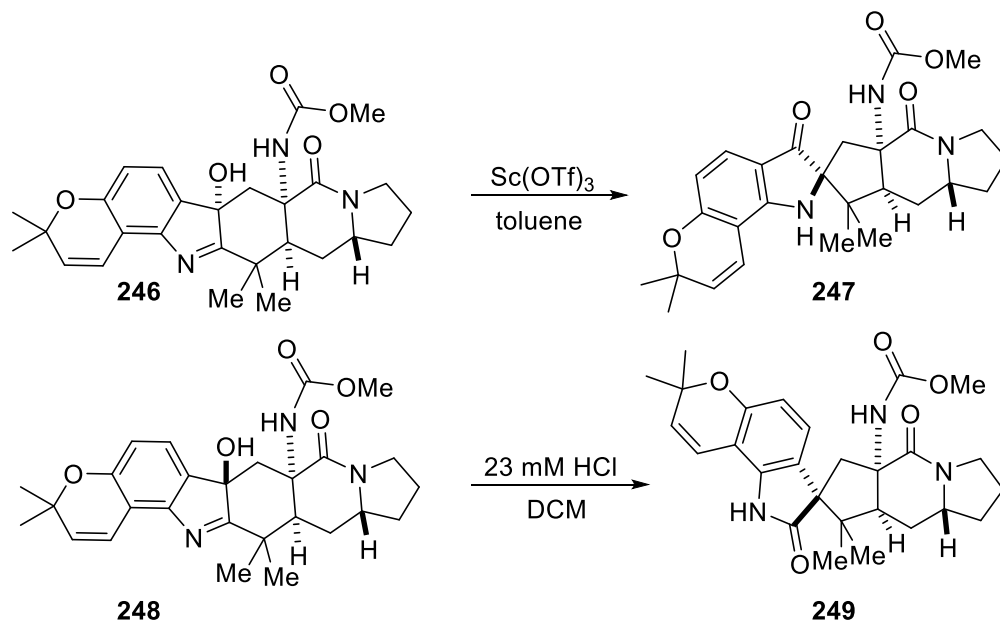


**Figure 3.24: Rearrangement favorability of hydroxyindolenine diastereomers 246 and 248.** The oxindole was not able to be formed from **246**, but readily was constructed from **249**.

For example, Ashenhurst's study on the oxidative rearrangement of tryptamine derivatives found that the indoxyl could easily be converted to the oxindole by heating in toluene with a catalytic amount of  $\text{Sc}(\text{OTf})_3$  (Figure 3.25).<sup>124</sup> The studies also demonstrated almost exclusive favoring of oxindole **252** formation when applying a variety of Lewis acids. It was later theorized that some favorable hydrogen-bonding interaction may be occurring to stabilize indoxyl over oxindole formation from **246**.<sup>5</sup>

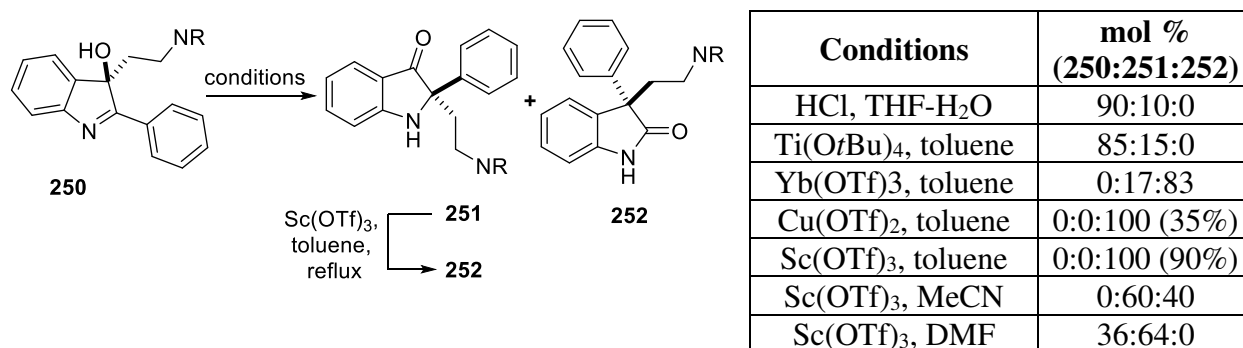


**Figure 3.25: Selectivity of oxindole or indoxyl formation from hydroxyindolenine 250.** R= Phthalimide.

Seeing that the use of Sc(OTf)<sub>3</sub> successfully converted hydroxyindolenine **246** to indoxyl **247**, the reagent was tested on hydroxyindolenine **45**. An equimolar amount of Sc(OTf)<sub>3</sub> was found to promote the semi-pinacol rearrangement of compound **45** to the fluorescent yellow indoxyl, (±) brevianamide A, in a 89% yield when refluxed in toluene (Figure 3.23). All NMR data collected for the synthetic sample matched that isolated from *P. brevicompactum* (Figure 3.26).

Having synthesized brevianamide A, attention was shifted towards synthesizing *syn*-indoxyl **204** that is believed to be the unknown indoxyl found in *bvnE-KO* study of *P. brevicompactum*. The necessary hydroxyindolenine (**216**) was obtained by oxidizing *syn*-cycloadduct **126** with mCPBA. When **216** was treated with NaOH in MeOH, only the oxindole, brevianamide X, was obtained (Figure 3.27). The oxindole was also created when hydroxyindolenine **216** was heated in Sc(OTf)<sub>3</sub>, whether the solvent was toluene or DMF.<sup>124</sup> As all conditions so far had led to the formation of the oxindole, new conditions were investigated.

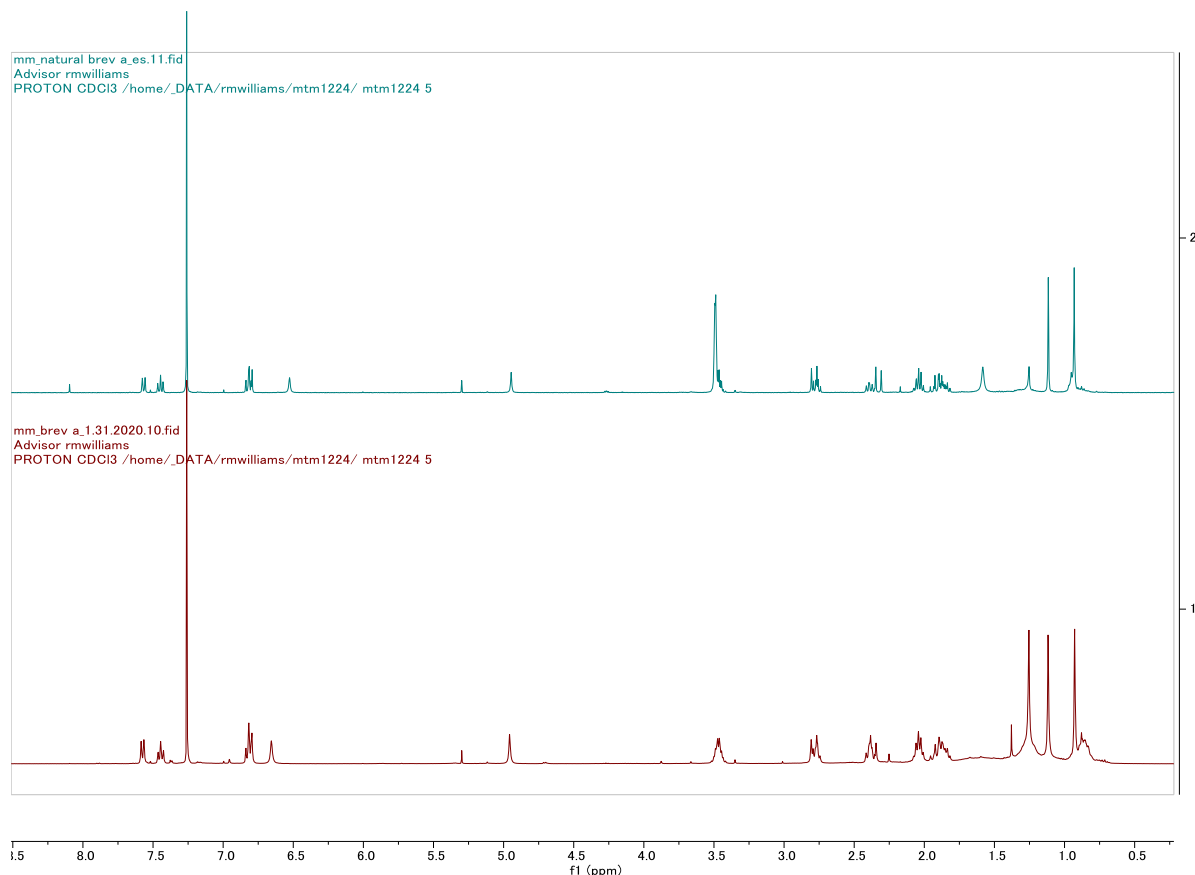


**Figure 3.26:  $^1\text{H-NMR}$  comparison of synthetic vs. isolated brevipanamide A.** Solvent for both spectra was  $\text{CDCl}_3$ . Synthetic spectra = red; isolated spectra = blue.

When studying the interconversion between a hydroxyindolenine and an indoxyl species, Nagase and co-workers found that DBU could catalyze the formation of the indoxyl when heated in DMF.<sup>125</sup> Care had to be taken, though, to prevent the reverse reaction from occurring, as almost any acidic conditions converted the indoxyl back to the hydroxyindolenine which then could then be converted to the oxindole. This gives evidence that the previously tested conditions could have formed the indoxyl, but if the reaction ran too long the hydroxyindolenine and/or the oxindole would be isolated instead. Upon heating in DMF with DBU, the *syn*-hydroxyindolenine did slowly convert to the indoxyl, but not fully (*Figure 3.27*). It was also difficult to completely purify the compound. Optimization of these conditions are still being investigated in the lab.

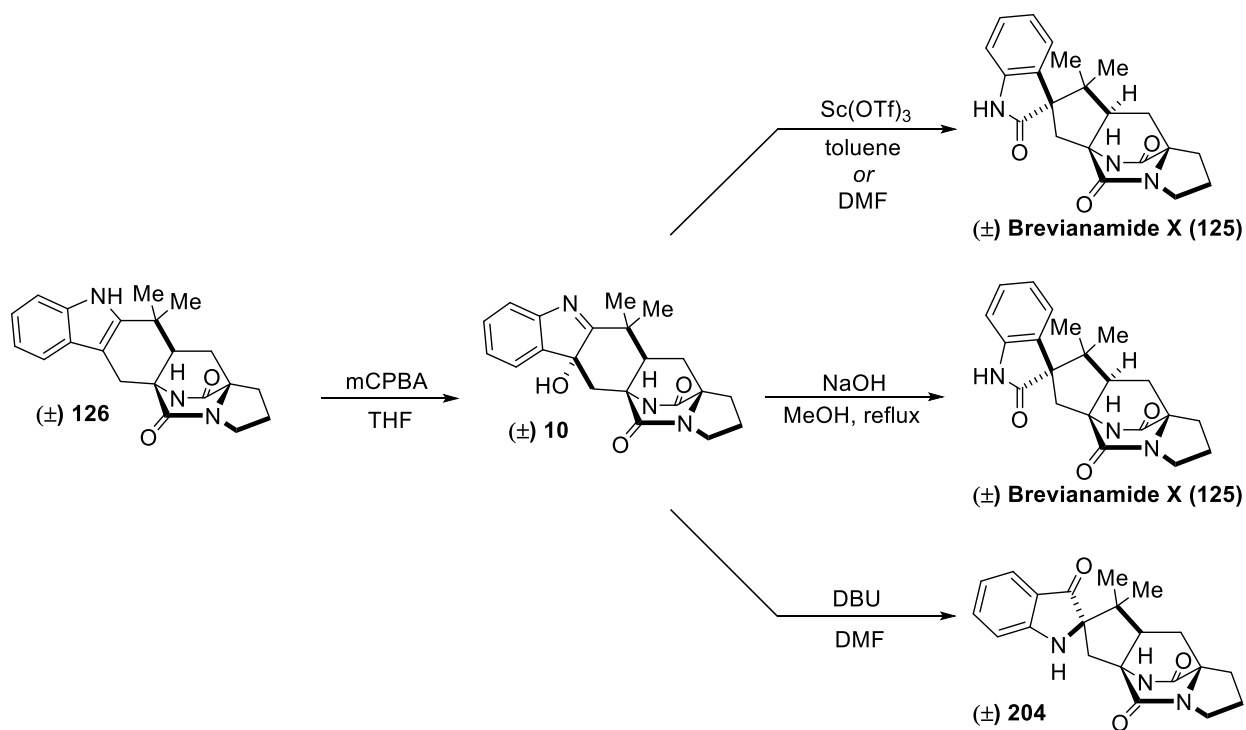


**Figure 3.27: Semi-pinacol rearrangement conditions tested on hydroxyindolenine 10.** Compounds synthesized were racemic mixtures.

### VIII. Computational Analysis

Density functional theory and coupled cluster theory calculations were applied to evaluate the intermediate and transition state structures in the newly identified brevianamide biosynthetic pathway. The innate regio- and stereochemical selectivity in key transformations were also explored both for the biosynthetic and lab synthesized transformations. The computational investigations were carried out by the Paton group at Colorado State University.

During the *P. brevicompactum* knock-out study with BvnE, the IMDA was shown to occur spontaneously on compound **203** to give hydroxyindolenine intermediates **45**, **46**, and **216** (Figure 3.2) The transformation was found to be energetically favorable (Figure 3.28). The 1,2-alkyl shift was only found to occur on hydroxyindolenines **46** and **216**, not compound **45**, in the KO study. Computational analysis confirmed that **45** would not perform a pinacol

rearrangement; the barrier for the tautomerization of hydroxyindolenine **45** was too high in energy (35.5 kcal•mol<sup>-1</sup> between **45** and **253**). The product distribution found in the *bvnE*-KO study agreed with calculated results where brevianamide Y and hydroxyindolenine **45** were the most favored products, followed by brevianamide X, and lastly brevianamides A and B based upon energetics (experimental ratio, Brevianamide Y: X: A: B: **45**, 9:5:1:1:7).

The pinacol rearrangement selectivity was found experimentally to be highly dependent on reaction conditions. The oxindole was formed when exposed to acid, while base was more often what would form the indoxyl. The acid/base selectivity was further confirmed computationally. It was found that general, or acidic, activation of the nitrogen resulted in a build-up of positive charge in the migrating group of the transition state, such that it favored a 1,2-prenyl migration ( $\Delta\Delta G^\ddagger$  8.8 kcal•mol<sup>-1</sup>) to the oxindole (*Figure 3.29*). Base activation appeared to activate the hydroxyl group instead, causing the selectivity to favor the migration of the diketopiperazine moiety ( $\Delta\Delta G^\ddagger$  0.7 kcal•mol<sup>-1</sup>). Exploration of the semi-pinacol rearrangement catalyzed by BvnE established the rearrangement to be exergonic and irreversibly favorable ( $\Delta G$  -11.6 kcal•mol<sup>-1</sup>). The regioselective biocatalytic conversion of native substrate **203** to **39** and conversion of synthetic derivative **222** to **223/224** under acid-base conditions gives strong evidence to Tyr113 or Tyr114 acting as a hydrogen-bond acceptor for the activation of the 3-hydroxyl group in BvnE during the key initiation step (*Figure 3.12*).

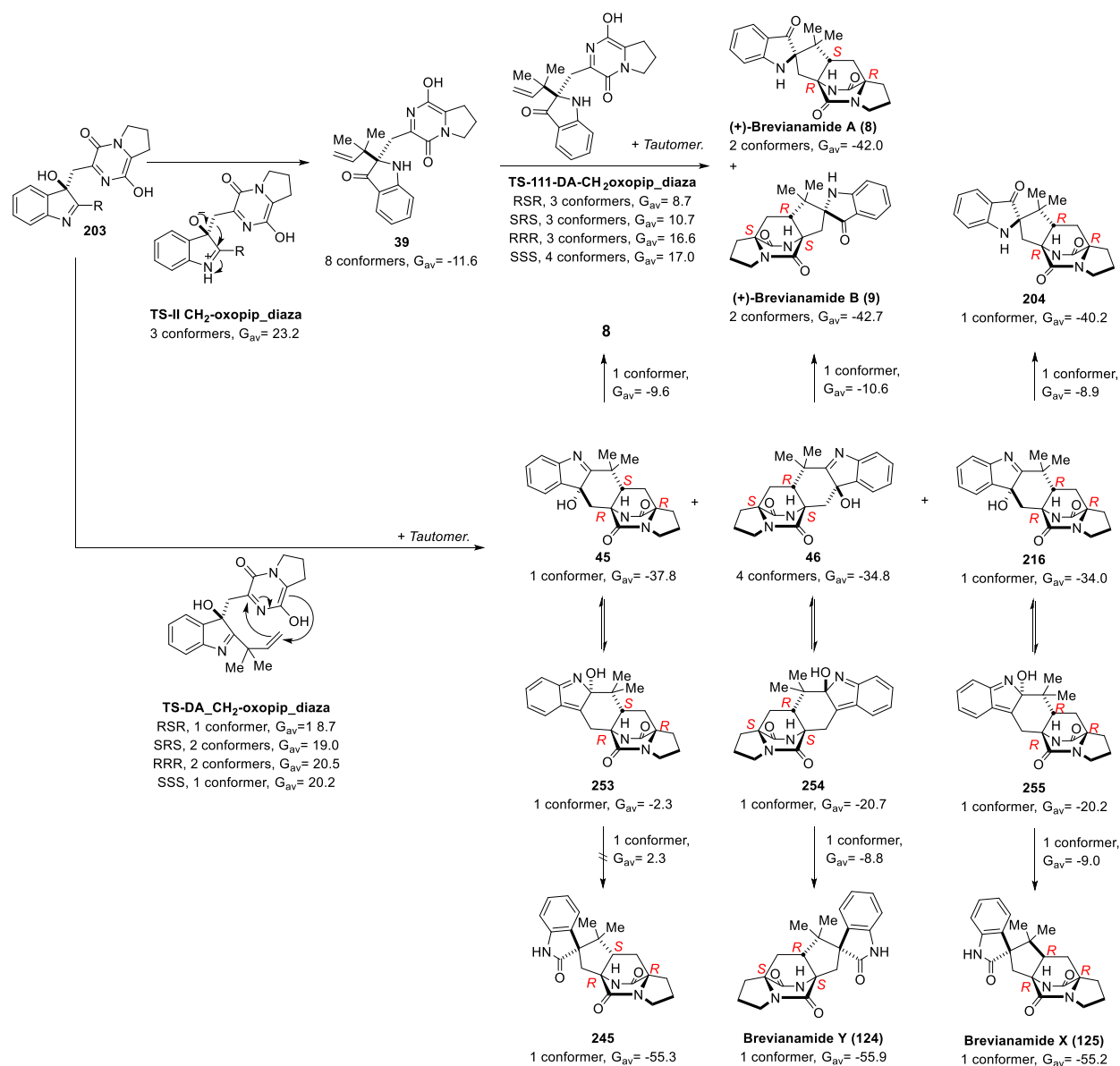


**Figure 3.28: Boltzmann weighted G of the main reaction pathways from compound 203.** The number of conformers found for each reaction step are included in the calculations. Computation data was collected by the Paton group

The selectivity of the IMDA cycloaddition was examined for the selectivity in wild and *bvnE*-KO *P. brevicompactum* strains (Figure 3.30 A). The *anti*- over *syn*-cycloaddition selectivity was controlled by a combination of favorable intramolecular hydrogen bonding and unfavorable steric interactions (Figure 3.30 B). While *syn*-cycloaddition is incredibly disfavored from indoxyl **39** relative to *anti*-cycloaddition, there were some C-H...O interactions from

hydroxyindolenine **203** that do allow *syn*-cycloaddition to occur (Figure 3.30 C).<sup>126,127</sup> As such, the selectivity for *anti*-cycloaddition from the indoxyl is incredibly high. Diastereoselectivity of the IMDA to form brevianamide A over its pseudo-enantiomer, brevianamide B, is derived from an intramolecular N-H•••O hydrogen bond that increases the preference by 2 kcal•mol<sup>-1</sup> (Figure 3.30 A).

Precursor		
Migrating Group		
Condition	$\Delta G$ of migration (kcal/mol)	
Acid	<b>18.7</b>	27.5
Neutral	<b>29.7</b>	36.0
Basic	19.2	<b>18.5</b>
Experimental selectivity	<b>2</b>	1
Experimental selectivity with BvnE	1	<b>20</b>

**Figure 3.29: Activation barriers in kcal/mol for the migration of the reverse-prenyl group and the -CH<sub>2</sub>-dioxopiperazine group.** Includes when using acid (R = H<sup>+</sup>, R' = H), neutral (R = lone electron pair, R' = H) and basic (R = lone electron pair, R' = negative charge) catalysis. Also, the experimental results of selectivity obtained from **37** with and without BvnE are shown.

The selectivity for the formation of the brevianamides in *P. brevicompactum* appears to arise from indoxyl preference through acid-base activation with BvnE and favorable hydrogen-bonding interactions driving the IMDA cycloaddition. The selectivity of only *anti*-cycloadducts in the total synthesis of brevianamide Y (chapter 3 section VI) and versicolamide B<sup>68</sup> was likely

a result of similar hydrogen bonding interactions. Further analysis of the selectivity is currently under investigation.

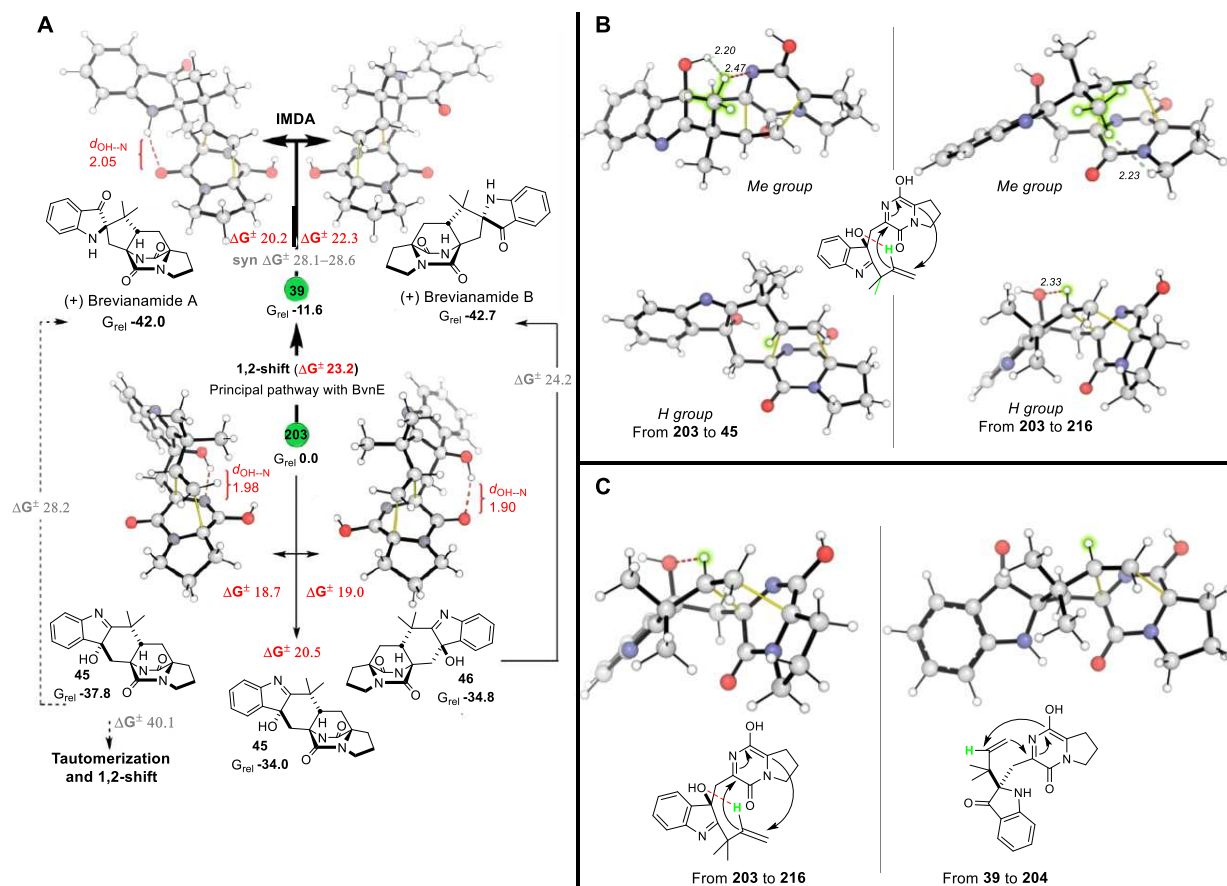


**Figure 3.30: Quantum chemical calculation and modeling results.** (A) anti-Selective IMDA transition structures and products accessible from **203** and **39**. Gibbs energies (kcal/mol); highlighted distances (Å). Normal lines follow the major pathways obtained under bvnE-KO conditions. Pathways in bold correspond to the major reactivity with BvnE (switch in reactivity). Dashed lines represent pathways with prohibitively high activation energies under the reaction conditions. (B) Main differences in the *anti*- and *syn*-IMDA transition states from compound **13**. The H and Me substituents that show relevant differences between the systems are highlighted in green. Relevant steric effects and hydrogen bonds are represented as green and red dashed lines, respectively. (C) Comparison of *syn*-IMDA transition states from compounds **203** and **39**. The key hydrogen bond formed in the IMDA from compound **203** is represented with a red dashed line. Computational data was all collected by the Paton group.

## IX. Conclusions and Future Directions

From a combination of biosynthetic techniques, total synthesis, and computational analysis, a revised biosynthesis of the brevianamides was elucidated with the identification of a new class of enzymes, co-factor independent pinacolases. The pinacolase, BvnE, was found to mediate diastereocontrol for the subsequent spontaneous IMDA cycloaddition to construct the bicyclo[2.2.2]diazaoctane core. Mechanistic questions remain for the BvnD enzyme; specifically, if the oxidation is to an azadiene species, as the product was too unstable to identify. Through the total synthesis of unstable hydroxyindolenine intermediates, a mechanistic study of BvnE was carried out through a *bvnE*-KO strain of *P. brevicompactum*.

A greater understanding of the pinacol rearrangement to the oxindole and semi-pinacol rearrangement to the indoxyl was explored. Of which total synthesis, completed by the author, played a crucial role in this understanding. The total synthesis of newly discovered oxindole metabolites, brevianamide X and Y, were achieved, and their absolute configurations elucidated. Optically active brevianamide Y was accessed through a pinacol rearrangement prior to the construction of the bicyclic ring. Brevianamide X was only able to be accessed from a hydroxyindolenine precursor and resulted in a mixture of enantiomers. Computations studies, performed by the Paton group, confirmed why the order of steps was important to construct each cycloadduct.

The second total synthesis of brevianamide A, which was accessed through hydroxyindolenine intermediate **45**, was completed through a semi-pinacol rearrangement catalyzed by a Lewis acid. The *syn*-indoxyl enantiomer of brevianamide A was also studied, but the rearrangement could only be accessed with a bulky base. Each set of conditions will be further tested to synthesize brevianamide B.

The new understanding of semi-pinacol and pinacol rearrangement of indole derivatives will assist in future syntheses of other prenylated indole alkaloid metabolites. For example, recently isolated oxindole metabolites, such as notoamide T3 or citrinalin C, could be more readily accessed synthetically with a better understanding of the pinacol rearrangement in this class of molecules. Also, as the spirocyclic scaffold has been experiencing increased utilization in drug development, this study could assist in efforts to access target spiro-compounds more readily.<sup>128</sup>

### I. Penicimutamide A-C: Isolation and Biosynthetic proposal<sup>17</sup>

Recent efforts to isolate new fungal metabolites have moved towards identifying methods that can activate previously silent biosynthetic pathways in the species. Environmental factors have the potential to trigger the previously silent pathways with strategies such as one-strain-many-compounds (OSMAC),<sup>75</sup> chemical epigenetics<sup>76</sup>, and co-cultivation<sup>77</sup>. Silent pathways in bacteria have had successful activation with ribosomal engineering<sup>78,79</sup> by selecting drug-resistant mutants with activated pathways under standard culture conditions.<sup>80,81</sup> The use of ribosomal engineering has been employed in recent years on fungi with pronounced success.<sup>82-86</sup> One recent pathway that has been developed out of this renaissance of mutagenesis was the use diethyl sulfate (DES) to activate silent fungal pathways.<sup>87-91</sup> Using DES to create a mutant of the *Penicillium purpurogenum* G59 strain, AD-2-1, three new alkaloids, penicimutamides A-C, were isolated (Figure 4.1).

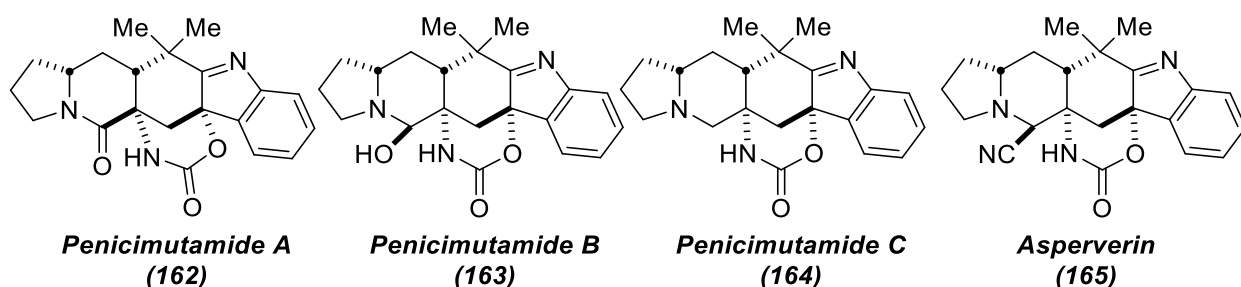


**Figure 4.1: Carbamate metabolites.** Penicimutamides A-C were newly isolated from *P. purpurogenum*. The structure of aspeverin was reevaluated and confirmed to match that of the penicimutamides.<sup>74</sup>

While prenylated indole alkaloids have been studied for over 50 years, only one other carbamate-containing alkaloid product, aspeverin, had previously been isolated.

<sup>17</sup> The work discussed can be found in reference 74.

Penicimutamides A-C all contain the non-prevalent carbamate ring system like aspeverin, an intriguing finding as they come from different fungal genus, *Penicillium* and *Aspergillus*.<sup>92</sup> From the study of the newly isolated penicimutamides, the absolute stereochemistry of aspeverin was reassigned to have a more similar stereochemistry to the newly isolated compounds. After full characterization of the penicimutamides, the parent, non-mutated strain of *P. purpurogenum* was screened for their presence. The results revealed that penicimutamides A-C were only found in the mutant strain.

A biosynthetic proposal was developed to explain the relationship between the penicimutamides, which was proposed to begin with deoxybrevianamide E (*Figure 4.2*). Oxidation and tautomerization to azadiene species **166**, followed by a DA reaction could yield *anti*-cycloadduct **167**. Formation of an epoxide (**168**) by oxidizing the C-2 positions of the indole would then suffer epoxide opening to give hydroxyindolenine **169**. Free amine **170** could be accessed by loss of CO<sub>2</sub> and addition of water. Carbonic acid could then be introduced and form the carbamate of penicimutamide A. Reduction of the amide to the alcohol would afford penicimutamide B, and further reduction would provide penicimutamide C. The selectivity of these reactions likely would necessitate some catalysts throughout the pathway.

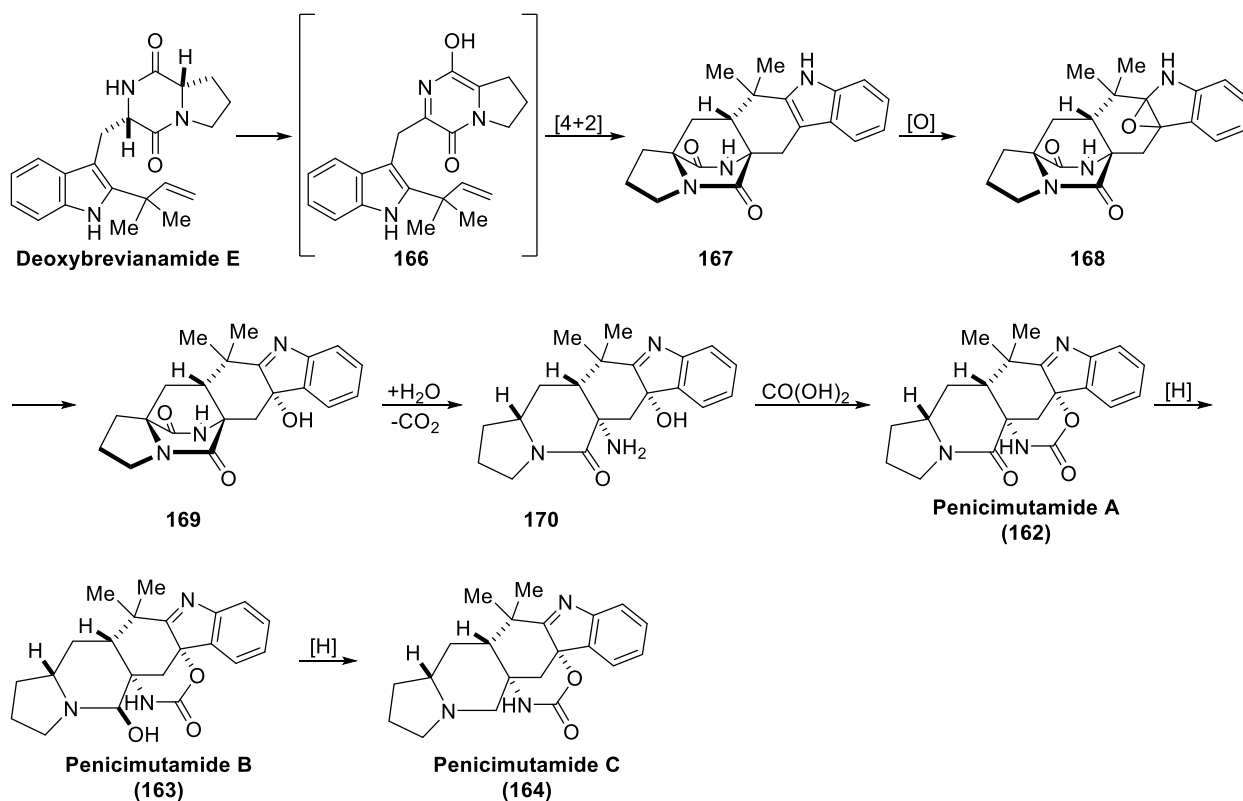


Figure 4.2: Biosynthetic proposal for penicimutamides A-C.

## II. Total Synthesis of the Enantiomers of Aspeverin and Penicimutamide A<sup>18</sup>

Emphasizing diastereoselectivity in the DA cycloaddition, the total synthesis of the enantiomers of aspeverin and penicimutamide A was carried out. Starting with pyrrolidinone **170**, reduction with DIBAL left a hemiaminal, which was allylated with allyltrimethylsilane (**171**) to produce a mixture of products (*Figure 4.3*). Carrying forward **172**, Boc deprotection was achieved with acid, and acylation with acryloyl chloride afforded amide **173**. Grubs' olefin metathesis with **174** was utilized to form the 6-membered ring of the indolizidine **175**. Iodination of the double bond, following Johnson and co-worker's procedure<sup>95</sup>, succeeded by Pd-catalyzed carbonylation produced compound **176**. The DA cycloaddition occurred between silyloxydiene

<sup>18</sup> The work discussed can be found in references 93 and 94.

**177** and **176** by a Lewis acid, ZnCl<sub>2</sub>, catalyzed reaction, giving a single diastereomer as the product (**178**). While the C:D:E ring system had been established, it is important to note the stereochemistry of the two hydrogens on **178** that should be *syn* to produce the natural products were *anti* at that time.

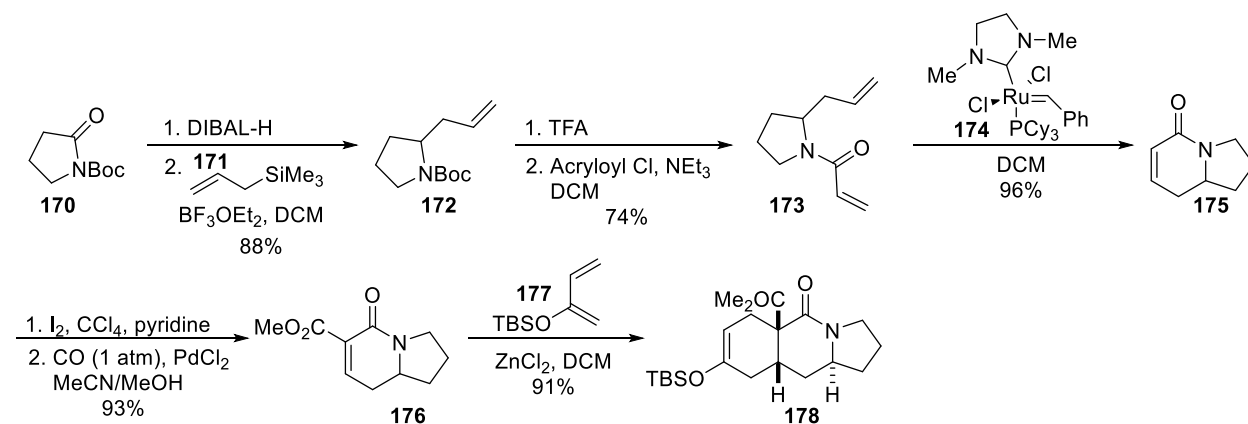


**Figure 4.3: Synthesis of the C:D:E ring system of the carbamate natural products.**

Regioselective installation of the indole ring system was possible by using a reagent developed by Rawal and co-workers, *o*-(nitrophenyl)phenyliodonium fluoride (**179**, NPIF), to overcome Fischer indole regioselectivity (*Figure 4.4*).<sup>96</sup> The reaction gave **180** as a single regioisomer with a diastereomeric mixture of 2:2:1 of inconsequential diastereomers. The nitroaryl ketone (**180**) underwent a reductive cyclization by two separate sets of conditions: treatment with SnCl<sub>2</sub> (54% yield) or reduction by H<sub>2</sub> and Pd/C in presence of Pd(PPh<sub>3</sub>)<sub>4</sub>.<sup>97,98</sup> With the 5 rings establish, attention moved towards epimerizing the hydrogen at the C-4 position, such that the stereochemistry of the two hydrogens could be *syn*, which was achieved through installation of a benzylic ketone.

Indole derivative **181** was able to undergo an  $\alpha$ -acetoxylation when treated with lead (IV) acetate in acetic acid.<sup>99</sup> The crude acetate (**182**) was subjected to transesterification to provide alcohol **183**. When exposed to MnO<sub>2</sub>, alcohol **183** was oxidized to ketone **184**. While a variety of

conditions for epimerizing the  $\alpha$ -stereocenter were tested, it was found that enolization with KHMDS at low temperatures and quenching at  $-70^\circ\text{C}$  with  $\text{NH}_4\text{Cl}$  afforded **185** with the desired stereochemistry at a 9.5:1 ratio while maintaining an 80% isolated yield.

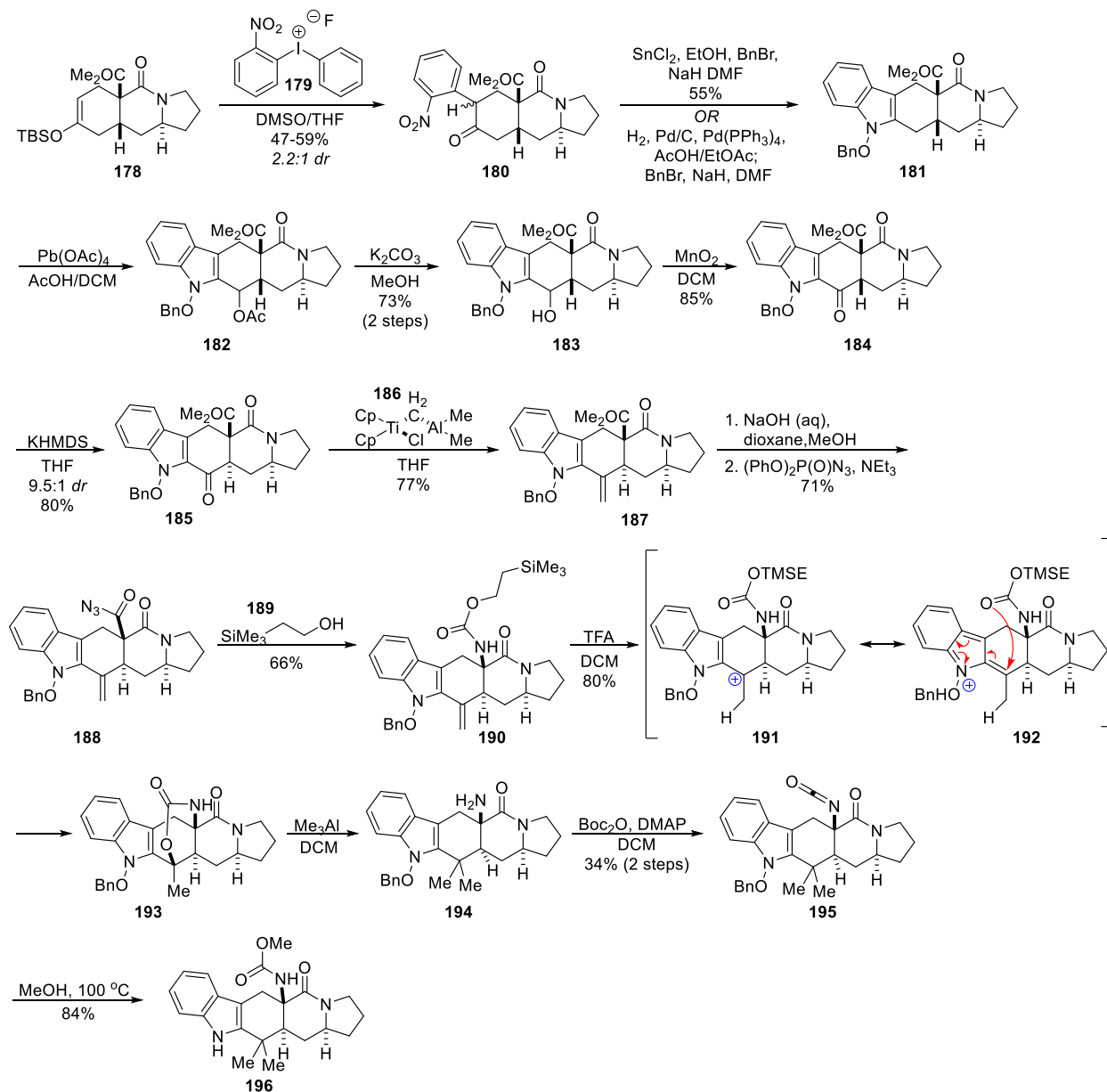


**Figure 4.4: Construction of A-E rings of the carbamate natural products while setting the subsequent stereocenters.**

With the stereochemistry now set in the A-E rings, attention was moved towards the formation of the carbamate and conversion of the ketone to a geminal dimethyl group. The

ketone was converted to a terminal olefin (**187**) with the use of Tebbe reagent (**186**).<sup>100</sup> Ester hydrolysis resulted in the free carboxylic acid that was immediately advanced through a Curtius rearrangement to **190**. The rearrangement occurred as follows: formation of the azide (**188**) with diphenylphosphoryl azide (DPPA) succeeded by thermolysis in the presence of 2-trimethylsilylethanol (**189**). When compound **190** was exposed to TFA protonation occurred at the exocyclic olefin, creating a carbocation (**191/192**), which the carbamate attacked to yield cyclic product **193**.<sup>101</sup> Having a single methyl group already installed, a Lewis acid, Me<sub>3</sub>Al, was utilized to render the carbamate a good leaving group and establish the second methyl of the geminal dimethyl group (**194**). Interestingly, when free amine **194** was treated with di-*tert*-butyl decarbonate (Boc<sub>2</sub>O) an isocyanate (**195**) was formed instead of the theorized *tert*-butyloxycarbamate. After heating **195** in MeOH, the isocyanate converted to methyl carbamate **196**. Having set the functionalized scaffold of the carbamate natural products, two related routes were taken to synthesize aspeverin and penicimutamide A (Figure 4.5).

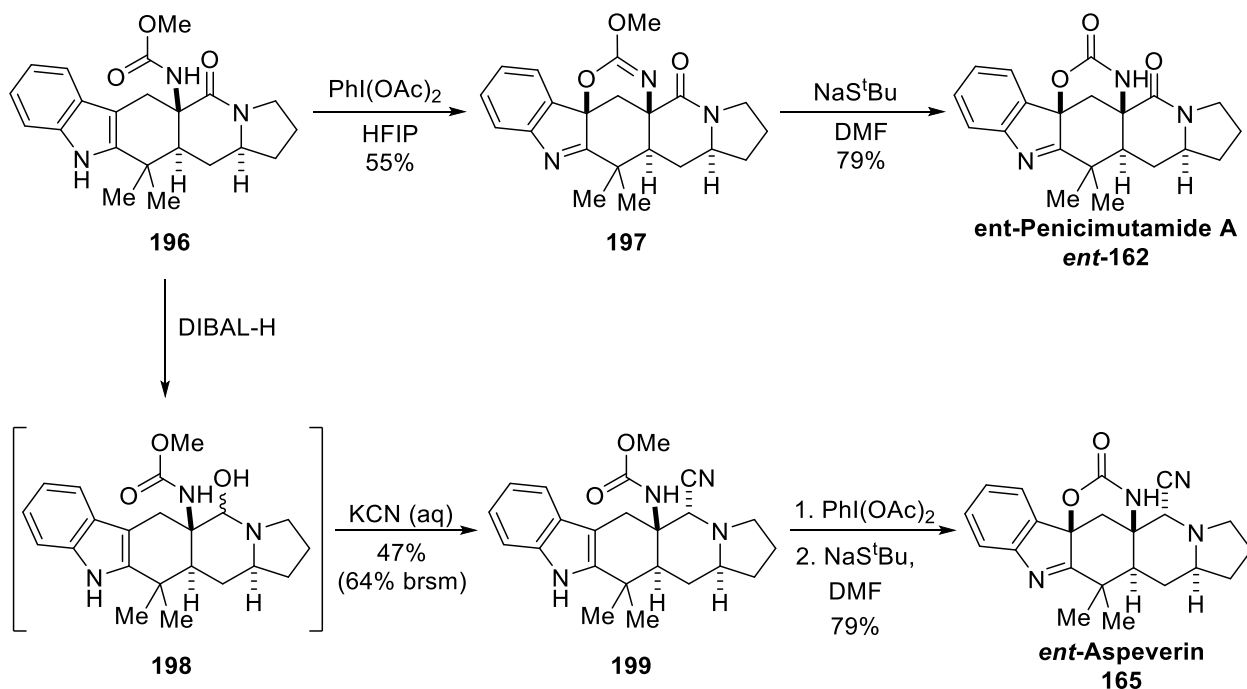


Figure 4.5: Late stage transformation to synthesize the enantiomers of Penicimutamide A (**162**) and Aspeverin (**165**).

The only structural component missing from compound **196** was the cyclic carbamate. To cyclize selectively, oxidation of the indole double bond was performed with  $\text{PhI}(\text{OAc})_2$  in hexafluoroisopropanol (HFIP) to create a hydroxyindolenine that immediately reacted with the methoxy-carbamate to form **197**.<sup>102,103</sup> The methylimidate of **197** was dealkylated with sodium 2-methyl-2-propanethiolate yielding the enantiomer of penicimutamide A.

Before the carbamate cyclization steps could be carried out to finish the synthesis of aspeverin, the cyano-group needed to be installed. This was achieved by DIBAL-H reduction of the amide to the free alcohol **198** and subsequent workup with potassium cyanide. After the carbamate was in place, the cyclization steps used for establishing the cyclic carbamate on penicimutamide A were applied to give the enantiomer of aspeverin.

### III. Isolation of Penicimutamides D-E<sup>19</sup>

Previously, penicimutamides A-C were isolated from a mutant strain of *Penicillium purpurogenum* G59. This was accomplished through the activation of formerly silent pathways in the organism with DES.<sup>74</sup> New penicimutamides D and E were isolated from the same strain. Unlike penicimutamides A-C, the new compounds were not carbamates, but instead monooxopiperazines (*Figure 4.6*). It is interesting to note that decarbonylated substrates were isolated from an organism that also yielded monooxopiperazines, as decarbonylated substrates (e.g. the penicimutamides and citrinalins) based on genetic implications had previously been assigned to the monooxopiperazine class of compounds. With the isolation of both monooxopiperazines and decarbonyled substrates from *P. purpurogenum*, more evidence is

---

<sup>19</sup> The work discussed can be found in reference 104.

provided to confirm that the decarboxylated substrates must be a part of the monoxopiperazine family of prenylated indole alkaloids.

Most fungi that produce prenylated indole alkaloids either contain *syn*- or *anti*-cycloadducts. In the case of the *P. purpurogenum* mutant, mostly *anti*-cycloadducts, but at least one *syn*-, have been isolated.<sup>1</sup> Both diastereomers of premalbrancheamide were identified in the fungi, with the new diastereomer being penicimutamide E.<sup>25,105</sup> Interestingly, premalbrancheamide was found as a racemic mixture in *P. purpurogenum*.<sup>106</sup>

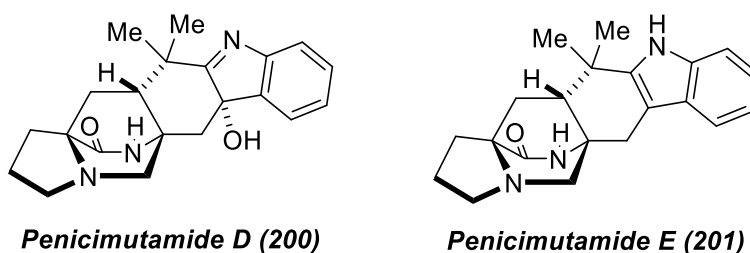


*Figure 4.6: Structures of new isolates from mutant P. purpurogenum.*

In recent years, a variety of hydroxyindolenine natural products have been isolated (e.g taichunamide A, taichunamide H, **45**, and **216**). Oftentimes, the hydroxyindolenine is an intermediate in the biosynthetic pathway to a more advanced natural product. For example, hydroxyindolenine **46** has been found to be an intermediate to brevianamide A in a mutant of *Penicillium brevicompactum*.<sup>107</sup> Also, synthetically the hydroxyindolenine has been used to establish indoxyls, oxindoles, and even carbamate rings at both advance and early stages in the synthetic plan.<sup>107,51,62</sup> As such, isolating penicimutamide D was an intriguing find, and has tremendous implications on the biosynthetic pathway of the penicimutamides.

#### IV. Conclusions

Through the application of activating previously silent biosynthetic pathways, a new class of prenylated indole alkaloid metabolites were identified. The penicimutamides contain the rare carbamate functionality and possess both *syn*- and *anti*-metabolites. While little is known about the penicimutamide metabolites, the biological applications of the only other carbamate-containing alkaloid metabolite strengthen the plausibility of the metabolites being biologically relevant. The total synthesis of the enantiomers of both penicimutamide A and aspeverin has been completed, but little is still known about the biochemical mechanisms that the producing fungi, *P. purogenum*, utilizes for the construction of the carbamate ring system. If the compounds prove to be biologically relevant, identifying the enzyme(s) responsible for the construction of the carbamate ring could allow for further derivatization of the penicimutamide metabolites to optimize possible biological responses.

## I. Introduction

The penicimutamides are a class of prenylated indole alkaloids that were recently isolated from a mutant strain of *P. purpurogenum*. The interest in the penicimutamides stems from the opened bicyclic core and the bridged carbamate, something that had previously only been seen in aspeverin. Aspeverin has displayed anticancer<sup>14,129-138</sup>, antibacterial<sup>139-142</sup>, anti-atherosclerotic<sup>143</sup>, and monoamine oxidase (MAO) inhibitor<sup>144</sup> properties to name a few. While biological testing of penicimutamides A-E has been minimal, the immense variety and success in the application of aspeverin gives possible precedent to applications of the carbamate-containing penicimutamides. Through the total synthesis of the penicimutamides being investigated by the author the goal is to determine the biosynthetic pathway to the metabolites and to access sufficient quantities of the metabolites to perform a thorough screening of their biological activities.

## II. Total synthesis of penicimutamide E and synthetic studies towards the synthesis of penicimutamide D

The approach to the synthesis of penicimutamide E began with *anti*-cycloadduct **34**. A protocol to selectively reduce the tertiary amide established in the total synthesis of VM55599<sup>145</sup> was followed to yield penicimutamide E. Diisobutylaluminum hydride (DIBAL-H) reduction of the tertiary amide to the free amine was accomplished with a 91% yield of (±) penicimutamide E (*Figure 5.1*). All data for the synthetic compound matched isolation data for penicimutamide E from *P. purpurogenum*.



**Figure 5.1: Synthesis of penicimutamide E and attempts towards penicimutamide D.** All compounds are racemic mixtures.

With penicimutamide E in hand, attempts to synthesize penicimutamide D were examined. Initial efforts to form the hydroxyindolenine by using the same conditions previously employed did not work (*see chapter 3 section III*). After further analysis, it appeared that the tertiary amine may be able to react with Davis oxaziridine more readily than the indole moiety; therefore, a method to yield the amine unreactive needed to be employed. In the total synthesis of marcfortine C, pyridinium toluene sulfonate (PPTS) was used to protonate the tertiary amine and render it unreactive.<sup>146</sup> When PPTS was applied to penicimutamide E followed by Davis oxaziridine, no desired product was isolated. It is possible that the PPTS group did not fully protonate the tertiary amine, was not removed by column chromatography like expected, or was deprotected prematurely. Further investigation to synthesize penicimutamide D is currently being carried out, with a focus on optimizing the protonation conditions.

### III. Towards the Total Synthesis of Penicimutamide A-C and Aspeverin

Previous members of the Williams group, Dr. Kimberly Klas and Dr. Kazutada Ikeuchi, investigated the opening of the bicycle of cycloadducts **126** and **34**.<sup>146</sup> The goal was to carry out a full model study for the synthesis of citrinalins A and B with a mixture of *anti*- and *syn*-cycloadduct **34** and **126**. The bridged amide was transformed to lactim ether **256** with  $\text{BF}_4\text{OEt}_3$  (*Figure 5.2*). Upon treatment with acid, the bicycle would continuously open and close, but to

assure the bicycle remained open, the resulting amine was protected by an acetyl group. Decarboxylation of **258** started by conversion to the carboxylic acid and a Curtius-type rearrangement with diphenylphosphoryl azide (DPPA). The resultant compound (**260**) was hydrogenated with  $\text{NaBH}_3\text{CN}$  to give a mixture of products (**261** and **262**). While the model study was not completed for the citrinalins, Dr. Klas and Dr. Ikeuchi were able to effectively open the bicycle in a manner that could mimic how the bicycle is opened in *P. purpurogenum*.

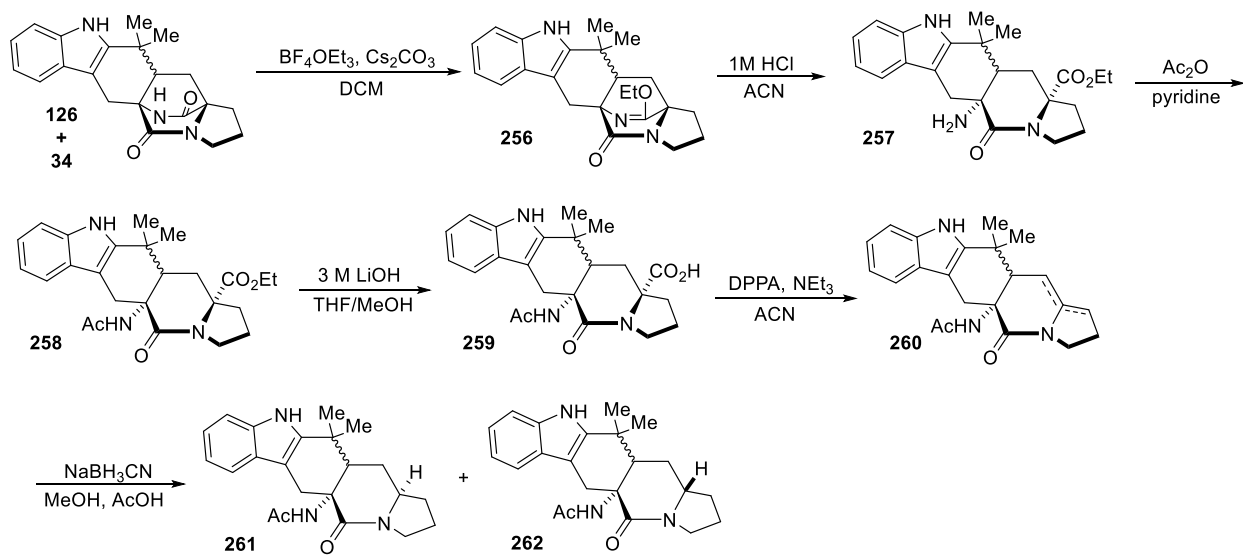


**Figure 5.2: Synthetic scheme for the opening of the bicyclic core.** Work was performed by Dr. Klas and Ikeuchi. Both syn and anti-cycloadducts (**126** and **34**) were brought forward; the ratio of syn-to-anti- was 2.1:1.

Applying the same conditions to open the bicycle, the total synthesis of penicimutamides A-C and aspeverin has commenced (*Figure 5.3*). Starting with *anti*-cycloadduct **34**, lactim ether **263** has been synthesized. Initial attempts to open the bicycle with 2 M HCl have proven to not be successful; instead of opening the bicycle the lactim ether is deprotected and *anti*-cycloadduct **34** is reformed. Optimization of acidic conditions appears to be a crucial point in effectively opening the bicycle without removing the lactam ether. This could be accomplished through either shorter reaction times or the use of a weaker acid.

Once the bicycle opening has been optimized, carbamate formation (**265**), instead of acetylation (**258**) could occur. This would be accomplished by using methyl chloroformate and an adequate base, like 1 M NaOH, NaHCO<sub>3</sub>, or diisopropylethylamine (DIEA).<sup>147-149</sup> The bridged carbamate moiety of penicimutamides A-C could be established by oxidizing the indole with Davis oxaziridine (**131**), which would suffer a subsequent attack from the carbamate, creating methylimidate **266**. Dealkylation with sodium 2-methyl-2-propanethiolate would give bridge carbamate **267**.<sup>93,94</sup> Decarboxylation of the ethyl ester could be accomplished by applying the same conditions mentioned above in the citrinalin model study (*Figure 5.2*); hydrolysis of the ester, decarbonylation, and Curtius-type rearrangement to provide penicimutamide A.<sup>93,94</sup>

In this synthetic plan penicimutamide A would act as the gateway compound by which penicimutamides B and C, as well as aspeverin, could be accessed.<sup>93,94</sup> By treating penicimutamide A with DIBAL-H the amide would be reduced to the alcohol, likely in a stereoselective manner due to the bridged carbamate, yielding penicimutamide B. The alcohol could be exposed to KCN and form aspeverin. Lastly, penicimutamide C could be accessed through further reduction of the free alcohol using tosyl-chloride (TsCl).

There are possible areas in this proposed synthetic plan that could prove to not react in the expected manner. For example, the initial reaction of chloroformate with free amine **264** may not be quick enough to trap the opened bicycle, and in turn leave **34** as the major product. If this were to be a problem, acetylation should occur first. Once decarboxylation was complete the acetyl group could be deprotected and the carbamate formed. It is also possible that treatment of penicimutamide A with DIBAL-H will fully reduce the amide to the free amine (penicimutamide C). If this is the case either different reduction conditions would need to be tested or a

rearrangement of reaction order should occur, such that the synthesis mirrors that of Levinson's total synthesis of the enantiomer of aspeverin.<sup>93</sup>

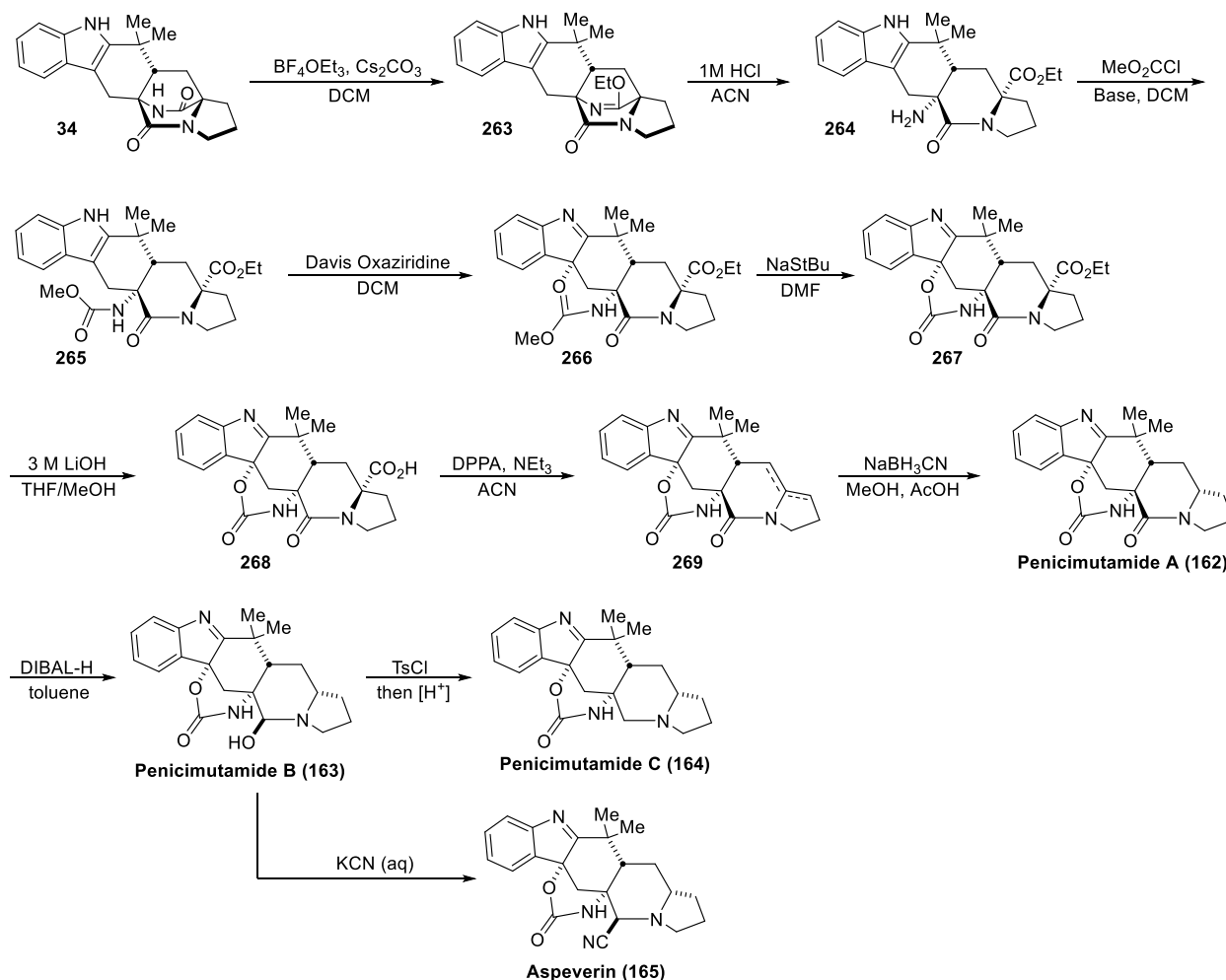


**Figure 5.3: Biomimetic Synthetic Proposal towards Pencimutamides A-C and Aspeverin.** The synthesis is based upon *Figure 5.2*. The products would all be racemic mixtures.

#### IV. Conclusions and Future direction

The biochemical mechanism for the decarbonylation of the bicyclo[2.2.2]diazaoctane core in *Penicillium purpurogenum* is not understood; therefore, by completing the synthesis of penicimutamide A, one would have access to possible biological intermediates to test by either feeding studies or screening for their presence. The total synthesis of penicimutamides A-C has

been commenced (by the author) but focus on opening the bicycle has been the current issue. By further studying the decarbonylation synthetically, and possibly analyzing the mechanism computationally, information on the intrinsic reactivity and facial bias of the decarbonylation could be obtained.

## References

1. Finefield, J.; Frisvad, J.C.; Sherman, D.H.; Williams, R.M. Fungal Origins of the bicyclo[2.2.2]diazaoctane Ring System of Prenylated Indole Alkaloids. *J. Nat. Prod.* **2012**, *75*, 812-833.
2. Finefield, J.; Sherman, D.H.; Kreitman, M.; Williams, R.M. Enantiomeric Natural Products: Occurrence and Biogenesis *Angew. Chem. Int. Ed.* **2012**, *51*, 4802-4836.
3. Klas, K.; Kato, H.; Frisvad, J.C.; Yu, F.; Newmister, S.; Fraley, A.; Sherman, D.H.; Williams, R.M.; Tsukamoto, S. Structural and stereochemical diversity in prenylated indole alkaloids containing the bicyclo[2.2.2]diazaoctane ring system from marine and terrestrial fungi. *Nat. Prod. Rep.* **2018**, *35*, 532-558.
4. Li, S.; Srinivasan, K.; Tran, H.; Yu, F.; Finefield, J.M.; Sunderhaus, J.D.; McAfoos, T.J.; Tsukamoto, S.; Williams, R.M.; Sherman, D.H. Comparative analysis of the biosynthetic systems for fungal bicyclo[2.2.2]diazaoctane indole alkaloids: the (+)/(-)-notoamide, paraherquamide and malbrancheamide pathways. *Med. Chem. Comm.* **2012**, *3*, 987-996.
5. Mercado-Marin, E. V.; Garcia-Reynaga, P.; Romminger, S.; Pimenta, E. F.; Romney, D. K.; Lodewyk, M. W.; Williams, D. E.; Anderson, R. J.; Miller, S. J.; Tantillo, D. J.; Berlinck, R. G. S.; Sarpong, R. Total synthesis and isolation of citrinalin and cyclopiamine congeners. *Nature* **2014**, *509*, 318-324.
6. Epe, C.; Kaminsky, R. New advancement in anthelmintic drugs in veterinary medicine. *Trends Parasitol.* **2013**, *29*, 129-134.
7. Polonsky, J.; Merrien, M-A.; Prange, T.; Pascard, C. Isolation and structure (X-ray analysis) of marcfortine A, a new alkaloid from *Penicillium roqueforti*. *J. Chem. Soc. Chem. Comm.* **1980**, 601-602.
8. Prange, T.; Billion, M-A.; Vuilhorgne, M.; Pascard, C.; Polonsky, J.; Moreau, S. Structures of marcfortine B and C (X-ray analysis), alkaloids from *Penicillium roqueforti*. *Tetrahedron Lett.* **1981**, *22*, 1977-1980.
9. Hayashi, H.; Nishimoto, Y.; Nozaki, H. Asperparaline A, a new paralytic alkaloid from *Aspergillus japonicus* JV-23. *Tetrahedron Lett.* **1997**, *38*, 5655-5658.

10. Banks, R.M.; Blanchflower, S.E.; Everett, J.R.; Manger, B.R.; Reading, C. Novel anthelmintic metabolites from an *Aspergillus* species; the aspergillimides. *J. Antibiot.* **1997**, *50*, 840-84
11. Paterson, R. R. M.; Simmonds, M. S. J.; Blaney, W. M. Mycopesticidal effects of characterized extracts of *Penicillium* isolates and purified secondary metabolites (including mycotoxins) on *Drosophila melanogaster* and *Spodoptera littoralis*. *I. Invertebr. Pathol.* **1987**, *50*, 124-133.
12. Paterson, R. R. M.; Simmonds, M. S. J.; Kimmelmeier, C.; Blaney, W. M. Effects of brevianamide A, its photolysis product brevianamide D, and ochratoxin A from two *Penicillium* strains on the insect pests *Spodoptera frugiperda* and *Heliothis virescens*. *Mycol. Res.* **1990**, *94*, 538-542.
13. Wang, X.; You, J.; King, J. B.; Powell, D. R.; Cichewicz, R. H. Waikialoid A Suppresses Hyphal Morphogenesis and Inhibits Biofilm Development in Pathogenic *Candida albicans*. *J. Nat. Prod.* **2012**, *75*, 707-715.
14. Luo, W. *Application of aspeverin in preparation of anticancer drugs against nasopharyngeal cancer*. China Patent 103,340,876 (A), Oct. 09, **2013**.
15. Fenical, W.; Jensen, P.R.; Cheng, X.C. *Avrainvillamide, a Cytotoxic Marine Natural Product and Derivatives Thereof*. U.S. Patent 6,066,635 (**2000**).
16. Sugie, Y.; Hirai, H.; Inagaki, T.; Ishiguro, M.; Kim, Y-J.; Kojima, Y.; Sakakibara, T.; Sakemi, S.; Sugiura, A.; Suzuki, Y.; Brennan, L.; Duignan, J.; Huang, L.H.; Sutcliffe, J.; Kojima, N. A new antibiotic CJ-17, 665 from *Aspergillus ochraceus*. *J. Antibiot.* **2001**, *54*, 911-916.
17. Kai, A.; Kato, H.; Sherman, D.H.; Williams, R.M.; Tsukamoto, S. Isolation of a new indoxyl alkaloid, Amoenamide B, from *Aspergillus amoenus* NRRL 35600: biosynthetic implications and correction of the structure of Speramide B *Tetrahedron Lett.* **2018**, *59*, 4236-4240.
18. Chang, Y-W.; Yuan, C-M.; Zhang, J.; Liu, S.; Cao, P.; Hua, H-M.; Di, Y-T.; Hao, X-J. Speramides A–B, two new prenylated indole alkaloids from the freshwater-derived fungus *Aspergillus ochraceus* KM007 *Tetrahedron Lett.* **2016**, *57*, 4952-4955.
19. Lin, Z.; Wen, J.; Zhu, T.; Fang, Y.; Gu, Q.; Zhu, W. Chrysogenamide A from an endophytic fungus associated with *Cistanche deserticola* and its neuroprotective effect on SH-SY5Y cells. *J. Antibiot.* **2008**, *61*, 81-85.
20. Wulff, J.E.; Herzon, S.B.; Siegrist, R.; Myers, A.G., Evidence for the rapid conversion of stephacidin B into the electrophilic monomer avrainvillamide in cell culture. *J. Am. Chem. Soc.* **2007**, *129*, 4898-4899.

21. Wulff, J.E.; Siegrist, R.; Myers, A.G. The natural product avrainvillamide binds to the oncoprotein nucleophosmin. *J. Am. Chem. Soc.* **2007**, *129*, 14444-14451.
22. Kato, H.; Kai, A.; Kawabata, T.; Sunderhaus, J.D.; McAfoos, T.J.; Finefield, J.M.; Sugimoto, Y.; Williams, R.M.; Tsukamoto, S. Enantioselective inhibitory abilities of enantiomers of notoamides against RANKL-induced formation of multinuclear osteoclasts. *Bioorg. Med. Chem. Lett.* **2017**, *27*, 4975-4978.
23. Martinez-Luis, S.; Rodriguez, R.; Acevedo, L.; Gonzalez, M. C.; Lira-Rocha, A.; Mata, R. Malbrancheamide, a new calmodulin inhibitor from the fungus *Malbranchea aurantiaca*. *Tetrahedron*, **2006**, *62*, 1817-1822.
24. Miller, K.A.; Williams, R.M. Synthetic approaches to the bicyclo [2.2. 2] diazaoctane ring system common to the paraherquamides, stephacidins and related prenylated indole alkaloids. *Chem. Soc. Rev.* 2009, *38*, 3160-3174.
25. Dan, Q.; Newmister, S. A.; Klas, K. R.; Fraley, A. E.; McAfoos, T. J.; Somoza, A. D.; Sunderhaus, J. D.; Ye, Y.; Shende, V. V.; Yu, F.; Sanders, J. N.; Brown, W. C.; Zhao, L.; Paton, R. S.; Houk, K. N.; Smith, J. L.; Sherman, D. H.; Williams, R. M. Fungal indole alkaloid biogenesis through evolution of a bifunctional reductase/Diels–Alderase. *Nat. Chem.* **2019**, *11*, 972-980.
26. Greshock, T. J.; Grubbs, A. W.; Jiao, P.; Wicklow, D. T.; Gloer, J. B.; Williams, R. M. Isolation, Structure Elucidation, and Biomimetic Total Synthesis of Versicolamide B, and the Isolation of Antipodal (–)-Stephacidin A and (+)-Notoamide B from *Aspergillus versicolor* NRRL 35600. *Angew. Chem., Int. Ed.* **2008**, *47*, 3573–3577.
27. Qian-Cutrone, J.; Huang, S.; Shu, Y.-Z.; Vyas, D.; Fairchild, C.; Menendez, A.; Krampitz, K.; Dalterio, R.; Klohr, S. E.; Gao, Q. Stephacidin A and B: two structurally novel, selective inhibitors of the testosterone-dependent prostate LNCaP cells. *J. Am. Chem. Soc.*, **2002**, *124*, 14556–14557.
28. Chen, M.; Shao, C-L.; Fu, X-M.; Xu, R-F.; Zheng, J-J.; Zhao, D-L.; Shi, Z-G.; Wang, C-Y. Bioactive Indole Alkaloids and Phenyl Ether Derivatives from a Marine-Derived *Aspergillus* sp. Fungus. *J. Nat. Prod.* **2013**, *76*, 547-553.
29. Klas, K.; Tsukamoto, S.; Sherman, D. H.; Williams, R. M. Natural Diels–Alderases: elusive and irresistible. *J. Org. Chem.* **2015**, *80*, 11672-11685.

30. Williams, R. M. Natural products synthesis: enabling tools to penetrate nature's secrets of biogenesis and biomechanism. *J. Org. Chem.* **2011**, *76*, 4221-4259.
31. Sunderhaus, J. D.; Williams, R.M., Studies on the biosynthesis of the stephacidin and notoamide natural products: a stereochemical and genetic conundrum. *Israel J. Chem.* **2011**, *3-4*, 442-452.
32. Birch, A. J.; Wright, J. J. The brevianamides: a new class of fungal alkaloid. *J. Chem. Soc. Chem. Comm.* **1969**, 644-645.
33. Birch, A. J.; Wright, J. J. Studies in relation to biosynthesis—XLII: The structural elucidation and some aspects of the biosynthesis of the brevianamides-A and-E. *Tetrahedron* **1970**, *26*, 2329-2344.
34. Baldas, J.; Birch, A. J.; Russell, R. A. Studies in relation to biosynthesis. Part XLVI. Incorporation of cyclo-L-tryptophyl-L-proline into brevianamide A. *J. Chem. Soc. Perkin Trans I* **1974**, 50-52.
35. Birch, A. J.; Wright, J. J. Studies in relation to biosynthesis—XLIV: Structural elucidations of brevianamides-B,-C,-D and-F. *Tetrahedron* **1972**, *28*, 2999-3008.
36. Porter A. E. A.; Sammes P. G. A Diels–Alder reaction of possible biosynthetic importance. *J. Chem. Soc. D* **1970**, *17*, 1103a.
37. Williams, R. M.; Glinka, T.; Kwast, E. Facial selectivity of the intramolecular SN<sup>2</sup>'cyclization: stereocontrolled total synthesis of brevianamide B. *J. Am. Chem. Soc.* **1988**, *110* (17), 5927-5929.
38. Williams, R. M.; Kwast, E.; Coffman, H.; Glinka, T. Remarkable, enantio-divergent biogenesis of brevianamide A and B. *J. Am. Chem. Soc.* **1989**, *111* (8), 3064-3065.
39. Williams, R. M.; Glinka, T.; Kwast, E.; Coffman, H.; Stille, J. K. Asymmetric, stereocontrolled total synthesis of (-)-brevianamide B. *J. Am. Chem. Soc.* **1990**, *112*, 808-821.
40. Seebach, D.; Boes, M.; Naef, R.; Schweizer, W. F. Alkylation of amino acids without loss of the optical activity: preparation of. alpha.-substituted proline derivatives. A case of self-reproduction of chirality. *J. Am. Chem. Soc.* **1983**, *105*, 5390.
41. Sanz-Cervera, J. F.; Glinka, T.; Williams, R. M. Biosynthesis of brevianamides A and B: in search of the biosynthetic Diels-Alder construction. *Tetrahedron* **1993**, *49*, 8471-8482.
42. Sanz-Cervera, J. F.; Glinka, T.; Williams, R. M. Biosynthesis of the brevianamides: quest for a biosynthetic Diels-Alder cyclization. *J. Am. Chem. Soc.* **1993**, *115*, 347-348.

43. Kametani, T.; Kanaya, N.; Ihara, M. Studies on the syntheses of heterocyclic compounds. Part 876. The chiral total synthesis of brevianamide E and deoxybrevianamide E. *J. Chem. Soc., Perkin Trans. I* **1981**, *1*, 959.
44. Kametani, T.; Kanaya, N.; Ihara, M. Asymmetric total synthesis of brevianamide E. *J. Am. Chem. Soc.* **1980**, *102*, 3974.
45. For a review, see: Grandberg, I. I.; Sorokin, V. I. The mode of cyclisation of the arylhydrazones and o-phenyl ethers of the oximes of asymmetric ketones under the conditions of the Fischer reaction. *Russ. Chem. Rev.* **1974**, *43*, 115.
46. Gibson, T. W.; Erman, W. F. Photochemistry of substituted 1, 5-hexadien-3-ones. *J. Org. Chem.*, **1972**, *37*, 1148–1154.
47. Williams, R. M.; Sanz-Cervera, J. F.; Sancenón, F.; Marco, A.; Halligan, K. Biomimetic Diels–Alder cyclizations for the construction of the brevianamide, paraherquamide sclerotamide, and VM55599 ring systems. *J. Am. Chem. Soc.* **1998**, *120*, 1090-1091.
48. Halligan, K. M. Synthetic and Biosynthetic Studies of the Brevianamides. PH.D thesis, Colorado State University, 2000.
49. Adams, L. A.; Valente, M. W. N.; Williams, R. M. A concise synthesis of d, l-brevianamide B via a biomimetically-inspired IMDA construction. *Tetrahedron* **2006**, *62*, 5195-5200.
50. Dauben, W. G.; Cogen, J. M.; Ganzer, G. A.; Behar, V. Photochemistry of 1, 5-hexadien-3-ones: wavelength-dependent selectivity in intramolecular enone-olefin photoadditions. *J. Am. Chem. Soc.* **1991**, *113*, 5817–5824.
51. Greshock, T. J.; Williams, R. M. Improved Biomimetic Total Synthesis of d,l-Stephacidin A. *Org. Lett.* **2007**, *9*, 4255-4258.
52. Stocking, E. M.; Sanz-Cervera, J. F.; Williams, R. M. Total Synthesis of VM55599. Utilization of an Intramolecular Diels–Alder Cycloaddition of Potential Biogenetic Relevance. *J. Am. Chem. Soc.* **2000**, *122*, 1675-1683.
53. Sans-Cervera, J. F.; Williams, R. M. Asymmetric total synthesis of (–)-VM55599: establishment of the absolute stereochemistry and biogenetic implications. *J. Am. Chem. Soc.* **2002**, *124*, 2556.
54. Frebault, F. C.; Simpkins, N. S. A cationic cyclisation route to prenylated indole alkaloids: synthesis of malbrancheamide B and brevianamide B, and progress towards stephacidin A. *Tetrahedron* **2010**, *66*, 6585-6596.

55. Fuchs, J. R.; Mitchell, M. L.; Shabangi, M.; Flowers, R. A., II. The effect of lithium bromide and lithium chloride on the reactivity of SmI<sub>2</sub> in THF. *Tetrahedron Lett.* **1997**, *38*, 8157.
56. Robins, J. G.; Kim, K. J.; Chinn, A. J.; Woo, J. S.; Scheerer, J. R. Intermolecular Diels–Alder Cycloaddition for the Construction of Bicyclo [2.2. 2] diazaoctane Structures: Formal Synthesis of Brevianamide B and Premalbrancheamide. *J. Org. Chem.* **2016**, *81*, 2293–2301.
57. Perkins, J. C.; Wang, X.; Pike, R. D.; Scheerer, J. D. Further investigation of the intermolecular Diels–Alder cycloaddition for the synthesis of bicyclo [2.2. 2] diazaoctane alkaloids. *J. Org. Chem.* **2017**, *82*, 13656–13662.
58. Laws, S. W.; Scheerer, J. R. Enantioselective synthesis of (+)-malbrancheamide B. *J. Org. Chem.* **2013**, *78*, 2422–2429.
59. Danishefsky, S.; Prisbylla, M. P.; Hiner, S. The use of trans-methyl. beta.-nitroacrylate in Diels–Alder reactions. *J. Am. Chem. Soc.* **1978**, *100*, 2918–2920.
60. Godfrey, R.; Green, N.; Nichol, G. S.; Lawrence, A. Total synthesis of brevianamide A. *Nat. Chem.* **2020**, *12*, 615–619.
61. Schkeryantz, J. M.; Woo, J. C. G.; Siliphaivanh, P.; Depew, K. M.; Danishefsky, S. J. Total synthesis of gypsetin, deoxybrevianamide E, brevianamide E, and tryprostatin B: Novel constructions of 2, 3-disubstituted indoles. *J. Am. Chem. Soc.* 1999, *121*, 11964– 11975.
62. Steyn, P. S. The structures of five diketopiperazines from *Aspergillus ustus*. *Tetrahedron* **1973**, *29*, 107–120.
63. Scott, P. M.; Kennedy, B. P. C.; Harwig, J.; Chen, Y-K. Formation of diketopiperazines by *Penicillium italicum* isolated from oranges. *Appl. Microbiol.* **1974**, *28*, 892–894.
64. Kaur, A.; Raja, H. A.; Deep, G.; Agarwal, R.; Oberlies, N. H. Pannorin B, a new naphthopyrone from an endophytic fungal isolate of *Penicillium* sp. *Magn. Reson. Chem.* **2016**, *54*, 164–167.
65. Domingo, L. R.; Sanz-Cervera, J. F.; Williams, R. M.; Picher, M. T.; Marco, J. A. Biosynthesis of the Brevianamides. An ab Initio Study of the Biosynthetic Intramolecular Diels–Alder Cycloaddition. *J. Org. Chem.* **1997**, *62*, 1662–1667.
66. Xu, X.; Zang, X.; Nong, X.; Wang, J.; Qi, S. Brevianamides and Mycophenolic Acid Derivatives from the Deep-Sea-Derived Fungus *Penicillium brevicompactum* DFFSCS025. *Mar. Drugs* **2017**, *15*, 43–52.

67. Cushing, T. D.; Sanz-Cervera, J. F.; Williams, R. M. Stereocontrolled total synthesis of (+)-paraherquamide B *J. Am. Chem. Soc.* **1996**, *118*, 557-579.
68. Miller, K. A.; Tsukamoto, S.; Williams, R. M. Asymmetric total syntheses of (+)- and (-)-versicolamide B and biosynthetic implications. *Nat. Chem.* **2009**, *1*, 63-68.
69. Williams, R. M.; Glinka, T.; Kwast, E. Synthetic studies on paraherquamide: Regioselectivity of indole oxidation. *Tetrahedron Lett.* **1989**, *30*, 5575-5578.
70. European patent 301742A, Merck and Co. **1987**.
71. Greshock, T. J.; Grubbs, A. W.; Tsukamoto, S.; Williams, R. W. A concise, biomimetic total synthesis of stephacidin A and notoamide B. *Angew. Chem. Int. Ed.* **2007**, *46*, 2262-2265.
72. Qin, W.; Xiao, T.; Zhang, D.; Deng, L.; Wang, Y.; Qin, Y. Total synthesis of (-)-depyranoversicolamide B. *Chem. Commun.* **2015**, *51*, 16143-16146.
73. Wang, Y.; Kong, C.; Du, Y.; Song, H.; Zhang, D.; Qin, Y. Silver-promoted Friedel-Crafts reaction: concise total synthesis of (-)-ardeemin, (-)-acetylardeemin and (-)-formylardeemin. *Org. Biomol. Chem.* **2012**, *10*, 2793-2797.
74. Li, C.; Wu, C.; Cui, C.; Xu, L.; Cao, F.; Zhu, H. Penicimutamides A-C: rare carbamate-containing alkaloids from a mutant of the marine-derived *Penicillium purpurogenum* G59. *RSC Adv.* **2016**, *6*, 73383-73387.
75. Bode, H. B.; Bethe, B.; Hofs, R.; Zeeck, A. Big effects from small changes: possible ways to explore nature's chemical diversity. *ChemBioChem*, **2002**, *3*, 619-627.
76. Williams, R. B.; Henrikson, J. C.; Hoover, A. R.; Lee, A. E.; Cichewicz, R. H. Epigenetic remodeling of the fungal secondary metabolome. *Org. Biomol. Chem.* **2008**, *6*, 1895-1897.
77. Marmann, A.; Aly, A. H.; Lin, W.; Wang, B.; Proksch, P. Co-Cultivation—A Powerful Emerging Tool for Enhancing the Chemical Diversity of Microorganisms. *Mar. Drugs* **2012**, *12*, 1043-1065.
78. Ochi, K.; Okamoto, S.; Tozawa, Y.; Inaoka, T.; Hosaka, T.; Xu, J.; Kurosawa, K. Ribosome engineering and secondary metabolite production. *Adv. Appl. Microbiol.* **2004**, *56*, 155-179.
79. Ochi, K. From microbial differentiation to ribosome engineering. *Biosci. Biotechnol. Biochem.* **2007**, *71*, 1373-1386.
80. Hosaka, T.; Ohnishi-Kameyama, M.; Muramatsu, H.; Murakami, K.; Tsurumi, Y.; Kodani, S.; Yoshida, M.; Fujie, A.; Ochi, K. Antibacterial discovery in actinomycetes strains with mutations in RNA polymerase or ribosomal protein S12. *Nat. Biotechnol.* **2009**, *27*, 462-464.

81. Fu, P.; Jamison, M.; La, S.; Macmillan, J. B. Inducamides A–C, Chlorinated Alkaloids from an RNA Polymerase Mutant Strain of *Streptomyces* sp. *Org. Lett.* **2014**, *16*, 5656-5659.
82. Chai, Y. J.; Cui, C. B.; Li, C. W.; Wu, C. J.; Tian, C. K.; Hua, W. Activation of the Dormant Secondary Metabolite Production by Introducing Gentamicin-Resistance in a Marine-Derived *Penicillium purpurogenum* G59. *Mar. Drugs* **2012**, *10*, 559-582.
83. Wu, C. J.; Yi, L.; Cui, C. B.; Li, C. W.; Wang, N.; Han, X. Activation of the Silent Secondary Metabolite Production by Introducing Neomycin-Resistance in a Marine-Derived *Penicillium purpurogenum* G59. *Mar. Drugs* **2015**, *13*, 2465-2487.
84. Dong, Y.; Cui, C. B.; Li, C. W.; Hua, W.; Wu, C. J.; Zhu, T. J.; Gu, Q. Q. Activation of Dormant Secondary Metabolite Production by Introducing Neomycin Resistance into the Deep-Sea Fungus, *Aspergillus versicolor* ZBY-3. *Mar. Drugs*, **2014**, *12*, 4326-4352.
85. Wang, N.; Cui, C. B.; Li, C. W. *Arch. Pharm. Sci. Res.* **2016**, 39762.
86. Yi, L.; Cui, C. B.; Li, C. W.; Peng, J. X.; Gu, Q. Q. Chromosulfine, a novel cyclopentachromone sulfide produced by a marine-derived fungus after introduction of neomycin resistance. *RSC Adv.* **2016**, *6*, 43975-43979.
87. Fang, S. M.; Wu, C. J.; Li, C. W.; Cui, C. B. A practical strategy to discover new antitumor compounds by activating silent metabolite production in fungi by diethyl sulphate mutagenesis. *Mar. Drugs* **2014**, *12*, 1788-1814.
88. Fang, S. M.; Cui, C. B.; Li, C. W.; Wu, C. J.; Zhang, Z. J.; Li, L.; Huang, X. J.; Ye, W. C. Purpurogemutant and Purpurogemutantidin, New Drimenyl Cyclohexenone Derivatives Produced by a Mutant Obtained by Diethyl Sulfate Mutagenesis of a Marine-Derived *Penicillium purpurogenum* G59 *Mar Drugs* **2012**, *10*, 1266-1287.
89. Xia, M. W.; Cui, C. B.; Li, C. W.; Wu, C. J.; Peng, J. X.; Li, D. H. Three new and eleven known unusual C25 steroids: activated production of silent metabolites in a marine-derived fungus by chemical mutagenesis strategy using diethyl sulphate. *Mar. Drugs* **2014**, *12*, 1545-1568.
90. Wu, C.-J.; Li, C.-W.; Cui, C. B. Seven New and Two Known Lipopeptides as well as Five Known Polyketides: The Activated Production of Silent Metabolites in a Marine-Derived Fungus by Chemical Mutagenesis Strategy Using Diethyl Sulphate. *Mar. Drugs* **2014**, *12*, 1815.

91. Xia, M. W.; Cui, C. B.; Li, C. W.; Wu, C. J.; Peng, J. X.; Li, D. H. Rare Chromones from a Fungal Mutant of the Marine-Derived *Penicillium purpurogenum* G59. *Mar. Drugs* **2015**, *13*, 5219.
92. Ji, N. J.; Liu, X. H.; Miao, F. P.; Qiao, M. F. Total synthesis of aspeverin via an iodine (III)-mediated oxidative cyclization. *Org. Lett.* **2013**, *15*, 2327.
93. Levinson, A. M. Total synthesis of aspeverin via an iodine (III)-mediated oxidative cyclization. *Org. Lett.* **2014**, *16*, 4904-4907.
94. Levinson, A. Part I: Total Synthesis Of Aspeverin And Penicimutamide A. Part II: Total Chemical Synthesis Of All-L And All-D Kras (G12V) And The Further Exploration Of Isonitrile Mediated Peptide Ligations. Ph. D. Dissertation, Cornell University, Ithaca, NY, 2017.
95. Johnson, C. R.; Adams, J. P.; Braun, M. P.; Senanayake, C. B. W.; Wovkulich, P. M.; Uskokovic, M. R. Direct  $\alpha$ -iodination of cycloalkenones. *Tetrahedron Lett.* **1992**, *33*, 917-918.
96. Kozmin, S. A.; Rawal, V. H. A General Strategy to Aspidosperma Alkaloids: Efficient, Stereocontrolled Synthesis of Tabersonine. *J. Am. Chem. Soc.* **1998**, *120*, 13523-13524.
97. Nicolaou, K. C.; Estrada, A. A.; Lee, S. H.; Freestone, G. C. Synthesis of Highly Substituted N-Hydroxyindoles through 1,5-Addition of Carbon Nucleophiles to In Situ Generated Unsaturated Nitrones. *Angew. Chem. Int. Ed.* **2006**, *45*, 5364-5368.
98. Belley, M.; Beaudoin, D.; St.-Pierre, G. A new general synthesis of N-hydroxyindoles. *Synlett* **2007**, *19*, 2999-3002.
99. Kametani, T.; Takahashi, K.; Kigawa, Y.; Ihara, M.; Fukumoto, K. Studies on the syntheses of heterocyclic compounds. Part 676. Synthesis of 1-substituted 7-methoxymitosenes. *J. Chem. Soc., Perkin Trans. 1* **1977**, 28-31.
100. Tebbe, F. N.; Parhall, G. W.; Reddy, G. S. Olefin homologation with titanium methylene compounds. *J. Am. Chem. Soc.* **1978**, *100*, 3611-3613.
101. Jiricek, J.; Blechert, S. Enantioselective synthesis of (-)-gilbertine via a cationic cascade cyclization. *J. Am. Chem. Soc.* **2004**, *126*, 3534-3538.
102. Braun, N. A.; Bray, J. D.; Ciufolini, M. A. Hypervalent iodine oxidation of indolic 2-oxazolines. *Tetrahedron Lett.* **1999**, *40*, 4985-4988

- 103.** Colomer, I.; Batchelor-McAuley, C.; Odell, B.; Donohoe, T. J.; Compton, R. G. Hydrogen bonding to hexafluoroisopropanol controls the oxidative strength of hypervalent iodine reagents. *J. Am. Chem. Soc.* **2016**, *138*, 8855-8861.
- 104.** Wu, C.-J.; Li, C.-W.; Gao, H.; Huang, X.-J.; Cui, C.-B. Penicimutamides D–E: two new prenylated indole alkaloids from a mutant of the marine-derived *Penicillium purpurogenum* G59. *RCS Adv.* **2017**, *7*, 24718-24722.
- 105.** Ding, Y.; Greshock, T. J.; Miller, K. A.; Sherman, D. H.; Williams, R. M. Premalbrancheamide: Synthesis, Isotopic Labeling, Biosynthetic Incorporation, and Detection in Cultures of *Malbranchea aurantiaca*. *Org. Lett.* **2008**, *10*, 4863.
- 106.** Watts, K. R.; Loveridge, S. T.; Tenney, K.; Media, J.; Valeriote, F. A.; Crews, P. Utilizing DART mass spectrometry to pinpoint halogenated metabolites from a marine invertebrate-derived fungus. *J. Org. Chem.* **2011**, *76*, 6201.
- 107.** Ye, Y.; Du, L.; Zhang, X.; Newmister, S. A.; McCauley, M.; Alegre-Requena, J. V.; Zhang, W.; Mu, S.; Minami, A.; Fraley, A. E.; Adrover-Castellano, M. L.; Carney, N.; Shende, V. V.; Qi, F.; Oikawa, H.; Kato, H.; Tsukamoto, S.; Paton, R. S.; Williams, R. M.; Li, S.; Sherman, D. H. Cofactor-Independent Pinacolase Directs Non-Diels-Alderase Biogenesis of the Brevianamides. *Nat. Catal.* **2020**, *3*, 497-506.
- 108.** Simpson, T. J.; Dejesus, A. E.; Steyn, P. S.; Vleggaar, R. *J. Chem. Soc. D* **1982**, *11*, 631-632.
- 109.** Marion, F.; Williams, D. E.; Patrick, B. O.; Hollander, I.; Mallon, R.; Kim, S. C.; Roll DM, Feldberg, L.; Van Soest, R.; Andersen, R. J. Liphagal, a Selective Inhibitor of PI3 Kinase  $\alpha$  Isolated from the Sponge *Aka coralliphaga*: Structure Elucidation and Biomimetic Synthesis. *Org. Lett.* **2006**, *8*, 321-324.
- 110.** Guo, H.; Benndorf, R.; Lechnitz, D.; Klassen, J. L.; Vollmers, J.; Goerls, H.; Steinacker M, Weigel, C.; Dahse, H. M.; Kaster, A. K.; Poulsen, M. Isolation, biosynthesis and chemical modifications of rubterolones AF: rare tropolone alkaloids from *Actinomadura* sp. 5-2. *Chem. Eur. J.* **2017**, *23*, 9338-9345.
- 111.** Hoefle, G.; Irschik, H. Isolation and Biosynthesis of Aurachin P and 5-Nitroresorcinol from *Stigmatella erecta*. *J. Nat. Prod.* **2008**, *71*, 1946-1948
- 112.** Vleggaar, R. Biosynthetic studies on some polyene mycotoxins. *Pure Appl. Chem.* **1986**, *58*, 239-256.

- 113.** Li, S.; Finefield, J. M.; Sunderhaus, J. D.; McAfoos, T. J.; Williams, R. M.; Sherman, D. H. Biochemical characterization of NotB as an FAD-dependent oxidase in the biosynthesis of notoamide indole alkaloids. *J. Am. Chem. Soc.* **2012**, *134*, 788-791.
- 114.** Katsuyama, Y.; Harmrolfs, K.; Pistorius, D.; Li, Y.; Mueller, R. A. A Semipinacol Rearrangement Directed by an Enzymatic System Featuring Dual-Function FAD-Dependent Monooxygenase *Angew. Chem. Int. Ed.* **2012**, *51*, 9437-9440.
- 115.** Davison, J.; al Fahad, A.; Cai, M.; Song, Z.; Yehia, S. Y. Genetic, molecular, and biochemical basis of fungal tropolone biosynthesis *Proc. Natl. Acad. Sci. U. S. A.* **2012**, *109*, 7642-7647.
- 116.** Mori, T.; Iwabuchi, T.; Hoshino, S.; Wang, H.; Matsuda, Y.; Abe, I. Molecular basis for the unusual ring reconstruction in fungal meroterpenoid biogenesis. *Nat. Chem. Biol.* **2017**, *13*, 1066-1073.
- 117.** Ding, Y.; de Wet, J. R.; Cavalcoli, J.; Li, S.; Greshock, T. J.; Miller, K. A. Genome-Based Characterization of Two Prenylation Steps in the Assembly of the Stephacidin and Notoamide Anticancer Agents in a Marine-Derived *Aspergillus* sp. *J. Am. Chem. Soc.* **2010**, *132*, 12733-12740.
- 118.** Maiya, S.; Grundmann, A.; Li, S. M.; Turner, G. The fumitremorgin gene cluster of *Aspergillus fumigatus*: identification of a gene encoding brevianamide F synthetase. *Chem. Bio. Chem.* 2006, *7* (7), 1062-1069.
- 119.** Li, S.; Finefield, J. M.; Sunderhaus, J. D.; McAfoos, T. J.; Williams, R. M.; Sherman, D. H. Biochemical characterization of NotB as an FAD-dependent oxidase in the biosynthesis of notoamide indole alkaloids. *J. Am. Chem. Soc.*, **2012**, *134*, 788-791.
- 120.** Somei, M.; Karasawa, Y.; Kaneko, C. Selective mono-alkylation of carbon nucleophiles with gramine. *Heterocycles* **1981**, *16*, 941.
- 121.** Davis, F. A.; Towson, J. C.; Vashi, D. B.; ThimmaReddy, R.; McCauley Jr, J. P.; Harakal, M. E.; Gosciniak, D. J. Chemistry of oxaziridines. 13. Synthesis, reactions, and properties of 3-substituted 1, 2-benzisothiazole 1, 1-dioxide oxides. *J. Org. Chem.* **1990**, *55*(4), 1254-1261.
- 122.** Grubbs, A.W.; Artman III, G. D.; Tsukamoto, S.; Williams, R. M. A concise total synthesis of the notoamides C and D. *Angew. Chem. Int. Ed.* **2007**, *46*, 2257-2261.
- 123.** Baran, P. S.; Hafensteiner, B. D.; Ambhaikar, N. B.; Guerrero, C. A.; Gallagher, J. D. Aerobic oxidation of indolomorphinan without the 4, 5-epoxy bridge and subsequent

- rearrangement of the oxidation product to spiroindolinonyl-C-normorphinan derivative. *J. Am. Chem. Soc.*, **2006**, *128*, 8678-8693.
- 124.** Movassaghi, M.; Schmidt, M. A.; Ashenurst, J. A. *Org. Lett.* **2008**, *10*, 4009-4012.
- 125.** Fujii, H.; Ogawa, R.; Ohata, K.; Nemoto, T.; Nakajima, M.; Hasebe, K.; Mochizuki, H.; Nagase, H. *Bioorg. Med. Chem.* **2009**, *17*, 5983-5988.
- 126.** Sutor, D. J. The C–H... O Hydrogen Bond in Crystals. *Nature* **1962**, *195*, 68-69.
- 127.** Schwalbe, C. H. June Sutor and the C–H... O hydrogen bonding controversy. *Crystallography Reviews* **2012**, *18*, 191-206.
- 128.** Zheng, Y. J.; Tice, C. M.; Singh, S. B. The use of spirocyclic scaffolds in drug discovery. *Bioorg. Med. Chem. Lett.* **2014**, *24* (16), 3673–3682.
- 129.** Zhao, Q. *Applications of aspeverin in the preparation of drugs for treatment of leukemia.* China Patent 103,356,634 (A), Oct. 23, **2013**.
- 130.** *Application of aspeverin in the preparation of drug for the treatment of ovarian cancer.* China Patent 103,251,624 (A), Aug. 21, **2013**.
- 131.** *Application of aspeverin in preparation of anticancer drugs for treating ileocecal cancer.* China Patent 103,251,613 (A), Aug. 21, **2013**.
- 132.** *Application of aspeverin in preparation of drug for treating laryngocarcinoma.* China Patent 103,251,615 (A), Aug. 21, **2013**.
- 133.** Duan, Z. *Aspeverin application in preparing medicines for treating pancreatic cancer.* China Patent 103,285,009 (A), Sep. 11, **2013**.
- 134.** *Application of aspeverin in preparation of medicine for treating bladder cancer.* China Patent 103,251,617 (A), Aug. 21, **2013**.
- 135.** *Application of aspeverin in preparation of medicine for treating tongue cancer.* China Patent 103,251,609 (A), Aug. 21, **2013**.
- 136.** Gao, Z. *Application of aspeverin in preparation of drugs for treating lung cancer.* China Patent 103,356,635 (A), Oct. 23, **2013**.
- 137.** Yan, J. *Application of Aspeverin in preparing medicine for treating cervical cancer.* China Patent 103,316,009 (A), Sep. 25, **2013**.
- 138.** *Application of aspeverin in manufacture of medicine for treating rectal cancer.* China Patent 103,316,008 (A), Sep. 25, **2013**.

139. He, Y. *Application of aspeverin in preparation of anti-Helicobacter pylori drugs*. China Patent 103,356,633 (A), Oct. 23, **2013**.
140. *Application of aspeverin in preparation of bactericides*. China Patent 103,251,611 (A), Aug. 21, **2013**.
141. Ji, N. Y.; Liu, X. H.; Miao, F. P.; Qiao, M. F. *Org. Lett.* **2013**, *15*, 2327-2329.
142. *Application of aspeverin in producing the medical formulations for treating tubercle bacillus*. China Patent 103,285,010 (A), Sep. 11, **2013**.
143. He, Y. *Application of aspeverin in the preparation of drugs for treatment of atherosclerosis*. China Patent 103,356,632 (A), Oct. 23, **2013**.
144. *Use of aspeverin in preparing monoamine oxidase MAO inhibitor*. China Patent 103,285,012 (A), Oct. 11, **2013**.
145. Stocking, E. M.; Sanz-Cervera, J. F.; Williams, R. M. Total Synthesis of VM55599. Utilization of an Intramolecular Diels–Alder Cycloaddition of Potential Biogenetic Relevance. *J. Am. Chem. Soc.* **2000**, *122*, 1675-1683.
146. Klas, K. Elucidation of the Biogenesis of the Paraherquamides, Malbrancheamides, Citrinalins, and Brevianamides. PH.D. Thesis. Colorado State University, Fort Collins, CO, 2019.
147. Greshock, T. J.; Grubbs, A. W.; Williams, R. M. Synthesis and antidepressant activity of optical isomers of 2-(4-benzylpiperazin-1-yl)-1-(5-chloro-6-methoxynaphthalen-2-yl) propan-1-ol (SIPI5056). *Tetrahedron* **2007**, *63*, 6124-6130.
148. Weng, Z.; Li, J. Synthesis and antidepressant activity of optical isomers of 2-(4-benzylpiperazin-1-yl)-1-(5-chloro-6-methoxynaphthalen-2-yl) propan-1-ol (SIPI5056). *Bioorg. Med. Chem. Lett.* **2010**, *20*, 1256-1259.
149. Hoemann, M.; Wilson, N.; Argiriadi, M.; Banach, D.; Burchat, A.; Calderwood, D.; Clapham, B.; Cox, P.; Duignan, D. B.; Konopacki, D.; Somal, G.; Vasudeva, A. Synthesis and optimization of furano [3, 2-d] pyrimidines as selective spleen tyrosine kinase (Syk) inhibitors. *Bioorg. Med. Chem. Lett.* **2016**, *26*, 5562-5567.
150. Hao, J.; Beck, J. P.; Schaus, J. M.; Krushinski, J. H.; Chen, Q.; Beadle, C. D.; Vidal, P.; Reinhard, M. R.; Dressman, B. A.; Massey, S. M.; Boulet, S. L.; Cohen, M. P.; Watson, B. M.; Tupper, D.; Gardiner, K. M.; Myers, J.; Johansson, A. M.; Richardson, J.; Richards, D. S.; Hembre, E. J.; Remick, D. M.; Coates, D. A.; Bhardwaj, R. M.; Diserod, B. A.; Bender, D.;

Stephenson, G.; Wolfangel, C. D.; Diaz, N.; Getman, B. G.; Wang, X.-S.; Heinz, B. A.; Cramer, J. W.; Zhou, X.; Maren, D. L.; Falcone, J. F.; Wright, R. A.; Mitchell, S. N.; Carter, G.; Yang, C. R.; Bruns, R. F.; Svennson, K. A. Synthesis and Pharmacological Characterization of 2-(2,6-Dichlorophenyl)-1-((1S,3R)-5-(3-hydroxy-3-methylbutyl)-3-(hydroxymethyl)-1-methyl-3,4-dihydroisoquinolin-2-(1H)-yl) ethan-1-one (LY3154207), a Potent, Subtype Selective, and Orally Available Positive Allosteric Modulator of the Human Dopamine D1 Receptor. *J. Med. Chem.* **2019**, *62*, 8711-8732.

## Appendix I: Contributions to Work

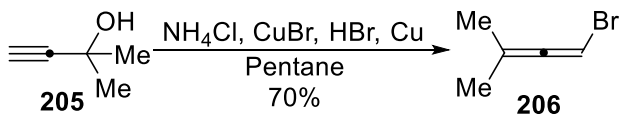
Chapter 3: All computational data was obtained by Juan V. Alegre-Requena from the Paton lab at Colorado State University. The biological data was collected by Ying Ye and fellow members of David Sherman's group at the University of Michigan.

## Appendix II: Supporting Information

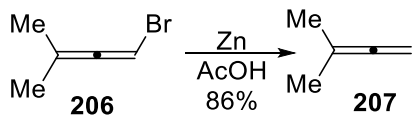
### Chapter 1: Experimental

#### *i. General Procedures*

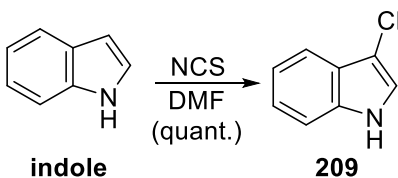
Flash column chromatography was performed with silica gel grade 60 (230-400 mesh) from Sorbent Technologies. Preparative TLC was performed with glassed backed precoated silica gel 60 F254 20 x 20 cm plates. Unless otherwise noted, materials were obtained from commercially available sources. Dichloromethane ( $\text{CH}_2\text{Cl}_2$ ), tetrahydrofuran (THF), N, N-dimethylformamide (DMF), acetonitrile (MeCN), triethylamine ( $\text{NEt}_3$ ), toluene, and methanol (MeOH) were all degassed with argon and passed through a solvent purification system containing alumina or molecular sieves in most cases. Optical rotations were taken on a Rudolph Research Analytical Autopol III Polarimeter operating at 589 nm at a room temperature of 23 °C. Solvents used to dilute polarimetry samples were obtained from the solvent system. All  $^1\text{H}$  and  $^{13}\text{C}$  spectra were obtained using 400 MHz or 500 MHz spectrometers. The chemical shifts are given in parts per million (ppm). Solvent residuals were relative to  $\text{CDCl}_3$   $\delta$  7.26 ppm,  $\text{CD}_3\text{OD}$   $\delta$  3.31 ppm, or  $(\text{CD}_3)_2\text{SO}$   $\delta$  2.50 ppm for proton spectra and relative to  $\text{CDCl}_3$   $\delta$  77.16 ppm,  $\text{CD}_3\text{OD}$   $\delta$  49.00,  $(\text{CD}_3)_2\text{SO}$   $\delta$  39.52 ppm for carbon spectra. Splitting patterns are described using the following abbreviations: s = singlet, br. s = broad singlet, d = doublet, t = triplet, q = quartet, quin = quintet, sext = sextet, sept = septet, m = multiplet. More than one abbreviation may be used to describe more complex splitting patterns, with the form “*ab*” denoting that splitting pattern *a* modifies pattern *b*. Mass spectra were obtained by the Colorado State University Central Instrument Facility on various TOF or QTOF spectrometers.



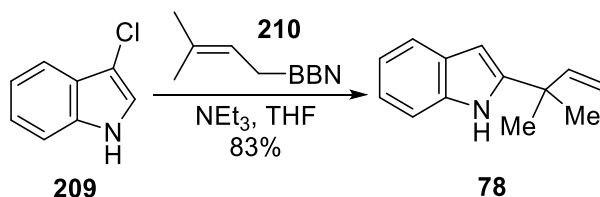
**1-bromo-3-methylbuta-1,2-diene (206):** NH<sub>4</sub>Br (37.35 g, 381 mmols), CuBr (46.65 g, 325 mmols), Cu (2.37 g, 37.29) and HBr (180 mL) were added to a 1L round bottom flask while a mixture of 2-methyl-3-butyn-2-ol **205** (90 mL, 928.7 mmols) and pentane (225 mL) was added dropwise over the course of 30 minutes. After addition, the flask was heat to 30°C and stirred for 3 additional hours. Once the solution was cooled to rt, the mixture was extracted with equal volumes of concentrated HBr (×2) and water (×3), dried overnight over MgSO<sub>4</sub> at 0 °C. The dried compound was run over a silica plug, eluting with pentane, and concentrated at 0 °C to yield a clear yellow liquid (94.61g, 69%). **206:** <sup>1</sup>H NMR (400 MHz, Chloroform-*d*) δ 5.83 (hept, *J* = 2.1 Hz, 1H), 1.84 (d, *J* = 2.1 Hz, 6H). <sup>13</sup>C NMR (101 MHz, Chloroform-*d*) δ 199.69, 106.72, 69.81, 20.23.



**3-methylbuta-1,2-diene (207):** Zn dust (37 g, 571 mmols) and AcOH (238 mL) were added to a multineck round bottom flask set-up with an additional and a short path distillation apparatus with the receiving flask set in a -78 °C bath. The flask was heated to 70 °C, and bromoallene (70g, 476 mmols) was added dropwise maintaining a distillation temperature below 45 °C. Once all of the bromoallene was added, the flask was heated to 75 °C. Once the distillation was complete, allene was isolated from any remaining AcOH by freezing off the AcOH to yield 20.0 g of allene (86 %). **207:** <sup>1</sup>H NMR (400 MHz, Chloroform-*d*) δ 4.52 (hept, *J* = 3.2 Hz, 2H), 1.69 (t, *J* = 3.2 Hz, 6H). <sup>13</sup>C NMR (101 MHz, Chloroform-*d*) δ 207.10, 93.86, 72.54, 20.10.

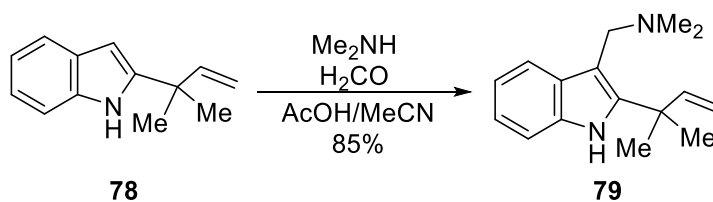


**3-chloroindole (209):** Recrystallized NCS (22.8 g, 170.8 mmols) was added to a solution of indole (20g, 170.8 mmols) in DMF (500 mL) at rt and stirred for 4 hours, keeping the reaction flask out of direct light. The solution was diluted with 250 mL of brine, extracted with EtOAc (3 × 250 mL), washed with 500 mL of water, 250 mL of NaHCO<sub>3</sub>, 250 mL of NH<sub>4</sub>Cl, and 500 mL of brine. The organics were dried over Na<sub>2</sub>SO<sub>4</sub>, filtered, and concentrated to a dark yellow oil. The oil was purified by a silica plug (10-20% EtOAc/Hexane) and recrystallized in EtOAc/Hexane giving a white crystal (25.8g, 170.8 mmols) in a quantitative yield. **209:** <sup>1</sup>H NMR (400 MHz, Chloroform-*d*) δ 8.17 (s, 1H), 7.77 (dt, *J* = 7.7, 1.0 Hz, 1H), 7.47 (dt, *J* = 8.2, 1.0 Hz, 1H), 7.42 – 7.28 (m, 2H). <sup>13</sup>C NMR (101 MHz, Chloroform-*d*) δ 135.06, 125.48, 123.22, 120.98, 120.57, 118.35, 111.63, 106.59.

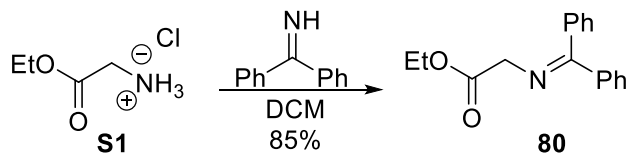


**2-(2-methylbut-3-en-2-yl)-1H-indole (78):** Allene **207** (5 mL, 50.43 mmols) was added to a 0.5 M solution of 9-BBN in THF (84.05 mL, 42.03 mL) at 0 °C and allowed to stir overnight at room temperature. Chlorinated indole (2.16 g, 14.245 mmols) was added to the solution at room temp 15 minutes before the addition of NEt<sub>3</sub> (5.17 mL, 42.45 mmols). The reaction mixture was stirred for 8 hours, monitoring by TLC (25% EtOAc/Hex) for full conversion. The solution was washed with 91 mL of 1M HCl and 46 mL of NaHCO<sub>3</sub>. The organics were brought to 0°C and a quick quench was performed in a -78 °C bath with 80 mL of 2M NaOH and 80 mL of H<sub>2</sub>O<sub>2</sub>

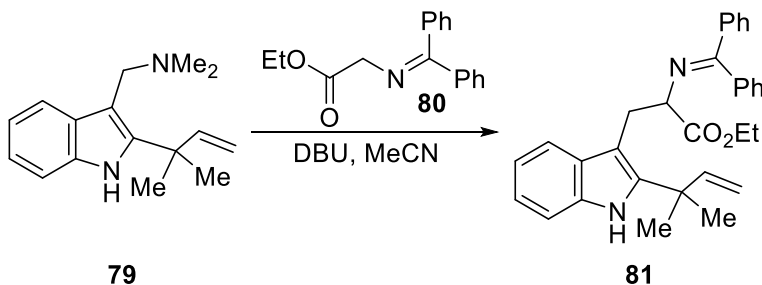
sequentially while maintaining an internal temperature between 0-5 °C. The organics were extracted with 182 mL of ether and washed with brine (2 × 91 mL), dried over MgSO<sub>4</sub>, filtered and concentrated. The crude material was purified by flash column chromatography (2-6% EtOAc/Hex) to yield a pale-yellow oil (2.20 g, 83%). **78**: <sup>1</sup>H NMR (400 MHz, Chloroform-*d*) δ 7.87 (s, 1H), 7.59 – 7.52 (m, 1H), 7.34 – 7.27 (m, 1H), 7.13 (ddd, *J* = 8.1, 7.1, 1.4 Hz, 1H), 7.07 (td, *J* = 7.4, 1.2 Hz, 1H), 6.32 (dd, *J* = 2.3, 0.9 Hz, 1H), 6.10 (s, 0H), 6.10 – 6.00 (m, 1H), 5.16 – 5.13 (m, 1H), 5.11 (s, 1H), 1.49 (s, 6H). <sup>13</sup>C NMR (101 MHz, Chloroform-*d*) δ 146.15, 145.85, 136.00, 128.64, 121.37, 120.22, 119.71, 112.30, 110.58, 98.08, 38.26, 27.50.



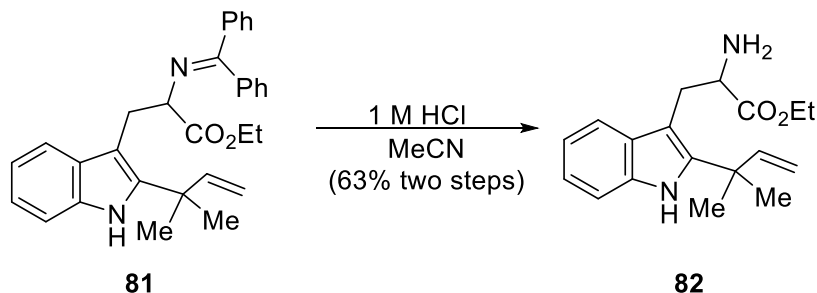
**N,N-dimethyl-1-(2-(2-methylbut-3-en-2-yl)-1H-indol-3-yl)methanamine (79)**: Me<sub>2</sub>NH (40 % in H<sub>2</sub>O, 1.11 mL, 8.79 mmols) and H<sub>2</sub>CO (37% in H<sub>2</sub>O, 0.63 mL, 8.49 mmols) were added to a solution of prenylated indole **78** (1.48 g, 7.99 mmols) in AcOH/MeCN (7.7 mL/0.77 mL) at 0 °C and ran at rt for 3 hours. The reaction was partitioned between 50 mL of 1M HCl and 100 mL of ether. The organics were washed with 1M HCl (2 × 50 mL). The aqueous was basified with 2M NaOH and washed with ether (2 × 195 mL). The organics were combined, washed with NaHCO<sub>3</sub> (2 × 50 mL), brine (2 × 195 mL), dried over MgSO<sub>4</sub>, filtered and concentrated to yield a bright orange oil (1.78 g, 92%).



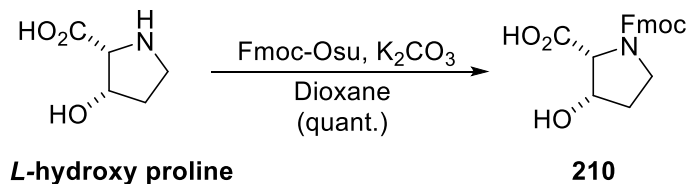
**ethyl 2-((diphenylmethylene)amino)acetate (80):** Benzophenone imine **S1** (12.98 g, 71.64 mmols) was added to a solution of glycine HCl (10.00 g, 71.64 mmols) in DCM (84.4 mL) at rt. A CaCl<sub>2</sub> tube was equipped to the flask and left to run for 24 hours. The salts were filtered off and the resulting solution was concentrated. The crude oil was taken up in ether (260 mL), washed with H<sub>2</sub>O (2 × 130 mL), dried over MgSO<sub>4</sub>, filtered, and concentrated to yield glycine derivative as a yellow solid (15.0 g, 78%). **80:** <sup>1</sup>H NMR (400 MHz, Chloroform-*d*) δ 7.69 – 7.63 (m, 2H), 7.50 – 7.43 (m, 3H), 7.43 – 7.38 (m, 1H), 7.37 – 7.31 (m, 2H), 7.24 – 7.15 (m, 2H), 4.26 – 4.16 (m, 4H), 1.27 (t, *J* = 7.1 Hz, 3H). <sup>13</sup>C NMR (101 MHz, Chloroform-*d*) δ 171.98, 170.79, 139.42, 136.16, 130.59, 128.96, 128.91, 128.82, 128.20, 127.82, 61.01, 55.88, 14.36.



**ethyl 2-((diphenylmethylene)amino)-3-(2-(2-methylbut-3-en-2-yl)-1H-indol-3-yl)propanoate (81):** DBU (1.61 mL, 10.87 mmols) was added to a solution of gramine **79** (1.95 g, 8.05 mmols) and glycine derivative **80** (2.04 g, 8.05 mmols) in MeCN (66.5 mL) at 0 °C. The reaction was refluxed overnight. The reaction mixture was washed with 46 mL of NH<sub>4</sub>Cl and ether (2 × 46 mL). The organics were combined and washed with brine (2 × 90 mL), dried over Na<sub>2</sub>SO<sub>4</sub>, filtered, and concentrated to yield a crude orange oil that was immediately carried forward.

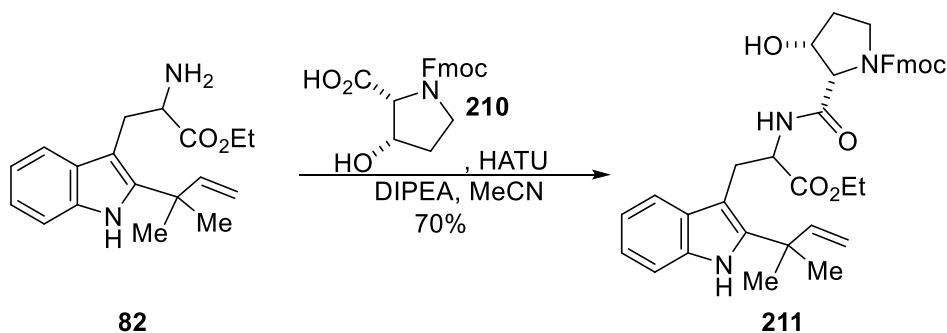


**ethyl 2-amino-3-(2-(2-methylbut-3-en-2-yl)-1H-indol-3-yl)propanoate (82):** To a solution of crude imine **81** (3.74 g, 8.06 mmols) in MeCN (49 mL), 1M HCl (23.4 mL) was added at 0 °C and ran for 3 hours at rt. The solution was cooled back to 0 °C and basified with 1M NaOH. The reaction mixture was extracted with ether (235 mL), washed with brine (2 × 123 mL), dried over MgSO<sub>4</sub>, filtered, and concentrated. The crude material was run through a silica plug first with DCM until disappearance of UV activity, then 3% MeOH/DCM was run through the plug to yield pure tryptophan as a bright yellow-orange oil (1.40 g, 58% over 2 steps). **82:** <sup>1</sup>H NMR (400 MHz, Chloroform-*d*) δ 7.92 (s, 1H), 7.56 (dd, *J* = 7.8, 1.2 Hz, 1H), 7.28 (dt, *J* = 8.1, 1.0 Hz, 1H), 7.13 (ddd, *J* = 8.1, 7.0, 1.3 Hz, 1H), 7.08 (ddd, *J* = 8.1, 7.0, 1.2 Hz, 1H), 6.15 (dd, *J* = 17.4, 10.6 Hz, 1H), 5.19 (dd, *J* = 8.2, 1.0 Hz, 1H), 5.16 (s, 1H), 4.12 (qq, *J* = 10.8, 7.1 Hz, 2H), 3.85 (dd, *J* = 9.5, 5.1 Hz, 1H), 3.33 (dd, *J* = 14.5, 5.0 Hz, 1H), 3.06 (dd, *J* = 14.5, 9.5 Hz, 1H), 1.57 (s, 6H), 1.52 (s, 2H), 1.18 (t, *J* = 7.1 Hz, 3H).

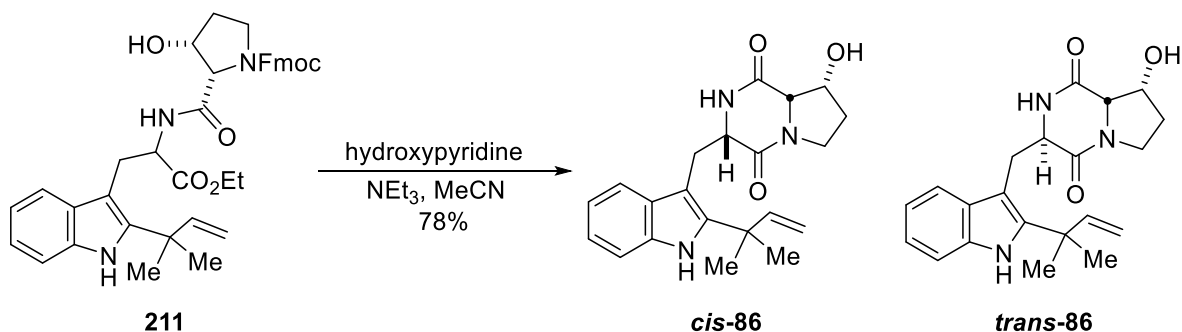


**(9H-fluoren-9-yl)methyl (2S,3S)-2-(formyloxy)-3-hydroxypyrrolidine-1-carboxylate (210):** K<sub>2</sub>CO<sub>3</sub> (26.26 g in 191 mL H<sub>2</sub>O) was added to a solution of enantiomerically pure hydroxy proline (5 g, 38.0 mmols) in dioxane, followed by the addition of Fmoc-Osu (14.66 g, 43.5 mmols). The reaction was stirred vigorously overnight (~18 hours). The solution was diluted

with 252 mL of water and extracted with ether (2 × 629 mL). The aqueous was acidified with 2M HCl (~220 mL) and extracted with EtOAc (1 × 629 mL, 2 × 315 mL). The organics were combined then washed with brine (2 × 629 mL), dried over MgSO<sub>4</sub>, filtered, and concentrated to yield a white solid (13.46 g, quant.).



**(9H-fluoren-9-yl)methyl (2S,3R)-2-((1-ethoxy-3-(2-(2-methylbut-3-en-2-yl)-1H-indol-3-yl)-1-oxopropan-2-yl)carbamoyl)-3-hydroxypyrrolidine-1-carboxylate (211):** HATU (2.53 g, 6.65 mmols) and DIPEA (2.60 mL, 15.0 mmols) were added to a solution of tryptophan **82** (1.50 g, 5.00 mmols) and proline **210** (2.29 g, 6.5 mmols) in MeCN (30 mL) at rt. The reaction was ran for 3 hours then concentrated. The crude oil was taken up in 63 mL of DCM and washed with 63 mL of 1M HCl. The aqueous was back extracted with DCM (2 × 24 mL). The organics were combined, washed with 40 mL of brine, dried over Na<sub>2</sub>SO<sub>4</sub>, filtered and concentrated. The oil was further purified by flash column chromatography (40-60% EtOAc/Hex) to yield diastereomers of rotomers as an off-white foam (2.54 g, 80%). Dipeptide **211** was carried forward without further characterization.



**(8*R*,8*aS*)-8-hydroxy-3-((2-(2-methylbut-3-en-2-yl)-1*H*-indol-3-**

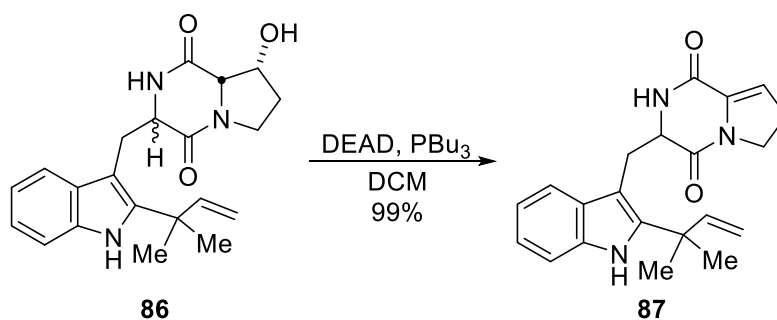
**yl)methyl)hexahydropyrrolo[1,2-*a*]pyrazine-1,4-dione (Cis- & trans 86):** 2-hydroxypyridine

(82.3 mg, 8.65 mmols) was added to a solution of NEt<sub>3</sub> (5.48 mL, 39.3 mmols) and dipeptide (2.5 g, 3.93 mmols) in MeCN (75 mL) at rt, then refluxed for 21 hrs. The reaction mixture was cooled to rt, concentrated, and partitioned between 1M HCl (96.4 mL) and DCM (195 mL). The aqueous layer was back extracted with DCM (48 mL × 2), the combined organics were washed with brine (195 mL), dried over Na<sub>2</sub>SO<sub>4</sub>, filtered and concentrated. Flash column

chromatography (0-3% MeOH/DCM) was used to separate and purify the diastereomers to yield

off *cis*-**86** (540 mg, 1.47 mmols, 37.5%) and *trans*-**86** (540 mg, 1.47 mmols, 37.5%). **Cis-86:** <sup>1</sup>H NMR (400 MHz, Chloroform-*d*) δ 8.06 (s, 1H), 7.49 (dd, *J* = 7.9, 1.1 Hz, 1H), 7.34 (dt, *J* = 8.1, 0.9 Hz, 1H), 7.18 (ddd, *J* = 8.2, 7.1, 1.2 Hz, 1H), 7.12 (ddd, *J* = 8.1, 7.1, 1.1 Hz, 1H), 6.19 – 6.08 (m, 1H), 5.85 (s, 1H), 5.21 (s, 1H), 5.17 (dd, *J* = 6.8, 0.9 Hz, 1H), 4.69 (dq, *J* = 3.9, 2.1 Hz, 1H), 4.43 (ddd, *J* = 11.8, 4.0, 1.8 Hz, 1H), 4.12 (t, *J* = 2.6 Hz, 1H), 3.89 (td, *J* = 11.2, 7.6 Hz, 1H), 3.77 (dd, *J* = 15.3, 4.0 Hz, 1H), 3.71 (ddd, *J* = 11.7, 10.4, 2.4 Hz, 1H), 3.20 (dd, *J* = 15.3, 11.7 Hz, 1H), 2.98 (t, *J* = 2.0 Hz, 1H), 2.24 – 2.13 (m, 1H), 2.04 (tdt, *J* = 14.1, 10.2, 2.1 Hz, 1H), 1.56 (d, *J* = 1.3 Hz, 6H). <sup>13</sup>C NMR (101 MHz, Chloroform-*d*) δ 167.73, 165.90, 145.65, 141.73, 134.48, 129.15, 122.39, 120.35, 117.98, 113.10, 111.06, 104.61, 71.01, 64.66, 55.01, 44.19, 39.15, 30.33, 28.09, 28.00, 26.30. **trans-86:** <sup>1</sup>H NMR (400 MHz, Chloroform-*d*) δ 7.99 (s, 1H),

7.55 – 7.48 (m, 1H), 7.24 (t,  $J = 1.2$  Hz, 1H), 7.10 (pd,  $J = 7.1, 1.3$  Hz, 2H), 6.12 (dd,  $J = 17.4, 10.5$  Hz, 1H), 5.92 (d,  $J = 4.0$  Hz, 1H), 5.20 (dd,  $J = 10.6, 1.0$  Hz, 1H), 5.18 – 5.15 (m, 1H), 4.59 (t,  $J = 3.7$  Hz, 1H), 4.29 (dt,  $J = 9.7, 3.9$  Hz, 1H), 3.85 (td,  $J = 11.1, 7.7$  Hz, 1H), 3.70 (d,  $J = 3.1$  Hz, 1H), 3.55 (ddd,  $J = 11.8, 10.0, 1.7$  Hz, 1H), 3.49 (dd,  $J = 14.7, 3.8$  Hz, 1H), 3.33 – 3.17 (m, 2H), 2.89 (s, 1H), 2.11 – 2.00 (m, 1H), 1.83 (dtd,  $J = 14.3, 10.3, 4.3$  Hz, 1H), 1.53 (d,  $J = 3.3$  Hz, 6H).  $^{13}\text{C}$  NMR (101 MHz, Chloroform-*d*)  $\delta$  167.29, 166.19, 146.08, 141.57, 134.33, 129.05, 122.11, 120.00, 118.62, 112.23, 110.70, 105.12, 71.11, 63.95, 58.63, 44.34, 39.23, 30.08, 29.72, 28.11, 27.91.

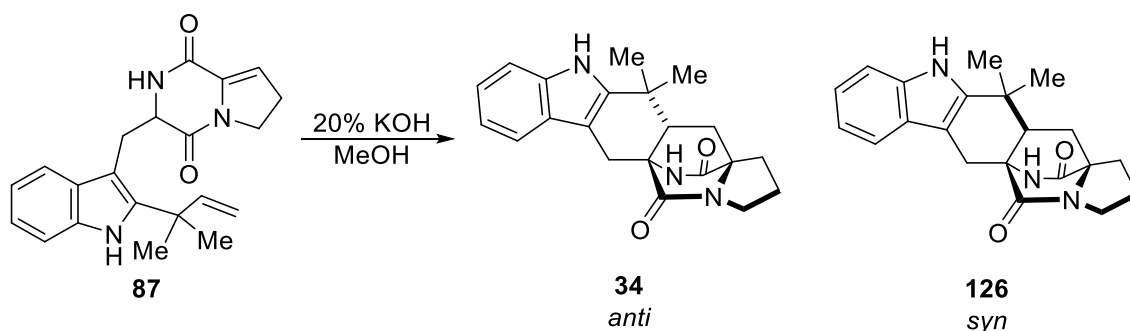


**3-((2-(2-methylbut-3-en-2-yl)-1H-indol-3-yl)methyl)-2,3,6,7-tetrahydropyrrolo[1,2-**

**a]pyrazine-1,4-dione (87):** DEAD (40% weight in toluene, 4.59 mL, 11.6 mmols) was added to a solution of **86** (1.42 g, 3.86 mmols) in DCM (77.4 mL) at rt and ran for 15 minutes before PBU<sub>3</sub> (2.90 mL, 11.6 mmols) was added to the solution. The reaction mixture stirred for 3 hours before being concentrated. The crude reaction mixture was purified by flash column chromatography with 60-100% ethyl acetate/hexane to give an off-white solid as product in a quantitative yield.

**87:**  $^1\text{H}$  NMR (400 MHz, Chloroform-*d*)  $\delta$  8.03 (s, 1H), 7.53 (d,  $J = 7.9$  Hz, 1H), 7.32 (d,  $J = 7.9$  Hz, 1H), 7.18 (ddd,  $J = 8.1, 7.0, 1.3$  Hz, 1H), 7.12 (td,  $J = 7.5, 7.0, 1.2$  Hz, 1H), 6.18 – 6.07 (m, 2H), 5.65 (s, 1H), 5.22 – 5.11 (m, 2H), 4.52 (d,  $J = 11.6$  Hz, 1H), 4.15 – 3.99 (m, 2H), 3.73 (dd,  $J = 14.6, 3.6$  Hz, 1H), 3.23 (dd,  $J = 14.6, 11.3$  Hz, 1H), 2.78 (ddd,  $J = 9.9, 8.1, 3.0$  Hz, 2H), 1.55 (d,  $J = 2.3$  Hz, 6H).  $^{13}\text{C}$  NMR (101 MHz, Chloroform-*d*)  $\delta$  162.68, 156.58, 145.78, 141.81,

134.41, 133.25, 128.93, 122.28, 120.27, 118.97, 118.33, 112.62, 110.92, 104.67, 57.57, 45.72, 39.17, 30.93, 28.08, 28.02, 27.93.



**(12a*S*)-12,12-dimethyl-2,3,11,12,12a,13-hexahydro-1*H*,5*H*,6*H*-5*a*,13*a*-**

**(epiminomethano)indolizino[7,6-*b*]carbazole-5,14-dione (*anti* **34** & *syn* **126**):** 20% KOH (74

mL) was added to a solution of **87** (1.36 g, 3.89 mmols) in MeOH (296 mL) at 0 °C. The

solution was slowly warmed to rt over the course of an hour, then ran for an additional 18 hours.

The solution was acidified with NH<sub>4</sub>Cl, extracted with DCM (×3), washed with brine, dried over

Na<sub>2</sub>SO<sub>4</sub>, filtered, and concentrated. The crude material was purified by flash column with 1%

MeOH/CHCl<sub>3</sub> to yield *syn*(**126**) :*anti*(**34**) in a 2.1:1 ratio as white solids (1.10 g, 81%). A small

amount of starting material was also recovered. **34**: <sup>1</sup>H NMR (400 MHz, Chloroform-*d*) δ 7.82

(s, 1H), 7.53 (dt, *J* = 7.8, 0.7 Hz, 1H), 7.33 (dt, *J* = 8.0, 1.0 Hz, 1H), 7.19 (ddd, *J* = 8.1, 7.1, 1.3

Hz, 1H), 7.13 (ddd, *J* = 8.1, 7.1, 1.1 Hz, 1H), 5.69 (s, 1H), 3.94 (d, *J* = 17.9 Hz, 1H), 3.60 – 3.52

(m, 2H), 2.92 (d, *J* = 18.0 Hz, 1H), 2.87 – 2.79 (m, 1H), 2.41 – 2.33 (m, 1H), 2.22 – 2.00 (m,

4H), 1.88 (dt, *J* = 13.0, 7.5 Hz, 1H), 1.34 (s, 3H), 1.31 (s, 3H). <sup>13</sup>C NMR (101 MHz,

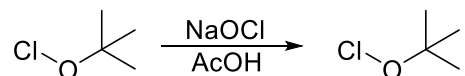
Chloroform-*d*) δ 172.85, 169.19, 139.76, 136.57, 127.35, 122.30, 119.88, 118.52, 110.85,

103.80, 67.25, 61.79, 45.91, 44.34, 34.67, 32.82, 29.33, 29.15, 25.46, 24.65, 24.11. IR: 3220,

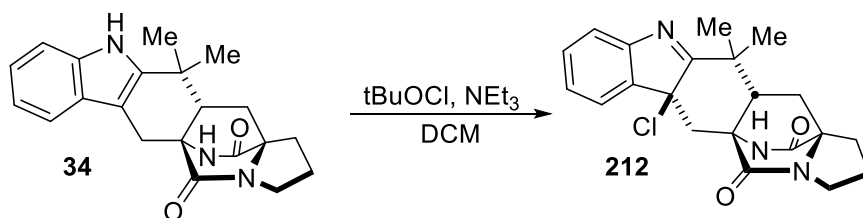
3100, 3062, 2994, 2878, 1697 cm<sup>-1</sup>. **126**: <sup>1</sup>H NMR (400 MHz, Chloroform-*d*) δ 7.50 (d, *J* = 7.6

Hz, 1H), 7.39 (q, *J* = 7.5 Hz, 2H), 7.22 (d, *J* = 7.3 Hz, 1H), 6.37 (s, 1H), 3.74 (dd, *J* = 10.0, 7.4

Hz, 1H), 3.49 (ddt,  $J = 18.4, 11.6, 6.2$  Hz, 2H), 2.94 (d,  $J = 16.1$  Hz, 1H), 2.80 (dt,  $J = 12.8, 6.6$  Hz, 1H), 2.31 (d,  $J = 16.2$  Hz, 1H), 2.21 (t,  $J = 11.5$  Hz, 1H), 2.09 – 1.93 (m, 2H), 1.87 (dt,  $J = 13.3, 7.7$  Hz, 2H), 1.36 (s, 3H), 1.16 (s, 3H).  $^{13}\text{C}$  NMR (101 MHz, Chloroform-*d*)  $\delta$  189.86, 173.45, 167.94, 139.37, 130.47, 126.66, 122.26, 121.13, 83.33, 67.17, 60.25, 48.55, 44.56, 38.66, 34.45, 31.59, 29.86, 29.61, 28.83, 24.63, 21.20. IR: 3320, 3187, 3058, 2971, 2880, 1680  $\text{cm}^{-1}$ .

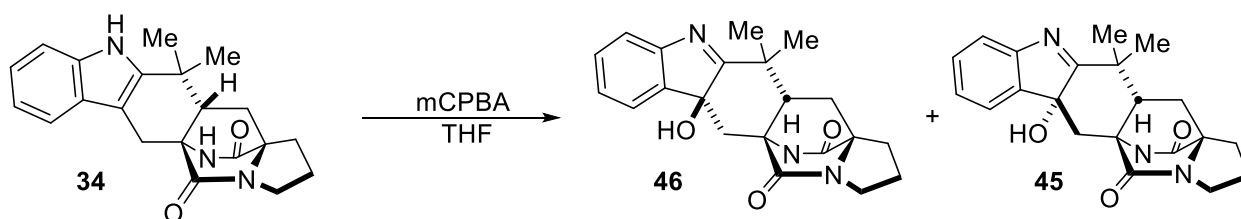


**Tert-butyl hypochlorite:** tBuOH (37 mL, 387 mmols) and AcOH (24.5 mL, 430 mmols) were added together to a 1 L flask containing NaOCl (6%, 442 mL, 395 mmols) when the temperature of the flask reached below 10 °C. While adding care was taken to keep the internal temperature below 20 °C. Ambient light was kept away from the reaction, and it was left to stir for an additional 10 minutes after addition. The reaction mixture was washed with 50 mL of 10%  $\text{Na}_2\text{CO}_3$ ,  $\text{H}_2\text{O}$ , and dried over  $\text{CaCl}_2$  in an amber glass bottle in the fridge as a bright yellow liquid.



**(5aR,12aS,13aR)-6a-chloro-12,12-dimethyl-2,3,6a,12,12a,13-hexahydro-1H,5H,6H-5a,13a-(epiminomethano)indolizino[7,6-b]carbazole-5,14-dione (212):** tBuOCl (25.9 mL, 0.23 mmols) and  $\text{NEt}_3$  (35.2 mL, 0.252 mmols) was added to a solution of **34** (20 mg, 0.057 mmols) in DCM (1.5 mL) at 0 °C and ran for 3 hours. The reaction mixture was warmed to rt before concentrating. The crude material was immediately purified by preparative TLC (6% MeOH/DCM) to yield a pale yellow unstable solid. **212**:  $^1\text{H}$  NMR (400 MHz, Chloroform-*d*)  $\delta$

7.56 (t,  $J = 7.4$  Hz, 2H), 7.40 (td,  $J = 7.6, 1.2$  Hz, 1H), 7.29 (t,  $J = 7.5$  Hz, 1H), 6.61 (s, 1H), 4.21 (d,  $J = 15.9$  Hz, 1H), 3.54 – 3.46 (m, 3H), 2.66 (dt,  $J = 13.0, 6.7$  Hz, 1H), 2.16 (dd,  $J = 13.3, 10.3$  Hz, 1H), 2.05 – 1.89 (m, 3H), 1.78 (dt,  $J = 12.9, 7.5$  Hz, 1H), 1.54 (d,  $J = 16.0$  Hz, 1H), 1.47 (s, 3H), 1.36 (s, 3H).  $^{13}\text{C}$  NMR (101 MHz, Chloroform-*d*)  $\delta$  187.21, 173.40, 168.64, 152.46, 140.05, 130.34, 127.06, 122.92, 121.13, 66.98, 66.54, 59.54, 44.61, 42.64, 39.11, 35.13, 31.05, 29.47, 29.22, 24.74, 23.87.

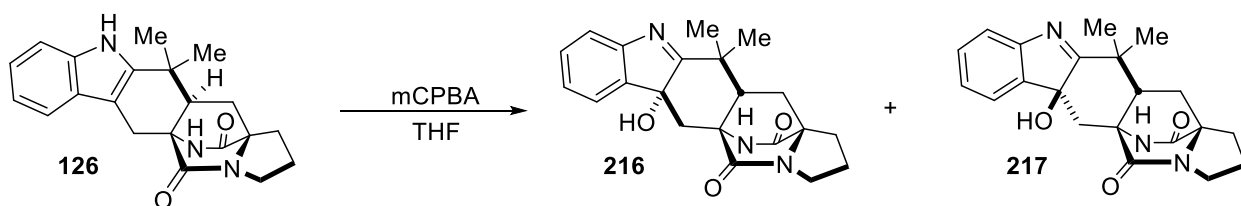


**(5aR,12aS,13aR)-6a-hydroxy-12,12-dimethyl-2,3,6a,12,12a,13-hexahydro-1H,5H,6H-**

**5a,13a-(epiminomethano)indolizino[7,6-b]carbazole-5,14-dione (45 & 46):**

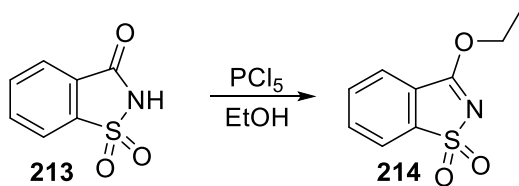
To a solution of compound **34** (30.0 mg, 0.087 mmols) in THF (3 mL) at rt was added mCPBA (19.2 mg, 0.111 mmols). The reaction was stirred vigorously for 2 hours or until TLC showed completion (6% MeOH/ $\text{CDCl}_3$ ). The reaction was quenched with  $\text{Me}_2\text{S}$  and concentrated under reduced pressure. The diastereomers were separated and purified by preparative TLC (6% MeOH/ $\text{CDCl}_3$ ) to yield pale yellow solids (70%) with **46** as the major and **45** as the minor product. **46**:  $^1\text{H}$  NMR (400 MHz, Chloroform-*d*)  $\delta$  7.49 (ddd,  $J = 7.0, 2.5, 1.2$  Hz, 2H), 7.36 (td,  $J = 7.6, 1.3$  Hz, 1H), 7.28 – 7.19 (m, 1H), 6.74 (s, 1H), 3.77 – 3.69 (m, 1H), 3.68 (s, 1H), 3.44 (dt,  $J = 11.3, 6.9$  Hz, 1H), 3.41 – 3.31 (m, 2H), 2.70 (dt,  $J = 13.4, 6.9$  Hz, 1H), 2.17 – 2.05 (m, 1H), 2.08 – 1.97 (m, 1H), 2.00 – 1.92 (m, 1H), 1.92 (dd,  $J = 13.2, 6.9$  Hz, 1H), 1.84 (dt,  $J = 13.8, 7.1$  Hz, 1H), 1.47 – 1.38 (m, 1H), 1.38 (s, 3H), 1.33 (s, 3H).  $^{13}\text{C}$  NMR (101 MHz, Chloroform-*d*)  $\delta$  189.78, 173.62, 170.55, 153.56, 139.89, 129.84, 126.48, 122.55, 120.69, 82.00, 67.14, 60.27, 44.38, 43.32, 39.03, 34.48, 30.70, 29.03, 28.32, 24.65, 23.25. **45**:  $^1\text{H}$  NMR (400 MHz, Chloroform-*d*)  $\delta$  7.56 (dd,  $J = 7.7, 1.0$

Hz, 1H), 7.45 (dt,  $J = 7.1, 1.0$  Hz, 1H), 7.39 (td,  $J = 7.6, 1.3$  Hz, 1H), 7.30 – 7.21 (m, 1H), 7.07 (s, 1H), 3.77 (s, 1H), 3.46 (t,  $J = 6.8$  Hz, 2H), 2.86 (d,  $J = 15.8$  Hz, 1H), 2.83 – 2.74 (m, 2H), 2.14 (d,  $J = 22.6$  Hz, 1H), 2.07 (dd,  $J = 3.2, 2.1$  Hz, 2H), 2.05 – 1.98 (m, 2H), 1.86 (dt,  $J = 13.1, 7.3$  Hz, 1H), 1.48 (s, 3H), 1.35 (s, 3H).  $^{13}\text{C}$  NMR (101 MHz, Chloroform-*d*)  $\delta$  188.06, 172.45, 168.37, 152.21, 140.41, 130.49, 126.81, 122.41, 121.36, 82.65, 67.34, 62.07, 50.54, 44.25, 40.58, 38.02, 32.74, 29.23, 27.46, 24.57, 20.23.

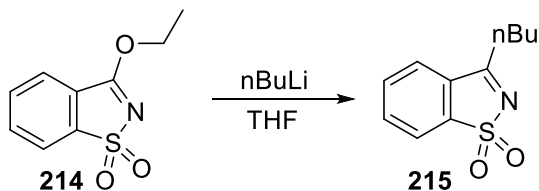


**(5aR,12aS,13aR)-6a-hydroxy-12,12-dimethyl-2,3,6a,12,12a,13-hexahydro-1H,5H,6H-**

**5a,13a-(epiminomethano)indolizino[7,6-b]carbazole-5,14-dione 216 & 217:** The synthesis of **216** and **217** was achieved by following the same protocol as for the synthesis of **45** and **46** with mCPBA. **216:**  $^1\text{H}$  NMR (400 MHz, Chloroform-*d*)  $\delta$  7.50 (d,  $J = 7.6$  Hz, 1H), 7.39 (q,  $J = 7.5$  Hz, 2H), 7.22 (d,  $J = 7.3$  Hz, 1H), 6.37 (s, 1H), 3.74 (dd,  $J = 10.0, 7.4$  Hz, 1H), 3.49 (ddt,  $J = 18.4, 11.6, 6.2$  Hz, 2H), 2.94 (d,  $J = 16.1$  Hz, 1H), 2.80 (dt,  $J = 12.8, 6.6$  Hz, 1H), 2.31 (d,  $J = 16.2$  Hz, 1H), 2.21 (t,  $J = 11.5$  Hz, 1H), 2.09 – 1.93 (m, 2H), 1.87 (dt,  $J = 13.3, 7.7$  Hz, 2H), 1.36 (s, 3H), 1.16 (s, 3H).  $^{13}\text{C}$  NMR (101 MHz, Chloroform-*d*)  $\delta$  189.86, 173.45, 167.94, 153.59, 139.37, 130.47, 126.66, 122.26, 121.13, 83.33, 67.17, 60.25, 48.55, 44.56, 38.66, 34.45, 31.59, 29.61, 28.83, 24.63, 21.20.

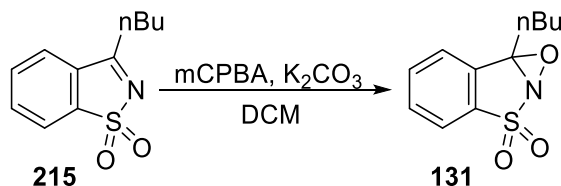


**3-ethoxybenzo[d]isothiazole 1,1-dioxide (214):**  $\text{PCl}_5$  (8.0 g, 39.0 mmols) and saccharin (5.49 g, 30.0 mmols) were added to a 500 mL round bottom flask connected to an air condenser. The reaction mixture was stirred vigorously while slowly heating the contents to 175 °C and run for 2 hours. The solution was concentrated, taken up in 400 mL of absolute ethanol, and refluxed for 1 hour. After reflux, the solution was cooled to rt and filtered. The filtrate was cooled to 0 °C and the solid was collected to yield 4.0 g of a needle-like solid (65%). **214:**  $^1\text{H}$  NMR (400 MHz, Chloroform-*d*)  $\delta$  7.89 (dd,  $J = 7.0, 1.5$  Hz, 1H), 7.79 – 7.67 (m, 3H), 4.67 (q,  $J = 7.1$  Hz, 2H), 1.53 (t,  $J = 7.1$  Hz, 3H).  $^{13}\text{C}$  NMR (101 MHz, Chloroform-*d*)  $\delta$  168.93, 143.34, 133.83, 133.22, 126.95, 123.14, 121.68, 68.04, 13.84.



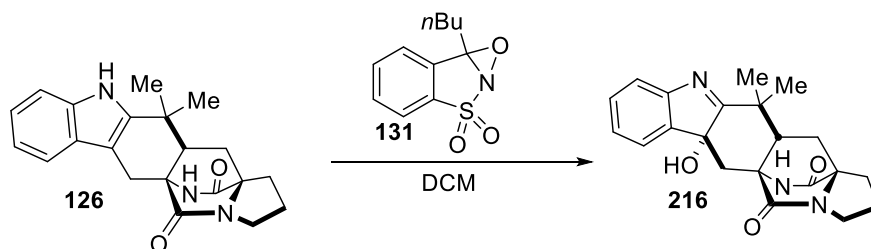
**3-butylbenzo[d]isothiazole 1,1-dioxide (215):** Fresh *n*-BuLi (1.6 M in hexanes, 3.85 mL, 6.15 mmols) was added to a solution of **214** (1.00 g, 4.73 mmols) in THF (95 mL) at -78 °C. Maintaining the -78 °C temperature, the reaction was left to run for 4 hours then quenched with  $\text{NH}_4\text{Cl}$ . The reaction mixture was extracted with EtOAc ( $\times 2$ ), washed with brine ( $\times 2$ ), dried over  $\text{MgSO}_4$ , filtered, and concentrated to give product as white crystals (0.864 g, 82%). **215:**  $^1\text{H}$  NMR (400 MHz, Chloroform-*d*)  $\delta$  7.95 – 7.85 (m, 1H), 7.81 – 7.64 (m, 3H), 4.66 (q,  $J = 7.1$  Hz, 1H), 3.01 – 2.93 (m, 2H), 1.93 – 1.85 (m, 1H), 1.85 (s, 0H), 1.58 – 1.50 (m, 1H), 1.54 – 1.44 (m,

2H), 0.99 (t,  $J = 7.4$  Hz, 2H).  $^{13}\text{C}$  NMR (101 MHz, Chloroform- $d$ )  $\delta$  176.47, 139.94, 134.00, 133.62, 131.46, 124.02, 122.58, 30.98, 27.58, 22.49, 13.90.



**7b-butyl-7bH-benzo[d][1,2]oxazireno[2,3-b]isothiazole 3,3-dioxide (Davis oxaziridine; 131):**

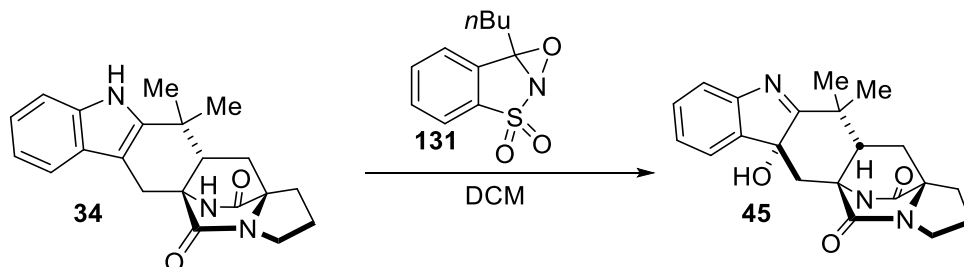
Imine **215** (624 mg, 2.79 mmols) was added to a mixture of saturated  $\text{K}_2\text{CO}_3$  (46.8 mL) and DCM (46.8 mL). While the mixture was stirred vigorously, mCPBA (1.45 g, 8.38 mmols) was dissolved in DCM (55 mL) and added dropwise over 30 minutes. The reaction was monitored by TLC for completion. Once the reaction was complete, the organic layer was separated, washed with  $\text{Na}_2\text{SO}_3$ ,  $\text{NaHCO}_3$ , and brine. The organic layer was dried over  $\text{Na}_2\text{SO}_4$ , filtered, and concentrated. The crude material was purified by column chromatography to yield a solid as product (500 mg, 75%). **131**:  $^1\text{H}$  NMR (400 MHz, Chloroform- $d$ )  $\delta$  7.82 – 7.76 (m, 1H), 7.75 – 7.68 (m, 3H), 2.60 (ddd,  $J = 15.1, 9.0, 6.1$  Hz, 1H), 2.24 (ddd,  $J = 14.9, 9.3, 6.6$  Hz, 1H), 1.66 – 1.49 (m, 2H), 1.49 – 1.37 (m, 2H), 0.94 (t,  $J = 7.2$  Hz, 3H).  $^{13}\text{C}$  NMR (101 MHz, Chloroform- $d$ )  $\delta$  134.63, 134.15, 133.59, 132.60, 126.00, 123.70, 86.43, 28.07, 25.64, 22.20, 13.64.



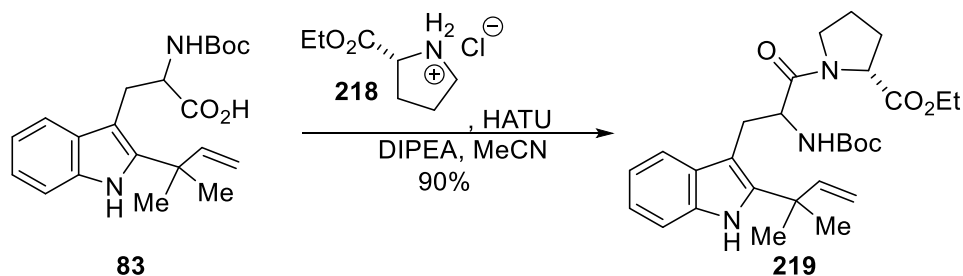
**(5aR,12aS,13aR)-6a-hydroxy-12,12-dimethyl-2,3,6a,12,12a,13-hexahydro-1H,5H,6H-**

**5a,13a-(epiminomethano)indolizino[7,6-b]carbazole-5,14-dione (216):** Davis oxaziridine was added to a solution of DA cycloadduct in DCM at rt. The reaction mixture was stirred overnight,

then concentrated. The crude oil was purified by flash column chromatography (6-10% MeOH/CHCl<sub>3</sub>). The material was further purified by preparative TLC with 6% MeOH/CHCl<sub>3</sub> to yield a pale yellow solid. Data for compound **216** is listed previously.

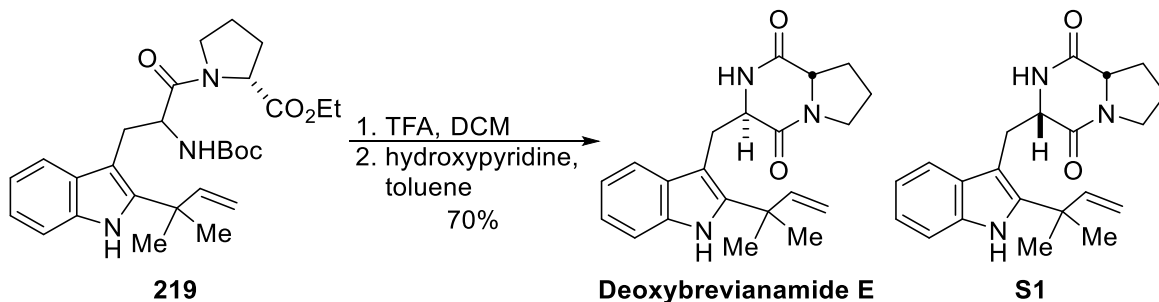


**(5aR,12aS,13aR)-6a-hydroxy-12,12-dimethyl-2,3,6a,12,12a,13-hexahydro-1H,5H,6H-5a,13a-(epiminomethano)indolizino[7,6-b]carbazole-5,14-dione (45)**: The synthesis of **45** was completed following the same procedure listed for the synthesis of **216** with Davis oxaziridine (**131**). All spectral data for **45** is listed previously.



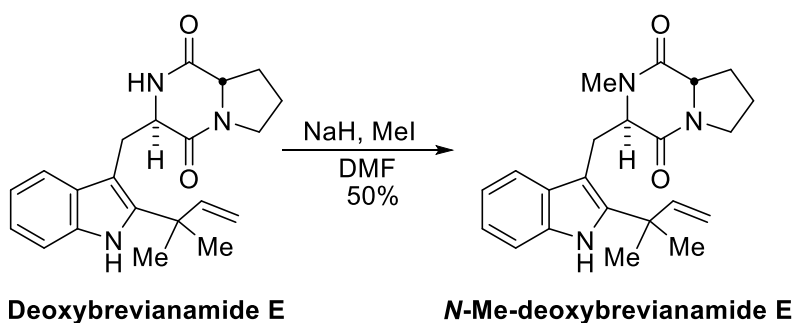
**ethyl (2-((tert-butoxycarbonyl)amino)-3-(2-(2-methylbut-3-en-2-yl)-1H-indol-3-yl)propanoyl)prolinate (219)**: HATU (1.35 g, 3.56 mmols) and DIPEA (1.39 mL, 8.04 mmols) were added to a solution of Boc-protected tryptophan **83** (1.00 g, 2.68 mmols) and proline salt (0.630 g, 3.484 mmols) in MeCN (16.0 mL) at rt and ran for 4 hours. The reaction was concentrated to an oil. The oil was partitioned between 34 mL of DCM and 34 mL of 1M HCl. The aqueous was re-extracted with DCM (2 × 13 mL). The organics were combined, washed with brine (2 × 21 mL), dried over Na<sub>2</sub>SO<sub>4</sub>, filtered and concentrated to a crude oil. The oil was purified by flash column chromatography (40-60% EtOAc/Hex) to yield an off-white foam

product (1.20 g, 90%) and carried forward immediately. **219**:  $^1\text{H}$  NMR (400 MHz, Chloroform-*d*)  $\delta$  7.87 (s, 1H), 7.56 – 7.45 (m, 1H), 7.29 – 7.18 (m, 1H), 7.12 – 7.06 (m, 1H), 7.09 – 6.99 (m, 1H), 6.13 (dd,  $J = 17.4, 10.5$  Hz, 1H), 5.60 (d,  $J = 8.1$  Hz, 1H), 5.26 – 5.14 (m, 3H), 4.73 – 4.42 (m, 1H), 4.20 – 4.01 (m, 3H), 3.46 – 3.07 (m, 4H), 1.63 (d,  $J = 6.4$  Hz, 6H), 1.44 (d,  $J = 3.3$  Hz, 9H), 1.26 (d,  $J = 2.4$  Hz, 3H), 1.24 – 1.15 (m, 3H).



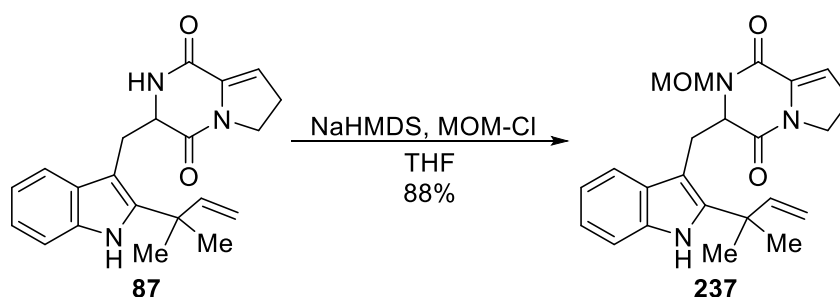
**Deoxybrevianamide E & S1:** TFA (5 mL) was added to a solution of dipeptide **219** (1.20 g, 2.00 mmols) in DCM (5 mL) at 0 °C then warmed to rt to run for 3 hours. The excess acid was quenched with  $\text{NaHCO}_3$ , extracted with EtOAc (2  $\times$  125 mL), dried over  $\text{Na}_2\text{SO}_4$ , filtered, and concentrated. The crude amine was taken up in toluene (20 mL) and 2-hydroxypyridine (38.25 mg, 0.403 mmols) was added to the solution. The reaction mixture was refluxed overnight then concentrated. The crude oil was partitioned between DCM and 1M HCl. The aqueous was extracted with DCM ( $\times 2$ ). The organics were combined, washed with brine, dried over  $\text{Na}_2\text{SO}_4$ , filtered, and concentrated. The material was purified by flash column chromatography (0-3% MeOH/DCM) to yield separable diastereomers as solids (492 mg, 70%). **Deoxybrevianamide E:**  $^1\text{H}$  NMR (400 MHz, Chloroform-*d*)  $\delta$  8.42 (s, 1H), 7.47 (dt,  $J = 7.8, 0.9$  Hz, 1H), 7.31 (dt,  $J = 8.1, 1.0$  Hz, 1H), 7.15 (ddd,  $J = 8.1, 7.1, 1.2$  Hz, 1H), 7.08 (ddd,  $J = 8.1, 7.0, 1.2$  Hz, 1H), 6.11 (dd,  $J = 17.5, 10.4$  Hz, 1H), 5.72 (s, 1H), 5.18 (d,  $J = 0.9$  Hz, 0H), 5.17 – 5.11 (m, 2H), 4.44 (ddd,  $J = 11.6, 4.1, 1.7$  Hz, 1H), 4.06 (ddd,  $J = 9.0, 6.7, 1.7$  Hz, 1H), 3.75 (dd,  $J = 15.3, 4.0$  Hz, 1H), 3.71 – 3.64 (m, 1H), 3.58 (ddd,  $J = 11.9, 8.8, 3.0$  Hz, 1H), 3.19 (dd,  $J = 15.3, 11.6$  Hz, 1H),

2.39 – 2.23 (m, 1H), 2.17 – 1.99 (m, 2H), 1.98 – 1.81 (m, 1H), 1.53 (d,  $J = 2.7$  Hz, 6H). **S1**:  $^1\text{H}$  NMR (400 MHz, Chloroform- $d$ )  $\delta$  8.35 (s, 1H), 7.54 – 7.47 (m, 1H), 7.29 – 7.22 (m, 1H), 7.07 (dddd,  $J = 21.0, 8.2, 7.0, 1.2$  Hz, 2H), 6.12 (dd,  $J = 17.4, 10.5$  Hz, 1H), 6.06 (d,  $J = 4.0$  Hz, 1H), 5.20 – 5.09 (m, 2H), 4.25 (ddd,  $J = 7.6, 5.8, 3.7$  Hz, 1H), 3.69 – 3.55 (m, 2H), 3.52 – 3.37 (m, 2H), 3.29 (dd,  $J = 14.6, 9.2$  Hz, 1H), 2.33 – 2.20 (m, 1H), 2.00 – 1.79 (m, 2H), 1.77 – 1.62 (m, 1H), 1.51 (d,  $J = 2.6$  Hz, 6H).



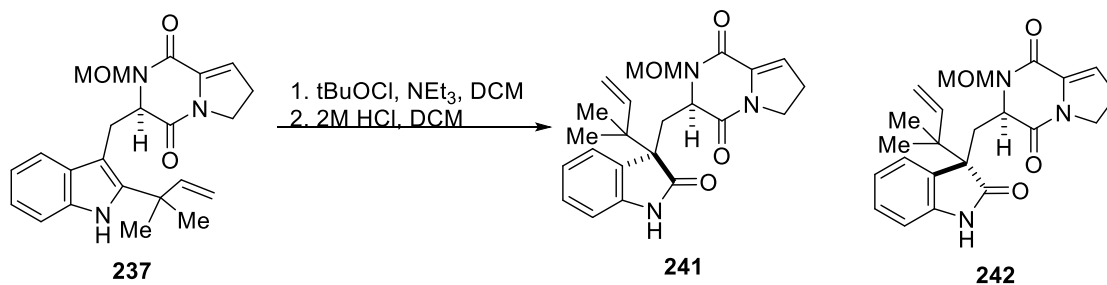
**N-methyl-deoxybrevianamide E**: NaH (60%, 69 mg, 1.72 mmol) was added to a solution of **deoxybrevianamide E** (400 mg, 1.14 mmols) in DMF (13 mL) at 0°C and ran for 30 minutes. MeI (~ 71 mL, 1.14 mmols) was added in 5 mL increments until TLC (3% MeOH/DCM) showed disappearance of starting material or appearance of double methylated material, keeping the temperature at 0 °C. The reaction mixture was partitioned between 57 mL of DCM and 57 mL of  $\text{NH}_4\text{Cl}$ . The aqueous layer was back-extracted with DCM (2 × 57 mL). The organics were combined, washed with 100 mL of brine, dried over  $\text{Na}_2\text{SO}_4$ , filtered, and concentrated. The crude material was purified by flash column chromatography (50-100% EtOAc/Hex) to yield 208 mg of product (50%). **N-methyl-deoxybrevianamide E**:  $^1\text{H}$  NMR (400 MHz, Chloroform- $d$ )  $\delta$  8.14 (s, 1H), 7.53 (dd,  $J = 7.7, 1.2$  Hz, 1H), 7.28 (dt,  $J = 8.2, 0.9$  Hz, 1H), 7.16 – 7.11 (m, 1H), 7.08 (ddd,  $J = 8.3, 7.0, 1.3$  Hz, 1H), 6.13 (dd,  $J = 17.5, 10.6$  Hz, 1H), 5.17 (dd,  $J = 14.6, 1.1$  Hz, 1H), 5.13 (dd,  $J = 7.7, 1.1$  Hz, 1H), 4.51 (dd,  $J = 8.9, 4.0$  Hz, 1H), 3.96 (dd,  $J = 11.1, 6.0$  Hz, 1H), 3.84 (dt,  $J = 12.1, 8.1$  Hz, 1H), 3.74 (dd,  $J = 15.1, 4.0$  Hz, 1H), 3.41 (s, 0H), 3.35 – 3.23 (m,

2H), 2.67 (s, 3H), 2.34 (dtd,  $J = 12.3, 6.2, 3.2$  Hz, 1H), 1.90 – 1.74 (m, 2H), 1.63 (dtd,  $J = 12.1, 11.2, 9.5$  Hz, 1H), 1.54 (d,  $J = 1.5$  Hz, 6H).  $^{13}\text{C}$  NMR (600 MHz,  $\text{CDCl}_3$ ):  $\delta$  166.8, 165.8, 146.0, 140.6, 134.3, 129.1, 122.1, 120.0, 118.6, 112.3, 110.8, 106.1, 63.1, 59.7, 45.1, 39.4, 34.3, 31.6, 29.3, 27.9, 27.8, 22.0.



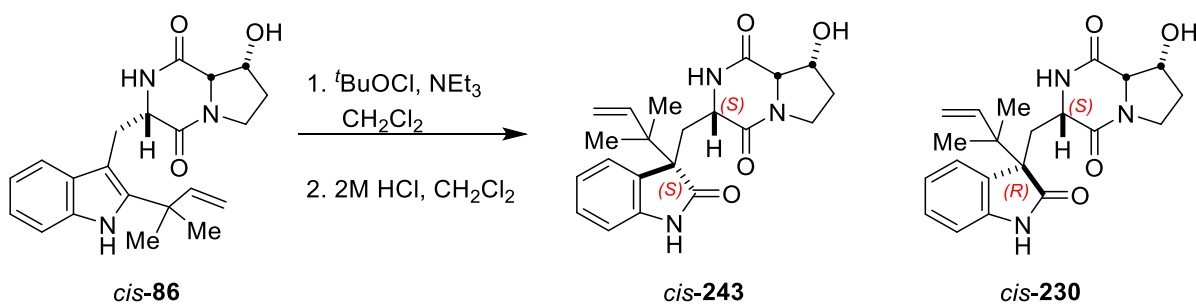
**2-(methoxymethyl)-3-((2-(2-methylbut-3-en-2-yl)-1H-indol-3-yl)methyl)-2,3,6,7-**

**tetrahydropyrrolo[1,2-a]pyrazine-1,4-dione (237):** NaHMDS (11.3 mL, 0.0913 mmols) was added to a solution of enamine **87** (29 mg, 0.083 mmols) in THF (1 mL) at  $-78$  °C. The bath was removed, and MOM-Cl was added in 1-3 mL increments every 10-15 minutes, checking TLC in-between to make sure double protection was not occurring.  $\text{NH}_4\text{Cl}$  was added to dilute the solution, and the solution was extracted with EtOAc ( $\times 2$ ), washed with brine, dried over  $\text{Na}_2\text{SO}_4$ , filtered, and concentrated to an oil. The crude oil was purified by preparative TLC (3% MeOH/DCM) to yield a pale-yellow solid (30 mg, 88%). **237:**  $^1\text{H}$  NMR (400 MHz, Chloroform-*d*)  $\delta$  7.92 (s, 1H), 7.50 – 7.46 (m, 1H), 7.30 – 7.24 (m, 1H), 7.14 (ddd,  $J = 8.0, 7.0, 1.4$  Hz, 1H), 7.09 (ddd,  $J = 8.2, 7.1, 1.3$  Hz, 1H), 6.16 (t,  $J = 3.1$  Hz, 1H), 6.10 (dd,  $J = 17.5, 10.5$  Hz, 1H), 5.25 – 5.13 (m, 2H), 5.08 (d,  $J = 10.3$  Hz, 1H), 4.58 (dd,  $J = 8.9, 4.6$  Hz, 1H), 4.00 (ddd,  $J = 12.8, 11.0, 5.5$  Hz, 1H), 3.85 (td,  $J = 11.7, 9.3$  Hz, 1H), 3.76 (d,  $J = 10.3$  Hz, 1H), 3.49 (dd,  $J = 14.7, 4.6$  Hz, 1H), 3.40 – 3.29 (m, 1H), 3.11 (s, 3H), 2.75 – 2.53 (m, 2H), 1.52 (d,  $J = 2.4$  Hz, 6H).



**(8R,8aS)-8-hydroxy-2-(methoxymethyl)-3-(((S)-3-(2-methylbut-3-en-2-yl)-2-oxoindolin-3-yl)methyl)hexahydropyrrolo[1,2-a]pyrazine-1,4-dione (241 & 242):** tBuOCl (58.8 mL, 0.518 mmols) was added to a solution of **237** (102 mg, 0.259 mmols) and NEt<sub>3</sub> (79.4 mL, 0.570 mmols) in DCM (4.65 mL) at 0 °C and ran for 2 hours. The reaction was concentrated to a yellow solid then immediately taken up in DCM (9.50 mL) and 2M HCl (9.50 mL) to run for 48 hours. The reaction mixture was basified with NaHCO<sub>3</sub>, extracted with DCM (×2), washed with brine, dried over Na<sub>2</sub>SO<sub>4</sub>, filtered, and concentrated. The material was purified by flash column chromatography (0-3% MeOH/DCM), then further purified by preparative TLC (3% MeOH/DCM) to yield separated diastereomers and a small amount of starting material. **242**: <sup>1</sup>H NMR (400 MHz, Chloroform-*d*) δ 8.23 (s, 1H), 7.19 (td, *J* = 7.7, 1.3 Hz, 1H), 7.10 (d, *J* = 7.4 Hz, 1H), 6.97 (td, *J* = 7.6, 1.1 Hz, 1H), 6.86 (d, *J* = 7.7 Hz, 1H), 6.13 – 6.01 (m, 2H), 5.12 (dd, *J* = 10.8, 1.2 Hz, 1H), 5.00 (dd, *J* = 17.4, 1.3 Hz, 1H), 4.85 (d, *J* = 10.4 Hz, 1H), 4.27 (d, *J* = 10.4 Hz, 1H), 4.16 (dd, *J* = 7.4, 4.8 Hz, 1H), 3.68 (td, *J* = 11.6, 8.5 Hz, 1H), 3.62 – 3.51 (m, 1H), 3.21 (s, 3H), 2.87 (dd, *J* = 14.8, 4.8 Hz, 1H), 2.77 – 2.53 (m, 2H), 2.33 (dd, *J* = 14.7, 7.5 Hz, 1H), 1.08 (s, 3H), 0.97 (s, 3H). **241**: <sup>1</sup>H NMR (400 MHz, Chloroform-*d*) δ 7.74 (s, 1H), 7.22 (d, *J* = 7.5 Hz, 1H), 7.17 (td, *J* = 7.7, 1.3 Hz, 1H), 6.95 (td, *J* = 7.6, 1.1 Hz, 1H), 6.74 (d, *J* = 7.8 Hz, 1H), 6.02 (dd, *J* = 17.5, 10.8 Hz, 1H), 5.75 (t, *J* = 3.0 Hz, 1H), 5.32 (d, *J* = 10.9 Hz, 1H), 5.11 (dd, *J* = 10.9, 1.2 Hz, 1H), 4.98 (dd, *J* = 17.4, 1.2 Hz, 1H), 4.47 (d, *J* = 10.9 Hz, 1H), 4.32 (dd, *J*

= 6.6, 2.1 Hz, 1H), 3.54 (dtd,  $J = 29.7, 12.1, 5.1$  Hz, 2H), 3.19 (s, 3H), 2.90 (dd,  $J = 15.1, 2.1$  Hz, 1H), 2.81 (dd,  $J = 15.1, 6.6$  Hz, 1H), 2.54 – 2.29 (m, 2H), 1.06 (s, 3H), 0.98 (s, 3H).

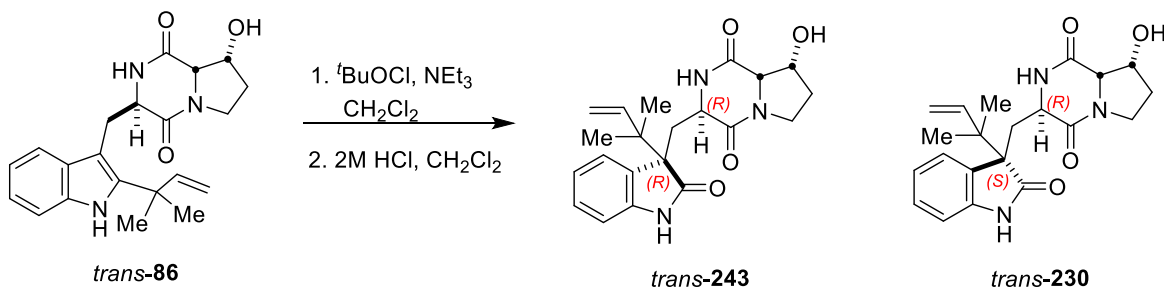


**(3S,8R,8aS)-8-hydroxy-3-(((S)-3-(2-methylbut-3-en-2-yl)-2-oxoindolin-3-yl)methyl)hexahydropyrrolo[1,2-a]pyrazine-1,4-dione & (3S,8R,8aS)-8-hydroxy-3-(((R)-3-(2-methylbut-3-en-2-yl)-2-oxoindolin-3-yl)methyl)hexahydropyrrolo[1,2-a]pyrazine-1,4-**

**dione (Cis-230 & 243):** tBuOCl (227  $\mu\text{L}$ , 2.18 mmols) and NEt<sub>3</sub> (334  $\mu\text{L}$ , 2.40 mmols) was added to a solution of *cis-86* (400 mg, 1.09 mmols) in DCM (20 mL) at 0 °C and run for 20-40 minutes maintaining the temperature. The reaction was concentrated before the addition of DCM (40 mL) and 2M HCl (40 mL), which then ran for 24 hours. Once complete, the reaction mixture was neutralized with NaHCO<sub>3</sub>, washed with DCM ( $\times 2$ ) and brine, dried over MgSO<sub>4</sub>, filtered and concentrated. The crude reaction mixture was purified by flash column chromatography (2-6% MeOH/DCM), to yield off-white solids (60% **230**, 5% **243**). *Cis-243*:  $[\alpha]_D^{23} -129$  (c 0.20, MeOH). <sup>1</sup>H NMR (400 MHz, Chloroform-*d*)  $\delta$  7.90 (s, 1H), 7.29 – 7.20 (m, 2H), 7.04 (td,  $J = 7.6, 1.1$  Hz, 1H), 6.88 (dt,  $J = 7.5, 0.9$  Hz, 1H), 6.65 (s, 1H), 6.03 (dd,  $J = 17.4, 10.8$  Hz, 1H), 5.13 (dd,  $J = 10.8, 1.1$  Hz, 1H), 5.02 (dd,  $J = 17.4, 1.1$  Hz, 1H), 4.61 (t,  $J = 3.7$  Hz, 1H), 3.96 – 3.88 (m, 1H), 3.71 (td,  $J = 11.3, 7.1$  Hz, 1H), 3.63 – 3.52 (m, 1H), 3.25 (dd,  $J = 15.1, 1.4$  Hz, 1H), 3.17 (d,  $J = 9.2$  Hz, 2H), 2.27 (dd,  $J = 15.0, 9.2$  Hz, 1H), 2.16 – 2.02 (m, 1H), 1.99 – 1.63 (m, 1H), 1.14 (s, 3H), 1.09 (s, 3H). <sup>13</sup>C NMR (101 MHz, Chloroform-*d*)  $\delta$  181.51, 168.33, 165.12, 142.36, 141.33, 129.59, 128.77, 126.34, 122.71, 114.82, 109.56, 70.85, 64.15, 58.04,

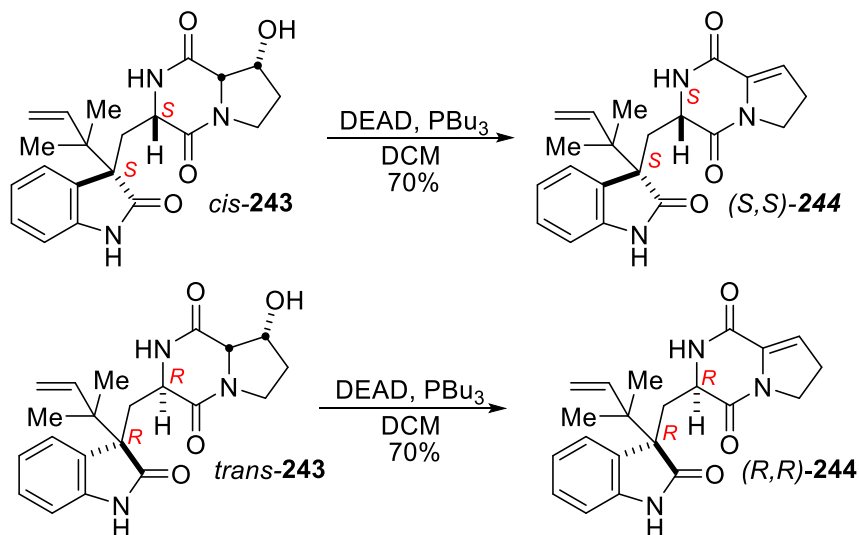
52.85, 44.41, 42.59, 30.28, 29.86, 22.54, 21.65. IR: 3274, 3086, 2955, 2922, 2852, 1682, 1619  $\text{cm}^{-1}$ . HRMS (ESI/Q-TOF)  $m/z$ :  $[M + H]^+$  Calcd for  $\text{C}_{21}\text{H}_{26}\text{N}_3\text{O}_4$  384.1918; Found 384.1909.

*Cis-230*:  $[\alpha]_D^{23}$  -45.6 ( $c$  0.50, MeOH)  $^1\text{H}$  NMR (400 MHz, Chloroform- $d$ )  $\delta$  8.77 (s, 1H), 7.30 (dd,  $J = 7.6, 1.2$  Hz, 1H), 7.25 – 7.20 (m, 1H), 7.03 (td,  $J = 7.6, 1.1$  Hz, 1H), 6.95 – 6.87 (m, 1H), 6.11 (s, 1H), 6.10 (dd,  $J = 17.4, 10.8$  Hz, 1H), 5.13 (dd,  $J = 10.9, 1.2$  Hz, 1H), 5.02 (dd,  $J = 17.5, 1.2$  Hz, 1H), 4.48 (q,  $J = 3.6, 3.1$  Hz, 1H), 4.06 (ddd,  $J = 6.5, 4.4, 1.9$  Hz, 1H), 3.91 (t,  $J = 2.7$  Hz, 1H), 3.57 – 3.46 (m, 2H), 3.00 (dd,  $J = 15.0, 4.5$  Hz, 1H), 2.63 – 2.51 (m, 2H), 2.03 – 1.80 (m, 2H), 1.14 (s, 3H), 1.05 (s, 3H).  $^{13}\text{C}$  NMR (101 MHz, Chloroform- $d$ )  $\delta$  180.97, 167.58, 164.89, 142.70, 141.74, 129.24, 129.04, 127.33, 121.67, 114.58, 110.32, 70.67, 63.99, 56.42, 54.02, 44.03, 43.03, 31.59, 30.29, 22.44, 21.60. IR: 3361, 3222, 3087, 2965, 2933, 2895, 1657, 1617  $\text{cm}^{-1}$ . HRMS (ESI/Q-TOF)  $m/z$ :  $[M + H]^+$  Calcd for  $\text{C}_{21}\text{H}_{26}\text{N}_3\text{O}_4$  384.1918; Found 384.1916.



**(3R,8R,8aS)-8-hydroxy-3-(((R)-3-(2-methylbut-3-en-2-yl)-2-oxindolin-3-yl)methyl)hexahydropyrrolo[1,2-a]pyrazine-1,4-dione & (3R,8R,8aS)-8-hydroxy-3-(((S)-3-(2-methylbut-3-en-2-yl)-2-oxindolin-3-yl)methyl)hexahydropyrrolo[1,2-a]pyrazine-1,4-dione (*Trans-230* & *243*):** The same procedure was followed as for the synthesis of *cis-230* and *cis-243* from *cis-86*. *Trans-230*:  $[\alpha]_D^{23}$  +82.3 ( $c$  0.265, MeOH)  $^1\text{H}$  NMR (400 MHz, Chloroform- $d$ )  $\delta$  10.76 (s, 1H), 8.44 (d,  $J = 5.1$  Hz, 1H), 7.23 (t,  $J = 7.4$  Hz, 2H), 7.04 (t,  $J = 7.5$

Hz, 1H), 6.90 (d,  $J = 7.8$  Hz, 1H), 6.06 (dd,  $J = 17.4, 10.8$  Hz, 1H), 5.14 (d,  $J = 10.8$  Hz, 1H), 5.03 (d,  $J = 17.4$  Hz, 1H), 4.54 (d,  $J = 3.8$  Hz, 1H), 4.20 (d,  $J = 3.2$  Hz, 1H), 3.71 – 3.60 (m, 2H), 3.43 (dt,  $J = 12.4, 4.3$  Hz, 1H), 2.82 (s, 1H), 2.48 (t,  $J = 13.2$  Hz, 1H), 2.40 (dd,  $J = 14.1, 3.7$  Hz, 1H), 2.17 – 2.07 (m, 1H), 2.06 – 1.94 (m, 1H), 1.15 (s, 3H), 1.05 (s, 3H).  $^{13}\text{C}$  NMR (101 MHz, Chloroform-*d*)  $\delta$  183.51, 169.99, 167.00, 142.70, 142.35, 128.14, 127.75, 126.28, 121.99, 114.66, 111.84, 70.86, 63.21, 56.60, 55.85, 44.34, 42.53, 33.96, 30.08, 22.07, 21.87. IR: 3207, 3083, 2961, 2927, 1702.1, 1660  $\text{cm}^{-1}$ . HRMS (ESI/Q-TOF)  $m/z$ :  $[\text{M} + \text{H}]^+$  Calcd for  $\text{C}_{21}\text{H}_{26}\text{N}_3\text{O}_4$  384.1918; Found 384.1921. *Trans*-**243**:  $[\alpha]_{\text{D}}^{23} -233$  ( $c$  0.33, MeOH);  $^1\text{H}$  NMR (400 MHz, Chloroform-*d*)  $\delta$  10.75 (s, 1H), 8.80 (s, 1H), 7.29 (td,  $J = 7.7, 1.3$  Hz, 1H), 7.19 (dd,  $J = 7.7, 1.3$  Hz, 1H), 7.09 – 6.89 (m, 2H), 6.02 (dd,  $J = 17.4, 10.8$  Hz, 1H), 5.11 (dd,  $J = 10.8, 1.1$  Hz, 1H), 4.98 (dd,  $J = 17.4, 1.2$  Hz, 1H), 4.23 – 4.15 (m, 1H), 3.93 (q,  $J = 8.6$  Hz, 1H), 3.46 (dt,  $J = 12.3, 8.5$  Hz, 1H), 3.14 (td,  $J = 12.4, 11.5, 2.9$  Hz, 1H), 3.00 – 2.88 (m, 2H), 2.77 (dd,  $J = 15.0, 7.5$  Hz, 1H), 2.19 – 2.07 (m, 1H), 1.60 – 1.41 (m, 2H), 1.10 (s, 3H), 0.97 (s, 3H).  $^{13}\text{C}$  NMR (101 MHz, Chloroform-*d*)  $\delta$  182.97, 169.04, 164.85, 143.50, 142.62, 129.08, 128.38, 128.15, 120.60, 114.52, 110.59, 72.10, 59.38, 56.26, 55.41, 42.88, 41.14, 33.19, 28.48, 22.01, 21.61. IR: 3212, 3084, 2963, 2928, 2893. HRMS (ESI/Q-TOF)  $m/z$ :  $[\text{M} + \text{H}]^+$  Calcd for  $\text{C}_{21}\text{H}_{26}\text{N}_3\text{O}_4$  384.1918; Found 384.1914



**(S)-3-(((S)-3-(2-methylbut-3-en-2-yl)-2-oxoindolin-3-yl)methyl)-2,3,6,7-**

**tetrahydropyrrolo[1,2-a]pyrazine-1,4-dione & (R)-3-(((R)-3-(2-methylbut-3-en-2-yl)-2-**

**oxoindolin-3-yl)methyl)-2,3,6,7-tetrahydropyrrolo[1,2-a]pyrazine-1,4-dione (**244**):** DEAD

(527  $\mu$ L, 1.16 mmols) was added to a solution of *cis* & *trans*-**243** (148 mg, 0.386 mmols) in

DCM (7.80 mL) at room temperature. After running for 15 minutes, PBU<sub>3</sub> (290  $\mu$ L, 1.16 mmols)

was added. The reaction was run until starting material was consumed (~ 3 hrs) and

concentrated. The crude material was purified by flash column chromatography eluting with 3-

10% MeOH/DCM to yield a pale yellow solid (70%). Each diastereomer was carried forward

separately. (*R,R*)-**244**:  $[\alpha]^{23}_D$  -25.8 (*c* 0.33, MeOH); <sup>1</sup>H NMR (400 MHz, Chloroform-*d*)  $\delta$  10.84

(s, 1H), 8.69 (s, 1H), 7.18 (d, *J* = 7.8 Hz, 1H), 7.12 (td, *J* = 7.6, 1.3 Hz, 1H), 6.94 – 6.84 (m, 2H),

6.08 (dd, *J* = 17.4, 10.8 Hz, 1H), 5.55 (t, *J* = 3.0 Hz, 1H), 5.10 (dd, *J* = 10.8, 1.2 Hz, 1H), 4.98

(dd, *J* = 17.4, 1.2 Hz, 1H), 4.31 (d, *J* = 7.2 Hz, 1H), 3.71 (t, *J* = 9.1 Hz, 2H), 3.08 – 2.99 (m, 1H),

2.75 (dd, *J* = 14.8, 7.4 Hz, 1H), 2.54 – 2.40 (m, 2H), 1.11 (s, 3H), 0.97 (s, 3H). <sup>13</sup>C NMR (101

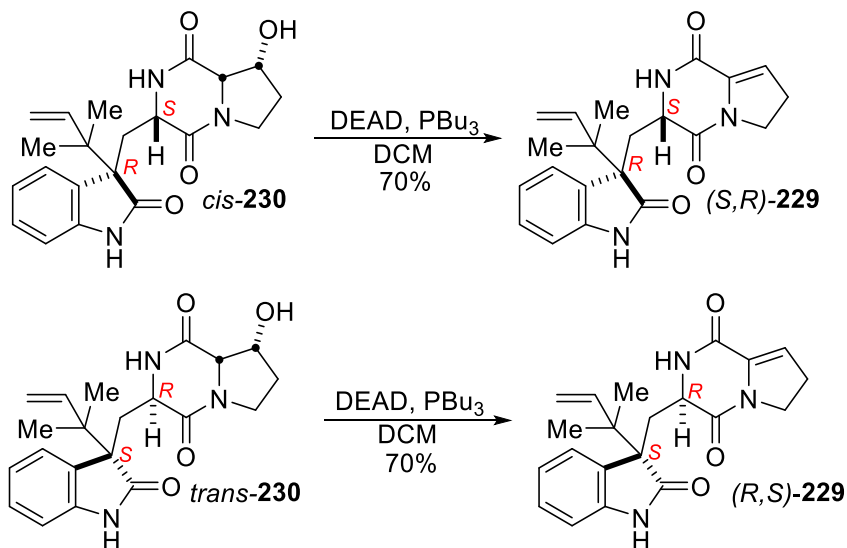
MHz, Chloroform-*d*)  $\delta$  183.09, 162.62, 157.56, 143.06, 132.14, 128.36, 128.06, 127.85, 120.46,

118.19, 114.16, 111.05, 56.25, 55.79, 45.25, 42.63, 33.75, 29.86, 27.50, 22.17, 21.61. IR: 3277,

2963, 2920, 2851, 1675, 1641, 1619, 1557  $\text{cm}^{-1}$ . HRMS (ESI/Q-TOF) *m/z*: [M + H]<sup>+</sup> Calcd for

C<sub>21</sub>H<sub>24</sub>N<sub>3</sub>O<sub>3</sub> 366.1812; Found 366.1811. (*S,S*)-**244**: [ $\alpha$ ]<sub>D</sub><sup>23</sup> +22.0 (*c* 0.10, MeOH). HRMS

(ESI/Q-TOF) *m/z*: [M + H]<sup>+</sup> Calcd for C<sub>21</sub>H<sub>24</sub>N<sub>3</sub>O<sub>3</sub> 366.1812; Found 366.1809.



**(S)-3-(((R)-3-(2-methylbut-3-en-2-yl)-2-oxoindolin-3-yl)methyl)-2,3,6,7-**

**tetrahydropyrrolo[1,2-a]pyrazine-1,4-dione & (R)-3-(((S)-3-(2-methylbut-3-en-2-yl)-2-**

**oxoindolin-3-yl)methyl)-2,3,6,7-tetrahydropyrrolo[1,2-a]pyrazine-1,4-dione (**229**):** The

synthesis of **229** was carried forward from *cis* & *trans*-**230** following the same procedure for the

synthesis of **229** from *cis/trans*-**230**. (*S,R*)-**229**: [ $\alpha$ ]<sub>D</sub><sup>23</sup> -177 (*c* 0.15, MeOH); HRMS (ESI/Q-

TOF) *m/z*: [M + H]<sup>+</sup> Calcd for C<sub>21</sub>H<sub>24</sub>N<sub>3</sub>O<sub>3</sub> 366.1812; Found 366.1817. (*R,S*)-**229**: [ $\alpha$ ]<sub>D</sub><sup>23</sup> +174

(*c* 0.25, MeOH). <sup>1</sup>H NMR (400 MHz, Chloroform-*d*)  $\delta$  10.41 (s, 1H), 7.65 (d, *J* = 3.9 Hz, 1H),

7.30 – 7.22 (m, 2H), 7.05 (td, *J* = 7.5, 1.1 Hz, 1H), 6.97 (dd, *J* = 8.1, 1.1 Hz, 1H), 6.06 (dd, *J* =

17.4, 10.8 Hz, 1H), 5.94 (t, *J* = 3.0 Hz, 1H), 5.14 (dd, *J* = 10.8, 1.1 Hz, 1H), 5.02 (dd, *J* = 17.4,

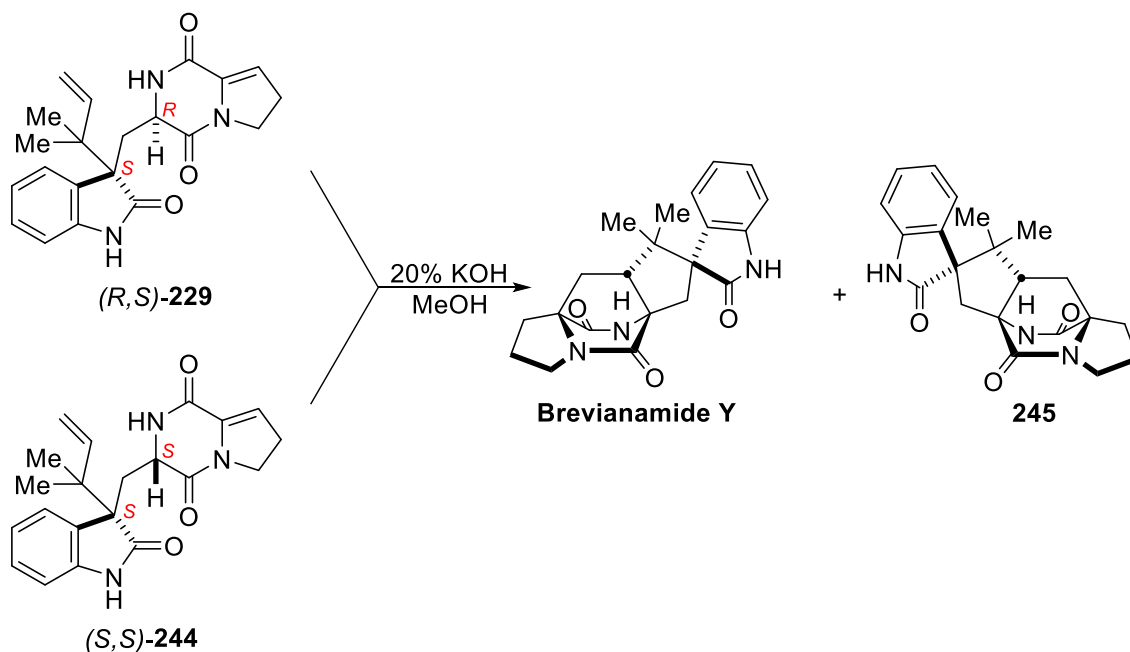
1.2 Hz, 1H), 4.05 (ddd, *J* = 12.4, 11.1, 5.4 Hz, 1H), 3.83 (td, *J* = 11.8, 8.3 Hz, 1H), 3.57 (dt, *J* =

11.9, 3.1 Hz, 1H), 2.81 (dddd, *J* = 19.1, 11.1, 8.3, 2.8 Hz, 1H), 2.67 (ddt, *J* = 19.5, 10.2, 3.1 Hz,

2H), 2.41 (dd, *J* = 13.9, 11.8 Hz, 1H), 1.16 (s, 3H), 1.05 (s, 3H). <sup>13</sup>C NMR (101 MHz,

Chloroform-*d*)  $\delta$  182.97, 163.64, 157.92, 142.75, 142.33, 133.37, 128.20, 127.92, 126.33,

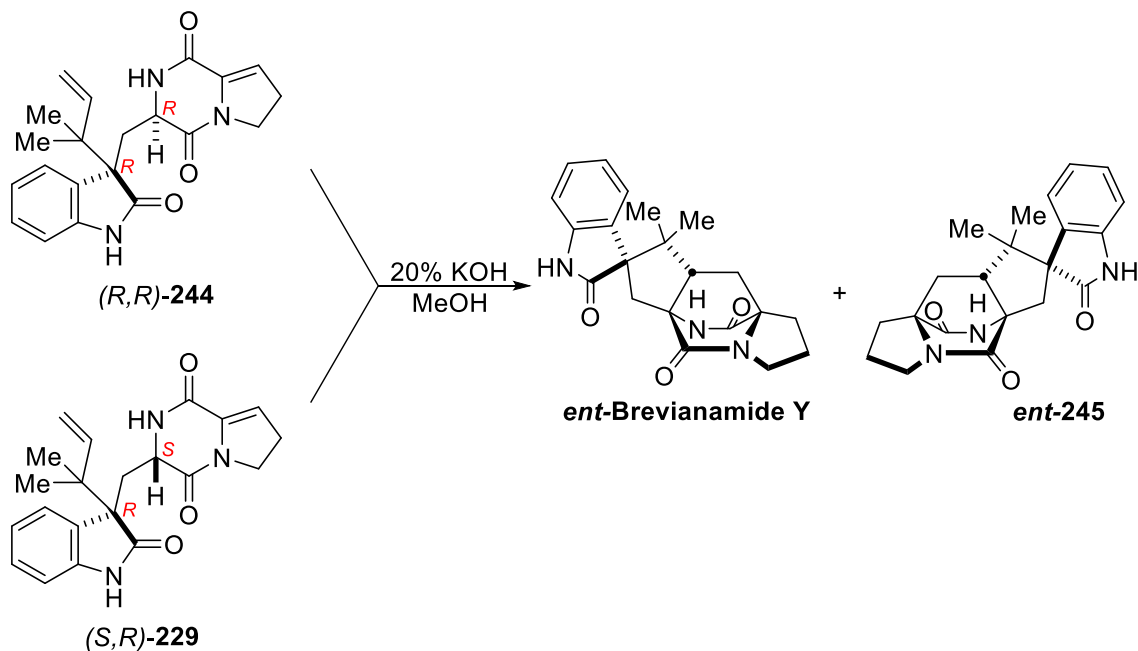
121.90, 118.90, 114.58, 112.07, 56.70, 55.86, 45.74, 42.61, 38.98, 28.01, 22.04, 21.90. IR: 3212, 3086, 2963, 2926, 2853, 1703, 1677, 1644, 1618  $\text{cm}^{-1}$ . HRMS (ESI/Q-TOF)  $m/z$ :  $[M + H]^+$  Calcd for  $\text{C}_{21}\text{H}_{24}\text{N}_3\text{O}_3$  366.1812; Found 366.1844.



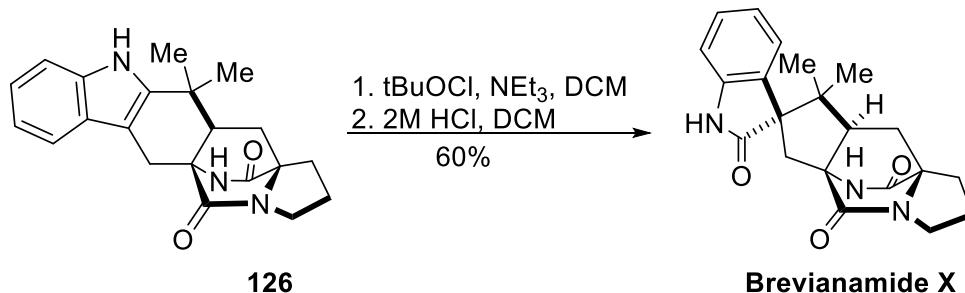
**Brevianamide Y & Compound 245:** A 20% aqueous solution of KOH (7.53 mL) was added to a solution of (R,S)-229 & (S,S)-244 (110 mg, 0.30 mmols) in MeOH (25 mL) at 0 °C and slowly warmed to rt over the course of an hour. The reaction was run at rt for an additional 12 hours. The reaction was quenched with  $\text{NH}_4\text{Cl}$ , and extracted with DCM ( $\times 3$ ). The combined organics were washed with brine, dried over  $\text{Na}_2\text{SO}_4$ , filtered and concentrated. The crude oil was purified by flash column chromatography with 1-6% MeOH/ $\text{CHCl}_3$  to yield a mixture of diastereomers as a white solid. The diastereomers could be partially separated by preparative TLC with 3% MeOH/ $\text{CDCl}_3$ . **Brevianamide Y:**  $^1\text{H}$  NMR (500 MHz,  $\text{DMSO}-d_6$ )  $\delta$  10.29 (s, 1H), 8.79 (s, 1H), 7.42 (d,  $J = 7.5$  Hz, 1H), 7.19 (td,  $J = 7.7, 1.2$  Hz, 1H), 6.98 (td,  $J = 7.5, 1.1$  Hz, 1H), 6.80 (d,  $J = 7.7$  Hz, 1H), 3.31 – 3.22 (m, 1H), 3.17 (dd,  $J = 10.4, 7.2$  Hz, 1H), 2.82 (d,  $J = 15.1$  Hz, 1H), 2.46 (dd,  $J = 12.1, 6.4$  Hz, 1H), 2.13 (d,  $J = 15.2$  Hz, 1H), 2.04 – 1.89 (m, 2H), 1.87 – 1.73 (m, 2H),

1.65 (dd,  $J = 13.0, 7.2$  Hz, 1H), 1.23 (s, 1H), 0.99 (s, 3H), 0.69 (s, 3H).  $^{13}\text{C}$  NMR (126 MHz, DMSO- $d_6$ )  $\delta$  181.86, 172.53, 169.08, 142.42, 129.78, 128.14, 126.30, 120.84, 109.05, 68.58, 67.17, 62.11, 50.04, 46.85, 43.25, 33.63, 28.44, 27.96, 24.45, 22.99, 20.41.  $^1\text{H}$  NMR (400 MHz, Methanol- $d_4$ )  $\delta$  7.42 – 7.36 (m, 1H), 7.23 (td,  $J = 7.7, 1.2$  Hz, 1H), 7.03 (td,  $J = 7.6, 1.1$  Hz, 1H), 6.88 (d,  $J = 7.9$  Hz, 1H), 3.49 – 3.38 (m, 3H), 3.06 (d,  $J = 15.5$  Hz, 1H), 2.66 (dt,  $J = 12.8, 6.2$  Hz, 1H), 2.18 (d,  $J = 15.5$  Hz, 1H), 2.14 – 1.87 (m, 4H), 1.79 (dd,  $J = 13.1, 7.4$  Hz, 1H), 1.10 (s, 3H), 0.82 (s, 3H).  $^{13}\text{C}$  NMR (101 MHz, Methanol- $d_4$ )  $\delta$  184.43, 175.64, 172.10, 143.63, 130.88, 129.60, 127.34, 122.72, 110.60, 70.85, 69.24, 64.37, 44.84, 35.24, 30.78, 29.86, 29.36, 25.86, 23.46, 21.05.  $[\alpha]_D^{23} +120$  ( $c$  0.10, MeOH). IR: 3245, 2925, 2854, 1677  $\text{cm}^{-1}$ . HRMS (ESI/Q-TOF)  $m/z$ :  $[\text{M} + \text{H}]^+$  Calcd for  $\text{C}_{21}\text{H}_{24}\text{N}_3\text{O}_3$  366.1812; Found 366.1822. **245**:  $^1\text{H}$  NMR (400 MHz, DMSO- $d_6$ )  $\delta$  10.29 (s, 1H), 8.70 (s, 1H), 7.17 (td,  $J = 7.6, 1.2$  Hz, 1H), 7.06 (d,  $J = 7.1$  Hz, 1H), 6.93 (td,  $J = 7.6, 1.1$  Hz, 1H), 6.82 (dd,  $J = 7.7, 1.1$  Hz, 1H), 3.32 – 3.23 (m, 1H), 3.17 (d,  $J = 5.2$  Hz, 1H), 2.67 – 2.54 (m, 2H), 2.45 (dd,  $J = 13.5, 5.9$  Hz, 2H), 2.06 – 1.88 (m, 2H), 1.90 – 1.72 (m, 2H), 1.65 (dd,  $J = 13.0, 7.4$  Hz, 1H), 1.05 (s, 3H), 0.41 (s, 3H).  $^{13}\text{C}$  NMR (126 MHz, DMSO- $d_6$ )  $\delta$  178.68, 172.33, 169.51, 141.52, 134.34, 127.88, 124.05, 121.07, 109.15, 68.53, 67.54, 62.44, 53.07, 47.79, 43.38, 33.12, 28.42, 27.31, 24.43, 23.18, 19.51.  $^1\text{H}$  NMR (400 MHz, Methanol- $d_4$ )  $\delta$  7.25 – 7.15 (m, 2H), 6.99 (td,  $J = 7.6, 1.1$  Hz, 1H), 6.91 – 6.83 (m, 1H), 3.52 (dt,  $J = 11.1, 6.9$  Hz, 1H), 3.48 – 3.40 (m, 1H), 2.85 (d,  $J = 15.4$  Hz, 1H), 2.81 – 2.76 (m, 1H), 2.66 (dt,  $J = 13.1, 6.6$  Hz, 1H), 2.49 (d,  $J = 15.4$  Hz, 1H), 2.18 – 2.07 (m, 1H), 2.07 – 2.00 (m, 2H), 1.96 – 1.87 (m, 1H), 1.79 (dd,  $J = 13.2, 7.2$  Hz, 1H), 1.16 (s, 3H), 0.55 (s, 3H).  $^{13}\text{C}$  NMR (101 MHz, Methanol- $d_4$ )  $\delta$  181.78, 175.20, 172.00, 142.63, 135.82, 129.30, 125.52, 122.97, 110.70, 70.89, 69.86, 64.54, 55.36, 44.92, 34.94, 30.79, 29.78, 29.21, 25.82, 24.43, 20.58.  $[\alpha]_D^{23} +212$  ( $c$

0.05, MeOH). IR: 3230, 2970, 2872, 1718  $\text{cm}^{-1}$ . HRMS (ESI/Q-TOF)  $m/z$ :  $[\text{M} + \text{H}]^+$  Calcd for  $\text{C}_{21}\text{H}_{24}\text{N}_3\text{O}_3$  366.1812; Found 366.1803.

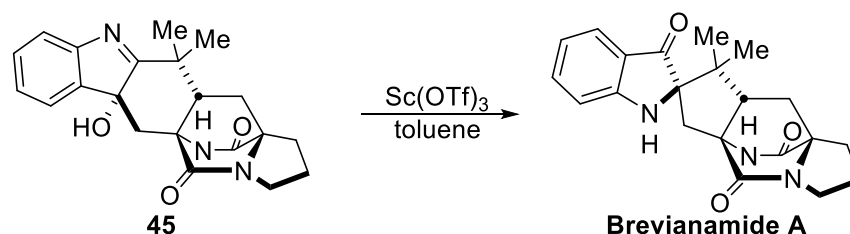


**Ent-Brevianamide Y & Ent-245:** The synthesis of *ent*-brevianamide Y and *ent*-245 that from *trans/cis*-245 was achieved following the same procedure as seen for the synthesis of **brevianamide Y** and **245** from (*R,R*)-244 & (*S,R*)-229. All spectra data matches that from **brevianamide Y** and **245**. *ent*-Brevianamide Y:  $[\alpha]_{\text{D}}^{23}$  -117 (*c* 0.15, MeOH). HRMS (ESI/Q-TOF)  $m/z$ :  $[\text{M} + \text{H}]^+$  Calcd for  $\text{C}_{21}\text{H}_{24}\text{N}_3\text{O}_3$  366.1812; Found 366.1807. *ent*-245:  $[\alpha]_{\text{D}}^{23}$  -136 (*c* 0.10, MeOH). HRMS (ESI/Q-TOF)  $m/z$ :  $[\text{M} + \text{H}]^+$  Calcd for  $\text{C}_{21}\text{H}_{24}\text{N}_3\text{O}_3$  366.1812; Found 366.1805.

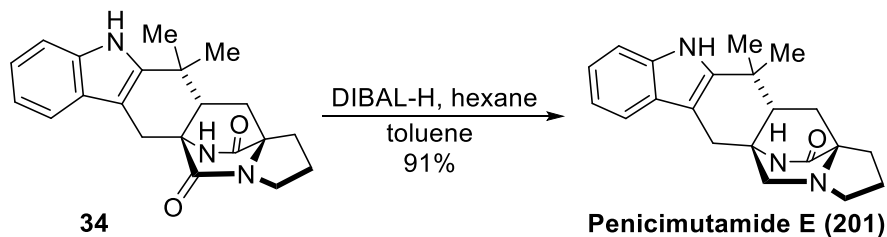


**Brevianamide X:** tBuOCl (64.7 mL, 0.57 mmols) and NEt<sub>3</sub> (88 mL, 0.63 mmols) was added to a solution of syn DA (50 mg, 0.143 mmols) in DCM (2.55 mL) at 0 °C and ran for 3 hours. The reaction mixture was warmed to rt before concentrating. The bright yellow solid is immediately taken up in DCM (5.25 mL) and 2M HCl (5.25 mL), and stirred vigorously for 48 hours. The mixture was quenched with NaHCO<sub>3</sub>, extracted with DCM (×2), washed with brine, dried over Na<sub>2</sub>SO<sub>4</sub>, filtered, and concentrated. The crude material was purified by flash column chromatography (2-10% MeOH/CHCl<sub>3</sub>) to yield a white solid product (65%, 34 mg). <sup>1</sup>H NMR (400 MHz, DMSO-*d*<sub>6</sub>) δ 10.34 (s, 1H), 9.10 (s, 1H), 7.22 (dd, *J* = 7.6, 1.2 Hz, 1H), 7.19 (td, *J* = 7.7, 1.2 Hz, 1H), 6.97 (td, *J* = 7.6, 1.1 Hz, 1H), 6.82 (dd, *J* = 7.7, 1.1 Hz, 1H), 3.40 (overlap with H<sub>2</sub>O, 2H), 3.22 (dd, *J* = 10.3, 8.2 Hz, 1H), 2.85 (d, *J* = 14.2 Hz, 1H), 2.50 (overlap with DMSO-D, 2H), 2.19 (d, *J* = 14.1 Hz, 1H), 2.05 – 1.89 (m, 2H), 1.87 – 1.71 (m, 3H), 0.73 (s, 3H), 0.71 (s, 3H). <sup>13</sup>C NMR (101 MHz, DMSO-*d*<sub>6</sub>) δ 182.37, 173.15, 169.45, 142.34, 130.59, 128.11, 126.02, 121.12, 109.23, 68.13, 65.68, 61.47, 55.48, 45.14, 43.44, 33.15, 29.45, 29.03, 24.38, 23.28, 19.75. <sup>1</sup>H NMR (400 MHz, Chloroform-*d*) δ 7.71 (s, 1H), 7.43 (d, *J* = 7.5 Hz, 1H), 7.22 (td, *J* = 7.7, 1.2 Hz, 1H), 7.06 – 7.02 (m, 1H), 7.00 (s, 1H), 6.86 (d, *J* = 7.7 Hz, 1H), 3.64 (ddd, *J* = 11.8, 7.5, 4.5 Hz, 1H), 3.51 (dt, *J* = 10.5, 7.8 Hz, 2H), 3.30 (d, *J* = 14.8 Hz, 1H), 2.85 – 2.74 (m, 1H), 2.21 (d, *J* = 14.8 Hz, 1H), 2.16 – 1.93 (m, 3H), 1.83 (dt, *J* = 13.2, 8.1 Hz, 1H), 1.72 (dd, *J* = 12.8, 8.4 Hz, 1H), 0.89 (s, 3H), 0.84 (s, 3H). <sup>13</sup>C NMR (101 MHz, Chloroform-*d*) δ 183.20, 174.12, 169.52, 140.87, 130.24, 128.32, 127.03, 122.31, 109.33, 68.83, 66.74, 62.33, 56.06, 46.15, 43.94,

34.56, 30.67, 29.71, 29.69, 24.86, 23.35, 19.88. HRMS (ESI/Q-TOF)  $m/z$ :  $[M + H]^+$  Calcd for  $C_{21}H_{24}N_3O_3$  366.1812; Found 366.1802.

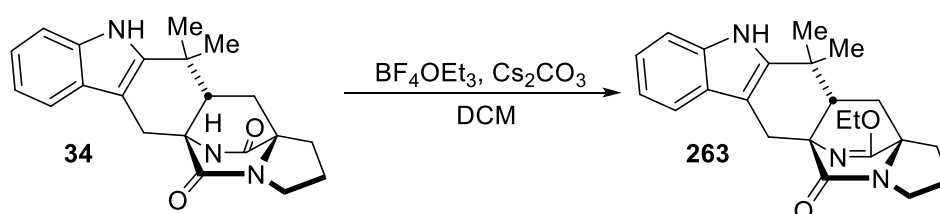


**Brevianamide A:** Sc(OTf)<sub>3</sub> (67 mg, 0.136 mmols) was added to a solution of hydroxyindolenine **45** (25 mg, 0.0684 mmols) in toluene (13.6 mL). The solution was heated to reflux, ran overnight, and cooled to room temperature. The fluorescent yellow reaction mixture was quenched with NaHCO<sub>3</sub>, extracted with DCM, and dried over Na<sub>2</sub>SO<sub>4</sub>, filtered, and concentrated. The crude material was purified by flash column using 3-6% MeOH/DCM to yield a fluorescent yellow solid (89%). **Brevianamide A:** <sup>1</sup>H NMR (400 MHz, Chloroform-*d*)  $\delta$  7.57 (d,  $J = 7.7$  Hz, 1H), 7.45 (ddd,  $J = 8.3, 7.0, 1.3$  Hz, 1H), 6.86 – 6.77 (m, 2H), 6.66 (s, 1H), 4.96 (s, 1H), 3.47 (td,  $J = 6.6, 4.3$  Hz, 2H), 2.77 (td,  $J = 10.8, 9.6, 6.1$  Hz, 2H), 2.44 – 2.32 (m, 2H), 2.04 (p,  $J = 7.3, 6.7$  Hz, 2H), 1.93 (dd,  $J = 13.3, 9.7$  Hz, 1H), 1.92 – 1.85 (m, 1H), 1.84 (dd,  $J = 8.5, 5.9$  Hz, 1H), 1.12 (s, 3H), 0.93 (s, 3H). <sup>13</sup>C NMR (101 MHz, Chloroform-*d*)  $\delta$  202.20, 172.43, 169.78, 160.17, 137.78, 124.84, 121.18, 119.37, 112.11, 78.86, 69.52, 67.82, 55.74, 48.46, 44.05, 37.42, 29.18, 28.96, 25.11, 24.09, 19.86. IR: 3324, 3262, 2922, 2852, 1671, 1618, 1487, 1463, 1390 cm<sup>-1</sup>. HRMS (ESI/Q-TOF)  $m/z$ :  $[M + Na]^+$  Calcd for  $C_{21}H_{23}N_3O_3Na$  388.1632; Found 388.1645.



**Penicimutamide E:** A 0.005 M solution of **34** (25 mg, 0.0715 mmols) was created in toluene (13.75 mL), then brought to 0 °C. To the cooled solution, 1M DIBAL in hexane (1.43 mL) and then allowed to warm to rt and run for 24 hrs. The reaction was quenched with Na<sub>2</sub>SO<sub>4</sub> • 10H<sub>2</sub>O (0.66 g) or until bubbling subsides. The reaction mix was run for an additional 30 minutes and then filtered through a fritted funnel. The solid residue was rinsed with ethyl acetate, and the combined filtrates were evaporated under reduced pressure. The product was isolated via flash silica gel column chromatography or PTLC using 2% MeOH/CHCl<sub>3</sub> as a white solid (22 mg, 91.7%). **Penicimutamide E:** <sup>1</sup>H NMR (400 MHz, Chloroform-*d*) δ 7.91 (s, 1H), 7.46 – 7.39 (m, 1H), 7.32 (dt, *J* = 8.1, 1.0 Hz, 1H), 7.17 (ddd, *J* = 8.1, 7.1, 1.3 Hz, 1H), 7.11 (ddd, *J* = 8.2, 7.2, 1.1 Hz, 1H), 5.76 – 5.71 (m, 1H), 3.19 (d, *J* = 10.3 Hz, 1H), 3.14 (s, 1H), 2.95 (d, *J* = 17.2 Hz, 1H), 2.81 (d, *J* = 17.2 Hz, 1H), 2.67 (d, *J* = 10.3 Hz, 1H), 2.64 – 2.55 (m, 1H), 2.38 (q, *J* = 8.6 Hz, 1H), 2.23 – 2.15 (m, 1H), 2.12 (d, *J* = 10.6 Hz, 1H), 1.95 (ddd, *J* = 12.6, 8.4, 3.8 Hz, 3H), 1.52 – 1.37 (m, 1H), 1.28 (s, 3H), 1.20 (s, 3H). <sup>1</sup>H NMR (400 MHz, Methanol-*d*<sub>4</sub>) δ 7.38 (dt, *J* = 7.6, 1.1 Hz, 1H), 7.27 (dt, *J* = 8.1, 1.0 Hz, 1H), 7.04 (ddd, *J* = 8.1, 7.1, 1.3 Hz, 1H), 6.96 (ddd, *J* = 8.0, 7.1, 1.1 Hz, 1H), 3.17 – 3.07 (m, 2H), 3.00 (d, *J* = 16.9 Hz, 1H), 2.86 (d, *J* = 17.0 Hz, 1H), 2.68 (d, *J* = 10.6 Hz, 1H), 2.59 – 2.47 (m, 1H), 2.45 – 2.34 (m, 1H), 2.21 (dd, *J* = 10.1, 3.4 Hz, 1H), 2.15 (dd, *J* = 13.1, 10.1 Hz, 1H), 1.93 (dddd, *J* = 13.2, 9.1, 5.0, 2.3 Hz, 3H), 1.47 (ddd, *J* = 12.5, 10.1, 7.6 Hz, 1H), 1.32 (s, 3H), 1.20 (s, 3H). <sup>13</sup>C NMR (101 MHz, Chloroform-*d*) δ 173.83, 141.60, 136.43, 127.11, 122.06, 119.74, 118.01, 110.96, 103.34, 65.44, 62.46, 56.00, 53.60, 46.17, 34.36, 29.85, 29.39, 27.97, 27.38, 24.96, 22.94. <sup>13</sup>C NMR (101 MHz, Methanol-*d*<sub>4</sub>) δ

175.90, 142.72, 138.41, 128.43, 121.95, 119.51, 118.49, 111.68, 103.67, 66.51, 62.38, 56.81, 54.28, 47.53, 35.57, 31.85, 29.12, 28.08, 28.06, 24.56, 23.34. IR: 3240, 3170, 3055, 2958, 2933, 2900, 2811, 1664, 1459, 1411, 1375, 1305, 1294, 1238, 1212, 1193, 1132  $\text{cm}^{-1}$ . HRMS (ESI/Q-TOF)  $m/z$ :  $[M + H]^+$  Calcd for  $\text{C}_{21}\text{H}_{26}\text{N}_3\text{O}$  336.2071; Found 336.2081.



**(5a*S*,12a*S*,13a*S*)-14-ethoxy-12,12-dimethyl-2,3,11,12,12a,13-hexahydro-1*H*,5*H*,6*H*-5a,13a-(azenometheno)indolizino[7,6-*b*]carbazol-5-one (263):**  $\text{BF}_4\text{OEt}_3$  (54.5 mg, 0.286) and  $\text{Cs}_2\text{CO}_3$  (140 mg, 0.43 mmols) to a solution of cycloadduct **34** (50 mg, 0.43 mmols) in DCM (10 mL) at 0 °C. The solution was warmed to rt then refluxed overnight. Once the reaction mixture cooled to rt, it was filtered over celite with a fritted funnel, and rinsed with DCM. The resulting solution was washed with  $\text{NH}_4\text{Cl}$  and brine, dried over  $\text{Na}_2\text{SO}_4$ , filtered and concentrated. The material was further purified by flash column chromatography with 2-6% MeOH/DCM (45 mg, 83%).

**263:**  $^1\text{H}$  NMR (400 MHz, Chloroform-*d*)  $\delta$  8.02 (s, 1H), 7.62 – 7.52 (m, 1H), 7.32 (s, 0H), 7.29 (dt,  $J = 8.1, 0.9$  Hz, 1H), 7.16 (s, 0H), 7.10 (dtd,  $J = 16.9, 7.1, 1.3$  Hz, 2H), 4.14 (ddt,  $J = 11.1, 7.1, 3.8$  Hz, 1H), 4.04 (dq,  $J = 10.7, 7.1$  Hz, 1H), 3.93 (d,  $J = 17.1$  Hz, 1H), 3.55 – 3.42 (m, 2H), 3.48 (d,  $J = 57.3$  Hz, 0H), 3.30 (d,  $J = 17.1$  Hz, 1H), 2.76 – 2.64 (m, 1H), 2.33 (dd,  $J = 9.8, 4.1$  Hz, 1H), 2.11 – 1.86 (m, 5H), 1.82 (dd,  $J = 12.9, 4.2$  Hz, 1H), 1.27 – 1.24 (m, 6H), 1.16 (s, 3H).  $^{13}\text{C}$  NMR (101 MHz, Chloroform-*d*)  $\delta$  172.49, 170.25, 140.01, 136.55, 128.11, 121.38, 119.14, 118.85, 110.50, 106.19, 67.27, 64.30, 62.86, 53.54, 45.92, 43.69, 35.01, 33.58, 29.24, 28.49, 26.26, 25.40, 24.80.



**(5aS,12aS,13aS)-14-ethoxy-12,12-dimethyl-2,3,11,12,12a,13-hexahydro-1H,5H,6H-5a,13a-(azenometheno)indolizino[7,6-b]carbazole (S4):**  $\text{BF}_4\text{OEt}_3$  (27.19 mg, 0.143 mmols) and  $\text{Cs}_2\text{CO}_3$  (70 mg, 0.215 mmols) was added to a solution of **penicimutamide E** (24 mg, 0.072 mmols) at 0 °C, then heated to reflux overnight. The reaction mixture was cooled to rt before filtering over celite in a fritted funnel, using DCM to wash. The organic solution was washed with  $\text{NH}_4\text{Cl}$ , brine, dried over  $\text{Na}_2\text{SO}_4$ , filtered, and concentrated. The crude material was purified with 1-5% MeOH/DCM to yield an off-white solid (15 mg, 58%). **S4:**  $^1\text{H}$  NMR (400 MHz, Chloroform-*d*)  $\delta$  7.80 (s, 1H), 7.49 – 7.43 (m, 1H), 7.29 (dd,  $J = 7.8, 1.1$  Hz, 1H), 7.12 (ddd,  $J = 8.1, 7.1, 1.4$  Hz, 1H), 7.06 (td,  $J = 7.4, 1.2$  Hz, 1H), 4.21 – 4.09 (m, 1H), 4.01 (dq,  $J = 10.6, 7.1$  Hz, 1H), 3.20 (d,  $J = 16.4$  Hz, 1H), 2.92 (d,  $J = 28.6$  Hz, 2H), 2.81 (d,  $J = 16.4$  Hz, 1H), 2.46 (ddd,  $J = 12.7, 9.2, 3.6$  Hz, 1H), 2.29 – 2.21 (m, 2H), 2.10 (q,  $J = 8.7$  Hz, 1H), 1.78 – 1.62 (m, 2H), 1.61 – 1.48 (m, 2H), 1.43 (p,  $J = 7.3$  Hz, 1H), 1.25 (s, 3H), 1.22 (s, 3H), 1.08 (s, 3H).

## Chapter 2: NMR Data

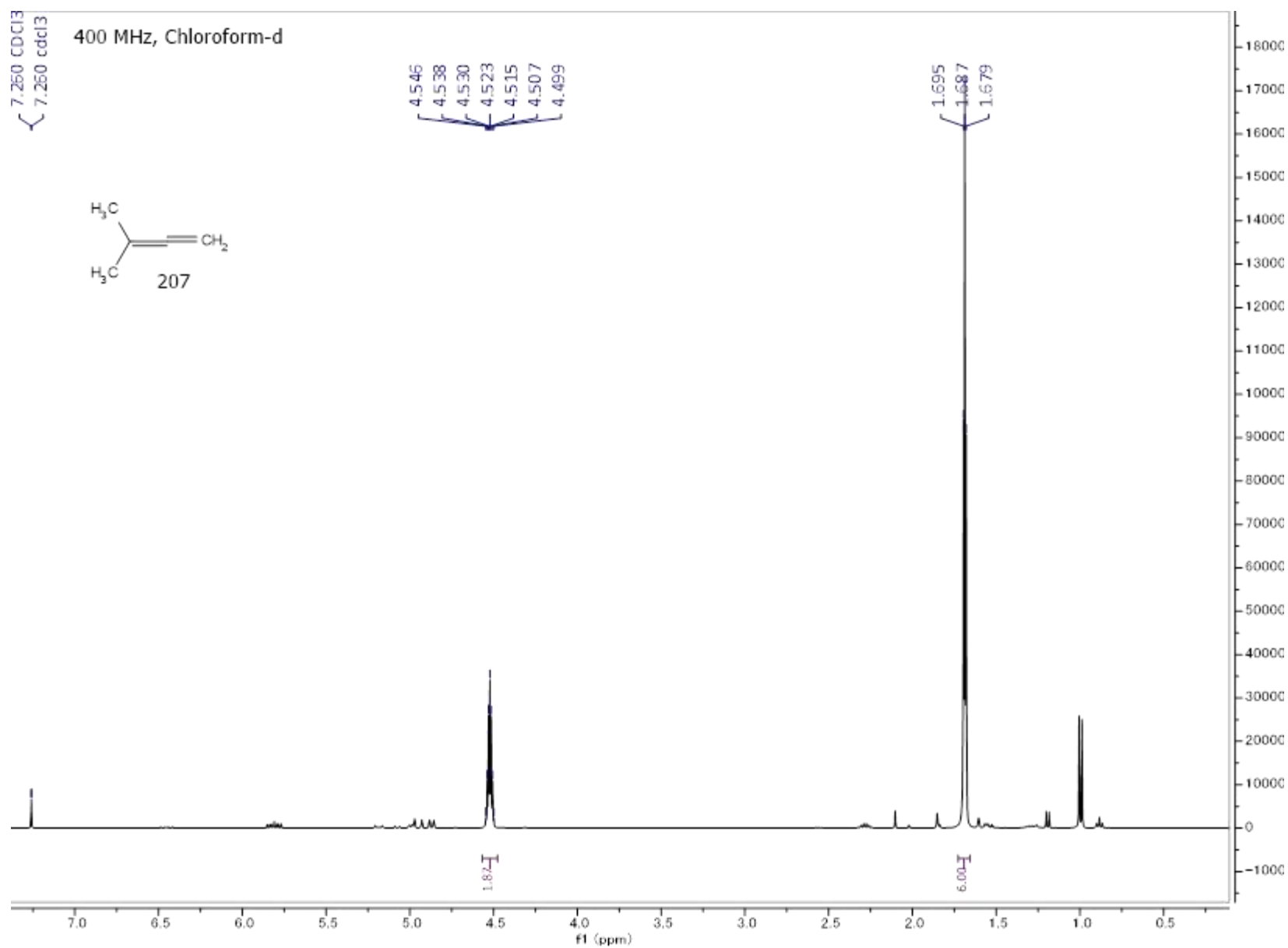


Figure A3: <sup>1</sup>H NMR spectrum of **207**.

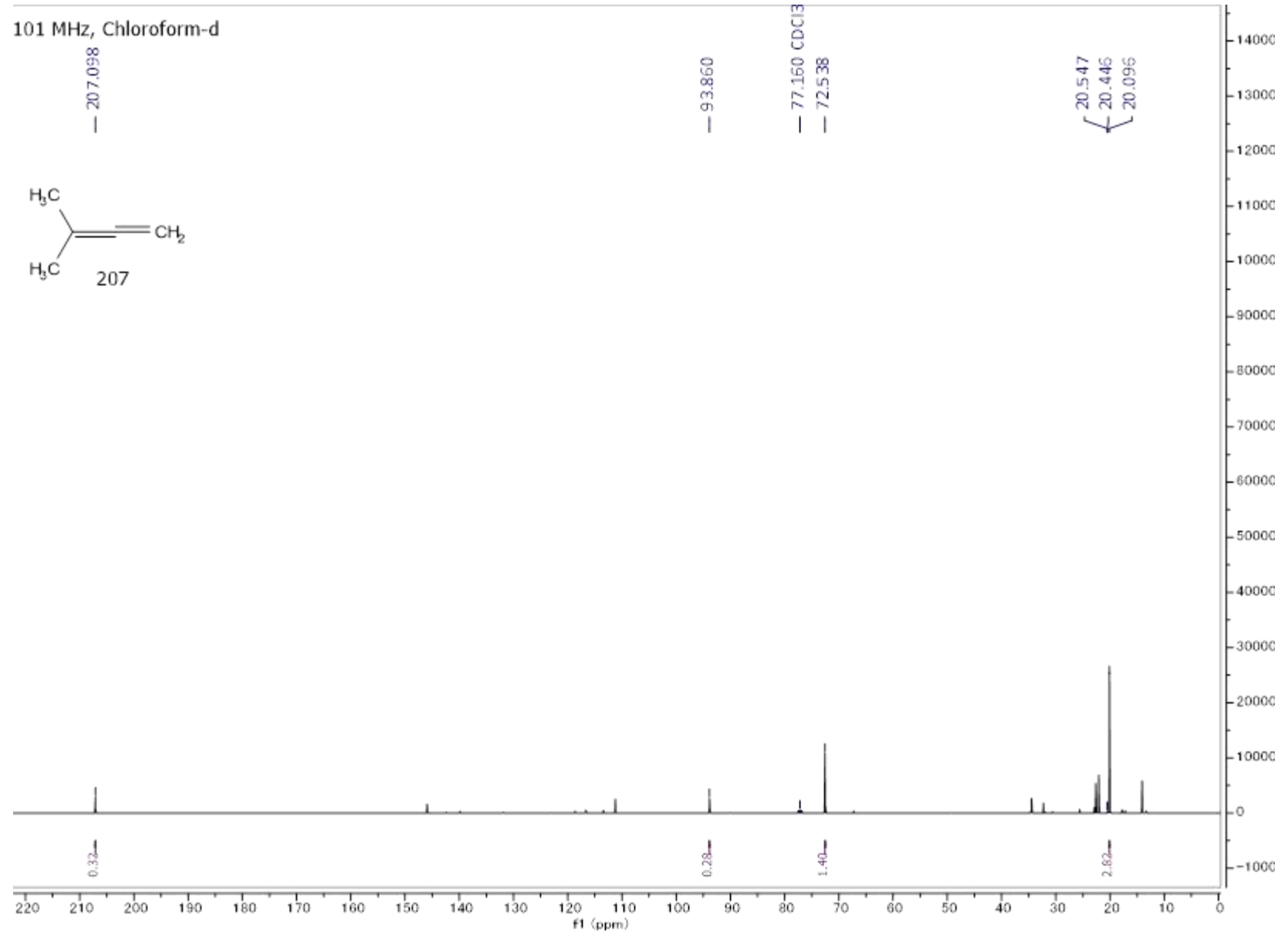


Figure A4: <sup>13</sup>C NMR spectrum of **207**.

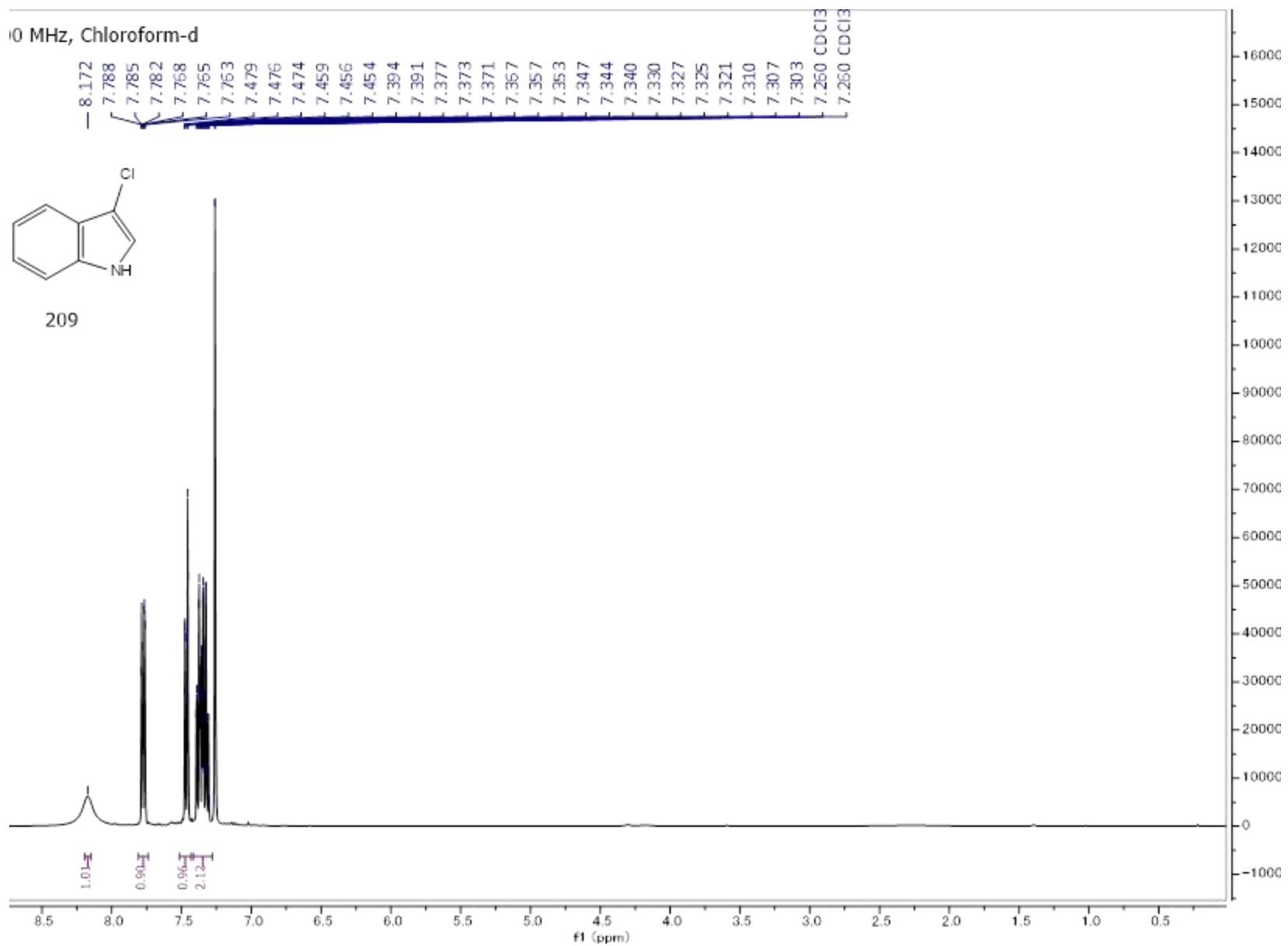


Figure A5:  $^1\text{H}$  NMR spectrum of **209**.

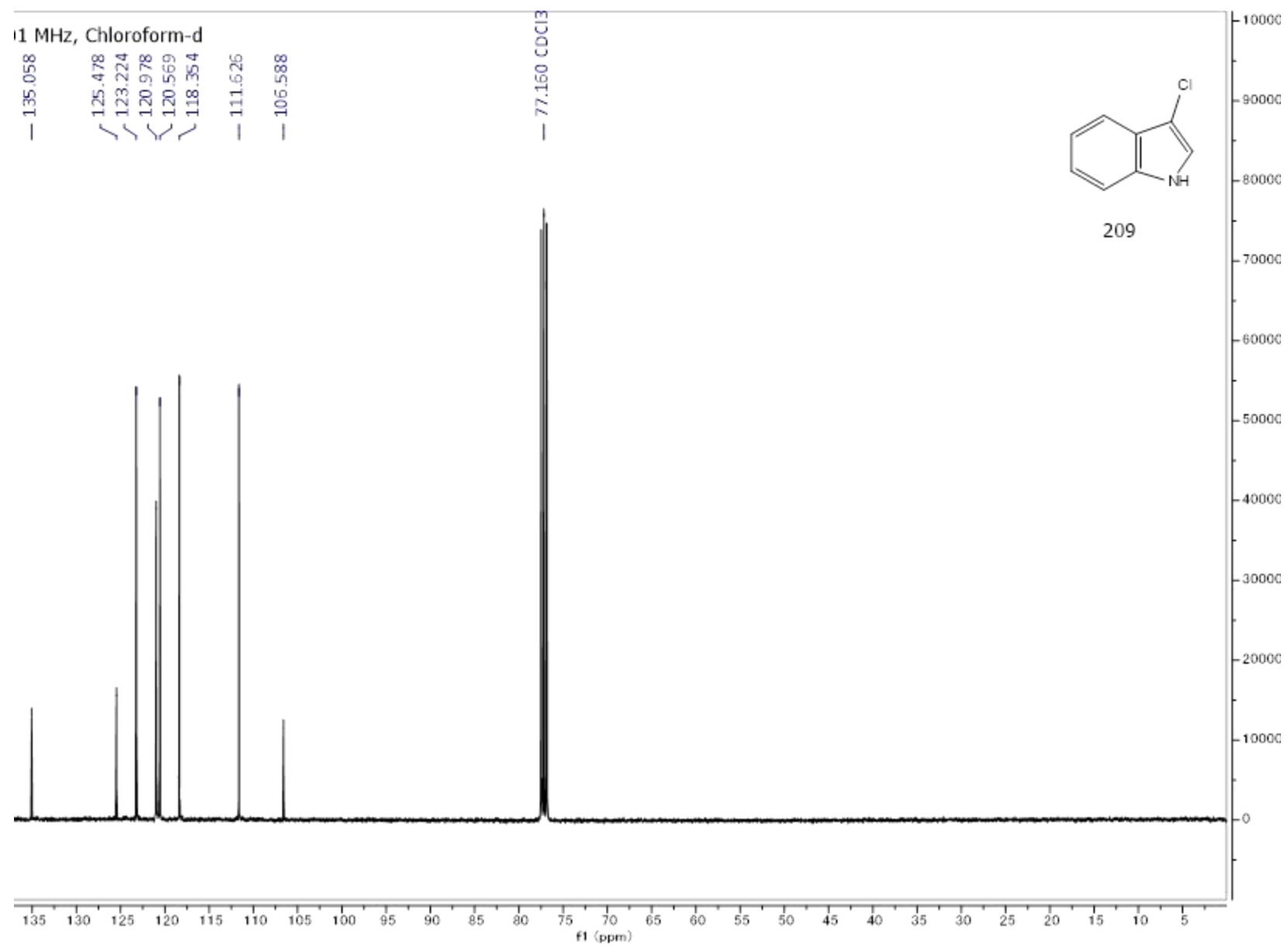


Figure A6: <sup>13</sup>C NMR spectrum of **209**.

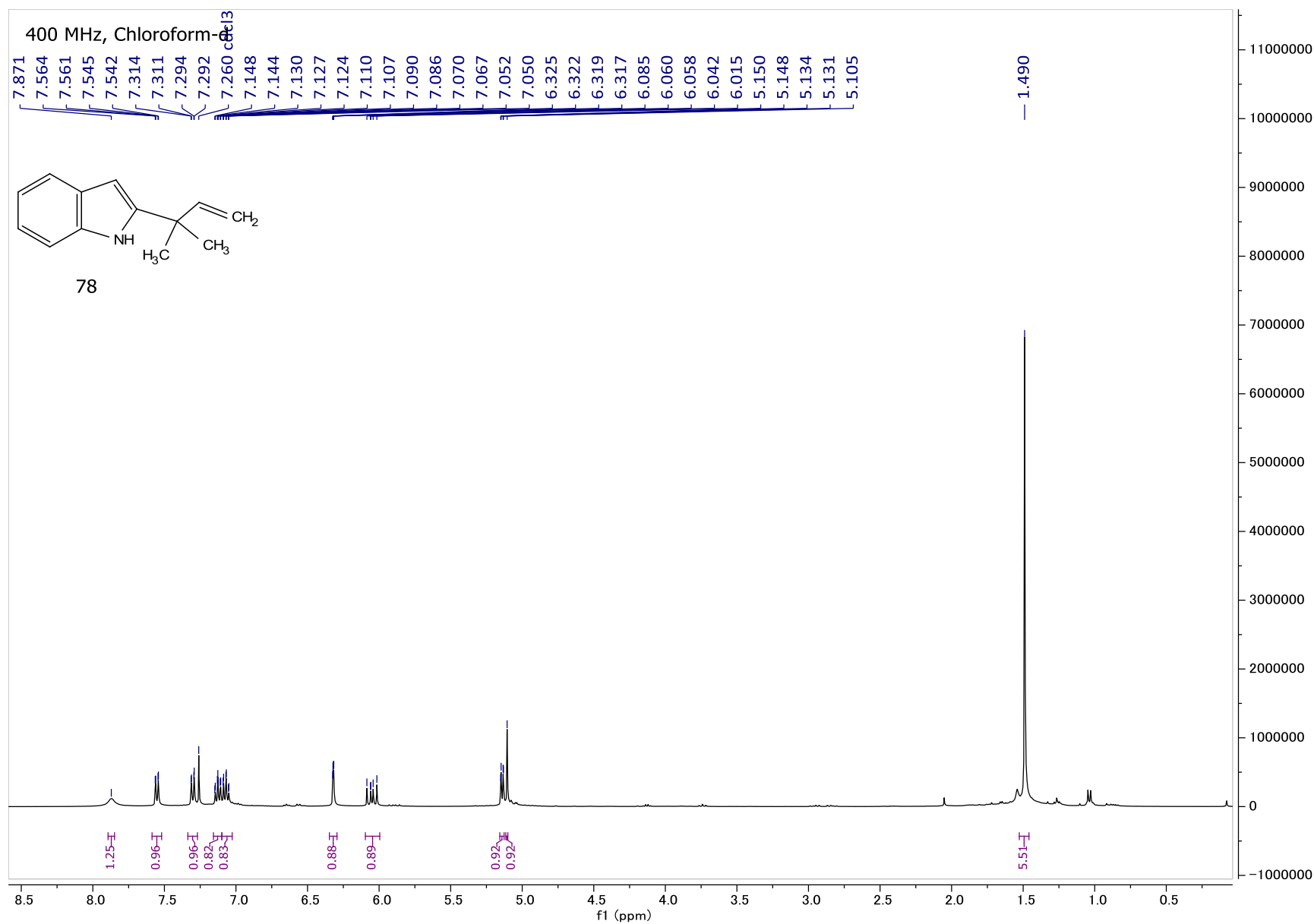


Figure A7: <sup>1</sup>H NMR spectrum of **78**.

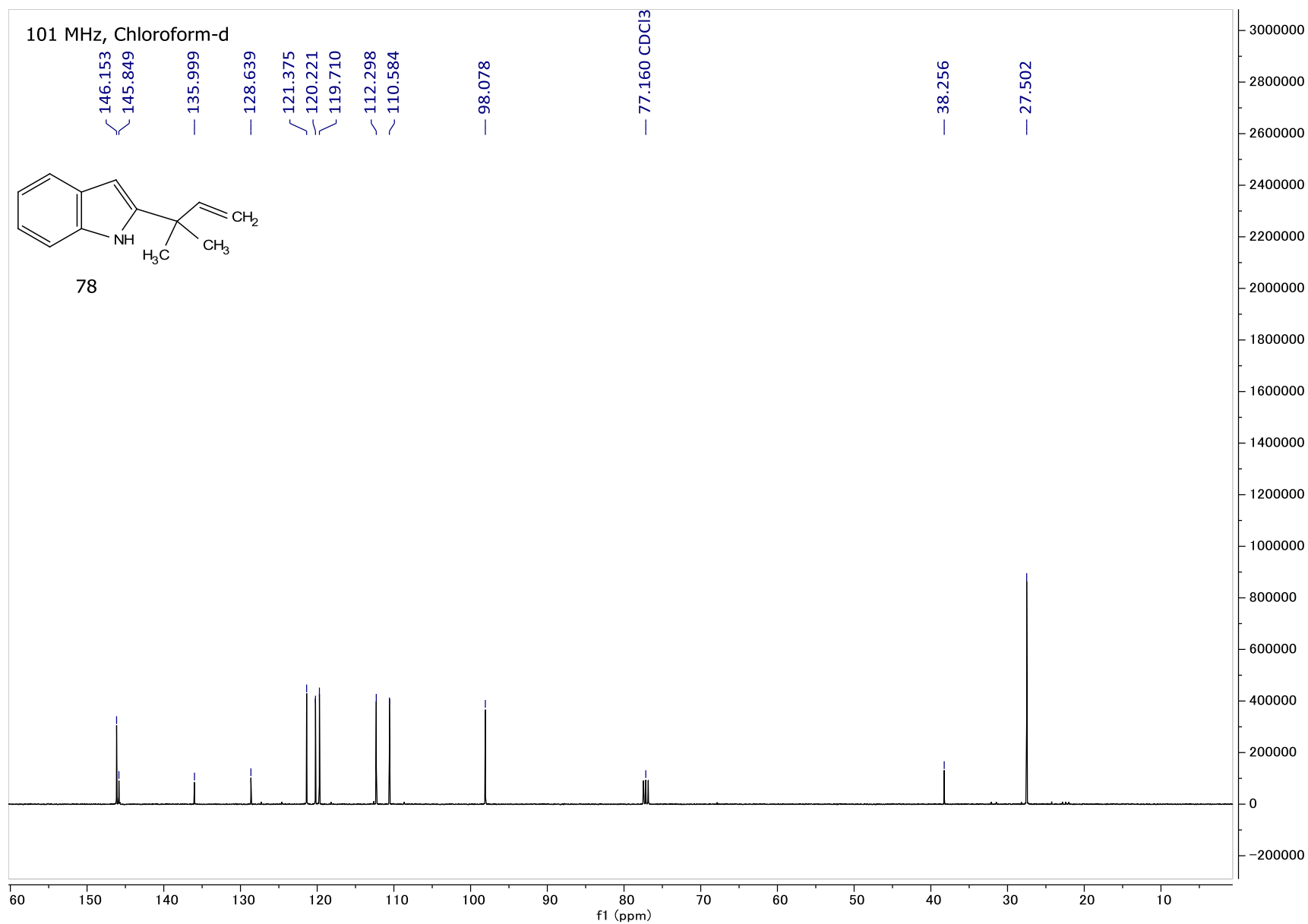


Figure A8: <sup>13</sup>C NMR spectrum of **78**.

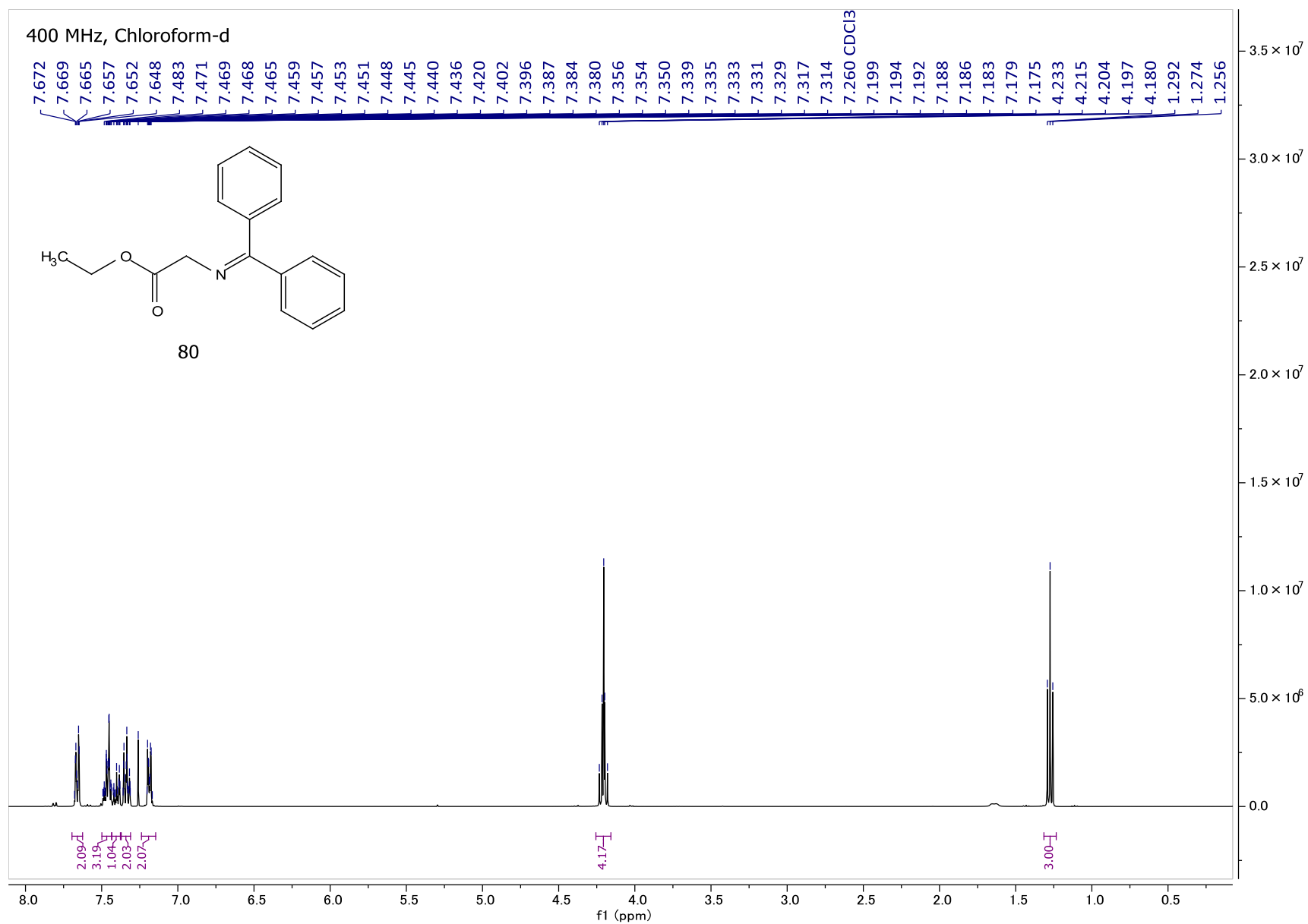


Figure A9:  $^1\text{H}$  NMR spectrum of **80**.

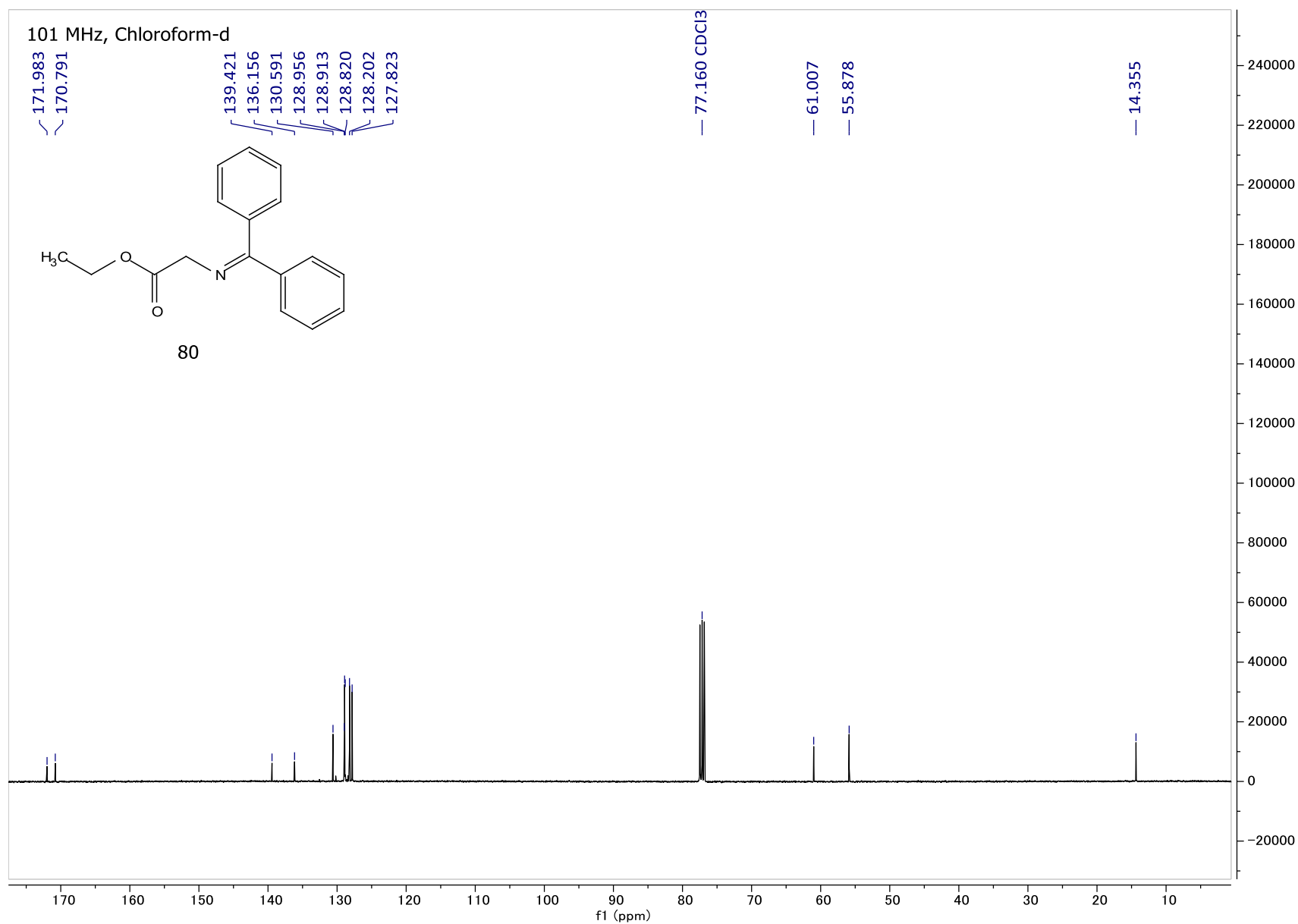


Figure A10: <sup>13</sup>C NMR spectrum of **80**.

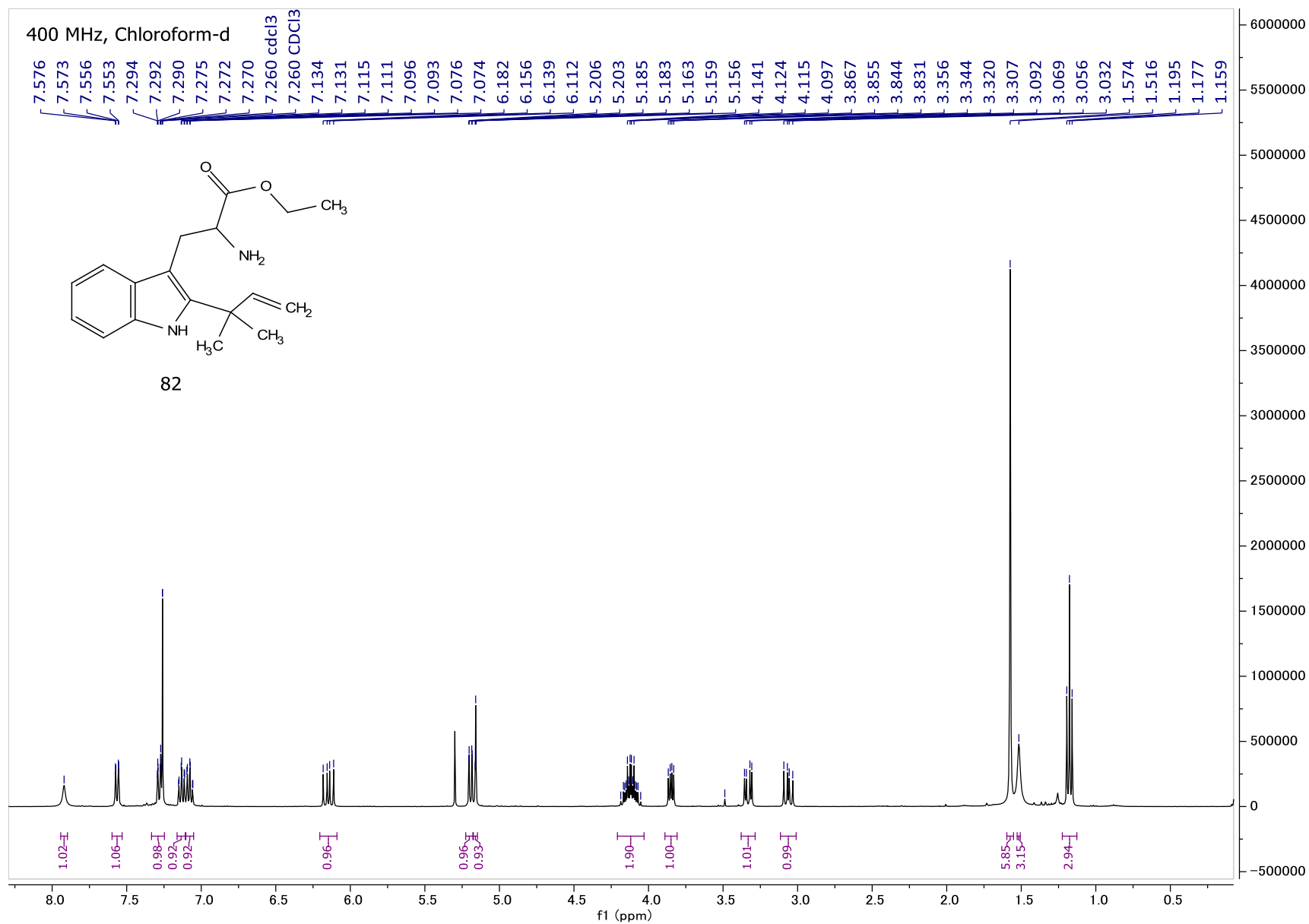


Figure A11:  $^1\text{H}$  NMR spectrum of **82**.

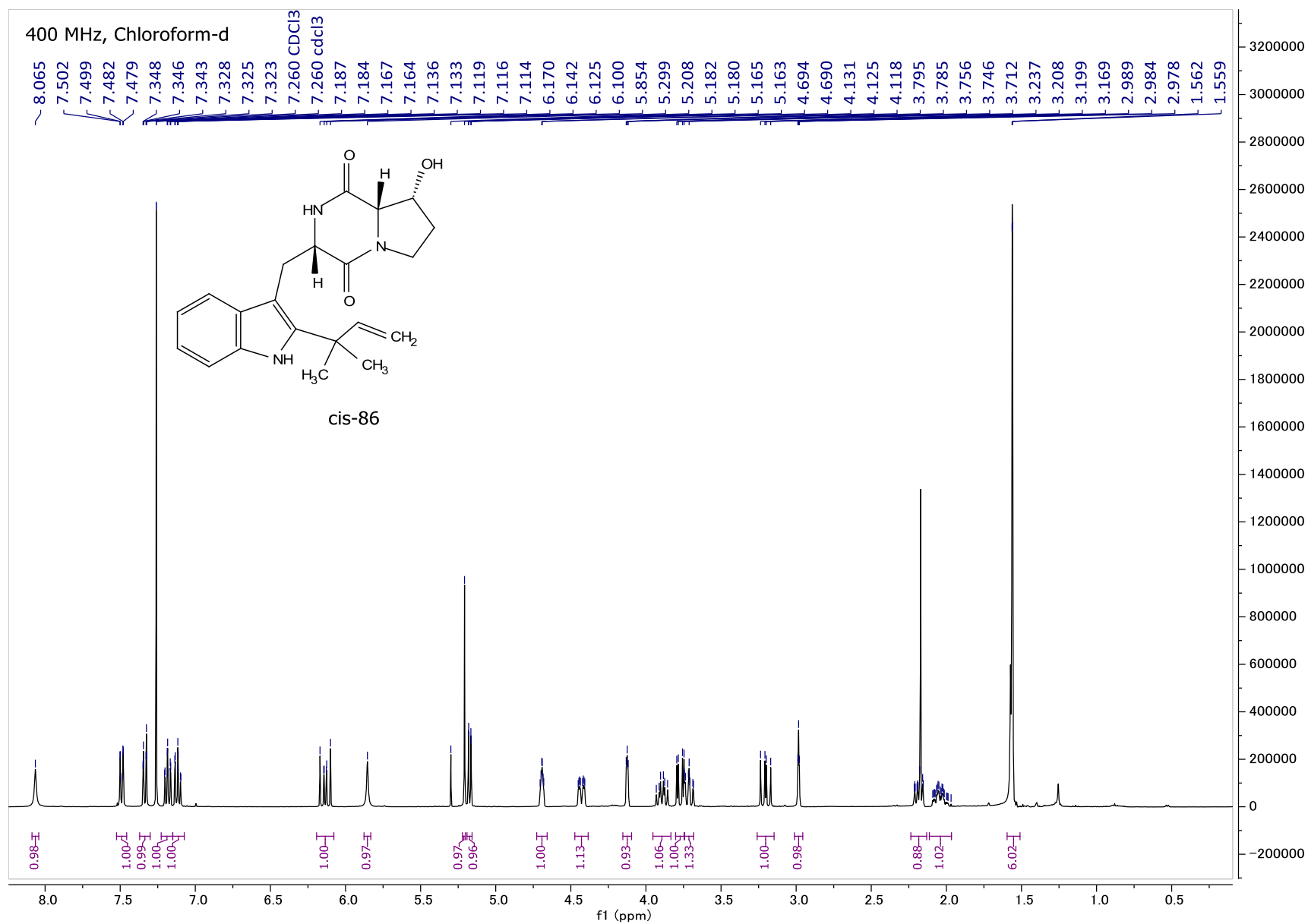


Figure A12:  $^1\text{H}$  NMR spectrum of **cis-86**.

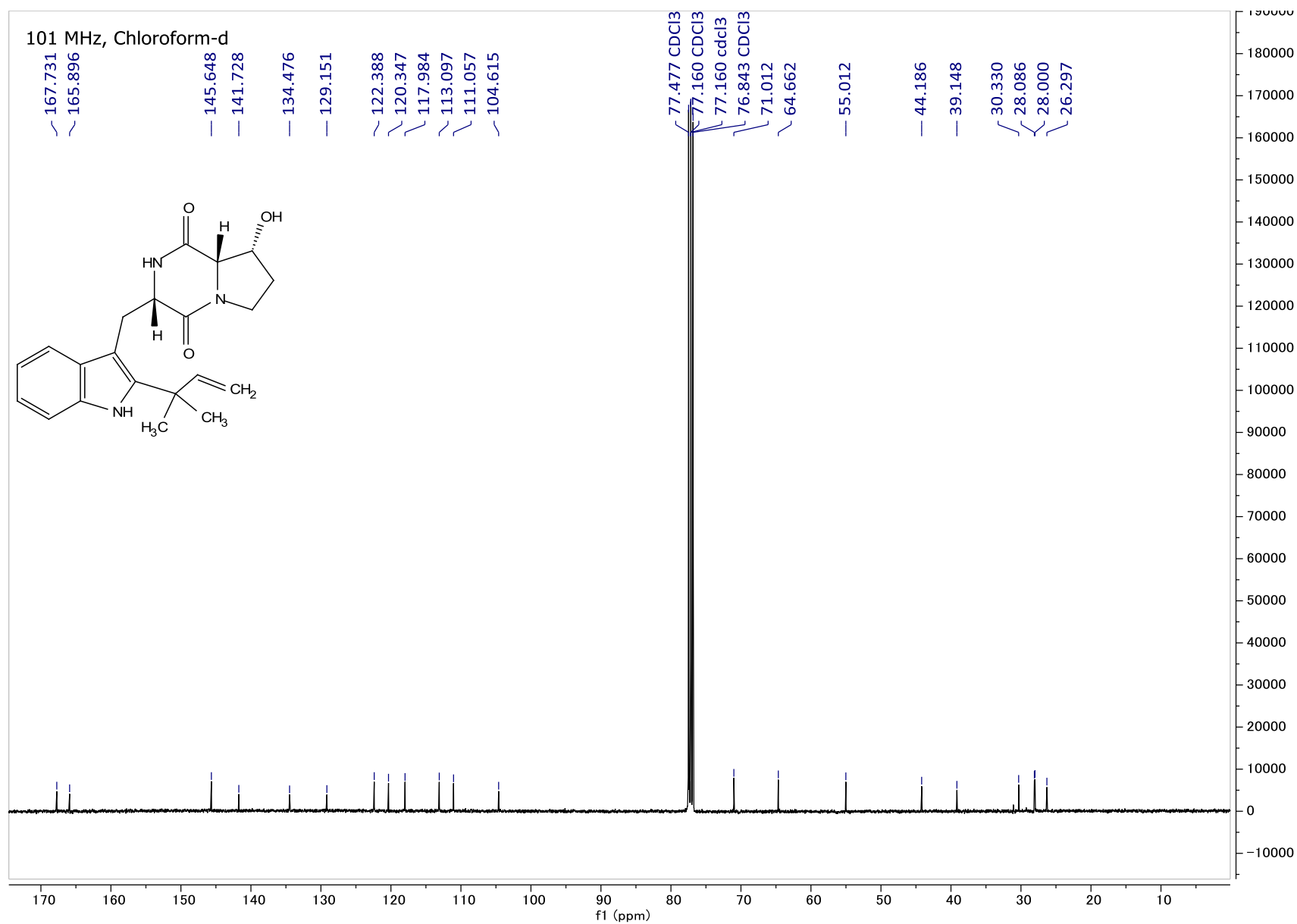


Figure A13:  $^{13}\text{C}$  NMR spectrum of *cis*-86.

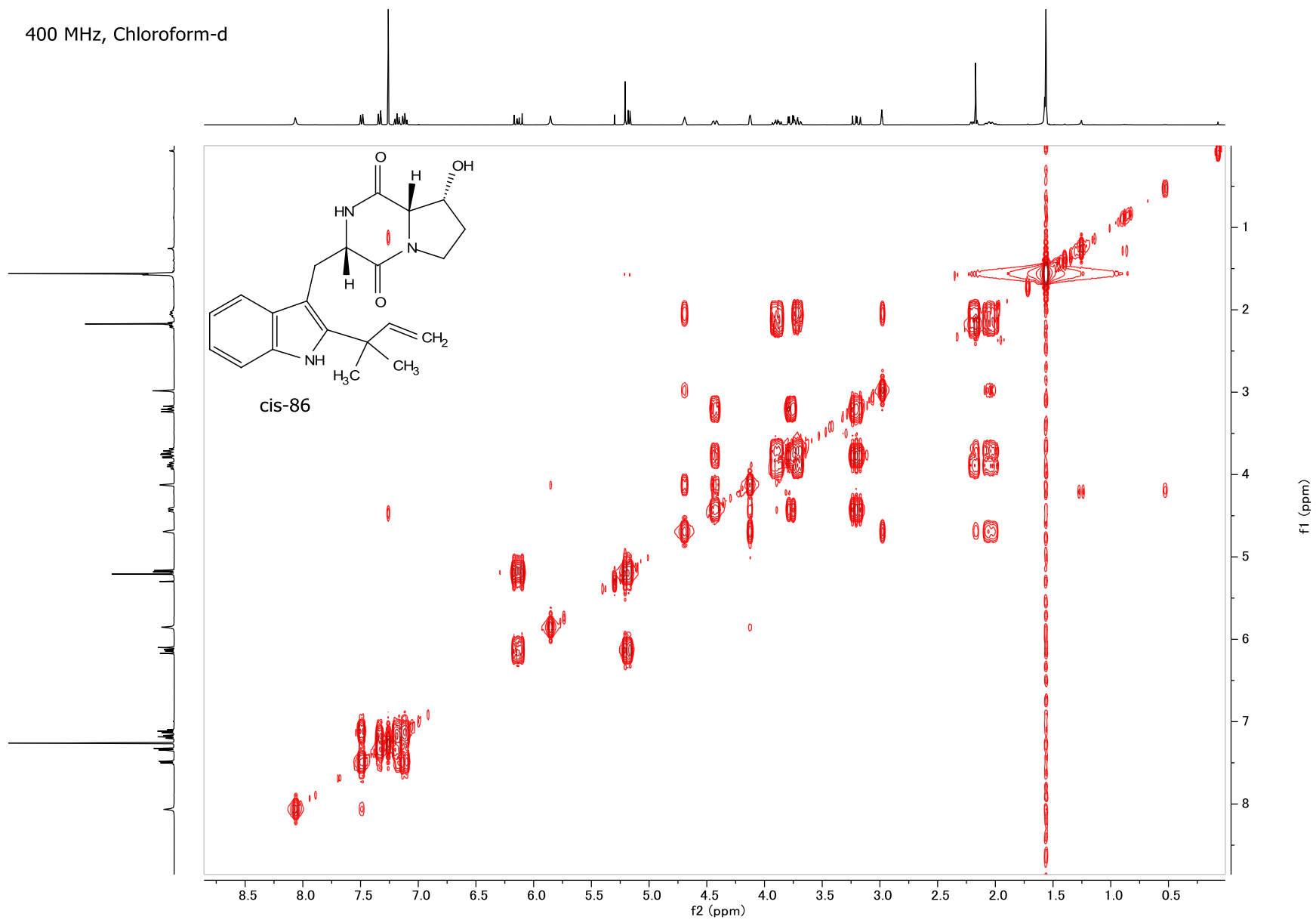


Figure A14: COSY NMR spectrum of *cis*-86.

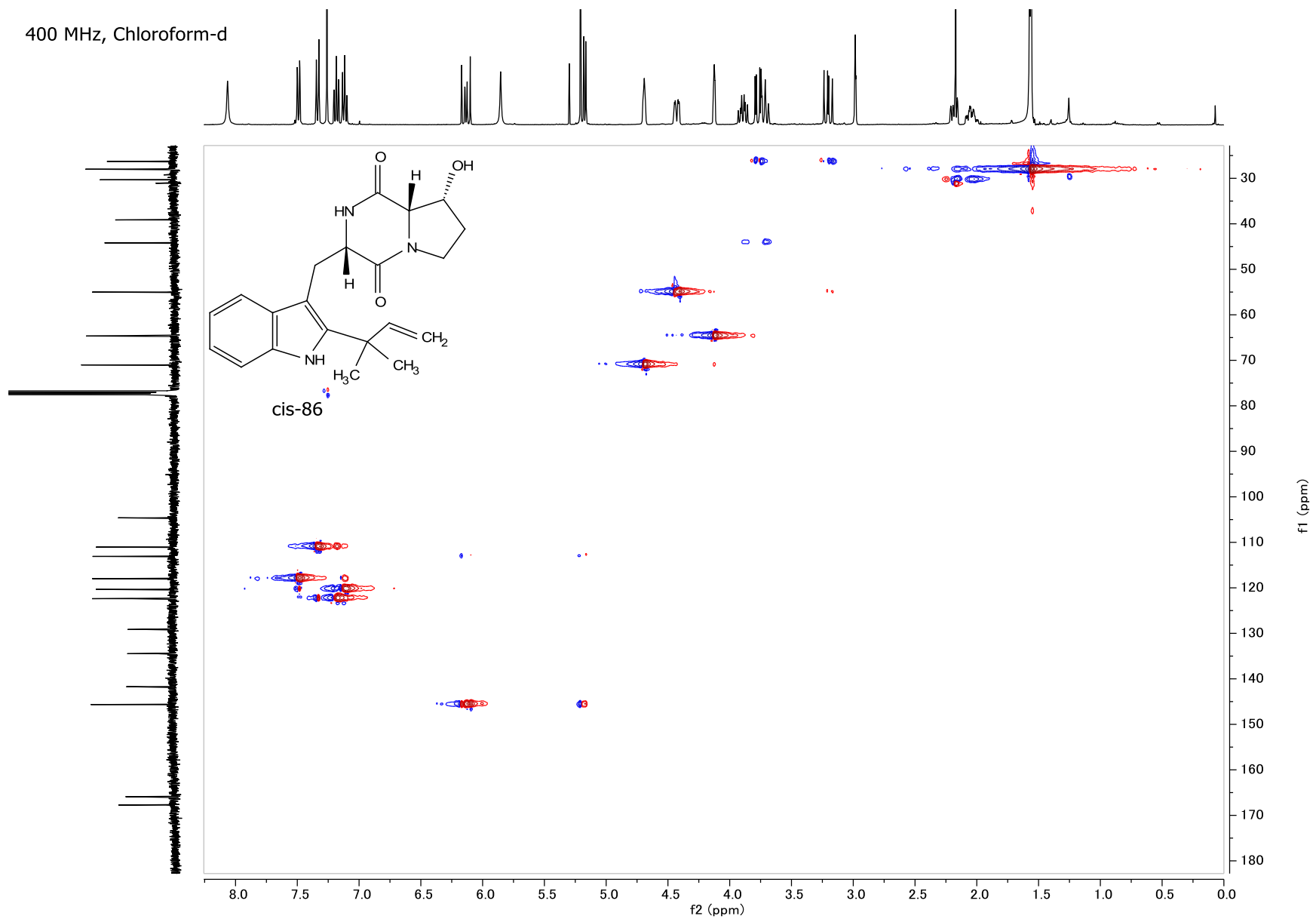


Figure A15: HSQC NMR spectrum of *cis-86*.

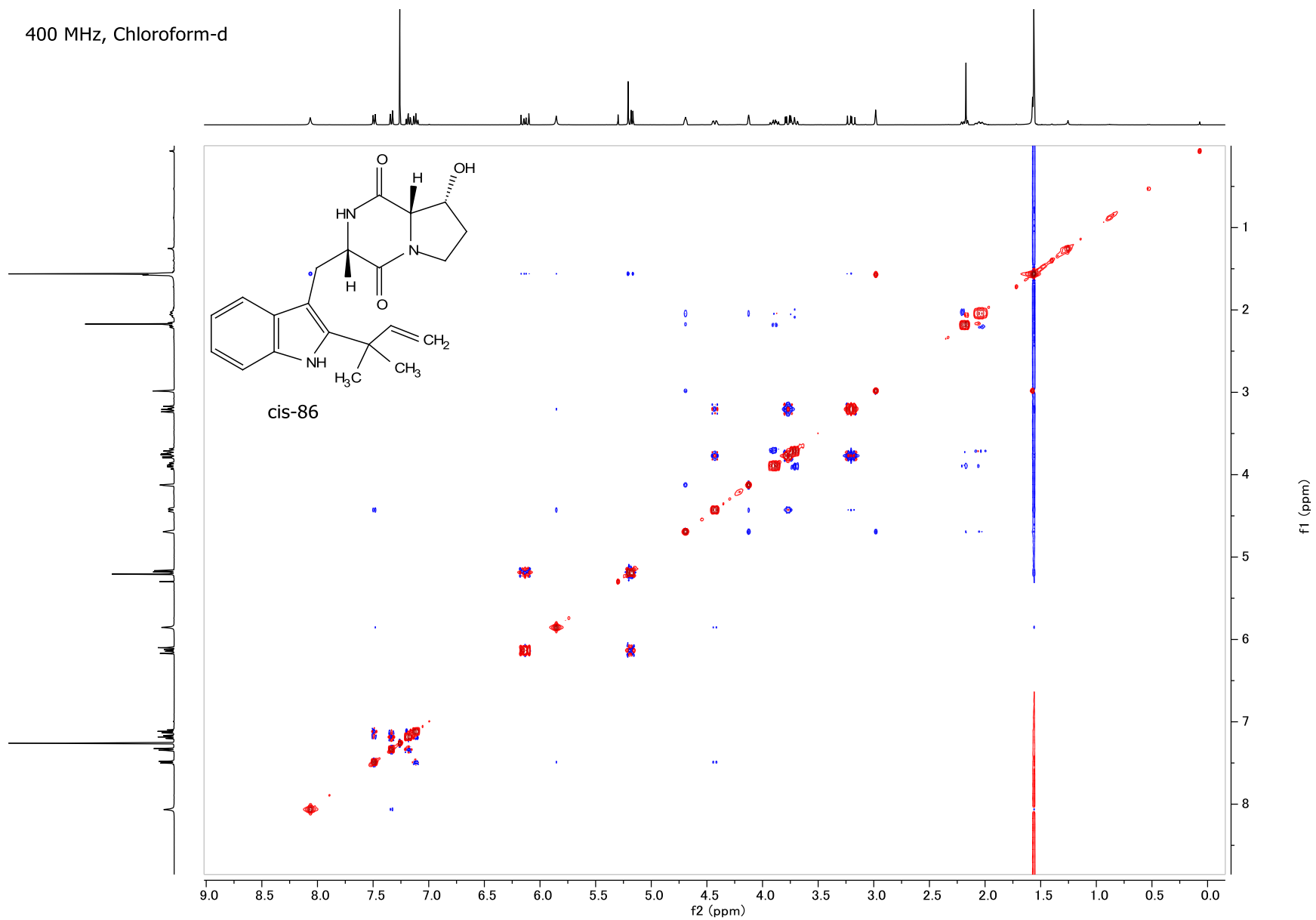


Figure A16: NOESY NMR spectrum of *cis*-86.

400 MHz, Chloroform-d

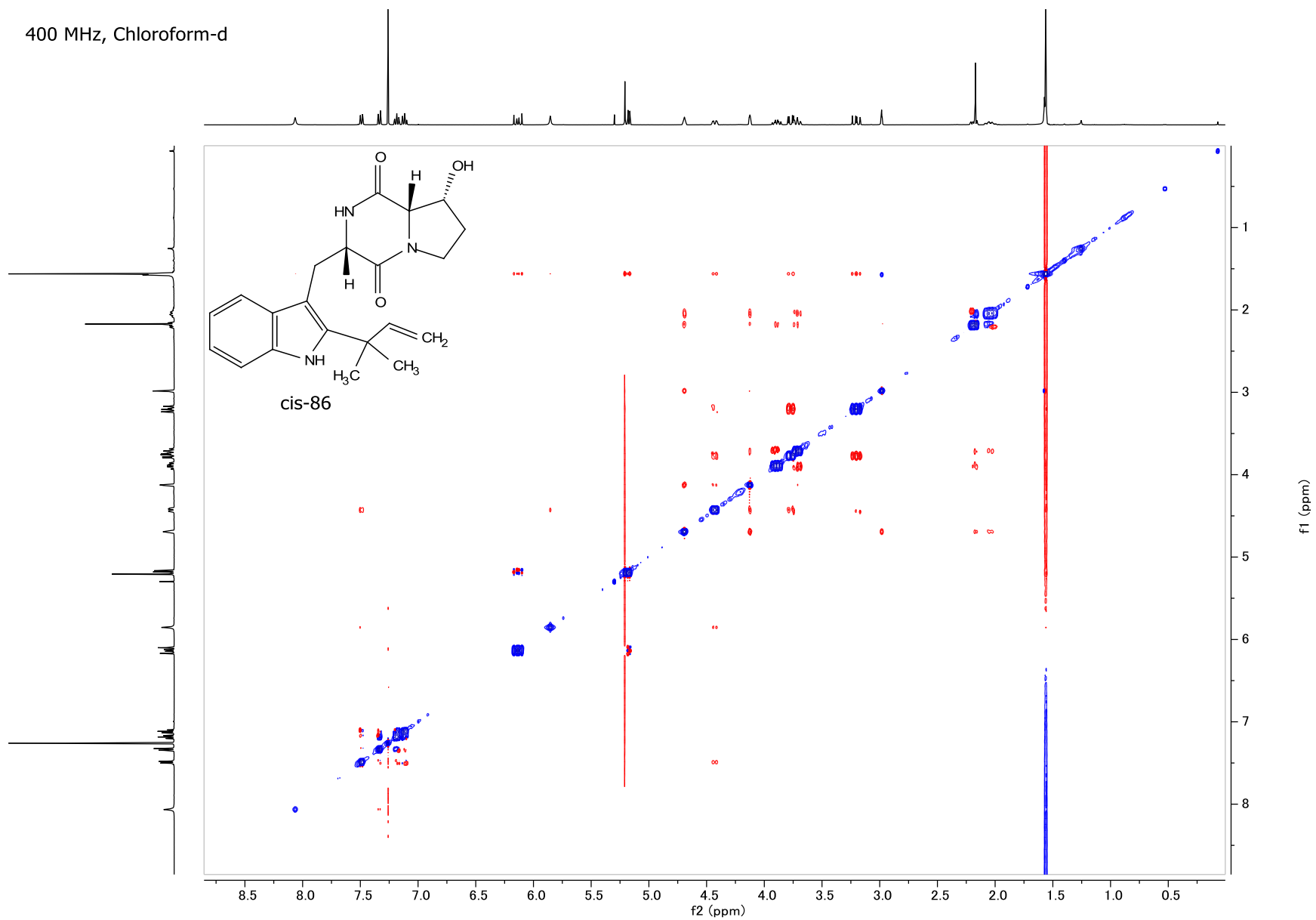


Figure A17: ROESY NMR spectrum of *cis*-86.

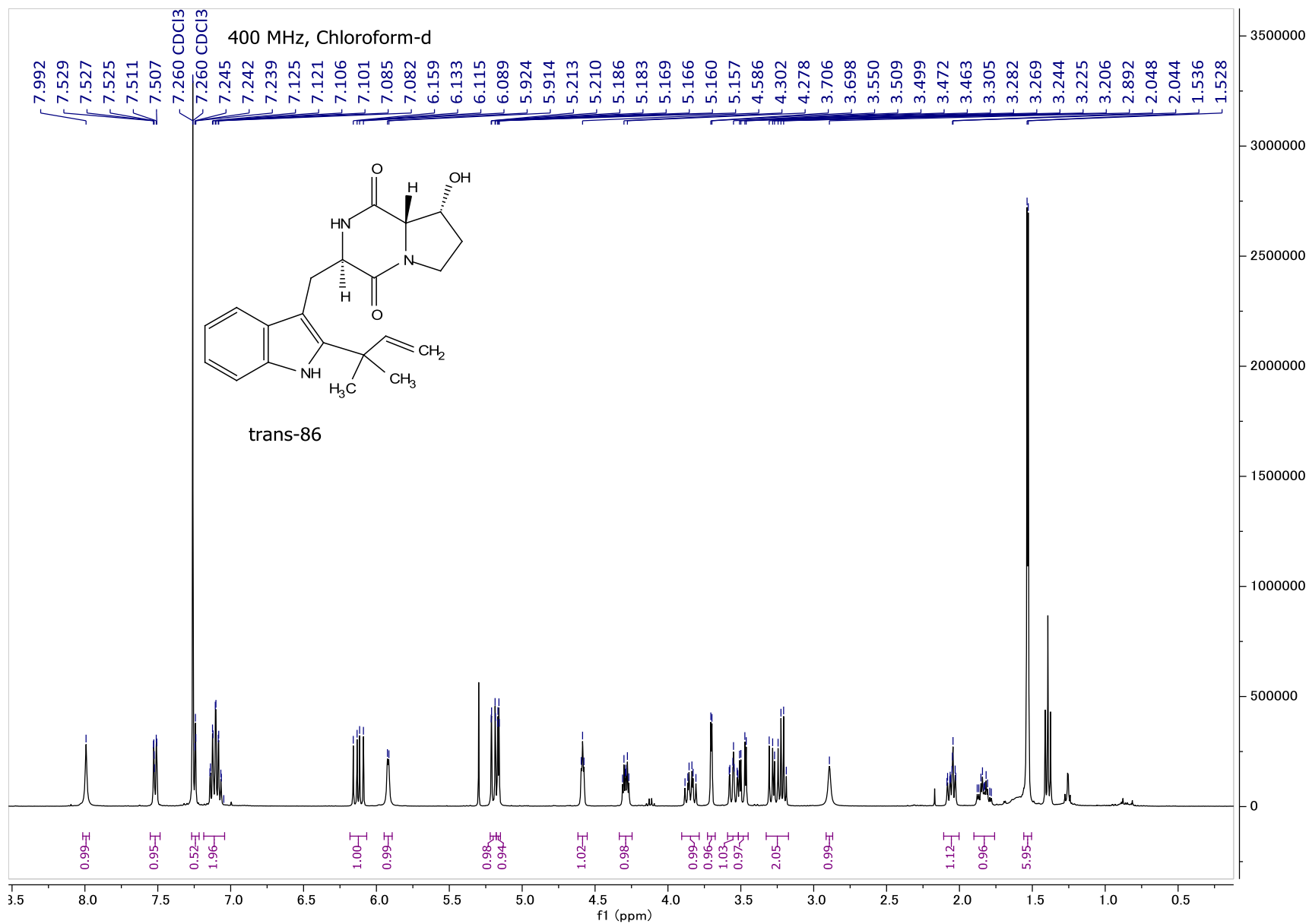


Figure A18:  $^1\text{H}$  NMR spectrum of *trans*-86.

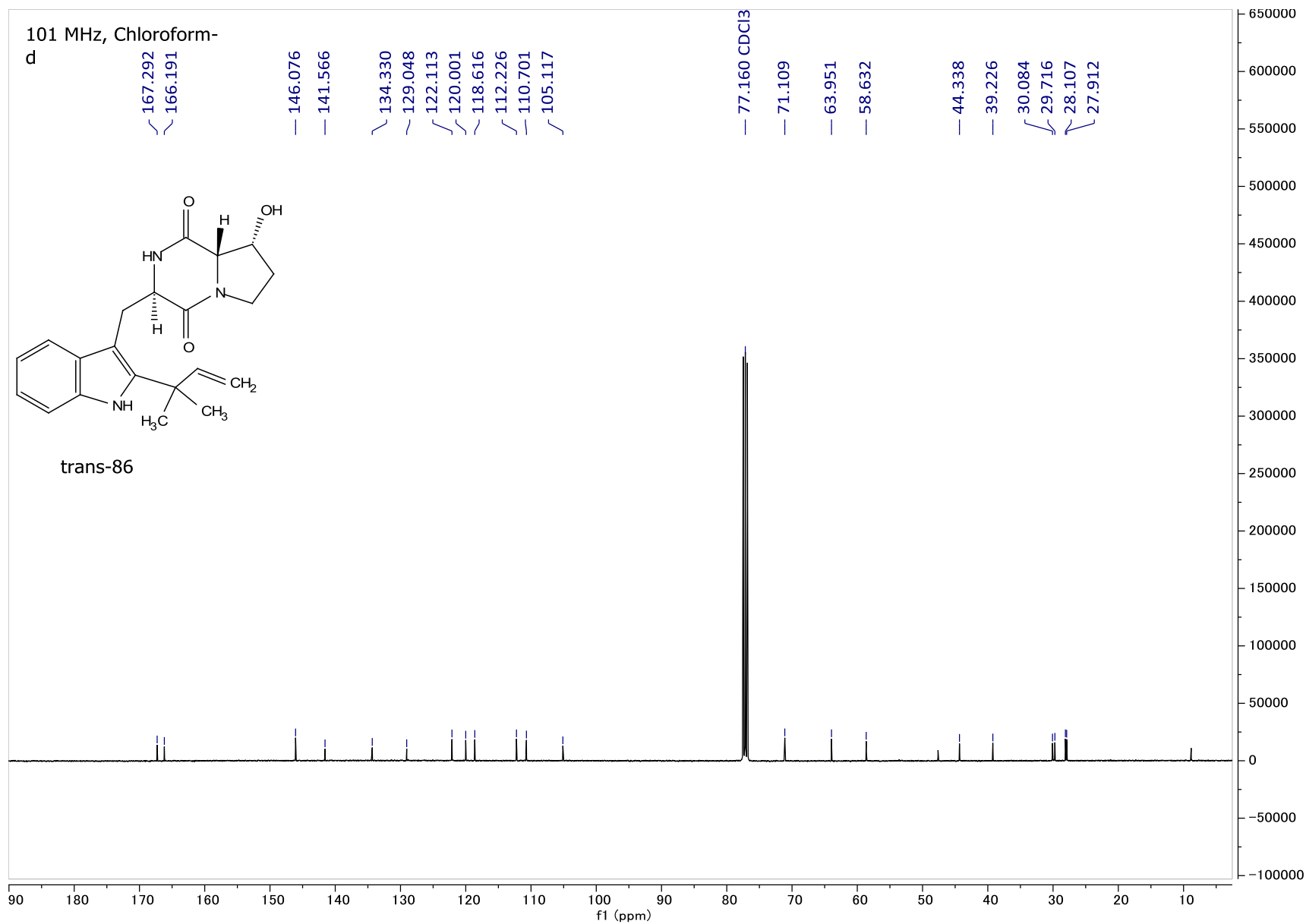


Figure A19: <sup>13</sup>C NMR spectrum of *trans*-86.

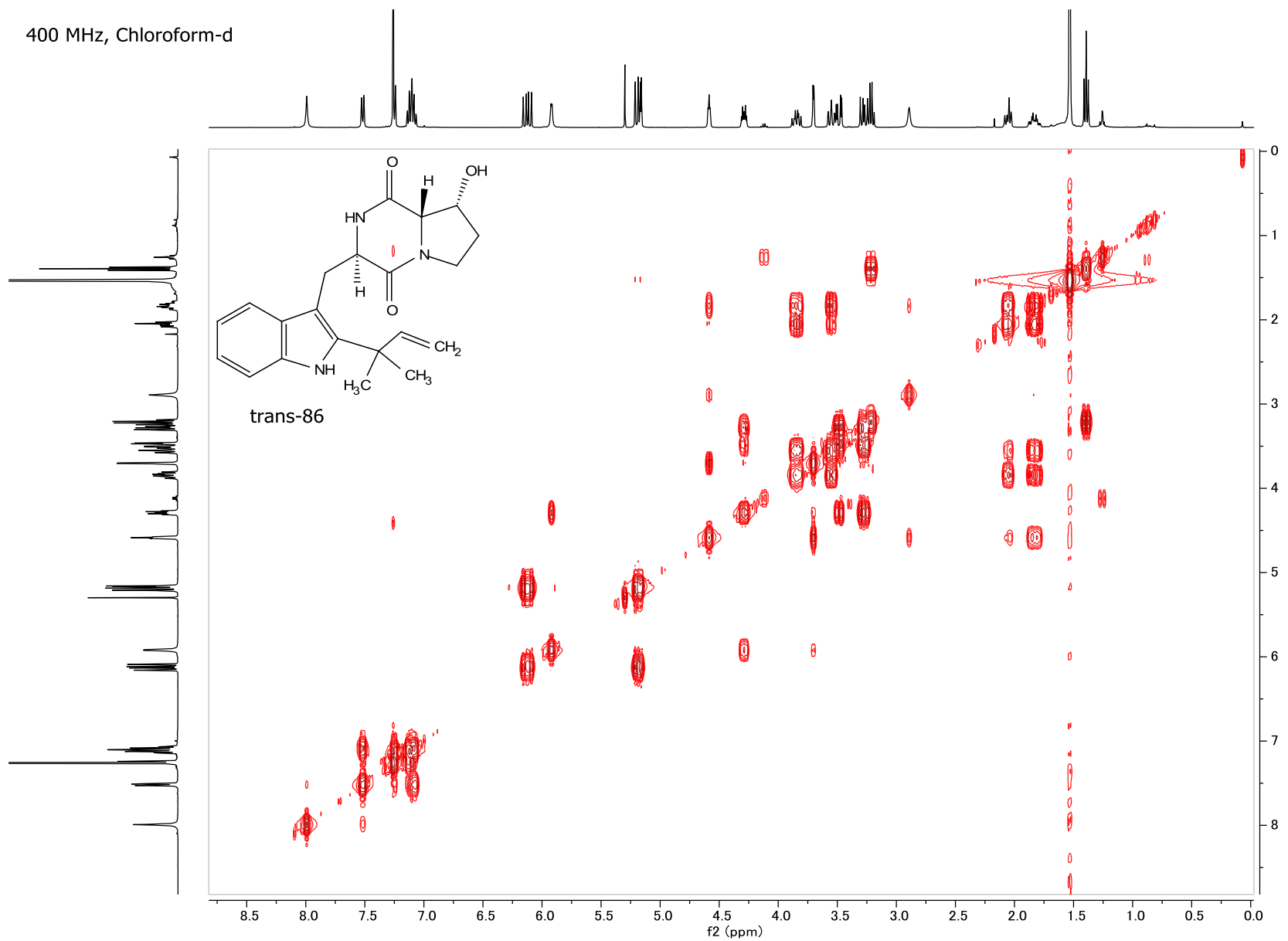


Figure A20: COSY NMR spectrum of *trans*-86.

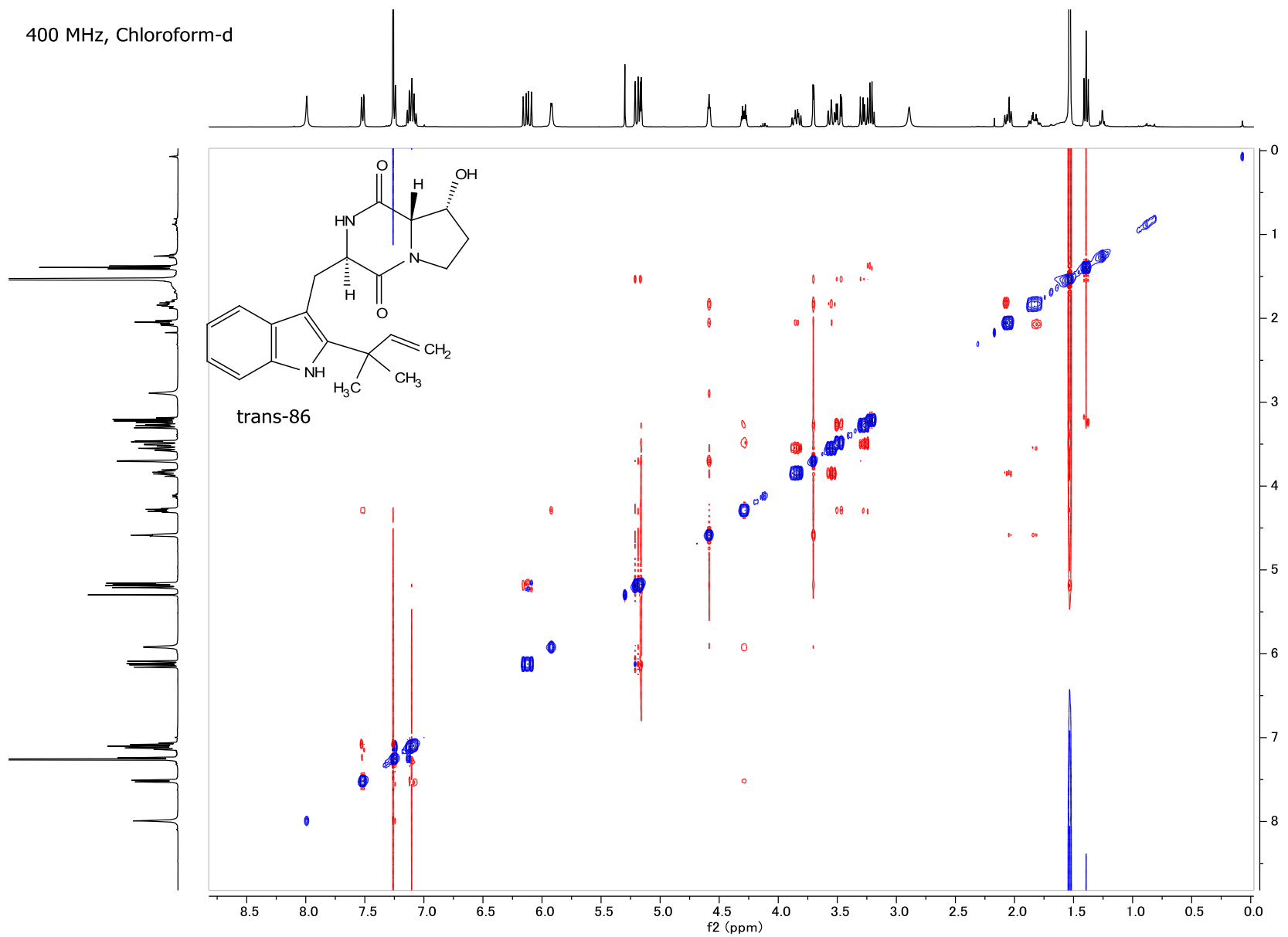


Figure A21: HSQC NMR spectrum of *trans*-86.

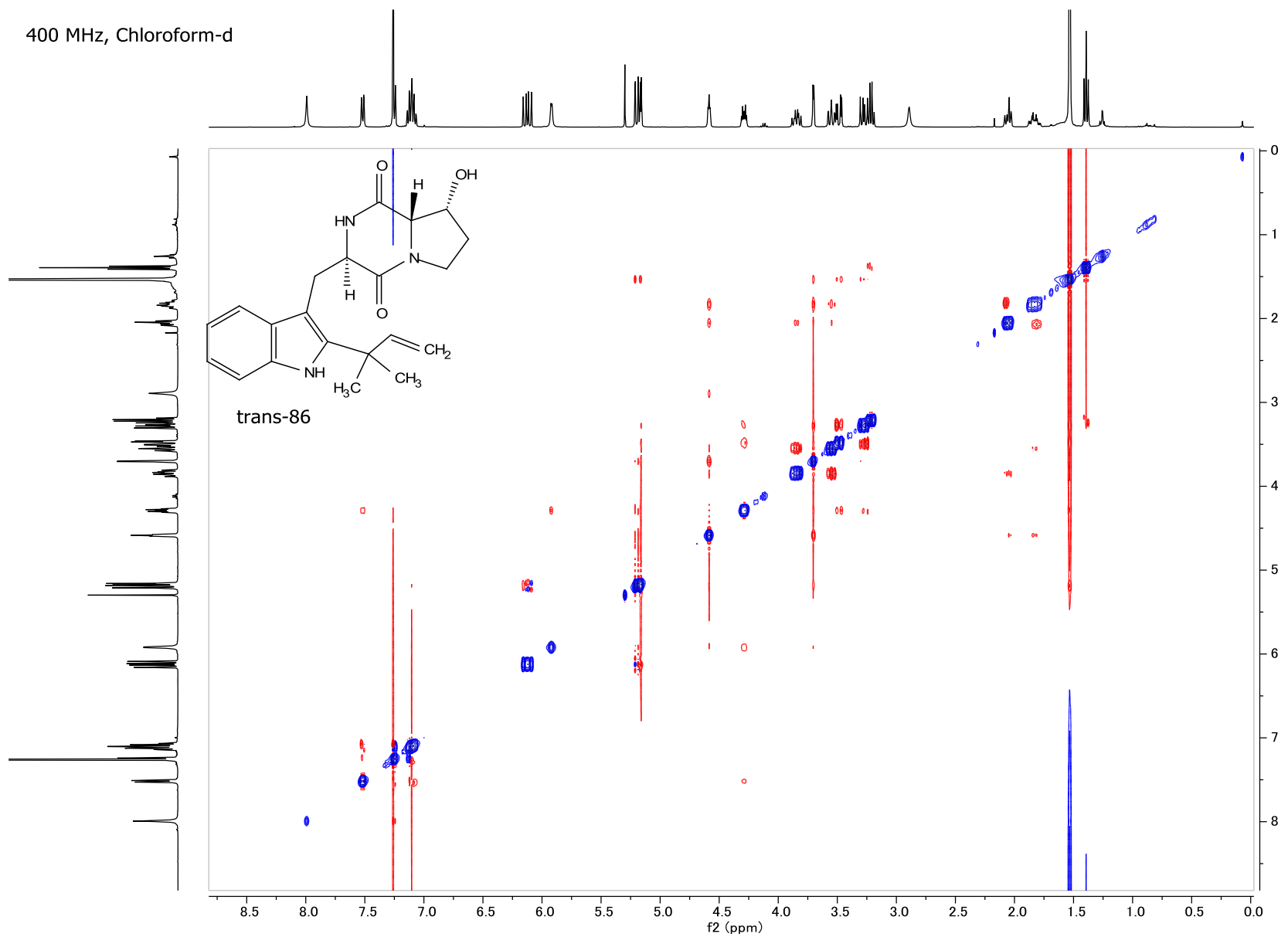


Figure A22: ROESY NMR spectrum of *trans*-86.

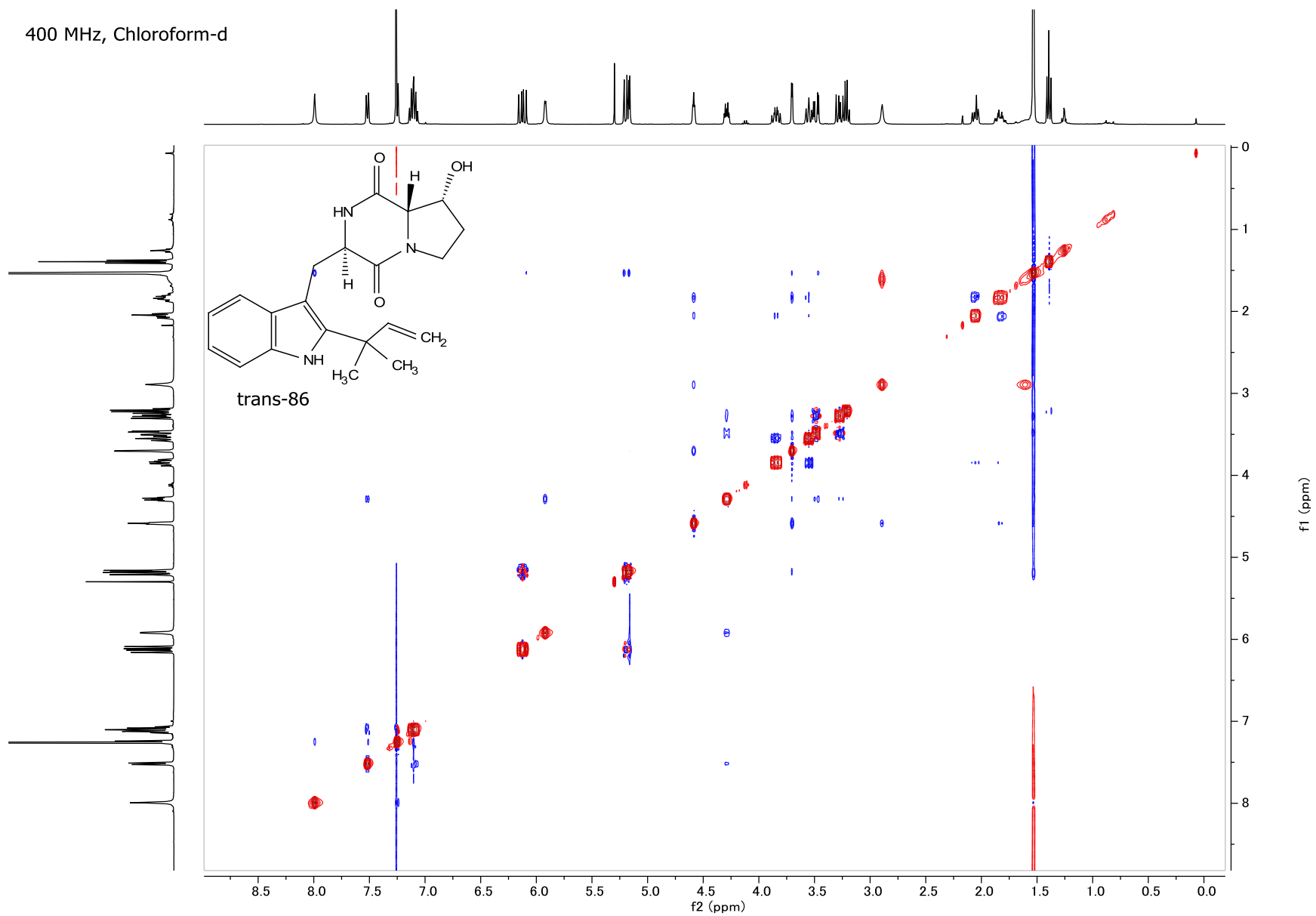


Figure A23: NOESY NMR spectrum of *trans*-86.

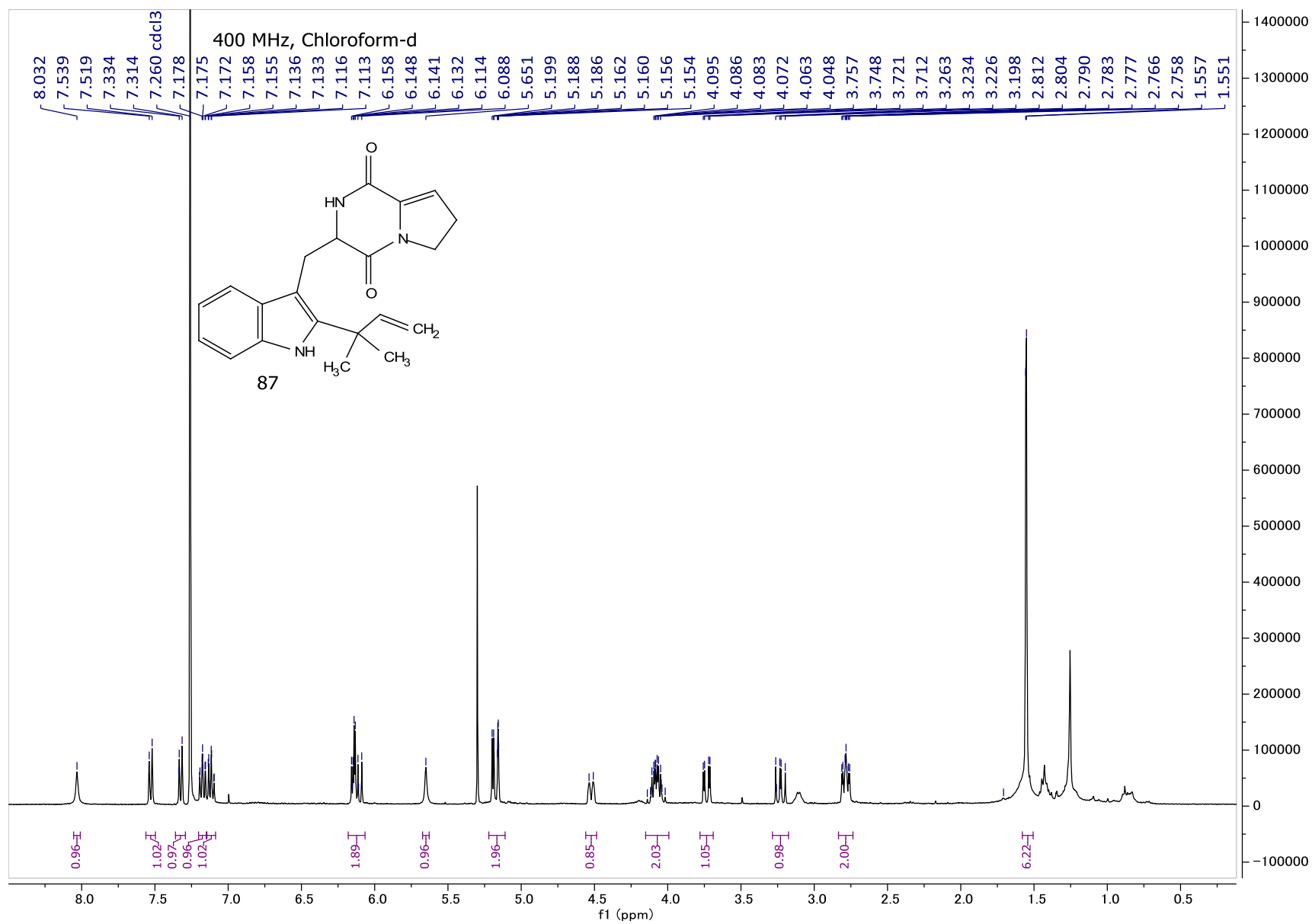


Figure A24:  $^1\text{H}$  NMR spectrum of **87**.

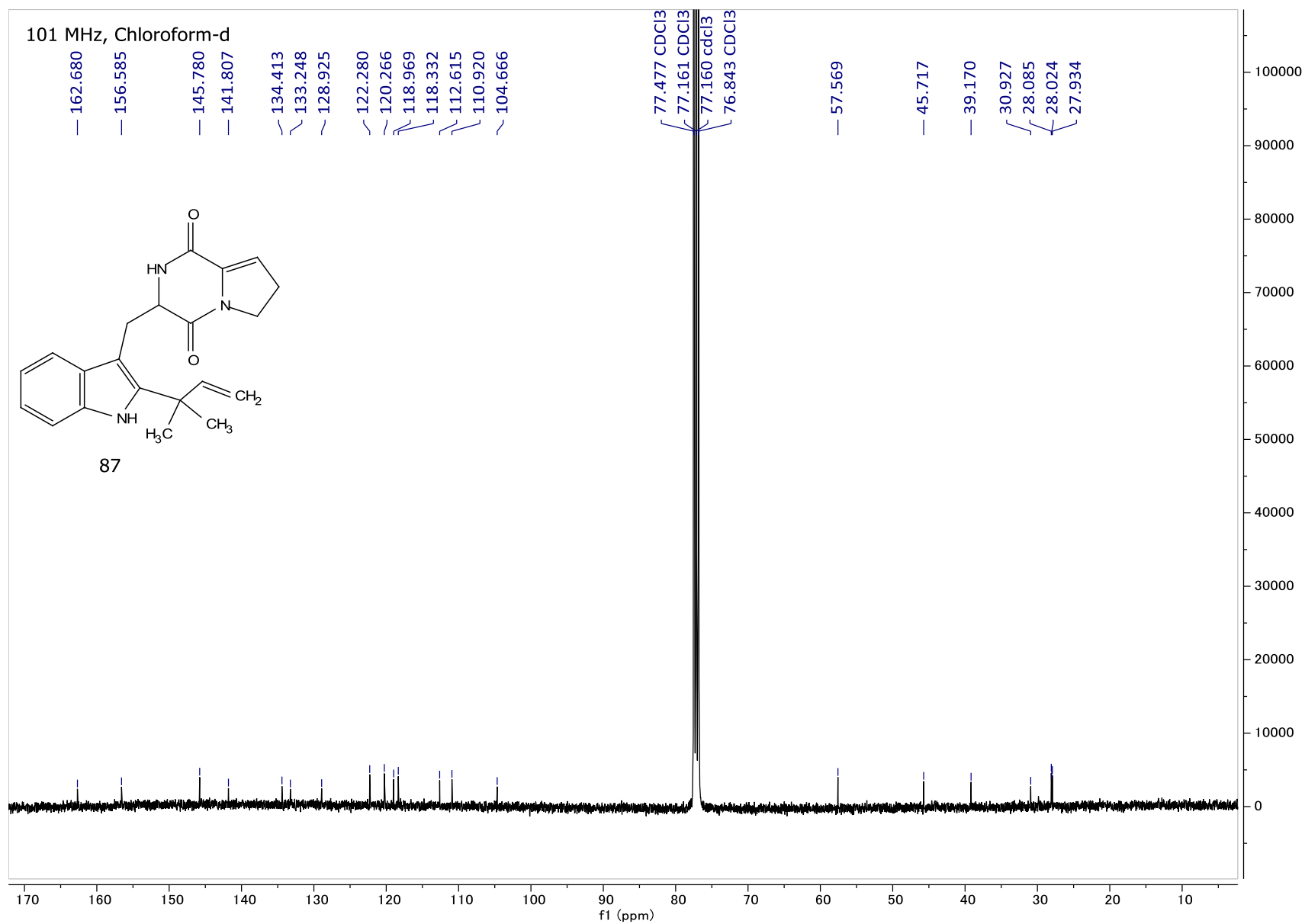


Figure A25: <sup>13</sup>C NMR spectrum of **87**.

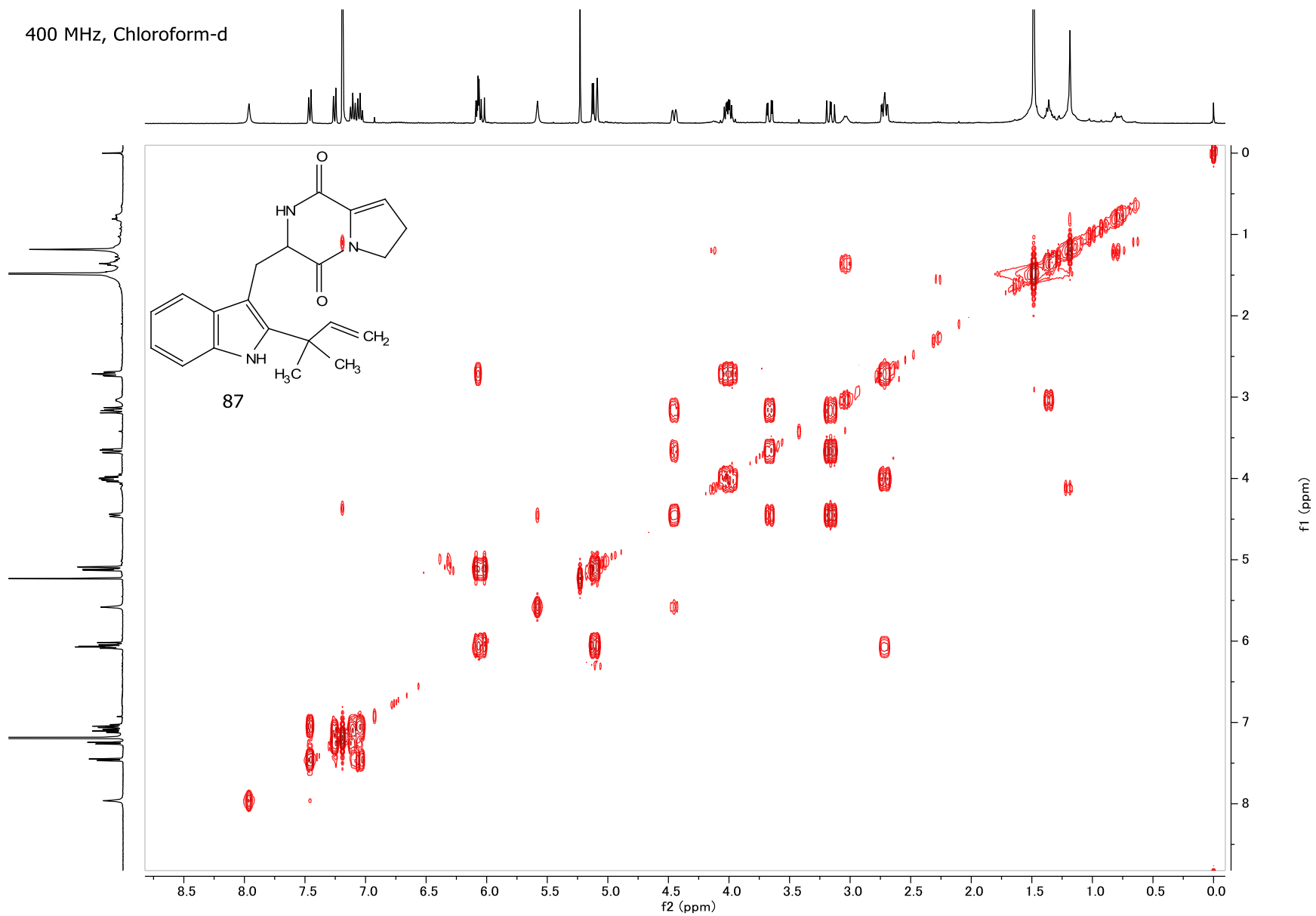


Figure A26: COSY NMR spectrum of **87**.

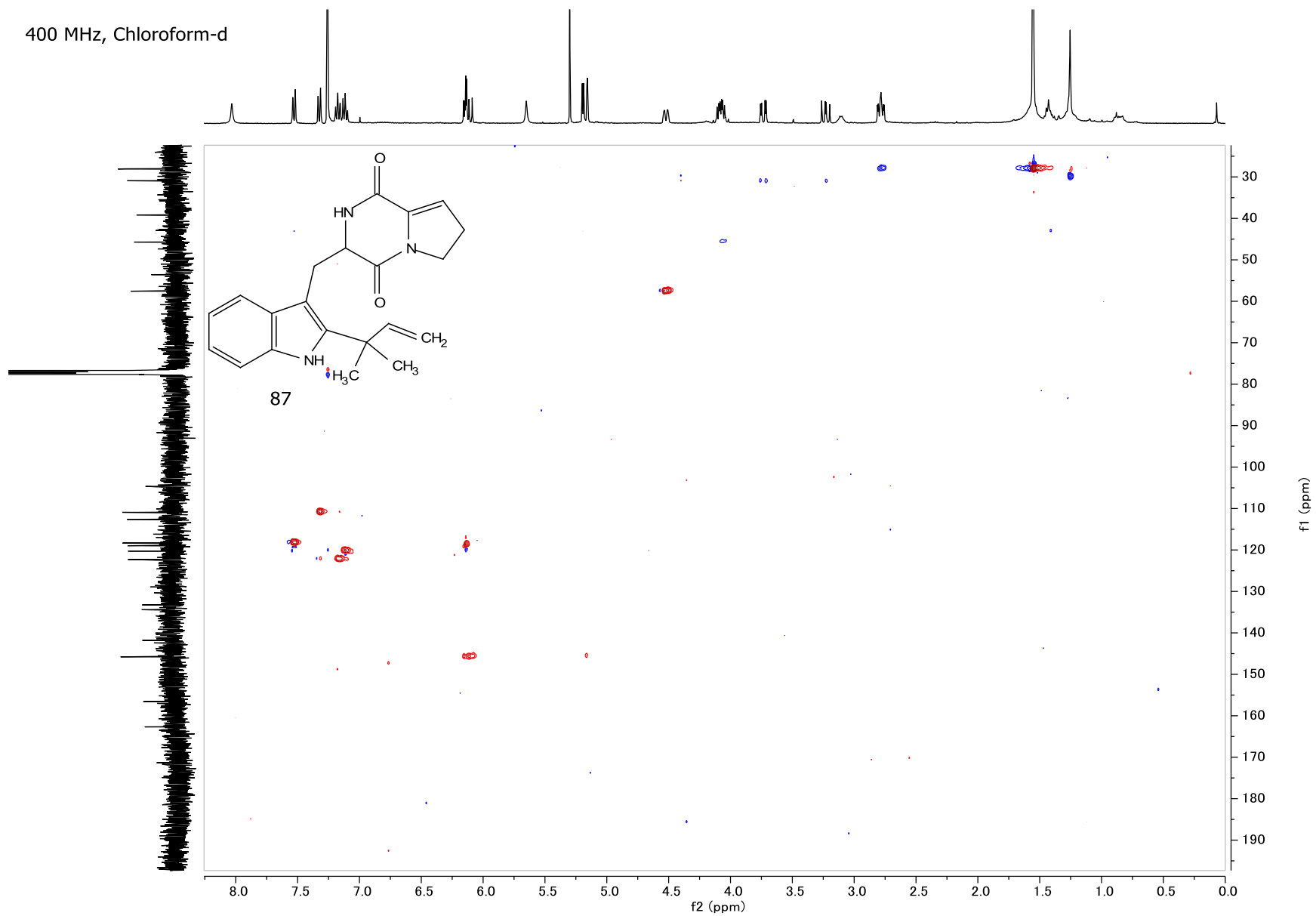


Figure A27: HSQC NMR spectrum of **87**.

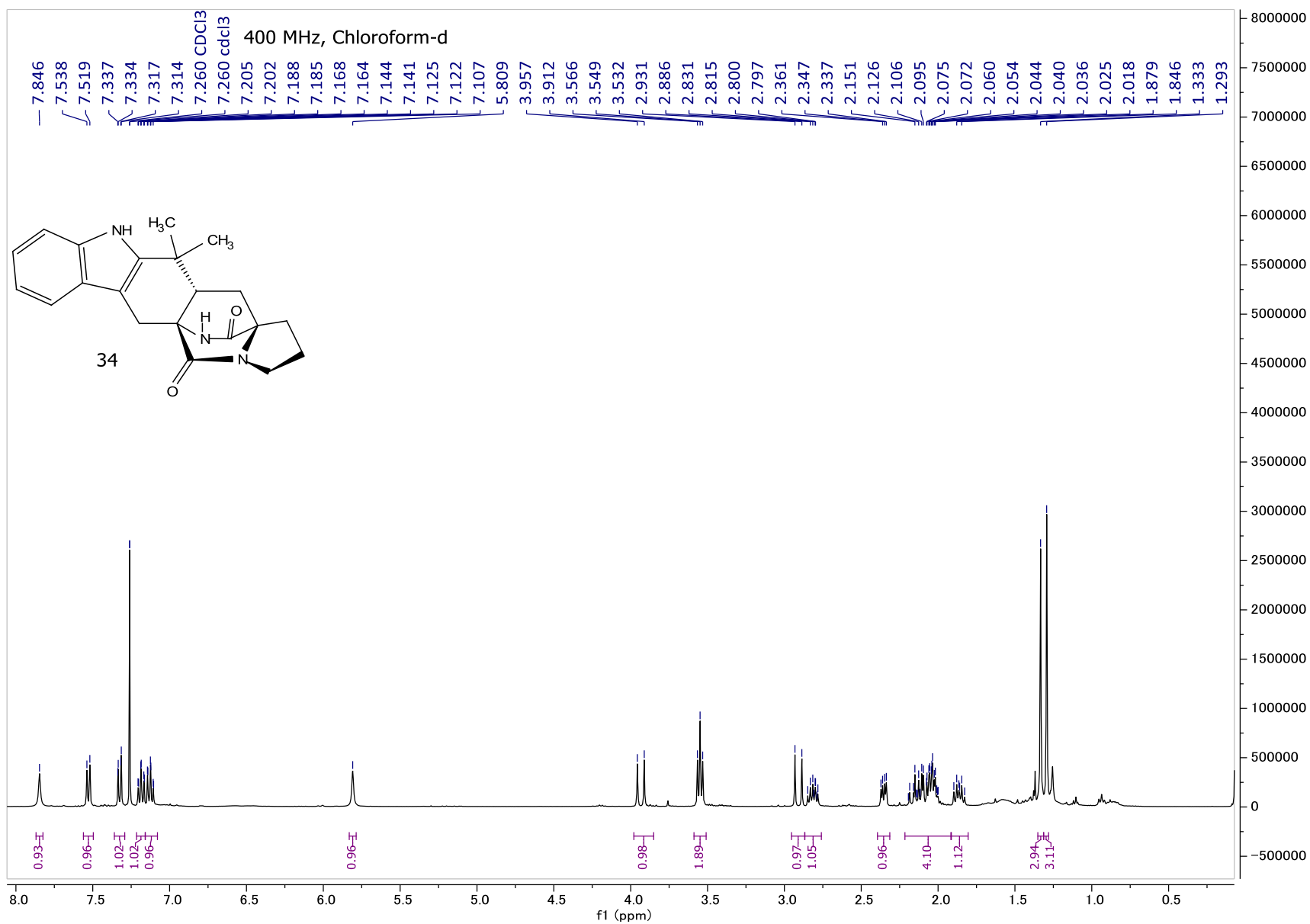


Figure A28: <sup>1</sup>H NMR spectrum of **34**.

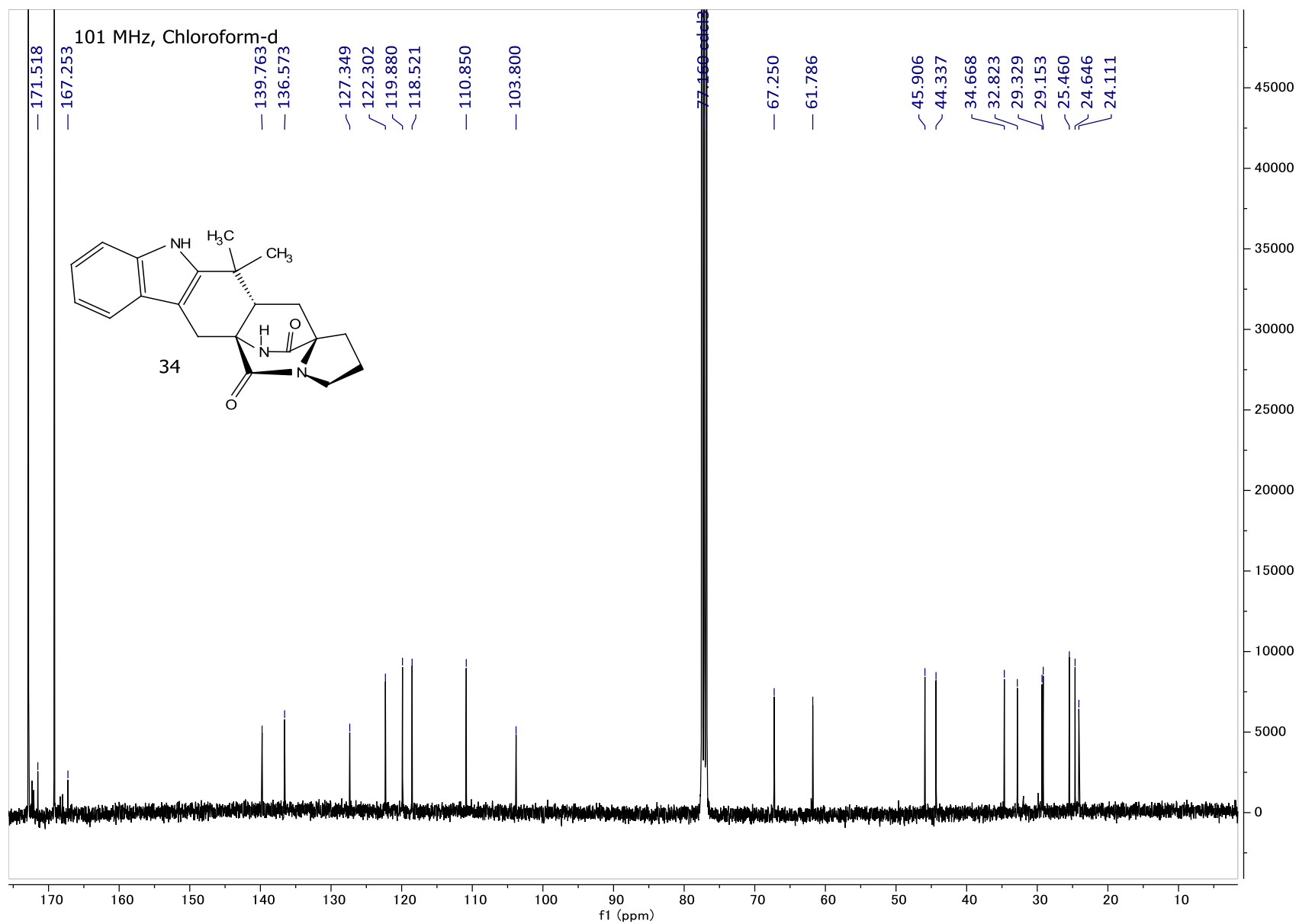


Figure A29: <sup>13</sup>C NMR spectrum of **34**.

400 MHz, Chloroform-d

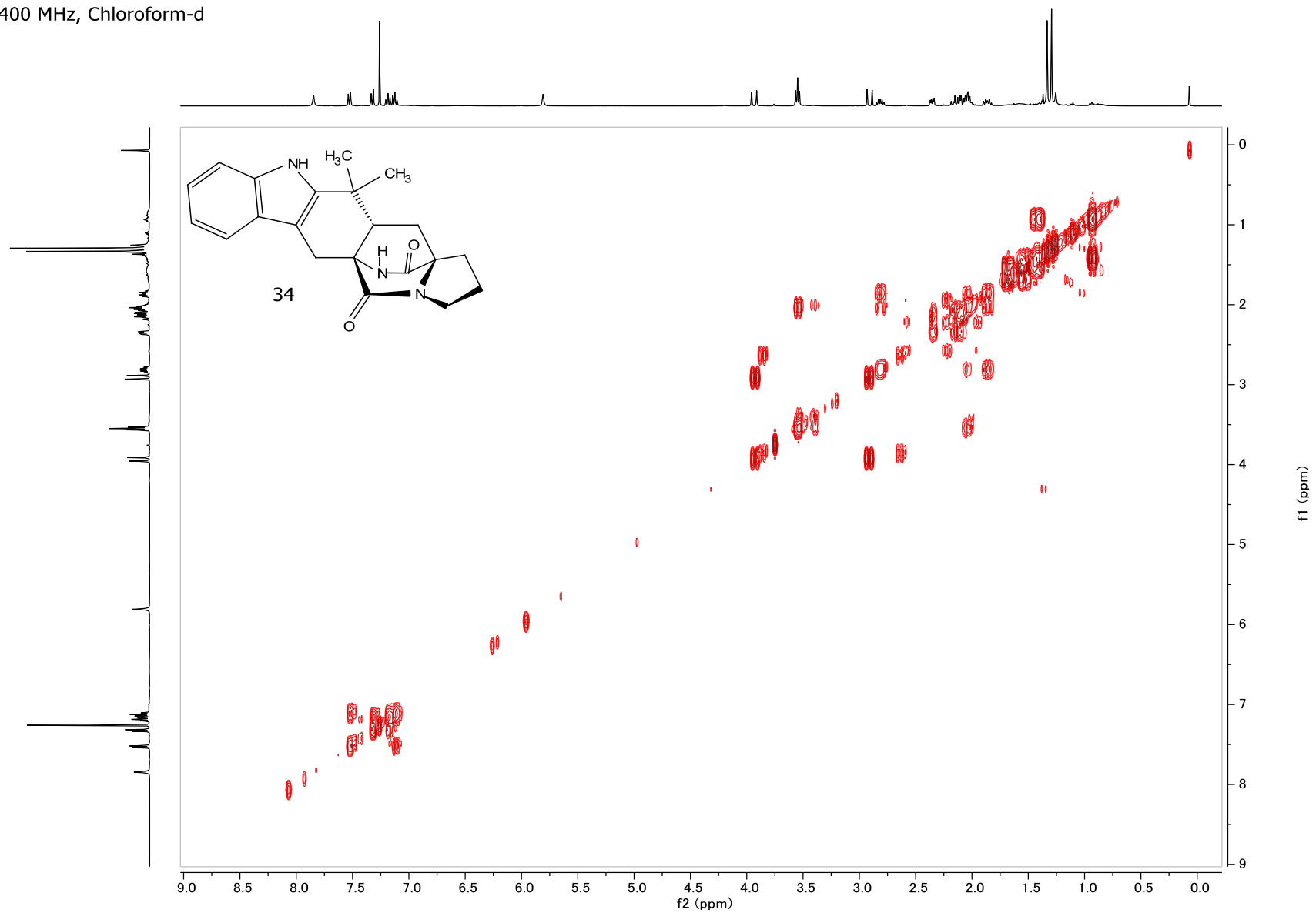


Figure A30: COSY NMR spectrum of **34**.

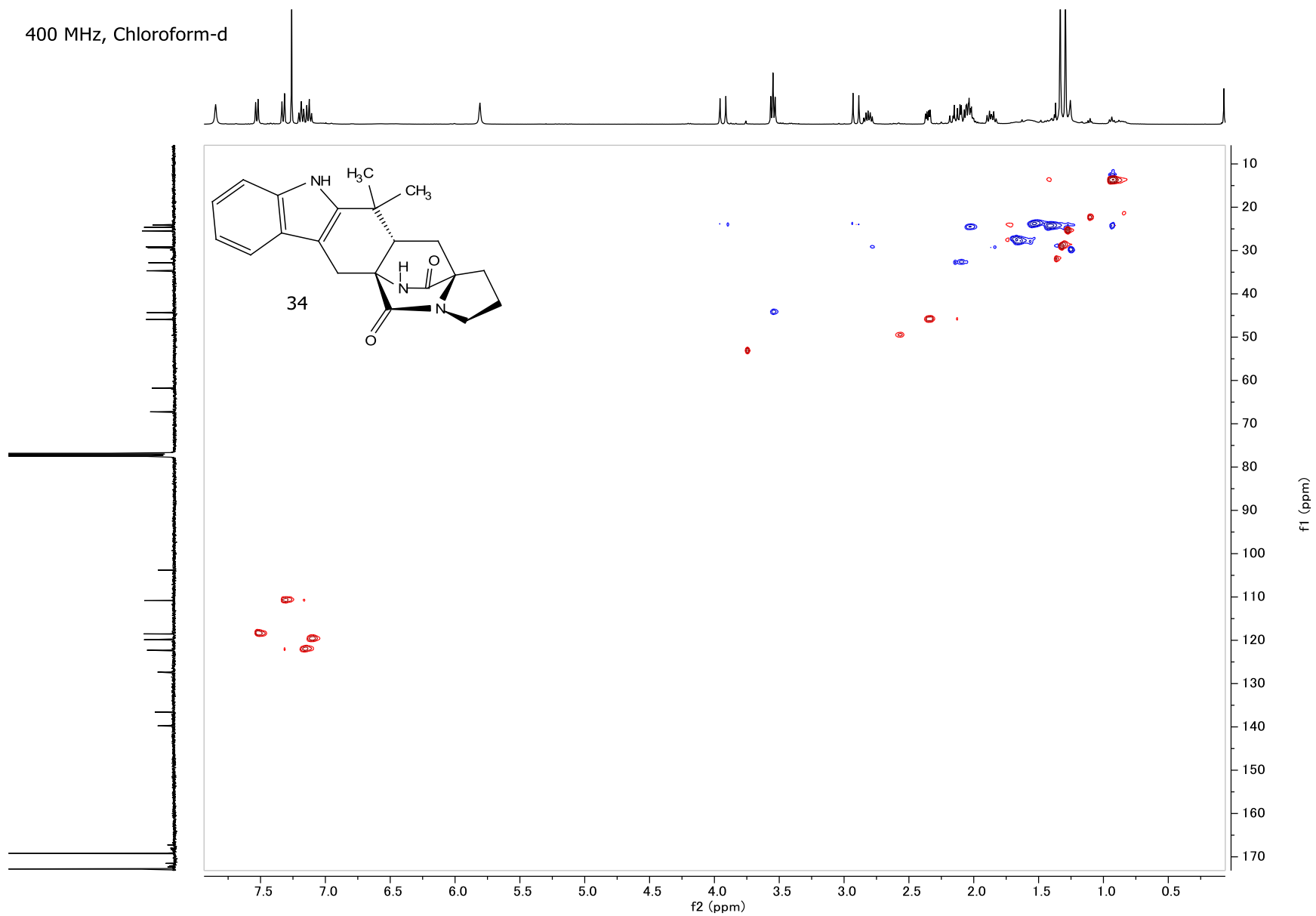


Figure A31: HSQC NMR spectrum of **34**.

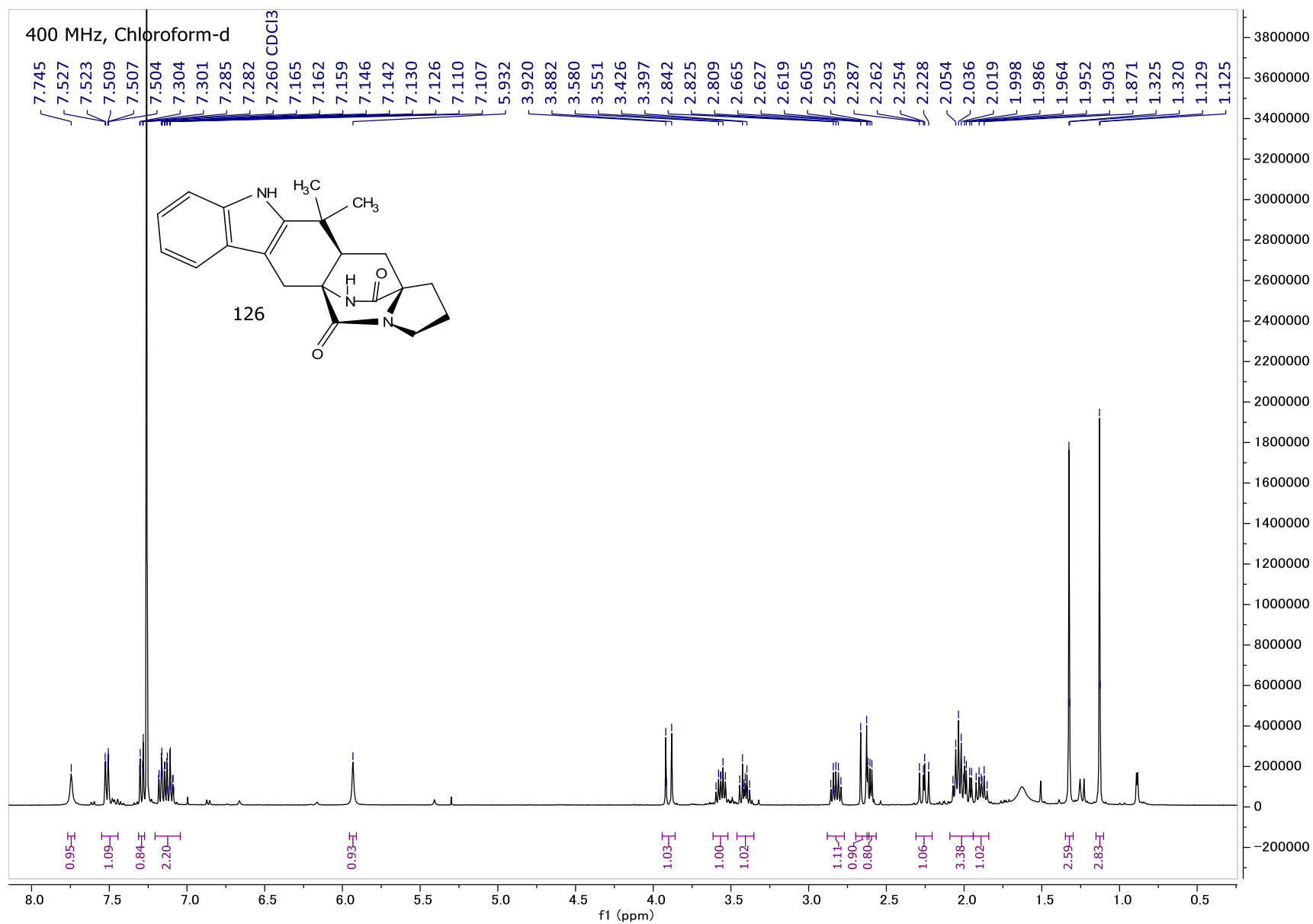


Figure A32: <sup>1</sup>H NMR spectrum of **126**.

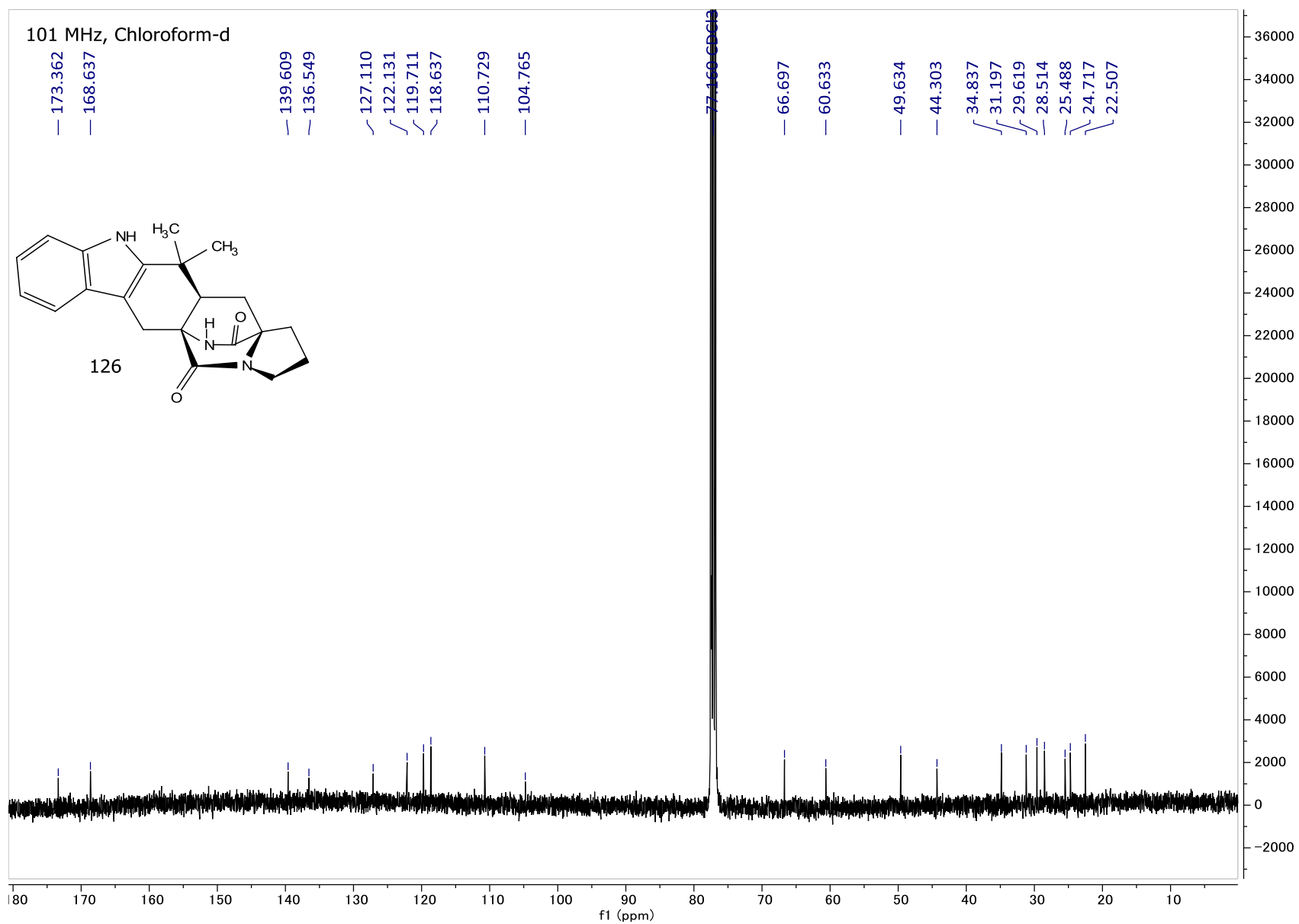


Figure A33: <sup>13</sup>C NMR spectrum of **126**.

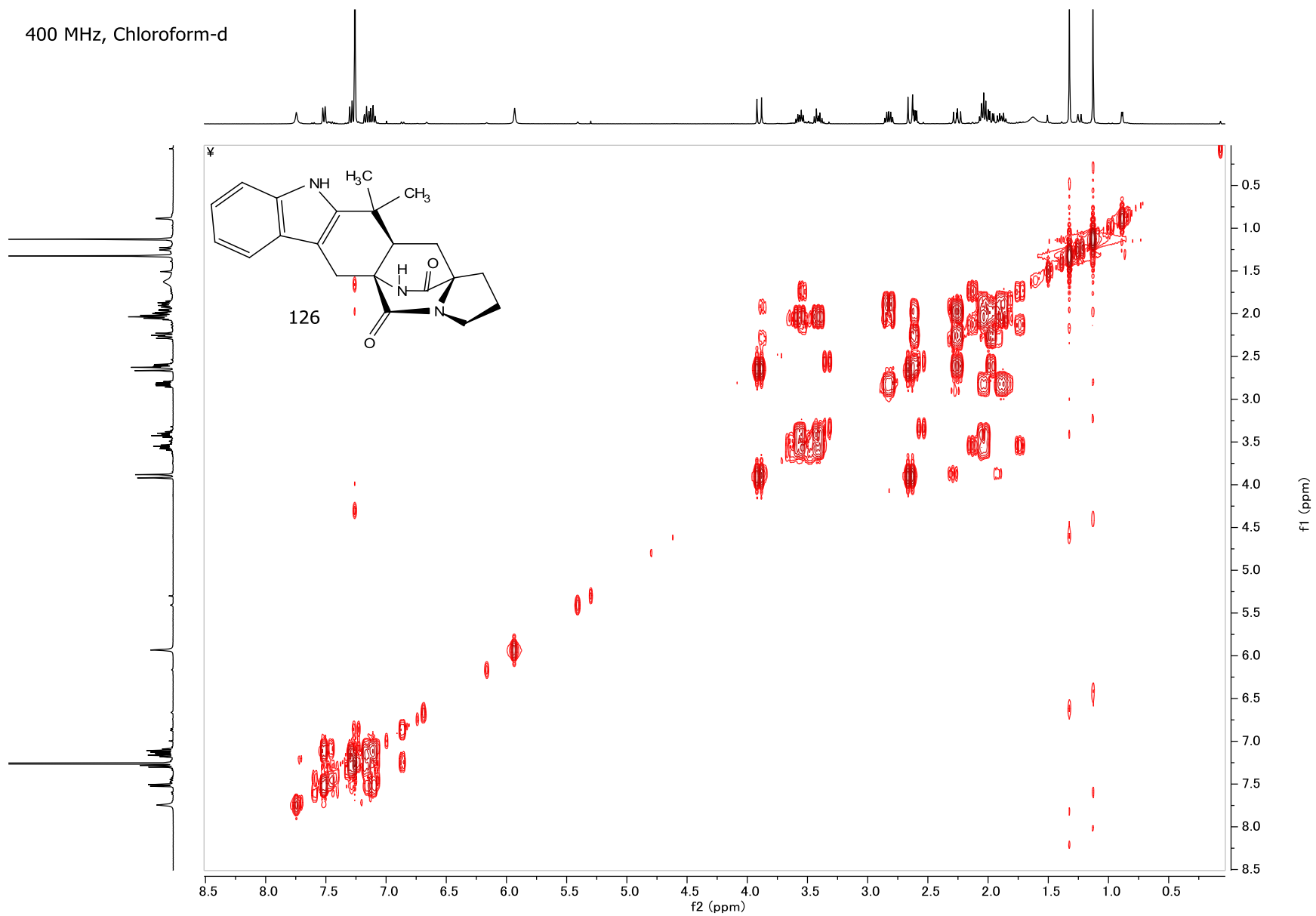


Figure A34: COSY NMR spectrum of **126**.

400 MHz, Chloroform-d

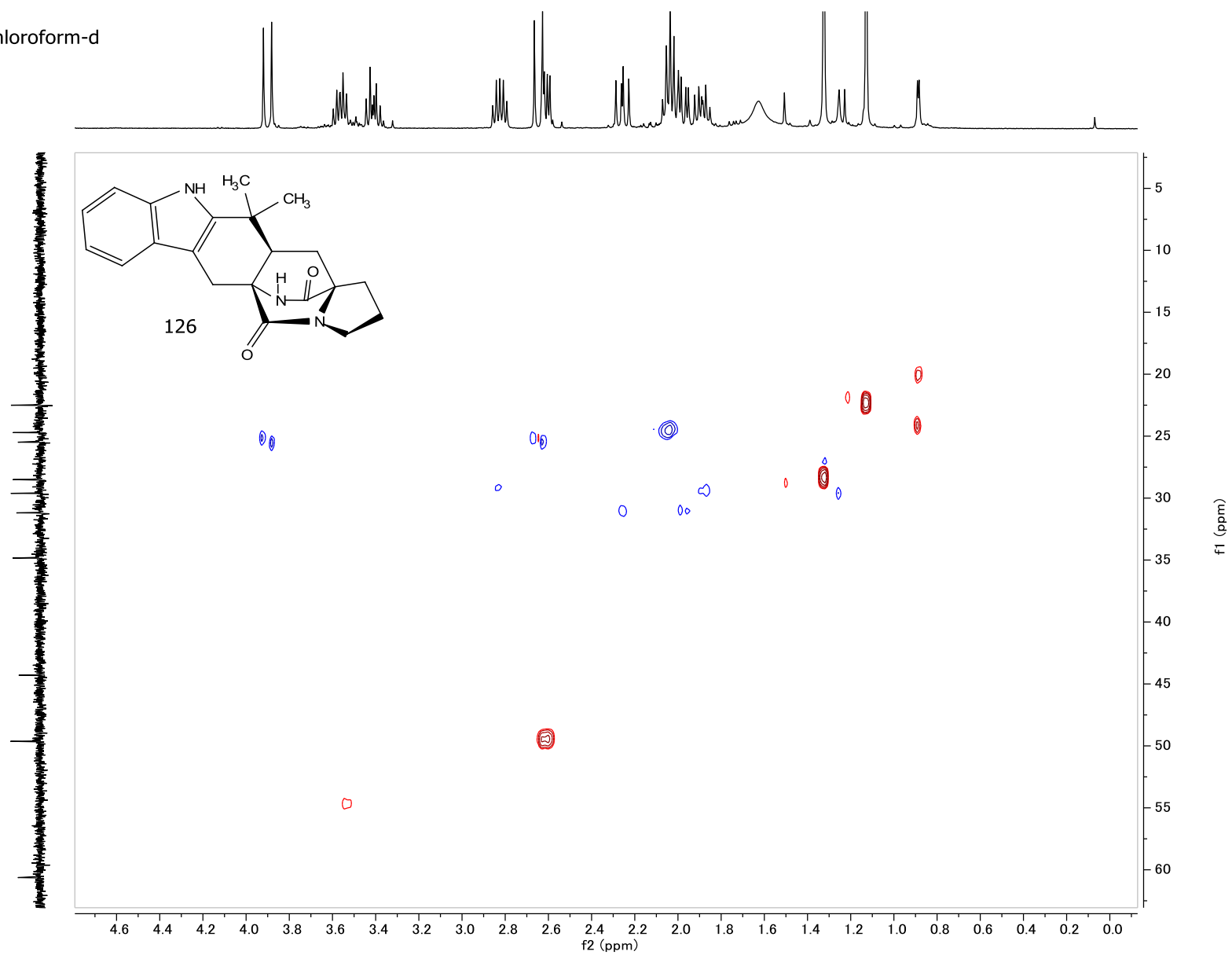


Figure A35: HSQC NMR spectrum of **126**.

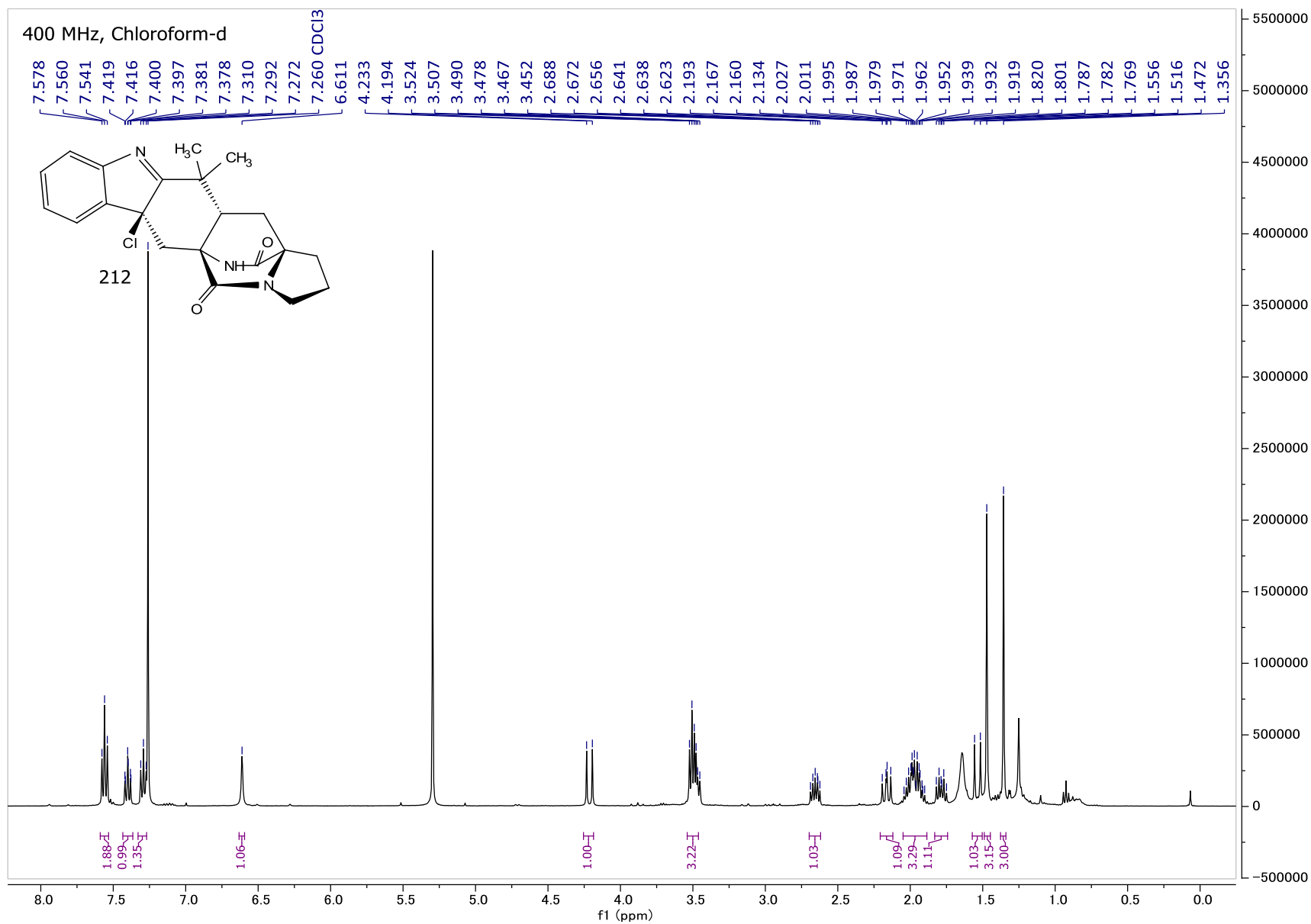


Figure A36: <sup>1</sup>H NMR spectrum of **212**.

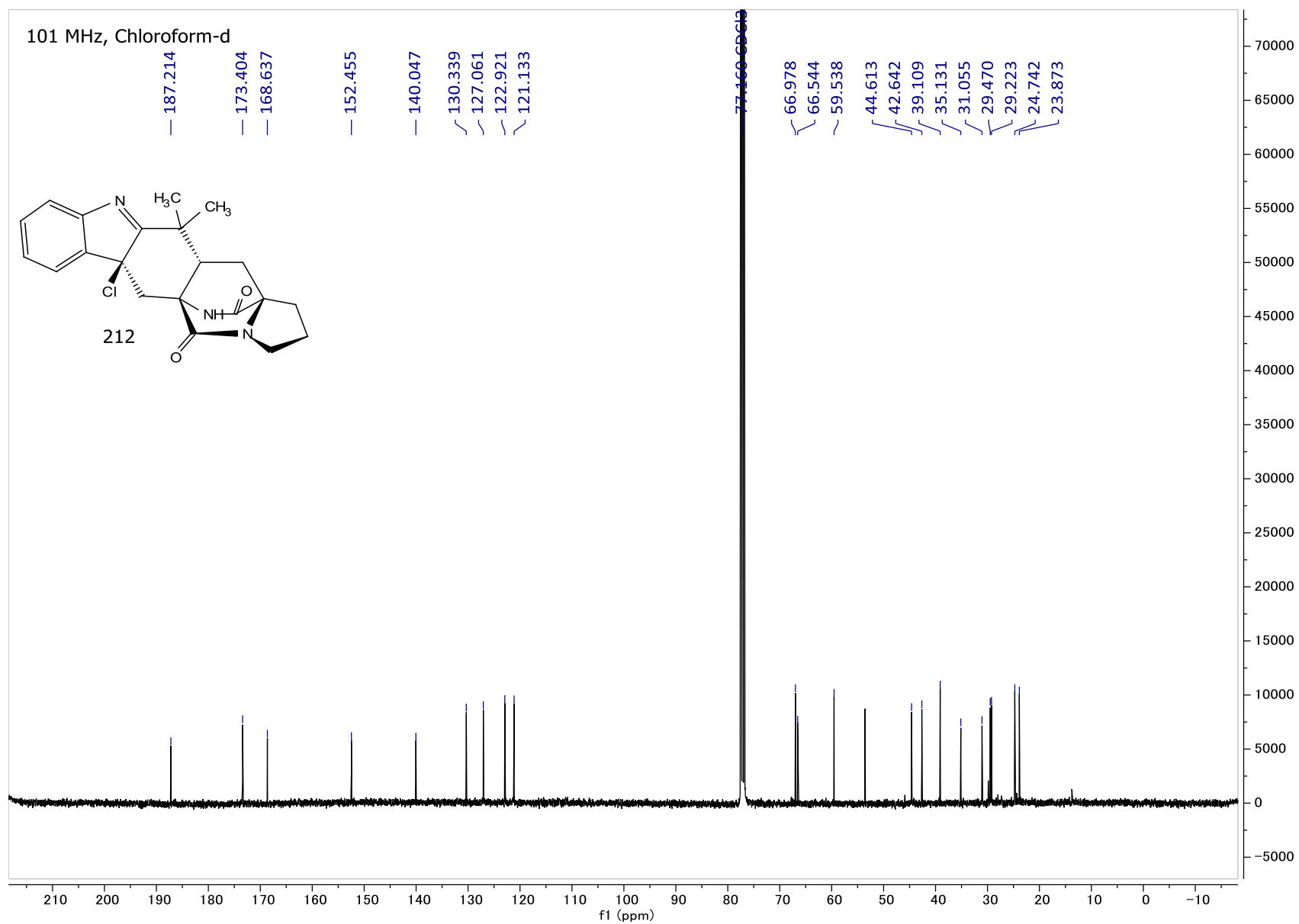


Figure A37:  $^{13}\text{C}$  NMR spectrum of **212**.

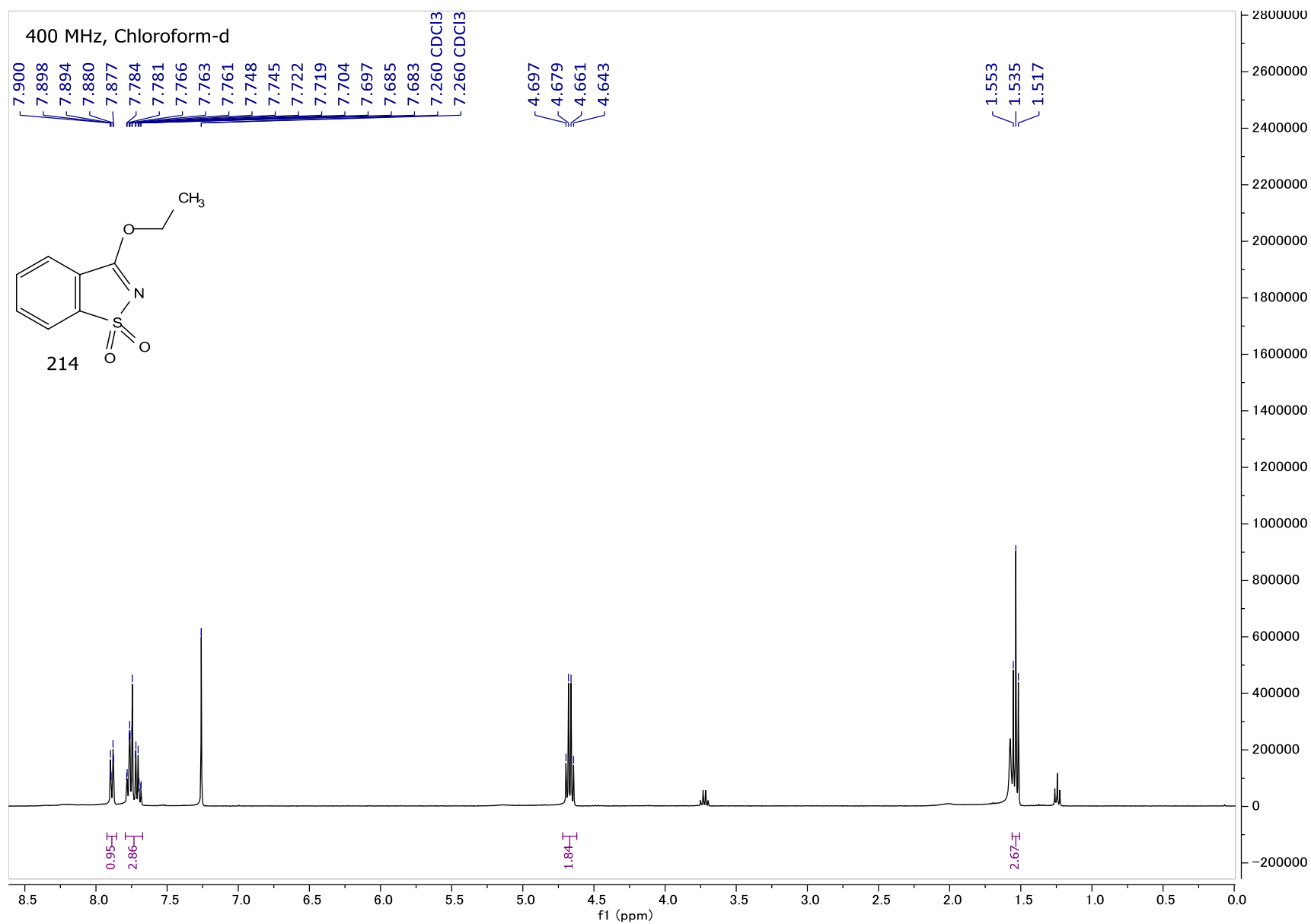


Figure A38: <sup>1</sup>H NMR spectrum of **214**.

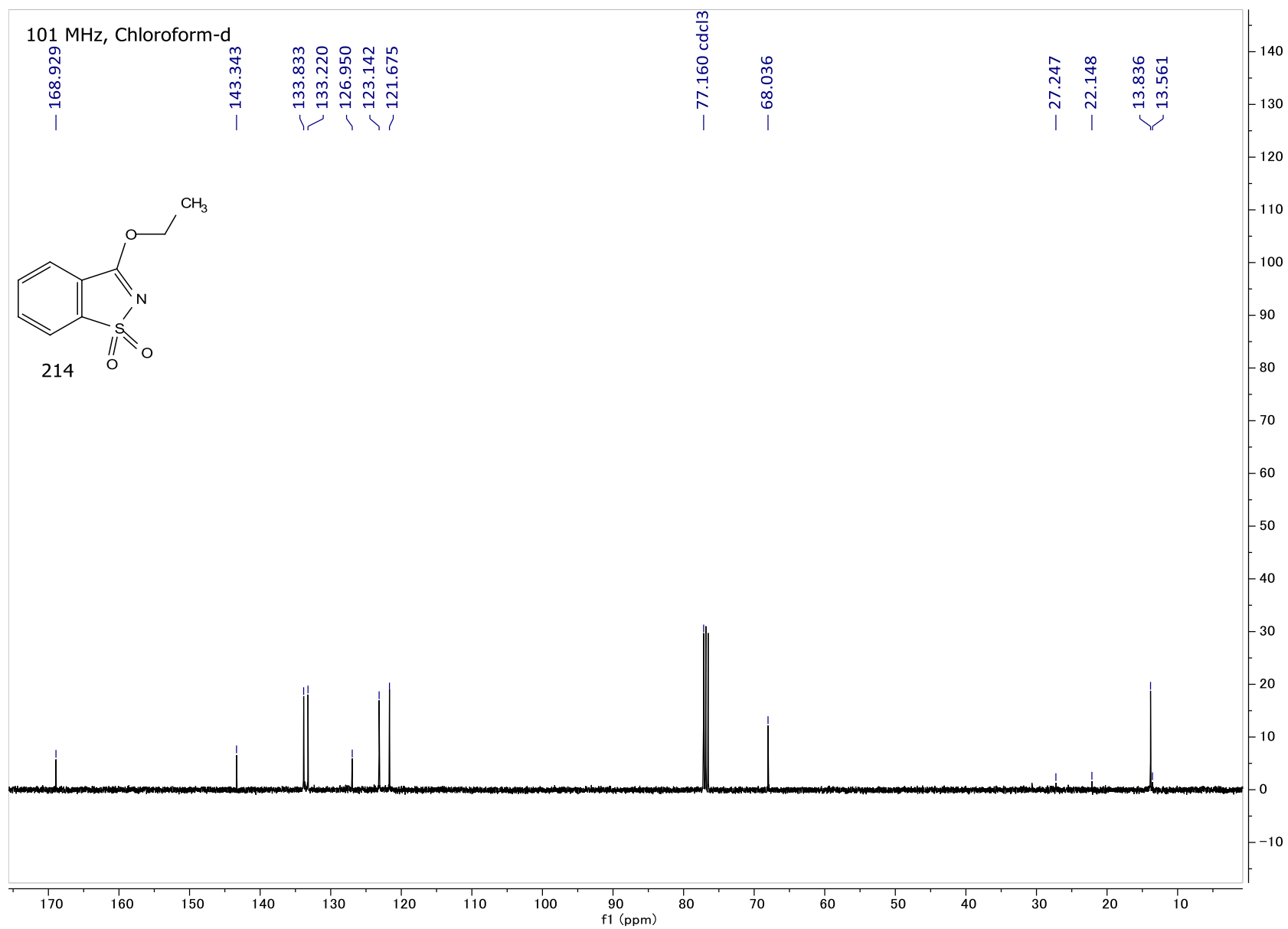


Figure A39:  $^{13}\text{C}$  NMR spectrum of **214**.

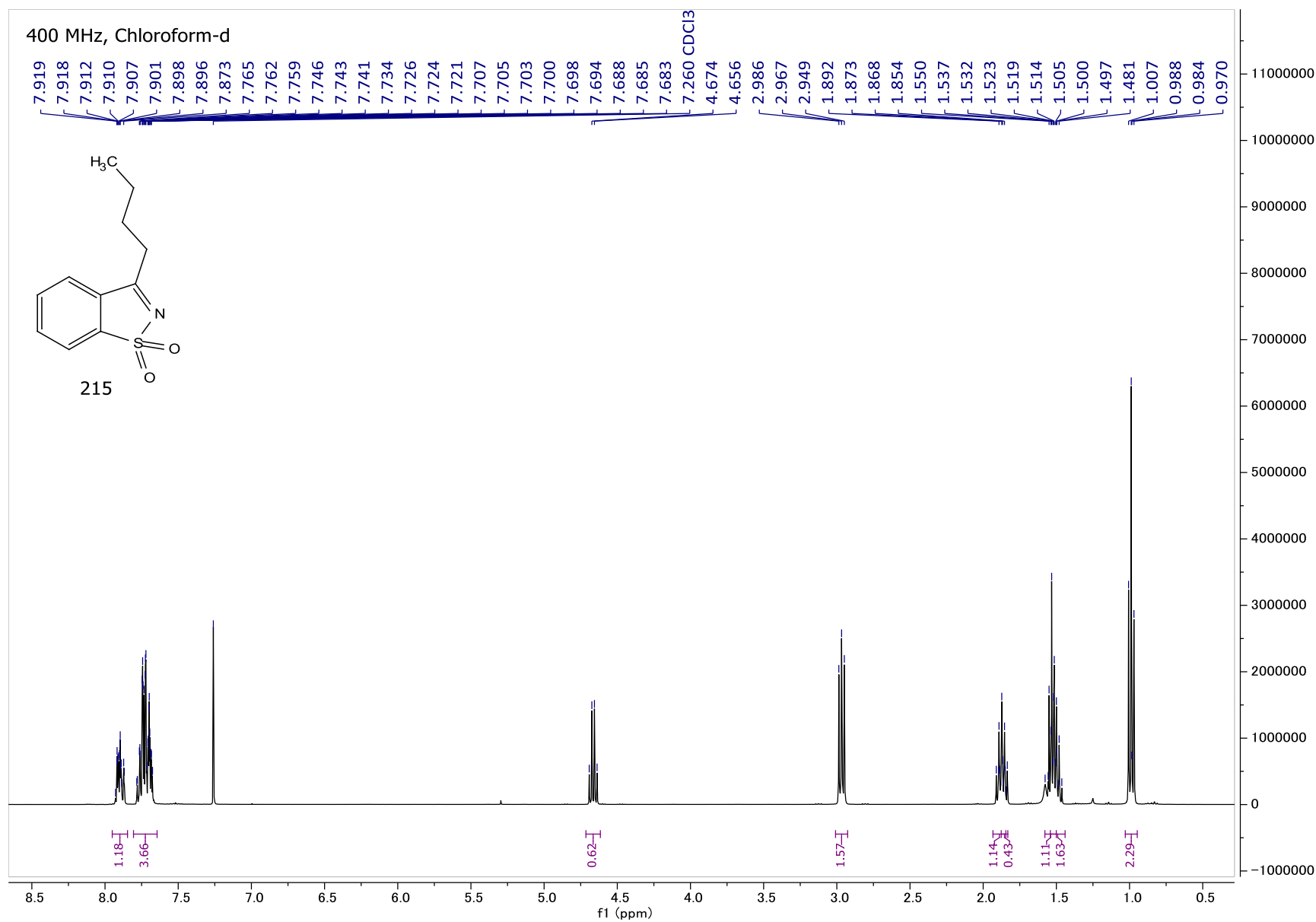


Figure A40: <sup>1</sup>H NMR spectrum of **215**.

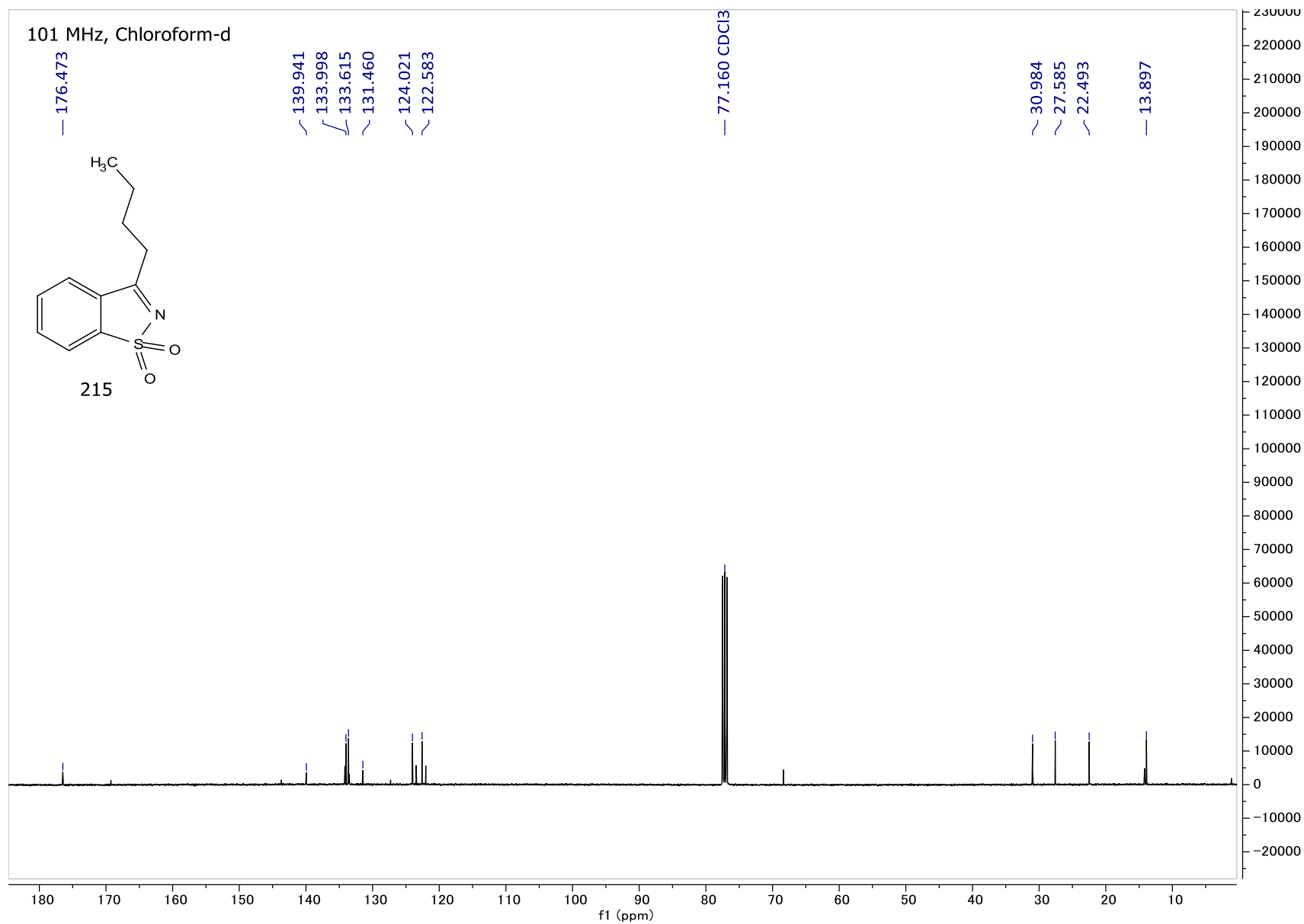


Figure A41: <sup>13</sup>C NMR spectrum of **215**.

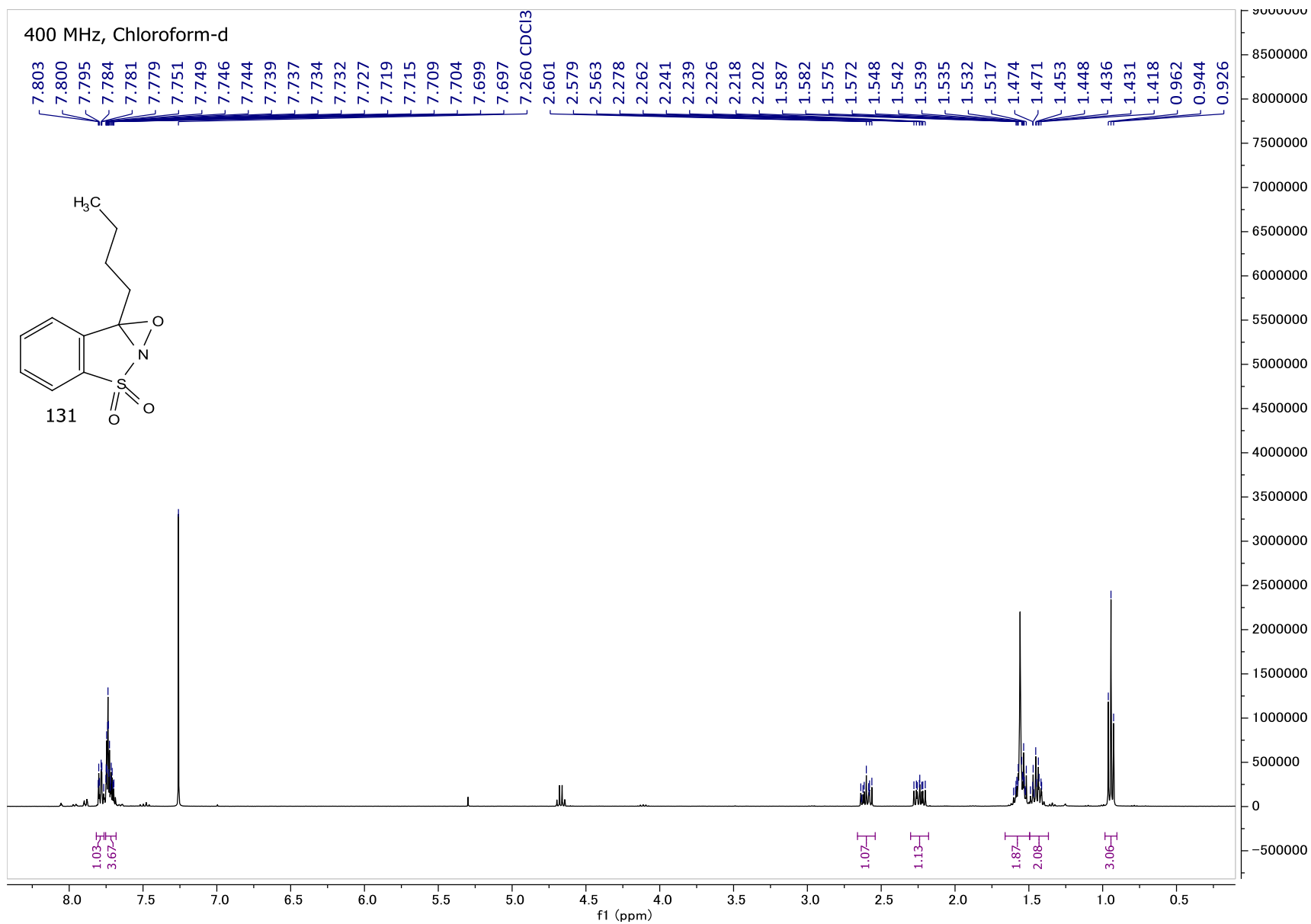


Figure A42: <sup>1</sup>H NMR spectrum of **131**.

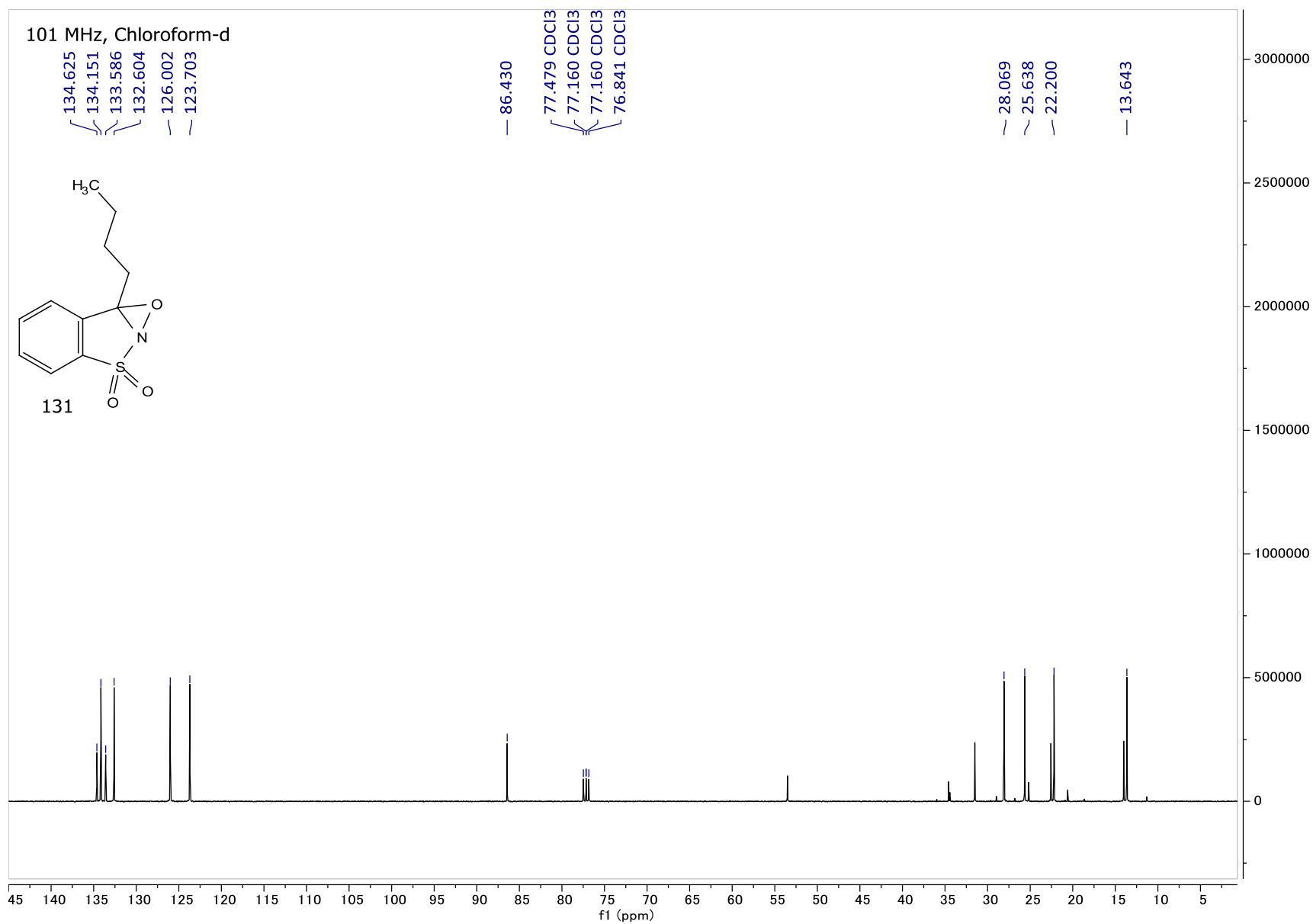


Figure A43: <sup>13</sup>C NMR spectrum of **131**.

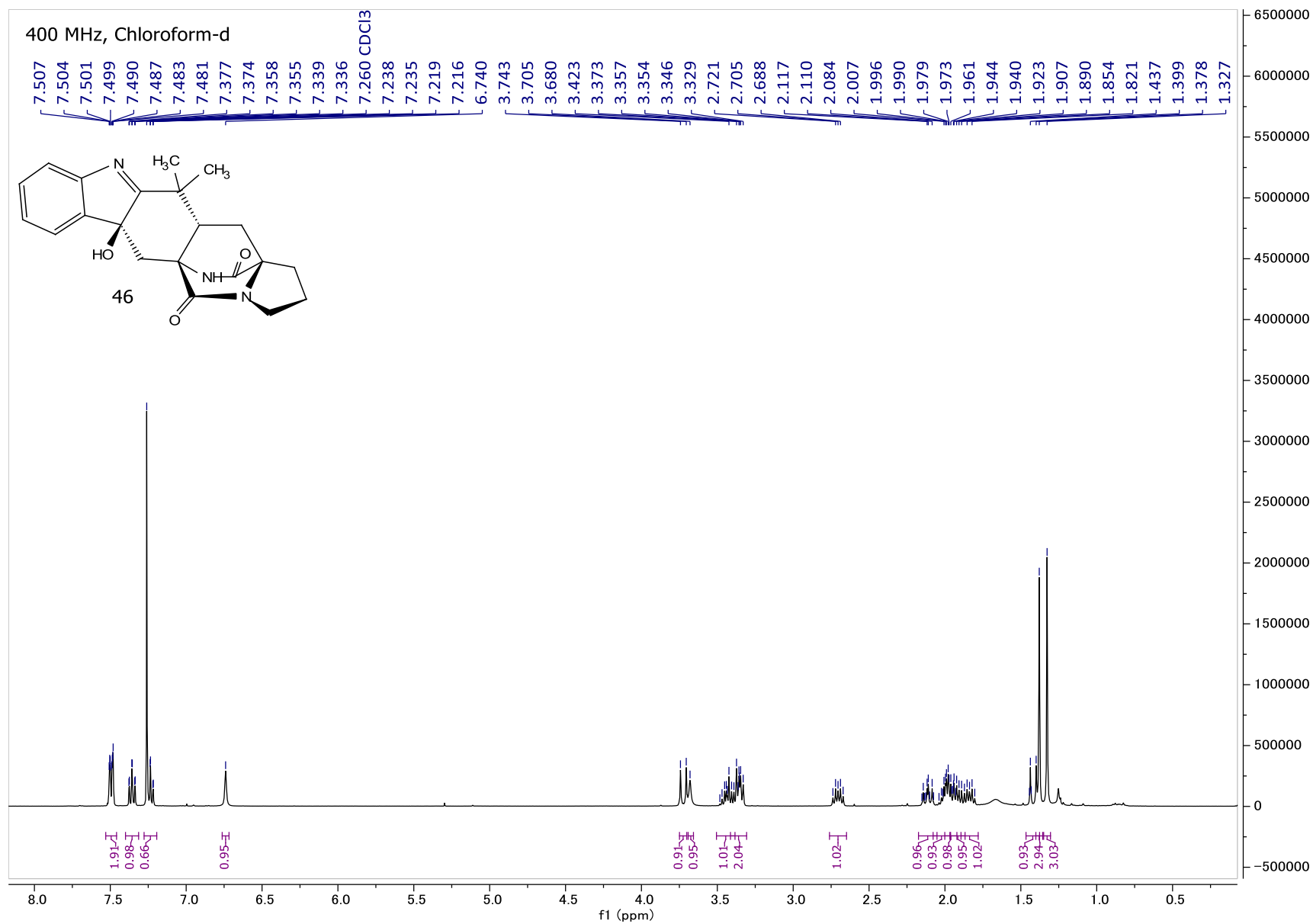


Figure A44: <sup>1</sup>H NMR spectrum of **46**.

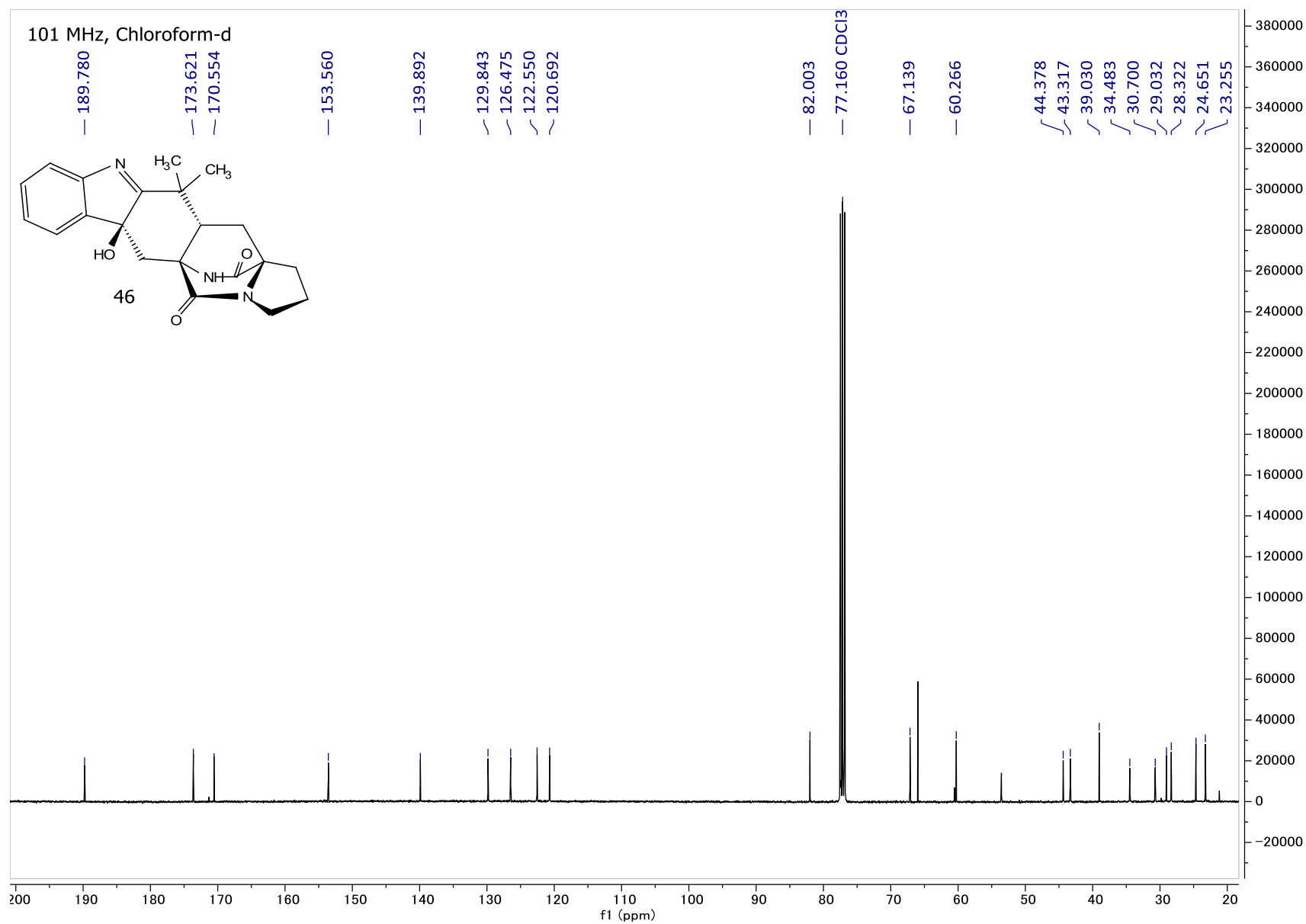


Figure A45:  $^{13}\text{C}$  NMR spectrum of **46**.

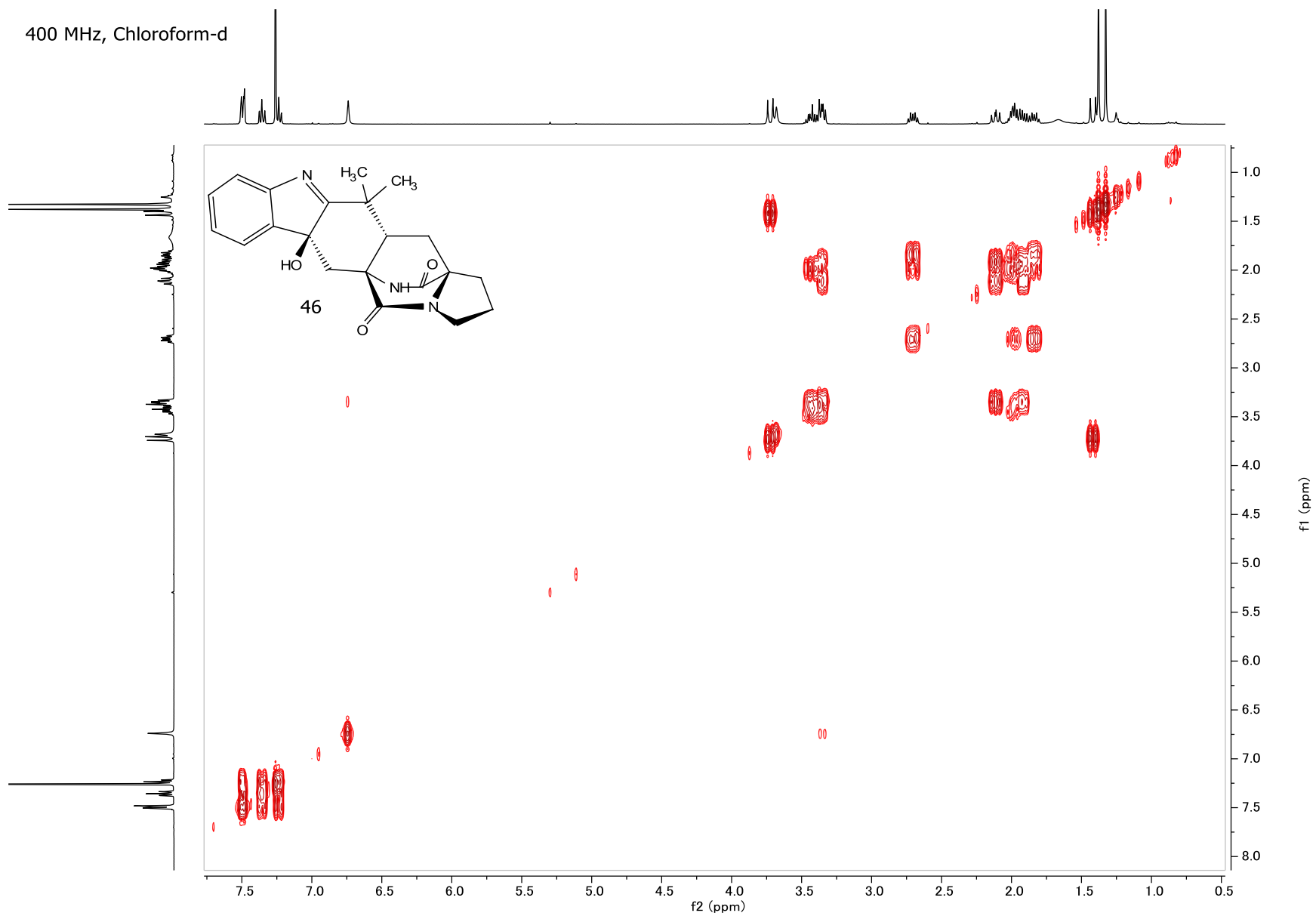


Figure A46: COSY NMR spectrum of **46**.

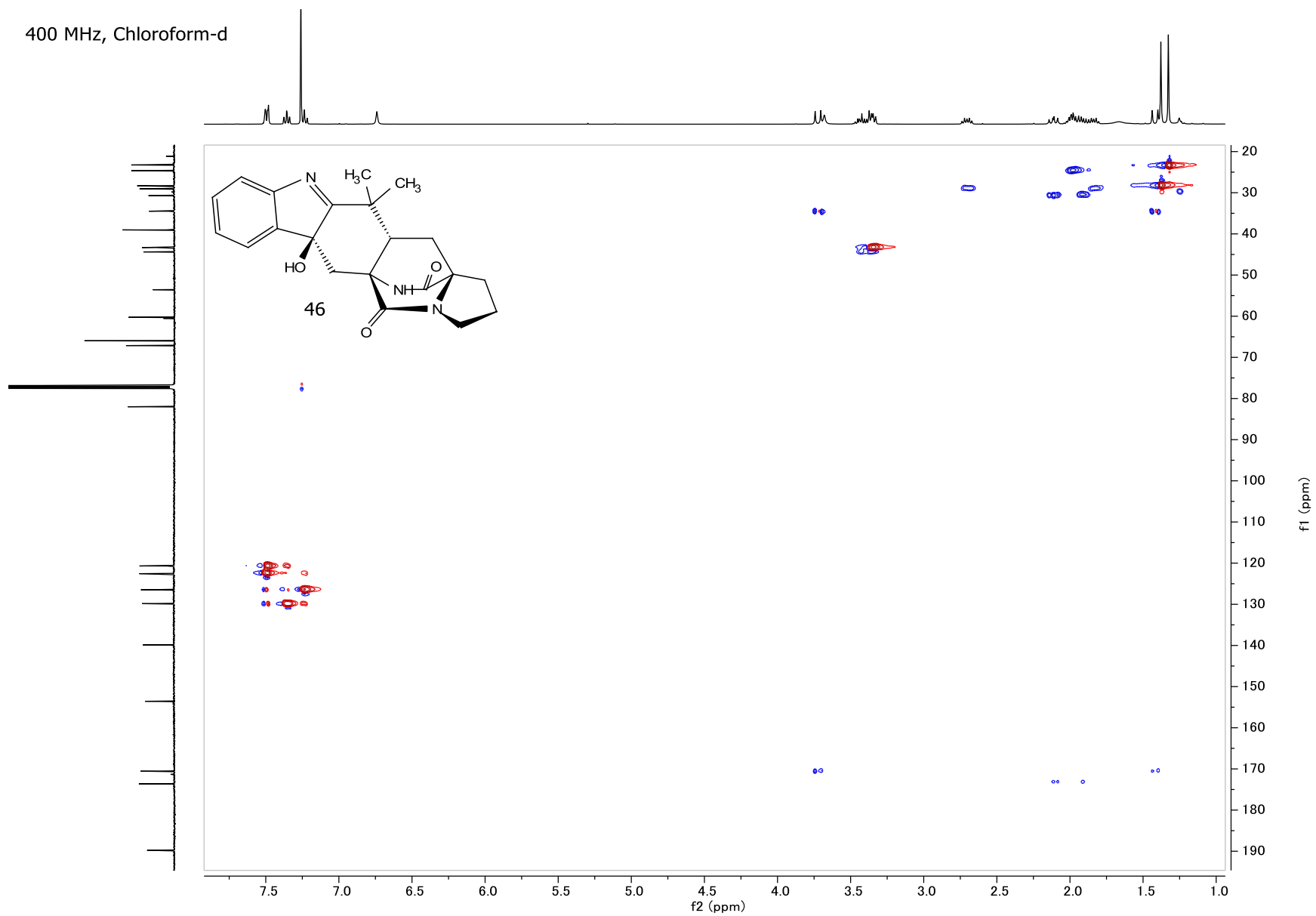


Figure A47: HSQC NMR spectrum of **46**.

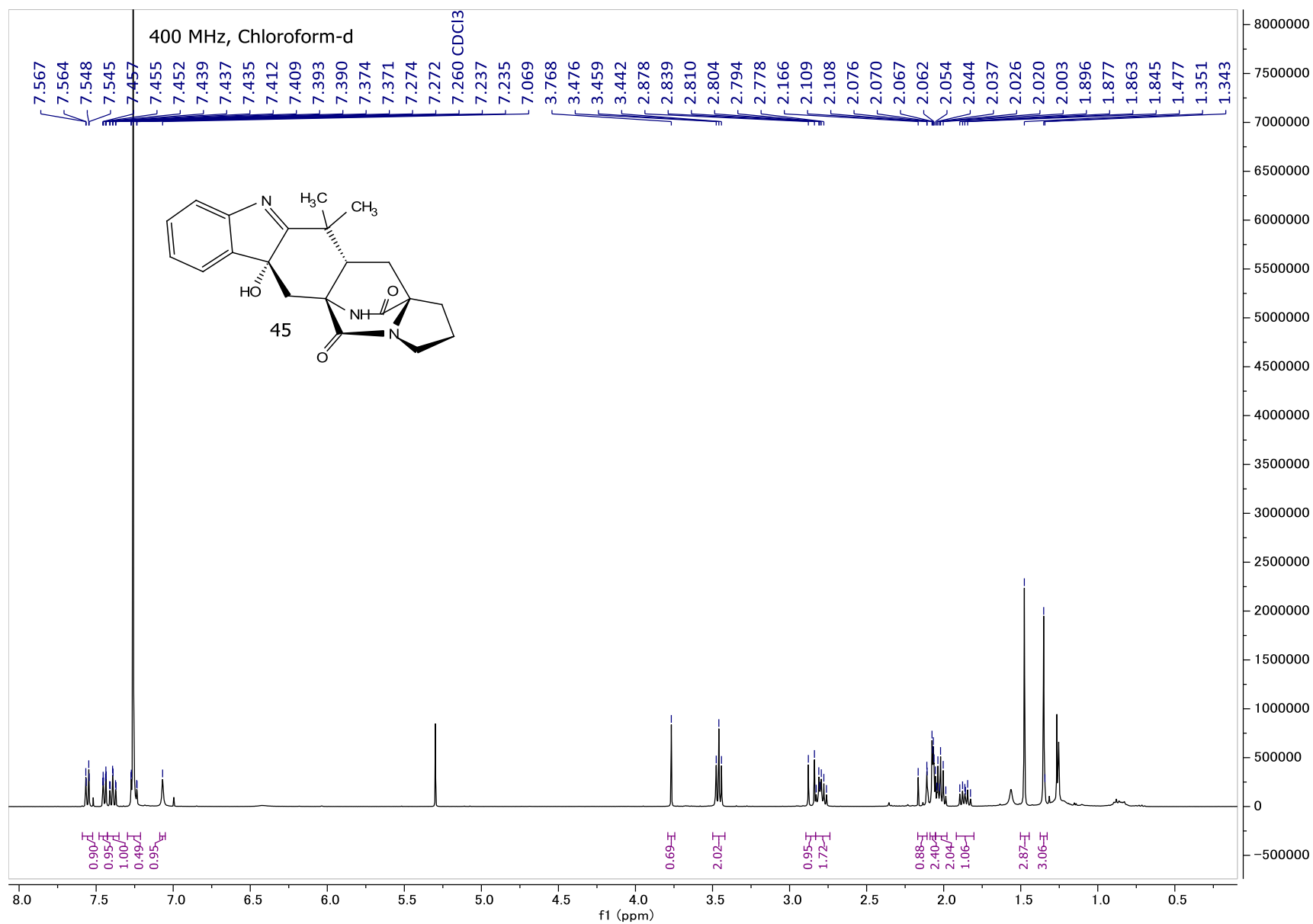


Figure A48: <sup>1</sup>H NMR spectrum of **45**.

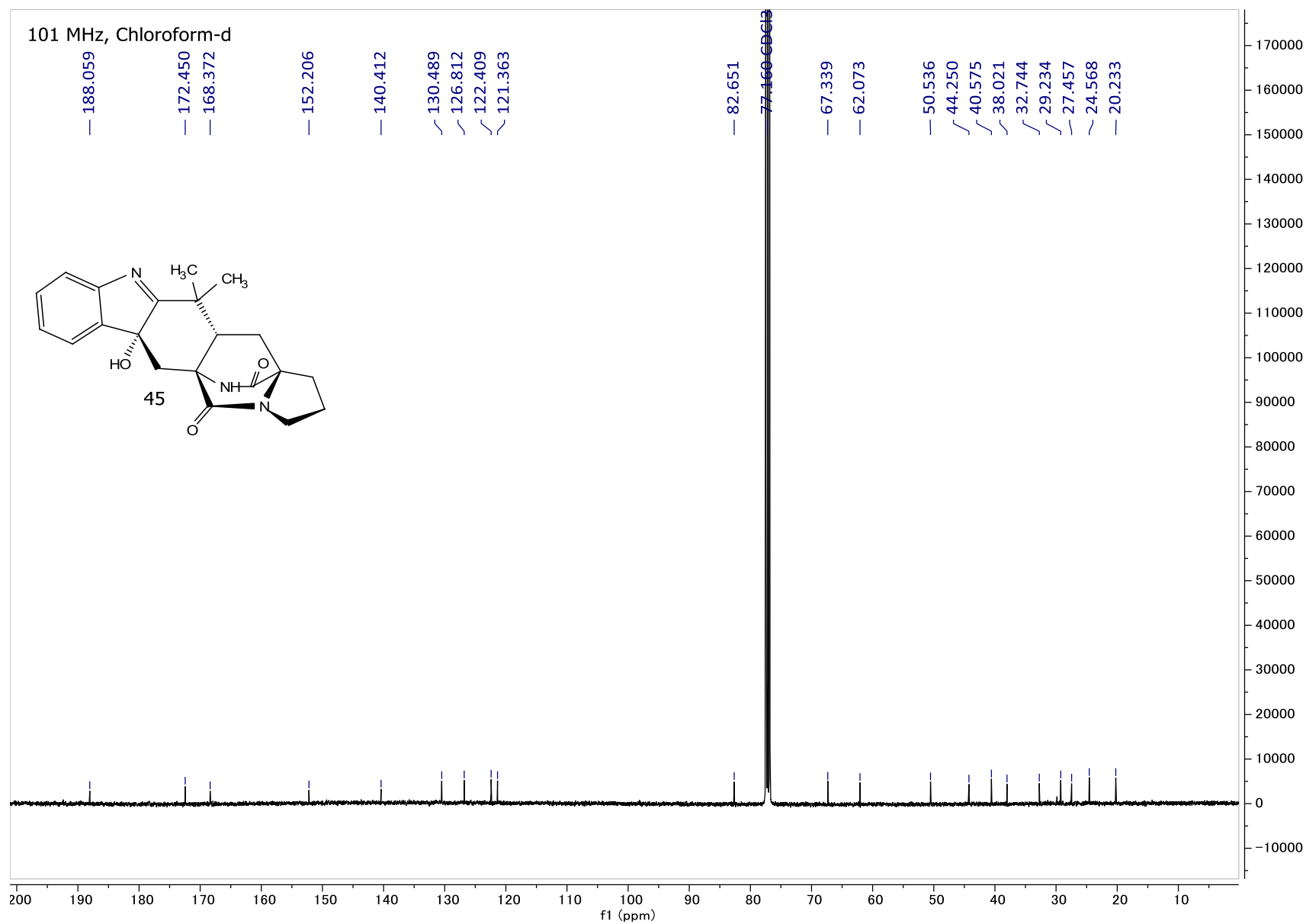


Figure A49: <sup>13</sup>C NMR spectrum of **45**.

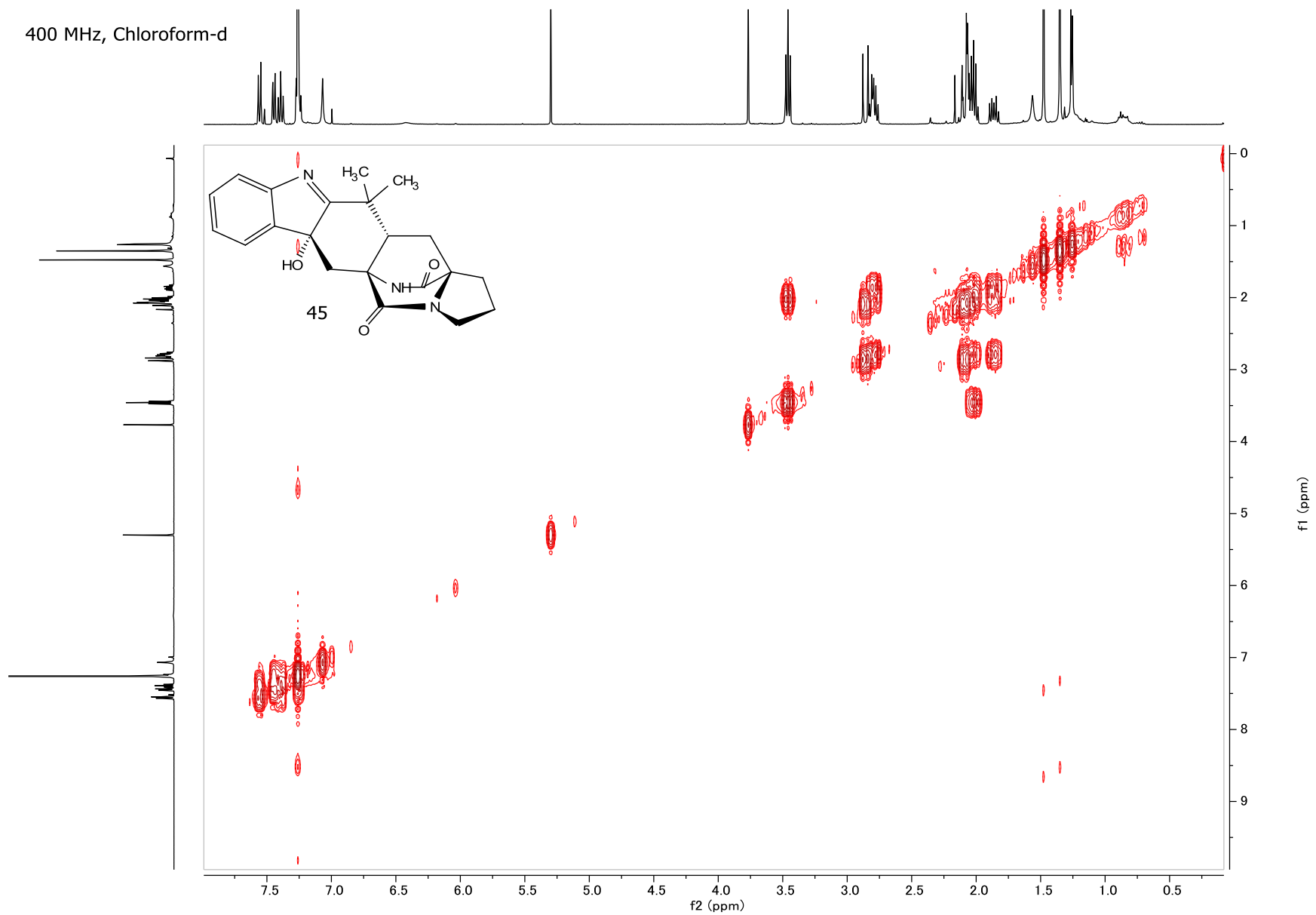


Figure A50: COSY NMR spectrum of **45**.

400 MHz, Chloroform-d

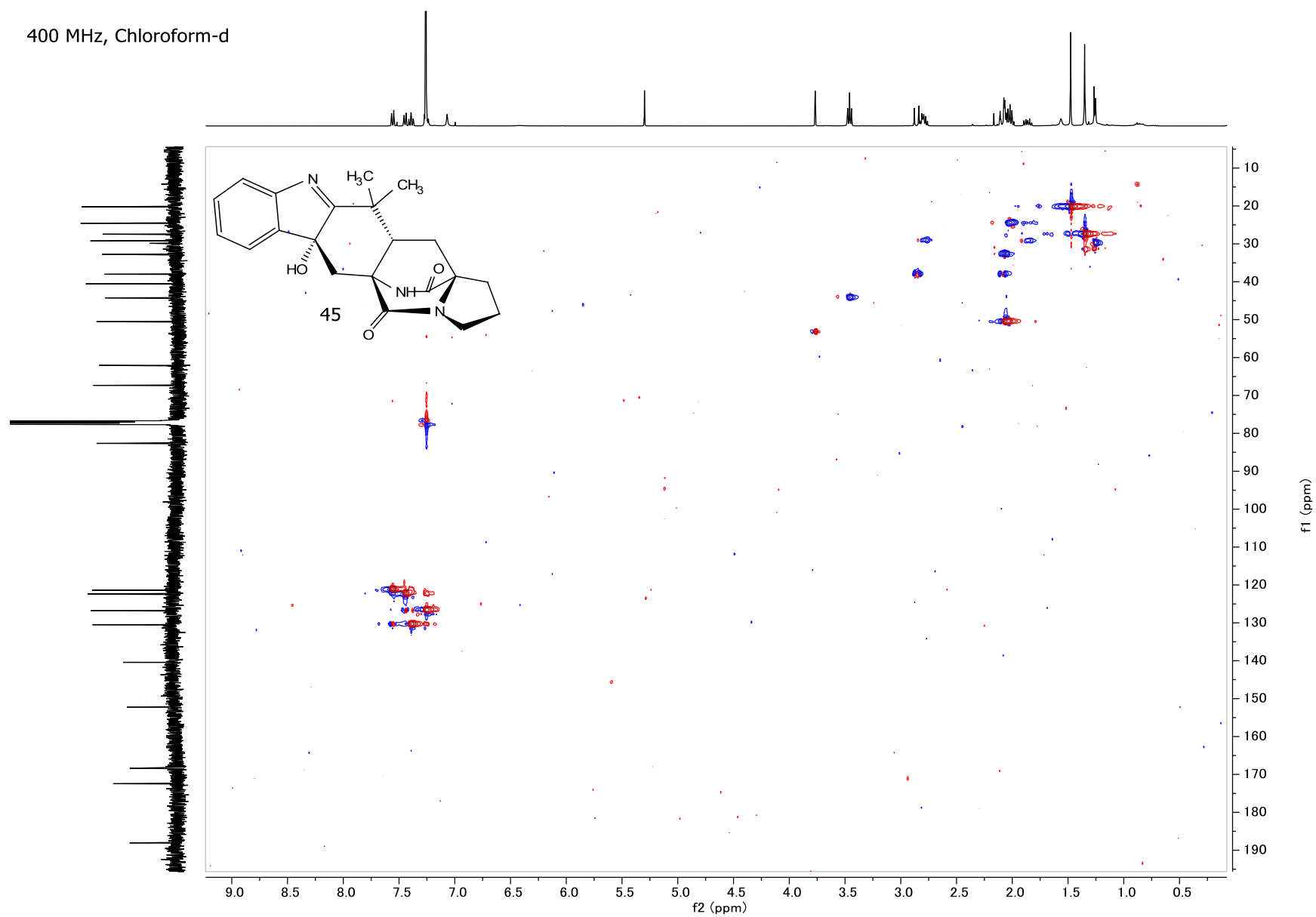


Figure A51: HSQC NMR spectrum of **45**.

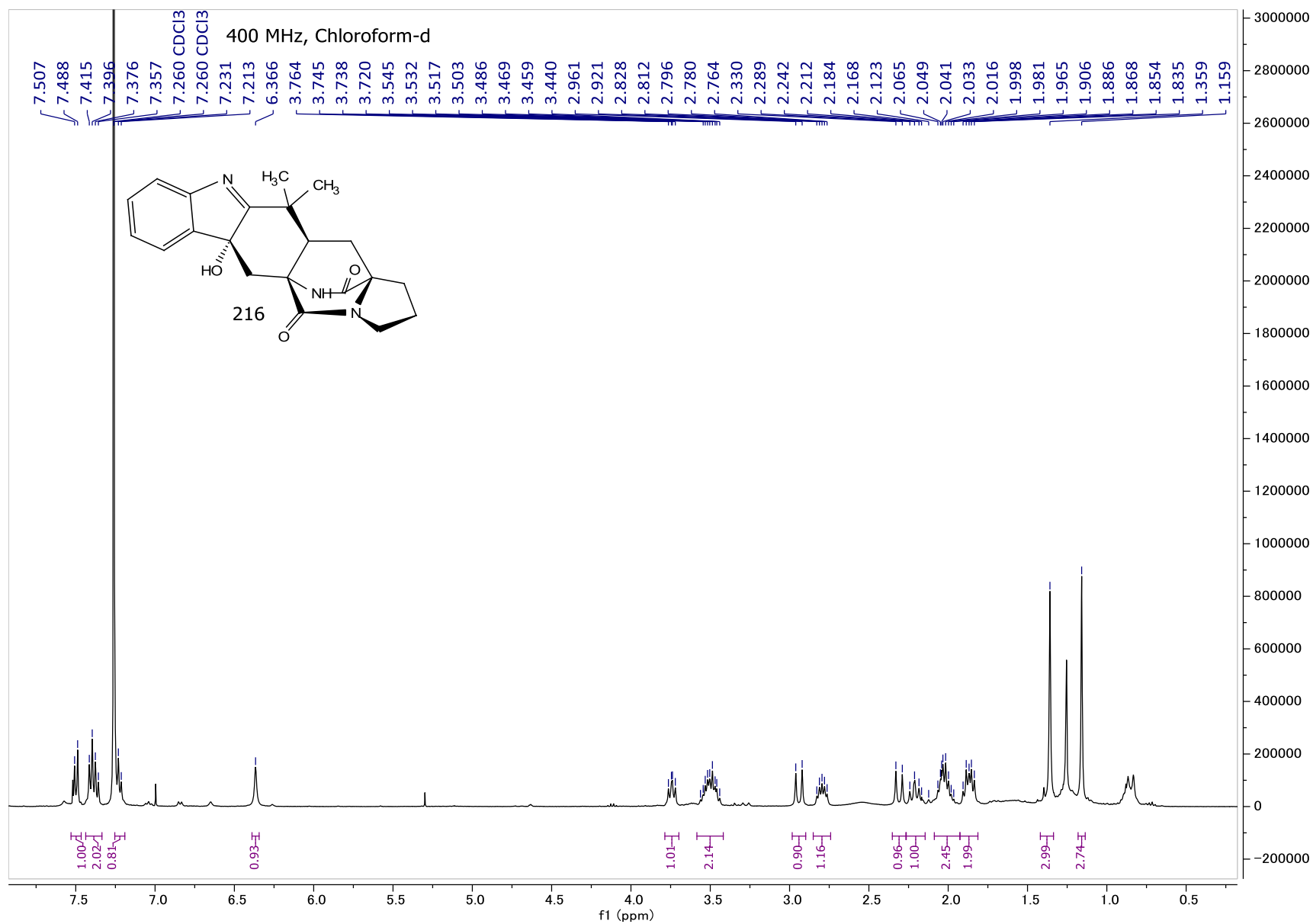


Figure A52:  $^1\text{H}$  NMR spectrum of 216.

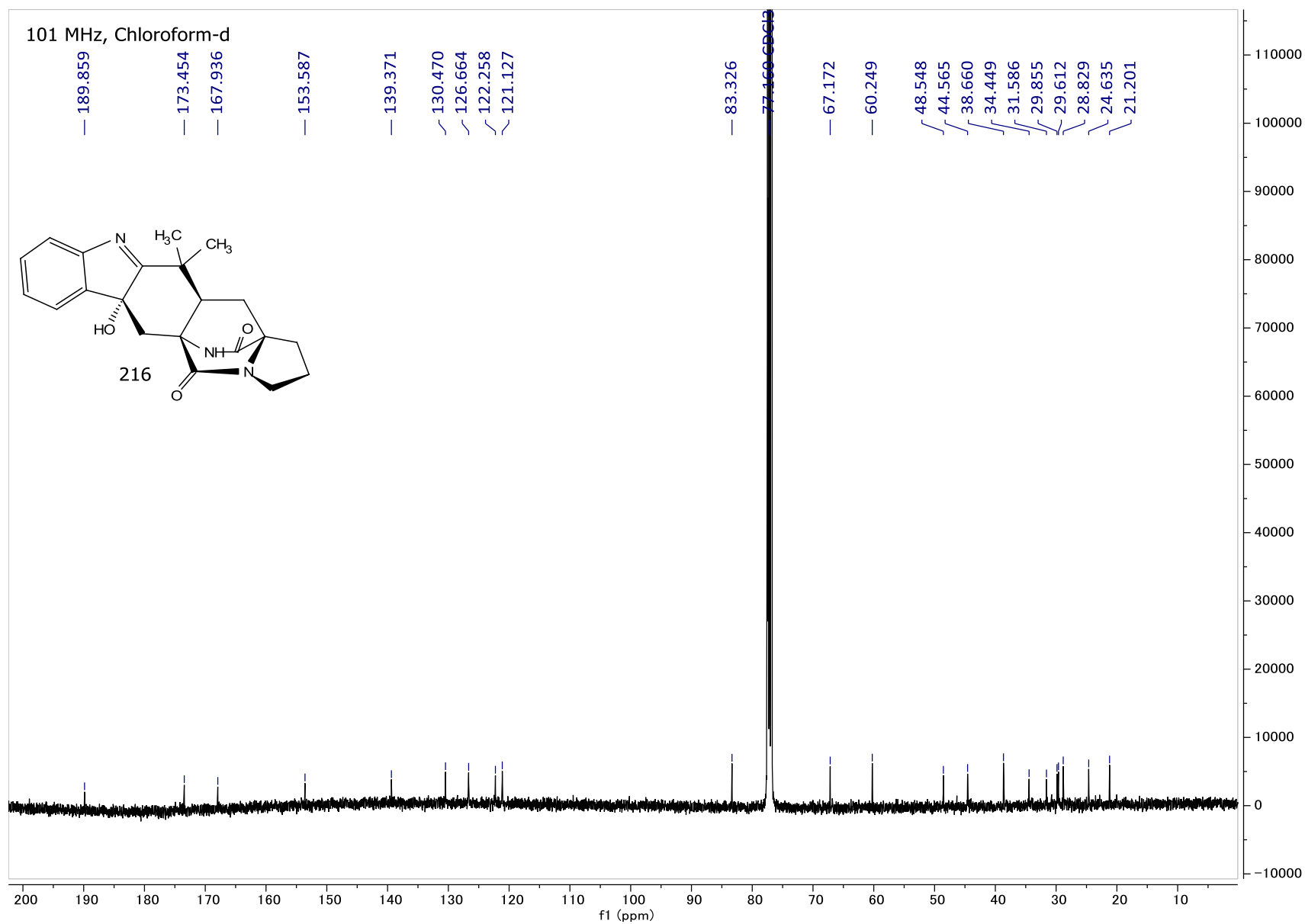


Figure A53: <sup>13</sup>C NMR spectrum of 216.

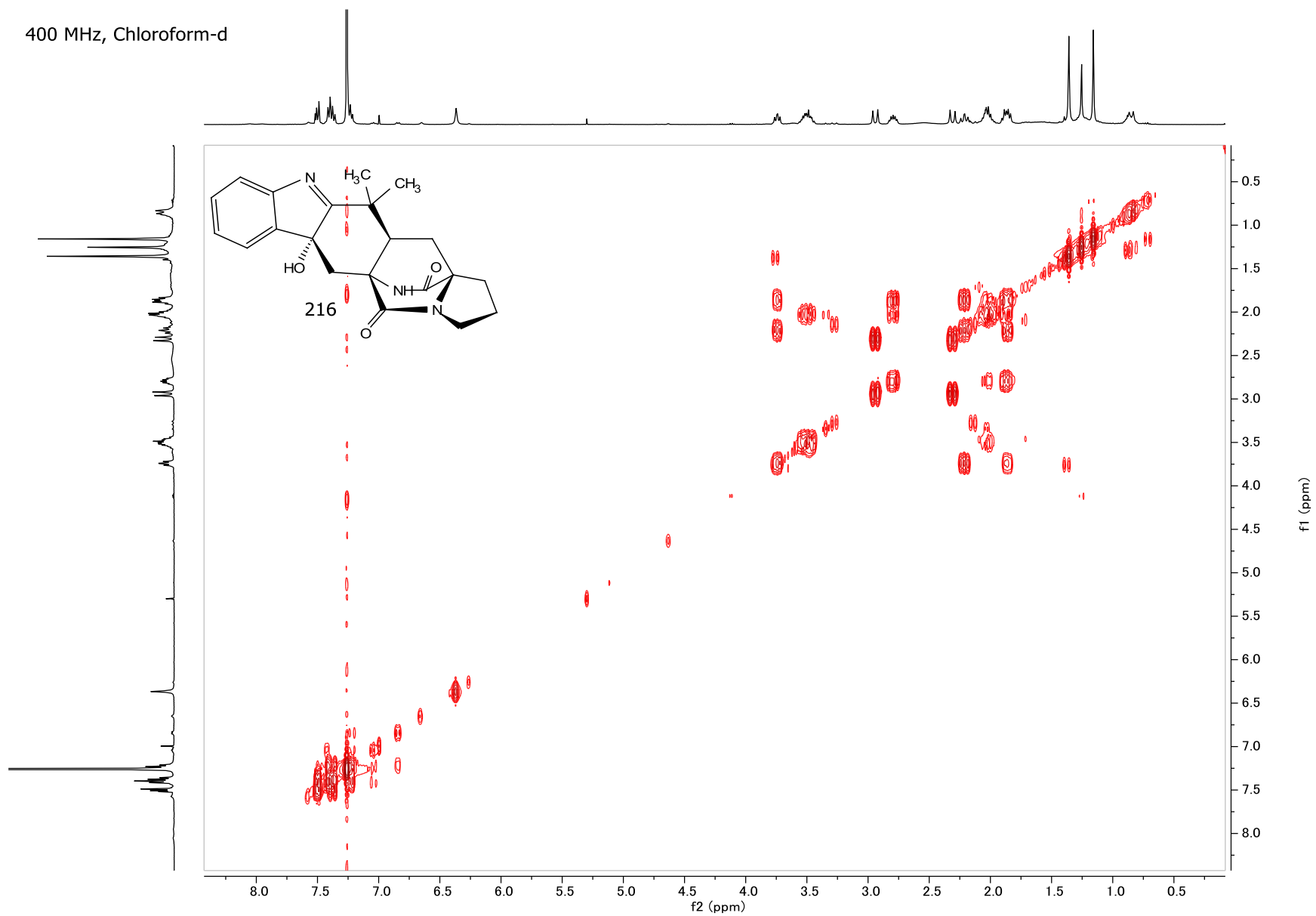


Figure A54: COSY NMR spectrum of **216**.

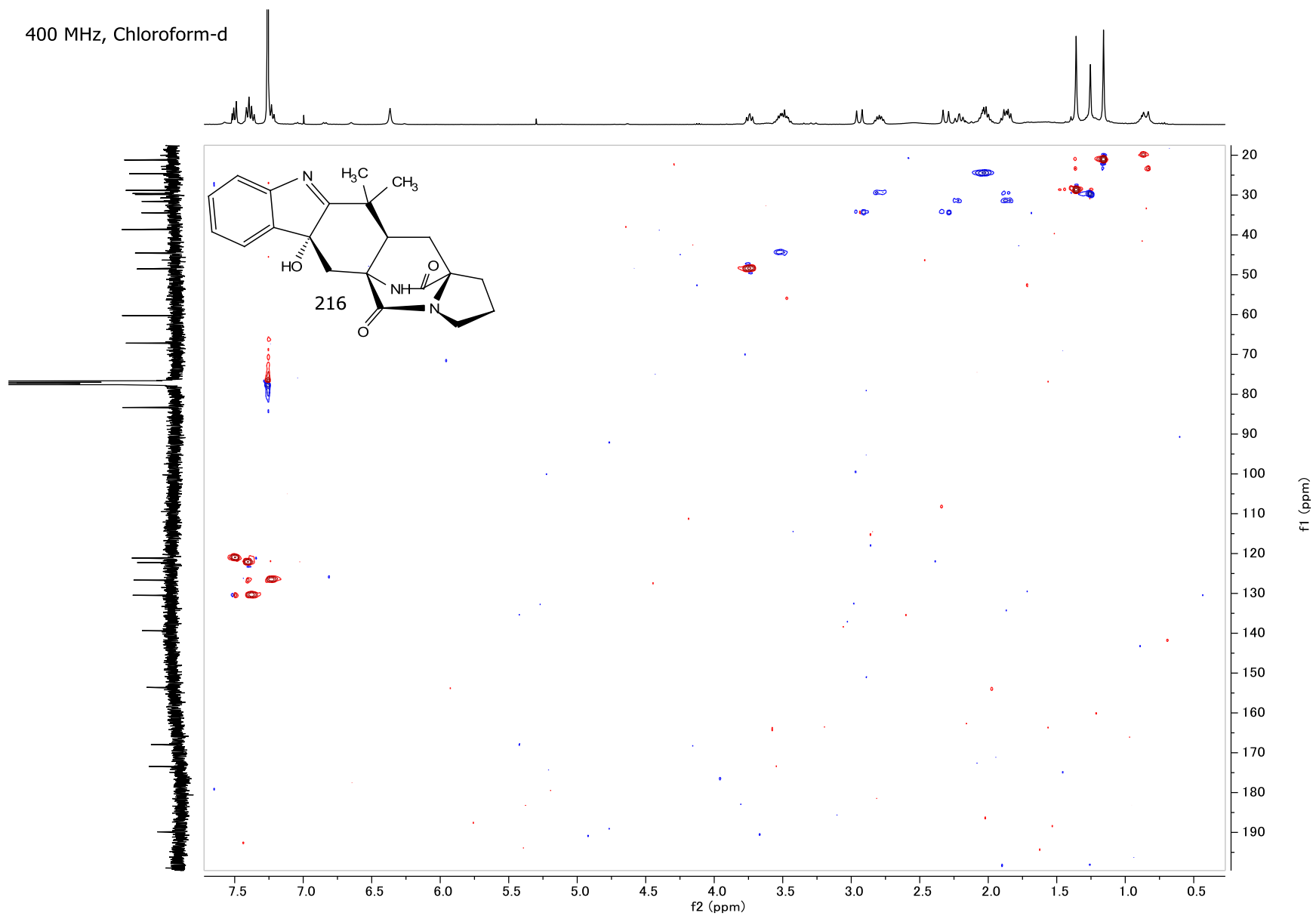


Figure A55: HSQC NMR spectrum of 216.

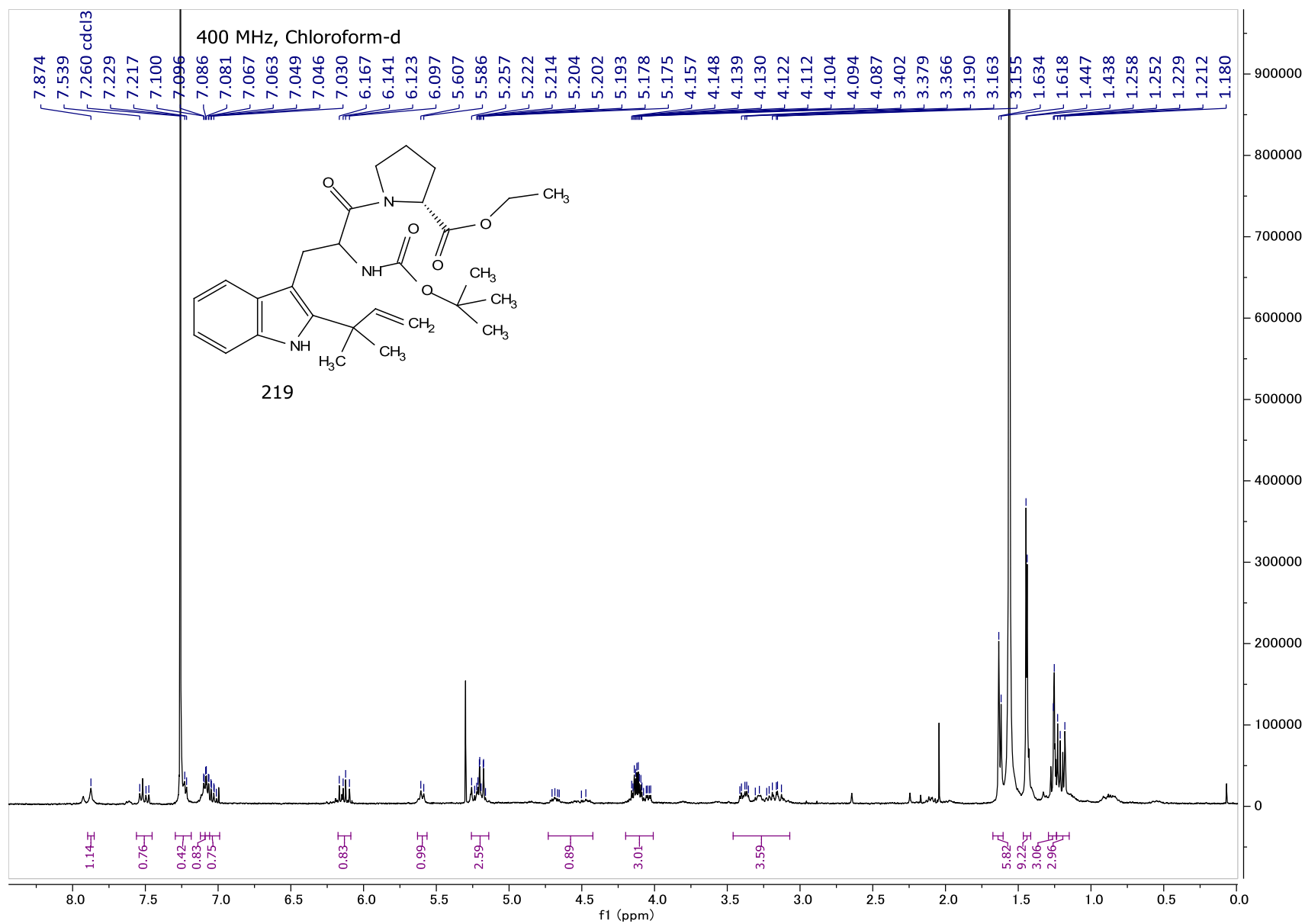


Figure A56: <sup>1</sup>H NMR spectrum of **219**.

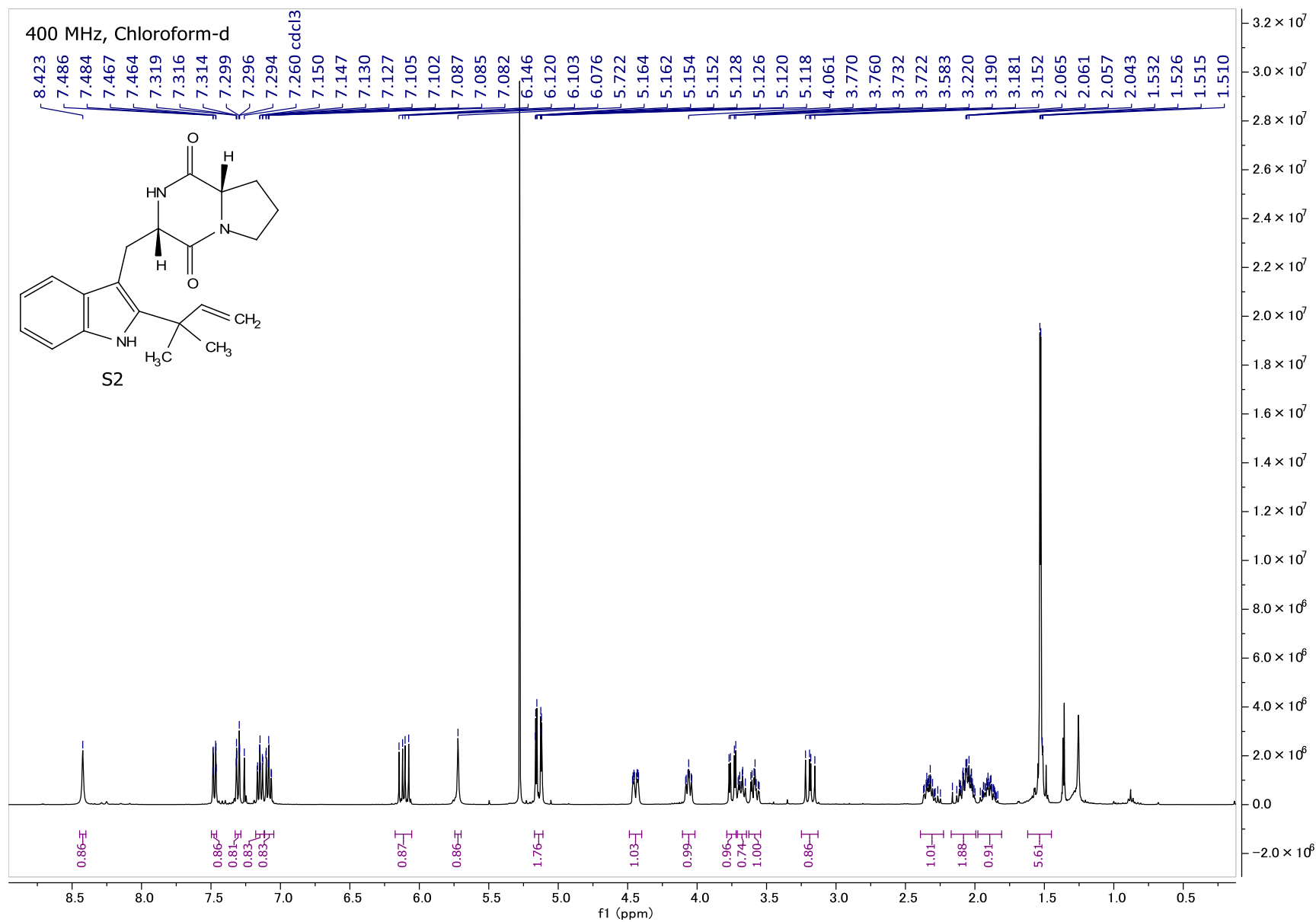


Figure A57:  $^1\text{H}$  NMR spectrum of S2.

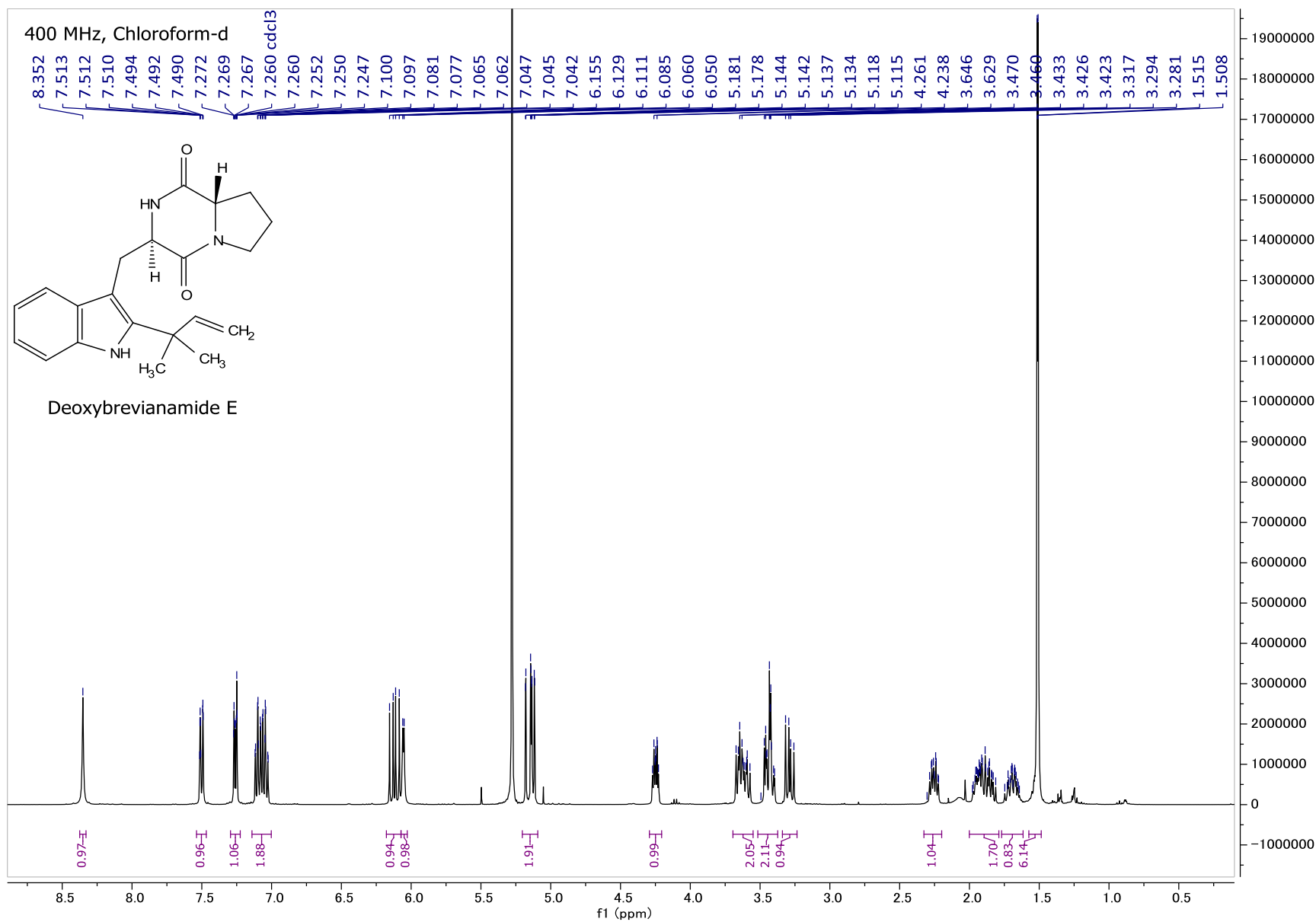


Figure A58:  $^1\text{H}$  NMR spectrum of Deoxybrevianamide E.

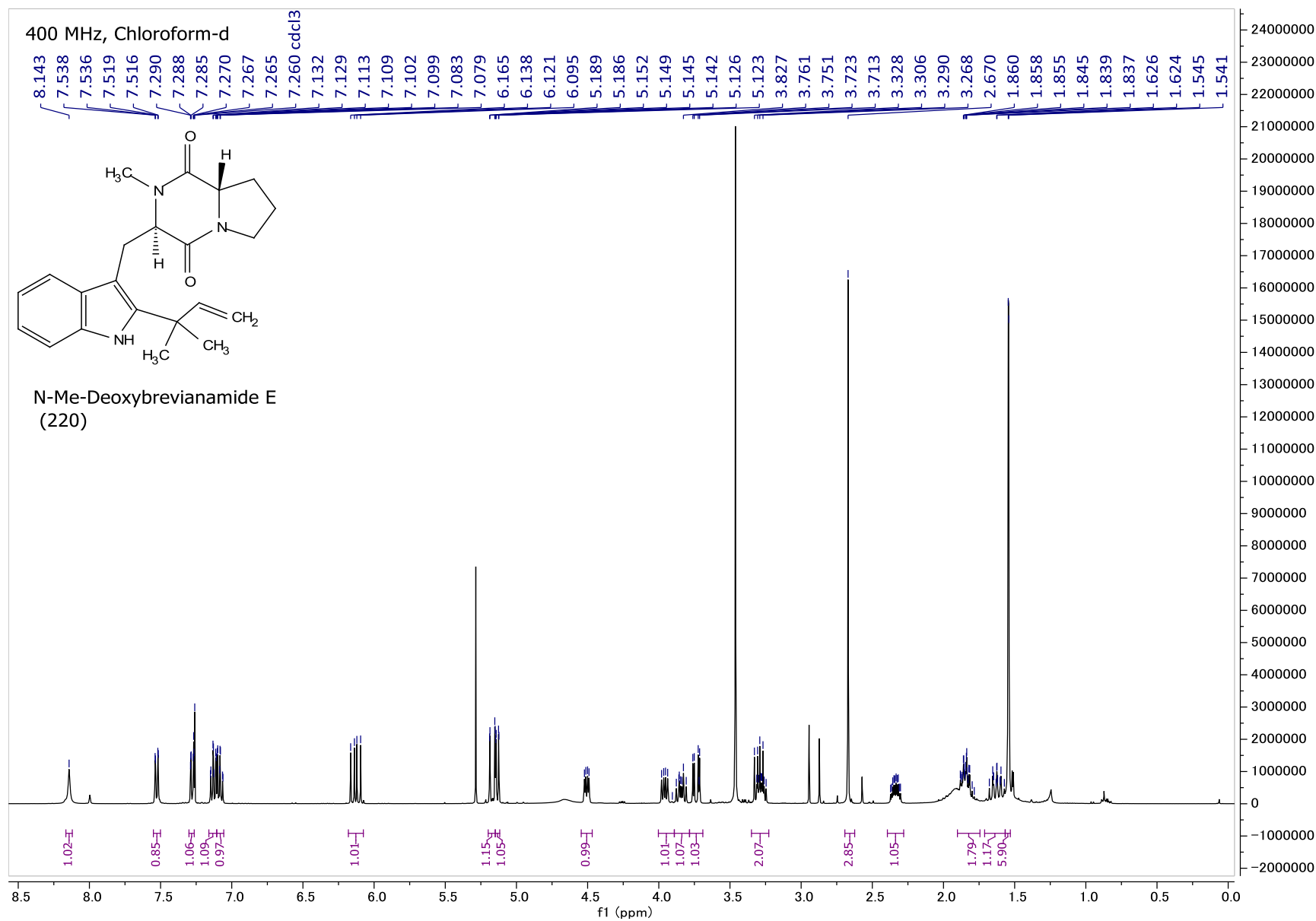


Figure A59:  $^1\text{H}$  NMR spectrum of N-methyl-deoxybrevianamide E.

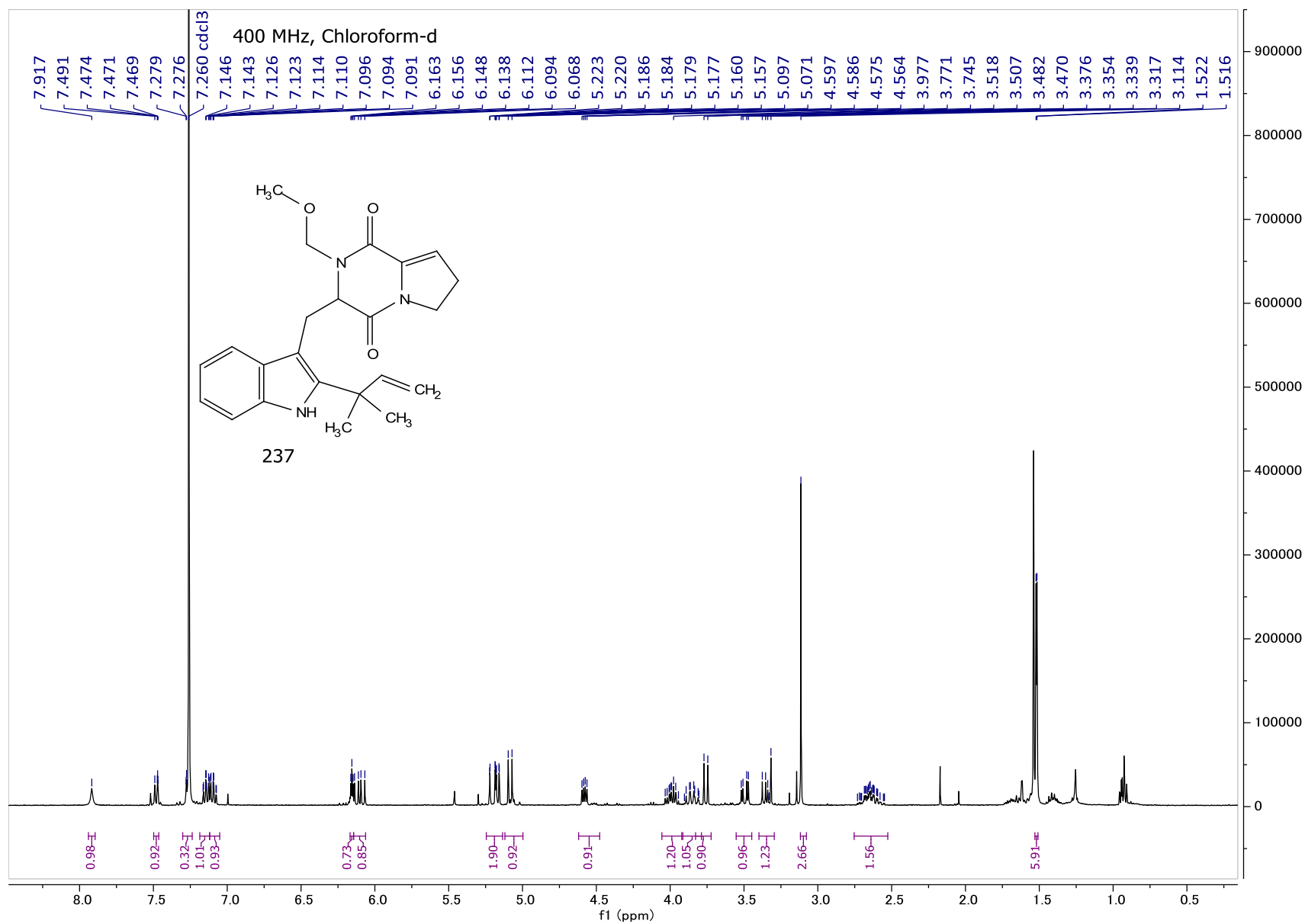


Figure A60:  $^1\text{H}$  NMR spectrum of **237**.

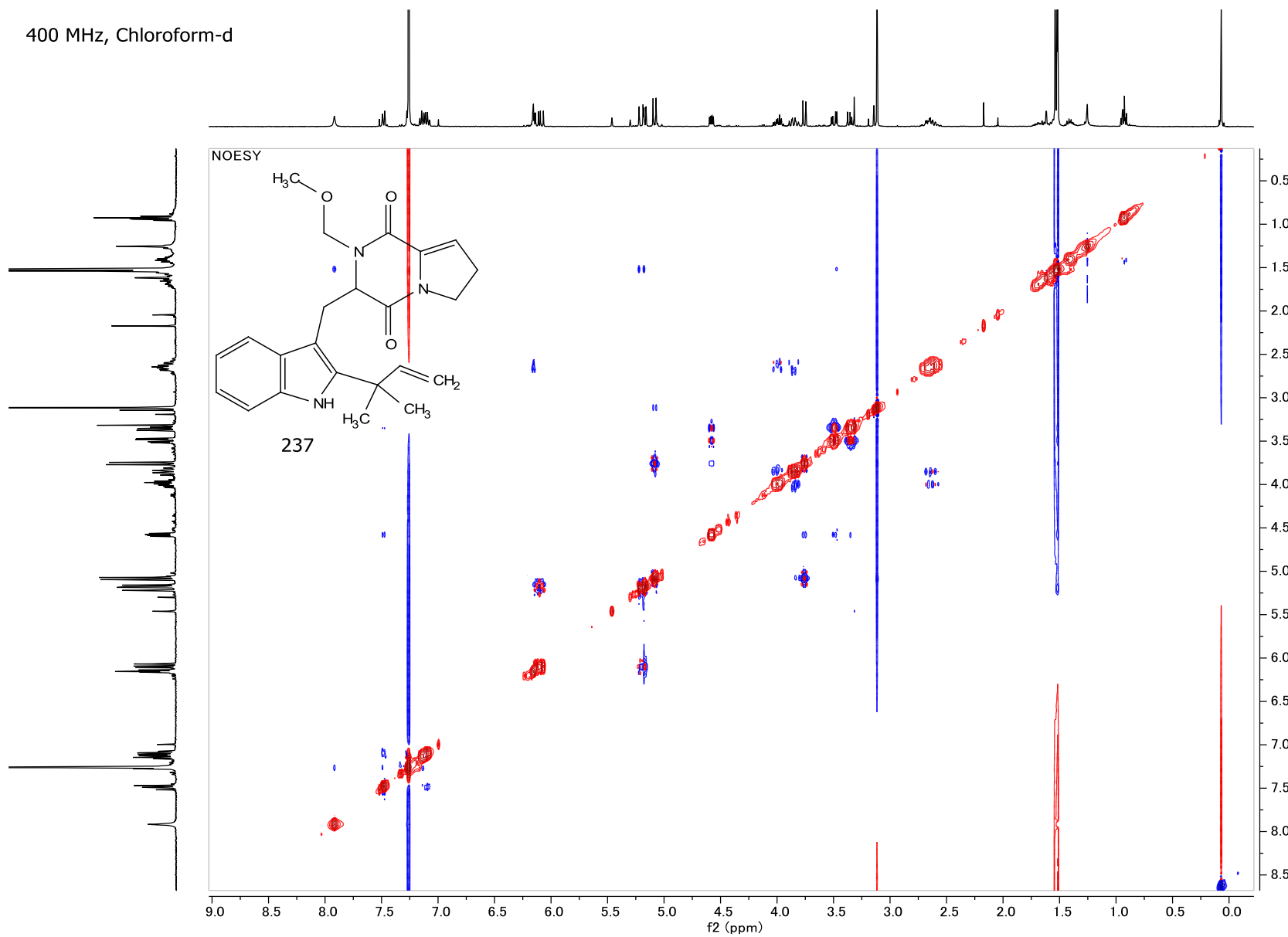


Figure A61: NOESY NMR spectrum of **237**.

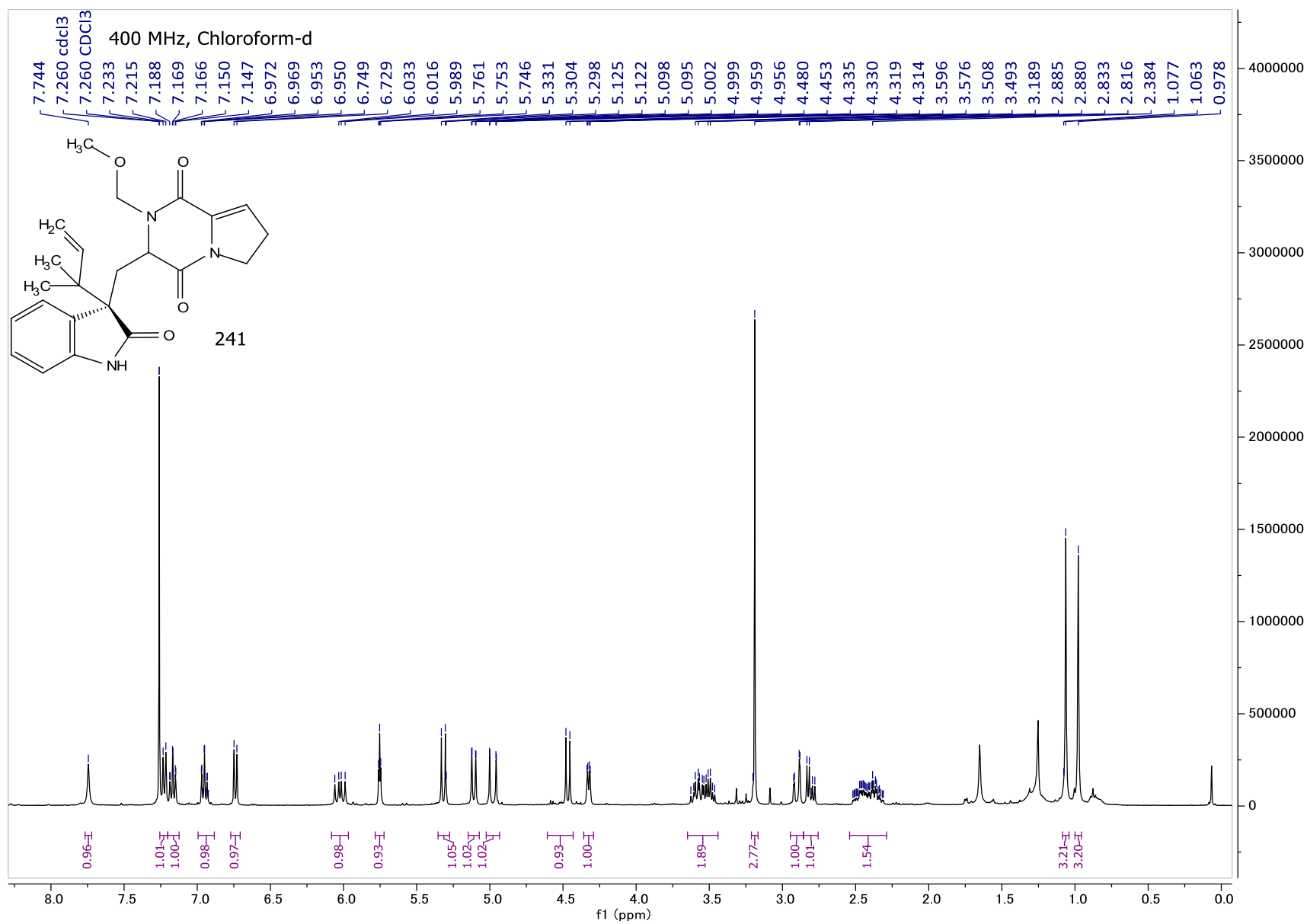


Figure A62:  $^1\text{H}$  NMR spectrum of **241**.

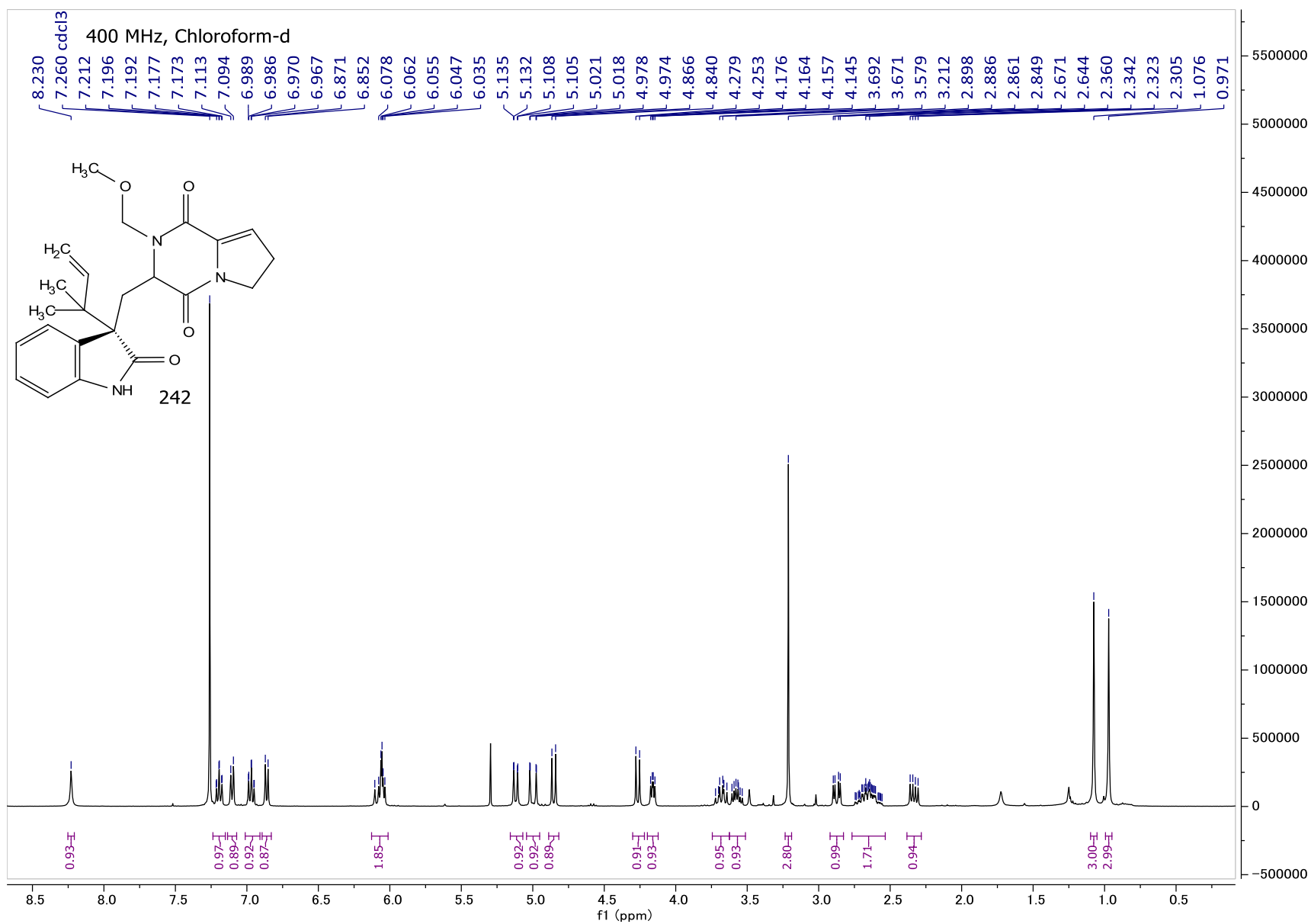


Figure A63:  $^1\text{H}$  NMR spectrum of **242**.

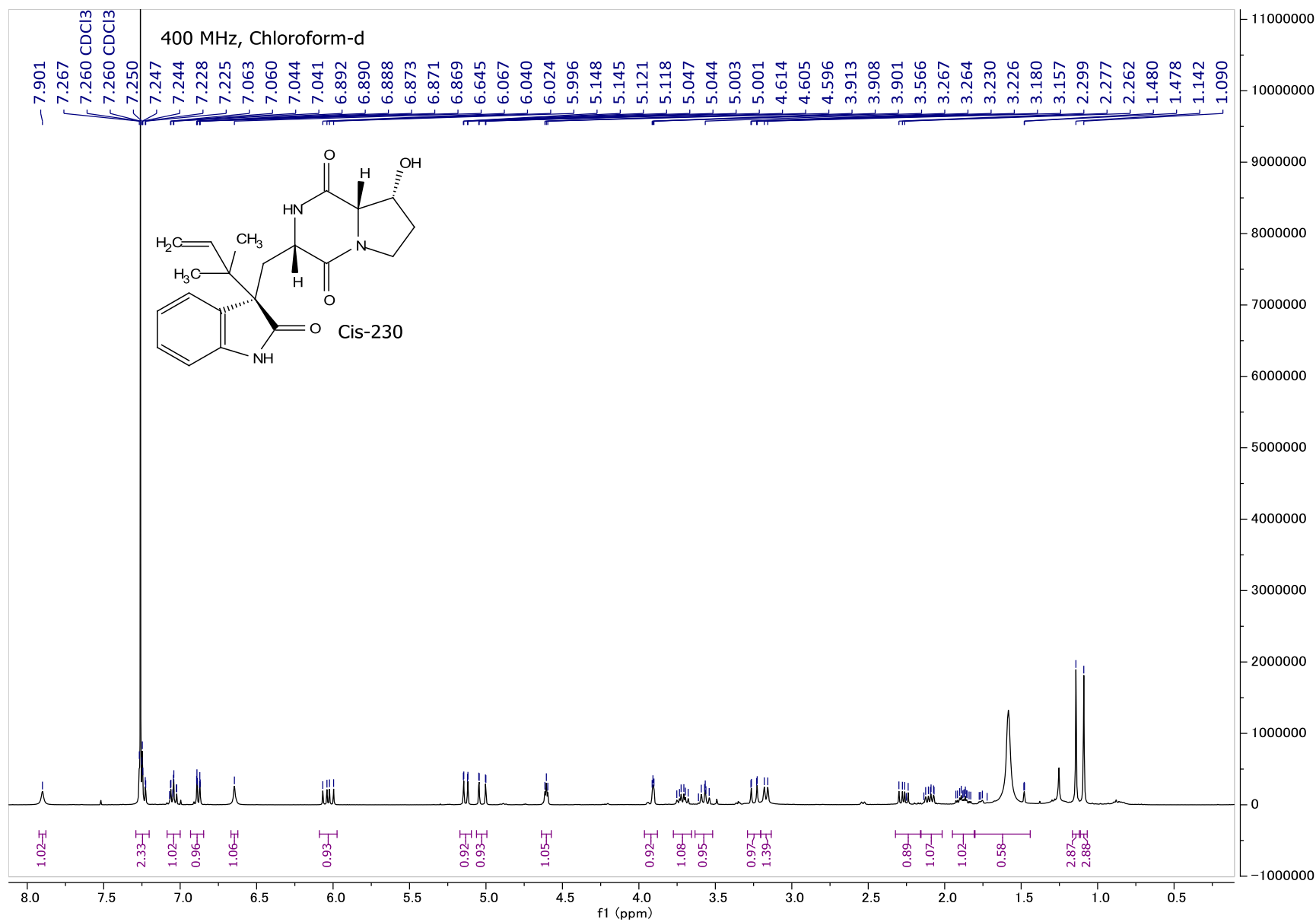


Figure A64: <sup>1</sup>H NMR spectrum of *cis*-230.

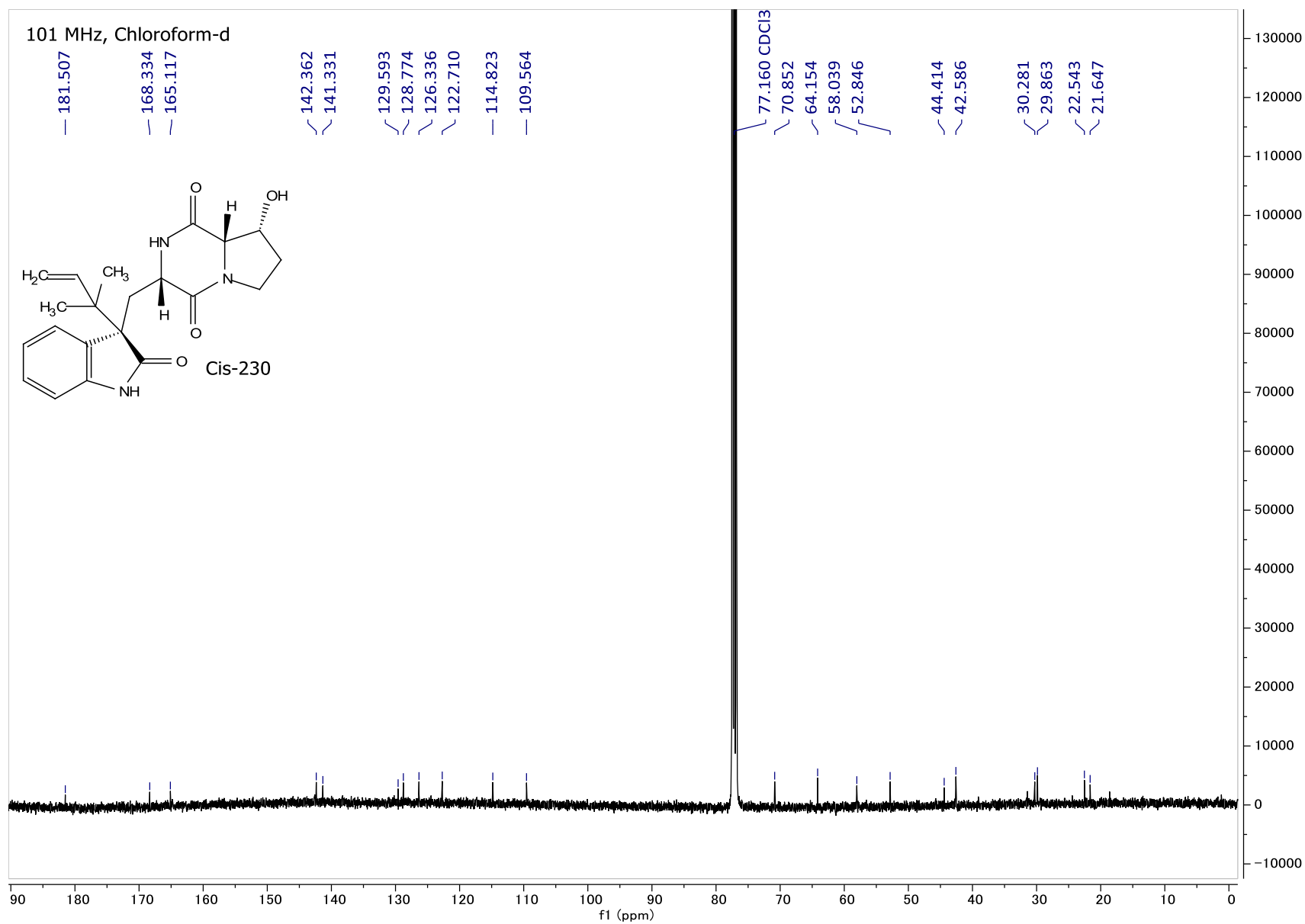


Figure A65: <sup>13</sup>C NMR spectrum of *cis*-230.

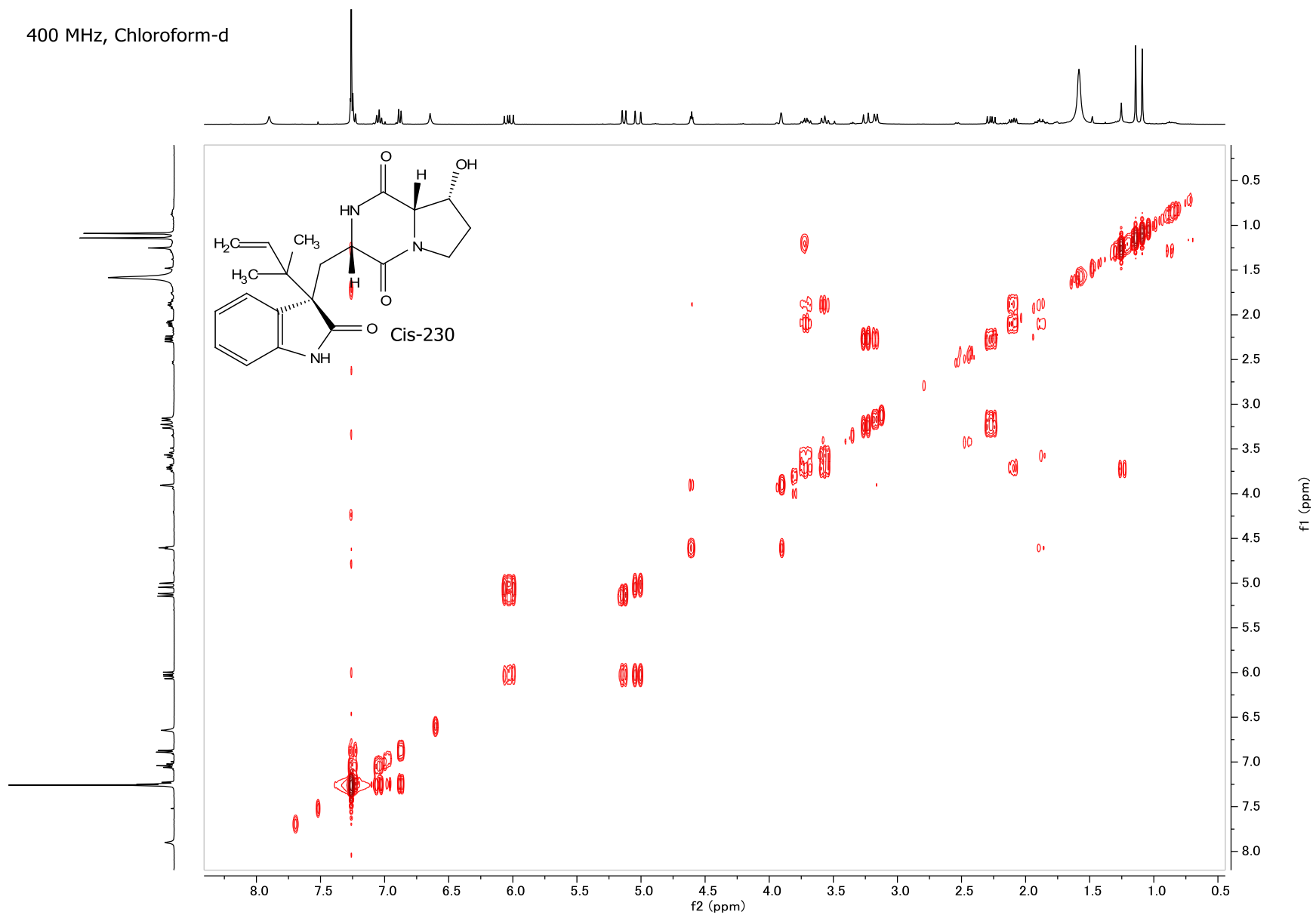


Figure A66: COSY NMR spectrum of *cis*-230.

400 MHz, Chloroform-d

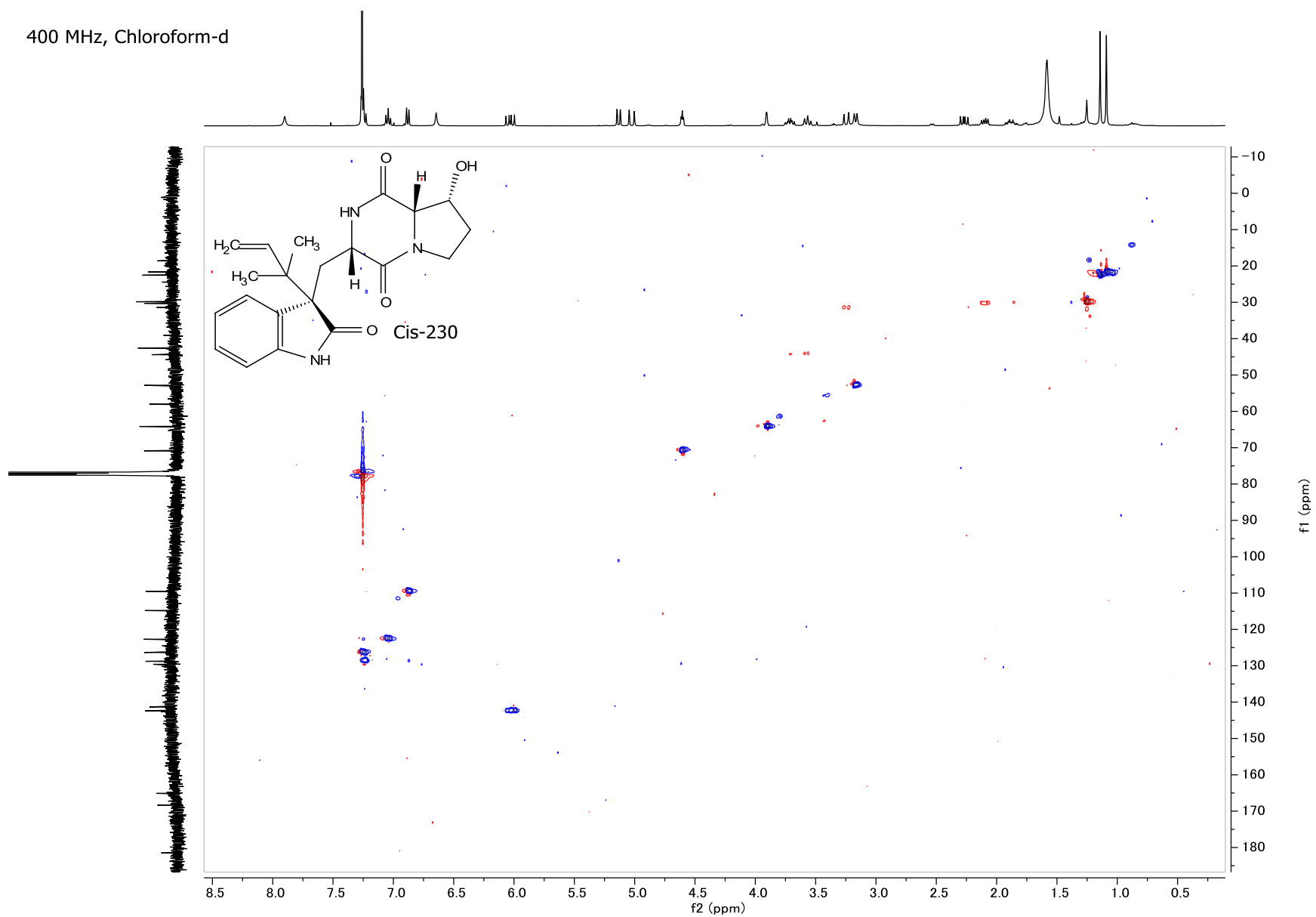


Figure A67: HSQC NMR spectrum of *cis*-230.

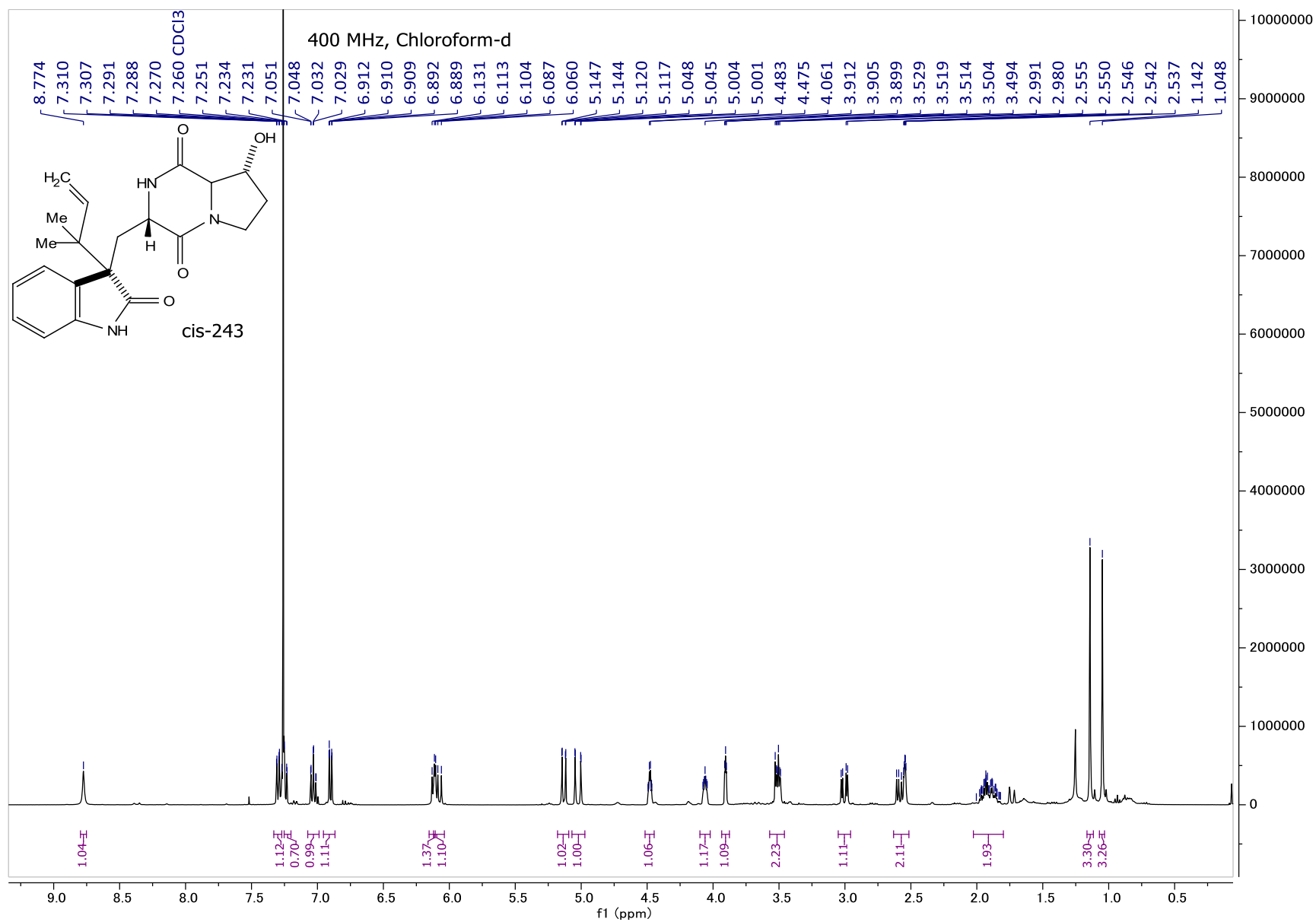


Figure A68: <sup>1</sup>H NMR spectrum of *cis*-243.

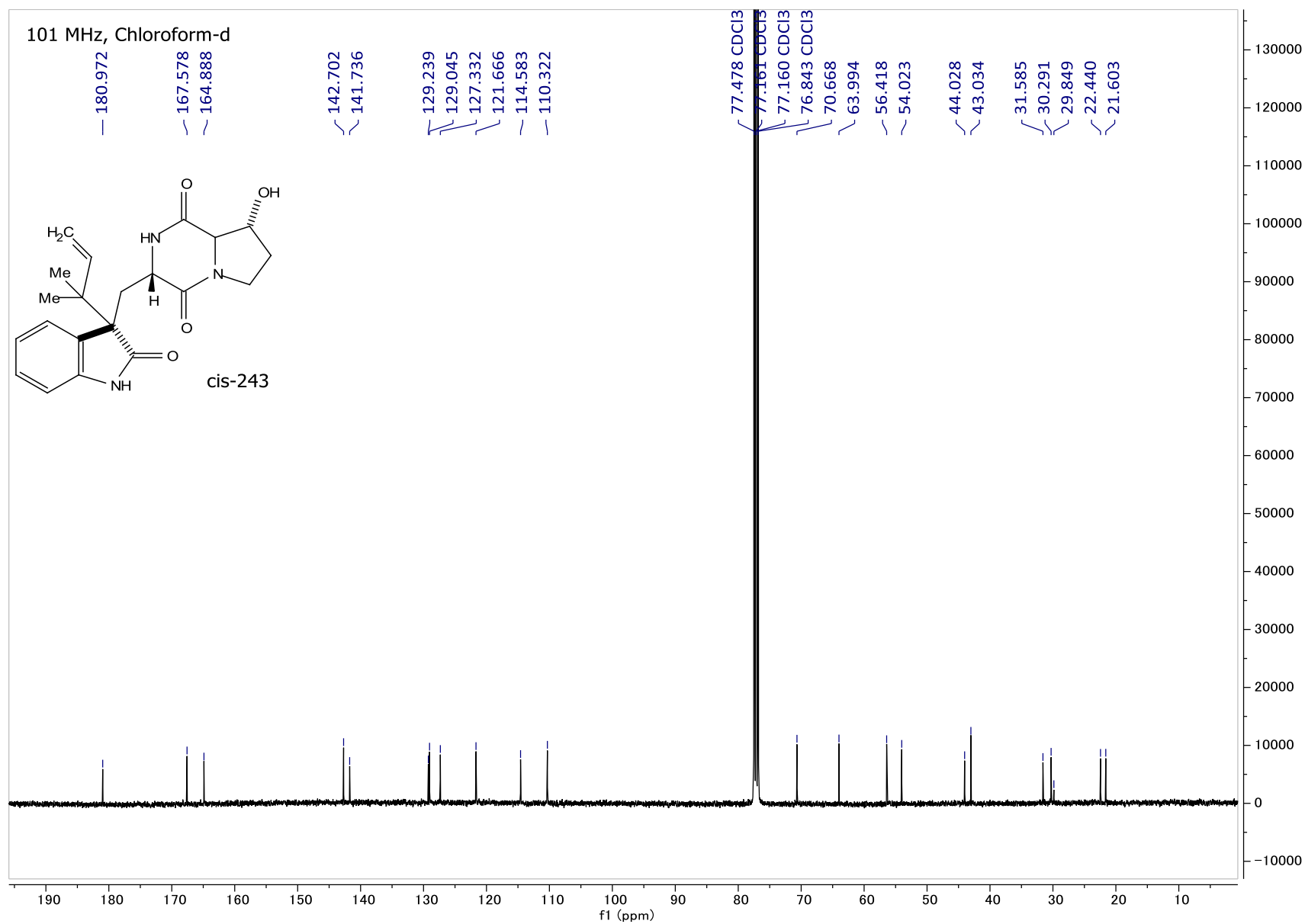


Figure A69:  $^{13}\text{C}$  NMR spectrum of *cis*-243.

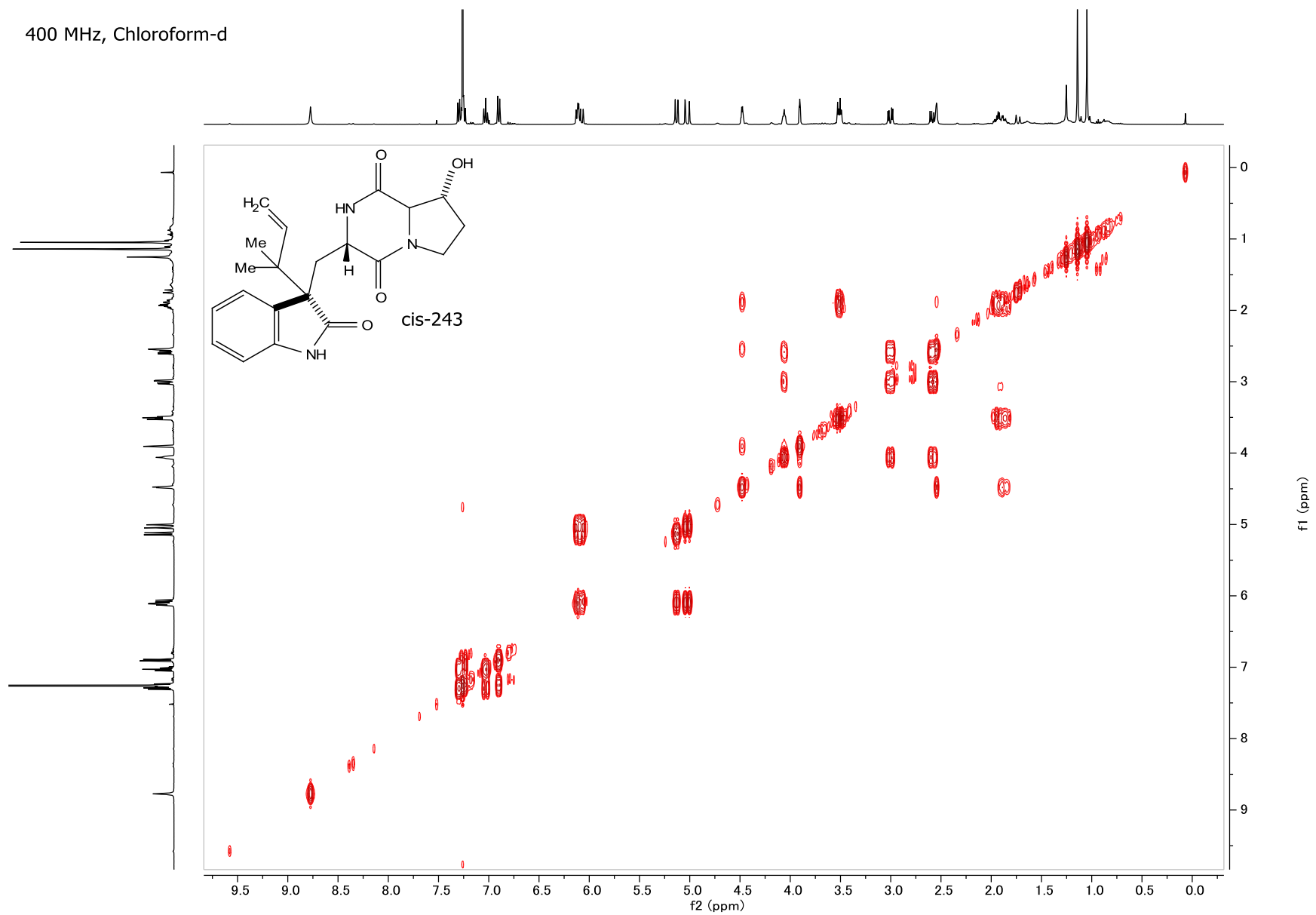


Figure A70: COSY NMR spectrum of *cis*-243.

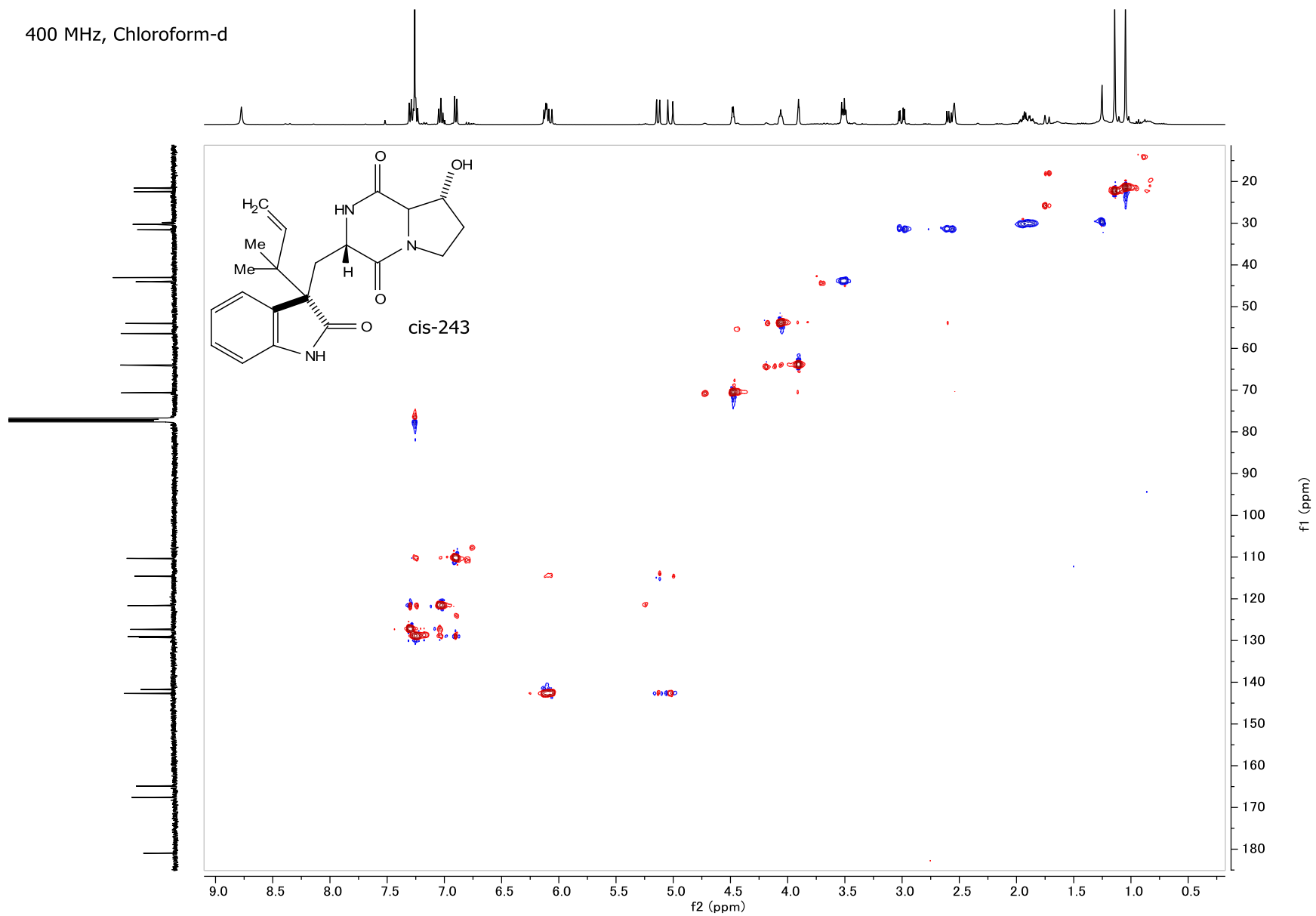


Figure A71: HSQC NMR spectrum of *cis*-243.

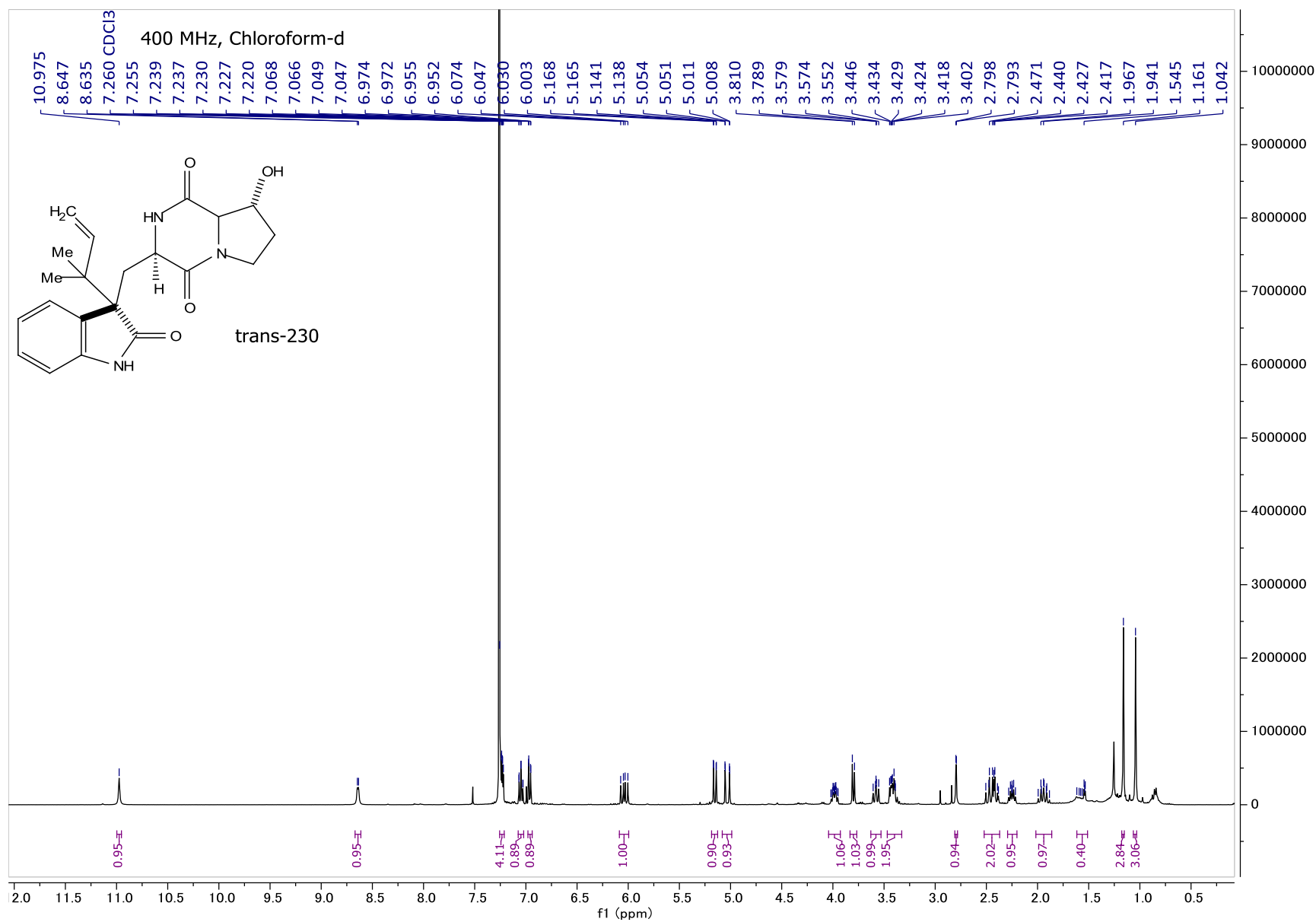


Figure A72:  $^1\text{H}$  NMR spectrum of *trans*-230.

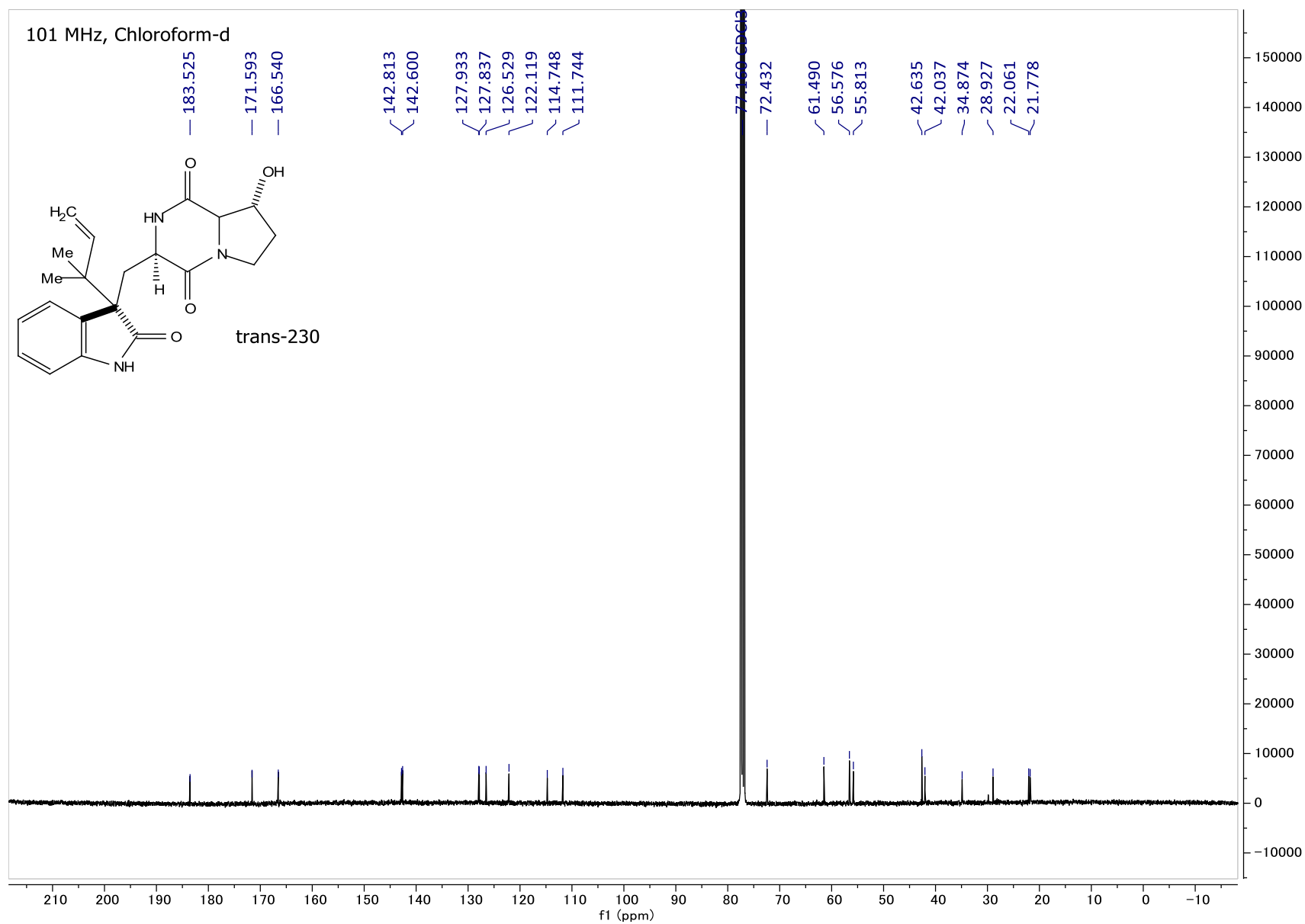


Figure A73:  $^{13}\text{C}$  NMR spectrum of *trans*-230.

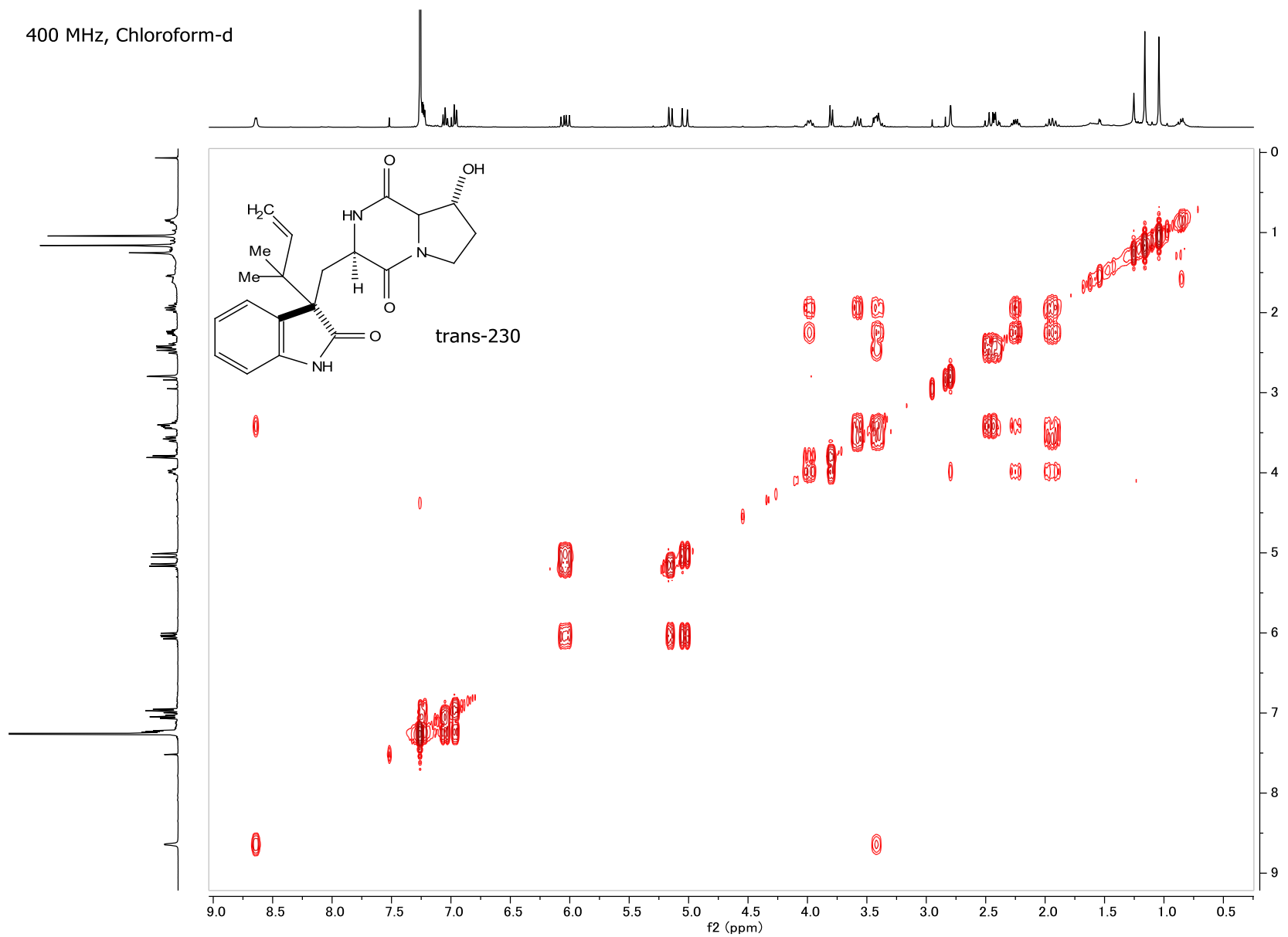


Figure A74: COSY NMR spectrum of *trans*-230.

400 MHz, Chloroform-d

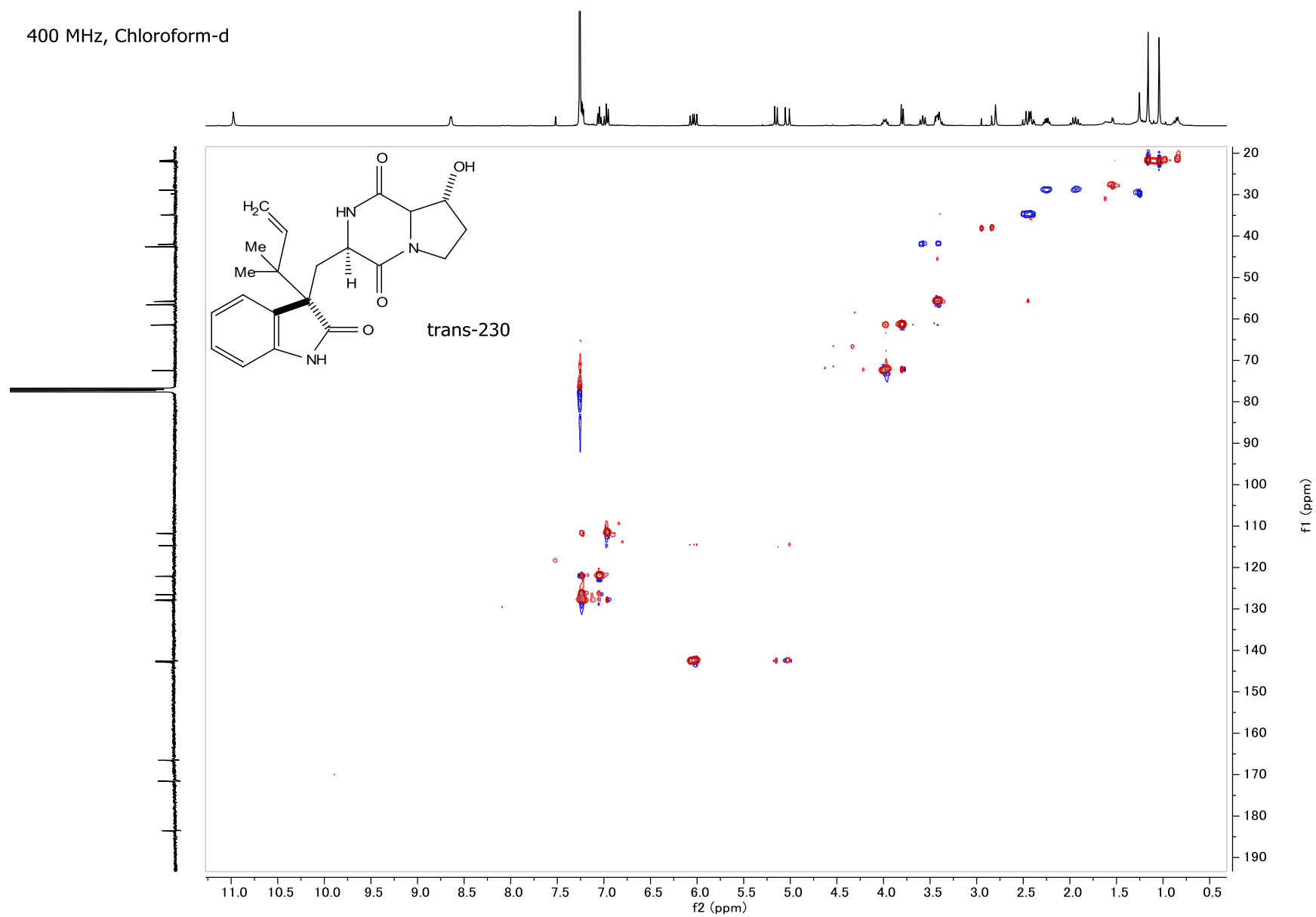


Figure A75: HSQC NMR spectrum of *trans*-230.

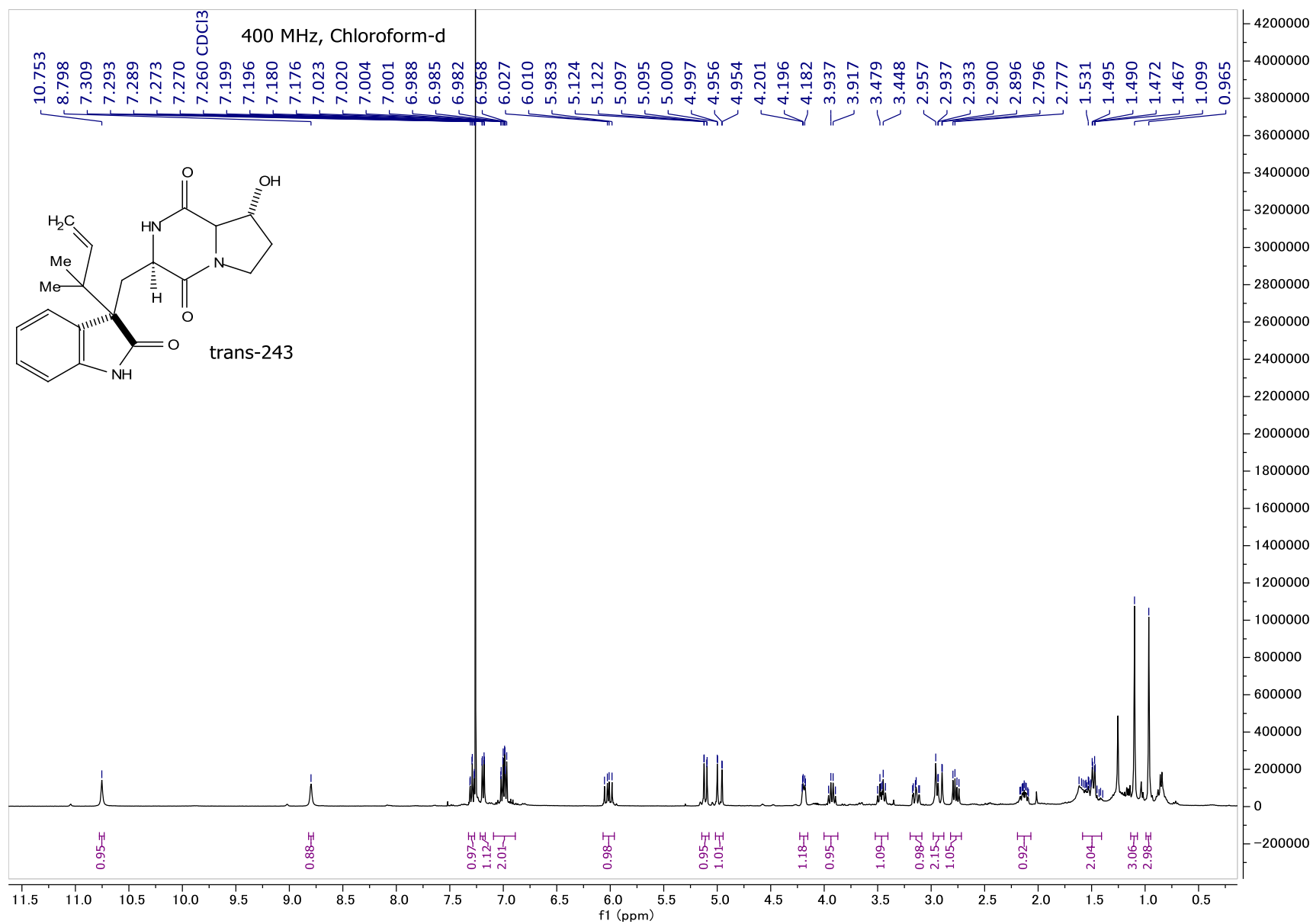


Figure A76:  $^1\text{H}$  NMR spectrum of *trans*-243.

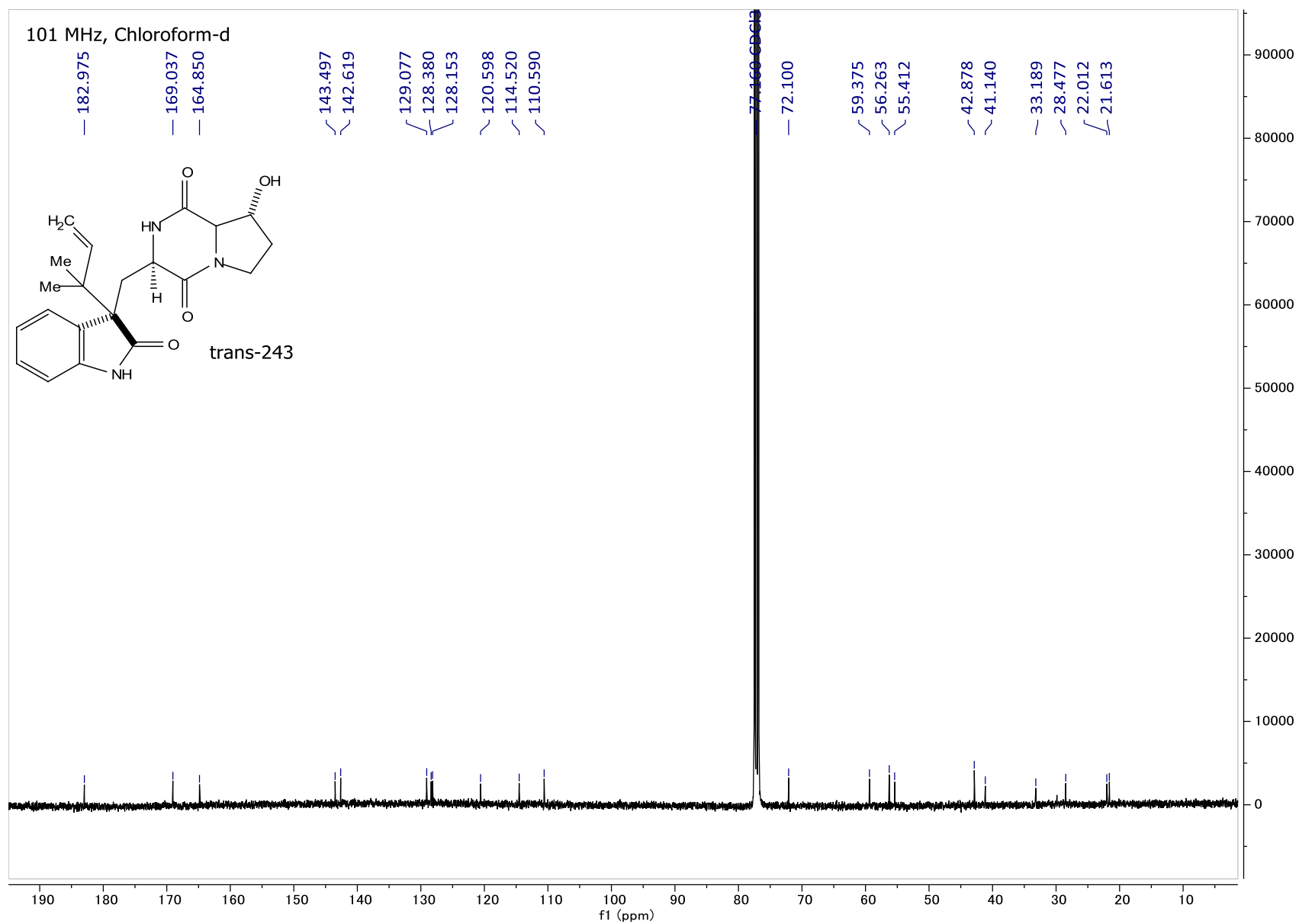


Figure A77:  $^{13}\text{C}$  NMR spectrum of *trans*-243.

400 MHz, Chloroform-d

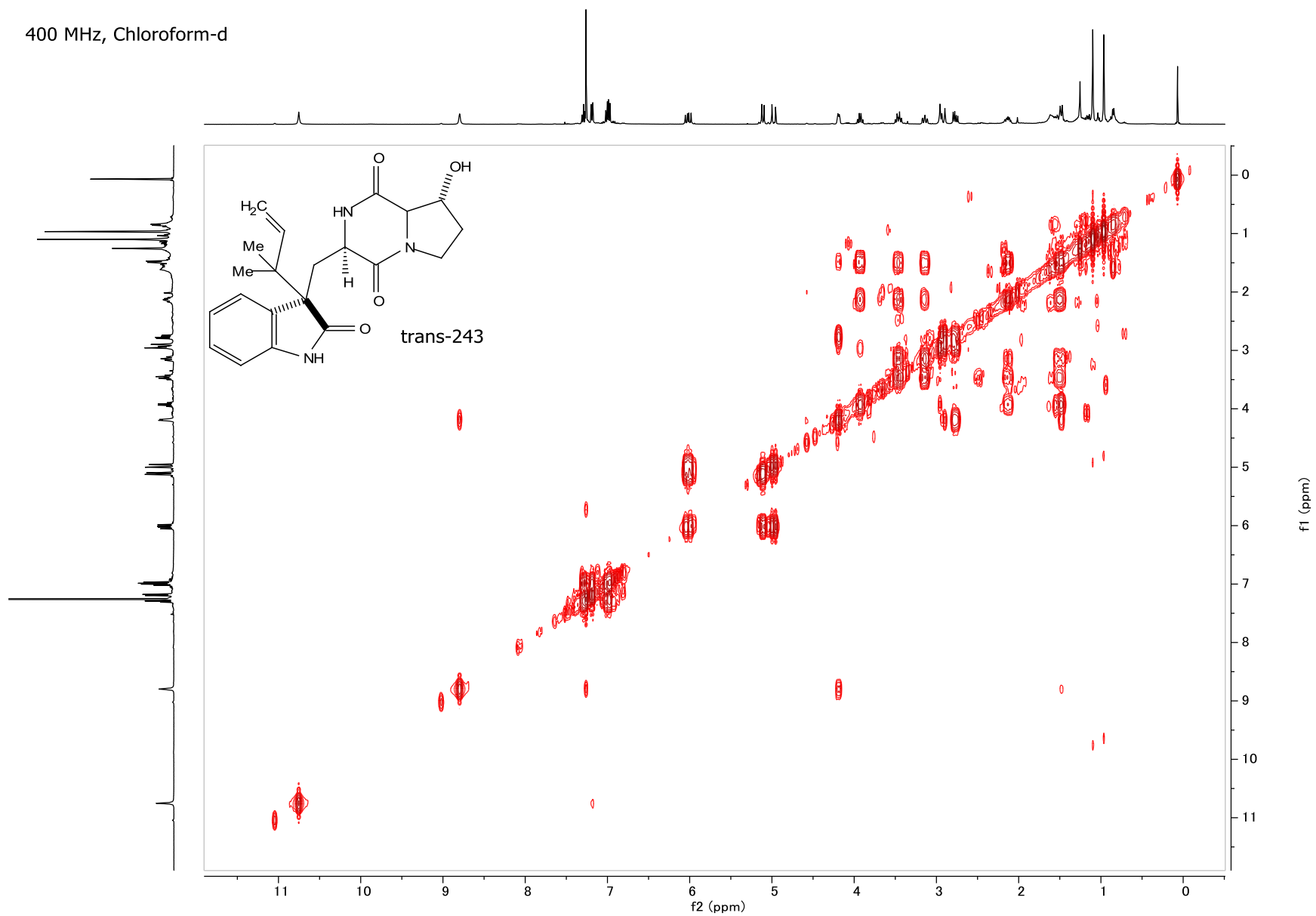


Figure A78: COSY NMR spectrum of *trans*-243.

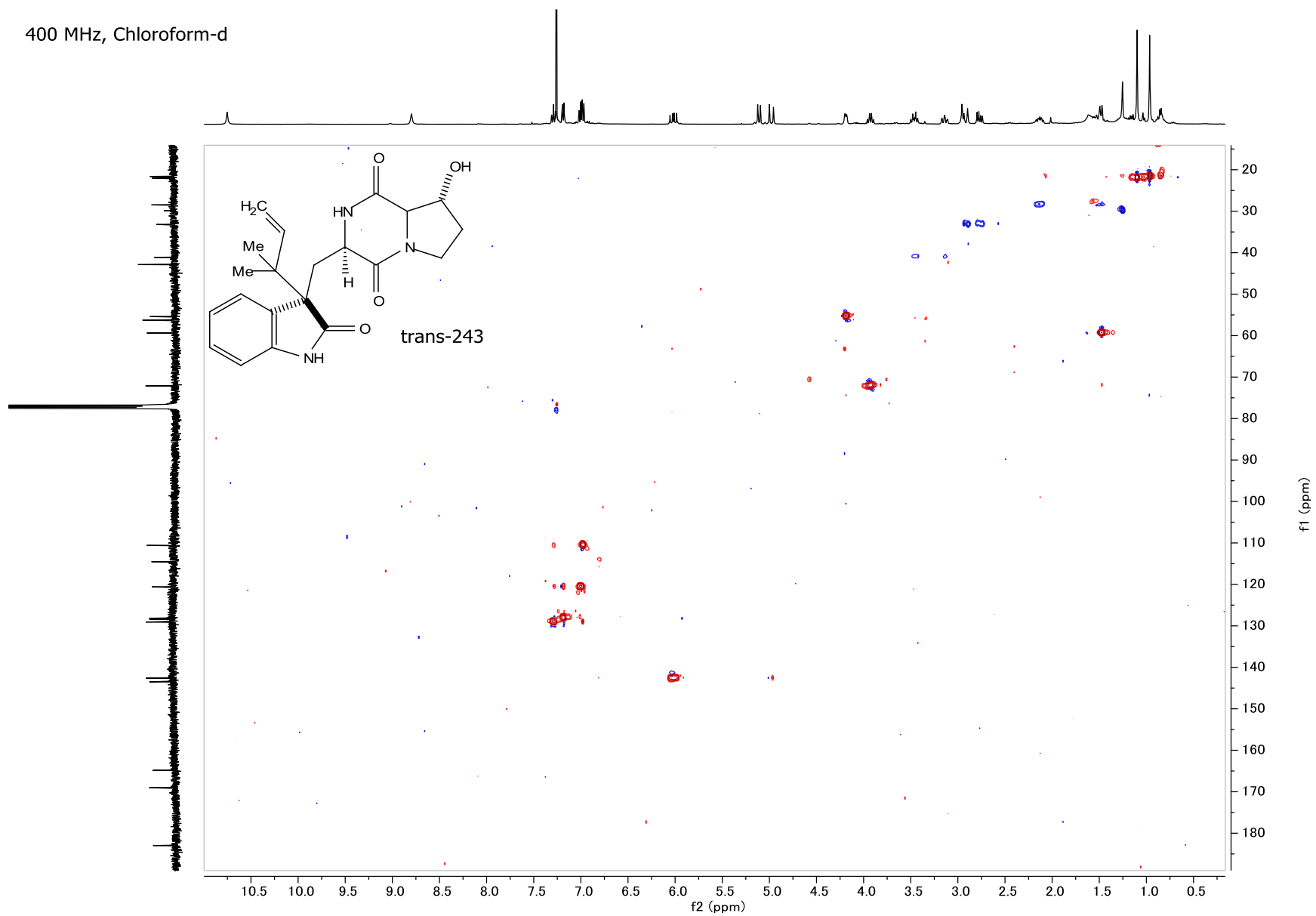


Figure A79: HSQC NMR spectrum of *trans*-243.

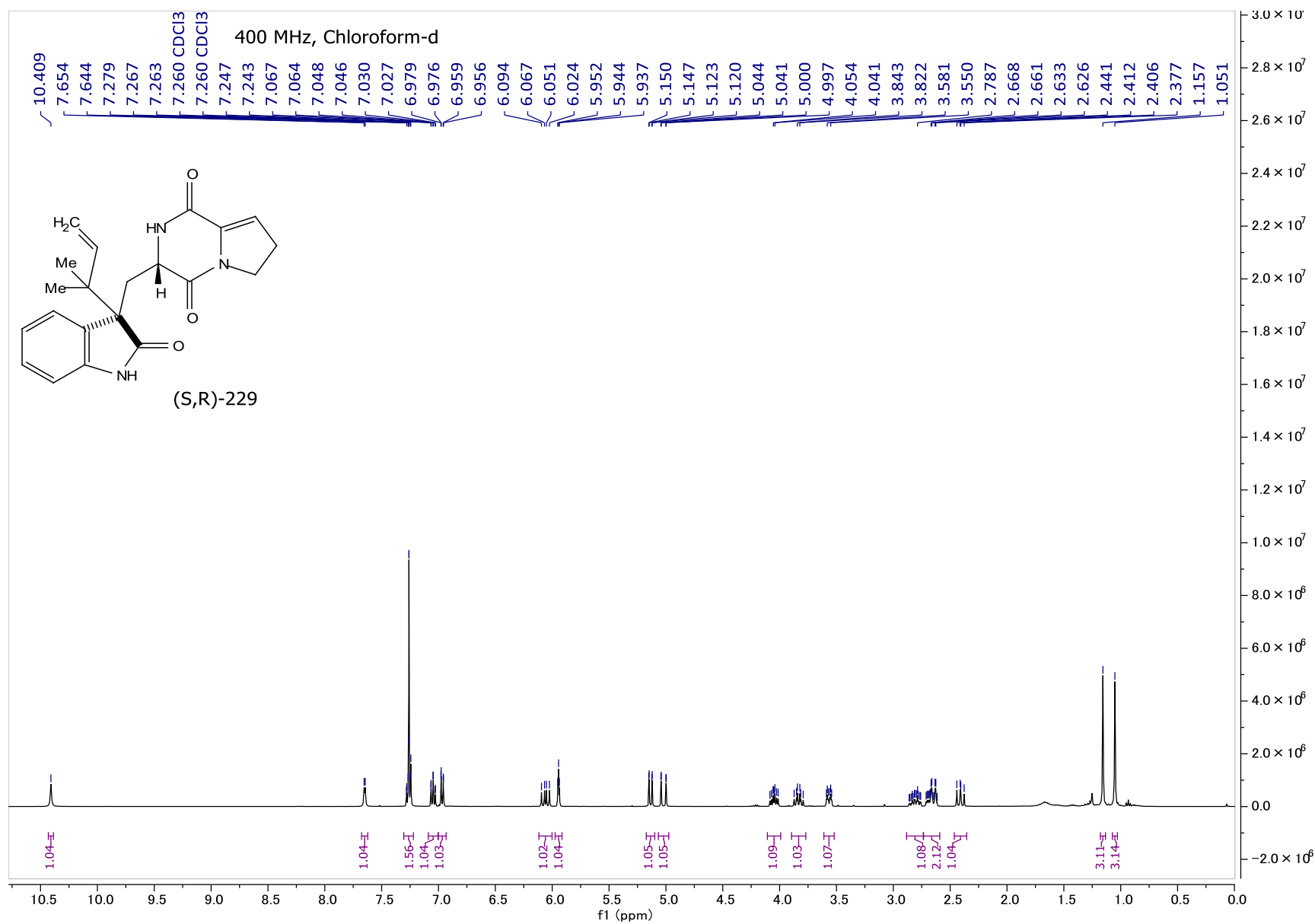


Figure A80:  $^1\text{H}$  NMR spectrum of (S,S) & (R,R)-229.

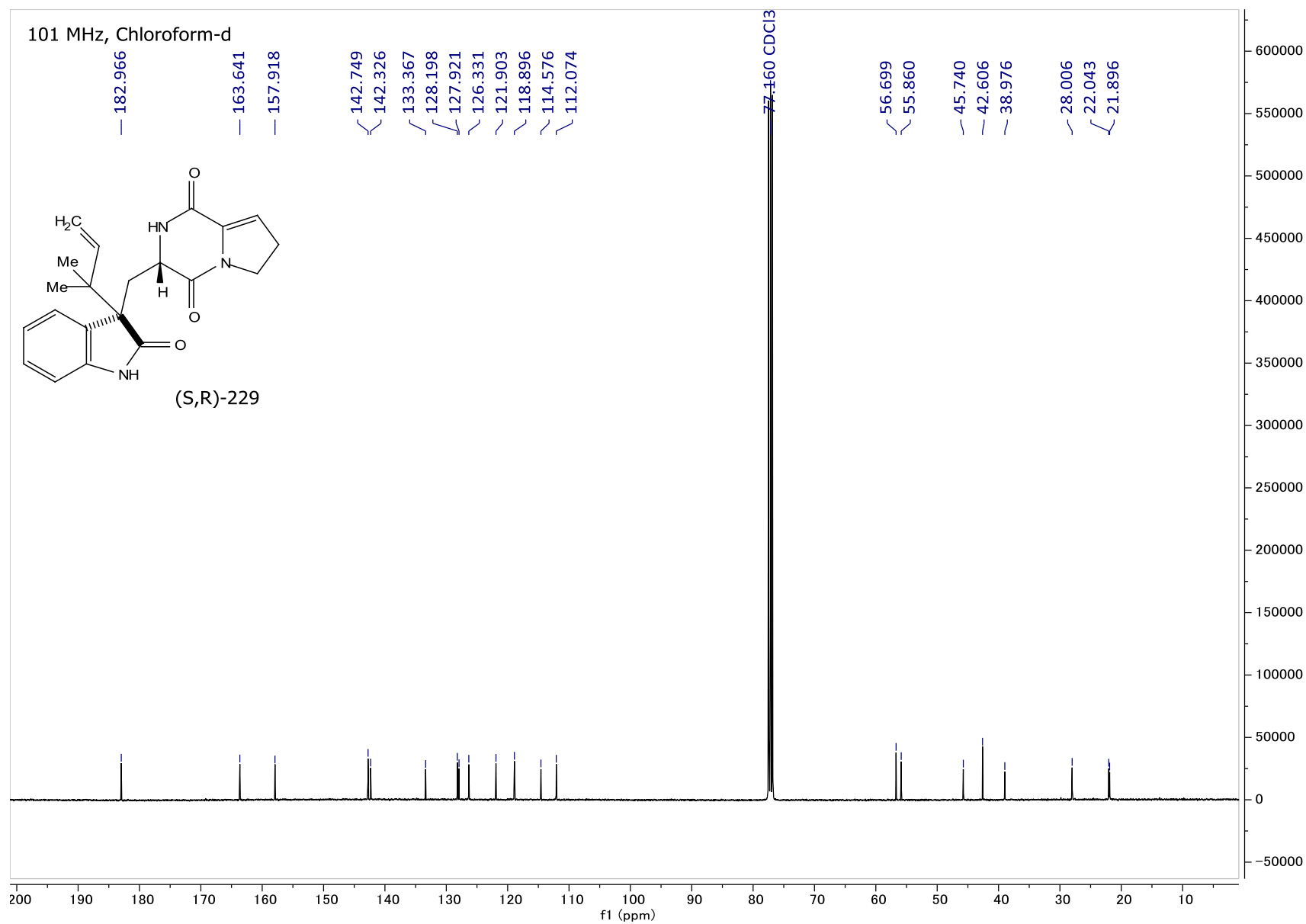


Figure A81:  $^{13}\text{C}$  NMR spectrum of (S,S)-229 & (R,R)-229.

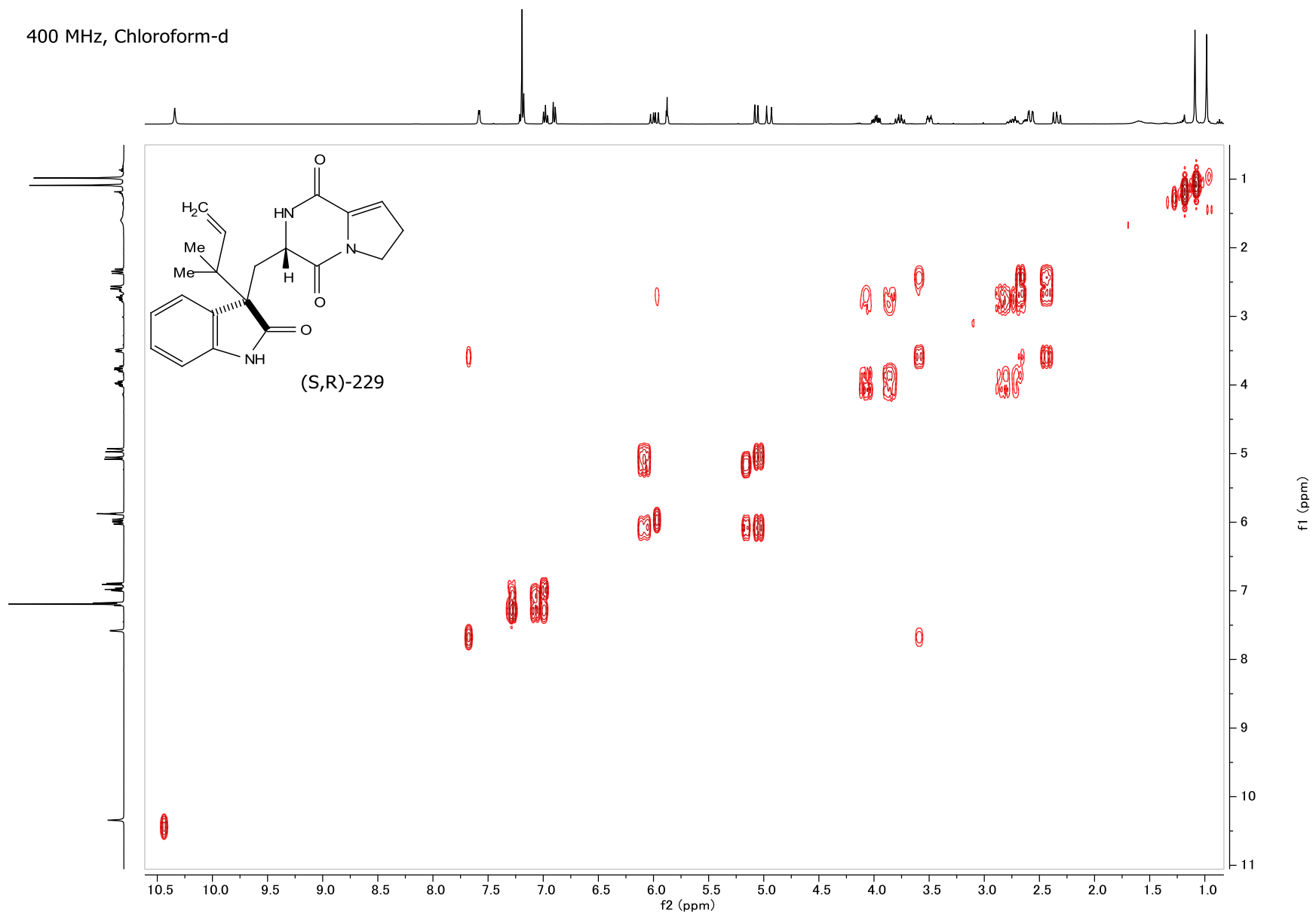


Figure A82: COSY NMR spectrum of (*S,S*) & (*R,R*)-**229**.

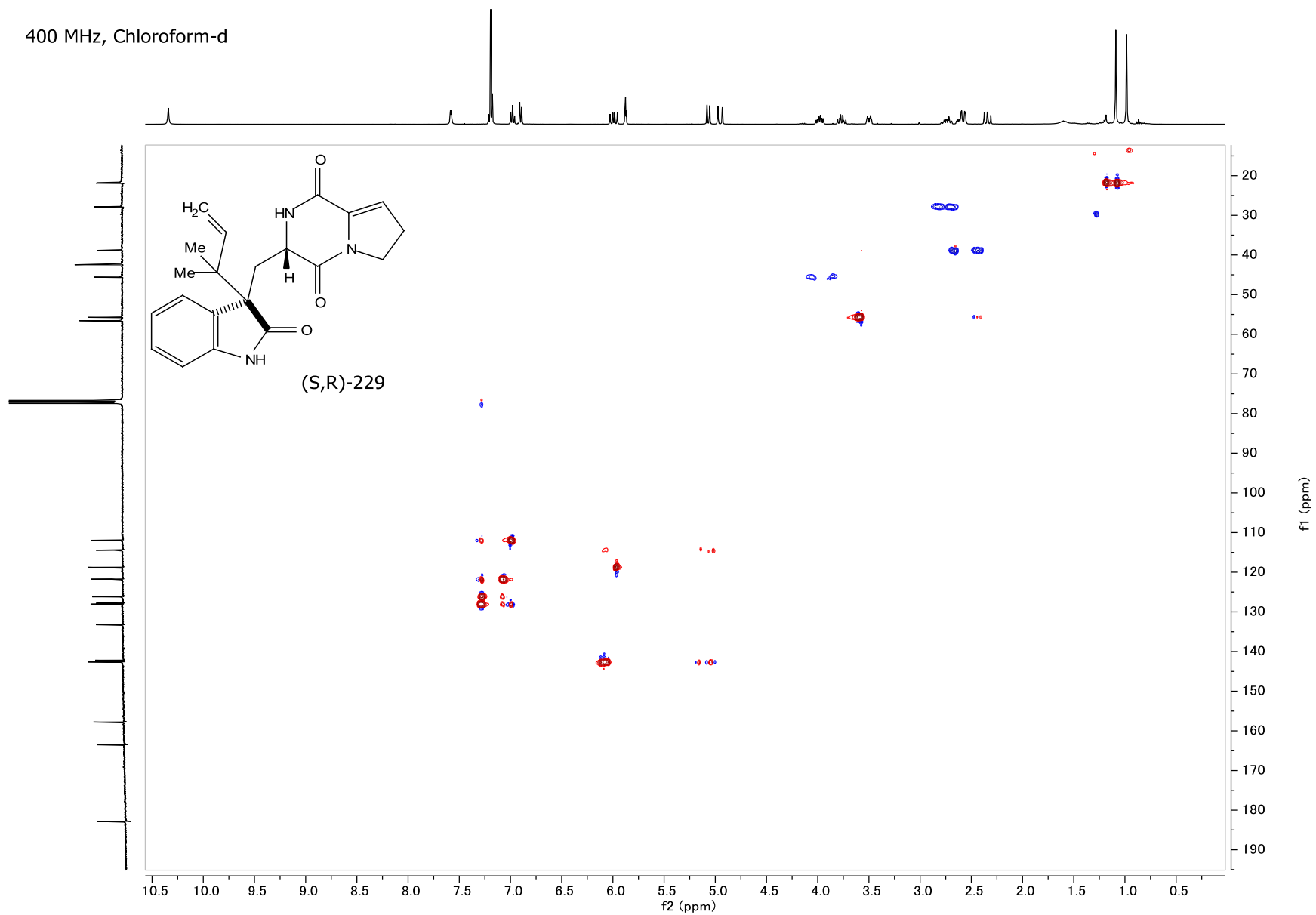


Figure A83: HSQC NMR spectrum of (*S,S*) & (*R,R*)-229.

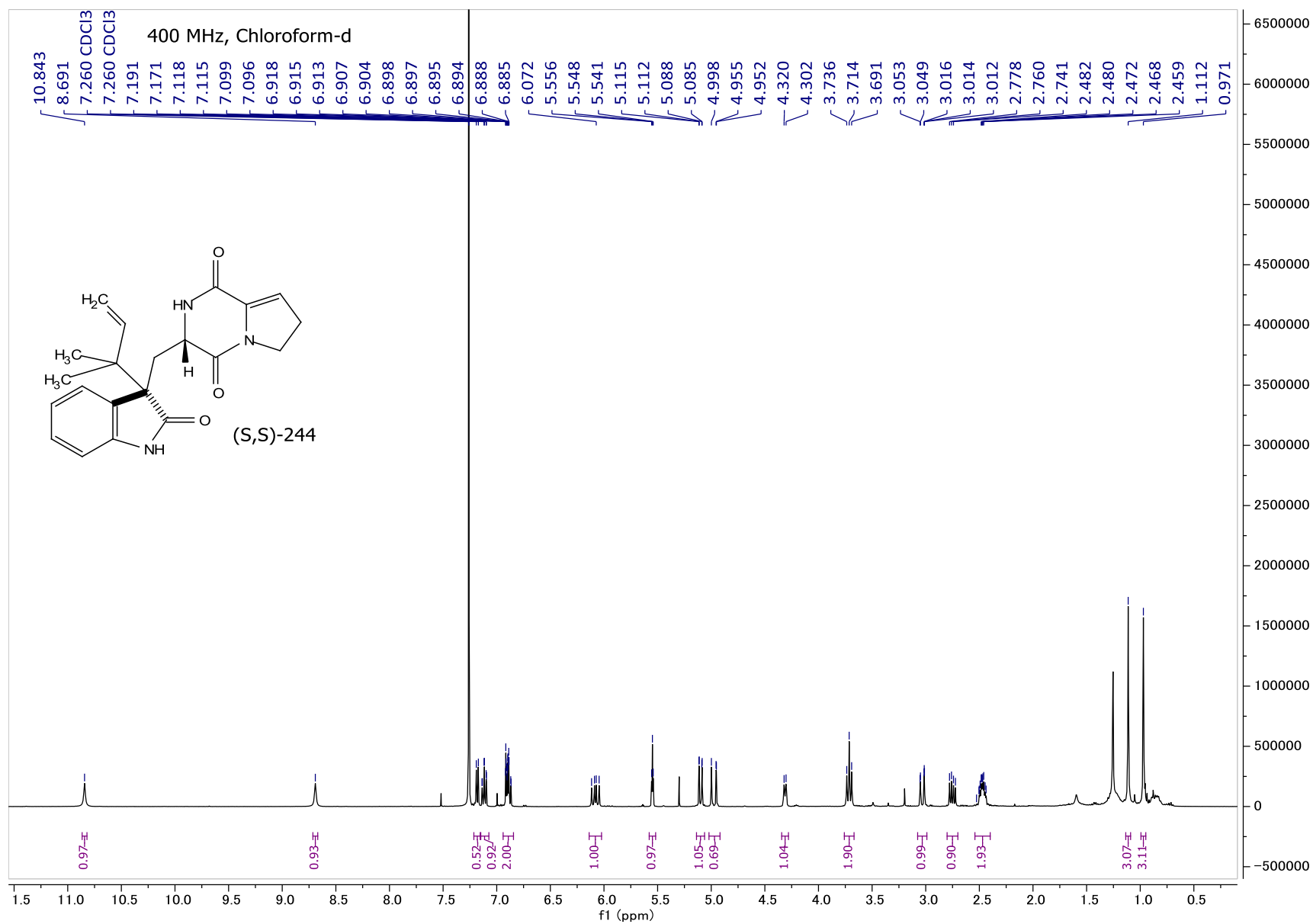


Figure A84:  $^1\text{H}$  NMR spectrum of (S,R)-244 & (R,S)-244.

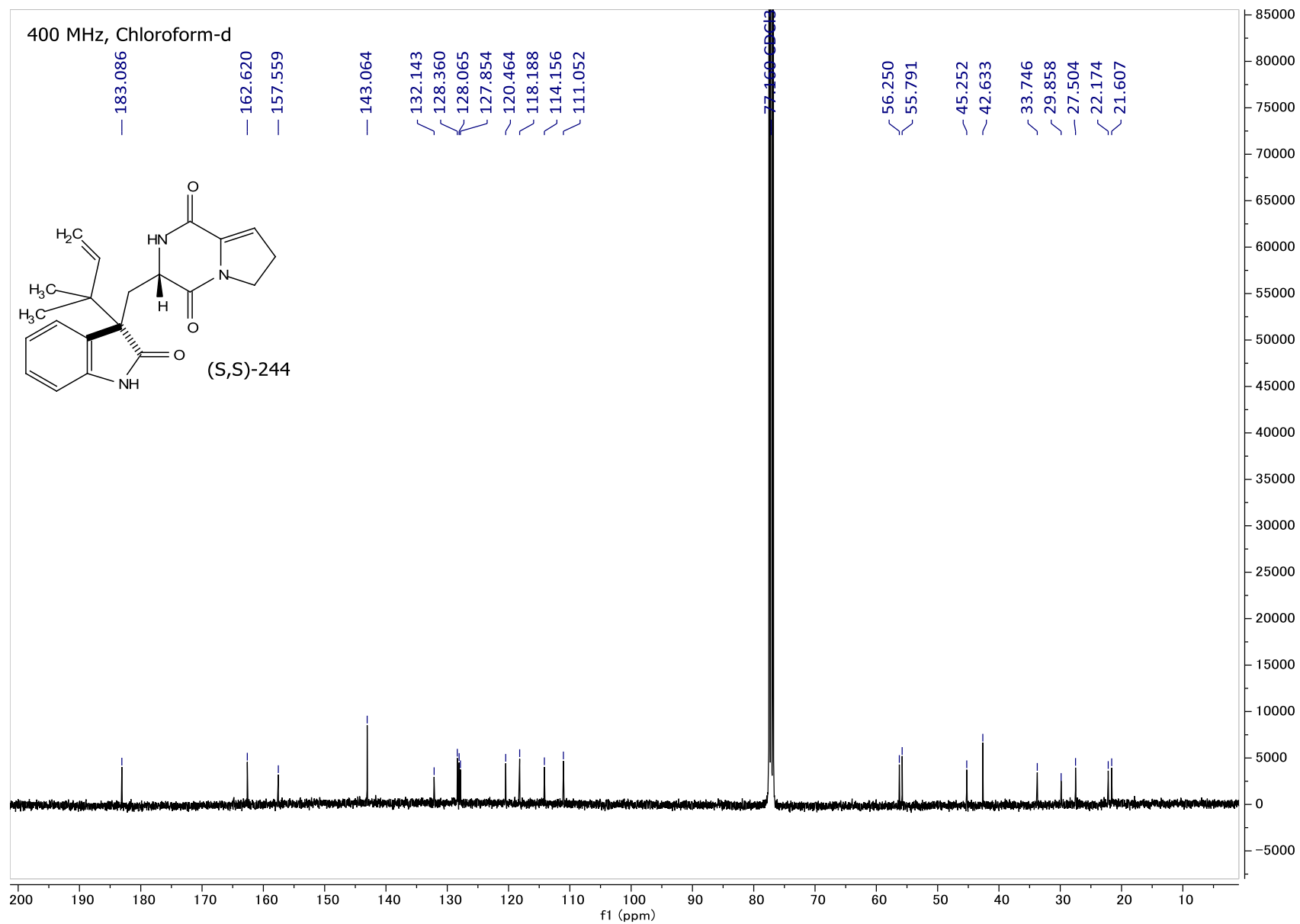


Figure A85:  $^{13}\text{C}$  NMR spectrum of (S,R)-244 & (R,S)-244.

400 MHz, Chloroform-d

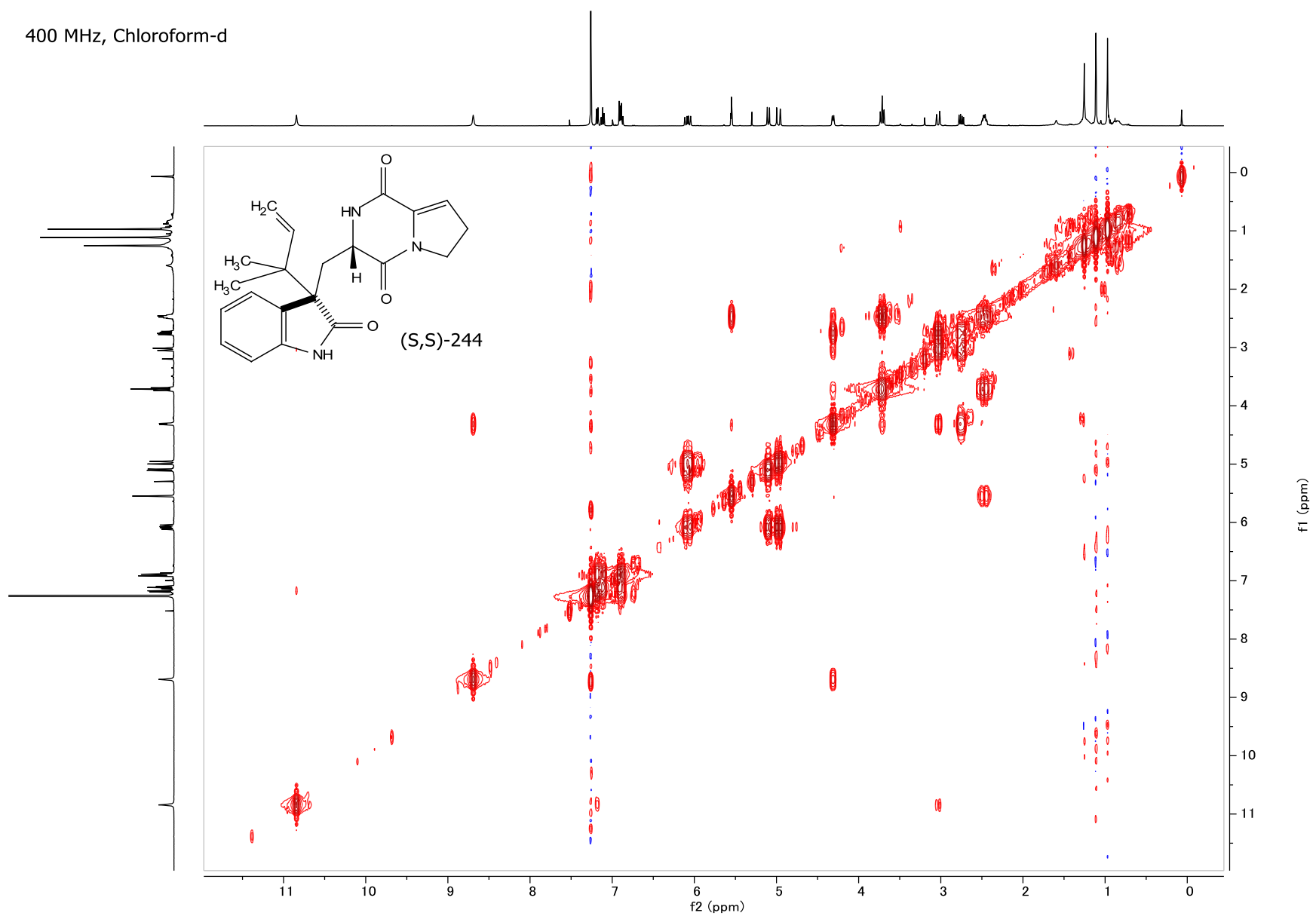


Figure A86: COSY NMR spectrum of (S,R)-244 & (R,S)-244.

400 MHz, Chloroform-d

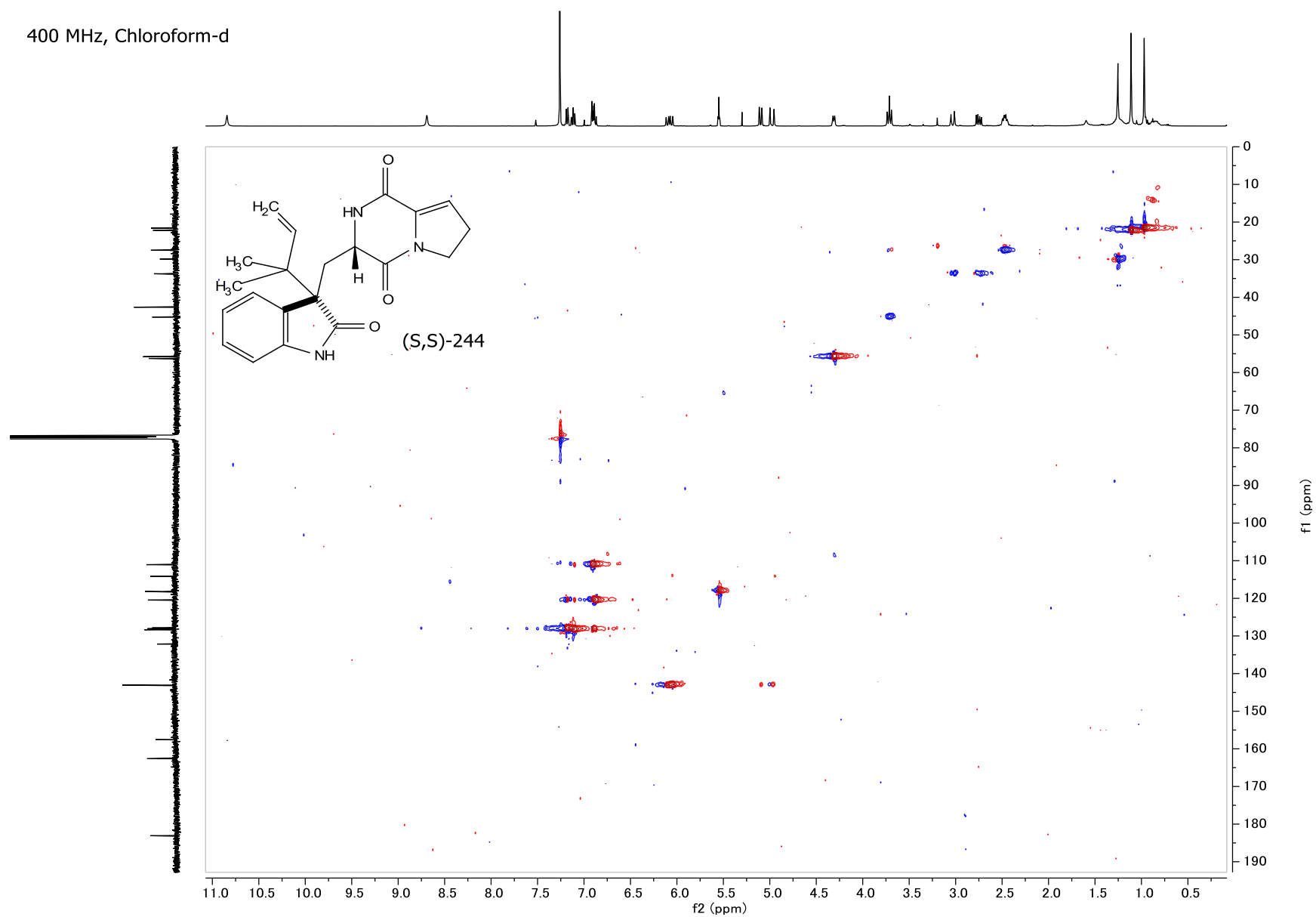


Figure A87: HSQC NMR spectrum of (S,R)-244 & (R,S)-244.

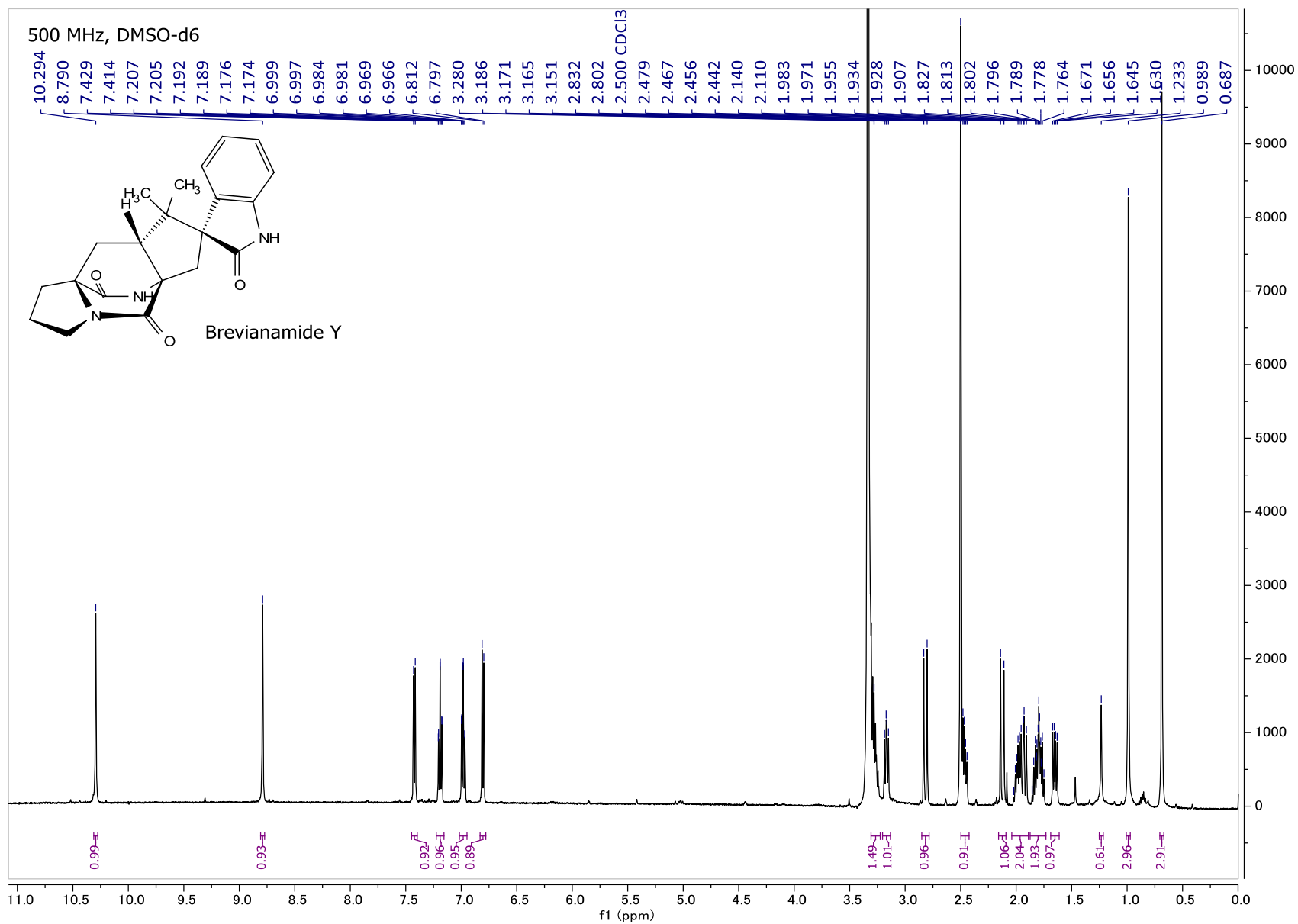


Figure A88: <sup>1</sup>H NMR spectrum of Brevianamide Y.

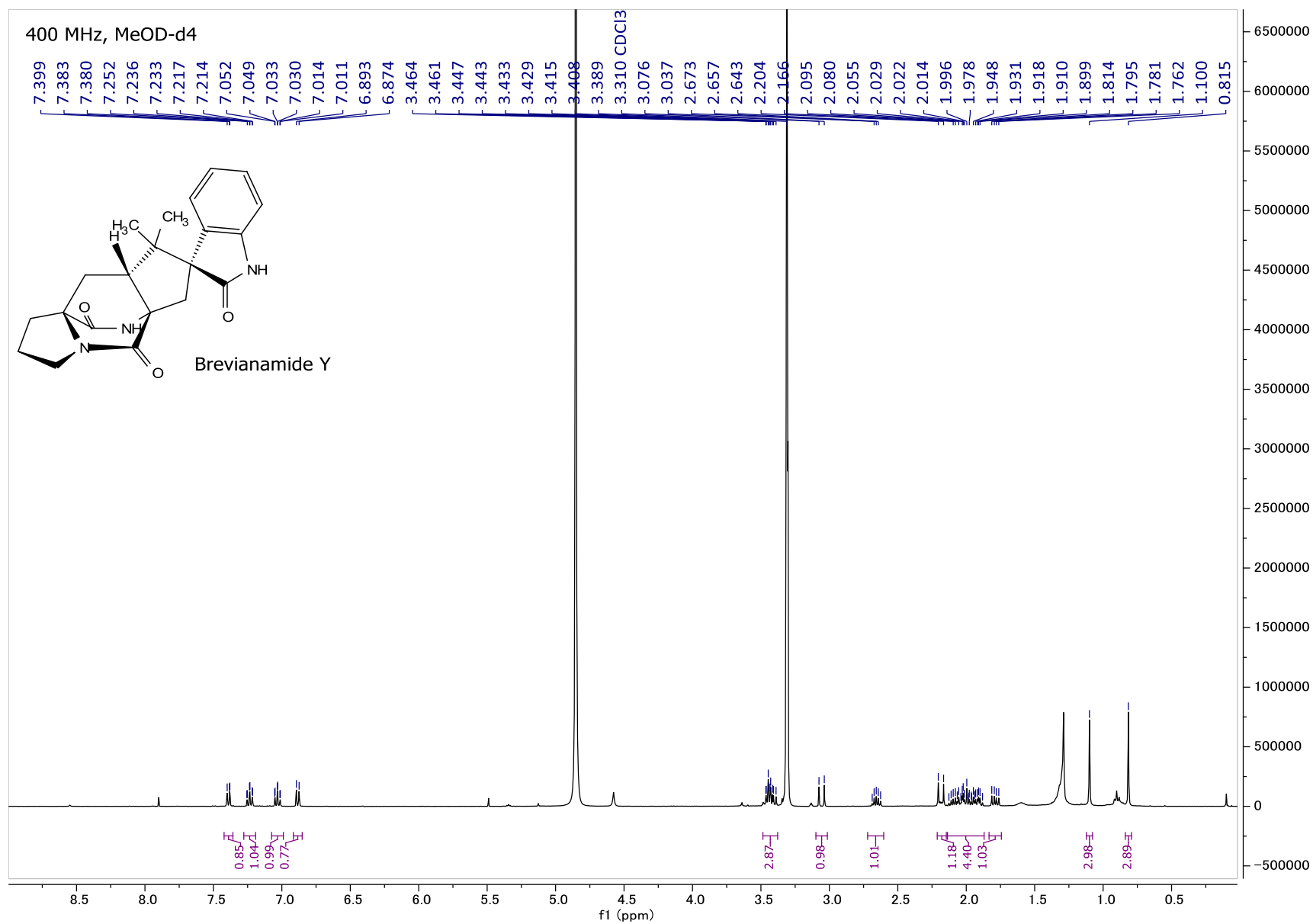


Figure A89: <sup>1</sup>H NMR spectrum of **Brevianamide Y** (MeOD).

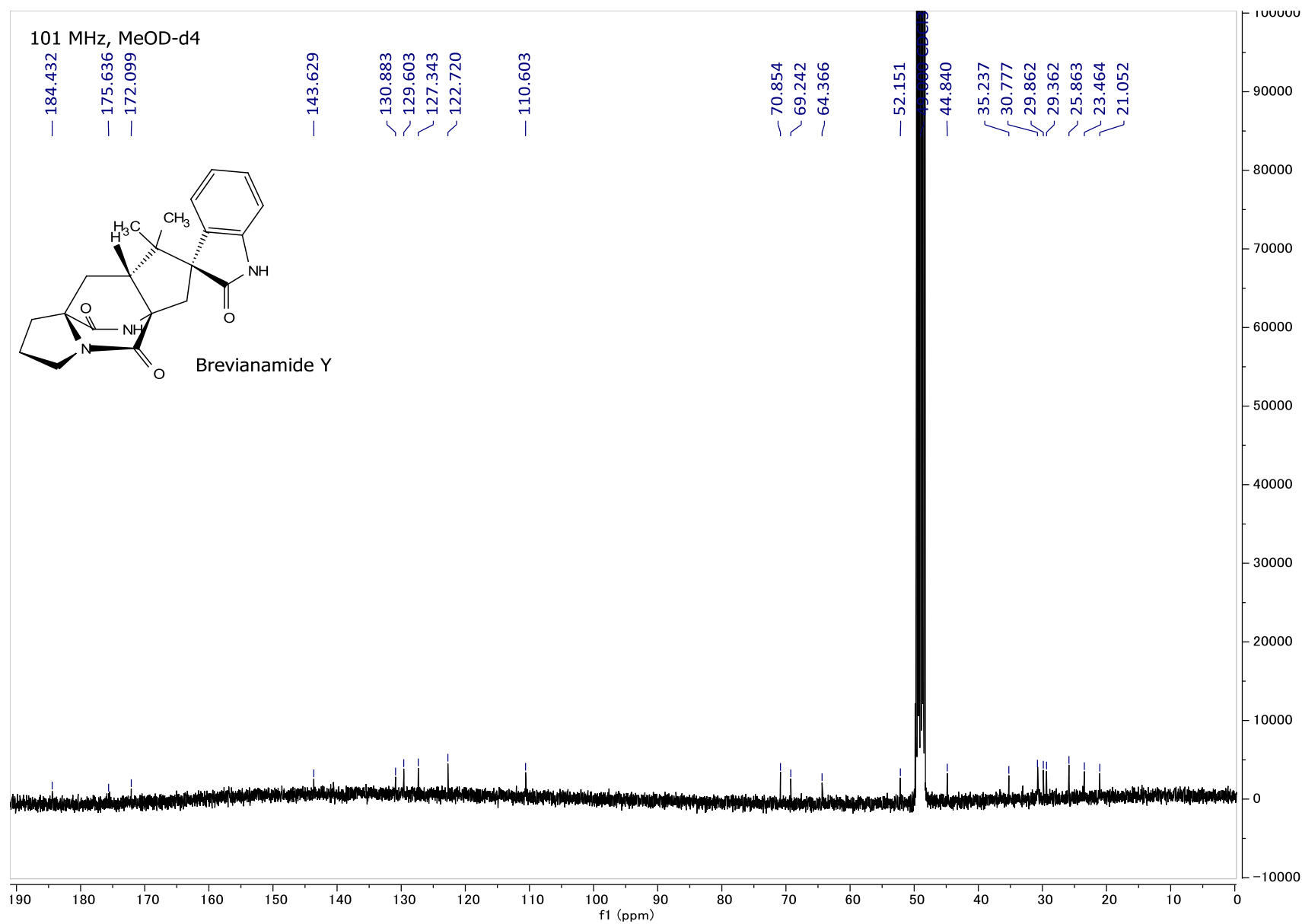


Figure A90:  $^{13}\text{C}$  NMR spectrum of **Brevianamide Y** (MeOD).

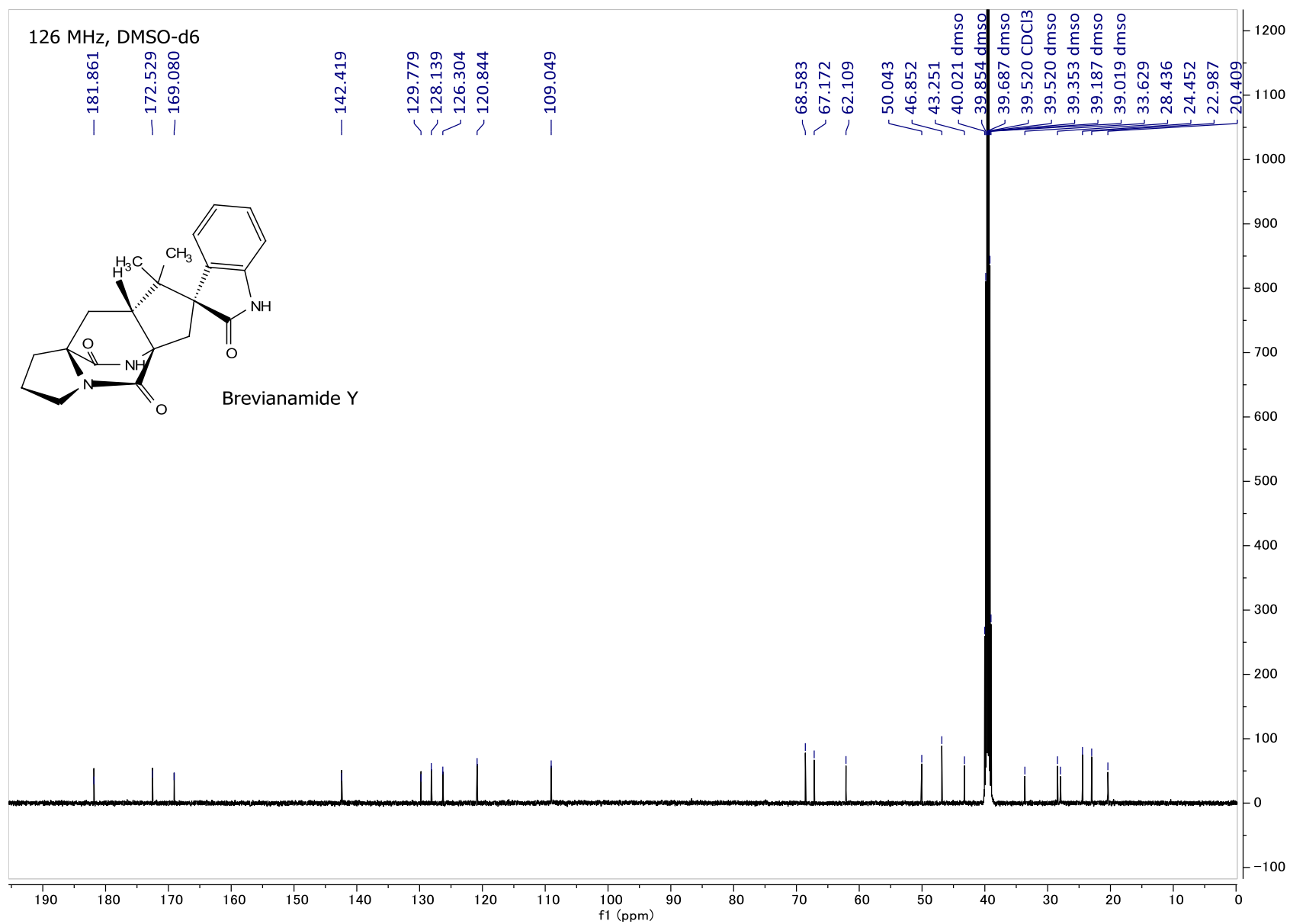


Figure A91: <sup>13</sup>C NMR spectrum of **Brevianamide Y** (DMSO).

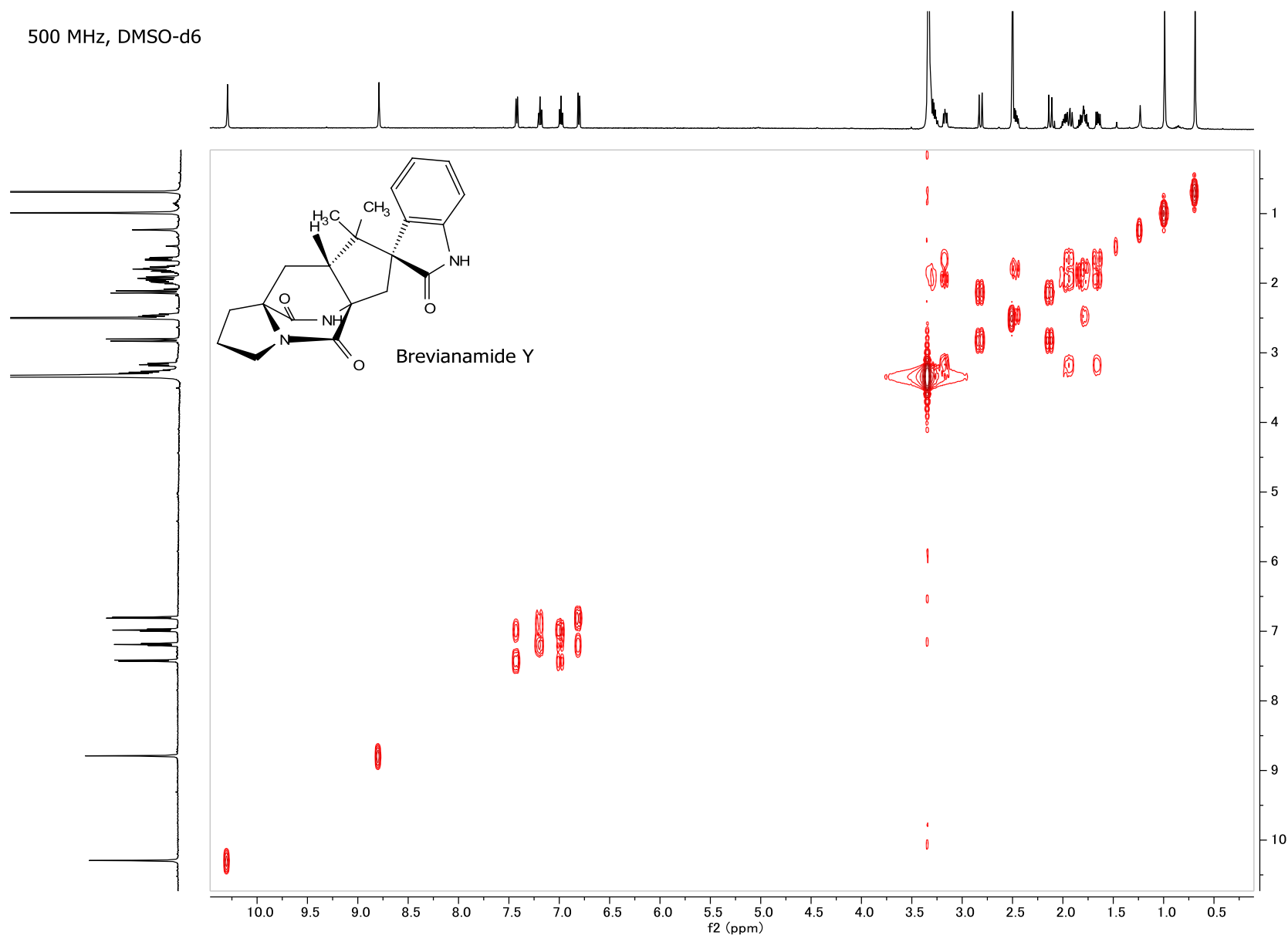


Figure A92: COSY NMR spectrum of **Brevianamide Y** (DMSO).

500 MHz, DMSO-d6

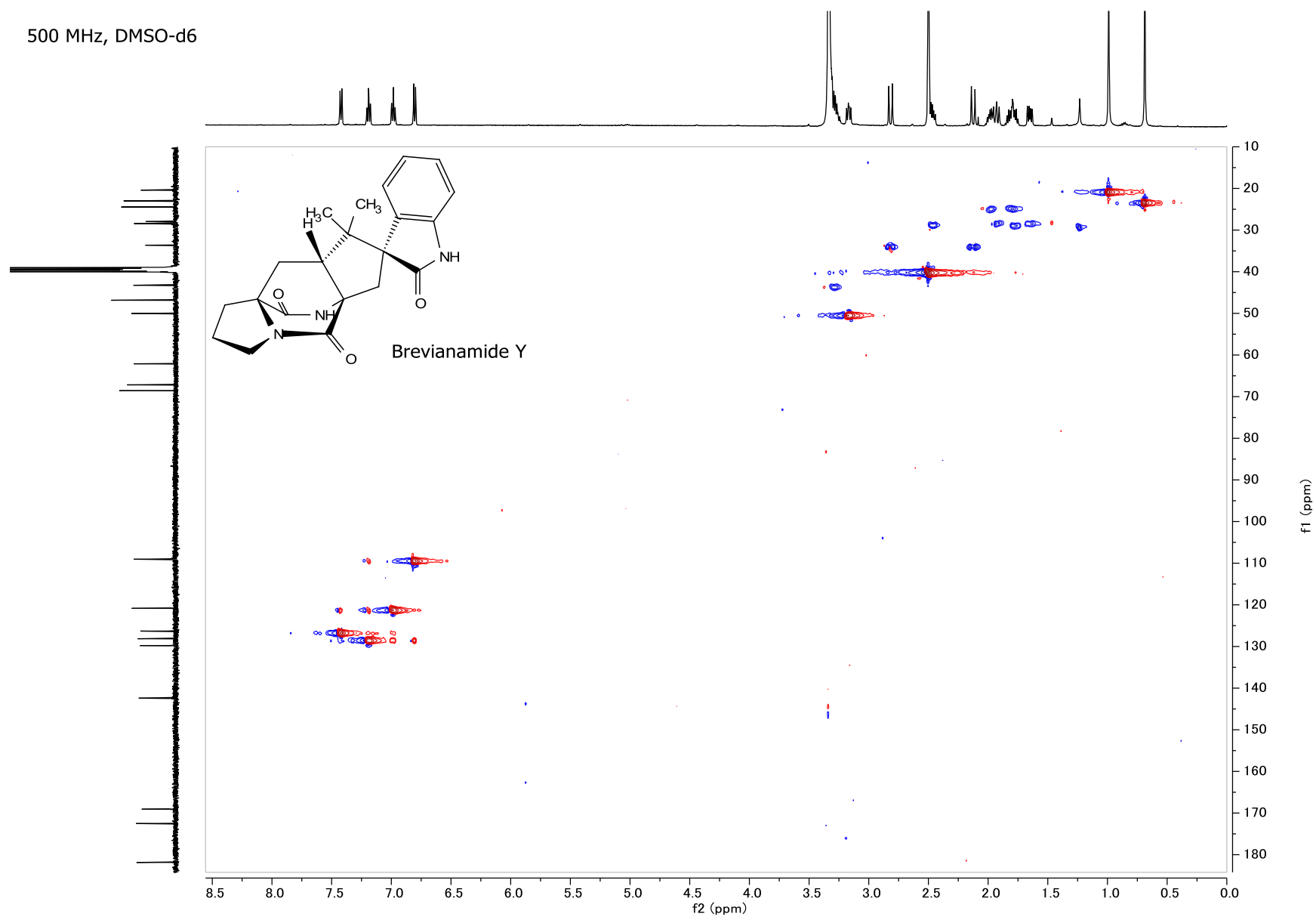


Figure A93: HSQC NMR spectrum of **Brevianamide Y** (DMSO).

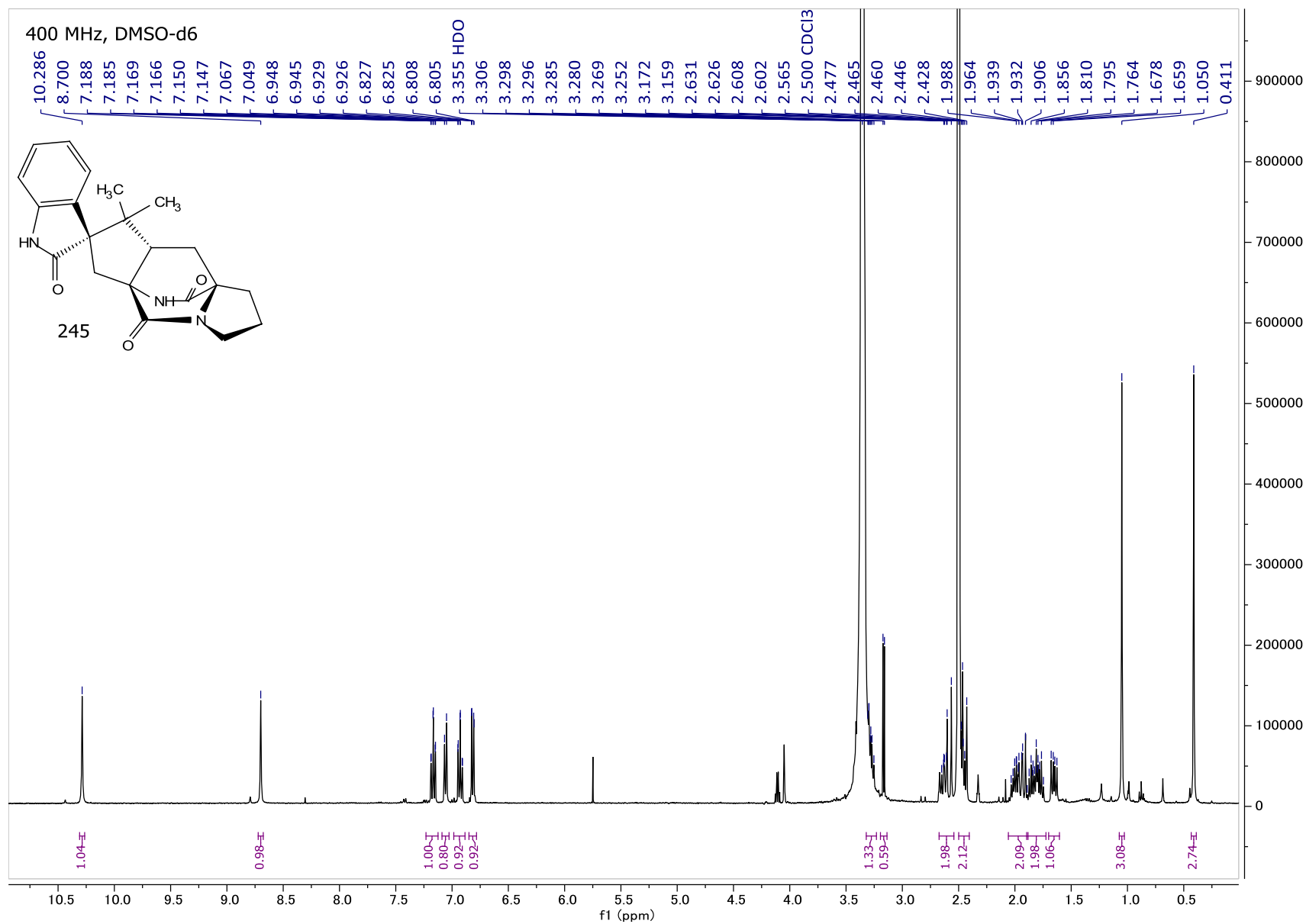


Figure A94:  $^1\text{H}$  NMR spectrum of **245** (DMSO).

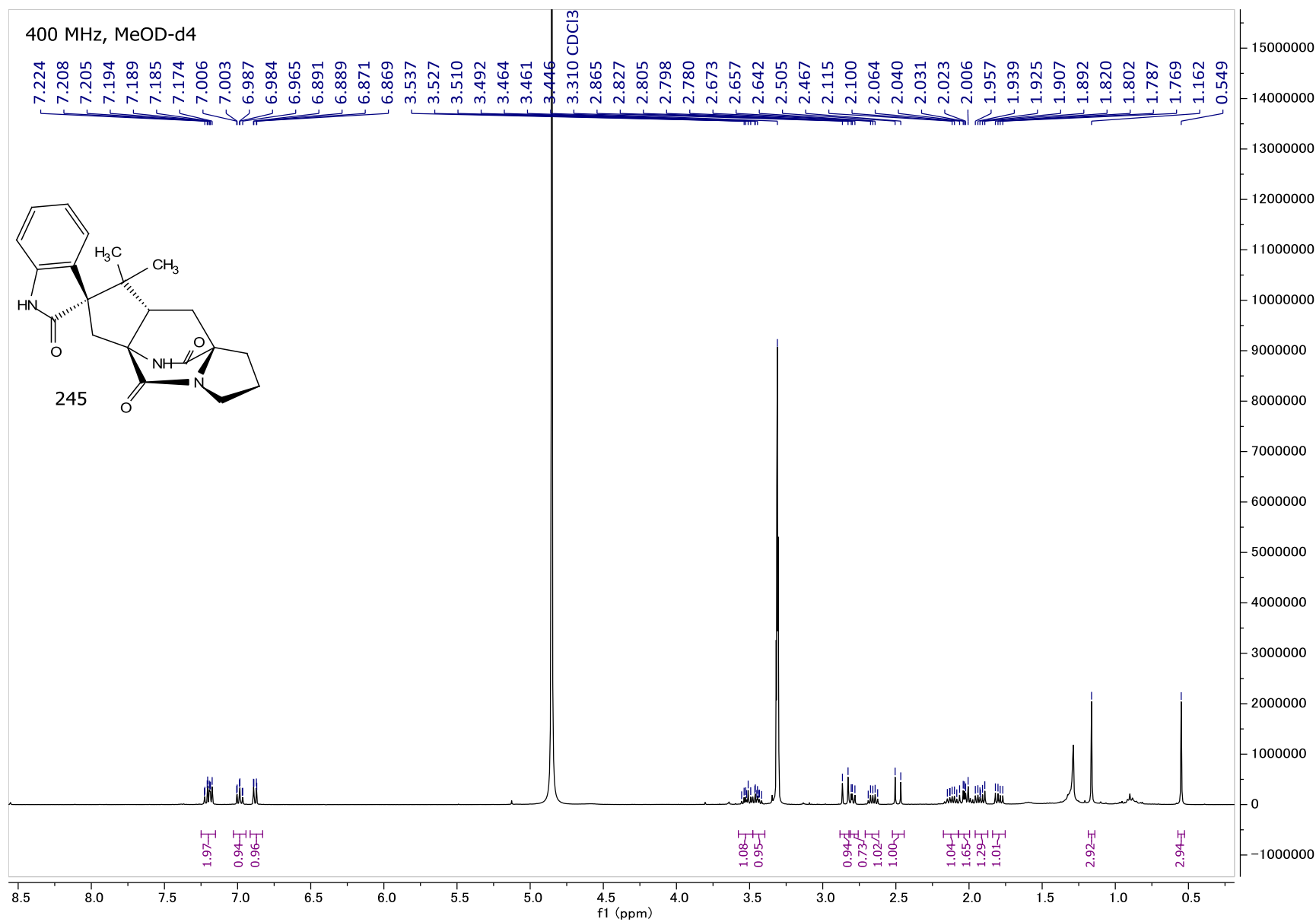


Figure A95: <sup>1</sup>H NMR spectrum of **245** (MeOD).

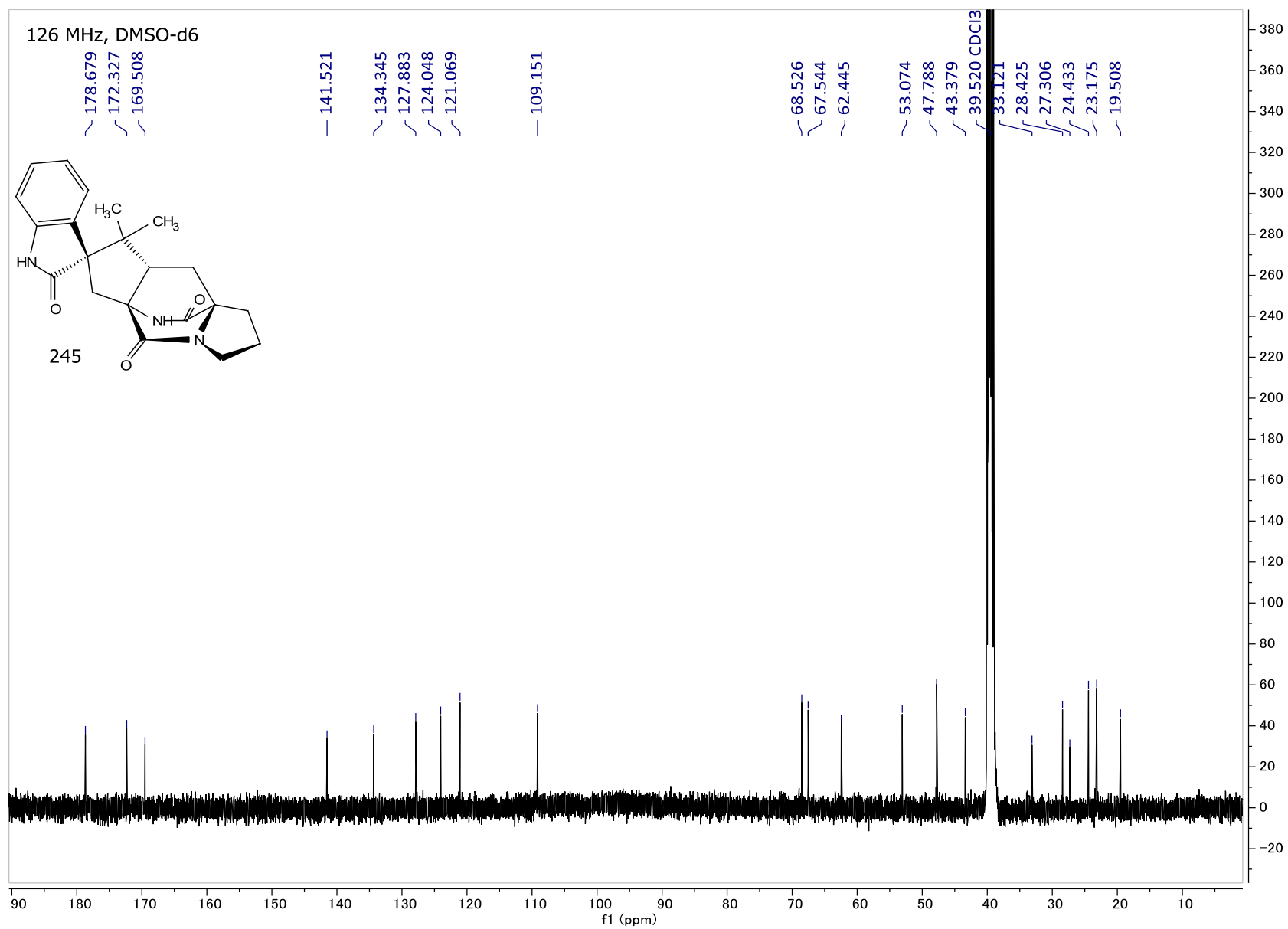


Figure A96: <sup>13</sup>C NMR spectrum of **245** (DMSO).

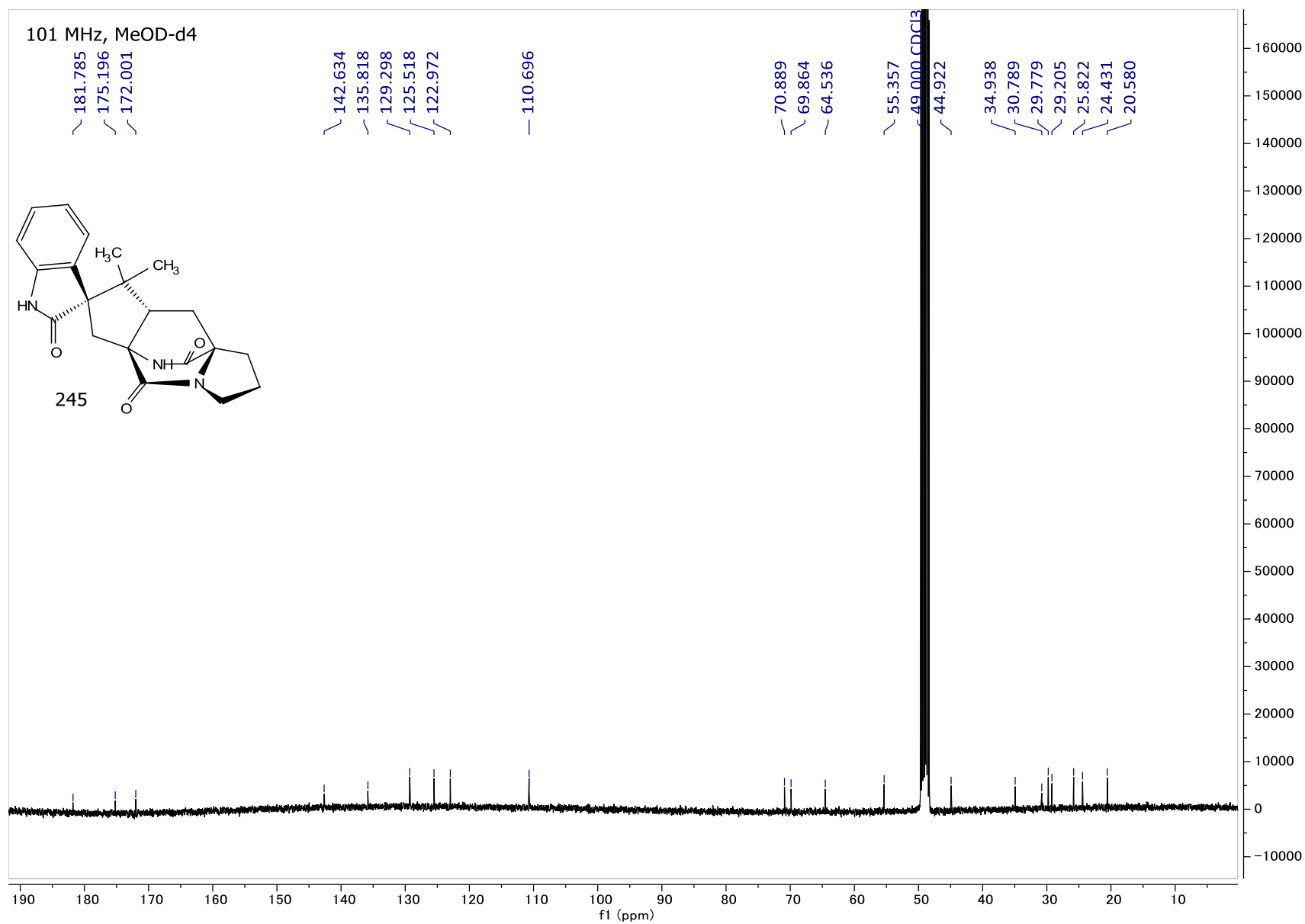


Figure A97: <sup>13</sup>C NMR spectrum of **245** (MeOD).

400 MHz, DMSO-d6

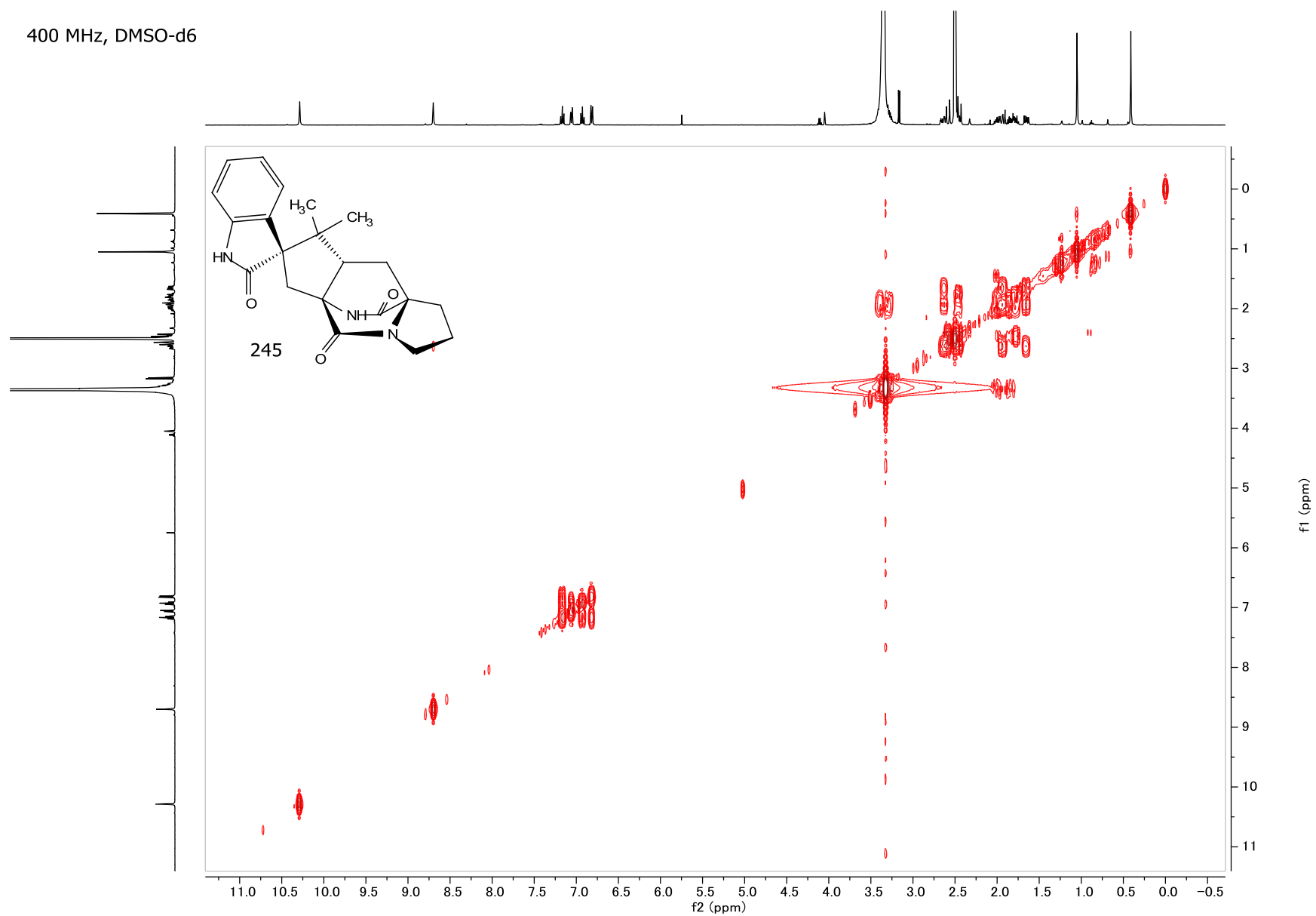


Figure A98: COSY NMR spectrum of **245** (DMSO).

400 MHz, DMSO-d6

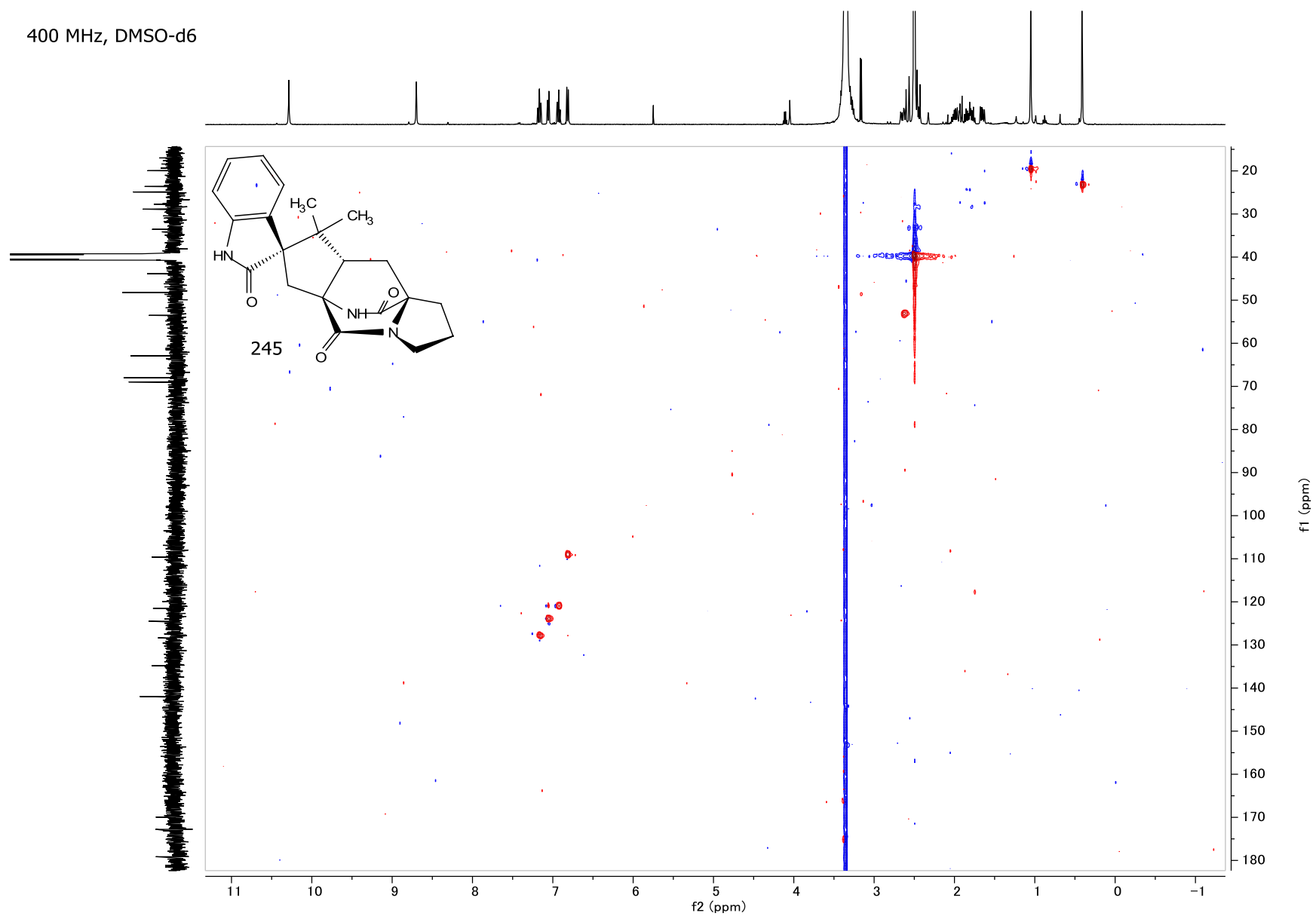


Figure A99: HSQC NMR spectrum of **245** (DMSO).

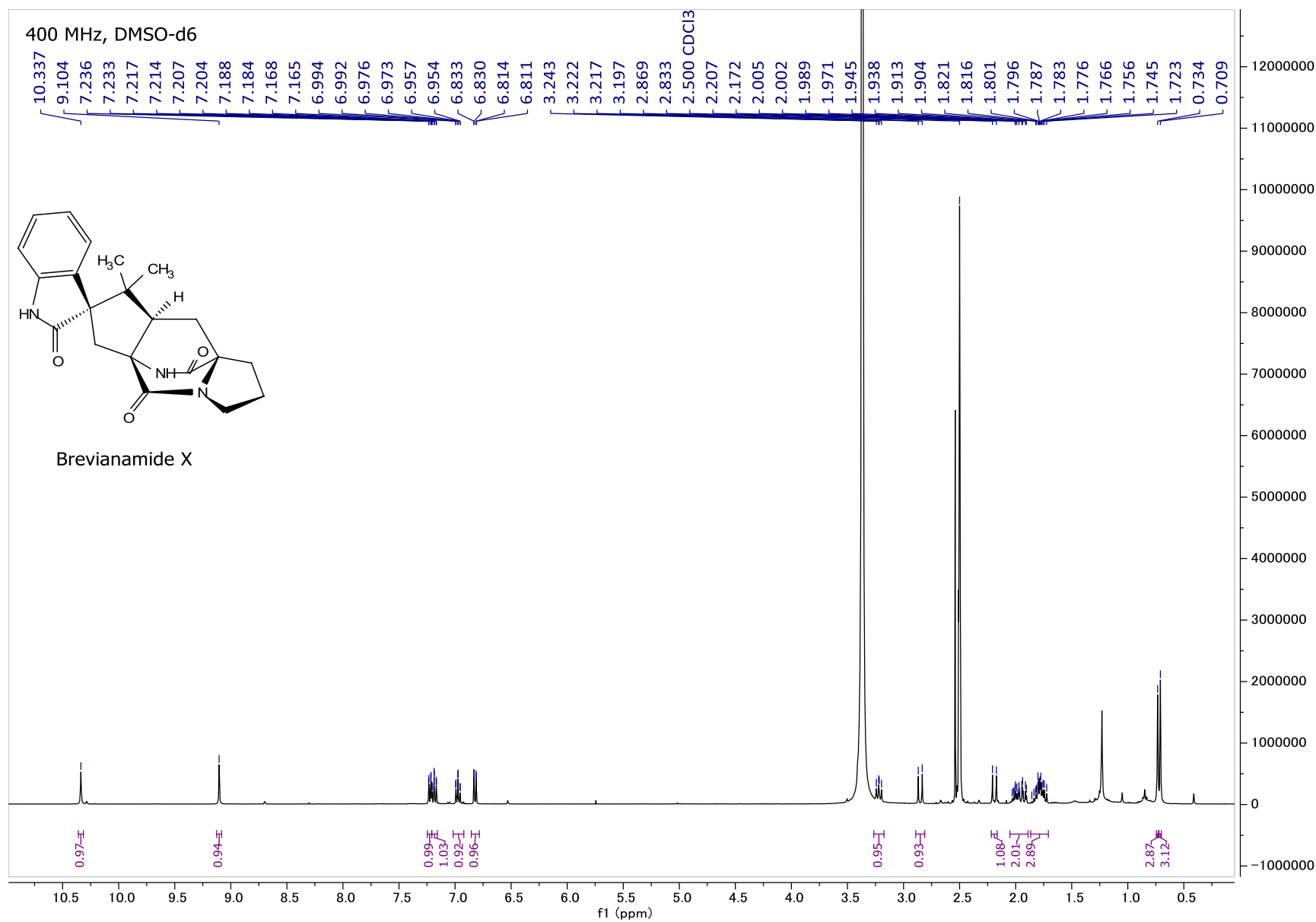


Figure A100: <sup>1</sup>H NMR spectrum of **Brevianamide X** (DMSO).

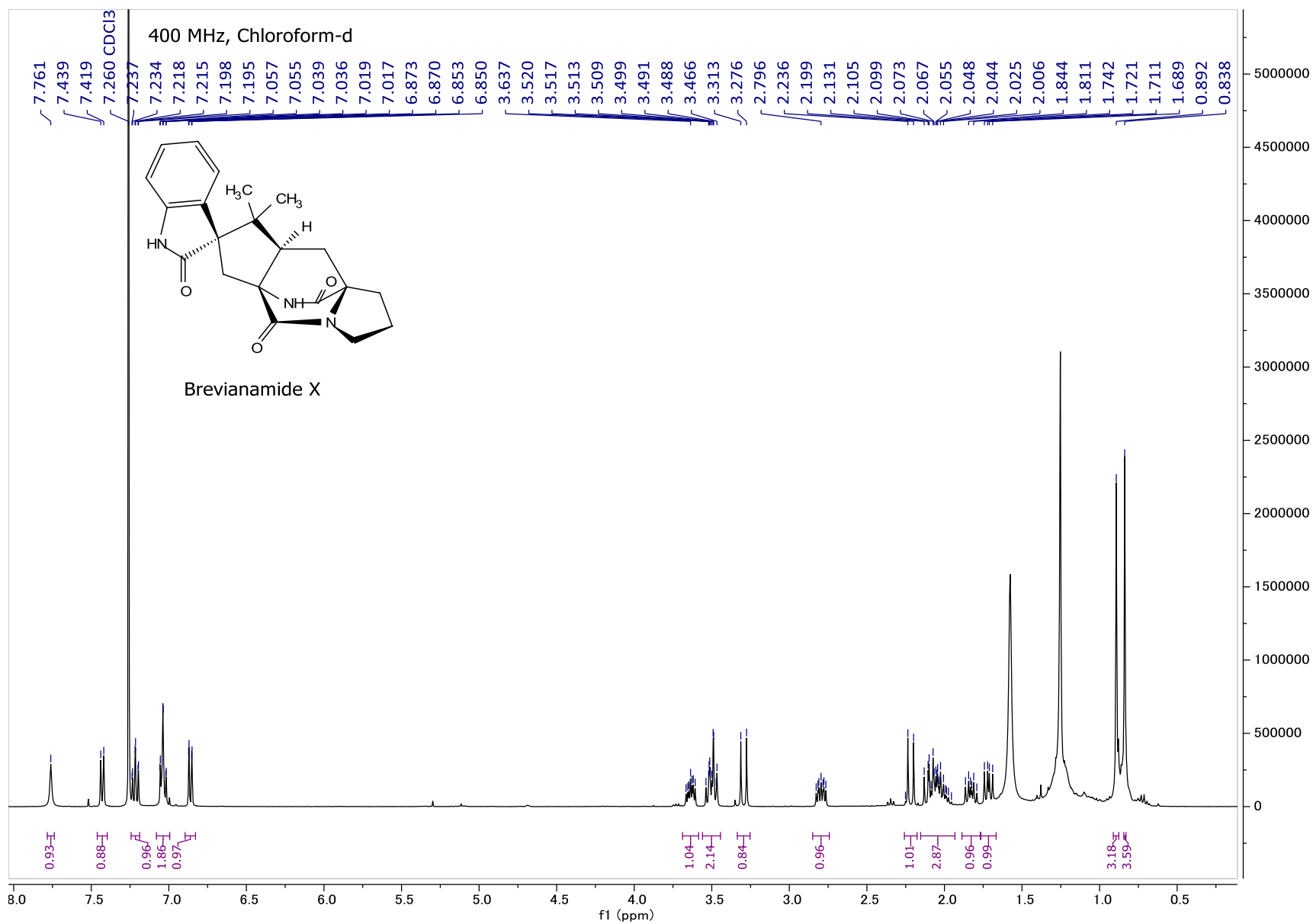


Figure A101: <sup>1</sup>H NMR spectrum of **Brevianamide X** (CDCl<sub>3</sub>).

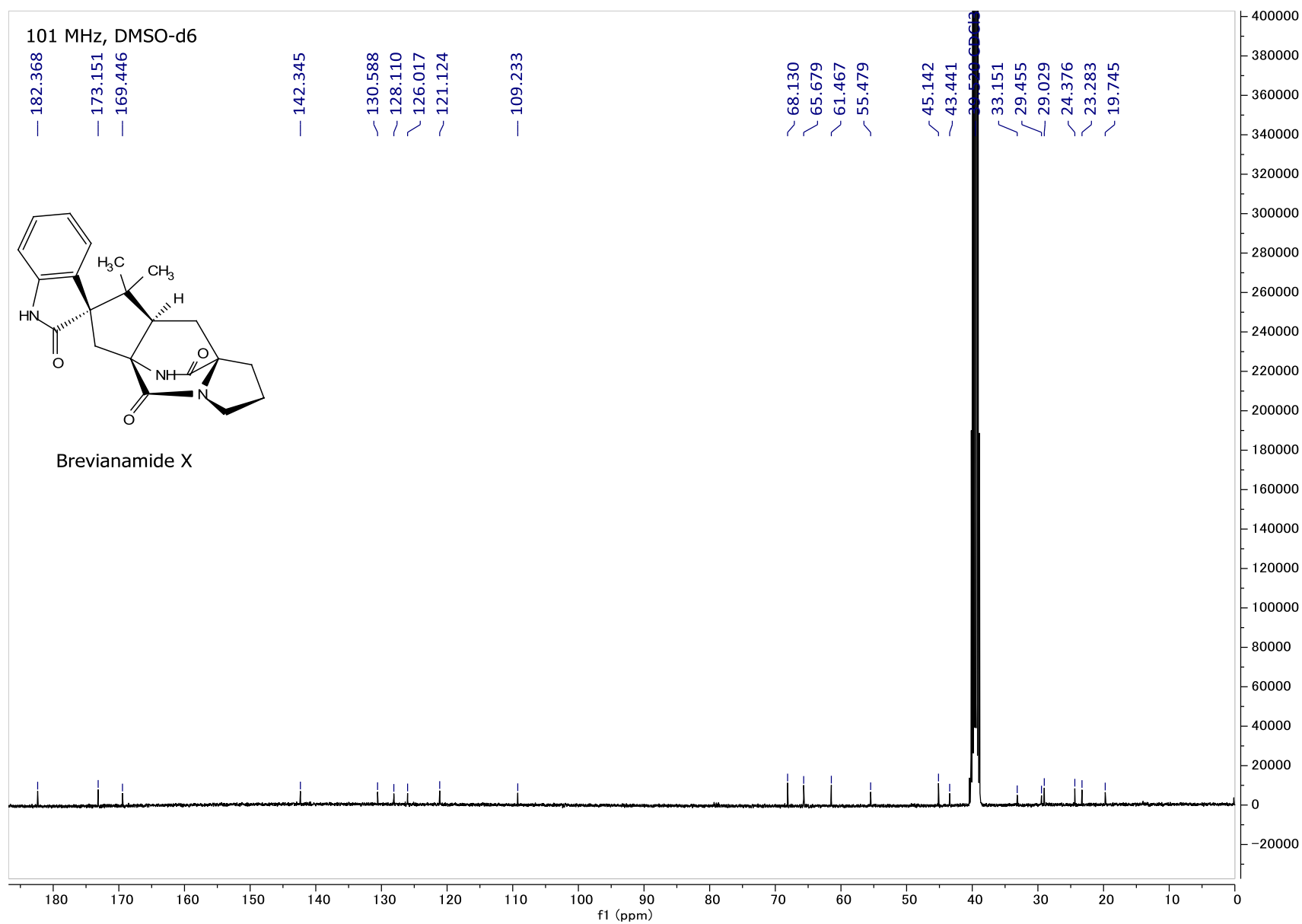


Figure A102: <sup>13</sup>C NMR spectrum of **Brevianamide X** (DMSO).

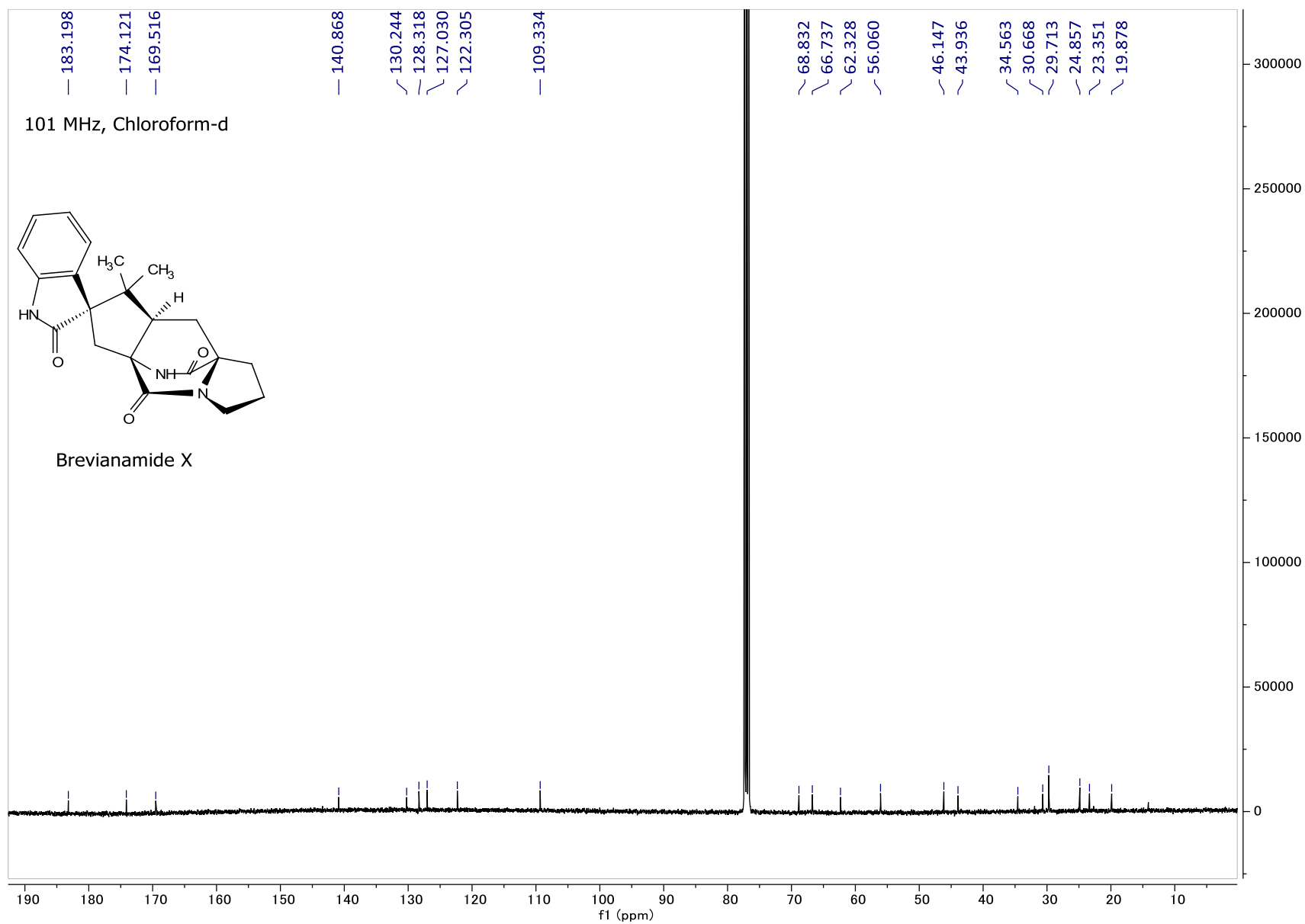


Figure A103:  $^{13}\text{C}$  NMR spectrum of **Brevianamide X** (DMSO).

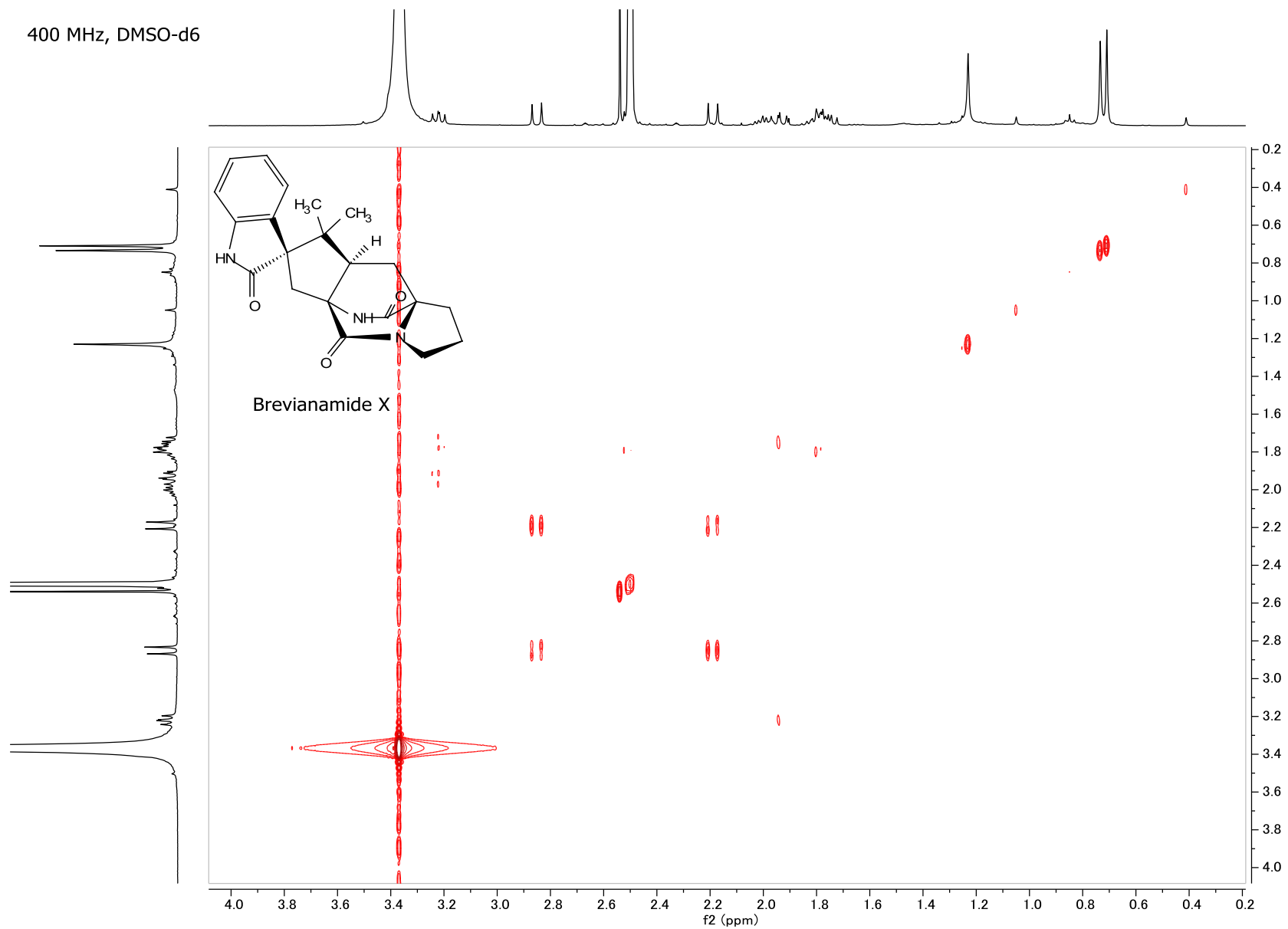


Figure A104: COSY NMR spectrum of **Brevianamide X** (DMSO).

400 MHz, DMSO-d6

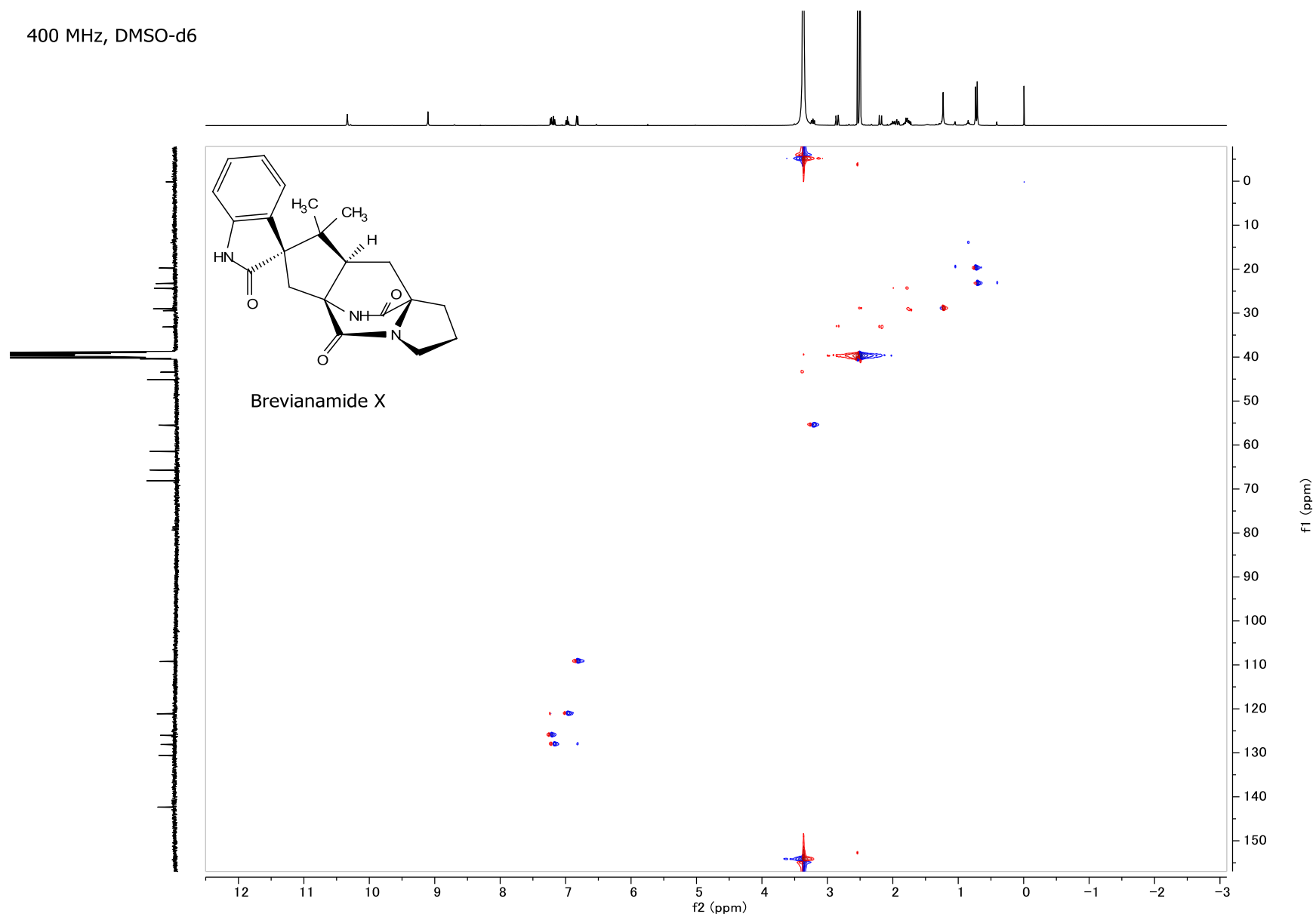


Figure A105: HSQC NMR spectrum of **Brevianamide X** (DMSO).

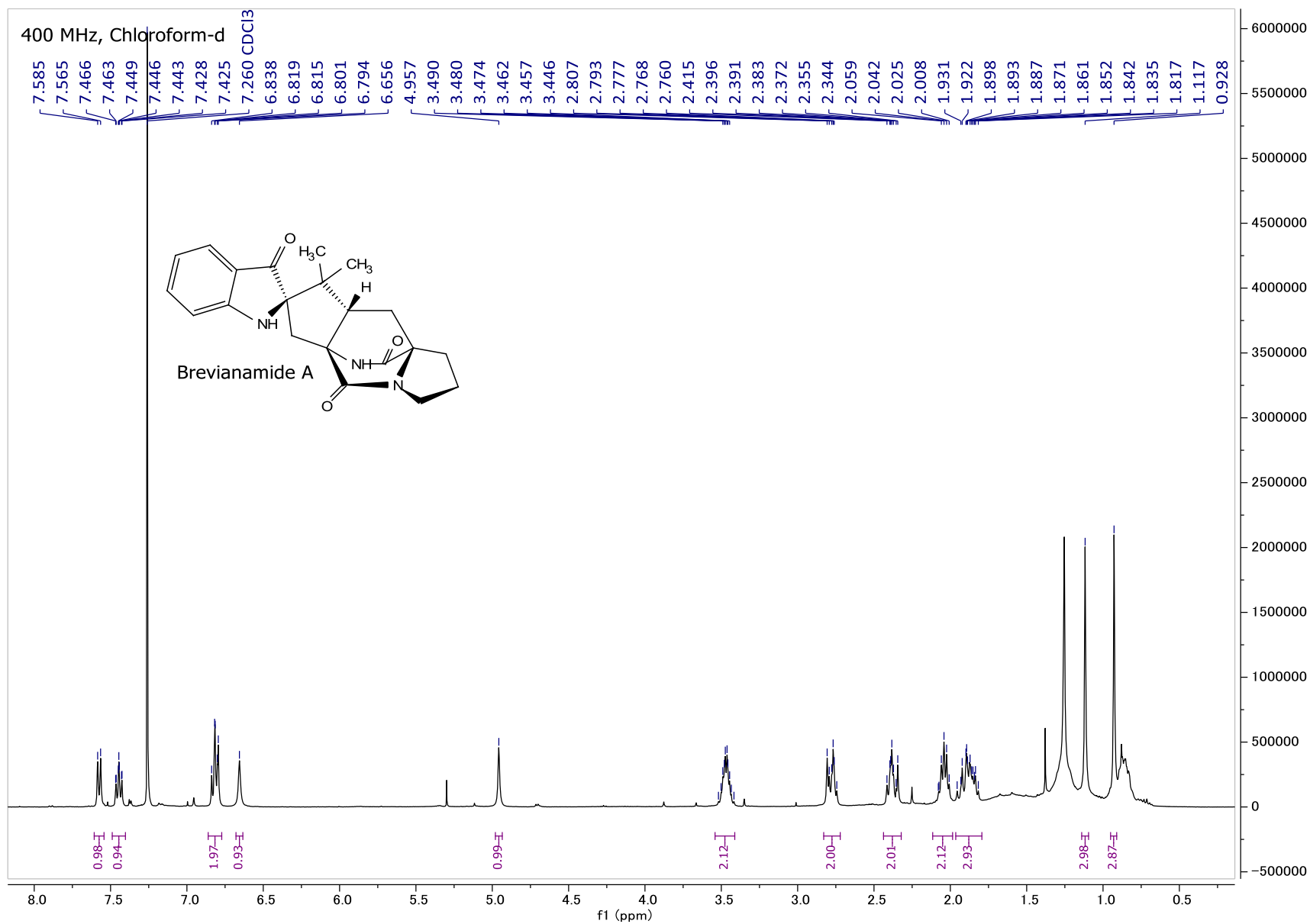


Figure A106: <sup>1</sup>H NMR spectrum of **Brevianamide A**.

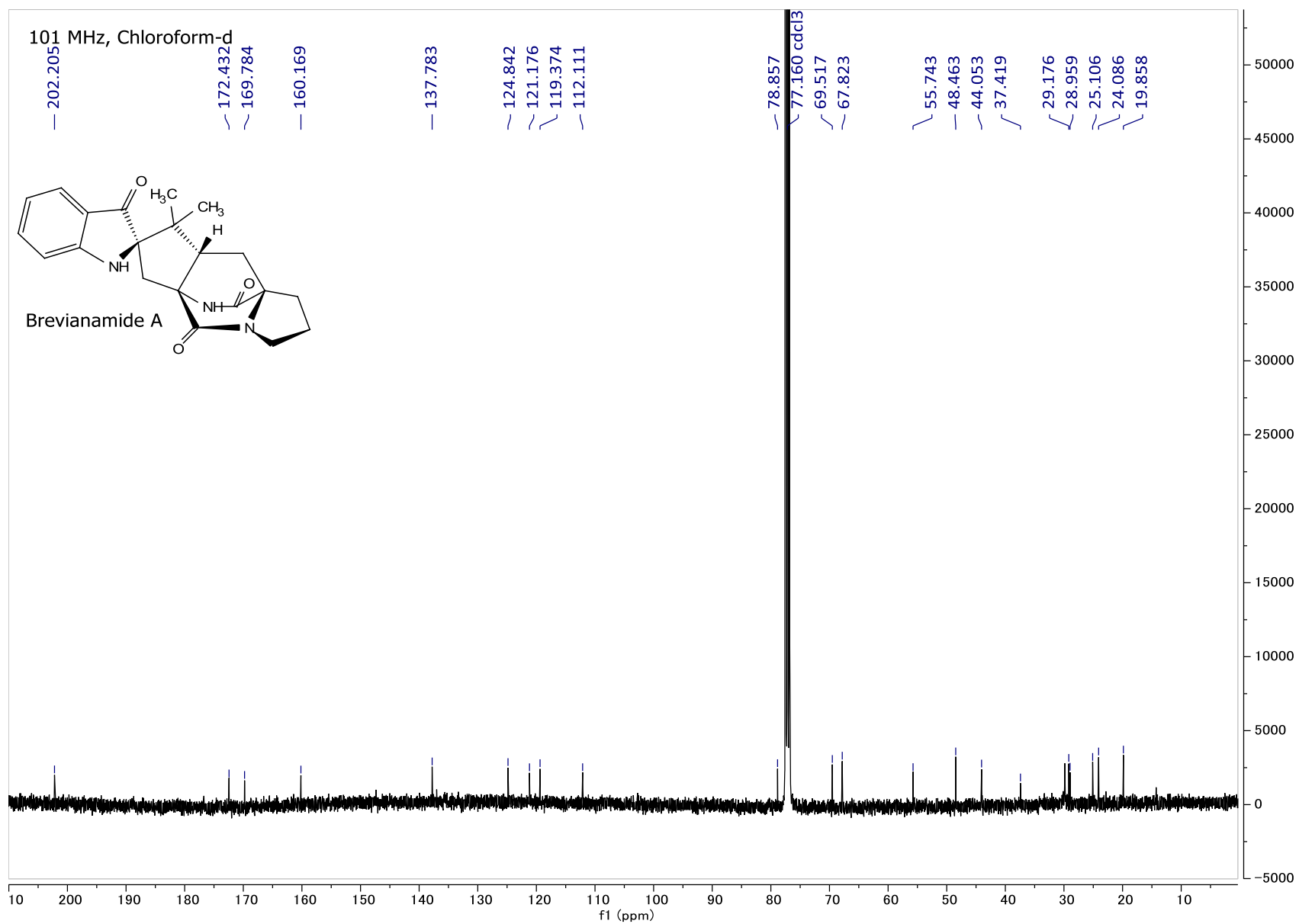


Figure A107:  $^{13}\text{C}$  NMR spectrum of Brevianamide A.

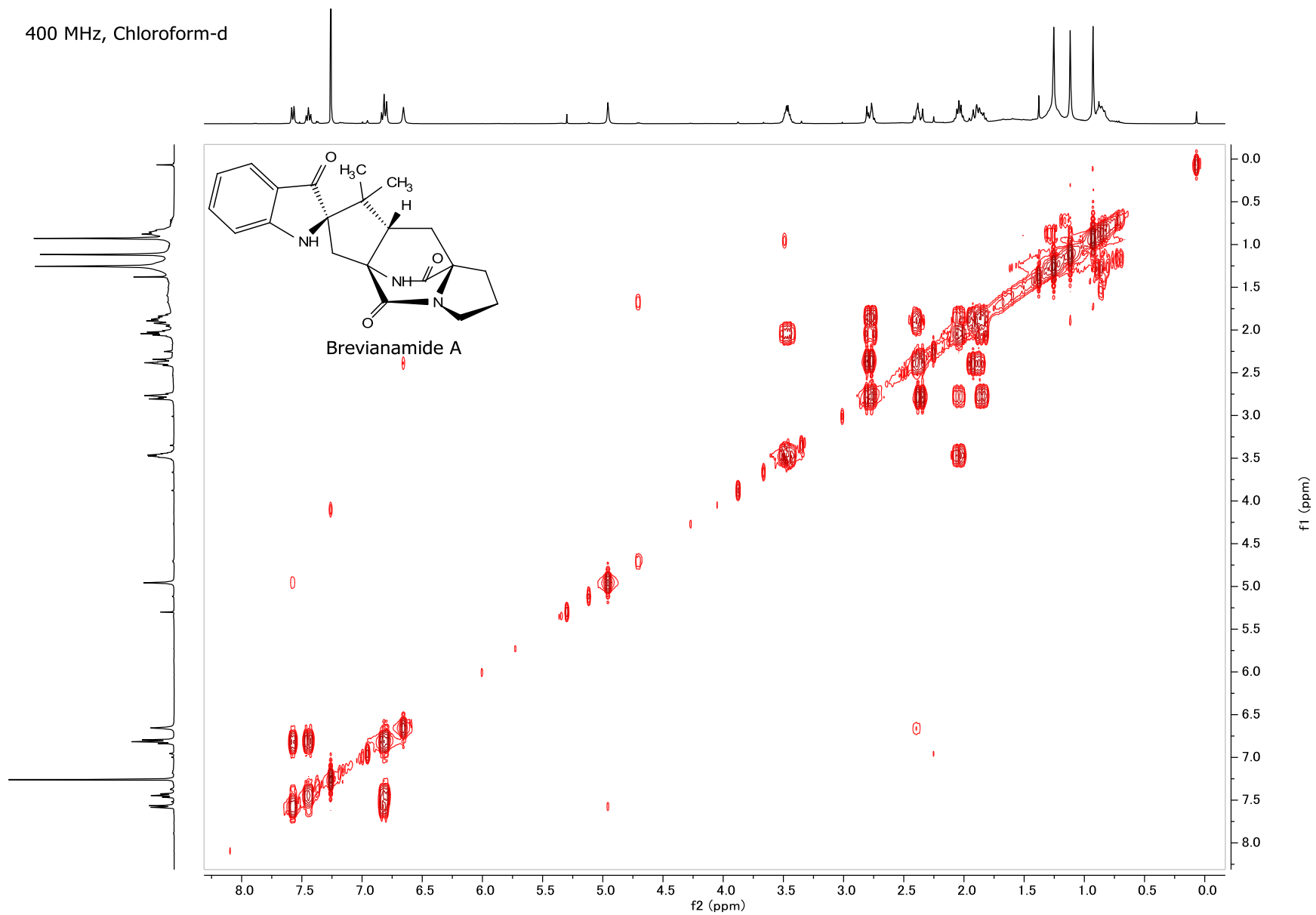


Figure A108: COSY NMR spectrum of **Brevianamide A**.

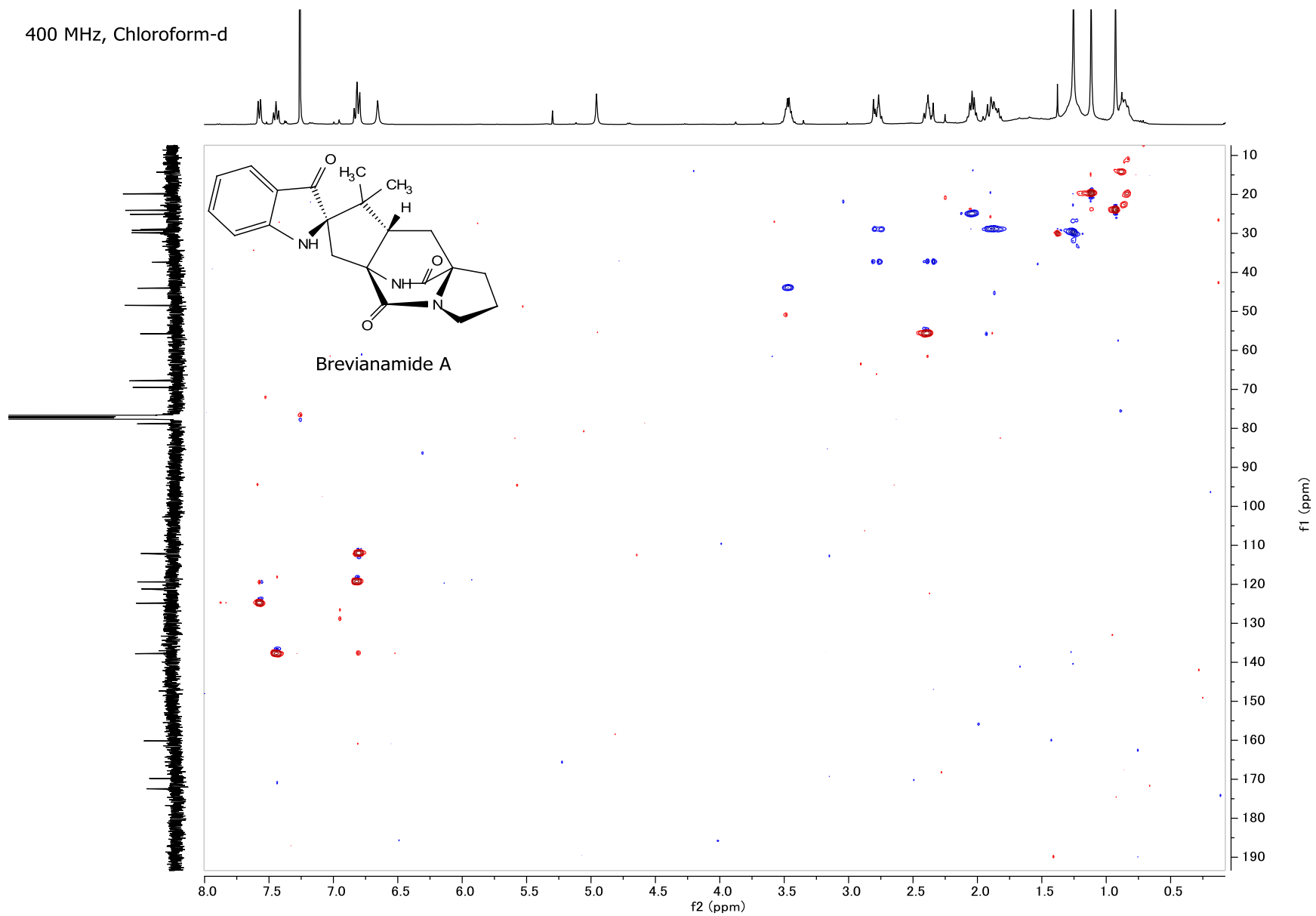


Figure A109: HSQC NMR spectrum of **Brevianamide A**.

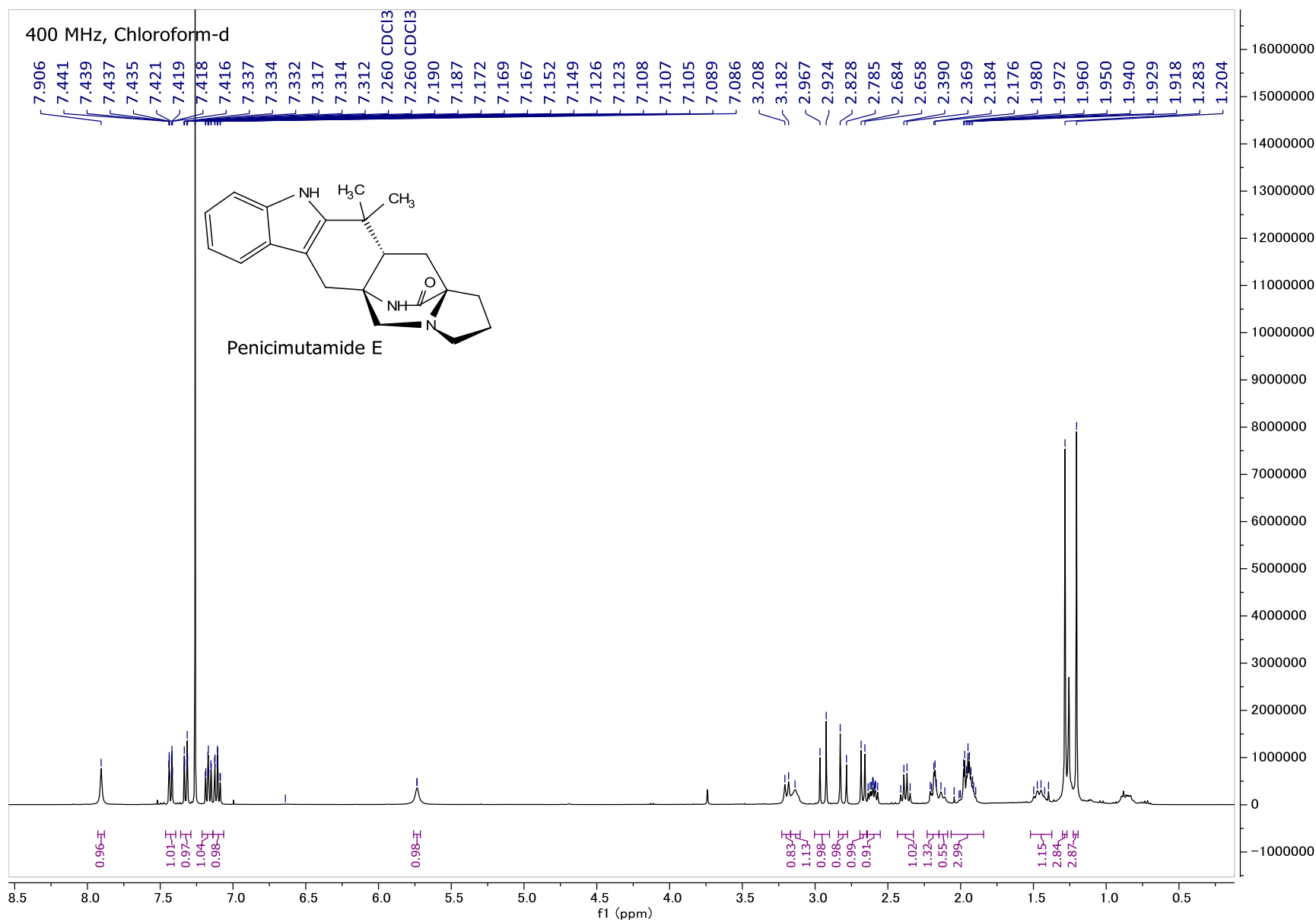


Figure A110:  $^1\text{H}$  NMR spectrum of **Penicimutamide E** in  $\text{CDCl}_3$ .

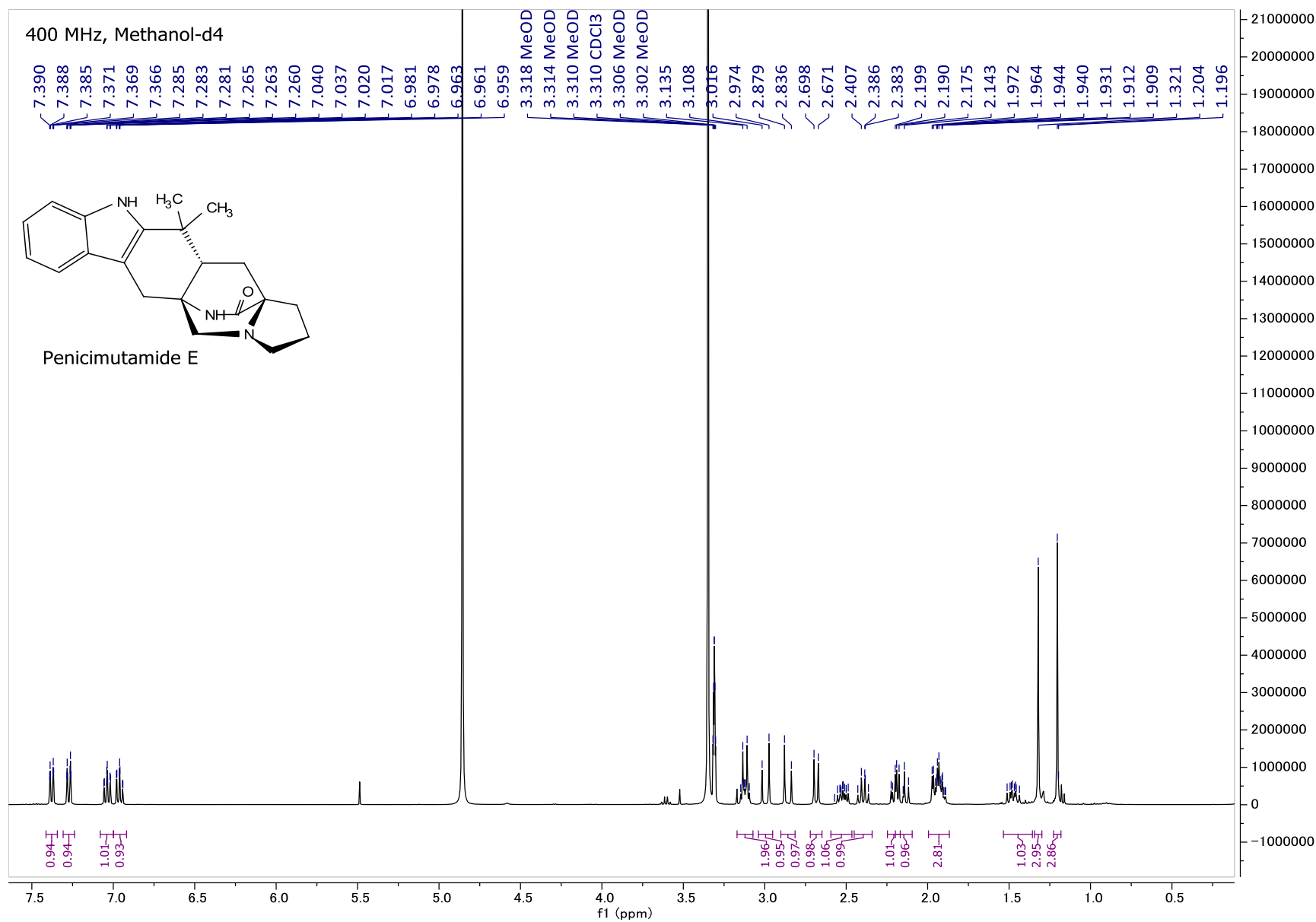


Figure A111: <sup>1</sup>H NMR spectrum of **Penicimutamide E** in MeOD.

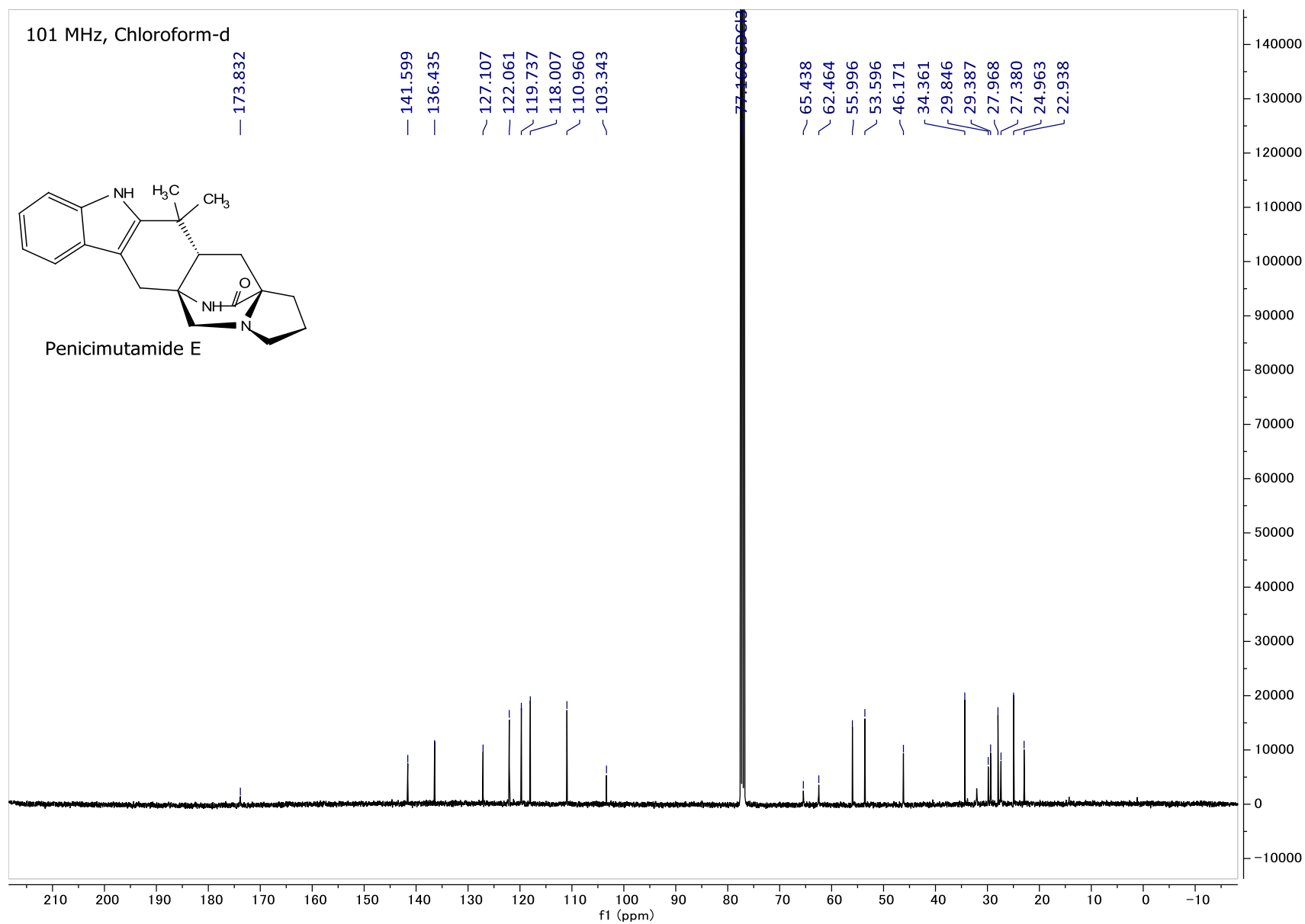


Figure A112:  $^{13}\text{C}$  NMR spectrum of **Penicimutamide E** in  $\text{CDCl}_3$ .

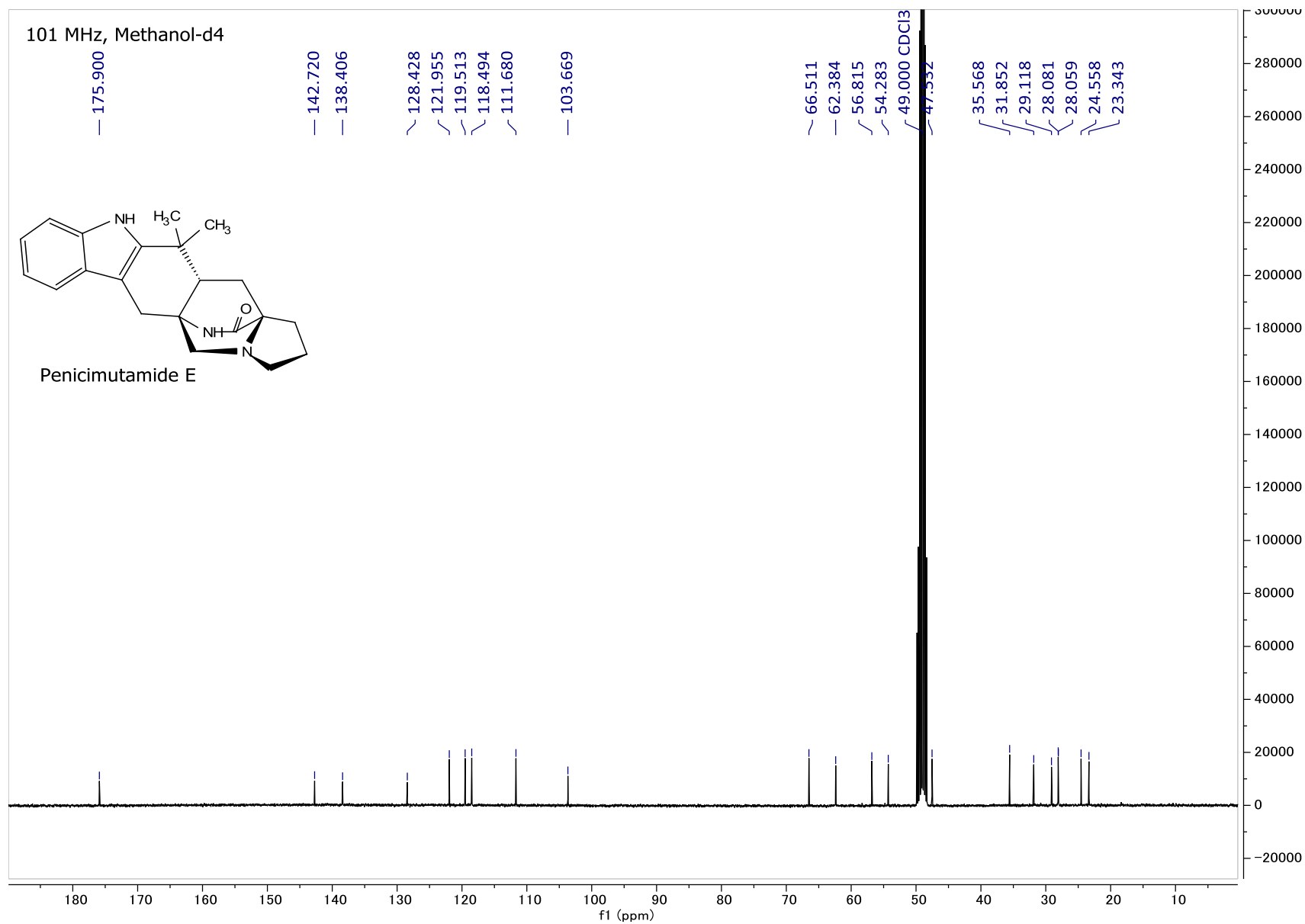


Figure A113:  $^{13}\text{C}$  NMR spectrum of **Penicimutamide E** in MeOD.

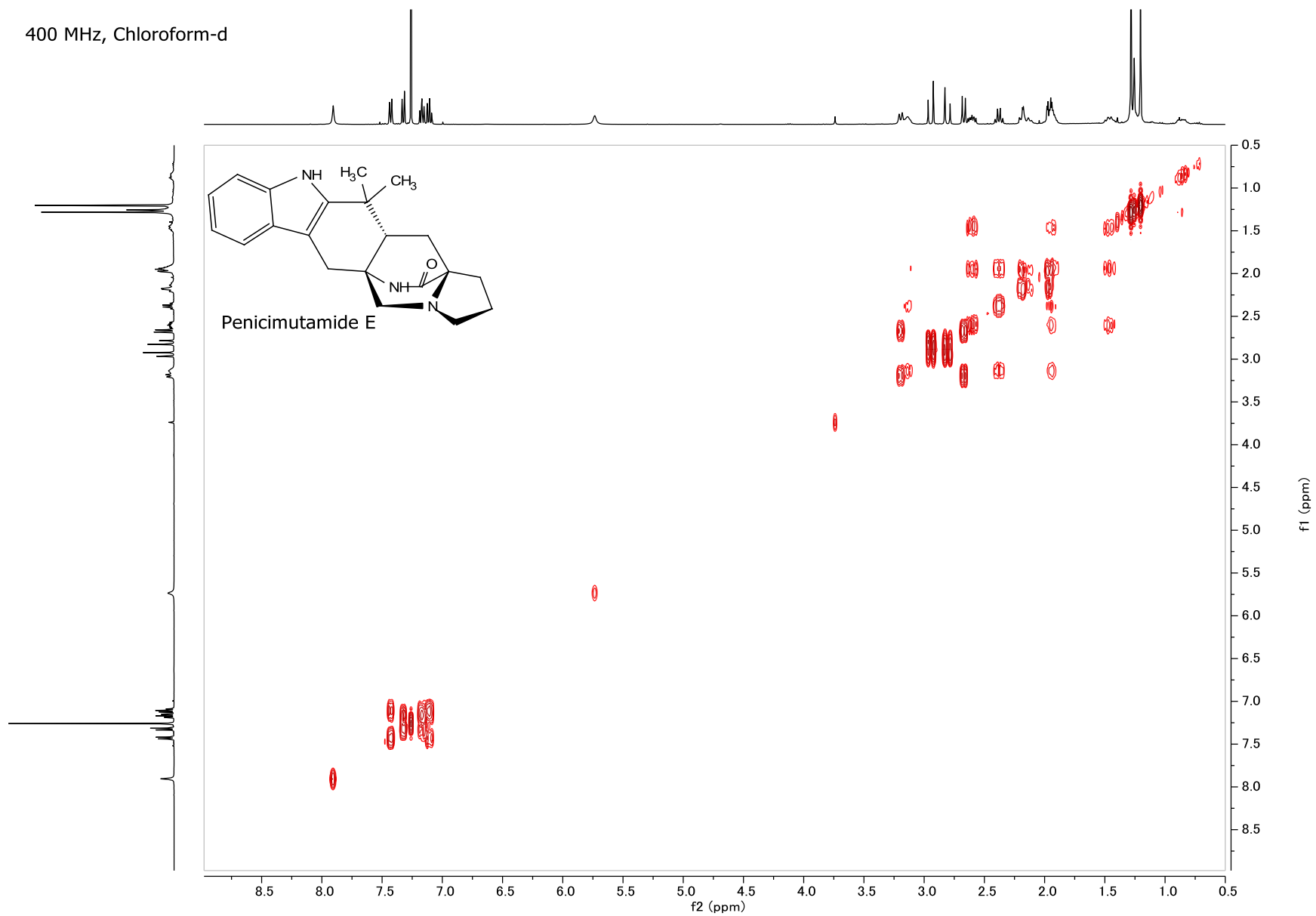


Figure A114: COSY NMR spectrum of **Penicimutamide E**.

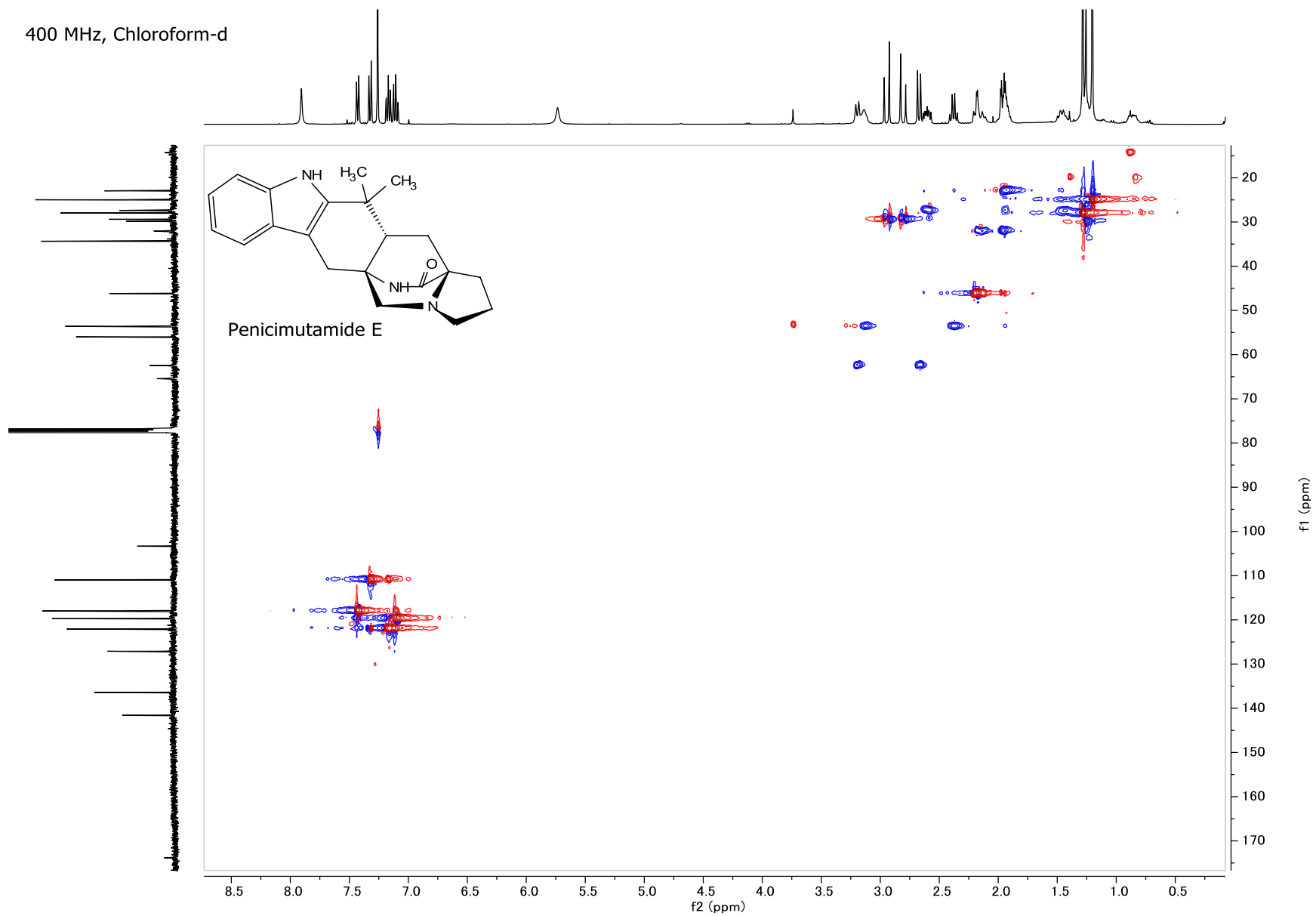


Figure A115: HSQC NMR spectrum of **Penicimutamide E**.

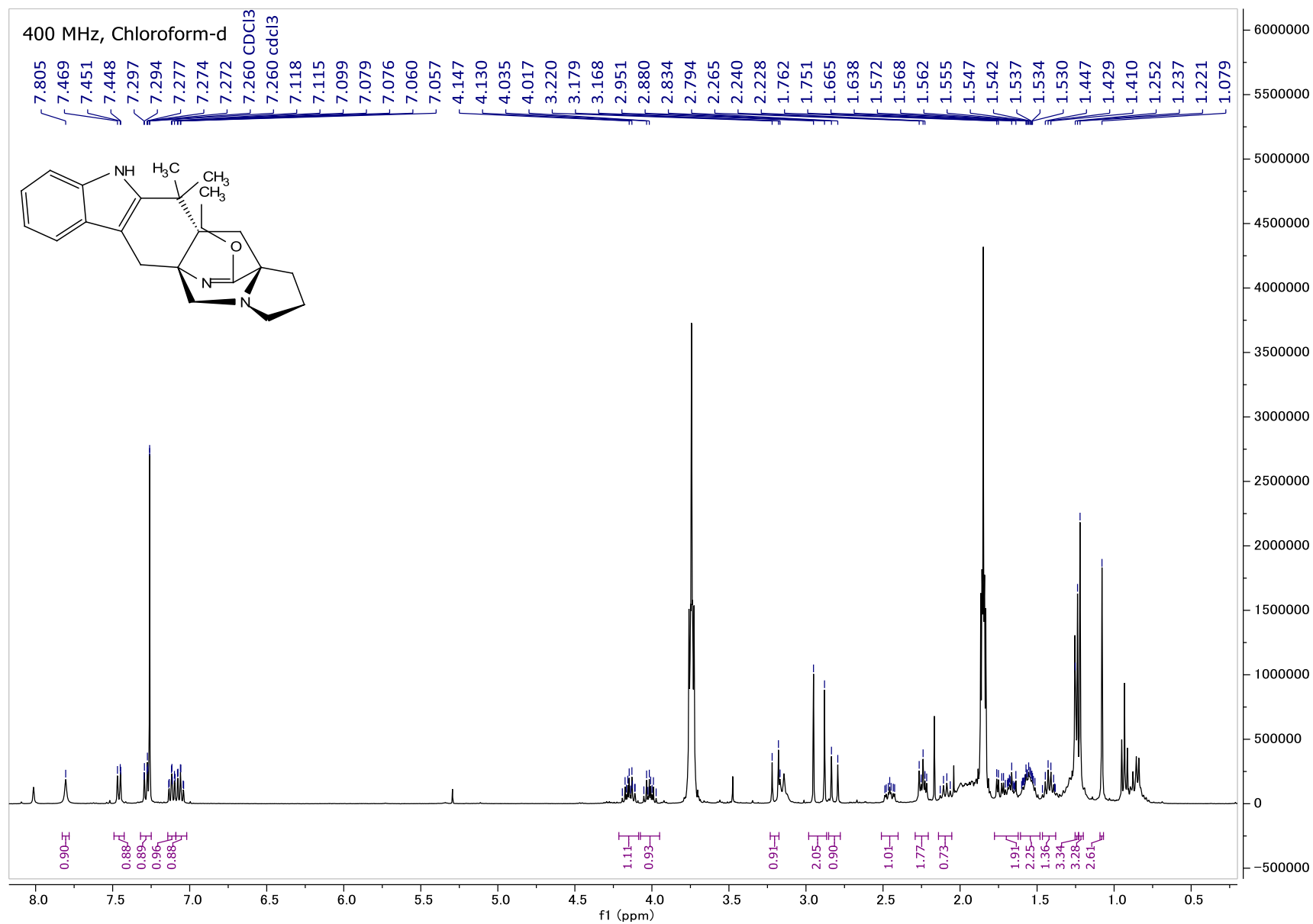


Figure A116:  $^1\text{H}$  NMR spectrum of S3.

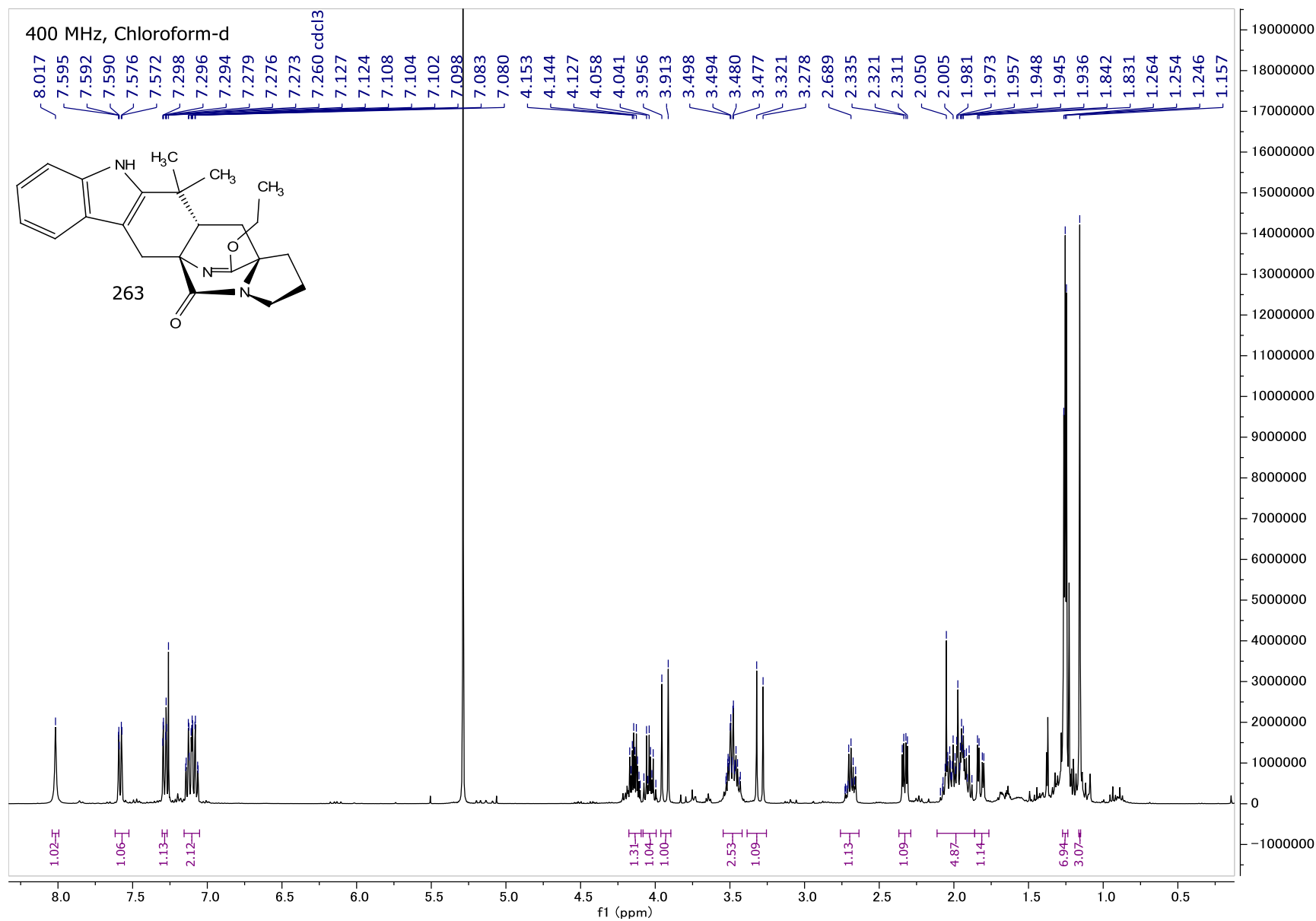


Figure A117:  $^1\text{H}$  NMR spectrum of **263**.

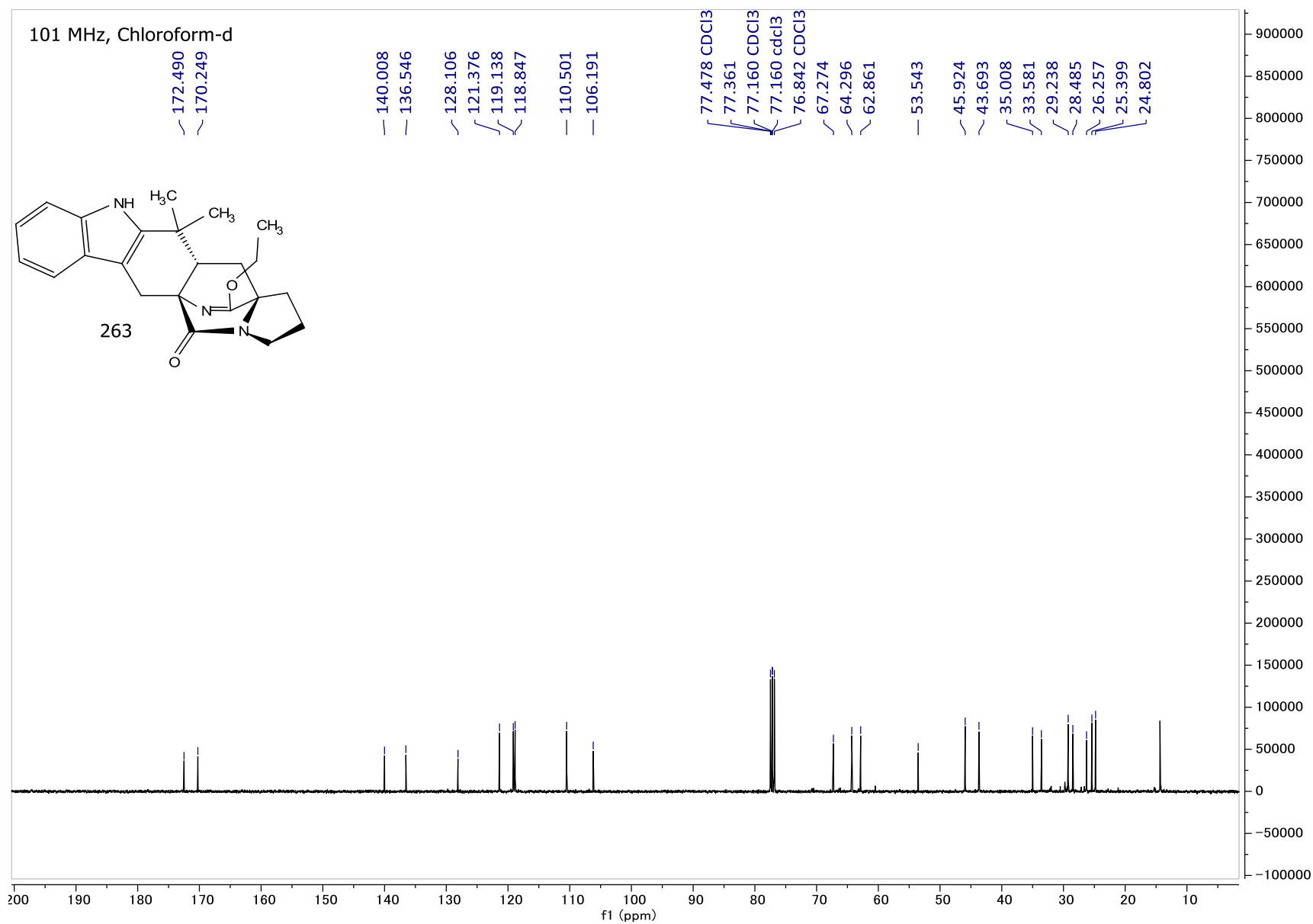
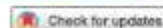


Figure A118: <sup>13</sup>C NMR spectrum of **263**.

## Appendix IV: Publications



# Fungal-derived brevianamide assembly by a stereoselective semipinacolase

Ying Ye<sup>1,2</sup>, Lei Du<sup>2,3,12</sup>, Xingwang Zhang<sup>2,4</sup>, Sean A. Newmister<sup>5</sup>, Morgan McCauley<sup>5</sup>, Juan V. Alegre-Requena<sup>5</sup>, Wei Zhang<sup>2</sup>, Shuai Mu<sup>6</sup>, Atsushi Minami<sup>7</sup>, Amy E. Fraley<sup>1</sup>, Maria L. Adrover-Castellano<sup>1</sup>, Nolan A. Carney<sup>1</sup>, Vikram V. Shende<sup>8</sup>, Feifei Qi<sup>2</sup>, Hideaki Oikawa<sup>7</sup>, Hikaru Kato<sup>8</sup>, Sachiko Tsukamoto<sup>8</sup>, Robert S. Paton<sup>5,9</sup>, Robert M. Williams<sup>5,10</sup>, David H. Sherman<sup>1,11</sup> and Shengying Li<sup>2,3,4</sup>

Fungal bicyclo[2.2.2]diazaoctane indole alkaloids represent an important family of natural products with a wide spectrum of biological activities. Although biomimetic total syntheses of representative compounds have been reported, the details of their biogenesis, especially the mechanisms for the assembly of diastereomerically distinct and enantiomerically antipodal metabolites, have remained largely uncharacterized. Brevianamide A represents a basic form of the subfamily bearing a dioxopiperazine core and a rare 3-spiro- $\psi$ -Indoxyl skeleton. In this study, we have identified the brevianamide A biosynthetic gene cluster from *Penicillium brevicompactum* NRRL 864 and elucidated the metabolic pathway. BvnE was revealed to be an essential isomerase/semipinacolase that specifies the selective production of the natural product. Structural elucidation, molecular modelling and mutational analysis of BvnE as well as quantum chemical calculations have provided mechanistic insights into the diastereoselective formation of the 3-spiro- $\psi$ -Indoxyl moiety in brevianamide A. This occurs through a BvnE-controlled semipinacol rearrangement and a subsequent spontaneous intramolecular [4+2] hetero-Diels-Alder cycloaddition.

Fungal indole alkaloids bearing the unusual bicyclo[2.2.2]diazaoctane core have drawn considerable attention from natural product, synthetic and biological chemists for decades. A wealth of studies on the discovery of analogues (including semi-synthetic, synthetic and natural) and their biological activities and biosynthetic mechanisms have been conducted<sup>1</sup>. The prominent representatives of this structural family have been recognized by our laboratories and others as belonging to two main biogenetic subfamilies (Extended Data Fig. 1). The first subfamily, the dioxopiperazines, includes the insecticidal brevianamides A and B (BA and BB) from *Penicillium brevicompactum*<sup>2</sup>, the anticancer agents (-)-notoamide A, isolated from *Aspergillus protuberus* (formerly *Aspergillus* sp. MF297-2), and (+)-notoamide A, from *Aspergillus amoensis* (formerly *Aspergillus versicolor* NRRL 35600), the anticancer agents stephacidins A and B from *Aspergillus ochraceus*, the sclerotiamides, versicolamides, taichunamides, antifungal waikalooids, amoenamide B, speramides and asperochramides. The second subfamily are the monooxopiperazines, which include the antiparasitic paraherquamides from *Penicillium* spp., the asperparalines, marcfortines, calmodulin-inhibiting malbrancheamides, chrysoenamides, mangrovamides, penioxalamine, penicimutamides and aspersiamides<sup>3,4</sup>.

The bicyclo[2.2.2]diazaoctane core structure has long been proposed to arise from an intramolecular [4+2] hetero-Diels-Alder

(IMDA) construction<sup>5–10</sup>. In our continuing pursuit of biocatalysts responsible for the [4+2] cycloaddition reaction that is essential for the assembly of diverse diastereomerically distinct and enantiomerically antipodal metabolites, we realized that dioxopiperazines and monooxopiperazines have distinct biosynthetic strategies for building their respective bicyclo[2.2.2]diazaoctane scaffold (Fig. 1a). For instance, we recently revealed that the bifunctional NADPH-dependent reductase/Diels-Alderase MalC (and PhqE) catalyses diastereo- and enantioselective IMDA cyclization via a zwitterionic intermediate for the assembly of the monooxopiperazines malbrancheamides (and paraherquamides)<sup>11</sup>. However, the biosynthetic gene clusters for dioxopiperazines such as notoamides lack a MalC/PhqE homologue (Extended Data Fig. 2), indicating alternative yet uncharacterized mechanisms for the generation of their bicyclo[2.2.2]diazaoctane system.

BA and BB are among the original natural alkaloids isolated that comprise the bicyclo[2.2.2]diazaoctane core (Fig. 1a)<sup>2</sup>. After we established the correct absolute configuration of natural (+)-BB through total synthesis<sup>12,13</sup>, it became evident that the biogenesis of BA and BB must accommodate the assembly of the core pseudo-enantiomeric tricyclic ring systems. Based on the pioneering proposal first suggested by Porter and Sammes in 1970 (ref. 14), several hypotheses for their biogenesis were proposed to accommodate the stereochemistry, presumably installed by a [4+2]

<sup>1</sup>Life Sciences Institute, University of Michigan, Ann Arbor, MI, USA. <sup>2</sup>State Key Laboratory of Microbial Technology, Shandong University, Qingdao, China. <sup>3</sup>Shandong Provincial Key Laboratory of Synthetic Biology, CAS Key Laboratory of Biofuels, Qingdao Institute of Bioenergy and Bioprocess Technology, Chinese Academy of Sciences, Qingdao, China. <sup>4</sup>Laboratory for Marine Biology and Biotechnology, Qingdao National Laboratory for Marine Science and Technology, Qingdao, China. <sup>5</sup>Department of Chemistry, Colorado State University, Fort Collins, CO, USA. <sup>6</sup>Tianjin Institute of Pharmaceutical Research, Tianjin, China. <sup>7</sup>Department of Chemistry, Faculty of Science, Hokkaido University, Sapporo, Japan. <sup>8</sup>Graduate School of Pharmaceutical Sciences, Kumamoto University, Kumamoto, Japan. <sup>9</sup>Chemical Research Laboratory, University of Oxford, Oxford, UK. <sup>10</sup>University of Colorado Cancer Center, Aurora, CO, USA. <sup>11</sup>Departments of Medicinal Chemistry, Chemistry and Microbiology & Immunology, University of Michigan, Ann Arbor, MI, USA. <sup>12</sup>These authors contributed equally: Ying Ye, Lei Du. <sup>13</sup>✉e-mail: robert.williams@colostate.edu; davidhs@umich.edu; lishengying@sdu.edu.cn

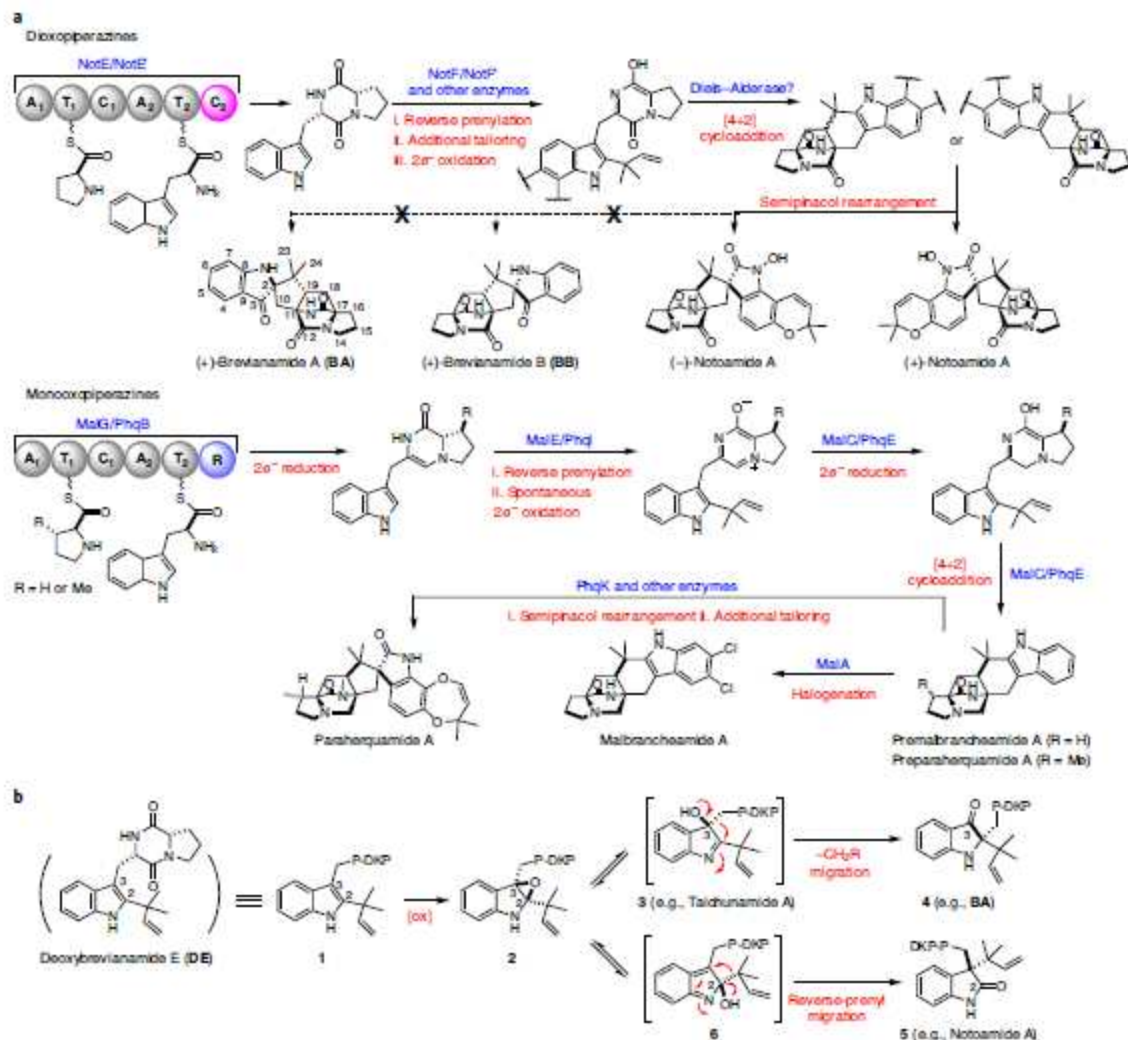


**Fig. 1** | Present knowledge on bicyclo[2.2.2]diazaoctane assembly and semipinacol rearrangements of indole 2,3-epoxide systems. **a**, Distinct biosynthetic strategies for the assembly of the bicyclo[2.2.2]diazaoctane core structure in dioxopiperazines and monooxopiperazines. **b**, Disparate fates of the indole 2,3-epoxide (**2**) and semipinacol rearrangements leading to a stable 3-hydroxyindolenine (**3**), an indoxyl (**4**) and an oxindole (**5**). P-DKP refers to the prolyl-dioxopiperazine moiety of **DE**. Diketopiperazine and dioxopiperazine are synonymous terms.

IMDA cycloaddition, and the unique 3-spiro- $\psi$ -indoxyl moiety. Specifically (Fig. 1b and Extended Data Fig. 3), a highly modified, reverse-prenylated indole (**1**, for example, deoxybrevianamide E (**DE**)) undergoes an apparent indole 2,3-epoxidation either before or after the IMDA cyclization. Ring-opening of epoxide **2** can form the 3-hydroxyindolenine (**3**), which in some instances is stable (for example, taichunamide A; ref. <sup>13</sup>) or suffers a spontaneous semipinacol rearrangement to ultimately generate a 3-spiro- $\psi$ -indoxyl (via intermediate **4**, for example, **BA**), or a spiro-2-oxindole (via intermediate **5**, for example, notoamide A; ref. <sup>14</sup>) via an alternative ring-opening intermediate **6** (refs. <sup>1,34</sup>).

Although spiro-2-oxindoles are frequently observed in the prenylated indole alkaloid family, only a small number of 3-spiro- $\psi$ -indoxyl species have been isolated so far, and very rarely are natural spiro-2-oxindoles and 3-spiro- $\psi$ -indoxyls co-produced

by a single microbe<sup>17,18</sup>. These co-metabolite profiles suggest that the semipinacol rearrangement might be differentially controlled in the partitioning of the putative indole 2,3-epoxides and implies a specific biocatalyst-controlled mechanism. Recently, the chemical synthesis of **BA**, a structure that contains both the dioxopiperazine and 3-spiro- $\psi$ -indoxyl moieties, was accomplished and suggested a Diels–Alderase-free biosynthesis<sup>19</sup>. However, the biocatalytic details and sequential timing for the putative indole oxidation, semipinacol rearrangement and IMDA cycloaddition (Extended Data Fig. 3) remain unresolved experimentally due to the lack of access to the key enzymes.

In this study, we have addressed these outstanding biosynthetic questions by elucidating the **BA** biosynthetic pathway through gene disruption, heterologous expression, precursor incorporation experiments and in vitro biochemical analysis. In particular, an

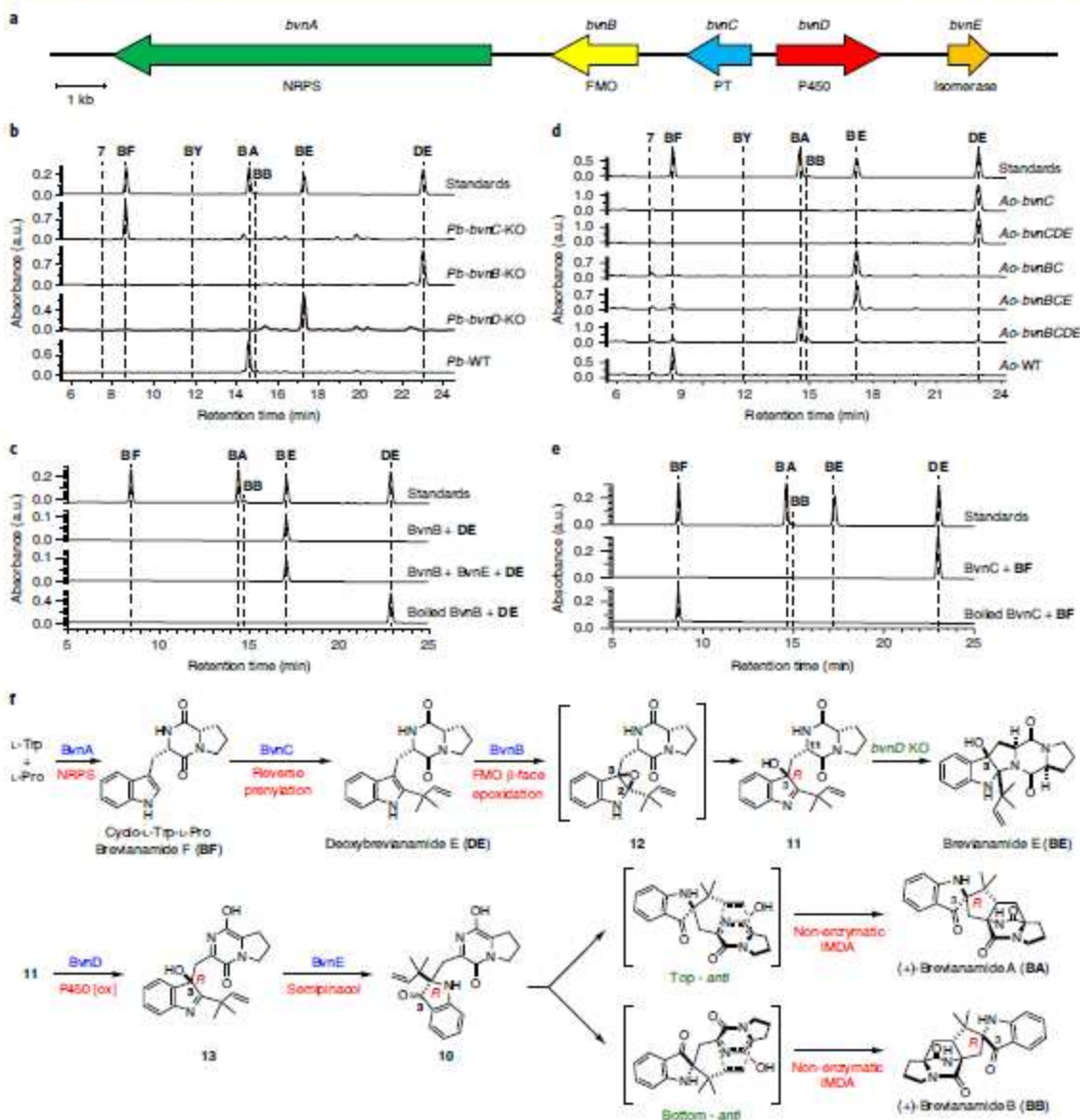


**Fig. 2 | Functional analysis of brevipanamide A biosynthetic genes and the proposed biosynthetic pathway. a**, Brevianamide A biosynthetic gene cluster (*bvn*) from *P. brevicompactum* NRRL 864. **b**, HPLC analysis (230 nm) of *Pb* KO mutants. **c**, HPLC analysis (230 nm) of the *in vitro* assays of *BvnB* and *BvnE*. **d**, HPLC analysis (230 nm) of the brevipanamide F (BF) feeding experiments with recombinant *A. oryzae* NSAR1 (Ao) strains expressing different *bvn* gene(s). **e**, HPLC analysis (230 nm) of *in vitro* assays using *BvnC*. **f**, Revised biosynthetic pathway for BA and BB.

isomerase/semipinacolase *BvnE* was revealed to catalyse an essential semipinacol rearrangement, thereby directing the diastereoselective assembly of BA by a spontaneous [4+2] IMDA cycloaddition reaction. Resolution of this 50-year-old mechanistic mystery together with our recent characterization of the Diels–Alderase-mediated biogenesis of monooxopiperazines<sup>11</sup> highlight the diversified biosynthetic strategies deployed by fungi for creating structurally diverse spiro-cyclized indole alkaloids.

## Results and discussion

**Identification of the brevipanamide A biosynthetic gene cluster.** Initially, genome mining of BA-producing strain *P. brevicompactum* NRRL 864 (*Pb*) was conducted using the notoamide non-ribosomal peptide synthetase (NRPS) gene *notE* as a probe to search for its homologue responsible for assembling the cyclodipeptide brevipanamide F (BF)<sup>1</sup>. A putative 16-kilobase (kb) BA biosynthetic gene cluster (*bvn*, GenBank accession number: MN401751) was revealed

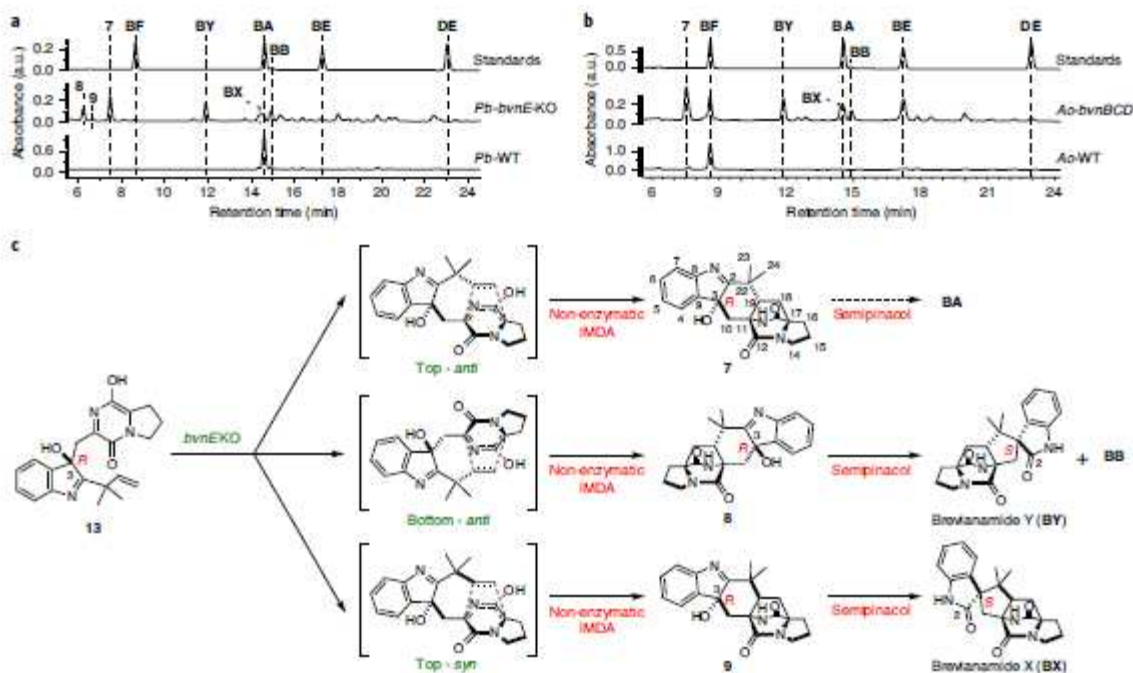


**Fig. 3 | Functional analyses of *bvnE*.** **a**, HPLC analysis (230 nm) of the *Pb-bvnE-KO* mutant. **b**, HPLC analysis (230 nm) of the **BF** feeding experiment of the *Ao-bvnB-CD* mutant. **c**, The putative spontaneous transformations in the absence of *BvnE*.

(Fig. 2a) that contains *bvnA* (NRPS), *bvnB* (flavin monooxygenase, FMO), *bvnC* (prenyltransferase, PT) and *bvnD* (cytochrome P450 monooxygenase, P450), all of which have homologues in the (+)-/(-)-notoamide A biosynthetic gene clusters<sup>1</sup>. The *bvnE* gene (465 bp) that encodes a putative isomerase shows low homology to *Trt14*, *Aush* and *PrhC* involved in meroterpenoid biosynthetic pathways<sup>20</sup>. Interestingly, the biosynthetic gene clusters of the spiro-2-oxindole-containing notoamides and paraherquamide<sup>2</sup> lack a *bvnE* homologue (Extended Data Fig. 2), and further mining of these corresponding genomes failed to identify homologous genes. Thus, we surmised that *BvnE* might play an important role in 3-spiro- $\psi$ -indoxyl formation.

**Functional analysis of brevianamide A biosynthetic genes.** In the *bvn* gene cluster, the bimodular NRPS encoded by *bvnA* is predicted to catalyse **BF** formation. This was confirmed by its heterologous expression in *Aspergillus oryzae* NSAR1 (*Ao*; Supplementary Fig. 1). To investigate the functions of *bvnB–E*, four individual single gene knockout (KO) strains of *Pb* were constructed. The resulting *Pb-bvnC-KO* strain accumulated **BF** (Fig. 2b) as the only product. The *Pb-bvnB-KO* and *Pb-bvnD-KO* strains accumulated **DE** and brevianamide E (**BE**; Fig. 2b), respectively. **BE** is proposed to be a rearranged shunt product resulting from the initial 2,3-indole epoxidation of **DE** by *BvnB* FMO (Fig. 2f). Indeed, the recombinant *N*-hexahistidine-tagged *BvnB* efficiently converted **DE** into **BE** in vitro (Fig. 2c), likely through a mechanism previously demonstrated for *NotB* (a *BvnB* homologue with 62%/75% identity/similarity) in notoamide biosynthesis<sup>21</sup>. Because *Pb-bvnD-KO* did not produce a bicyclo[2.2.2]diazooctane structure, we reasoned that *BvnD* is a key enzyme for the proposed IMDA reactions.

When *bvnE* was deleted from *Pb*, five detectable substances were observed in addition to low levels of **BA** (Supplementary Table 1 and

Supplementary Figs. 2 and 3) and **BB** (Fig. 3a), all showing the same molecular weight of 365 Da (Supplementary Fig. 4). These include three previously unknown 3-hydroxyindolenine derivatives 7–9 and the two reported spiro-2-oxindoles brevianamide X (**BX**) and brevianamide Y (**BY**). The planar structure of 7 was constructed on the basis of one- and two-dimensional NMR analyses (Supplementary Table 2 and Supplementary Figs. 5–10): the key heteronuclear multiple bond correlations (HMBCs) of C23/24-H<sub>2</sub> to C2/19/22, C10-H<sub>2</sub> to C2/3/11/19 and H4 to C3 (Supplementary Fig. 9) readily pointed to the hexatomic ring neighbouring the indole base, the C2=N double bond was deduced from the chemical shift of C2 (189.29 ppm) and the  $\alpha$ -configuration of 3-OH was determined from a nuclear Overhauser effect spectroscopy (NOESY) analysis (Supplementary Fig. 10). The absolute configuration of 7 was determined by comparison of the experimental and computational electronic circular dichroism (ECD) spectra (Extended Data Fig. 4). The structures of **BX** and **BY** were determined by high-resolution mass spectrometry (Supplementary Fig. 4), NMR analyses (Supplementary Table 1 and Supplementary Figs. 11–22) and comparison with the corresponding synthesized authentic standards (see Supplementary Methods). Their absolute configurations were established by single-crystal X-ray diffraction analysis (CCDC nos. 1973959 (**BX**) and 1973957 (**BY**); Extended Data Fig. 4 and Supplementary Table 3). The ratio of **BA**/**BB**/**7**/**BX**/**BY** was determined to be 1:1:7:5:9 (Supplementary Table 4). The instability of 8 and 9 prevented direct structural determination of these isomers. Nonetheless, the observations that 8 quickly collapsed to **BY** and **BB** and 9 collapsed to **BX** (Supplementary Fig. 23), as well as their similar UV spectra to that of 7, suggested the structures of these two unstable metabolites were 3-hydroxyindolenines (Fig. 3c and Supplementary Fig. 24). To determine the structures of 8 and 9, we chemically synthesized their hypothetical structures (see Supplementary Methods and

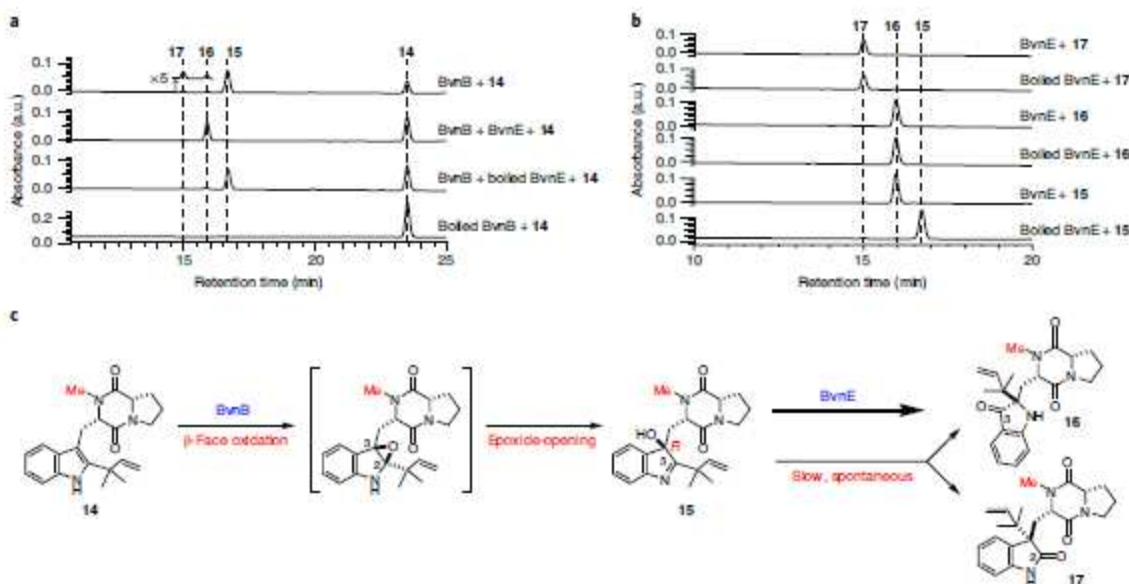


**Fig. 4 | Probing the functionality of BvnE using substrate mimics. a**, HPLC analysis (230 nm) of the in vitro assays of BvnB and BvnE. **b**, HPLC analysis (230 nm) of the in vitro assays of BvnE with the *N*-methylated substrates. **c**, The reaction scheme.

Supplementary Figs. 25–28). The matching UV spectra and HPLC retention times, as well as the same decomposition behaviour of the synthetic standards as the isolated samples (Supplementary Fig. 29), confirmed their structures.

To validate the function of *bvn* genes and also to clarify the order of biosynthetic steps, we conducted heterologous expression with different gene combinations in *Ao*. As expected, BF was converted into DE by either *Ao-bvnC* in vivo (Fig. 2d) or purified BvnC in vitro in the presence of dimethylallyl pyrophosphate (DMAPP) and  $Mg^{2+}$  (Fig. 2e). Thus, PT BvnC is a deoxybrevianamide E synthase, as previously demonstrated for NotF<sup>22</sup>. *Ao-bvnCDE* produced DE exclusively in the feeding experiment, whereas *Ao-bvnBC* and *Ao-bvnBCE* both accumulated BE exclusively (Fig. 2d). These results indicate that the presumed indole epoxidation catalysed by BvnB FMO occurs prior to the P450 BvnD-mediated step and preceding the BvnE-catalysed step. Upon the introduction of BF to the *Ao-bvnBCD* culture, five products with identical  $m/z = 366$  ( $[M+H]^+$ ) were observed (Fig. 3b and Supplementary Fig. 4). Their relative abundance (BA/BB/7/BX/BY = 1:1.5:2:6) was qualitatively consistent with the observations for *Pb-bvnE-KO* (Fig. 3a and Supplementary Table 4) except that derivatives 8 and 9 were not detected, probably due to their instability. Finally, when *bvnE* was incorporated and the *Ao-bvnBCDE* strain grown in the presence of exogenous BF, we observed BA and BB in a ratio of ~10:1 (Fig. 2d and Supplementary Table 4), which is consistent with the product profile of wild-type *Pb* (*Pb*-WT; Fig. 2b).

These results demonstrated that the metabolites generated through *Ao* biotransformations and individual *Pb* knockout mutants correlated directly with one another. The reaction sequence of each enzyme in the pathway can now be deduced as BvnA → BvnC → BvnB → BvnD → BvnE (Fig. 2f). Both systems showed a BvnE-dependent change of product profile, suggesting that BvnE might function to mediate the formation of the 3-oxo species 10, and directly impact the diastereo-outcome of the presumed IMDA reactions. With respect to BvnD activity, intensive attempts to produce this P450 enzyme in *Escherichia coli* and

*Saccharomyces cerevisiae* were unsuccessful, thus preventing direct functional analysis. Nonetheless, the results showing that *Ao-bvnBCD* transformed BF into multiple IMDA products (Fig. 3b) and that *Ao-bvnCDE* was unable to recognize DE as a substrate (Fig. 2d), along with the principles for P450 enzymes and Diels–Alder reactions, together suggest that BvnD might oxidize non-isolable intermediate 11 (derived from ring-opening of the indole epoxide 12) to 13, thereby generating the diene moiety required for IMDA cyclization (Fig. 2f). In the absence of BvnD, compound 11 would collapse to BE through an energetically favoured N–C ring closure (Supplementary Fig. 30).

Although we cannot exclude the possibility that BvnD might directly desaturate the N–C bond in the dioxopiperazine ring of 11 (ref. 23), it is more likely that BvnD first catalyses the hydroxylation of 11 and then undergoes spontaneous dehydration/tautomerization to yield 13 (Fig. 2f). Regarding the position on 11 likely oxidized by BvnD, bond dissociation energy calculations (Supplementary Fig. 31) indicated that the most probable hydroxylation site is the tertiary C–H bond at C11, which is supported by the following two facts: firstly, FtmG, a BvnD homologue with 47%/64% protein sequence identity/similarity in the fumitremorgin biosynthetic pathway, has been experimentally confirmed to catalyse the hydroxylation of an analogous position<sup>27</sup> and secondly, the fungal dioxopiperazine structure asperversiamide 1 was recently discovered to contain a hydroxylated C11, which might have been installed by an unidentified BvnD homologue<sup>24</sup>.

**Probing the catalytic mechanism of the isomerase/pinacolase BvnE.** Based on the results obtained with *Pb-bvnE-KO* and *Ao-bvnBCD* (Fig. 3), BvnE appears to be a central enzyme for controlling the product profile in brevianamide biogenesis. To assess this unique isomerase in vitro, the *N*-hexahistidine-tagged BvnE was produced in *E. coli* BL21(DE3) and purified to homogeneity (Supplementary Fig. 32). Next, we sought to identify the potential natural substrate of BvnE from *Pb-bvnE-KO*. Compounds 7–9, BX, BY and BE were tested as substrates, but failed to be transformed (Supplementary

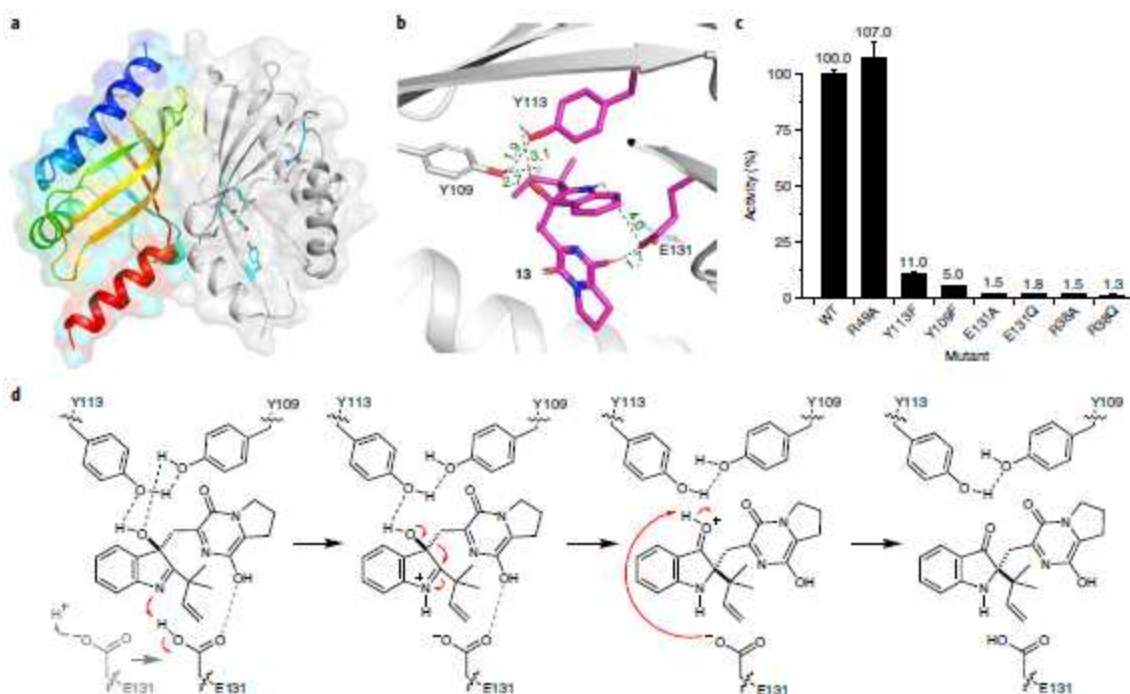


**Fig. 5 | BvnE crystal structure, docking and the proposed catalytic mechanism.** **a**, Structural overview of BvnE: the left chain shows in rainbow colours the N terminus (blue) to the C terminus (red), and the right chain in grey cartoon representation shows putative catalytic acid/basic residues (cyan) and water molecules in the active site (red spheres). **b**, The docked BvnE-**13** complex with the key residues, and hydrogen bonding distances shown in Å. **c**, Site-directed mutagenesis results. The data represent the average of independent experiments performed in triplicate (central values represent means, error bars represent standard deviations and  $n=3$ ). **d**, The proposed reaction mechanism for the isomerization of **13** catalysed by BvnE. Glu131-mediated proton transfer could be assisted by Arg38, which interacts with Glu131 through an ordered water network (Extended Data Fig. 6c). Indirect deprotonation of the oxonium intermediate via bound solvent molecules rather than a direct interaction with Glu131 cannot be excluded.

Figs. 33 and 34). Thus, we hypothesized that **13** might be the native substrate of BvnE. Considering the inaccessibility of this unstable intermediate, we elected to chemoenzymatically synthesize **15** (see Supplementary Methods), a stable analogue of **13** (Fig. 4c), to block the dioxipiperazine nitrogen from N-C ring closure and prevent the formation of the unstable azadiene intermediate upon spontaneous dehydration. The mechanistic probe **15** was prepared through BvnB-catalysed *in vitro* conversion of the chemically synthesized *N*-methyl-deoxybrevianamide **E** (**14**; Supplementary Figs. 35–43), and the absolute configuration of **15** was determined by single-crystal X-ray diffraction analysis (CCDC no. 1973958; Extended Data Fig. 4). Interestingly, two minor products, **16** and **17**, were also generated from **14** along with the predominant product **15** (Fig. 4a). Structural determination indicated that **16** and **17** are 3-oxo and 2-oxo isomers of **15**, respectively (Supplementary Table 5 and Supplementary Figs. 35 and 44–55). Their absolute configurations were determined by comparison of their experimental and calculated ECD spectra (Extended Data Fig. 4), which were consistent with the structures arising from the semipinacol rearrangement of **15**. Moreover, when **15** was incubated with BvnE, it was completely converted into **16** (Fig. 4b). These results indicate that BvnE functions as a semipinacolase responsible for the selective formation of the 3-spiro- $\psi$ -indoxyl substructure (in **16**) from the 3-hydroxypyrrrole moiety (in **15**). The spontaneous conversion of **15** into **16** and **17** at room temperature could also occur slowly (Fig. 4c and Supplementary Fig. 56). Loss of stereocontrol of the IMDA cycloaddition reaction in terms of top/bottom (7/9/BA/BX

vs 8/BY/BB) and *anti/syn* selectivity (7/8/BA/BB/BY vs 9/BX) in the absence of BvnE strongly suggests that these isomers are generated from non-enzymatic IMDA reactions. Moreover, the observed product profile (Fig. 3 and Supplementary Table 6) is quantitatively consistent with the calculated product distribution (see below). With respect to the catalytic properties of BvnE (Extended Data Fig. 5), the apparent  $k_{cat}$  and  $K_m$  values of BvnE towards **15** were determined to be  $0.013 \text{ min}^{-1}$  and  $822 \mu\text{M}$ , respectively, under the optimal pH (6.5) and temperature ( $30^\circ\text{C}$ ). The low catalytic efficiency ( $k_{cat}/K_m = 1.58 \times 10^{-5} \text{ min}^{-1} \mu\text{M}^{-1}$ ) is probably because **15** is not the native substrate.

As a key component in controlling product outcome in brevianamide biosynthesis, we sought to determine how BvnE catalyses the formation of the 3-spiro- $\psi$ -indoxyl species. BvnE is related to the NTF2-like superfamily enzymes that have been studied in fungal meroterpenoid biogenesis<sup>20</sup>. We solved the crystal structure of BvnE at 1.8 Å resolution (Fig. 5a and Supplementary Table 7; Protein Data Bank (PDB) ID: 6U9I) by molecular replacement using PrhC (PDB ID: 5X9J) as search model<sup>21</sup> (Supplementary Fig. 57). BvnE is a symmetric homodimer that adopts an  $\alpha$ - $\beta$ -barrel fold with the presumed active sites at the end of each barrel. This cavity has a hydrophobic interior and also contains several polar residues that could be involved in the acid/base chemistry reported for this family of enzymes (Fig. 5a and Supplementary Fig. 58).

Docking of the presumed native substrate **13** (Fig. 5b and Extended Data Fig. 6a) helped to reveal the BvnE active site.

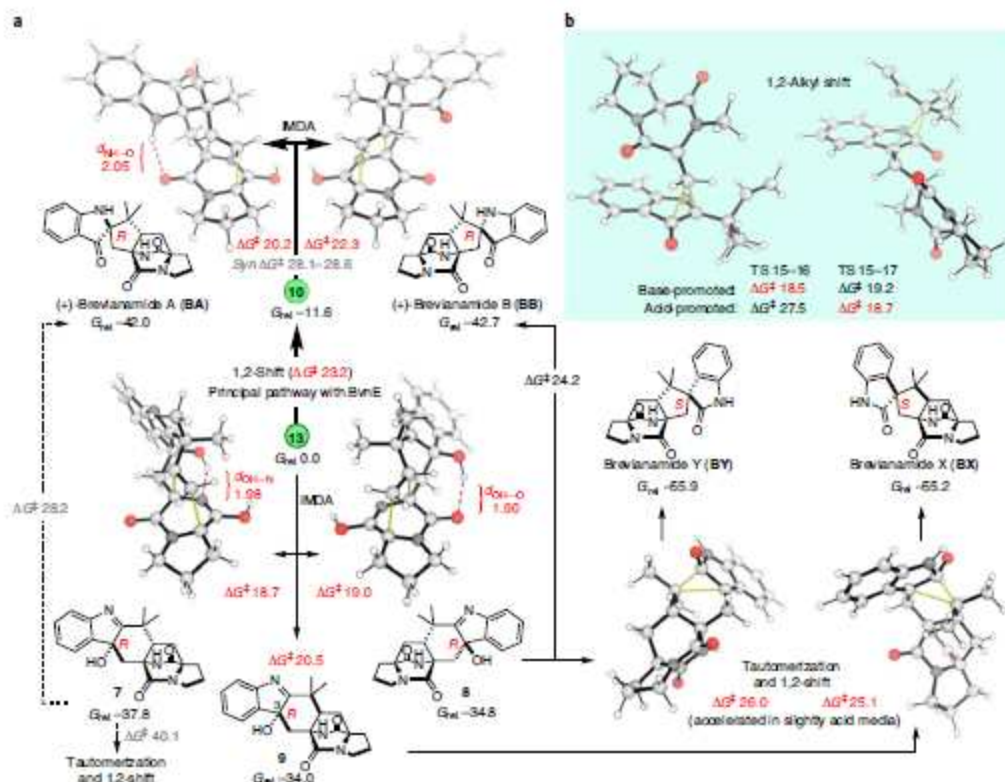


**Fig. 6 | Results of the quantum chemical calculations.** **a** The *anti*-selective IMDA transition-state structures and products accessible from Intermediates **13** and **10**. **b** The 1,2-alkyl shift (semipinacol) transition-state structures for the migration of  $\text{CH}_2$ -dioxopiperazine (left) and reverse-phenyl (right) groups. The computed Gibbs energies are given in  $\text{kcal mol}^{-1}$  and the highlighted distances in Å. Normal lines represent the major pathways obtained under *Pb-bvnE-KO* conditions. Pathways in bold correspond to the major reaction obtained when using *BvnE* (switch in reactivity). Dashed lines represent pathways with prohibitively high activation energies under the reaction conditions.

We identified Arg38, Tyr109, Tyr113 and Glu131 as candidates for site-directed mutagenesis and *in vitro* enzyme assays with **15**. In each case, mutation of these residues caused severely attenuated activity (Fig. 5c). All the CD spectra of the *BvnE* mutants matched the wild-type protein (Extended Data Fig. 6b), indicating that these point mutations did not significantly impact protein folding. The electron density data indicate that Arg38, Tyr113 and Glu131 adopt multiple conformations in the *BvnE* crystal lattice. Therefore, these residues were designated as flexible in molecular docking (Extended Data Fig. 6c). In the lowest-energy output of the *BvnE*-**13** docking complex, the reverse-phenyl group of the substrate is packed into a hydrophobic pocket (Extended Data Fig. 6a), and Tyr109 and Tyr113 interact with the 3-OH of **13** (Fig. 5b). Glu131 is positioned to interact with the indole nitrogen and the C18 oxygen of **13**, suggesting its key role in the semipinacol rearrangement (Fig. 5d). On the basis of these docking studies, we propose that the reaction mechanism involving *BvnE* includes Glu131-mediated proton transfer to initiate the semipinacol rearrangement and provide charge stabilization of the intermediate, and hydrogen-bond-assisted activation of the semipinacol rearrangement through Tyr109/Tyr113 (Fig. 5d). Arg38, which is essential for activity, does not directly interact with the docked ligands or active site residues. However, the structure reveals two ordered water molecules in a hydrogen-bonding network between Arg38 and Glu131 (Extended Data Fig. 6c),

suggesting that it may assist in proton transfer by regenerating the carboxylate form of E131.

**Quantum chemical calculations.** Next, we used density functional theory and coupled cluster theory calculations (SMD-DLPNO-CCSD(T)/cc-pV(DT)Z//M06-2X-D3/6-31+G(d,p); see Supplementary Methods) to evaluate the intermediate and transition-state (TS) structures in the revised brevianamide biosynthetic pathway (Figs. 2f and 3c), and to explore the innate regio- and stereochemical preferences associated with the key steps (Fig. 6a). Accordingly, under *Pb-bvnE-KO* conditions, the IMDA reactions that transform **13** into **7–9** are favoured. In the calculated mechanism, only two diastereomers of **7** (**8** and **9**) undergo a subsequent 1,2-alkyl shift to irreversibly generate **BY** and **BB** (from **8**) and **BX** (from **9**). Before the shifts that lead to the formation of the ring system, an initial tautomerization that switches the position of the OH group between C3 and C2 proceeds quickly (Supplementary Fig. 59). The reason **7** fails to undergo subsequent transformation is likely due to the high energy required for the tautomerization process ( $35.5 \text{ kcal mol}^{-1}$  between **7** and its tautomer; Supplementary Fig. 60). In the computed kinetic profile, the initial irreversible IMDA (from **13** to **7–9**) and  $\text{CH}_2$ -dioxopiperazine shift (from **13** to **10**) determine the selectivity of the process and their activation barriers are consistent with room-temperature reactivity

over the course of minutes and hours. Considering that **BY** and **BX** are the major products obtained from **8** and **9**, respectively, the calculated results agree qualitatively with the experimental results: the two most favourable products are **7** and **BY**, followed by **BX**, with **BA** and **BB** being minor products (experimental ratio **BY/7/BX/BA/BB** = 9:7:5:1:1; Supplementary Table 4).

The semipinacol rearrangement to form 3-spiro- $\psi$ -indoxyl **10** is favourably exergonic and irreversible ( $\Delta G = -11.6 \text{ kcal mol}^{-1}$ ). Competition between the two possible non-enzymatic semipinacol rearrangements ( $\text{CH}_2$ -dioxopiperazine vs reverse-prenyl shifts) was found computationally to depend strongly on whether the reaction undergoes basic activation of the hydroxy group or acidic activation of the imine group (Fig. 6b): whereas general/specific acidic activation of the nitrogen results in a buildup of positive charge in the migrating group in the TS, favouring 1,2-prenyl migration ( $\Delta \Delta G^\ddagger = 8.8 \text{ kcal mol}^{-1}$ ), basic activation of the hydroxy group has the opposite effect, inverting the selectivity to favour migration of the dioxopiperazine-containing group ( $\Delta \Delta G^\ddagger = 0.7 \text{ kcal mol}^{-1}$ ). The contrast between the regioselective biocatalytic conversion of **13** into **10** and the spontaneous conversion of **15** into **16/17** under acid/base conditions corroborates the involvement of the hydrogen-bond acceptors Tyr113 or Tyr109 as a likely candidate for the activation of the 3-hydroxy group by BvnE (Fig. 5d and Supplementary Fig. 61) during this key step.

Next, we investigated the distinct IMDA cyclization reactions from **10** and **13** (Fig. 6a). In each case, there are four possible stereochemical outcomes. The selectivity for *anti* over *syn* cycloadducts is controlled by the balance between stabilizing intramolecular hydrogen bonds and unfavourable steric interactions (Supplementary Fig. 62). Whereas the *syn* pathways from **10** are highly disfavoured relative to the *anti* pathways, those from **13** form C–H...O interactions<sup>26,27</sup>, making them more competitive (Supplementary Fig. 63). In this regard, the levels of IMDA diastereoselectivity of **10** are exceptional, displaying high selectivity for the formation of **BA** (20.2 kcal mol<sup>-1</sup>) over the pseudo-enantiomeric bicyclo[2.2.2] diazoctane **BB** (22.3 kcal mol<sup>-1</sup>) due to an intramolecular N–H...O hydrogen bond, with a very large ( $-6 \text{ kcal mol}^{-1}$ ) preference for the two *anti*-configured products (**BA** and **BB**) over their *syn* diastereomers (28.1–28.6 kcal mol<sup>-1</sup>) (Fig. 6a). The stereospecific conversion of **7** into **BA** through a ring contraction was found to be more challenging than the earlier 1,2-rearrangements (activation barrier of 28.2 kcal mol<sup>-1</sup>); however, this process is exergonic by 4 kcal mol<sup>-1</sup>. Accordingly, this ring contraction can be accomplished under laboratory conditions by treating **7** with sodium hydroxide in water (Fig. 3c and Supplementary Fig. 64).

## Conclusions

We have characterized and fully reconstituted the biosynthesis of **BA** and **BB** and identified a key semipinacolase, BvnE, that mediates diastereocontrol for subsequent spontaneous [4+2] cycloaddition for the biogenesis of the brevianamides. The formation of the dioxopiperazine bicyclo[2.2.2]diazoctane core construct has also been demonstrated and the computational data support a spontaneous [4+2] pericyclic reaction. Resolution of this mechanistic mystery together with our recent characterization of the Diels–Alderase-mediated biogenesis of monooxopiperazines<sup>1</sup> highlight the diversified biosynthetic strategies deployed by fungi for creating structurally diverse spiro-cyclized indole alkaloids. However, several important mechanistic questions remain, including what are the mechanistic details of the BvnD-catalysed two-electron oxidation required for azadiene formation to enable the IMDA reaction, and what, if any, biogenetic relationships exist between the brevianamides and other dioxopiperazine families comprising the bicyclo[2.2.2]diazoctane system, such as (+)/(–)-notoamide **A**, whose producer genomes lack apparent *bvnE* homologues?

**Note added in proof:** During production of this Article the total synthesis of brevianamide **A** which supports a spontaneous intramolecular [4+2] Diels–Alder construction by R. C. Godfrey et al. was published<sup>15</sup>.

## Methods

**Strains and culture conditions.** All *E. coli* strains were grown at 37 °C unless otherwise specified. The *E. coli* DH5 $\alpha$  strain was used for vector construction and plasmid isolation using Luria–Bertani (LB) agar plates or LB liquid media. The *E. coli* BL21(DE3) strain was used for protein production and purification, and cultured in Terrific Broth (TB: 1.2% tryptone, 2.4% yeast extract, 0.94% K<sub>2</sub>HPO<sub>4</sub>, 0.22% KH<sub>2</sub>PO<sub>4</sub>, 4% glycerol) media. *P. brevicompactum* NRRL 864 (*Pb*) was obtained from the Agricultural Research Service Culture Collection (NRRL) collection. *Pb* was cultured on potato dextrose agar (PDA) plates at 28 °C for 7 d before spore collection and preservation. For the fermentation of the brevianamides, solid Czapek–Dox agar (CDA) media were inoculated with the spore suspension and incubated at 28 °C for 6 d. *A. oryzae* NSAR1 (*Ao*) was a gift from Professor Oikawa's laboratory. *Ao* and its different transformants were grown on DPY (dextrin–polypeptide–yeast extract: 2% dextrin, 1% polypeptide, 0.5% yeast extract, 2% agar) agar plates at 30 °C for 7 d. For metabolite production, CMP liquid media (Czapek–Dox broth supplemented with 3% maltose and 1% peptone) were used. Upon inoculation, cultures were incubated at 28 °C for 5 d with shaking at 200 r.p.m. All the strains and vectors used in this study are listed in Supplementary Table 8.

**Protein expression and purification of BvnB, BvnC and BvnE.** For protein expression, the *E. coli* BL21(DE3) strain carrying a target gene expression plasmid was used. A single colony was picked, inoculated and cultured overnight at 37 °C in LB broth with appropriate selective antibiotics (commonly 50  $\mu\text{g ml}^{-1}$  kanamycin unless otherwise specified). The overnight seed culture was inoculated (1:100) into 11 TB medium containing 4% glycerol, selective antibiotics and 0.1% rare salt solution (0.68% FeCl<sub>3</sub>, 0.05% ZnCl<sub>2</sub>, 0.05% CoCl<sub>2</sub>, 0.05% Na<sub>2</sub>MoO<sub>4</sub>, 0.025% CuCl<sub>2</sub>, 0.047% CaSO<sub>4</sub>, 0.013% H<sub>2</sub>BO<sub>3</sub>). The culture was then incubated at 37 °C with shaking at 220 r.p.m. Protein expression was induced by adding isopropyl- $\beta$ -D-thiogalactoside (IPTG) to a final concentration of 0.2 mM, when the optical density at 600 nm (OD<sub>600</sub>) reached  $\sim 0.6$  (typically  $\sim 3$  h after inoculation). The cells were grown for an additional 20 h at 18 °C at 220 r.p.m. After collecting the cells by centrifugation (4,000g, 15 min) at 4 °C, they were frozen at  $-20$  °C for 30 min and then melted at ambient temperature. All protein purification procedures were conducted at 4 °C. Briefly, 40 ml lysis buffer (50 mM NaH<sub>2</sub>PO<sub>4</sub>, 300 mM NaCl, 10% glycerol, 5 mM imidazole, pH 7.5) was used to re-suspend the cell pellet by vortexing, and a Model 500 Sonic Dismembrator was used for ultrasonic cell lysis (5 s on, 5 s off, 1 h in total). After centrifugation at 12,000g for 30 min, the supernatant was collected, to which 1 ml nickel nitrilotriacetic acid (Ni-NTA) resin (Qtagen) was added and incubated on a shaker at 30 r.p.m. at 4 °C for 30 min. The slurry was then loaded onto an empty column. Then, 100–300 ml wash buffer (50 mM NaH<sub>2</sub>PO<sub>4</sub>, 300 mM NaCl, 10% glycerol, 10 mM imidazole, pH 7.5) was used to wash the protein-bound resin until no protein was detectable in flow-through in a Coomassie Brilliant Blue G-250 assay. Target proteins were eluted with 5 ml elution buffer (50 mM NaH<sub>2</sub>PO<sub>4</sub>, 300 mM NaCl, 10% glycerol, 250 mM imidazole, pH 7.5) and concentrated using an Amicon Ultra centrifugal filter with an appropriate molecular weight cutoff (Merck) at 5,000g for 30 min. The concentrated fraction ( $< 1$  ml) was loaded onto a PD-10 column (GE Healthcare) pre-equilibrated with 25 ml desalting buffer (50 mM NaH<sub>2</sub>PO<sub>4</sub>, 10% glycerol, pH 7.5) for buffer exchange. Aliquots of the desalted fraction (100  $\mu\text{l}$  per tube) were flash-frozen using liquid N<sub>2</sub> and stored at  $-80$  °C for later use.

**Gene knockout in *Pb*.** For targeted gene disruption in *Pb*, two specific homologous arms ( $\sim 1$  kb) were designed and amplified from *Pb* genomic DNA. Knockout vectors were constructed using common ligation or recombinase strategies, assembling the two arms respectively into the two multi-cloning sites (MCS) of the plasmid pRSF-hyg (Supplementary Fig. 65), which contains a hygromycin resistance marker for the selection of knockout mutants. The primers used in this study are listed in Supplementary Table 9. Gene knockout was performed using the *split-marker strategy*<sup>28</sup>. Briefly, two knockout cassette fragments were PCR-amplified using the primers x-up-F/hyg-R (x indicates the target gene to be knocked out) and hyg-F/x-down-R, and subsequently concentrated to  $> 200 \text{ ng } \mu\text{l}^{-1}$ . About 10  $\mu\text{l}$  of each of the two concentrated samples were mixed and transformed into *Pb* protoplasts. The protoplast preparation and poly(ethylene glycol) (PEG)-mediated transformation were performed by following the procedures developed by Heneghan et al. with some minor modifications<sup>29</sup>. Specifically, PDA and potato dextrose broth were used as solid and liquid media, respectively. The protoplasts were collected immediately after lysing by enzyme digestion. The PEG-mediated protoplast transformation was conducted on PDA plates containing 1 M sorbitol and 100  $\mu\text{g ml}^{-1}$  hygromycin as the selection antibiotic. The genotypes of the knockout mutants derived from homologous recombination were verified through PCR reaction with the appropriate primers listed in Supplementary Table 9.

**Heterologous gene expression in *Ao*.** A spore suspension of *Ao*-WT or an *Ao* mutant ( $1.0 \times 10^8$  cells) was inoculated into 100 ml DPY medium (2% dextrin, 1%

polypeptide, 0.5% yeast extract) supplemented with appropriate nutrients. After incubation for 3 d at 30°C and 200 r.p.m., mycelia were collected by filtration and washed with double-distilled H<sub>2</sub>O. Protoplasting was performed using Yatalase (Takara; 5.0 mg ml<sup>-1</sup>) in Solution 1 (0.8 M NaCl, 10 mM NaH<sub>2</sub>PO<sub>4</sub>, pH 6.0) at 30°C for 2 h. The protoplasts were centrifuged at 900g (Beckman JLA10.500) for 5 min and washed with 0.8 M sterile NaCl solution. Then, the protoplasts were adjusted to 2.0 × 10<sup>8</sup> cells ml<sup>-1</sup> by adding Solution 2 (0.8 M NaCl, 10 mM CaCl<sub>2</sub>, 10 mM Tris-HCl, pH 8.0) and Solution 3 (40% (w/v) PEG-4000, 50 mM CaCl<sub>2</sub>, 50 mM Tris-HCl, pH 8.0) in a 4:1 volume ratio. The appropriate plasmid (13 µg) was added to the protoplast solution (200 µl). The aliquot was incubated on ice for 20 min, and then Solution 3 (1 ml) was added. After 20 min incubation at room temperature, Solution 2 (10 ml) was added to the mixture and the mixture was centrifuged at 900g (Beckman JLA10.500) for 5 min. The transformation mixture was poured onto CDA plates supplemented with 0.8 M NaCl and appropriate nutrients, and then overlaid with the soft-top agar (1.2 M sorbitol, 3.5% Caspex-Dox broth, 0.6% agar). The plates were incubated at 30°C for 3–7 d until colonies showed up.

**In vitro enzyme assays.** Unless otherwise specified, all enzymatic assays were carried out in 100 µl of 50 mM Tris-HCl buffer (pH 7.5) at 30°C for 2 h. The enzyme reaction mixture contained 1 mM substrate(s) (BF and DMAPP for BvnE, DE or I4 for BvnI, 15 for BvnE or its mutants), necessary cofactors (10 mM Mg<sup>2+</sup> for BvnC, 2 mM NADPH for BvnI) and 10 µl of each purified enzyme.

**Mutagenesis of BvnE.** The mutagenesis PCR reaction was performed with 50 ng pET28b-bvnE as template, 0.2 µM primer (in our system, one primer is sufficient for successful mutagenesis), 2.5 µl 10× Pfu buffer, 0.5 µl dNTP mix (25 mM of each dNTP), 1 ml dimethyl sulfoxide and 0.5 µl PfuUltra II fusion HS DNA polymerase (Agilent) in a total volume of 25 µl. The PCR cycles were set as follows: (1) 95°C for 3 min, (2) 95°C for 30 s, (3) 53°C for 1 min and (4) 65°C for 2 min, with steps 2–4 repeated for 30 cycles. DpnI digestion was performed with 1 µl of 2 U µl<sup>-1</sup> DpnI and 25 µl PCR reaction solution for 2 h at 37°C. From the digested solution, 1 µl was used to transform 30 µl DH10β Electrocompetent Competent cells (Takara). The mutant plasmids were purified and subjected to sequencing at the University of Michigan DNA Sequencing Core.

**BvnE protein expression and purification for crystallization.** *E. coli* BL21(DE3)-pRARE2 was transformed with the plasmid (BvnE\_pET28b-MBP-T) and grown in 1 l TB medium with 50 µg ml<sup>-1</sup> kanamycin and 100 µg ml<sup>-1</sup> spectinomycin at 37°C to OD<sub>600</sub> ≈ 1. The culture was cooled to 20°C over 1 h, induced with 0.25 mM IPTG and incubated for 24 h (20°C, 225 r.p.m. shaking). The cells were collected by centrifugation (4°C, 5,000g) and stored at -20°C. All BvnE purification steps were performed at 4°C. The cell pellet was re-suspended in lysis buffer (50 mM Tris pH 7.5, 300 mM NaCl, 20 mM imidazole, 10% glycerol, 0.5 mg ml<sup>-1</sup> lysozyme, 0.05 mg ml<sup>-1</sup> DNase, 5 mM MgCl<sub>2</sub>) and lysed by sonication followed by high-speed centrifugation (4°C, 60,000g, 25 min). The lysate was filtered (0.45 µm) and loaded onto a 5-ml Ni-NTA HiTrap column of a fast protein liquid chromatograph (FPLC) and washed with 20 column volumes of Ni-NTA buffer (50 mM Tris pH 7.5, 300 mM NaCl, 20 mM imidazole, 10% glycerol) at 3 ml min<sup>-1</sup>. BvnE was eluted with elution buffer (50 mM Tris pH 7.5, 300 mM NaCl, 500 mM imidazole, 10% glycerol). The pooled fractions were incubated with His-tagged tobacco etch virus (TEV) protease in a 1:20 molar ratio to remove the His-maltose binding protein (MBP) tag. The protein was dialysed overnight against 50 mM Tris pH 7.5, 300 mM NaCl and 2 mM dithiothreitol, and passed through a Ni-NTA column to remove TEV protease and MBP. Further purification was accomplished by size-exclusion chromatography using a Superdex 75 10/300 GL column equilibrated with 50 mM Tris pH 7.5 and 300 mM NaCl. SDS-PAGE was used to assess protein homogeneity; BvnE was determined to be >95% pure. The protein was concentrated using an Amicon Ultra centrifugal concentrator (10,000 nominal molecular weight limit) to 29 mg ml<sup>-1</sup>. The concentration was determined by UV spectrophotometry using the calculated molar extinction coefficient.

**Crystallization and structure determination.** BvnE was screened for initial crystallization conditions using the Midwest Center Structural Genomics (MCSG) screen at 25 and 4°C. Single, diffraction-quality crystals of BvnE were grown by the sitting drop vapour diffusion method at 4°C by mixing 29 mg ml<sup>-1</sup> BvnE with the well solution (26% PEG3350, 0.1 M Tris pH 8.5, 4% v/v pentaerythritol ethoxylate (3/4 EO/OH)) in a 1:1 ratio. Sitting droplets were nucleated from an earlier spontaneous crystallization using a cat whisker. Then, 8 µl of cryoprotectant (12.75% glycerol, 26% PEG3350, 0.1 M Tris pH 8.5, 4% v/v pentaerythritol ethoxylate (3/4 EO/OH), 50 mM Tris pH 7.5, 300 mM NaCl) was added directly to the sitting drops, and the crystals were collected using nylon loops and verified by rapid plunging into liquid nitrogen. Diffraction data were collected at beamline 23-ID-B at the Advanced Photon Source (APS) using an X-ray wavelength of 1.033 Å (360° of data, 0.2° image width, 100 K). The data were integrated and scaled with XDS<sup>38</sup>. The structure was solved by molecular replacement using PhC (PDB ID: 5X9I) as search model (Phaser-MR)<sup>39</sup>. The final model was completed using alternate cycles of manual model building using Coot<sup>40</sup> and refinement using PHENIX.refine<sup>41</sup>. The structure was validated with MolProbity<sup>42</sup>. The data collection and refinement details are presented in Supplementary Table 7.

**Molecular docking of BvnE with compound 13.** Compound 13 was docked into the BvnE structure using the automated docking software Autodock4 (ref. 43). The conformational heterogeneity of the key active site residues Arg38, Tyr113 and Glu131 experimentally observed in the electron density/crystal structure was incorporated into the docking model. Docking was performed with Arg38, Tyr113 and Glu131 as flexible residues in an effort to obtain the lowest-energy conformations.

**Reporting Summary.** Further information on research design is available in the Nature Research Reporting Summary linked to this article.

### Data availability

The sequence data referenced in this study are available in GenBank with the accession number MN401751. Coordinates and associated structure factors have been deposited in the Protein Data Bank (PDB) with PDB ID 6U9I (BvnE) and in the Cambridge Crystallographic Data Centre (CCDC) with the CCDC numbers 1973959 (BX), 1973957 (BY) and 1973958 (15). Molecular coordinates as well as absolute and relative thermochemistry data have been provided for the computational studies. All other data are available from the corresponding authors on reasonable request.

Received: 5 October 2019; Accepted: 16 March 2020;

Published online: 18 May 2020

### References

- Klax, K. R. et al. Structural and stereochemical diversity in prenylated indole alkaloids containing the bicyclo[2.2.2]diazaoctane ring system from marine and terrestrial fungi. *Nat. Prod. Rep.* **35**, 532–558 (2018).
- Ittich, A. J. & Wright, J. I. The brevitaminamides: a new class of fungal alkaloid. *J. Chem. Soc. D* 644b–645b (1969).
- Li, S. et al. Comparative analysis of the biosynthetic systems for fungal bicyclo[2.2.2]diazaoctane indole alkaloids: the (+)/(-)-notoamide, paraherquamide and malbrancheamide pathways. *Mol. Cell. Proteom.* **3**, 987–996 (2012).
- Finefield, J. M., Frisvad, J. C., Sherman, D. H. & Williams, R. M. Fungal origins of the bicyclo[2.2.2]diazaoctane ring system of prenylated indole alkaloids. *J. Nat. Prod.* **75**, 812–833 (2012).
- Sanz-Cervera, J. F., Glinka, T. & Williams, R. M. Biosynthesis of the brevitaminamides: quest for a biosynthetic Diels–Alder cyclization. *J. Am. Chem. Soc.* **115**, 347–348 (1993).
- Sanz-Cervera, J. F., Glinka, T. & Williams, R. M. Biosynthesis of brevitaminamides A and B: in search of the biosynthetic Diels–Alder construction. *Tetrahedron* **49**, 8471–8482 (1993).
- Williams, R. M., Sanz-Cervera, J. F., Sancenon, F., Marco, J. A. & Halligan, K. Biomimetic Diels–Alder cyclizations for the construction of the brevitaminamide, paraherquamide sclerotamide, and VMS5599 ring systems. *J. Am. Chem. Soc.* **120**, 1090–1091 (1998).
- Adams, L. A., Valente, M. W. N. & Williams, R. M. A concise synthesis of d,l-brevitaminamide B via a biomimetically-inspired IMDA construction. *Tetrahedron* **62**, 5195–5200 (2006).
- Williams, R. M. & Cox, R. J. Paraherquamides, brevitaminamides, and asperparalines: laboratory synthesis and biosynthesis. An interim report. *Acc. Chem. Res.* **36**, 127–139 (2003).
- Stocking, E. M. & Williams, R. M. Chemistry and biology of biosynthetic Diels–Alder reactions. *Angew. Chem. Int. Ed.* **42**, 3078–3115 (2003).
- Dun, Q. et al. Fungal indole alkaloid biogenesis through evolution of a bifunctional reductase/Diels–Alderase. *Nat. Chem.* **11**, 972–980 (2019).
- Williams, R. M., Glinka, T. & Kwast, E. Facial selectivity of the intramolecular SN<sup>2</sup> cyclization: stereocontrolled total synthesis of brevitaminamide B. *J. Am. Chem. Soc.* **110**, 5927–5929 (1988).
- Williams, R. M., Kwast, E., Coffman, H. & Glinka, T. Remarkable, enantio-divergent biogenesis of brevitaminamide A and B. *J. Am. Chem. Soc.* **111**, 3064–3065 (1989).
- Porter, A. E. A. & Sammes, P. G. A Diels–Alder reaction of possible biosynthetic importance. *J. Chem. Soc. D* 1103a (1970).
- Li, F. et al. Determination of tatchuanamide H and structural revision of tatchuanamide A. *Org. Lett.* **20**, 1138–1141 (2018).
- Greshock, T. J. et al. Isolation, structure elucidation, and biomimetic total synthesis of vericolumamide B, and the isolation of antipodal (-)-stephacidin A and (+)-notoamide B from *Aspergillus versicolor* NRRL 35600. *Angew. Chem. Int. Ed.* **47**, 3573–3577 (2008).
- Kat, A., Kato, H., Sherman, D. H., Williams, R. M. & Tsukamoto, S. Isolation of a new indoxyl alkaloid, Amoenamide B, from *Aspergillus amoensis* NRRL 35600: biosynthetic implications and correction of the structure of Speramide B. *Tetrahedron Lett.* **59**, 4236–4240 (2018).
- Xu, X., Zhang, X., Nong, X., Wang, J. & Qi, S. Brevitaminamides and mycophenolic acid derivatives from the deep-sea-derived fungus *Penicillium brevicompactum* DFFSC025. *Mar. Drugs* **15**, 43 (2017).

19. Godfrey, R. C., Green, N. J., Nichol, G. S. & Lawrence, A. L. Total synthesis of brevianamide A. *Nat. Chem.* <https://doi.org/10.1038/s41557-020-0442-3> (2020).
20. Mori, T. et al. Molecular basis for the unusual ring reconstruction in fungal meroterpenoid biogenesis. *Nat. Chem. Biol.* **13**, 1066–1073 (2017).
21. Li, S. et al. Biochemical characterization of NotB as an FAD-dependent oxidase in the biosynthesis of notoamide indole alkaloids. *J. Am. Chem. Soc.* **134**, 788–791 (2012).
22. Ding, Y. et al. Genome-based characterization of two prenylation steps in the assembly of the stephacidin and notoamide anticancer agents in a marine-derived *Aspergillus* sp. *J. Am. Chem. Soc.* **132**, 12733–12740 (2010).
23. Kato, N. et al. Identification of cytochrome P450s required for fumitremorgin biosynthesis in *Aspergillus fumigatus*. *ChemBioChem* **10**, 920–928 (2009).
24. Li, H. et al. HPLC-DAD-directed isolation of linearly fused prenylated indole alkaloids from a soil-derived *Aspergillus versicolor*. *J. Nat. Prod.* **82**, 2181–2188 (2019).
25. Matsuda, Y. et al. Discovery of key dioxygenases that diverged the paraherquoin and acetoxydehydroaustin pathways in *Penicillium brassiabanum*. *J. Am. Chem. Soc.* **138**, 12671–12677 (2016).
26. Sutor, D. J. The C–H–O hydrogen bond in crystals. *Nature* **195**, 68–69 (1962).
27. Schwalbe, C. H. June Sutor and the C–H–O hydrogen bonding controversy. *Crystallogr. Rev.* **18**, 191–206 (2012).
28. Goswami, R. S. Targeted gene replacement in fungi using a split-marker approach. *Methods Mol. Biol.* **835**, 255–269 (2012).
29. Heneghan, M. N. et al. First heterologous reconstruction of a complete functional fungal biosynthetic multigene cluster. *ChemBioChem* **11**, 1508–1512 (2010).
30. Kabach, W. XDS. *Acta Crystallogr. D* **66**, 125–132 (2010).
31. McCoy, A. J. et al. Phaser crystallographic software. *J. Appl. Crystallogr.* **40**, 658–674 (2007).
32. Emsley, P., Lohkamp, B., Scott, W. G. & Cowtan, K. Features and development of Coot. *Acta Crystallogr. D* **66**, 486–501 (2010).
33. Adams, P. D. et al. PHENIX: a comprehensive Python-based system for macromolecular structure solution. *Acta Crystallogr. D* **66**, 213–221 (2010).
34. Chen, V. B. et al. MolProbity: all-atom structure validation for macromolecular crystallography. *Acta Crystallogr. D* **66**, 12–21 (2010).
35. Morris, G. M. et al. AutoDock4 and AutoDockTools4: automated docking with selective receptor flexibility. *J. Comput. Chem.* **30**, 2785–2791 (2009).

### Acknowledgements

This work was supported by the National Key Research and Development Program (2019YFA0905100 and 2019YFA0706900), the National Natural Science Foundation of China (21472204 and 31872729 to S.L. and 31800041 to L.D.), the National Institutes of Health R35 GM118101, the Hans W. Vahlteich Professorship (to D.H.S.), R01 CA070375 (to R.M.W. and D.H.S.), the Shandong Provincial Natural Science

Foundation (ZR2019ZD20 to S.L. and ZR201807060986 to L.D.), the National Postdoctoral Innovative Talents Support Program (BX20180325 to L.D.), the China Postdoctoral Science Foundation (2019M652500 to L.D.) and funding from the NSF (grant no. CHE-0840456, for X-ray instrumentation). GM/CA@APS is supported by the National Institutes of Health, the National Institute of General Medical Sciences (AGM-12006) and the National Cancer Institute (ACB-12002). We thank J. L. Smith from the University of Michigan for her assistance with the structure determination of Bvnl. R.S.P. acknowledges computational resources from the RMACC Summit supercomputer supported by the National Science Foundation (ACI-1532235 and ACI-1532236), the University of Colorado Boulder and Colorado State University, and the Extreme Science and Engineering Discovery Environment (XSEDE) through allocation TG-CHE180056. XSEDE is supported by the National Science Foundation (ACI-1548562). The authors thank X. Li and H. Sai from The State Key Laboratory of Microbial Technology, Shandong University for their assistance with single-crystal X-ray diffraction.

### Author contributions

Y.Y., L.D., R.M.W., D.H.S. and S.L. contributed to the experimental design. Y.Y., L.D., W.Z. and F.Q. performed molecular cloning, fungal genetics and compound purification. Y.Y., L.D. and X.Z. performed structural assignment (NMR analysis). Y.Y., L.D., S.A.N., A.E.F. and M.L.A.-C. performed molecular cloning, protein expression and purification. Y.Y. and L.D. performed enzymatic assays, and LC-MS and HPLC analyses. S.A.N. and M.L.A.-C. carried out all crystallographic experiments and structural analyses. Y.Y. performed structure-based site-directed mutagenesis. W.Z. performed genome mining of the gene cluster. M.M., N.A.C., V.V.S. and S.M. synthesized and validated the compounds described in this study. I.V.A.-R and R.S.P. performed DFT calculations. A.M. and H.O. supplied the heterologous expression system. H.K. and S.T. performed ECD measurements and calculations. Y.Y., L.D., S.A.N., R.S.P., R.M.W., D.H.S. and S.L. analysed the data and prepared the manuscript.

### Competing interests

The authors declare no competing interests.

### Additional information

Extended data is available for this paper at <https://doi.org/10.1038/s41929-020-0454-9>.

Supplementary information is available for this paper at <https://doi.org/10.1038/s41929-020-0454-9>.

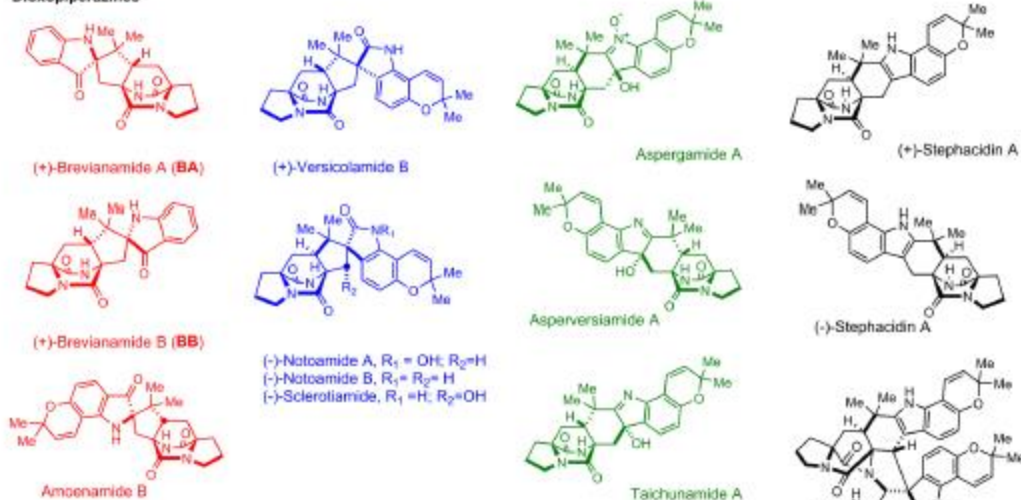
Correspondence and requests for materials should be addressed to R.M.W., D.H.S. or S.L.

Reprints and permissions information is available at [www.nature.com/reprints](http://www.nature.com/reprints).

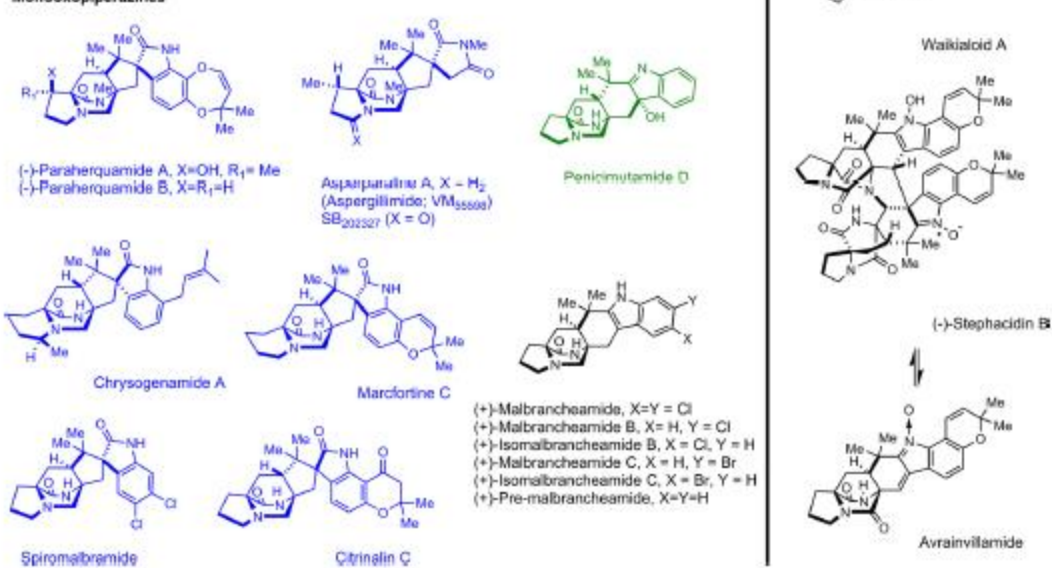
Publisher's note Springer Nature remains neutral with regard to jurisdictional claims in published maps and institutional affiliations.

© The Author(s), under exclusive licence to Springer Nature Limited 2020

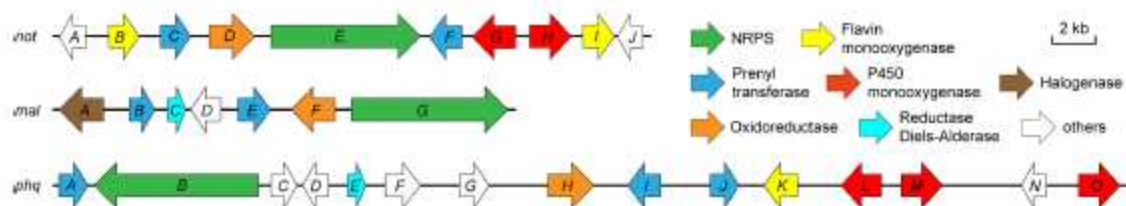
## Dioxopiperazines



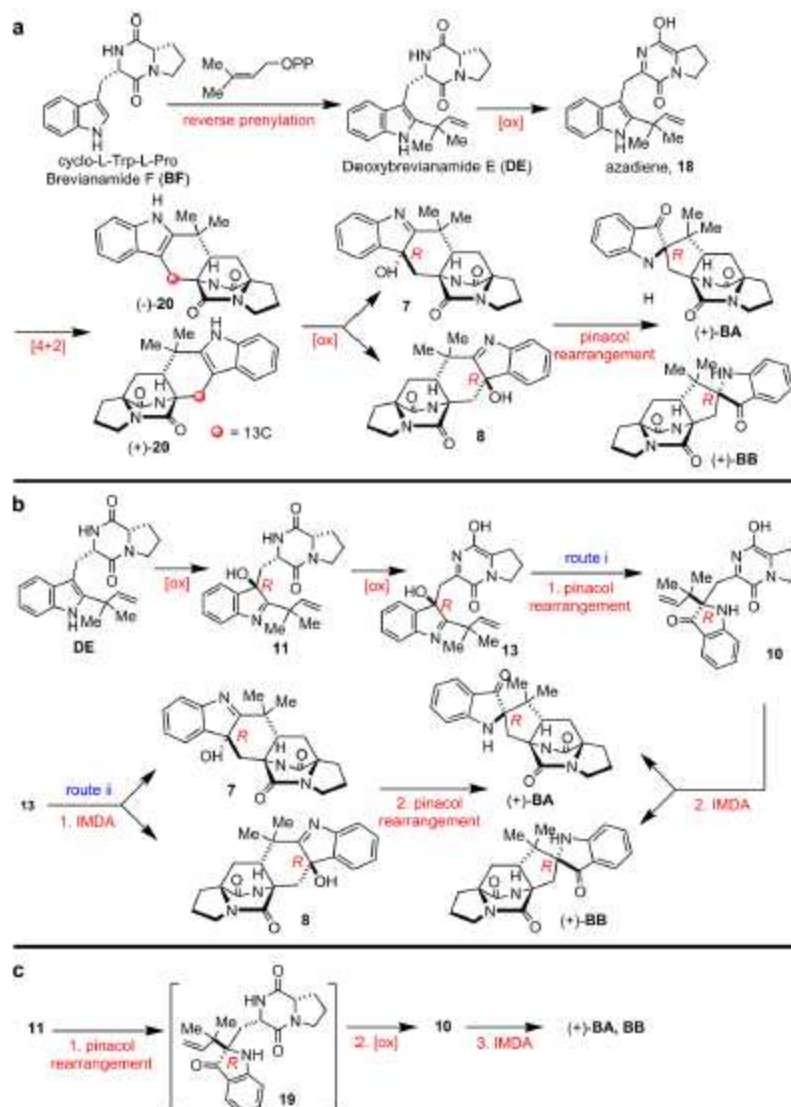
## Monooxopiperazines



**Extended Data Fig. 1 | Representative fungal bicyclo[2.2.2]diazaoctane indole alkaloids.** Compounds with 3-spro- $\psi$ -Indoxyls, spro-2-oxIndoles and 3-hydroxyindolenines are presented in red, blue and green, respectively.

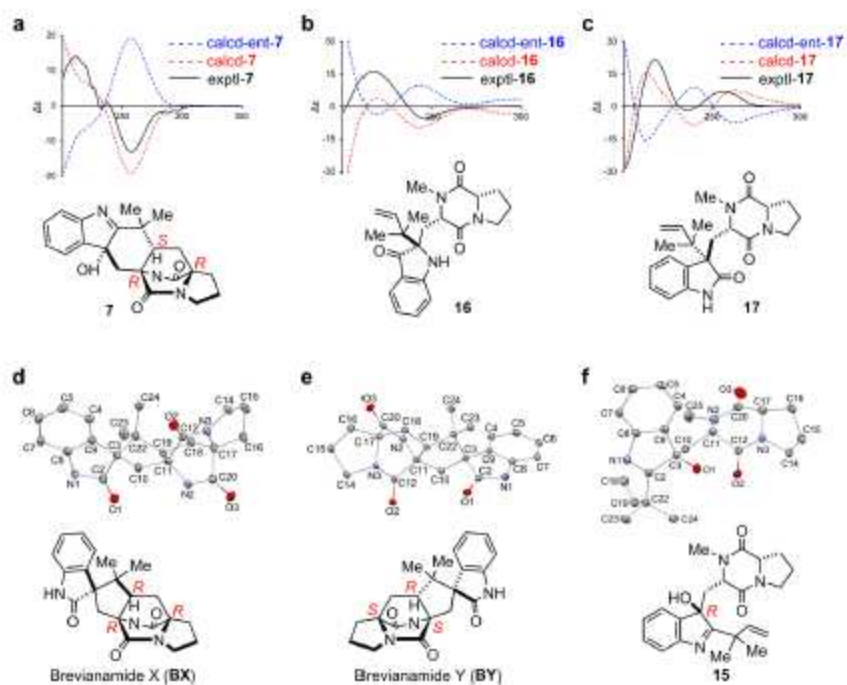


**Extended Data Fig. 2 |** The biosynthetic gene clusters for representative fungal bicyclo[2.2.2]indole alkaloids. The gene clusters *not*, *mal* and *phq* are responsible for biosynthesis of notoamides, malbrancheamides and parapherquamides, respectively.

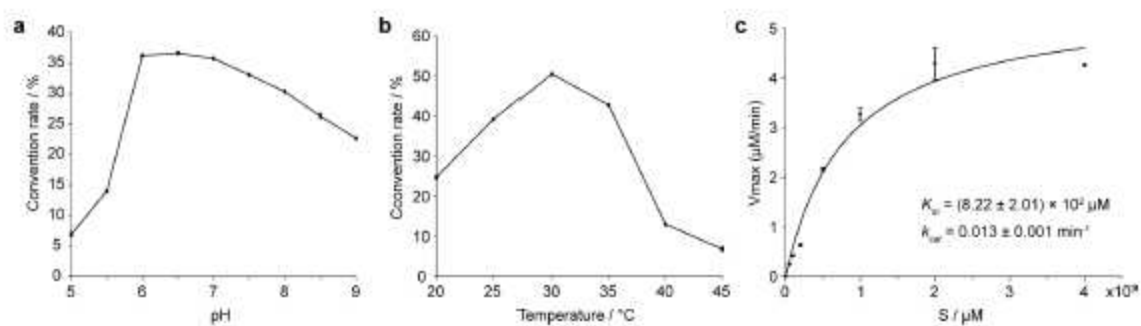


**Extended Data Fig. 3 | Biogenetic proposals for Brevianamide A (BA) and Brevianamide B (BB).** **a**, Early biosynthetic proposal suggested and interrogated by Williams *et al.*<sup>36</sup>. **b**, Original biogeneses proposed by Porter and Sammes (via 7)<sup>34</sup>. **c**, More recent biosynthetic proposals suggested by Williams *et al.*<sup>34,35</sup>. Several biogenetic hypotheses based on the pioneering proposal first suggested by Porter and Sammes in 1970<sup>34</sup> reasoned that the bicyclo[2.2.2]diazaoctane core arises via an intramolecular [4+2] hetero-Diels-Alder (IMDA) construction<sup>35,36</sup>. We experimentally interrogated the biogenetic proposal **a**, through the synthesis of <sup>13</sup>C-labeled putative Diels-Alder products ( $\pm$ )-20, but could not detect incorporation into either **BA** or **BB** in cultures of *Pb*. Based on these results, we then suggested the biosynthetic pathways illustrated in **b** and **c**. The fundamental difference between the biogeneses described in **a**, and that in **b** and **c** is the sequential timing of the indole oxidation, the semipinacol rearrangement and the crucial IMDA reactions. Thus, it remained conceivable that oxidation of **DE** to the (*R*)-hydroxyindolenine provides species **11**, which can suffer several fates. One is N-C ring closure to co-metabolite Brevianamide E (**BE**); a second possibility shown in **b** is oxidation and tautomerization to the azadiene species **13**, which can suffer IMDA cyclization providing **7** and **8**, then undergo a final semipinacol rearrangement to furnish **BA** and **BB** (route *i*). Alternatively, azadiene **13** could first suffer semipinacol rearrangement to **10**, which then undergoes the IMDA construction to generate **BA** and **BB** (route *ii*). Another possibility **c** involves (*R*)-hydroxyindolenine **11**, which proceeds through a semipinacol rearrangement to the indoxy species **19**, followed by further oxidation to the azadiene species **10** and subsequent IMDA to furnish **BA** and **BB**. Experimental supports to distinguish between these proposed pathways, all of which embrace the relative and absolute stereochemistry of **BA** and **BB**, have remained unresolved until this work.

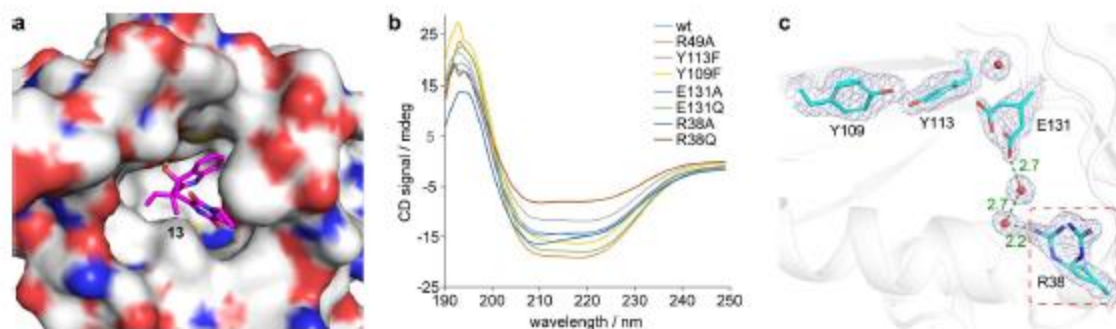
36. Williams, R. M., Sanz-Cervera, J. F., Sancenon, F., Marco, J. A. & Halligan, K. M. Biomimetic Diels-Alder cyclizations for the construction of the brevianamide, paraherquamide, sclerotamide, asperpsaltrin and VM55599 ring systems. *Borg. Med. Chem.* 6, 1233–1241 (1998).



**Extended Data Fig. 4 | Elucidation of absolute configurations.** **a**, Experimental and computational CD spectra of **7**. **b**, Experimental and computational CD spectra of **16**. **c**, Experimental and computational CD spectra of **17**. **d**, X-ray ORTEP diagram of **BX**. **e**, X-ray ORTEP diagram of **BY**. **f**, X-ray ORTEP diagram of **15**.



**Extended Data Fig. 5 | Enzyme properties of BvnE using compound 15 as a substrate. a,** pH dependency. **b,** temperature dependency. **c,** Michaelis-Menten kinetic analysis (centre values, means: error bars, standard deviations:  $n = 2$ ).



**Extended Data Fig. 6 | Docking results and CD spectra of BvnE.** **a**, Docking complex of BvnE with compound **13** (magenta). **b**, CD spectra of purified wild-type and mutant BvnE proteins. **c**, Electron density ( $2F_o - F_c$ ,  $1\sigma$ ) for the active site residues of BvnE (PDB ID code: 6U9I) shows conformational flexibility at Arg38 and Glu131 suggestive of potential active site remodeling during catalysis. Arg38 (red box) which is essential for catalytic activity does not make direct interactions with the docked ligand or active site residues. However, the structure reveals two ordered water molecules (red spheres) in a hydrogen bonding network between Arg38 and Glu131. These binding poses reveal possible key interactions between the ligand and BvnE.

## List of Abbreviations

Ac <sub>2</sub> O	Acetic Anhydride
AcOH	Acetic Acid
AIBN	Azobisisobutyronitrile
<i>Ao</i>	<i>Aspergillus oryzae</i>
9-BBN	9-Borabicyclo[3.3.1]nonane
BBr <sub>3</sub>	Boron tribromide
Boc	<i>tert</i> -Butoxycarbonyl
Boc <sub>2</sub> O	Di- <i>tert</i> -butyl dicarbonate
BF <sub>4</sub> OMe <sub>3</sub>	Trimethyloxonium tetrafluoroborate
Bn	Benzyl
BOP-Cl	Biphosphinic chloride
BuLi	Butyllithium
CDCl <sub>3</sub>	Deuterated Chloroform
CHCl <sub>3</sub>	Chloroform
CO <sub>2</sub> H	Formaldehyde
Cs <sub>2</sub> CO <sub>3</sub>	Cesium Carbonate
DA	Diels-Alder
DBU	1,8-diazabicyclo[5.4.0]undec-7-ene
DCC	N,N'-Dicyclohexylcarbodiimide

DCM	Dichloromethane
DDQ	2,3-dichloro-5,6-dicyano-1,4-benzoquinone
DEAD	Diethyl azocarboxylate
DES	Diethyl sulfate
DIBAL	Diisobutylaluminum hydride
DIPEA	Diisopropylethylamine
DMF	Dimethylformamide
DMSO	Dimethylsulfoxide
DO	Davis' Oxadizidine
EDC	N-(3-Dimethylaminopropyl)-N'-ethylcarbodiimide hydrochloride
Et	Ethyl
EtOAc	Ethyl acetate
Et <sub>2</sub> O	Diethyl ether
EtOH	Ethanol
Fmoc	Fluorenylmethyloxycarbonyl
FmocOsu	Fluorenylmethoxycarbonyloxy succinimide
HATU	<i>O</i> -(7-Azabenzotriazol-1-yl)- <i>N,N,N',N'</i> -tetramethyluronium
HFIP	Hexafluoroisopropanol
HPLC	High Performance Liquid Chromatography
IMDA	IMDA Intramolecular Diels-Alder
K <sub>2</sub> CO <sub>3</sub>	Potassium carbonate
KHMDS	KHMDS Potassium (bis)trimethylsilyl amide
KO	Knock-out

LDA	Lithium diisopropylamide
<i>m</i> CPBA	<i>m</i> CPBA <i>meta</i> -Chloroperbenzoic acid
Me	Methyl
MeI	Methyl iodide
MeCN	Acetonitrile
MeOH	Methanol
MOM	Methoxymethyl
MOM-Cl	Chloromethyl methyl ether
Ms	Methanesulfonyl (mesylate)
MsCl	Methanesulfonyl chloride
NaBH <sub>4</sub>	Sodium borohydride
NaBH <sub>3</sub> CN	Sodium cyanoborohydride
NADH	Nicotinamide adenine dinucleotide
NADPH	Nicotinamide adenine dinucleotide phosphate
NaH	Sodium Hydride
NaS <sup>t</sup> Bu	Sodium 2-methyl-2-propanethiolate
NCS	N-chlorosuccinimide
NHMDS (or NaHMDS)	Sodium (bis)trimethylsilyl amide
NHMe <sub>2</sub>	Dimethylamine
NHPI	N-Hydroxyphthalimide
NMR	Nuclear magnetic resonance
NRPS	Nonribosomal peptide synthetase
NTF2	Nuclear transport factor 2

PBu <sub>3</sub>	Tributylphosphine
PCl <sub>5</sub>	Phosphorus pentachloride
PhMe	Toluene
PhNHNH <sub>2</sub>	Phenylhydrazine
pMB	<i>p</i> -Methoxybenzyl
PPTS	Pyridinium <i>p</i> -toluenesulfonate
pTLC	pTLC Preparative thin layer chromatography
<i>i</i> -Pr	<i>i</i> -Pr Isopropyl
Py. or Pyr	Pyridine
Red-Al	Sodium bis(2-methoxyethoxy)aluminum dihydride
Sc(OTf) <sub>3</sub>	Scandium Triflate
SM	Starting Material
taut	Tautomerize
TBAF	Tetrabutylammonium fluoride
<i>t</i> -Bu	<i>Tert</i> -butyl
<i>t</i> BuOCl	<i>Tert</i> -butyl hypochlorite
TFA	Trifluoroacetic acid
THF	Tetrahydrofuran
TLC	Thin layer chromatography
TMS	Trimethylsilyl
TMSCl	Trimethylsilyl chloride
TMSOTf	Trimethylsilyl trifluoromethanesulfonate
TMSI	1-(Trimethylsilyl)imidazole

pTLC

Preparative thin layer chromatography

*i*-Pr

Isopropyl

2-OH-py

2-Hydroxypyridine